

# NON-LINEAR MASS TRANSFER AND HYDRODYNAMIC STABILITY

$$\rho(c)W(c).gradc =$$



$$= \operatorname{div}[\rho(c)D(c)gradc] + kc''$$

CHR. B. BOYADJIEV  
V. N. BABAK

ELSEVIER

**NON-LINEAR  
MASS TRANSFER  
AND  
HYDRODYNAMIC  
STABILITY**

This Page Intentionally Left Blank

# **NON-LINEAR MASS TRANSFER AND HYDRODYNAMIC STABILITY**

**Christo Boyanov Boyadjiev**

Institute of Chemical Engineering, Bulgarian Academy of Sciences,  
Acad. G. Bontchev Str. Bl. 103,  
1113 Sofia, Bulgaria

**Vladislav Nikolaevich Babak**

Institute of Problems of Chemical Physics, Russian Academy of Sciences,  
Chernogolovka, 142432 Moscow area, Russia

2000



**ELSEVIER**

Amsterdam - Lausanne - New York - Oxford - Shannon - Singapore - Tokyo

**ELSEVIER SCIENCE B.V.**  
Sara Burgerhartstraat 25  
P.O. Box 211, 1000 AE Amsterdam, The Netherlands

© 2000 Elsevier Science B.V. All rights reserved.

This work is protected under copyright by Elsevier Science, and the following terms and conditions apply to its use:

**Photocopying**

Single photocopies of single chapters may be made for personal use as allowed by national copyright laws. Permission of the Publisher and payment of a fee is required for all other photocopying, including multiple or systematic copying, copying for advertising or promotional purposes, resale, and all forms of document delivery. Special rates are available for educational institutions that wish to make photocopies for non-profit educational classroom use.

Permissions may be sought directly from Elsevier Science Global Rights Department, PO Box 800, Oxford OX5 1DX, UK; phone: (+44) 1865 843830, fax: (+44) 1865 853333, e-mail: permissions@elsevier.co.uk. You may also contact Global Rights directly through Elsevier's home page (<http://www.elsevier.nl>), by selecting 'Obtaining Permissions'.

In the USA, users may clear permissions and make payments through the Copyright Clearance Center, Inc., 222 Rosewood Drive, Danvers, MA 01923, USA; phone: (978) 7508400, fax: (978) 7504744, and in the UK through the Copyright Licensing Agency Rapid Clearance Service (CLARCS), 90 Tottenham Court Road, London W1P 0LP, UK; phone: (+44) 171 631 5555; fax: (+44) 171 631 5500. Other countries may have a local reprographic rights agency for payments.

**Derivative Works**

Tables of contents may be reproduced for internal circulation, but permission of Elsevier Science is required for external resale or distribution of such material. Permission of the Publisher is required for all other derivative works, including compilations and translations.

**Electronic Storage or Usage**

Permission of the Publisher is required to store or use electronically any material contained in this work, including any chapter or part of a chapter.

Except as outlined above, no part of this work may be reproduced, stored in a retrieval system or transmitted in any form or by any means, electronic, mechanical, photocopying, recording or otherwise, without prior written permission of the Publisher.

Address permissions requests to: Elsevier Global Rights Department, at the mail, fax and e-mail addresses noted above.

**Notice**

No responsibility is assumed by the Publisher for any injury and/or damage to persons or property as a matter of products liability, negligence or otherwise, or from any use or operation of any methods, products, instructions or ideas contained in the material herein. Because of rapid advances in the medical sciences, in particular, independent verification of diagnoses and drug dosages should be made.

**First edition 2000**

**Library of Congress Cataloging in Publication Data**

A catalog record from the Library of Congress has been applied for.

ISBN: 0 444 50428 1

⊗ The paper used in this publication meets the requirements of ANSI/NISO Z39.48-1992 (Permanence of Paper).  
Printed in The Netherlands.

This book is dedicated to our dear friend and teacher  
professor V. S. Krylov

Prof. Chr. B. Boyadjiev

Assoc. prof. V. N. Babak

*Chr. B. Boyadjiev, V. N. Babak*

## **Non-Linear Mass Transfer and Hydrodynamic Stability**

### **Abstract**

The kinetics of the non-linear mass transfer and its effect on the hydrodynamic stability in systems with intensive interphase mass transfer are surveyed in this book. The influence of the big concentration gradients, the high concentrations and the temperature is presented.

Non-linear mass transfer, as a result of intensive interphase mass transfer in gas (liquid)-solid, gas-liquid and liquid-liquid systems, is discussed in the approximations of the diffusion boundary layer and in a rectangular channel with the longitudinal diffusion taken into account. It is demonstrated that the direction of the intensive interphase mass transfer influences the rates of the mass transfer, heat transfer and multicomponent mass transfer.

Non-linear mass transfer in electrochemical systems with high current density is discussed on the examples of the anode dissolving of metals in the electrolyte flow and the electrode position of metals out of concentrated solutions.

Non-linear mass transfer in chemically reacting systems is discussed both in cases of non-linearity of the equations of chemical reactions kinetics and in the cases of either intensive interphase mass transfer or thermocapillary effects as a result of chemical reactions.

The kinetics of mass transfer, accompanied by a chemical reaction in non-stationary two-phase systems, is discussed for arbitrary contact times between the phases.

Linear analysis of the hydrodynamic stability of systems in which the non-linear mass transfer leads to change in the velocity distribution in the laminar boundary layers is performed.

One is demonstrated that the mass transfer direction affect the mass transfer rate and hydrodynamic stability in gas(liquid)-solid, gas-liquid and liquid-liquid systems.

## CONTENTS

<b>PREFACE</b>	<b>xi</b>
<b>Introduction</b>	<b>1</b>
<b>LINEAR MASS TRANSFER THEORY</b>	
1. Model theories	2
2. Boundary layer theory	4
3. Immobile phase boundary	5
4. Moving phase boundary	7
6. Counter-current flow	10
References	15
<b>PART 1</b>	
<b>Systems with Intensive Interphase Mass Transfer</b>	<b>17</b>
<b>CHAPTER 1.1.</b>	<b>SPECIFICS OF THE HYDRODYNAMIC CONDITIONS OF THE INTENSIVE INTERPHASE MASS TRANSFER</b>
1.1.1.	Influence of the intensive interphase mass transfer on hydrodynamics
1.1.2.	Boundary conditions of the non-linear mass transfer problem
<b>CHAPTER 1.2.</b>	<b>GAS (LIQUID)-SOLID SYSTEM</b>
1.2.1.	Non-linear mass transfer in the boundary layer
1.2.2.	Heat transfer in the conditions of non-linear mass transfer
1.2.3.	Multicomponent mass transfer
1.2.4.	Non-linear mass transfer in the entrance region of a channel
<b>CHAPTER 1.3.</b>	<b>GAS-LIQUID AND LIQUID-LIQUID SYSTEMS</b>
1.3.1.	Non-linear mass transfer in the gas and in the liquid boundary layer
1.3.2.	Multicomponent interphase mass transfer in the case of an intensive mass transfer in the gas
1.3.3.	Non-linear interphase mass transfer between two liquids
<b>CHAPTER 1.4.</b>	<b>GAS-FALLING LIQUID FILM-SOLID SURFACE SYSTEM</b>
1.4.1.	Non-linear interphase mass transfer between the gas and the falling liquid film
1.4.2.	Non-linear effects in the case of a multicomponent interphase mass transfer between the gas and the liquid film
<b>CHAPTER 1.5.</b>	<b>EFFECTS OF CONCENTRATION AND TEMPERATURE ON THE NON-LINEAR MASS TRANSFER</b>
1.5.1.	Concentration effects
1.5.2.	Influence of the high concentration on the mass transfer rate
1.5.3.	Non-linear mass transfer and Marangoni effect
References	107

**PART 2**

<b>Electrochemical Systems With High Intensity Electric Currents</b>	<b>111</b>	
<b>CHAPTER 2.1.</b>	<b>FUNDAMENTALS OF THE KINETIC THEORY OF TRANSPORT OF MASS AND CHARGE IN ELECTRIC SYSTEMS</b>	
2.1.1.	Method of the self-consistent field	111
2.1.2.	Transport of neutral molecules in the self-consistent field of the double electric layer	112
2.1.3.	Method of the local thermodynamic equilibrium	114
<b>CHAPTER 2.2.</b>	<b>ANODIC METAL DISSOLUTION IN AN ELECTROLYTE FLOW</b>	<b>116</b>
2.2.1.	Dissolution of surfaces equi-accessible with respect the ionic mass transfer	118
2.2.2.	Ionic mass transfer due to an anodic dissolution complicated with a reaction of complex formation	122
2.2.3.	Comparison between the theoretical predictions and the experimental data	127
2.2.4.	Ionic mass transfer effects on the hydrodynamics during dissolution of a rotating disk electrode surface	132
2.2.5.	Anodic dissolution of metals in concentrated solutions with variable physical properties	134
2.2.6.	Effect of saturation of near-anode layer by electrode reaction products	137
2.2.7.	Electrochemical dissolution of metal inclusions in channels	141
2.2.8.	Dissolution of rectangular channel walls	142
<b>CHAPTER 2.3.</b>	<b>ELECTROCHEMICAL RECOVERY OF METALS FROM CONCENTRATED SOLUTIONS</b>	<b>146</b>
2.3.1.	Method for the establishment of the effects of the apparent diffusion coefficient of the salt	157
<b>CHAPTER 2.4.</b>	<b>EFFECT OF THE NON-ISOTHERMAL CONDITIONS AND THE GAS EVOLUTION</b>	<b>158</b>
2.4.1.	Non-isothermal effects on potential distributions in an injection flow electrochemical cell	161
2.4.2.	Gas evolution	164
	References	165
<b>PART 3</b>		
<b>Chemically Reacting Gas-Liquid Systems</b>	<b>171</b>	
<b>CHAPTER 3.1.</b>	<b>INTERPHASE MASS TRANSFER MECHANISM</b>	<b>172</b>
3.1.1.	Irreversible chemical reactions	178
3.1.2.	Homogenous catalytic reactions	184
3.1.3.	Reversible chemical reactions	187
3.1.4.	Relationships between the chemical and physical equilibriums during absorption	191
<b>CHAPTER 3.2.</b>	<b>MACROKINETICS OF THE CHEMICAL TRANSFORMATIONS</b>	<b>193</b>
3.2.1.	Chemosorption in a falling liquid film	195

3.2.2.	Sulphuric acid alkylation process in a film flow reactor	198
3.2.3.	Non-linear mass transfer in a falling liquid film	203
<b>CHAPTER 3.3.</b>	<b>EFFECTS OF THE PHYSICAL PARAMETERS</b>	207
3.3.1.	Concentration effects	207
3.3.2.	Temperature effects	210
	References	223
<b>PART 4</b>		
<b>Non-Stationary Interphase Mass Transfer with Chemical Reactions</b>		225
<b>CHAPTER 4.1.</b>	<b>NON-STATIONARY PHYSICAL ABSORPTION</b>	227
4.1.1.	Problem solution	230
4.1.2.	Solutions at short contact times	232
4.1.3.	Interphase mass transfer resistance located in one of the phases	233
4.1.4.	Solution on the line $\beta = 1$	234
4.1.5.	Solution in the upper part of $X - Y$ plane	235
4.1.6.	Solution in the lower part of the $X - Y$ plane	236
4.1.7.	Solution in the left part of $X - Y$ plane	237
4.1.8.	Solution in the right part of $X - Y$ plane	239
4.1.9.	Numerical solutions	240
4.1.10.	Approximations of the numerical solutions	246
4.1.11.	Physical absorption	249
4.1.12.	Non-stationary interphase heat transfer	252
4.1.13.	Interphase heat transfer regimes	256
<b>CHAPTER 4.2.</b>	<b>NON-STATIONARY TWO-PHASE ABSORPTION COMPLICATED WITH FIRST ORDER CHEMICAL REACTION</b>	261
4.2.1.	Solution in $X - Y$ plane at $\varepsilon \ll 1, \varepsilon\beta \ll 1$	265
4.2.2.	Solution in the area with $\varepsilon \gg 1, \varepsilon\beta \ll 1$	268
4.2.3.	Solution at $\varepsilon \gg 1$ and $\varepsilon\beta \gg 1$	269
4.2.4.	Solution in the area with $\varepsilon \ll 1, \varepsilon\beta \gg 1$	269
4.2.5.	Solution at $\beta^2 = 1$	271
4.2.6.	Common properties of the solutions	271
4.2.7.	Numerical investigation of the two-phase chemosorption in the initial time interval	277
4.2.8.	Numerical investigation of the chemosorption outside the initial interval	288
4.2.9.	Methodology of the chemosorption design	290
<b>CHAPTER 4.3.</b>	<b>NON-STATIONARY ABSORPTION WITH SECOND ORDER CHEMICAL REACTION</b>	291
4.3.1.	Mass transfer in the liquid at short contact times	294
4.3.2.	Transformation of the problem of two-phase chemosorption to a two-phase absorption problem with non-linear boundary conditions	303
4.4.3.	Solution with parameters $\varepsilon N \leq 1, \varepsilon\beta N \leq 1$	307

4.3.4.	<b>Solution with parameters <math>\varepsilon N \geq 1</math> and <math>\varepsilon \beta N \geq 1</math></b>	328
4.3.5.	<b>Investigations in the fourth quadrant of the plane <math>X_N - Y_N</math></b>	343
4.3.6.	<b>Investigations in the second quadrant on the plane <math>X_N - Y_N</math></b>	357
4.3.7.	<b>Analysis of the basis relations of the two-phase absorption</b>	367
4.3.8.	<b>Applications</b>	375
	<b>References</b>	386
<b>PART 5</b>		
<b>Hydrodynamic Stability in Systems with Intensive Interphase</b>		
<b>Mass Transfer</b>		389
<b>CHAPTER 5.1.</b>	<b>STABILITY THEORY</b>	389
5.1.1.	<b>Evolution equations</b>	389
5.1.2.	<b>Bifurcation theory</b>	394
5.1.3.	<b>Eigenvalue problems</b>	398
<b>CHAPTER 5.2</b>	<b>HYDRODYNAMIC STABILITY</b>	399
5.2.1.	<b>Fundamental equations</b>	399
5.2.2.	<b>Power theory</b>	400
5.2.3.	<b>Linear theory</b>	403
5.2.4.	<b>Stability, bifurcation and turbulence</b>	405
5.2.5.	<b>Stability of parallel flows</b>	407
<b>CHAPTER 5.3</b>	<b>ORR-SOMMERFELD EQUATION</b>	407
5.3.1.	<b>Parallel flows</b>	408
5.3.2.	<b>Almost parallel flows</b>	409
<b>CHAPTER 5.4.</b>	<b>LINEAR STABILITY AND NON-LINEAR MASS TRANSFER</b>	410
5.4.1.	<b>Gas (liquid) –solid system</b>	410
5.4.2.	<b>Gas – liquid system</b>	424
5.4.3.	<b>Liquid-liquid system</b>	429
5.4.4.	<b>Gas-liquid film flow systems.</b>	435
5.4.5.	<b>Effect of concentration</b>	440
5.4.6.	<b>Effect of temperature</b>	449
<b>CHAPTER 5.5.</b>	<b>MECHANISM AND KINETICS OF THE TRANSPORT PROCESSES IN SYSTEMS WITH INTENSIVE INTERPHASE MASS TRANSFER</b>	451
5.5.1.	<b>Mass and heat transfer kinetics</b>	452
5.5.2.	<b>Linear stability analysis</b>	462
5.5.3.	<b>Comparison with experimental data</b>	470
5.5.4.	<b>Comparative analysis of the absorption and desorption rates</b>	472
	<b>References</b>	483
<b>Conclusion</b>		487
	<b>INDEX</b>	491

## PREFACE

The linear theory of mass transfer is characterised by three basic features:

1. The mass transfer rate does not depend on the direction of mass exchange between phases (for example absorption and desorption rates are equal).
2. The Sherwood number does not depend on concentration.
3. Mass transfer does not influence the hydrodynamics.

Experimental studies of many authors show considerable deviations from the linear theory. Several references (see references of Introduction [1 - 10]) indicate influence of the interphase mass transfer direction on the mass transfer rate in the phase. The influence of concentration on the Sherwood number is noticed in a number of cases, when the mass transfer is accompanied by a chemical reaction [11]. Most often the deviations of the experimental data from the linear theory are in the cases of increasing the mass transfer rate, which is explained by spontaneous (surface, interphase) turbulency, Marangoni effect, self-organising dissipate structures, etc. [1, 2, 5 – 8, 10 - 13].

All deviations of the experimental data from mass transfer linear theory, mentioned above, are result of different non-linear effects that will be discussed in this book.

The problems of non-linear mass transfer appear in connection with the examination of systems with intensive mass transfer. A series of non-linear effects in the mass transfer kinetics occur under these conditions as a result of the development of big concentration gradients in the transferred material. These effects have various manifestations, but their influence on the mass transfer rate can always be regarded as interconnected.

The theoretical analysis of the mass transfer kinetics permits the differentiation of a number of main effects, which differ from one another in principle. Some of them could be regarded as quantitative only, i.e. with impact on the mass transfer rate. Of greater interest are the qualitative effects, because they influence the mass transfer mechanism.

The case, when the dependence of the mass flux density from the transferred material concentration gradient is non-linear, could be considered as a first example of a non-linear effect. Under these conditions models are usually used, where the diffusivity coefficient depends on the transferred material concentration [14], i.e. the Fick's law is non-linear. This non-linear effect is significant in liquid systems, but not in gases. For the purposes of technical calculations this effect can be accounted for by the relationship between the activity and the transferred material concentration, if the chemical potential gradient is substituted in the Fick's equation [15].

Another non-linear effect, which shows up also when the concentration gradients are not very big, is connected with the dependence of the viscosity on the transferred material concentration. This effect influences the convective mass transfer in liquids (including those with complex rheology), but its impact on the process rate is not strong enough as to change the mass transfer kinetics in a qualitative way. Thus, for instance, it has been shown in [16] that taking into account the dependence of the viscosity and the diffusivity coefficients on the concentrations can not lead to a change in the mass transfer mechanism.

The most interesting from theoretical and practical points of view non-linear effect is associated with the generation of a secondary flow under conditions of intensive interphase mass transfer [17, 18], i.e. of a new mass flux which takes part in the overall balance of the transferred material, thus changing the mass transfer mechanism. In this way the intensive

interphase mass transfer affects the hydrodynamics of the flow as well as the kinetics of the mass transfer. This non-linear effect has various manifestations, the most interesting being the impact of the direction of the intensive interphase mass transfer on the rates of mass transfer, heat transfer and multicomponent mass transfer. The secondary flows at the phase boundary can be normal (non-linear mass transfer effect) or tangential (Marangoni effect).

Another effect of interest is connected with the existence of a non-linear source or sink of the diffusing substance as a result of chemical reactions in the volume of the phases. The influence of this non-linearity could practically be regarded as quantitative effect, so far as the non-linearity of the chemical reaction's kinetics does not change the mass transfer mechanism significantly.

The non-linear effects in the systems with intensive interphase mass transfer lead to changes in the hydrodynamics of the systems and their hydrodynamic stability. As a result stable self-organising dissipate structures are created, that are the basic reason for the most significant differences between the linear theory and the experimental data.

Surveyed in this book are the kinetics of the non-linear mass transfer in systems with intensive interphase mass transfer, in electrochemical systems with high current density, in chemically reacting systems and the hydrodynamic stability in these systems.

In Part I the non-linear mass transfer as a result of an intensive interphase mass transfer in the gas (liquid)-solid surface, gas-liquid and liquid-liquid systems is considered in the diffusion boundary layer approximation as well as in flat channel taking the longitudinal diffusion into account. The influence of the direction of the intensive interphase mass transfer on the heat transfer and the multi-component mass transfer is illustrated.

Part II discusses the non-linear mass transfer in electrochemical systems with high current density on the examples of the anode dissolving of metals in the electrolyte flow and the electro-separation of metals out of concentrated solutions. The theory of the measured electrochemical treatment of metals and alloys, which is a method of a wide practical use, has been elaborated on this basis.

In Part III the non-linear mass transfer in the chemically reacting systems is considered in the cases of: non-linearity of the equations of the chemical reaction's kinetics and intensive interphase mass transfer or thermo-capillary effect due to chemical reactions. On this basis, the mechanisms and the macro-kinetics of the chemical transformations in the gas-liquid systems are discussed.

Part IV is dedicated to the chemical reaction kinetics in stationary two phase systems at an arbitrary contact time between phases.

The big concentration gradients induce secondary flows at the phases interface, which, depending on the direction of the interphase mass transfer, represent suction from or injection into the boundary layer, which enhances or lowers the hydrodynamic stability of the flow in the boundary layer. In Part V these effects are considered in the approximations of the linear theory of the hydrodynamic stability of almost parallel flows.

In the systems with intensive interphase mass transfer besides the effect of non-linear mass transfer the Marangoni effect could also show up. A comparative analysis of these two effects is made in the book.

A part from the results presented in the book are obtained with a financial support from the National Fund "Scientific Research" of the Republic of Bulgaria (Contracts No. TH-154/87, TH-89/91, TH-508/95).

The authors take advantage of the possibility to express here their honour and respect for Prof. V. S. Krylov, whose scientific investigations in the second part of the book are one of the first and founding contributions in the non-linear mass transfer theory.

The authors would like to thank to: Assoc. Prof. Jordan Hristov, Ph.D, Assoc. Prof. Natasha Vaklieva-Bancheva, Ph.D and Assist. Prof. Maria Petkova, Ph.D for their help in preparation of this book.

Christo B. Boyadjiev  
Vladislav N. Babak

This Page Intentionally Left Blank

## Introduction

The contemporary development of the chemical, power, biotechnological and other industries, and especially the creation of apparatuses with big unit power, pose the problem of decreasing the equipment size. This can be achieved by introducing high rate processes.

The implementation in industry of apparatuses for highly intensive heat and mass transfer processes is prevented by the fact that under conditions of interphase mass transfer significant differences are noticed between the actual process rate and the rate, predicted by the linear theory of mass transfer. This makes difficult their optimal design.

The basic reasons for the deviations from the linear theory are the occurrence of several non-linear effects as a result of the gradients of pressure (Stephan flow), density (natural convection), concentration (non-linear mass transfer), and surface tension (Marangoni effect). The appearance of the temperature and concentration dependencies of the parameters in the equations of momentum, mass and heat transfer, as well as the chemical reactions (especially if their order is higher than unity), lead to other type of non-linear effects.

All these effects represent the influence of the temperature and concentration on the flow rate of a fluid, in which heat and / or mass transfer takes place. They may occur in two ways. In the first case the changes in the field of velocity lead to changes in the fields of concentration and temperature, and therefore to changes in the kinetics of the mass and heat transfer. In the second case the change in the velocity field leads to loss of stability of the flow, appearance of stable dissipative or turbulent structures, which on their hand lead to a new mechanism of heat and mass transfer and to an essential increase of the heat and mass transfer rate.

In most cases the models of non-linear processes will be treated as a superposition of the linear theory and the separate non-linear effects, which gives a reason for a short statement of the linear theory.

## LINEAR MASS TRANSFER THEORY

A balance of the convective and the diffusive transfer determines the mass transfer in a moving fluid. If are marked by  $u(x, y, z)$  and  $c(x, y, z)$  the fields of velocity and concentration, the mass flow ( $j$ ) through an unit surface of a given elementary volume is the sum of the convective and the diffusive flows:

$$j = uc - D \operatorname{grad} c, \quad (0.1)$$

where  $D$  is a diffusivity.

In the cases of stationary processes and absence of a volume source (stock) of a substance, the material balance of the substance in the elementary volume is obtained through integration of the flow over the whole surface of this volume:

$$\operatorname{div} j = 0. \quad (0.2)$$

From (0.1) and (0.2) one is directly obtained:

$$\mathbf{u} \cdot \nabla c = D \nabla^2 c . \quad (0.3)$$

From (0.3) one possible problem for a mass transfer in a two-dimensional area with dimensions  $L$  and  $h$ , where  $y = 0$  is the surface, through which the mass transfer with another phase (solid, liquid, gas) takes place, may be formulated:

$$\begin{aligned} u \frac{\partial c}{\partial x} + v \frac{\partial c}{\partial y} &= D \left( \frac{\partial^2 c}{\partial x^2} + \frac{\partial^2 c}{\partial y^2} \right); \\ x = 0, y > 0, c &= c_0, x = L, 0 \leq y < h, c = c^*; \\ y = 0, & 0 \leq x < L, c = c^*; \quad y = h, c = c_0. \end{aligned} \quad (0.4)$$

From (0.4) the rate of mass transfer  $J$  through the coefficient of mass transfer ( $k$ ) and the local mass flux  $i$  could be determined:

$$J = k(c^* - c_0) = \frac{h}{L} \int_0^L i \, dx, \quad i = -D \left( \frac{\partial c}{\partial y} \right)_{y=0}. \quad (0.5)$$

As a final result the Sherwood number can be determined:

$$Sh = \frac{kL}{D} = - \frac{1}{c^* - c_0} \int_0^L \left( \frac{\partial c}{\partial y} \right)_{y=0} \, dx. \quad (0.6)$$

From (0.5) and (0.6) it is directly seen that for determination of the mass transfer rate it is necessary to find the mass transfer coefficient or the Sherwood number, i.e. to solve the problem (0.4). A basic difficulty in its solution is to determine the velocity by solving of the system of non-linear equations of Navier – Stokes [19]. This difficulty is avoided in some model theories of mass transfer.

## 1. Model theories

The roughest approximation in the solution of the problem (0.4) is made in the film theory [20], where it is assumed that mass transfer takes place in a thin immobile layer  $h$ :

$$u = v = 0, \quad h \ll L. \quad (0.7)$$

In this way from (0.4) one is obtained:

$$\frac{\partial^2 c}{\partial y^2} = 0; \quad y = 0, c = c^*; \quad y = h, c = c_0, \quad (0.8)$$

i.e.

$$c = \frac{c_0 - c^*}{h} y + c^*, \quad k = \frac{D}{h}. \quad (0.9)$$

The basic disadvantages of this theory are the linear dependence of  $k$  on  $D$ , which is not confirmed experimentally, and the unknown thickness of the film  $h$ , which does not allow theoretical determination of the mass transfer coefficient. In spite of that some prerequisites and consequences of the theory are still valid. Examples for that are the assumptions that mass transfer takes place in a thin layer at the phase boundary, the existence of a thermodynamical equilibrium at the interphase, as well as the basic consequence of the theory regarding the additivity of the diffusion resistances [17, 21].

Another approximation is used in the penetration theory [22] and in some related theories, where it is assumed that the mass transfer takes place in a thin layer  $\delta$  with a constant fluid velocity  $u_0$ :

$$u = u_0, \quad v = 0, \quad \delta \ll h < L. \quad (0.10)$$

In this case from (0.4) is obtained:

$$\begin{aligned} u_0 \frac{\partial c}{\partial x} &= D \frac{\partial^2 c}{\partial y^2}; \\ x = 0, \quad c &= c_0; \quad y = 0, \quad c = c^*; \quad y \rightarrow \infty, \quad c = c_0. \end{aligned} \quad (0.11)$$

The solution of (0.11) is obtained through the Green function [5, 35]:

$$c = c_0 + (c^* - c_0) \operatorname{erfc} y \sqrt{\frac{u_0}{4Dx}}, \quad (0.12)$$

i.e.

$$Sh = \frac{2}{\sqrt{\pi}} Pe^{1/2}, \quad Pe = \frac{u_0 L}{D}. \quad (0.13)$$

In fact, the velocity in the thin layer is usually variable [17, 21, 23, 24] and (0.13) presents only the zero approximation in the solution of the problem.

Several other model theories of linear mass transfer exist, that do not differ principally from the ones discussed above, and have the same disadvantage of insufficient physical reasoning of their basic prerequisites. In this sense, the theory of mass transfer in the approximations of the boundary layer has the best physical reasoning.

## 2. Boundary layer theory

The linear theory of mass transfer in the approximations of the boundary layer [19, 25] treats the equation of convection diffusion together with the equations of momentum transfer (Navier – Stokes equations):

$$\begin{aligned} u \frac{\partial u}{\partial x} + v \frac{\partial u}{\partial y} &= -\frac{1}{\rho} \frac{\partial p}{\partial x} + \nu \left( \frac{\partial^2 u}{\partial x^2} + \frac{\partial^2 u}{\partial y^2} \right), \\ u \frac{\partial v}{\partial x} + v \frac{\partial v}{\partial y} &= -\frac{1}{\rho} \frac{\partial p}{\partial y} + \nu \left( \frac{\partial^2 v}{\partial x^2} + \frac{\partial^2 v}{\partial y^2} \right), \end{aligned} \quad (0.14)$$

where  $\rho$  is the density,  $\nu = \mu / \rho$ ,  $p$  – pressure,  $\mu$  - viscosity.

If are marked by  $u_0$  the character velocity of the flow and by  $L$  and  $\delta$  the character linear scales in directions  $x$  and  $y$ , where the basic change of velocity takes place, the variables in (0.14) may be presented in the following dimensionless form:

$$x = LX, \quad y = \delta Y, \quad u_x = u_0 U, \quad u_y = \frac{u_0 \delta}{L} V, \quad p = \rho u_0^2 P. \quad (0.15)$$

The substitution of (0.15) in (0.14) leads to

$$\begin{aligned} U \frac{\partial U}{\partial X} + V \frac{\partial U}{\partial Y} &= -\frac{\partial P}{\partial X} + \frac{\nu L}{u_0 \delta^2} \left( \frac{\delta^2}{L^2} \frac{\partial^2 U}{\partial X^2} + \frac{\partial^2 U}{\partial Y^2} \right), \\ \frac{\delta^2}{L^2} \left( U \frac{\partial V}{\partial X} + V \frac{\partial V}{\partial Y} \right) &= -\frac{\partial P}{\partial Y} + \frac{\nu L}{u_0 \delta^2} \left( \frac{\delta^4}{L^4} \frac{\partial^2 V}{\partial X^2} + \frac{\delta^2}{L^2} \frac{\partial^2 V}{\partial Y^2} \right), \\ \frac{\partial U}{\partial X} + \frac{\partial U}{\partial Y} &= 0. \end{aligned} \quad (0.16)$$

If is assumed that  $\delta$  is the thickness of the layer, in which the basic velocity change takes place as a result of the balance of inertial and viscous forces, in (0.16) could be defined:

$$\frac{\nu L}{u_0 \delta^2} = 1, \quad \delta = \sqrt{\frac{\nu L}{u_0}}. \quad (0.17)$$

From (0.17) it follows that:

$$\frac{\delta}{L} = Re^{-1/2}, \quad Re = \frac{u_0 L}{\nu}. \quad (0.18)$$

For the cases of practical interest the Reynolds number is big and  $\delta / L \ll 1$ , i.e. the basic change of velocity takes place in a thin layer (a laminar boundary layer) and the equations of momentum transfer (in the laminar boundary layer) take the form:

$$\begin{aligned} U \frac{\partial U}{\partial X} + V \frac{\partial U}{\partial Y} &= - \frac{\partial P}{\partial Y} + \frac{\partial^2 U}{\partial Y^2}, \quad \frac{\partial P}{\partial Y} = 0, \\ \frac{\partial U}{\partial X} + \frac{\partial V}{\partial Y} &= 0. \end{aligned} \quad (0.19)$$

An analogous transformation may be performed in (0.4), where it is assumed that the basic change of concentration takes place in the diffusion boundary layer  $\delta_D$ :

$$U \frac{\partial C}{\partial X} + Sc^{1/2} V \frac{\partial C}{\partial Y} = \frac{DL}{u_0 \delta_D^2} \left( \frac{\delta_D^2}{L^2} \frac{\partial^2 C}{\partial X^2} + \frac{\partial^2 C}{\partial Y^2} \right), \quad Sc = \frac{\nu}{D}, \quad (0.20)$$

where  $Sc$  is a Shmidt number.

If is accepted that  $\delta_D$  is the thickness of the layer, where the change of concentration is a result of the convective and the diffusion mass transfer, from (0.20) it directly follows that:

$$\frac{DL}{u_0 \delta_D^2} = 1, \quad \delta_D = \sqrt{\frac{DL}{u_0}}, \quad \frac{\delta_D}{L} = Re^{-1/2} \cdot Sc^{-1/2} \ll 1. \quad (0.21)$$

From (0.18) and (0.21) is directly seen that for gases  $\delta \approx \delta_0$  ( $Sc \approx 1$ ), while for liquids  $\delta \ll \delta_0$ , because  $Sc \approx 10^2$ . The substitution of (0.21) in (0.20) leads to:

$$U \frac{\partial C}{\partial X} + Sc^{1/2} V \frac{\partial C}{\partial Y} = \frac{\partial^2 C}{\partial Y^2}. \quad (0.22)$$

Equations (0.19) and (0.21) are the basis of the linear theory of mass transfer in the approximations of the boundary layer. They are used in the different cases with appropriate boundary conditions.

### 3. Immobile phase boundary

The interphase mass transfer in gas (liquid)-solid systems [19, 26, 27] is realized through an immobile phase boundary. Below, it will be discussed a potential flow with a constant velocity  $u_0$  on a semi - infinite flat plate. In this case from (0.19) and (0.22) is directly obtained:

$$u \frac{\partial u}{\partial x} + v \frac{\partial u}{\partial y} = v \frac{\partial^2 u}{\partial y^2},$$

$$\frac{\partial u}{\partial x} + \frac{\partial v}{\partial y} = 0,$$

$$u \frac{\partial c}{\partial x} + v \frac{\partial c}{\partial y} = D \frac{\partial^2 c}{\partial y^2};$$

$$\begin{aligned} x = 0, \quad u = u_0, \quad c = c_0; \\ y = 0, \quad u = 0, \quad v = 0, \quad c = c^*; \\ y \rightarrow \infty, \quad u = u_0, \quad c = c_0, \end{aligned} \quad (0.23)$$

where the boundary conditions express a thermodynamical equilibrium at the phase boundary ( $y = 0$ ) and depending on the sign of the difference ( $c^* - c_0$ ) a process of solution or crystallization takes place. The problem (0.23) has a solution if the following similarity variables are used:

$$\begin{aligned} u = 0.5u_0\varepsilon\phi', \quad v = 0.5\left(\frac{u_0v}{x}\right)^{0.5}(\eta\phi' - \phi), \\ c = c_0 + (c^* - c_0)\psi, \quad y = \eta\left(\frac{u_0}{4Dx}\right)^{-0.5}, \\ \varepsilon = Sc^{0.5}, \quad \phi = \phi(\eta), \quad \psi = \psi(\eta). \end{aligned} \quad (0.24)$$

The introduction of (0.24) into (0.23) leads to:

$$\begin{aligned} \phi''' + \varepsilon^{-1}\phi\phi'' = 0, \quad \phi'' + \varepsilon\phi\psi' = 0, \\ \phi(0) = 0, \quad \phi'(0) = 0, \quad \psi(0) = 1, \quad \phi'(\infty) = 2\varepsilon^{-1}, \quad \psi(\infty) = 0. \end{aligned} \quad (0.25)$$

The solution of (0.25) is obtained [26] through the Blasius function:

$$\begin{aligned} \phi(\eta) &= f(z), \quad z = \frac{2}{\varepsilon}\eta, \\ \psi(\eta) &= 1 - \frac{1}{\varphi_0} \int_0^z E(\varepsilon, p) dp, \\ E(\varepsilon, p) &= \exp\left[-\frac{\varepsilon^2}{2} \int_0^p f(s) ds\right], \\ \varphi &= \int_0^\infty E(\varepsilon, p) dp \approx \begin{cases} 3.01 Sc^{-0.35} & \text{for gases} \\ 3.12 Sc^{-0.34} & \text{for liquids} \end{cases}, \end{aligned} \quad (0.26)$$

where the function of Blasius is the solution of the problem

$$\begin{aligned} 2f''' + ff'' = 0, \\ f(0) = 0, \quad f'(0) = 0, \quad f''(0) = 0.33205 \end{aligned} \quad (0.27)$$

and its values are given in [28].

The introducing of (0.26) in (0.6) allows to determine the Sherwood number:

$$Sh = \frac{kL}{D} = -Pe^{0.5}\psi'(0) \approx \frac{2}{3}\sqrt{Re}\sqrt{Sc}. \quad (0.28)$$

#### 4. Moving phase boundary

The mass transfer in gas – liquid and liquid – liquid systems is realized at a moving phase boundary. In the approximations of the boundary layer the problem has the form:

$$\begin{aligned} u_j \frac{\partial u_j}{\partial x} + v_j \frac{\partial u_j}{\partial y} &= v_j \frac{\partial^2 u_j}{\partial y^2}, \\ \frac{\partial u_j}{\partial x} + \frac{\partial v_j}{\partial y} &= 0, \\ u_j \frac{\partial c_j}{\partial x} + v_j \frac{\partial c_j}{\partial y} &= D_j \frac{\partial^2 c_j}{\partial y^2}, \quad j = 1, 2, \end{aligned} \quad (0.29)$$

with boundary conditions, taking into account the continuity of velocity, stress tensor and mass flux at the phase boundary:

$$\begin{aligned} x = 0, \quad u_j &= u_{j0}, \quad c_j = c_{j0}, \quad j = 1, 2; \\ y = 0, \quad u_1 &= u_2, \quad \mu_1 \frac{\partial u_1}{\partial y} = \mu_2 \frac{\partial u_2}{\partial y}, \\ c_1 &= \chi c_2, \quad D_1 \frac{\partial c_1}{\partial y} = D_2 \frac{\partial c_2}{\partial y}, \quad v_j = 0, \quad j = 1, 2; \\ y \rightarrow \infty, \quad u_1 &= u_{10}, \quad c_1 = c_{10}; \\ y \rightarrow -\infty, \quad u_2 &= u_{20}, \quad c_2 = c_{20}; \end{aligned} \quad (0.30)$$

where the first phase ( $j = 1$ ) is a gas or a liquid, and the second one ( $j = 2$ ) – liquid. At the phase boundary the existence of phase equilibrium is assumed and  $\chi$  is the coefficient of Henry (gas – liquid) or the coefficient of separation (liquid – liquid).

The average rate of the mass transfer between the phases is determined in an analogous way, as well as the rate of mass transfer through finding the average of the local mass fluxes:

$$\begin{aligned} J &= K_1(c_{10} - \chi c_{20}) = \frac{1}{L} \int_0^L I_1 dx = k_1(c_{10} - c_1^*) = \\ &= K_2 \left( \frac{c_{10}}{\chi} - c_{20} \right) = \frac{1}{L} \int_0^L I_2 dx = k_2(c_2^* - c_{20}), \quad c_1^* = \chi c_2^*. \end{aligned} \quad (0.31)$$

where  $K_j$  ( $j=1, 2$ ) are the interphase mass transfer coefficients,  $k_j$  ( $j=1, 2$ ) – mass transfer coefficients,  $c_i^*$  and  $c_2^*$  - the concentrations in the two phases at the phase boundary ( $y = 0$ ). The local mass fluxes

$$I_j = -D_j \left( \frac{\partial c_j}{\partial y} \right)_{y=0}, \quad j = 1, 2 \quad (0.32)$$

are obtained after the solution of (0.29, 0.30).

From (0.31) and (0.32) the Sherwood numbers are obtained:

$$Sh_j = \frac{K_j L}{D_j} = \frac{\chi^{j-1}}{c_{j0} - \chi c_{20}} \int_0^L \left( \frac{\partial c_j}{\partial y} \right)_{y=0} dx, \quad j = 1, 2. \quad (0.33)$$

From (0.31) the law of additivity of the diffusion resistances is directly obtained:

$$\begin{aligned} K_1^{-1} &= k_1^{-1} + \chi k_2^{-1}; \quad \chi = 0, \quad K_1 = k_1; \\ K_2^{-1} &= (\chi k_1)^{-1} + k_2^{-1}; \quad \chi \rightarrow \infty, \quad K_2 = k_2. \end{aligned} \quad (0.34)$$

From (0.34) it can be seen that when the interphase mass transfer rate is limited by the diffusion resistance in one of the phases, the interphase mass transfer coefficient is equal to the mass transfer coefficient in this phase.

The problem (0.29, 0.30) has a solution after introducing the following similarity variables:

$$\begin{aligned} u_j &= 0.5 j u_{j0} \varepsilon_j \phi'_j, \\ u_j &= (-I)^{j-1} 0.5 j \left( \frac{u_{j0} v_j}{x} \right)^{0.5} (\eta_j \phi'_j - \phi_j), \\ c_j &= c_{j0} - (-\chi)^{1-j} (c_{j0} - \chi c_{20}) \psi_j, \\ \phi_j &= \phi_j(\eta_j), \quad \psi_j = \psi_j(\eta_j), \\ \eta_j &= (-I)^{j-1} y \left( \frac{u_{j0}}{4 D_j x} \right)^{0.5}, \\ \varepsilon_j &= Sc_j^{0.5}, \quad Sc_j = \frac{v_j}{D_j}, \quad j = 1, 2. \end{aligned} \quad (0.35)$$

As a result one is directly obtained:

$$\begin{aligned} \phi_j''' + j \varepsilon_j^{-1} \phi_j'' &= 0, \\ \psi_j'' + j \varepsilon_j \phi_j \psi_j' &= 0, \\ \phi_j(0) &= 0, \quad \phi_j'(\infty) = \frac{2}{j \varepsilon_j}, \quad \psi_j(\infty) = 0, \quad j = 1, 2, \\ \phi'_1(0) &= 2 \theta_1 \frac{\varepsilon_2}{\varepsilon_1} \phi'_2(0), \end{aligned}$$

$$\begin{aligned}
\phi_2''(0) &= -0,5\theta_2 \left( \frac{\varepsilon_1}{\varepsilon_2} \right)^2 \phi_1''(0), \\
\psi_2'(0) &= \frac{\chi}{\varepsilon_0} \psi_2'(0), \quad \psi_1(0) + \psi_2(0) = 1, \\
\theta_1 &= \frac{u_{20}}{u_{10}}, \quad \theta_2 = \left( \frac{\mu_1}{\mu_2} \right) \left( \frac{V_1}{V_2} \right)^{-0.5} \left( \frac{u_{10}}{u_{20}} \right)^{1.5}, \\
\varepsilon_0 &= \left( \frac{D_2}{D_1} \frac{u_{20}}{u_{10}} \right)^{0.5}. \tag{0.36}
\end{aligned}$$

The solution of (0.36) allows the determination of the interphase mass transfer rate between two phases with moving phase boundary:

$$Sh_j = -\sqrt{Pe_j} \psi_j'(0), \quad Pe_j = \frac{u_{j0}L}{D_j}, \quad j = 1, 2. \tag{0.37}$$

The problem (0.36) is solved numerically [29], but for the systems gas - liquid asymptotic solutions are found [30, 31] in a series of the orders of the small parameters  $\theta_1$  and  $\theta_2$  and for  $\psi_j'(0)$  ( $j = 1, 2$ ) the following expressions are obtained in first approximation, regarding the small parameters  $\theta_1$  and  $\theta_2$ :

$$\begin{aligned}
\psi_1'(0) &= -\frac{2}{\varepsilon_1 \varphi_{10}} \frac{1}{1+a} - \frac{2\theta_1}{\alpha \varphi_{10}^2 \varepsilon_1} \frac{1}{(1+a)^2} - 8\theta_2 \alpha \frac{\varepsilon_2}{\varepsilon_1} \frac{\bar{\varphi}_2}{\varphi_{10}} \frac{a}{(1+a)^2}, \\
\psi_2'(0) &= -\frac{2}{\sqrt{\pi}} \frac{a}{1+a} - \theta_1 \frac{2}{\sqrt{\pi} \alpha \varphi_{10}} \frac{a}{(1+a)^2} - 8\theta_2 \frac{\alpha \varepsilon_2 \bar{\varphi}_2}{\sqrt{\pi}} \frac{a^2}{(1+a)^2}, \tag{0.38}
\end{aligned}$$

where

$$\begin{aligned}
\varphi_{10} &\approx \frac{3}{\sqrt[3]{Sc}}, \quad a = \frac{\chi \sqrt{\pi}}{\varepsilon_0 \varepsilon_1 \varphi_{10}}, \quad \alpha = 0,33205, \\
\bar{\varphi}_2 &= \frac{1}{8} \sqrt{\frac{\pi}{Sc_2}}. \tag{0.39}
\end{aligned}$$

In the cases when the interphase mass transfer is limited by the mass transfer in the gas phase  $\chi / \varepsilon_0 \rightarrow 0$ ,  $a \rightarrow 0$  and for the Sherwood number may be written:

$$Sh_1 = \sqrt{Pe_1} \left( \frac{2}{\varepsilon_1 \varphi_{10}} + \frac{2\theta_1}{\varepsilon_1 \alpha \varphi_{10}^2} \right). \tag{0.40}$$

The Sherwood number can be determined in a similar way when the interphase mass transfer is limited by the mass transfer in the liquid phase:

$$Sh_2 = \sqrt{Pe_2} \left( \frac{2}{\sqrt{\pi}} + 8\theta_2 \frac{\alpha \varepsilon_2 \bar{\varphi}_2}{\sqrt{\pi}} \right). \quad (0.41)$$

The results obtained for the hydrodynamics and the mass transfer in co-current flows for a gas – liquid system are in a good agreement with the experimental data [29, 32 – 34].

## 6. Counter-current flow

The chemical technologies based on opposite-current flows in gas-liquid systems are widely distributed in practice. The theoretical analysis of such flows [35] demonstrates that there is a possibility to obtain asymptotic solutions for gas-liquid systems which are in a conformance with the experimental data, obtained from thermo-anemometrical measurements in the boundary layer. The correctness of the proposed asymptotic method [35] was confirmed by numerical experiments, as a result of the exact solution of the problem by means of numerical simulation [36]. The theoretical analysis of the counter-current flow shows [37], that it is a non-classical problem of mathematical physics which is not sufficiently discussed in the literature. A prototype of such problem is the parabolic boundary value problem with changing direction of time [38,39]. It was shown [37] that this non-classical problem can be described as consisting of several classical problems.

The mathematical description of the opposite-current flows in the approximation of boundary layer theory has the following form:

$$\begin{aligned} u_j \frac{\partial u_j}{\partial x} + v_j \frac{\partial u_j}{\partial y} &= v_j \frac{\partial^2 u_j}{\partial y^2}, \quad \frac{\partial u_j}{\partial x} + \frac{\partial v_j}{\partial y} = 0, \quad j = 1, 2; \\ x = 0, \quad y \geq 0, \quad u_1 &= u_1^\infty; \quad x = L, \quad y \leq 0, \quad u_2 = -u_2^\infty; \\ y \rightarrow \infty, \quad 0 \leq x \leq L, \quad u_1 &= u_1^\infty; \quad y \rightarrow -\infty, \quad 0 \leq x \leq l, \quad u_2 = -u_2^\infty; \\ y = 0, \quad 0 < x < L, \quad u_1 &= u_2, \quad \mu_1 \frac{\partial u_1}{\partial y} = \mu_2 \frac{\partial u_2}{\partial y}, \quad v_1 = v_2 = 0. \end{aligned} \quad (0.42)$$

The problem (0.42) can be presented in dimensionless form using two different coordinate systems for the two phases, so that the flow in each phase is oriented to the longitudinal coordinate, and the following dimensionless variables and parameters are introduced:

$$\begin{aligned} x = LX_1 &= L - LX_2, \quad y = \delta_1 Y_1 = -\delta_2 Y_2, \\ u_1 = u_1^\infty U_1, \quad v_1 &= u_1^\infty \frac{\delta_1}{L} V_1, \\ u_2 = -u_2^\infty U_2, \quad v_2 &= -u_2^\infty \frac{\delta_2}{L} V_2, \end{aligned}$$

$$\delta_j = \sqrt{\frac{v_j L}{u_j^\infty}}, \quad j = 1, 2, \quad \theta_1 = \frac{u_2^\infty}{u_1^\infty}, \quad \theta_2 = \left( \frac{\rho_1 \mu_1}{\rho_2 \mu_2} \right)^{1/2} \left( \frac{u_1^\infty}{u_2^\infty} \right)^{3/2}. \quad (0.43)$$

In the new coordinate systems the model of opposite-current flows takes the following form:

$$\begin{aligned} U_j \frac{\partial U_j}{\partial X_j} + V_j \frac{\partial U_j}{\partial Y_j} &= \frac{\partial^2 U_j}{\partial Y_j^2}, \quad \frac{\partial U_j}{\partial X_j} + \frac{\partial V_j}{\partial Y_j} = 0; \\ X_j = 0, \quad U_j &= I; \quad Y_j \rightarrow \infty, \quad U_j = I; \\ Y_1 = Y_2 = 0, \quad U_1 &= -\theta_1 U_2, \quad \theta_2 \frac{\partial U_1}{\partial Y_1} = \frac{\partial U_2}{\partial Y_2}, \quad V_j = 0; \quad j = 1, 2. \end{aligned} \quad (0.44)$$

The problem (0.44) can not be solved directly, because the velocities  $U_i$  ( $i = 1, 2$ ) change their directions in the ranges  $0 \leq X_i \leq 1, 0 \leq Y_i < \infty$ , ( $i = 1, 2$ ). This non-classical problem of mathematical physics can be presented as a classical one after the introduction of the following similarity variables:

$$U_j = f'_j, \quad V_j = \frac{1}{2\sqrt{X_j}}(\eta_j f'_j - f_j), \quad f_j = f_j(\eta_j), \quad \eta_j = \frac{Y_j}{\sqrt{X_j}}. \quad (0.45)$$

The substitution of (0.45) into (0.44) leads to:

$$\begin{aligned} 2f''_j + f_j f'_j &= 0, \\ f_j(0) &= 0, \quad f_j(\infty) = I, \quad j = 1, 2, \\ f'_1(0) &= -\theta_1 f'_2(0), \quad \theta_2 \sqrt{\frac{X_2}{X_1}} f''_1(0) = f''_2(0), \quad X_1 + X_2 = I. \end{aligned} \quad (0.46)$$

It is obvious from (0.46), that the problem (0.44) has no solution in similarity variables. However the problem (0.46) can be solved after the introduction of new parameter  $\bar{\theta}_2$  for each  $X_1 \in (0, 1)$ :

$$\bar{\theta}_2 = \theta_2 \sqrt{\frac{I-X_1}{X_1}}, \quad (0.47)$$

i.e. the problem has local similarity solution. In this way the problem (0.46) is substituted by several separate problems for each  $X_1 \in (0, 1)$ .

The solutions of these separate problems can be obtained after the introduction of function  $F$ :

$$F(a, b) = \int_{\delta}^{\gamma} (f'_1 - 1)^2 d\eta_1 + \int_{\delta}^{\gamma} (f'_2 - 1)^2 d\eta_2, \\ a = f'_1(0), \quad b = f'_2(0). \quad (0.48)$$

The solution of (0.46) for each  $X_1 \in (0,1)$  is obtained after searching the minimum of the function  $F(a, b)$ , where at each step of the minimization procedure the boundary problem has to be solved:

$$2f_j''' + f_j f_j'' = 0, \quad f_j(0) = 0, \quad j = 1, 2, \\ f'_1(0) = a, \quad f'_2(0) = -\frac{a}{\theta_1}, \quad f''_1(0) = b, \quad f''_2(0) = \bar{\theta}_2 b. \quad (0.49)$$

The problem (0.49) was solved numerically for opposite-current gas and liquid flows for the following parameters values  $\theta_1 = 0.1$  and  $\theta_2 = 0.152$ . In accordance with the requirement for minimum of  $F(a, b)$  in (0.48), the boundary conditions  $a, b$  and  $F(a, b)$  were determined [36].

The mathematical model of mass transfer in gas-liquid systems with counter-current flow in a laminar boundary layer with flat phase boundary takes the following form:

$$u_j \frac{\partial c_j}{\partial x} + v_j \frac{\partial c_j}{\partial y} = D_j \frac{\partial^2 c_j}{\partial y^2}, \quad j = 1, 2; \\ x = 0, \quad y \geq 0, \quad c_1 = c_1^\infty; \\ x = L, \quad y \leq 0, \quad c_2 = c_2^\infty; \\ y \rightarrow \infty, \quad 0 \leq x \leq L, \quad c_1 = c_1^\infty; \\ y \rightarrow -\infty, \quad 0 \leq x \leq L, \quad c_2 = c_2^\infty; \\ y = 0, \quad 0 < x < L, \quad c_1 = \chi c_2, \quad D_1 \frac{\partial c_1}{\partial y} = D_2 \frac{\partial c_2}{\partial y}, \quad (0.50)$$

where  $u_i$  and  $v_i$  ( $i = 1, 2$ ) are the velocity components in the gas and in the liquid phase determined after the solution of (0.49).

The soloving of problem (0.50) should be carried out [40] after the following similarity variables are introduced:

$$\eta_j = (-1)^{j+1} y \sqrt{\frac{u_j^\infty}{v_j L X_j}}, \quad X_1 = \frac{x}{L}, \quad X_2 = \frac{L-x}{L}, \quad X_1 + X_2 = 1, \\ u_j = (-1)^{j+1} u_j^\infty f'_j, \quad v_j = (-1)^{j+1} \frac{1}{2} \sqrt{\frac{v_j u_j^\infty}{L X_j}} (\eta_j f'_j - f_j), \quad f_j = f_j(\eta_j), \\ c_j = c_j^\infty - \chi^{1-j} (c_1^\infty - \chi c_2^\infty) \psi_j, \quad \psi_j = \psi_j(\eta_j), \quad j = 1, 2. \quad (0.51)$$

The substitution of equations (0.51) into equations (0.50) leads to:

$$\begin{aligned} 2f_j''' + f_j f_j'' &= 0, \quad 2\psi_j'' + Sc_j f_j \psi_j' = 0, \quad j = 1, 2, \\ f_1(0) &= 0, \quad f_1'(0) = a, \quad f_1''(0) = b, \\ f_2(0) &= 0, \quad f_2'(0) = -\frac{a}{\theta_1}, \quad f_2''(0) = \bar{\theta}_2 b, \\ \psi_1(0) + \psi_2(0) &= 1, \quad \bar{\theta}_3 \psi_1'(0) = \psi_2'(0), \quad \psi_j(\infty) = 0, \quad j = 1, 2, \end{aligned} \quad (0.52)$$

where

$$\begin{aligned} Sc_j &= \frac{\nu_j}{D_j} \quad (j = 1, 2), \quad \theta_1 = \frac{u_2^\infty}{u_1^\infty}, \quad \theta_2 = \left( \frac{\rho_1 \mu_1}{\rho_2 \mu_2} \right)^{1/2} \left( \frac{u_1^\infty}{u_2^\infty} \right)^{3/2}, \\ \bar{\theta}_2 &= \theta_2 \sqrt{\frac{X_2}{X_1}}, \quad \theta_3 = \chi \frac{D_1}{D_2} \sqrt{\frac{u_1^\infty \nu_2}{u_2^\infty \nu_1}}, \quad \bar{\theta}_3 = \theta_3 \sqrt{\frac{X_2}{X_1}}. \end{aligned} \quad (0.53)$$

and the boundary conditions  $a$  and  $b$  are determined after solving the (0.49).

It is clearly seen from equations (0.52) that it is possible to obtain the similarity solution for different values of  $X_1 = 1 - X_2$ .

The solution of (0.52) was carried out at new boundary conditions for  $\psi_j$  ( $j = 1, 2$ ):

$$\begin{aligned} \psi_1(0) &= \alpha, \quad \psi_1'(0) = \beta, \\ \psi_2(0) &= 1 - \alpha, \quad \psi_2'(0) = \bar{\theta}_3 \beta, \end{aligned} \quad (0.54)$$

where  $\alpha$  and  $\beta$  are determined for different values of  $X_1 = 1 - X_2$  so that the conditions  $\psi_j(\infty) = 0$ , ( $j = 1, 2$ ) be fulfilled.

The Sherwood number may be obtained analogously to (0.33):

$$Sh_j = -\sqrt{Re_j} \int_0^1 \frac{\psi_j'(0)}{\sqrt{X_j}} dX_j, \quad Re_j = \frac{u_j^\infty L}{\nu_j}, \quad j = 1, 2, \quad (0.55)$$

where the dimensionless diffusion flux has the form:

$$J_j = -\int_0^1 \frac{\psi_j'(0)}{\sqrt{X_j}} dX_j, \quad j = 1, 2. \quad (0.56)$$

The average diffusion flux values for gas of high ( $\theta_3 = 0$ ), low ( $\theta_3 \rightarrow \infty$ ) and medium solubility ( $\theta_3 = 1$ ) are shown in Table 0.1.

For the purpose of comparison between the counter-current flow mass transfer rate with the co-current one, equation (0.52) should be solved using parameters' values corresponding to co-current flow:

$$\begin{aligned}\theta_1 &= -0.1, & \theta_2 &= 0.152, \\ f'_1(0) &= 0.0908, & f'_2(0) &= 0.37265, \\ \bar{\theta}_3 &= \theta_3, & J_j^* &= -2\psi'_j(0), \quad j = 1, 2.\end{aligned}\tag{0.57}$$

**Table 0.1.**  
Comparison of the mass transfer rate in co-current and counter-current flow.

$\theta_3 = 0$		$\theta_3 \rightarrow \infty$		$\theta_3 = 1$			
$J_1$	$J_1^*$	$J_2$	$J_2^*$	$J_1$	$J_1^*$	$J_2$	$J_2^*$
0.554	0.720	4.380	4.822	0.432	0.626	0.432	0.626

The results obtained for  $J_j^*$  ( $j = 1, 2$ ) are shown in Table 0.1. The comparison of these results with values corresponding to co-current flow shows that the co-current flow mass transfer rate is higher than in case of counter current flow.

The theoretical analysis of the linear mass transfer shows that this process occurs when the equation of convective diffusion (0.4) is linear, i.e. the velocity ( $u, v$ ) and the diffusivity ( $D$ ) do not depend on the concentration ( $c$ ) of the transferred substance. These conditions are valid for systems, in which the mass transfer does not influence the hydrodynamics and the dependence of the mass flux on the concentration gradient is linear. The linear theory of mass transfer, built on this basis, has two main consequences: the mass transfer coefficient does not depend on the concentration and the interphase mass transfer direction does not influence the mass transfer rate.

Any deviation of experimental data from these two consequences shows the availability of non-linear effects, that can occur as a result of secondary flows, caused by the mass transfer, or the dependence of viscosity, diffusion constant and density on concentration. The secondary flows can appear as a result of the concentration gradient (non-linear mass transfer), surface tension gradient (Marangoni effect) and density gradient (natural convection). These secondary flows may influence the mass transfer rate through a change in the velocity field and therefore in the balance between the convective and diffusive transfer in the equation of convective diffusion. This effect may increase many times, if as a result of secondary flows the system loses stability and reaches a new state, becoming a self-organizing dissipation structure. The present book tries to solve part of these problems in industrial systems with intensive interphase mass transfer.

The results obtained up to now represent the linear theory of mass transfer in the approximations of the boundary layer with a flat phase boundary. In an analogous way these

problems can be solved for different form of the interphase surface (wave, sphere, cylindrical, etc.) in the processes in film flows, droplets, bubbles, jets, etc.

These results will be used in the following chapters of the book, where the linear theory of mass transfer will be discussed as a zero order approximation in the non-linear theory, regarding the parameters that take into consideration the separate non-linear effects.

## References

1. V. I. Kosortov at all , Theoretical Fundamentals of Chemical Technology (Russia), 5 (1971) 912.
2. V. I. Kosortov at all , Theoretical Fundamentals of Chemical Technology (Russia), 5 (1971) 474.
3. V. M. Ramm, Gas Absorption, Publ. House Chemistry, Moscow, 1976 (in Russian).
4. P. Grassman and G. Anders, Chem. Eng. Techn., Bd. 31, No 3 (1959), 154.
5. C. V. Sternling and L. E. Scriven, AIChE J., 5, (1959) 514.
6. A. Linde, E. Schwarz and K. Groeger, Chem. Eng. Sci., 22 (1967), 823.
7. F. Ruckenstein and C. Berbente, Chem. Eng. Sci., 19 (1964), 329.
8. W. J. Thomas and E. Mc K. Nicholl, Trans. Inst. Chem. Eng., 47 (1969), 325.
9. V. V. Dilman, N. N. Kulov, V. A. Lothov, V. A. Kaminski and V. I. Najdenov, Theoretical Fundamentals of Chemical Technology (Russia), 32 (1998), 337.
10. K. E. Porter, A. D. C. Cantwell and C. McDermott, AIChE J., 17 (1971), 536.
11. G. Astarita, Mass Transfer with a Chemical Reaction, Elsevier, New York, 1967.
12. D. L. Brian, J. E. Vivian and D. C. Matiatos, AIChE J., 13 (1967), 28.
13. U. V. Fumer, U. V. Axelrod at all, Theoretical Fundamentals of Chemical Technology (Russia), 5 (1971) 134.
14. R. B. Bird, W. E. Stewart and E. N. Lightfoot, Transport Phenomena, Willey, New York, 1960.
15. T. K. Sherwood, R. L. Pigford and C. R. Wilke, Mass Transfer, McGraw – Hill, New York, 1975.
16. Chr. Boyadjiev, Int. J. Heat Mass Transfer, 27 (1984), 1277.
17. Chr. Boyadjiev and V. Beshkov, Mass Transfer in Following Liquid Films, Publ. House Mir, Moscow, 1988. (in Russian)
18. V. S. Krylov, Success of Chemistry, 49 (1980) 118 (in Russian).
19. H. Schlichting, Grenzschicht – Theorie, Verlag G. Braun, Karlsruhe, 1965.
20. W. K. Lewis and W. G. Whitman, Ind. Eng. Chem., 16 (1924), 1215.
21. Chr. Boyadjiev and V. Beshkov, Mass Transfer in Liquid Film Flows, Publ. House Bulg. Acad. Sci., Sofia, 1984.
22. R. Higbie, Trans. Am. Inst. Chem. Eng., 31 (1935) 365.
23. Chr. Boyadjiev, V. G. Levich and V. S. Krylov, Int. Chem. Eng., 8 (1968) 393.
24. Chr. Boyadjiev, Int. Chem. Eng., 11 (1971) 459.
25. V. G. Levich, Physicochemical Hydrodynamics, Prentice-Hall, New York, 1962.
26. Chr. Boyadjiev and E. Toshev, Hung. J. Ind. Chem., 17 (1989) 457.
27. E. Pohlhausen, ZAMM, 1 (1921) 115.
28. Chr. Boyadjiev and M. Piperova, Int. Chem. Eng., 11 (1971) 479.
29. Chr. Boyadjiev and Pl. Mitev, Chem. Eng. J., 14 (1977) 225.

30. Chr. Boyadjiev, Int. Chem. Eng., 11 (1971) 459.
31. Chr. Boyadjiev and N. Vulchanov, Int. J. Heat Mass Transfer, 31 (1988) 795.
32. Chr. Boyadjiev, Pl. Mitev and Tsv. Sapundjiev, Int. J. Multiphase Flow, 3 (1976) 51.
33. Pl. Mitev and Chr. Boyadjiev, Int. J. Multiphase Flow, 3 (1976) 57.
34. Pl. Mitev and Chr. Boyadjiev, Letters Heat Mass Transfer, 5 (1978) 349.
35. Chr. Boyadjiev, Pl. Mitev and V. Beshkov, Int. J. Multiphase Flow, 3 (1976) 61.
36. Chr. Boyadjiev and M. Doichinova, Int. J. Heat Mass Transfer, in press.
37. Chr. Boyadjiev and P. Vabishchevich, Journal of Theoretical Applied Mechanics (Bulgaria), 23 (1992)114.
38. S. A. Tersenov, Parabolic Equations with Changing Direction of Time, Science, Novosibirsk, 1985, (in Russian).
39. I. A. Larkin, V. A. Novikov, and N. N. Ianenko, Nonlinear Equations From Changed Type, Science, Novosibirsk, 1983 (in Russian).
40. M. Doichinova and Chr. Boyadjiev, Int. J. Heat Mass Transfer, in press.

## PART 1

### Systems with Intensive Interphase Mass Transfer

The modern development of power, chemical, oil processing, food processing and other industries calls for creation of systems with intensive mass transfer. For this purpose it is possible to use the mass transfer processes in two-phase systems at large concentration gradients of the transferred substance. Under these conditions big mass fluxes of substance through the phase boundary induce secondary flows at the interphase surface. This fact leads to a change in the flow hydrodynamics, that influences significantly the mechanism and the kinetics of mass transfer.

#### CHAPTER 1.1. SPECIFICS OF THE HYDRODYNAMIC CONDITIONS OF THE INTENSIVE INTERPHASE MASS TRANSFER

The analysis of the mechanism and kinetics of convective mass transfer in two-phase systems in many cases is often possible, if the velocity distribution is determined in the beginning and then, after its substitution in the equation of convective diffusion, the rate of interphase mass transfer is found. However this procedure can not be used for systems with large concentration gradients due to the flow at the interphase surface, induced by the mass transfer. The velocity of this flow is perpendicular to the interphase surface and is directed towards the mass transfer direction. The physical cause of this movement is the mechanical impulse that is transferred from one phase to the other through the particles, responsible for the mass transfer. In the linear theory of mass transfer this impulse is considered insignificant. However at big mass fluxes through the interphase surface in cases of intensive mass transfer it should be considered. Since the transferred impulse is proportional to the diffusive flux of particles, taking part in the mass transfer, the velocity field close to the interphase boundary depends on the field of concentrations. The concrete form of this dependency is determined by the system of equations of the joint transfer of mass and quantity of movement, as well as by the boundary conditions, connecting the fluxes of mass and quantity of movement at the interphase boundary.

##### 1.1.1. Influence of the intensive interphase mass transfer on hydrodynamics

The velocity of the induced flow at the interphase surface is determined by the hydrodynamic effect of the intensive mass transfer. This effect reflects, first of all, on the boundary conditions to the equations of hydrodynamics and mass transfer, i.e. these equations can not be solved separately, unlike the case of systems with low rates of the interphase mass transfer. In order to find the connection between the velocity of the induced flow at the phase boundary and the rate of the interphase mass transfer, an example of an isothermal process of transfer of a dissolved substance from phase 1 into phase 2 will be discussed. It is assumed that each of the phases is a two-component mixture (a solution of the substance  $m$  in the corresponding solvent), and that the two solvents do not mix with each other. The diffusion

flux  $j_m^{(i)}$  of the substance  $m$  at each point of the space inside the phase  $i$  is determined in the following way:

$$j_m^{(i)} = M_m c_m^{(i)} (v_m^{(i)} - v^{(i)}), \quad i = 1, 2. \quad (1.1)$$

Here  $c_m^{(i)}$  is the molar concentration of the transferred substance in phase  $i$ ,  $M_m$  – the molecular mass of this substance,  $v_m^{(i)}$  – the average statistical velocity of movement of particles of the substance  $m$  in arbitrary, but fixed coordinate system;  $v^{(i)}$  – velocity of the mass center of the whole liquid mixture in the same coordinate system. Velocity  $v^{(i)}$  is defined by the system of equations of hydrodynamics (in the case of laminar flow – the system of equations of Navier – Stokes). Besides, by definition this velocity is connected to the velocities of movement of the mixture components through the relationship:

$$\rho^{(i)} v^{(i)} = M_m c_m^{(i)} v_m + M_0 c_0^{(i)} v_0^{(i)}, \quad (1.2)$$

where variables with subscript  $(0)$  refer to the corresponding solvent,  $\rho^{(i)} = M_m c_m^{(i)} + M_0 c_0^{(i)}$  is the summarized density of the solution in the phase  $i$  (in the general case this density is a function of the space coordinates and time). Let present each of the velocities in equation (1.2) as a sum of the velocity of movement at the interphase surface  $dr_s / dt$  ( $r_s$  – radius-vector of an arbitrary point at the phase boundary) and the velocity of movement in regard to this surface  $v_k^{(i)}$  ( $k = m, 0$ ). Due to the fact that the two solvents do not mix, the normal components of velocities  $v_{r0}^{(i)}$  and  $v_{r0}^{(2)}$  at the interphase boundary must be equal to zero. That is why equation (1.2), being projected in the normal direction to the interphase boundary, has at each point of this boundary the following form:

$$\rho^{(i)} (v_r^{(i)}, \mathbf{n}) = M_m c_m^{(i)} (v_{rm}^{(i)}, \mathbf{n}). \quad (1.3)$$

Analogously the projection of equation (1.1) on the normal direction  $\mathbf{n}$  (taking into account the relationship (1.3)) leads to the equation:

$$(v_s^{(i)}, \mathbf{n}) = \left( \frac{dr_s}{dt}, \mathbf{n} \right) + \frac{(j_{ms}^{(i)}, \mathbf{n})}{\rho_s^{(i)} - M_m c_{ms}^{(i)}}. \quad (1.4)$$

This equation is correct for each point at the interphase surface. The subscript "s" here means that the corresponding variable refers to the phase boundary. If the form of the surface is described by the equation

$$y = f_1(x, t), \quad z = f_2(r, t), \quad r = f_3(\theta, t),$$

then for the first term in the right part of (1.4) the following expressions are correct:

$$\left( \frac{dr_s}{dt}, \mathbf{n} \right) = \begin{cases} I + \left( \frac{\partial f_1}{\partial x} \right)^{-1/2} \frac{\partial f_1}{\partial t} & \text{in Decart coordinate system,} \\ I + \left( \frac{\partial f_2}{\partial r} \right)^{-1/2} \frac{\partial f_2}{\partial t} & \text{in cylindrical coordinate system,} \\ I + \left( \frac{\partial f_3}{f_3 \partial \theta} \right)^{-1/2} \frac{\partial f_3}{\partial t} & \text{in spherical coordinate system.} \end{cases}$$

From (1.4) it follows that in the case of high enough interphase mass transfer rates, the hydrodynamic problem has no solution in spite of the problem of convective diffusion.

In the literature a lot of systems of practical interest are described, in which intensive mass transfer leads to a significant change in the hydrodynamic conditions of mass transfer. Good examples of such systems are: condensation of vapors on a cooled wall [13, 26], evaporation of liquids from the surface of droplets and bubbles [8, 48, 50, 56, 57], crystallization and solution of salts [9, 51, 53, 54, 62], heat and mass transfer under conditions of intensive injection (suction) of gases through a porous wall [24, 55, 58, 60, 66]. It is necessary to mention that the effects of non-linear mass transfer that are further discussed, are a result of the big concentration gradient (in liquids) or the partial pressure (in gases) of the transferred substance, i.e. the mass flux through the phase boundary in these cases is determined by the velocity of convective diffusion. In this sense they differ from the Stephan flows [20, 22] and the effects of injection or suction of vapors or gases on a solid surface, which are effects from the gradient of the general pressure.

### 1.1.2. Boundary conditions of the non-linear mass transfer problem

The mathematical formulation of the mass transfer problem, taking into account the influence of mass transfer on the hydrodynamics, was given for the first time in [14, 15, 16]. Equation (1.4) presents the basic conclusion, where the velocity of the induced flow is determined with the help of the mass flux through the phase boundary. For the concrete cases in (1.4) a factual expression of the mass flux should be placed.

In the general case one of the phases in a two-phase system in Decart coordinates can be discussed [5], where  $y = h(x)$  is the phase boundary. Differentiating from (1.4) will be assumed that the interface surface is constant with time, i.e. wave surfaces and surfaces of growing droplets and bubbles will not be considered. The mass flux of the transferred substance at each point of the discussed phase can be expressed by means of the average statistical velocity of this substance (molecules, atoms, ions)  $v$  and the mass center velocity of the mixture (phase) particles  $v_I$ :

$$j = Mc(v - v_I). \quad (1.5)$$

The velocity  $v_I$  should satisfy the hydrodynamic equations and should be connected with the velocities of the mixture (phase) components through the equation

$$\rho v_I = M_0 c_0 v_0 + Mcv, \quad (1.6)$$

where  $\rho$  is the phase (mixture) velocity, and the subscript  $(0)$  marks the phase (mixture) parameters in the absence of a transferred substance. In this way for the density of the discussed phase it can be written:

$$\rho = M_0 c_0 + M c = \rho_0 + M c . \quad (1.7)$$

The projection of the vector equation (1.6) on the normal at the interface surface (vector  $n$ ) gives

$$\rho^*(v_i^*, n) = M c^*(v^*, n), \quad (1.8)$$

where the superscript  $(*)$  denotes the value of the function at the phase boundary. In order to obtain (1.8), the condition for complete mutual insolubility of both phases is used:

$$(v_0, n) = 0. \quad (1.9)$$

Equation (1.9) expresses the availability of a normal component of the liquid or phase velocity  $(v_i^*, n)$  at the interface velocity, which is determined by the diffusion rate  $(v^*, n)$ , and the velocity at the interface surface has only a tangent component.

The occurrence of an induced flow at the interphase surface creates a convective flow, i.e. the mass flux of the transferred substance through the interphase surface has convective and diffusive components:

$$I = -MD\left(\frac{\partial c}{\partial n}\right)_{y=h} + M c^*(v_i^*, n), \quad (1.10)$$

where  $\partial / \partial n$  is the derivative in direction normal to the interface surface.

The diffusion component may be expressed by means of projection of the vector equation (1.5) of the normal vector to the surface

$$(j^*, n) = -MD\left(\frac{\partial c}{\partial n}\right)_{y=h} = M c^*(v, n) - M c^*(v_i^*, n). \quad (1.11)$$

From equations (1.8) – (1.11) it is obtained:

$$I = \rho^*(v_i^*, n) = -\frac{\rho^*}{\rho^* - M c^*} MD\left(\frac{\partial c}{\partial n}\right)_{y=h}, \quad (1.12)$$

where

$$\rho^* = M_0 c_0^* + M c^* = \rho_0^* + M c^*. \quad (1.13)$$

For small concentrations of the transferred substance

$$\dot{\rho}_0 \approx \rho_0. \quad (1.14)$$

The expression (1.12) may be presented in the form:

$$I = \rho^* \frac{v^* - h' u^*}{\sqrt{1 + h'^2}} = \frac{MD\rho^*}{\dot{\rho}_0} \frac{h' \left( \frac{\partial c}{\partial x} \right)_{y=h} - \left( \frac{\partial c}{\partial y} \right)_{y=h}}{\sqrt{1 + h'^2}}, \quad (1.15)$$

where  $u^*$  and  $v^*$  are the components of the velocity  $v_i$  along the  $x$  and  $y$  axes correspondingly.

Equation (1.15) gives the relation between the gas or liquid velocity at the interface surface and the concentration gradient of the transferred substance and will be further used as a boundary condition for the Navier – Stokes equations. In the approximations of the linear theory of mass transfer (1.15) represents the condition of “non-leakage” at the interface surface:

$$\frac{v^* - h' u^*}{\sqrt{1 + h'^2}} = 0. \quad (1.16)$$

## CHAPTER 1.2. GAS (LIQUID)-SOLID SYSTEM

The processes of non-linear mass transfer, heat transfer and multicomponent mass transfer in gas (liquid) – solid surface systems will be discussed on the example of the longitudinal streaming of a semi-infinite flat plate in the approximations of the boundary layer theory. The non-linear effect is taken into account through the introduction of the velocity of the induced flow  $v^*$  at the interface  $y = 0$ . This velocity is obtained directly from (1.15), if  $u^* = 0$  at  $h \equiv 0$  is taken into account:

$$v^* = - \frac{MD}{\dot{\rho}_0} \left( \frac{\partial c}{\partial y} \right)_{y=0}. \quad (1.17)$$

### 1.2.1. Non-linear mass transfer in the boundary layer

The kinetics of the non-linear mass transfer in the approximations of the boundary layer [40, 41, 46, 65] will be discussed on the basis of the solution of the equations of hydrodynamics and convective diffusion, with boundary conditions that take into consideration the influence of the mass transfer on the hydrodynamics. In a rectangular coordinate system, where  $y = 0$  corresponds to the interphase surface gas (liquid) – solid, the mathematical description of the non-linear mass transfer has the form:

$$u \frac{\partial u}{\partial x} + v \frac{\partial u}{\partial y} = v \frac{\partial^2 u}{\partial y^2},$$

$$\begin{aligned}
& \frac{\partial u}{\partial x} + \frac{\partial v}{\partial y} = 0, \\
& u \frac{\partial c}{\partial x} + v \frac{\partial c}{\partial y} = D \frac{\partial^2 c}{\partial y^2}; \\
& x = 0, \quad u = u_0, \quad c = c_0; \\
& y = 0, \quad u = 0, \quad v = -\frac{MD}{\rho_0^*} \frac{\partial c}{\partial y}, \quad c = c^*; \\
& y \rightarrow \infty, \quad u = u_0, \quad c = c_0,
\end{aligned} \tag{1.18}$$

where a potential flow, with a velocity  $u_0$  along a plate, and a concentration ( $c_0$ ) of the transferred substance are assumed. As a result of the rapid establishment of thermodynamic equilibrium, the concentration  $c^*$  is always constant on the solid surface. The normal component of the velocity at the interphase is determined from equation (1.17), as a consequence of intensive interphase mass transfer.

The mass transfer rate for a plate of length  $L$  could be determined from the average mass flux:

$$J = Mk(c^* - c_0) = \frac{I}{L} \int_0^L I dx, \tag{1.19}$$

where  $k$  is the mass transfer coefficient and  $I$  can be expressed from (1.15) as follows:

$$I = -\frac{MD\rho^*}{\rho_0^*} \left( \frac{\partial c}{\partial y} \right)_{y=0}. \tag{1.20}$$

In order to solve problem (1.18), it is necessary to introduce the similarity variables:

$$\begin{aligned}
u &= 0.5u_0 \varepsilon \phi', \\
v &= 0.5 \left( \frac{u_0 v}{x} \right)^{0.5} (\eta \phi' - \phi), \\
c &= c_0 + (c^* - c_0) \psi, \\
y &= \eta \left( \frac{u_0}{4Dx} \right)^{-0.5},
\end{aligned} \tag{1.21}$$

where

$$\varepsilon = Sc^{0.5}, \quad Sc = v/D, \quad \phi = \phi(\eta), \quad \psi = \psi(\eta). \tag{1.22}$$

As a result of these substitutions problem (1.18) gets the following form:

$$\begin{aligned}\phi''' + \varepsilon^{-1} \phi \phi'' &= 0, \quad \psi'' + \varepsilon \phi \psi' = 0, \\ \phi(0) &= \theta \psi'(0), \quad \phi'(0) = 0, \quad \phi'(\infty) = 2\varepsilon^{-1}, \\ \psi(0) &= 1, \quad \psi(\infty) = 0,\end{aligned}\tag{1.23}$$

where

$$\theta = \frac{M(c^* - c_0)}{\varepsilon \rho_0}. \tag{1.24}$$

$\theta$  is a small parameter, that reflects the effect of the non-linear mass transfer. In the linear theory of the diffusion boundary layer  $\theta = 0$ .

Considering the new variables and equation (1.19), is obtained:

$$Sh = \frac{kL}{D} = -\frac{\dot{\rho}}{\dot{\rho}_0} Pe^{0.5} \psi'(0), \tag{1.25}$$

where

$$Pe = \frac{u_0 L}{D}. \tag{1.26}$$

It is seen from (1.25), that mass transfer kinetics is determined by the dimensionless diffusion flux  $\psi'(0)$ , which can be obtained solving the problem (1.23). The solution has been found utilising a perturbation method after presenting  $\phi$  and  $\psi$  as a series in power of the small parameter  $\theta$  [43]:

$$\begin{aligned}\phi &= \phi_0 + \theta \phi_1 + \theta^2 \phi_2 + \dots, \\ \psi &= \psi_0 + \theta \psi_1 + \theta^2 \psi_2 + \dots.\end{aligned}\tag{1.27}$$

If (1.27) is substituted in (1.23), a series of boundary problems that have been solved in [40], could be obtained and for the functions in (1.27) could be written:

$$\begin{aligned}\phi_0(\eta) &= f(z), \quad z = \frac{2}{\varepsilon} \eta, \\ \psi_0(\eta) &= 1 - \frac{1}{\phi_0} \int_0^z E(\varepsilon, p) dp, \\ E(\varepsilon, p) &= \exp \left[ -\frac{\varepsilon^2}{2} \int_0^p f(s) ds \right], \\ \phi_1(\eta) &= -\frac{2}{\varepsilon \phi_0} \varphi(z),\end{aligned}$$

$$\begin{aligned}
\psi_1(\eta) &= \frac{\varepsilon\varphi_3}{\varphi_0^3} \int_0^z E(\varepsilon, p) dp - \frac{\varepsilon}{\varphi_0^2} \int_0^z \left[ \int_0^p \varphi(s) ds \right] E(\varepsilon, p) dp, \\
\phi_2(\eta) &= -\frac{2\varphi_3}{\varphi_0^3} \varphi(z) - \frac{4}{\varepsilon^2 \varphi_0^2} \bar{\varphi}(z), \\
\psi_2(\eta) &= \left( -\frac{2\varepsilon^2 \varphi_3^2}{\varphi_0^5} + \frac{\varepsilon^2 \varphi_{33}}{2\varphi_0^4} + \frac{2\bar{\varphi}_{33}}{\varphi_0^4} \right) \int_0^z E(\varepsilon, p) dp + \\
&\quad + \frac{2\varepsilon^2 \varphi_3}{\varphi_0^4} \int_0^z \left[ \int_0^p \varphi(s) ds \right] E(\varepsilon, p) dp - \\
&\quad - \frac{\varepsilon^2}{2\varphi_0^3} \int_0^z \left[ \int_0^p \bar{\varphi}(s) ds \right]^2 E(\varepsilon, p) dp - \frac{2}{\varphi_0^3} \int_0^z \left[ \int_0^p \bar{\varphi}(s) ds \right] E(\varepsilon, p) dp. \tag{1.28}
\end{aligned}$$

In (1.28) the functions  $f$ ,  $\varphi$  and  $\bar{\varphi}$  are solutions of the boundary problems:

$$\begin{aligned}
2f''' + f'' &= 0, \\
2\varphi''' + f\varphi'' + f''\varphi &= 0, \\
2\bar{\varphi}''' + f\bar{\varphi}'' + f''\bar{\varphi} &= \varphi\varphi''; \\
f(0) &= 0, \quad f'(0) = 0, \quad f'(\infty) = 1, \quad (f''(0) = 0.33205), \\
\varphi(0) &= 1, \quad \varphi'(0) = 0, \quad \varphi'(\infty) = 0, \\
\bar{\varphi}(0) &= 0, \quad \bar{\varphi}'(0) = 0, \quad \bar{\varphi}'(\infty) = 0. \tag{1.29}
\end{aligned}$$

In (1.28) the parameters  $\varphi_0, \varphi_3, \varphi_{33}, \bar{\varphi}_{33}$  are functions of the Schmidt number:

$$\begin{aligned}
\varphi_0 &= \int_0^\infty E(\varepsilon, p) dp \approx \begin{cases} 3.01 Sc^{-0.35} & \text{for gases,} \\ 3.12 Sc^{-0.34} & \text{for liquids,} \end{cases} \\
\varphi_3 &= \int_0^\infty \left[ \int_0^p \varphi(s) ds \right] E(\varepsilon, p) dp \approx \begin{cases} 6.56 Sc^{-0.80} & \text{for gases,} \\ 5.08 Sc^{-0.67} & \text{for liquids,} \end{cases} \\
\varphi_{33} &= \int_0^\infty \left[ \int_0^p \bar{\varphi}(s) ds \right]^2 E(\varepsilon, p) dp \approx \begin{cases} 24.0 Sc^{-1.3} & \text{for gases,} \\ 12.2 Sc^{-1.0} & \text{for liquids,} \end{cases} \\
\bar{\varphi}_{33} &= \int_0^\infty \left[ \int_0^p \bar{\varphi}(s) ds \right] E(\varepsilon, p) dp \approx \begin{cases} 0.326 Sc^{-1.63} & \text{for gases,} \\ 0.035 Sc^{-1.1} & \text{for liquids.} \end{cases} \tag{1.30}
\end{aligned}$$

The dimensionless diffusion flux, expressed by the Sherwood number (1.25) is obtained directly from (1.28):

$$\psi'(0) = -\frac{2}{\varepsilon \varphi_0} + \theta \frac{2\varphi_3}{\varphi_0^3} + \theta^2 \left( -\frac{4\varepsilon \varphi_3^2}{\varphi_0^5} + \frac{\varepsilon \varphi_{33}}{\varphi_0^4} + \frac{4\bar{\varphi}_{33}}{\varepsilon \varphi_0^4} \right). \tag{1.31}$$

Equation (1.31) shows that the precision of this basic result from the asymptotic theory of the diffusion boundary layer significantly depends on  $\theta$  and  $\varepsilon$ . If it is necessary to obtain a theoretical result with an error less than 10 %, the second order approximation of the small parameter  $\theta$  should be smaller than one tenth of its zero order approximation, i.e.

$$\left| \theta^2 \left( -\frac{4\varepsilon\varphi_3^2}{\varphi_0^5} + \frac{\varepsilon\varphi_{33}}{\varphi_0^4} + \frac{4\bar{\varphi}_{33}}{\varepsilon\varphi_0^4} \right) - (0.1) \right| < \left| -\frac{2}{\varepsilon\varphi_0} \right|. \quad (1.32)$$

From (1.32) it follows:

$$\varepsilon = 1, \quad \theta < 0.41;$$

$$\varepsilon = 2, \quad \theta < 0.23;$$

$$\varepsilon = 10, \quad \theta < 0.056;$$

$$\varepsilon = 20, \quad \theta < 0.025.$$

In order to check the precision of the asymptotic theory of non-linear mass transfer in a diffusion boundary layer, the finite problem (1.23) was solved through a numerical method [41] and the results are shown on Fig. 1.1 – 1.3.

In Table 1.1 results of the asymptotic theory  $\psi'(0)$  are compared with the results of the numerical experiment  $\psi'_N(0)$ . The missing data in the table corresponds to the cases when the singular disturbances in the numerical solution of the problem increase. From (1.33) it is obvious that these cases go beyond the limits of the accepted precision of the asymptotic theory.

Table 1.1.

Comparison of the results of the asymptotic theory  $\psi'(0)$  with the results of the numerical experiment  $\psi'_N(0)$

$\theta$	$\varepsilon = 1$		$\varepsilon = 2$		$\varepsilon = 10$		$\varepsilon = 20$	
	$-\psi'_N(0)$	$-\psi'(0)$	$-\psi'_N(0)$	$-\psi'(0)$	$-\psi'_N(0)$	$-\psi'(0)$	$-\psi'_N(0)$	$-\psi'(0)$
0.00	0.664	0.664	0.535	0.535	0.314	0.305	0.250	0.246
+0.03	0.650	0.650	0.515	0.516	0.270	0.265	0.190	0.199
-0.03	0.679	0.679	0.553	0.555	0.384	0.365	0.406	0.363
+0.05	0.641	0.641	0.503	0.504	0.248	0.250	0.166	0.205
-0.05	0.689	0.689	0.572	0.570	0.459	0.415	-	0.479
+0.10	0.620	0.620	0.475	0.478	0.207	0.250	-	0.355
-0.10	0.716	0.7162	0.616	0.611	-	0.581	-	0.903
+0.20	0.581	0.584	0.429	0.442	0.160	0.418	-	1.229
-0.20	0.779	0.776	0.736	0.707	-	1.080	-	2.325
+0.30	0.548	0.555	0.393	0.425	-	0.808	-	2.868
-0.30	0.855	0.843	0.936	0.822	-	1.800	-	4.512

The obtained results show that the direction of the intensive mass transfer significantly influences the mass transfer kinetics and this can not be predicted in the approximations of the

linear theory ( $\theta = 0$ ). When the mass transfer is directed from the volume towards the phase boundary ( $\theta < 0$ ), the increasing of the concentration gradient in the diffusion boundary layer ( $c^* - c_0$ ) leads to an increase in the diffusion mass transfer. In the cases when the mass transfer is directed from the phase boundary towards the volume ( $\theta > 0$ ), the increasing of the concentration gradient leads to a decrease in the diffusion mass transfer.

The non-linear effects in the mass transfer kinetics under conditions of intensive mass transfer occur in a thin layer on the surface of the phase separation (Fig. 1.1), which thickness is approximately three times smaller than the one of the diffusion boundary layer. At the boundary of this "layer of non-linear mass transfer" the character of the non-linear effect changes, i.e. the local diffusion flux depends on the concentration gradient, and on the value of the parameter  $\theta$  correspondingly. In the "non-linear mass transfer layer" for  $\theta < 0$  ( $\theta > 0$ ) the flux increases (decreases) with the increase of the absolute value of  $\theta$ , and out of this layer this dependence turns to the opposite.

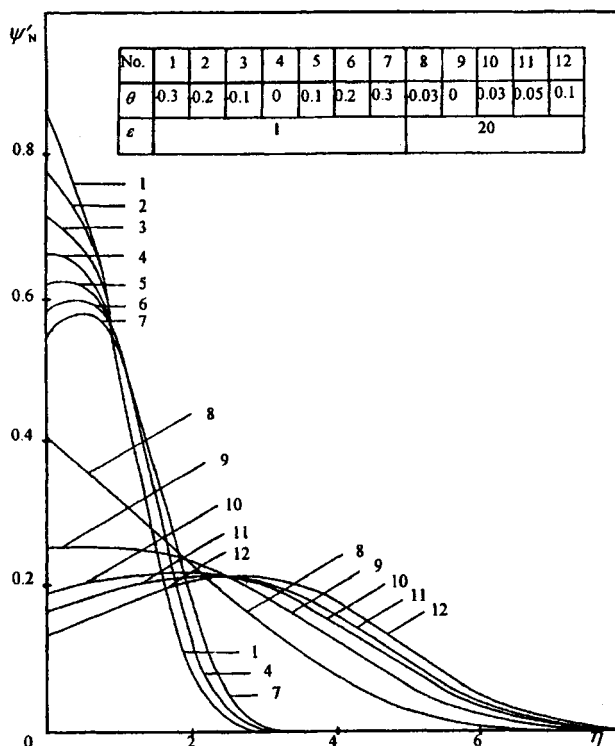
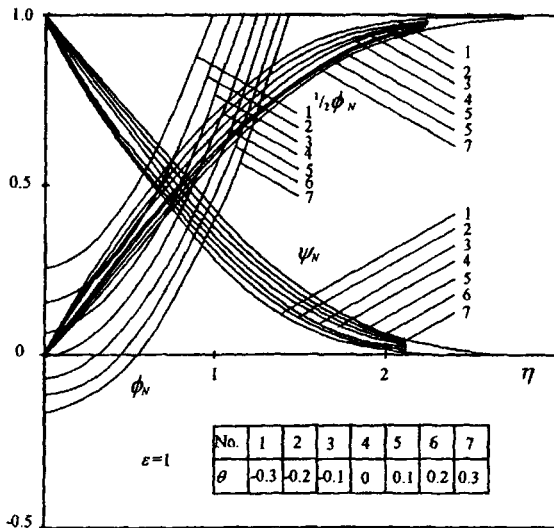


Fig. 1.1. Dimensionless diffusion flux (numerical experiment).



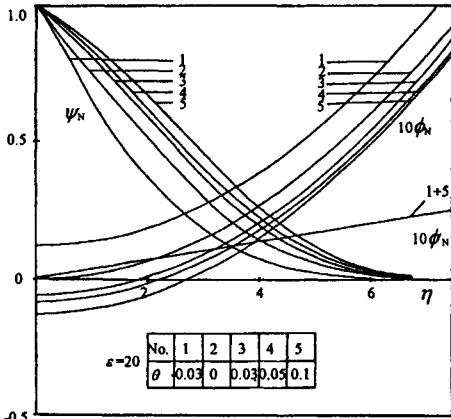


Fig. 1.3. Distribution of the dimensionless velocity ( $\phi'_N$ ) and dimensionless concentration ( $\psi_N$ ) in the boundary layer for liquids (numerical experiment).  $\phi'_N(0)$  is dimensionless velocity of the induced secondary flow.

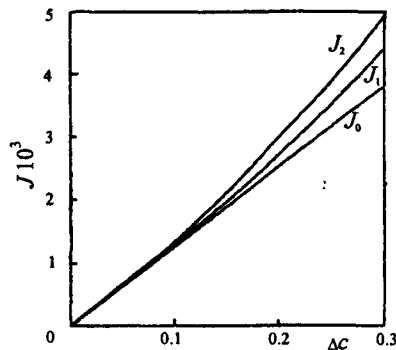


Fig. 1.4. Influence of the dimensionless concentration difference on the mass transfer rate.

The first term in (1.25) takes into consideration the convective transfer as a result of the induced secondary flow (1.17). This effect is essential for big concentrations at the boundary of the phase separation and is negligible for smaller concentration gradients or in the cases when  $c^* = 0$  ( $\theta < 0$ ).

In the cases when  $\theta > 0$  the mass transfer rate depends on  $\rho^* / \rho_0^*$ , and the change in  $\Delta c$  leads to a change in  $\theta$ .

Having all this in mind, it is interesting to compare the mass transfer rate at the same concentration gradients and different mass transfer directions.

The mass transfer rate in the approximations of the linear theory  $J_0$  is determined by (1.25), if it is assumed that  $\theta = 0$  and  $\rho^* / \rho_0^* = 1$ .

The non-linear mass transfer rate from the interphase surface towards the volume of the phase  $J_1$  is determined by (1.25), when  $\theta > 0$ .

The non-linear mass transfer rate from the phase volume towards the interphase surface  $J_2$  is determined by (1.25) for  $c^* = 0$ , when  $\theta = 0$  and  $\rho^* / \rho_0^* = 1$ .

The influence of the concentration gradient and the direction of the mass transfer on its rate, as well as the separate effects of the non-linear mass transfer for  $u_0 = 1$  m/s,  $L = 0.1$  m,  $D = 2.19 \cdot 10^{-5}$  m<sup>2</sup>/s,  $\varepsilon = 1$ , are illustrated on Fig. 1.4 [44]. As it is obvious, the increasing of the concentration gradient at  $\theta > 0$  leads to increase of  $\rho^* / \rho_0^*$  and to decrease of  $\psi'(0)$ . However, the mass transfer rate  $J_1$  grows and is always greater than the rate  $J_0$ , obtained in the approximations of the linear theory ( $\theta = 0$ ). At  $\theta < 0$  the mass transfer rate  $J_2$  is always

greater than the rate  $J_1$ . These results are correct in cases of mass transfer in gases (for example, diffusion of water vapour in air). In liquids the non-linear mass transfer may occur only at infinite solubility of the diffusing substance. Under ordinary conditions the maximum concentration gradients do not influence noticeably the mass transfer, as practically  $\theta = 0$ .

The theoretical results (1.31) obtained show in the first place that the direction of the interphase mass transfer influence its kinetics in the diffusion boundary layer. This effect is hydrodynamical, i.e the intensive mass transfer induces a flow directed normally to the boundary of phase separation, which leads to change in the velocity distribution in the diffusion boundary layer. All these facts provide some reason to expect analogous effects in the heat transfer kinetics.

### 1.2.2. Heat transfer in the conditions of non-linear mass transfer

The intensive mass transfer leads to a change of the velocity distribution in the boundary layer. As a result, its influence on the heat and mass transfer should be analogous. The theoretical analysis of the heat transfer kinetics, that is accompanied by a non-linear mass transfer, was carried out [32, 42] for cases, where the thermodiffusion and the diffusion thermal conductivity are not considered.

The influence of the non-linear mass transfer on the heat transfer may be determined, if the problem (1.8) is completed with the equation of the convective heat transfer in the approximations of the boundary layer:

$$\begin{aligned} u \frac{\partial t}{\partial x} + v \frac{\partial t}{\partial y} &= \alpha \frac{\partial^2 t}{\partial y^2}; \\ x = 0, \quad t &= t_0; \\ y = 0, \quad t &= t^*; \\ y \rightarrow \infty, \quad t &= t_\theta, \end{aligned} \tag{1.34}$$

where  $t_0$  and  $t^*$  are the temperatures in the volume and on the solid surface,  $\alpha$  is the thermal diffusivity.

In (1.34) it is necessary to introduce similarity variables (1.21) and the result is obtained:

$$\begin{aligned} T'' + \bar{\varepsilon}_t \phi T' &= 0, \\ T(0) = 1, T(\infty) &= 0, \end{aligned} \tag{1.35}$$

where

$$T = T(\eta) = \frac{t - t_0}{t^* - t_0}; \quad \bar{\varepsilon}_t = \varepsilon \alpha_t; \quad \alpha_t = \frac{D}{a} = Le^{-l}. \tag{1.36}$$

In (1.35) it is necessary to substitute  $\phi(\eta)$  from (1.27) and (1.28), which allows to seek  $T(\eta)$  in the form of a series of the orders of the small parameter  $\theta$ :

$$T = T_0 + \theta T_1 + \theta^2 T_2 + \dots . \tag{1.37}$$

In this way a series of finite problems for the separate approximations [32] is obtained and their solutions have the form:

$$\begin{aligned}
 T_0(\eta) &= I - \frac{1}{\varphi_{0t}} \int_0^x E(\varepsilon_t, p) dp, \quad z = \frac{2}{\varepsilon} \eta, \\
 T_1(\eta) &= \frac{\bar{\varepsilon}_t \varphi_{3t}}{\varphi_0 \varphi_{0t}^2} \int_0^z E(\varepsilon_t, p) dp - \frac{\bar{\varepsilon}_t^2}{\varphi_0 \varphi_{0t}} \int_0^z \left[ \int_0^p \varphi(s) ds \right] E(\varepsilon_t, p) dp, \\
 T_2(\eta) &= - \left[ \frac{\bar{\varepsilon}_t \varepsilon \varphi_{3t}}{\varphi_0^2 \varphi_{0t}^2} \left( \frac{\varphi_3}{\varphi_0} + \frac{\bar{\varepsilon}_t \varphi_{3t}}{\varepsilon \varphi_{0t}} \right) - \frac{\bar{\varepsilon}_t^2 \varphi_{33t}}{2\varphi_0^2 \varphi_{0t}^2} - \frac{\bar{\varepsilon}_t \bar{\varphi}_{33t}}{2\varepsilon \varphi_0^2 \varphi_{0t}^2} \right] \int_0^z E(\varepsilon_t, p) dp + \\
 &+ \frac{\bar{\varepsilon}_t \varepsilon}{\varphi_0^2 \varphi_{0t}} \left( \frac{\varphi_3}{\varphi_0} + \frac{\bar{\varepsilon}_t \varphi_{3t}}{\varepsilon \varphi_{0t}} \right) \int_0^z \left[ \int_0^p \varphi(s) ds \right] E(\varepsilon_t, p) dp - \frac{\bar{\varepsilon}_t^2}{2\varphi_0^2 \varphi_{0t}} \int_0^z \left[ \int_0^p \varphi(s) ds \right] E(\varepsilon_t, p) dp - \\
 &- \frac{\bar{\varepsilon}_t}{2\varepsilon \varphi_0^2 \varphi_{0t}} \int_0^z \left[ \int_0^p \bar{\varphi}(s) ds \right] E(\varepsilon_t, p) dp,
 \end{aligned} \tag{1.38}$$

where

$$\begin{aligned}
 \varepsilon_t &= (\varepsilon \bar{\varepsilon}_t)^{0.5}, \\
 E(\varepsilon_t, p) &= \exp \left[ - \frac{\varepsilon_t^2}{2} \int_0^p f(s) ds \right], \\
 \varphi_{0t} &= \int_0^\infty E(\varepsilon_t, p) dp \approx 3.01 \varepsilon_t^{-0.7}, \\
 \varphi_{3t} &= \int_0^\infty \left[ \int_0^p \varphi(s) ds \right] E(\varepsilon_t, p) dp \approx 6.56 \varepsilon_t^{-1.6}, \\
 \varphi_{33t} &= \int_0^\infty \left[ \int_0^p \varphi(s) ds \right]^2 E(\varepsilon_t, p) dp \approx 24 \varepsilon_t^{-2.6}, \\
 \bar{\varphi}_{33t} &= \int_0^\infty \left[ \int_0^p \bar{\varphi}(s) ds \right] E(\varepsilon_t, p) dp \approx 0.326 \varepsilon_t^{-3.26}.
 \end{aligned} \tag{1.39}$$

The expressions (1.38) and (1.39) are correct for gases only. In [42] it was shown that for big values of the Lewis number for liquids ( $\alpha \approx 10^{-2}$ ) the non-linear mass transfer does not influence the heat transfer, because the thickness of the diffusion boundary layer is much lower than the thickness of the temperature boundary layer. The non-linear mass transfer influences the hydrodynamics only in the thin diffusion boundary layer and this influence is not essential for the heat transfer in the thick temperature boundary layer. This result may be obtained from (1.35), where the big hydrodynamic effects of the intensive mass transfer ( $\phi(0) \neq 0$ ) for high values of the Lewis number may be ignored.

The transfer rate in the gas at the boundary with a solid surface with length  $L$  is determined by the average value of the heat flux:

$$J_t = k_i(t^* - t_0) = \frac{I}{L} \int_0^L I_t dx, \quad (1.40)$$

that has a convective component as a result of the induced flow:

$$I_t = -\lambda \left( \frac{\partial t}{\partial y} \right)_{y=0} + \rho_0^* c_p (vt)_{y=0}. \quad (1.41)$$

Using (1.21), (1.36), (1.40) and (1.41), an expression for the Nusselt number can be obtained:

$$Nu = \frac{k_i L}{\lambda} = -Pe^{0.5} \left[ T'(0) + \theta \bar{\epsilon}_t \frac{t^* - t_0}{t^*} \psi(0) \right]. \quad (1.42)$$

where  $Pe$  is determined from (1.26). In (1.42)  $\psi'(0)$  is determined from (1.31), and  $T'(0)$  is obtained from (1.37) and (1.38):

$$T'(0) = -\frac{2}{\varepsilon \varphi_{0t}} + \theta \frac{2\alpha_i \varphi_{3t}}{\varphi_0^2 \varphi_{0t}^2} - \theta^2 \left[ \frac{2\bar{\epsilon}_t \varphi_{3t}}{\varphi_0^2 \varphi_{0t}^2} \left( \frac{\varphi_3}{\varphi_0} + \frac{\alpha_i \varphi_{3t}}{\varphi_{0t}} \right) - \frac{\alpha_i \bar{\epsilon}_t \varphi_{33t}}{\varphi_0^2 \varphi_{0t}^2} - \frac{\alpha_i \bar{\varphi}_{33t}}{\varepsilon \varphi_0^2 \varphi_{0t}^2} \right]. \quad (1.43)$$

The check for the accuracy of the asymptotic theory for the joint heat mass transfer in the boundary layer under conditions of intensive mass transfer was carried out in the solution of the problem (1.35) through a numerical method [42]. The results obtained are shown on Fig. 1.5.

Table 1.2.

Comparison of the asymptotic theory prediction ( $T'(0)$ ) with results from numerical experiments ( $T'_N(0)$ ).

$\varepsilon = 1,$	$\alpha_i = 2,$	$\bar{\epsilon}_t = 2$
$\theta$	$-T'_N(0)$	$-T'(0)$
0.0	0.864	0.847
+0.1	0.762	0.765
-0.1	0.943	0.945
+0.2	0.690	0.700
-0.2	1.063	1.059
+0.3	0.633	0.652
-0.3	1.212	1.190

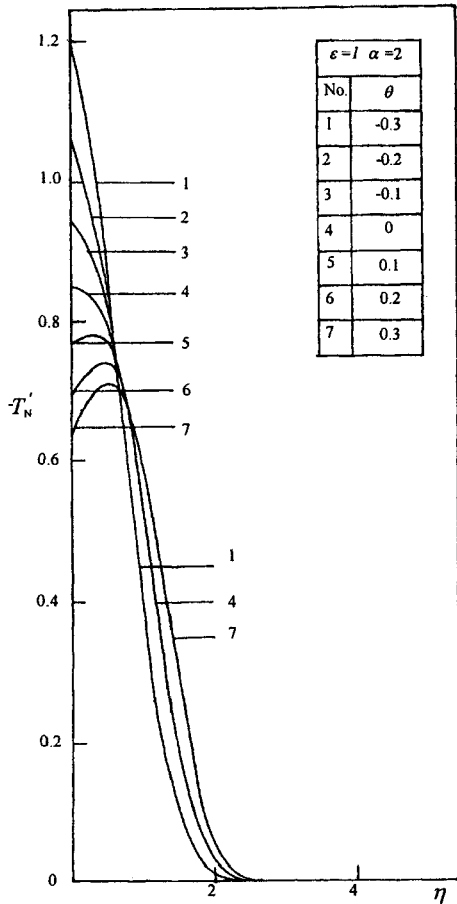


Fig. 1.5. Dimensionless heat flux (numerical results).

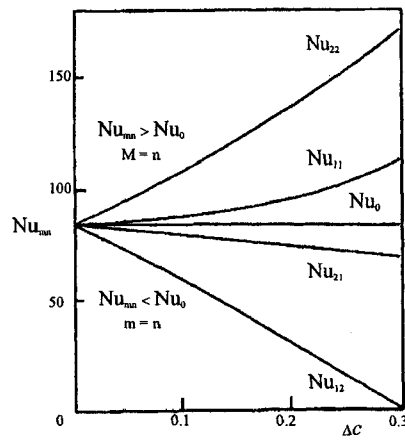


Fig. 1.6. Influence of the heat and mass transfer direction on the heat transfer rate.

The results of the asymptotic theory  $T'(\theta)$  are in good agreement with the results of the numerical experiment  $T'_N(\theta)$  (Table 1.2). It is obvious, that under conditions of intensive mass transfer ( $\theta \neq 0$ ) the non-linear mass and heat transfer are not independent on each other, as it follows from the linear theory ( $\theta = 0$ ) for small concentration gradients. In the cases where the non-linear mass transfer is directed a rigid wall ( $\theta < 0$ ), the increase of the concentration gradient leads to an increase of  $T'(\theta)$ . On the contrary, the increase of  $\theta$  leads to a decrease of  $T'(\theta)$  when the intensive interphase mass transfer is from the solid wall toward the gas ( $\theta > 0$ ).

The mass transfer kinetics under conditions of non-linear mass transfer is determined by the equations (1.40), (1.42), (1.43) and (1.31). The analysis of these expressions shows that

beside the concentration gradient, the direction of the mass transfer should also be considered. Having in mind that  $t^*$  and  $t_0$  are the temperatures at the borders of the temperature boundary layer,  $(t^* - t_0)$  may be treated as an average value of the temperature gradient in the temperature boundary layer. This assumption makes possible to determine the dimensionless temperature gradient  $\Delta t = (t^* - t_0)/t^*$  and its influence on the heat transfer rate [44].

Equation (1.42) shows that the Nusselt number depends on the temperature concentration gradients, i.e.  $Nu_{mn} = Nu(\theta_m, \Delta t_n)$ , where  $m = 1, 2; n = 1, 2$ ,  $\theta_1 = \theta > 0, \theta_2 = \theta < 0, \Delta t_1 = \Delta t > 0, \Delta t_2 = \Delta t < 0$ . In the cases when  $m=n$ , the directions of the heat and the mass transfer are the same, and when  $m \neq n$ , the directions are opposite to each other.

The comparison of the results for  $Nu_{mn}$  ( $m = 1, 2; n = 1, 2$ ) with the results of the linear theory  $Nu_0$  ( $\theta = 0$ ) for the same concentration gradients is displayed on Fig. 1.6. The data [44] is obtained for  $Pe = 10^4, \varepsilon = 1, \alpha_i = 2, \Delta t_n = (-1)^{n-1}, (n = 1, 2)$ . It can be clearly seen that non-linear effects (as a result of intensive interphase mass transfer under high concentration gradients) compared to the linear theory ( $Nu_0$ ) lead to a rise in the heat transfer rate ( $Nu_{mn}$ ), when mass transfer and heat transfer are unidirectional ( $m = n$ ), and to a decrease in the heat transfer rate, when these two processes are not unidirectional ( $m \neq n$ ).

### 1.2.3. Multicomponent mass transfer

The hydrodynamic nature of the non-linear effect in the mass transfer kinetics under conditions of intensive mass transfer gives reason to assume that an analogous effect may occur under conditions of multicomponent mass transfer for all components, if there is a mass transfer of one of them in conditions of a very big concentration gradient.

The theory of diffusion in a multicomponent systems [22, 59] shows that independent diffusion approximation is valid in two cases: when the concentrations of the components are low and when their diffusive components do not considerably differ. This together with the mass transfer at a high concentration gradient provides a sufficient basis to discuss in an analogous way the mass transfer of the other components, for which the concentration gradients  $c_i$  ( $i = 1, \dots, n$ ) are low. With this aim the following should be added to equation (1.18):

$$\begin{aligned} u \frac{\partial c_i}{\partial x} + v \frac{\partial c_i}{\partial y} &= D_i \frac{\partial^2 c_i}{\partial y^2}; \\ x = 0, \quad c_i &= c_{0i}; \\ y = 0, \quad c_i &= c_i^*; \quad y \rightarrow \infty, \quad c_i = c_{0i}; \quad i = 1, \dots, n. \end{aligned} \quad (1.44)$$

Using the dimensionless variables (1.21), the equation (1.23) is completed as follows:

$$\begin{aligned} \psi_i'' + \bar{\varepsilon}_i \phi \psi_i' &= 0 \\ \psi_i(0) = 1, \quad \psi_i(\infty) &= 0, \quad i = 1, \dots, n, \end{aligned} \quad (1.45)$$

where

$$\bar{\varepsilon}_i = \varepsilon \alpha_i, \quad \alpha_i = \left( \frac{\varepsilon_i}{\varepsilon} \right)^2, \quad \varepsilon_i = Sc_i^{0.5},$$

$$Sc_i = \frac{V}{D_i}, \quad \psi_i = \psi_i(\eta) = \frac{c_i - c_{0i}}{c_i^* - c_{0i}}, \quad i = 1, \dots, n. \quad (1.46)$$

In (1.45) the function  $\phi(\eta)$  is determined (1.27) in the form of a series of the orders of the small parameter  $\theta$ , which allows seeking the solution of (1.45) analogously:

$$\psi_i = \psi_i^{(0)} + \theta \psi_i^{(1)} + \theta^2 \psi_i^{(2)} + \dots, \quad i = 1, \dots, n. \quad (1.47)$$

The separate problems for the determination of the unknown functions in (1.47) are solved through the method of disturbances, where for  $\phi_0$ ,  $\phi_1$  and  $\phi_2$  (1.28) is used. In this way the following expressions are obtained [34]:

$$\begin{aligned} \psi_i^{(0)}(\eta) &= 1 - \frac{1}{\varphi_{0i}} \int_0^z E(\varepsilon_i, p) dp, \\ \psi_i^{(1)}(\eta) &= \frac{\bar{\varepsilon}_i \varphi_{3i}}{\varphi_0 \varphi_{0i}^2} \int_0^z E(\varepsilon_i, p) dp - \frac{\bar{\varepsilon}_i}{\varphi_0 \varphi_{0i}} \int_0^z \left[ \int_0^p \varphi(s) ds \right] E(\varepsilon_i, p) dp, \\ \psi_i^{(2)}(\eta) &= - \left[ \frac{\bar{\varepsilon}_i \varepsilon \varphi_{3i}}{\varphi_0^2 \varphi_{0i}^2} \left( \frac{\varphi_3 + \bar{\varepsilon}_i \varphi_{3i}}{\varepsilon \varphi_{0i}} \right) - \frac{\bar{\varepsilon}_i^2 \varphi_{33i}}{2 \varphi_0^2 \varphi_{0i}^2} - \frac{\bar{\varepsilon}_i \bar{\varphi}_{33i}}{2 \varepsilon \varphi_0^2 \varphi_{0i}^2} \right] \int_0^z E(\varepsilon_i, p) dp + \\ &+ \frac{\bar{\varepsilon}_i \varepsilon}{\varphi_0^2 \varphi_{0i}} \left( \frac{\varphi_3 + \bar{\varepsilon}_i \varphi_{3i}}{\varepsilon \varphi_{0i}} \right) \int_0^z \left[ \int_0^p \varphi(s) ds \right] E(\varepsilon_i, p) dp - \frac{\bar{\varepsilon}_i^2}{2 \varphi_0^2 \varphi_{0i}} \int_0^z \left[ \int_0^p \varphi(s) ds \right] E(\varepsilon_i, p) dp - \\ &- \frac{\bar{\varepsilon}_i}{2 \varepsilon \varphi_0^2 \varphi_{0i}} \int_0^z \left[ \int_0^p \bar{\varphi}(s) ds \right] E(\varepsilon_i, p) dp, \\ i &= 1, \dots, n, \end{aligned} \quad (1.48)$$

where

$$E(\varepsilon_i, p) = \exp \left[ - \frac{\varepsilon_i^2}{2} \int_0^p f(s) ds \right],$$

$$\varphi_{0i} = \int_0^\infty E(\varepsilon_i, p) dp \approx \begin{cases} 3,01 Sc_i^{-0.35} & \text{for gases,} \\ 3,12 Sc_i^{-0.34} & \text{for liquids,} \end{cases}$$

$$\varphi_{3i} = \int_0^\infty \left[ \int_0^p \varphi(s) ds \right] E(\varepsilon_i, p) dp \approx \begin{cases} 6,56 Sc_i^{-0.8} & \text{for gases,} \\ 5,08 Sc_i^{-0.67} & \text{for liquids,} \end{cases}$$

$$\varphi_{33i} = \int_0^\infty \left[ \int_0^p \varphi(s) ds \right]^2 E(\varepsilon_i, p) dp \approx \begin{cases} 24 Sc_i^{-1.3} & \text{for gases,} \\ 12,2 Sc_i^{-1} & \text{for liquids,} \end{cases}$$

$$\bar{\varphi}_{33i} = \int_0^p \left[ \int_0^p \bar{\varphi}(s) ds \right] E(\varepsilon_i, p) dp \approx \begin{cases} 0.326 Sc_i^{-1.63} & \text{for gases,} \\ 0.035 Sc_i^{-1.1} & \text{for liquids,} \end{cases} \\ i = 1, \dots, n. \quad (1.49)$$

The multicomponent mass transfer rate in gases (liquids) at a boundary with a solid surface with length  $L$  is determined by the average value of the mass flux:

$$J_i = M_i k_i (c_i^* - c_{0i}) = \frac{I}{L} \int_0^L I_i dx_i, \quad i = 1, \dots, n, \quad (1.50)$$

which has a convective component as well as a result of the induced flow:

$$I_i = -M_i D_i \left( \frac{\partial c_i}{\partial y} \right)_{y=0} + M_i (c_i v) = -M_i D_i \left[ \left( \frac{\partial c_i}{\partial y} \right)_{y=0} + \frac{M_i \alpha_i}{\rho_0} \left( c_i \frac{\partial c}{\partial y} \right)_{y=0} \right], \quad i = 1, \dots, n. \quad (1.51)$$

The expression for the Sherwood number is derived from (1.21), (1.46), (1.50) and (1.51):

$$Sh_i = \frac{k_i L}{D_i} = Pe^{0.5} \left[ \psi'_i(0) + \theta \bar{\varepsilon}_i \frac{c_i^*}{c_i^* - c_{0i}} \psi'(0) \right], \quad i = 1, \dots, n, \quad (1.52)$$

where  $\psi'(0)$  is determined from (1.31), while  $\psi'_i(0)$  is determined from equation (1.48):

$$\psi'_i(0) = -\frac{2}{\varepsilon \varphi_{0i}} + \theta \frac{2\bar{\varepsilon}_i \varphi_{3i}}{\varepsilon \varphi_0 \varphi_{0i}^2} - \theta^2 \left[ \frac{2\bar{\varepsilon}_i \varphi_{3i}}{\varphi_0^2 \varphi_{0i}^2} \left( \frac{\varphi_3}{\varphi_0} + \frac{\bar{\varepsilon}_i \varphi_{3i}}{\varepsilon \varphi_{0i}} \right) - \frac{\bar{\varepsilon}_i^2 \varphi_{33i}}{\varepsilon \varphi_0^2 \varphi_{0i}^2} - \frac{\bar{\varepsilon}_i \bar{\varphi}_{33i}}{\varepsilon^2 \varphi_0^2 \varphi_{0i}^2} \right], \\ i = 1, \dots, n. \quad (1.53)$$

**Table 1.3.**  
Comparison of the asymptotic theory ( $\psi'_i(0)$ ) with the numerical experiments ( $\psi'_{in}(0)$ ),  $i = 1, \dots, n$ , for gases.

$\varepsilon = 1,$	$\alpha_i = 2,$	$\bar{\varepsilon}_i = 2$
$\theta$	$-\psi'_i(0)$	$-\psi'_{in}(0)$
0.0	0.845	0.847
+0.1	0.762	0.765
-0.1	0.943	0.945
+0.2	0.689	0.700
-0.2	1.060	1.061
+0.3	0.633	0.652
-0.3	1.212	1.190

The accuracy of the basic result (1.53) of the asymptotic theory for the multicomponent mass transfer under conditions of intensive mass transfer depends on the parameters  $\theta, \varepsilon$  and  $\varepsilon_i$  ( $i = 1, \dots, n$ ). The limits of validation of this theory may be determined through an expression of the type (1.32). For example, for  $\varepsilon = 20$  and  $\bar{\varepsilon}_i = 10$  the admissible values for  $\theta$  are  $\theta < 0.033$ .

Table 1.4.

Comparison of the asymptotic theory ( $\psi'_i(0)$ ) with the numerical experiments ( $\psi'_{in}(0)$ ),  $i=1, \dots, n$ , for liquids.

$\varepsilon = 20$	$\alpha_i = 0.5$	$\bar{\varepsilon}_i = 10$
$\theta$	$-\psi'_i(0)$	$-\psi'_{in}(0)$
0.00	0.198	0.194
+0.03	0.167	0.169
-0.03	0.275	0.250
+0.05	0.154	0.170
+0.10	0.132	0.234

Evaluation of the accuracy of an asymptotic theory of the multicomponent mass transfer (1.53) (under conditions of interphase mass transfer for one of the components) has been made using numerical solution of problems (1.23) and (1.24). The comparison of the results of the numerical experiment  $\psi'_{in}(0)$  [34] with the asymptotic theory data  $\psi'_i(0)$  is shown in Tables 1.3 and 1.4. It can be clearly seen that intensive interphase mass transfer of one of the components from the volume toward the solid surface ( $\theta < 0$ ) increases the diffusive mass transfer for all of the components. In the cases where the direction of intensive interphase mass transfer is from the solid surface toward the volume ( $\theta > 0$ ) the multicomponent mass transfer decreases. These effects do not depend on the change in the direction of the interphase mass transfer for components with low concentration gradients.

The multicomponent mass transfer kinetics in the cases of non-linear mass transfer of one of the components (as a result of the high gradient of its concentration) is determined by equations (1.50), (1.52), (1.53) and (1.31). The analysis of these equations shows that the multicomponent mass transfer kinetics is influenced not only by the high concentration gradient, but also by the direction of the mass transfer of the separate components [44].

In equation (1.52) it is possible to introduce a dimensionless concentration gradient of the different components:

$$\Delta c_i = (c_i^* - c_{i0}) / c_i^*, \quad i = 1, \dots, n.$$

In this way the Nusselt number depends on the two concentration gradients:

$$Sh_{imq} = Nu_i(\theta_m, \Delta s_{iq}), \quad (i = 1, \dots, n; \quad m = 1, 2; \quad q = 1, 2).$$

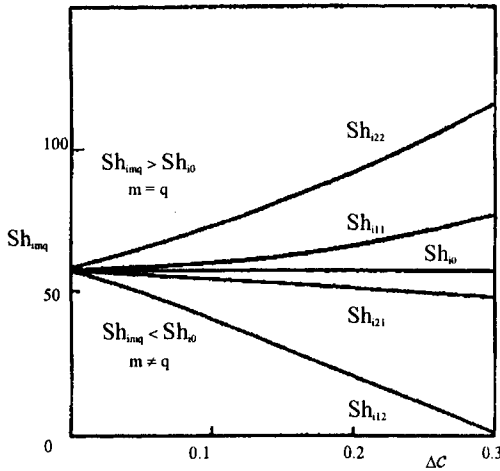


Fig. 1.7. Influence of the mass transfer direction on the mass transfer rate.

In the cases when  $m=q$ , the direction of the non-linear mass transfer and the multicomponent mass transfer is one and the same, and when  $m \neq q$ , the directions are opposite.

The comparison of the values of  $Sh_{imq}$  ( $i=1,\dots,n$ ;  $m=1,2$ ;  $q=1,2$ ) and  $Sh_{i\theta}$  ( $\theta=0$ ) for the same concentration gradients  $\Delta c$  is displayed on Fig. 1.7. These results [44] are obtained for  $Pe = 4566$ ,  $\varepsilon = 1$ ,  $\alpha_i = 1$ ,  $\Delta c_{iq} = (-1)^{q-1}$ , ( $n=1,\dots,n$ ;  $q=1,2$ ). It can be seen that the increase of the concentration gradient leads to an increase of the multicomponent mass transfer rate in the cases, where its direction is the same as the one of the non-linear mass transfer ( $m=q$ ). In the opposite case ( $m \neq q$ ) the multicomponent mass transfer rate decreases.

#### 1.2.4. Non-linear mass transfer in the entrance region of a channel

The non-linear mass transfer in a flat parallel channel is interesting in connection with the study of the intensive mass transfer kinetics in a number of chemical and electrochemical technologies, where processes of solution (sedimentation) of substances on the walls of a pipe with a circle or rectangular cross section take part. This problem was solved [12] in the approximations of the Poiseuille flow.

The non-linear mass transfer in the entrance region of a channel is of theoretical and practical interest, where the effects of the formation of the velocity profile of Poiseuille are added to the effects from the induced secondary flow due to the high concentration gradient.

Assume that a gas (liquid) with an average velocity  $u_0$  is moving in a flat parallel channel with a  $2b$  width and a  $L_0$  length. Having in mind that the problem is symmetrical, the complete system of equations has the form:

$$\begin{aligned}
U \frac{\partial U}{\partial X} + V \frac{\partial U}{\partial Y} &= -\frac{\partial P}{\partial X} + \frac{I}{\alpha_0 Re} \left( \alpha_0^2 \frac{\partial^2 U}{\partial X^2} + \frac{\partial^2 U}{\partial Y^2} \right), \\
\alpha^2 \left( U \frac{\partial V}{\partial X} + V \frac{\partial V}{\partial Y} \right) &= -\frac{\partial P}{\partial Y} + \frac{\alpha_0}{Re} \left( \alpha_0^2 \frac{\partial^2 V}{\partial X^2} + \frac{\partial^2 V}{\partial Y^2} \right), \\
\frac{\partial U}{\partial X} + \frac{\partial V}{\partial Y} &= 0, \\
U \frac{\partial C}{\partial X} + V \frac{\partial C}{\partial Y} &= \frac{1}{\alpha_0^2 Pe} \left( \alpha_0^2 \frac{\partial^2 C}{\partial X^2} + \frac{\partial^2 C}{\partial Y^2} \right), \\
X = 0, \quad U = 0, \quad V = 0, \quad P = 1, \quad C = 0; \\
Y = 0, \quad U = 0, \quad V = -\theta_0 \frac{\partial C}{\partial Y}, \quad P = 1, \quad C = 1; \\
Y = L, \quad \frac{\partial U}{\partial Y} = 0, \quad V = 0, \quad \frac{\partial C}{\partial Y} = 0,
\end{aligned} \tag{1.54}$$

where

$$\begin{aligned}
U &= \frac{u}{u_0}, \quad V = \frac{v}{\alpha_0 u_0}, \quad P = \frac{p}{\rho_0 u_0^2}, \quad C = \frac{c - c_0}{c^* - c_0}; \\
X &= \frac{x}{L_0}, \quad Y = \frac{y}{b}, \quad \alpha_0 = \frac{b}{L_0}, \quad Re = \frac{u_0 b}{v}, \quad Pe = \frac{\varepsilon^2}{\alpha_0} Re, \quad \theta_0 = \frac{\theta}{\alpha_0 \varepsilon Re}.
\end{aligned} \tag{1.55}$$

To the problem (1.54) boundary conditions for  $x \rightarrow \infty$  are to be added. Having in mind that equation (1.54) may be solved through numerical methods only, for most values of  $x$  a condition, expressing the achievement of asymptotic values of all functions can be used.

The solution of the problem of a flat flow in the entrance region of the channel was found by H. Shlichting [84] and the condition  $x \rightarrow \infty$  in the considered case will be  $x > 0,16b Re$ , i.e.  $\alpha_0 > 6,25 \cdot 10^{-3}$ .

The Sherwood number may be determined from (1.19), (1.20) and (1.55):

$$Sh = \frac{kL}{D} = -\frac{I}{\alpha_0 \rho_0^*} \int_0^{L/L_0} \left( \frac{\partial C}{\partial Y} \right)_{Y=0} dX = \frac{I}{\alpha_0 \rho_0^*} F(L), \tag{1.56}$$

where  $L < L_0$ .

The solution of the problem (1.54) was obtained [61] through the ADI method. The non-stationary problem was solved by means of fraction steps according to the Peaceman – Rachford schemes [19, 21, 25, 49].

The results for  $F(L)$  in (1.56) were obtained for the cases of gas movement when  $Re = 10^3$ ,  $\alpha_0 = 10^{-2}$ ,  $\varepsilon = 1$ ,  $Pe = 10^5$  and  $-0,5 \leq \theta \leq 0,5$ .

The influence of the mass transfer direction on its rate is illustrated on Fig. 1.8.

Equations (1.56) and (1.25) may be compared with the help of the function:

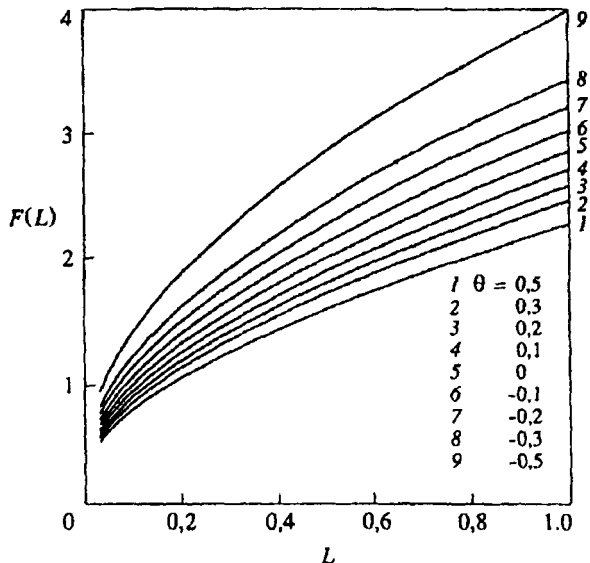


Fig. 1.8. Influence of the mass transfer direction and intensity ( $\theta$ ) on the rate of mass transfer ( $F$ ).

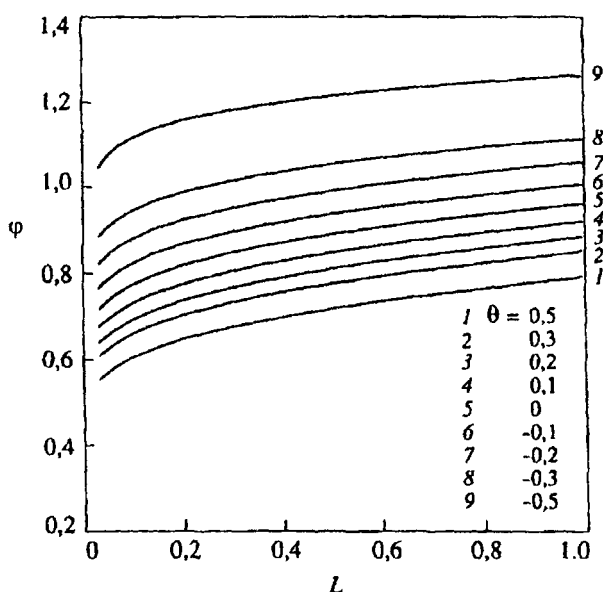


Fig. 1.9. Change of the diffusive transfer rate  $\varphi(L, \theta)$  along a channel of length  $L$ .

$$\varphi(X, \theta) = \frac{2\sqrt{X}}{\sqrt{\alpha_0 Pe}} \left( \frac{\partial C}{\partial Y} \right)_{Y=0}, \quad (1.57)$$

which does not depend on X in the approximations of the boundary layer:

$$\varphi(\theta) = \psi'(0). \quad (1.58)$$

The displayed on Fig. 1.9 function  $\varphi = \varphi(L, \theta)$  may be compared with  $\psi'(0) = 0,664$  for  $\theta = 0$ . As it is clearly seen, for  $L > 0,02$  the formation of the Poiseuille profile considerably influences the mass transfer rate.

### CHAPTER 1.3. GAS-LIQUID AND LIQUID-LIQUID SYSTEMS

The interphase mass transfer in the gas-liquid and the liquid-liquid systems is associated primarily with the industrial absorption and extraction processes. The process intensification through generation of big concentration gradients in the gas and the liquid leads to manifestation of non-linear effects in the kinetics of the mass transfer in the gas and liquid phases. In this way the interphase mass transfer in the gas-liquid and the liquid-liquid systems becomes non-linear.

#### 1.3.1. Non-linear mass transfer in the gas and in the liquid boundary layer

The industrial gas absorption is most frequently realized in packed bed columns. The sizes of packings used being small, the interphase transfer of the absorbed material is effected through the thin layers bordering the phase boundary between the gas and the liquid. The main change in the absorbed material concentration takes place in these layers, which allows the theoretical analysis of the kinetics of non-linear interphase mass transfer to be performed making use of the approximation of the diffusion boundary layer.

The kinetics of the non-linear interphase mass transfer in the cases of a flat phase interface and co-current movement of the gas and the liquid [5, 17] will be discussed. If the gas and the liquid are designated as a first and a second phase respectively, the equations (1.18) take the form:

$$\begin{aligned} u_j \frac{\partial u_j}{\partial x} + v_j \frac{\partial u_j}{\partial y} &= v_j \frac{\partial^2 u_j}{\partial y^2}, \\ \frac{\partial u_j}{\partial x} + \frac{\partial v_j}{\partial y} &= 0, \\ u_j \frac{\partial c_j}{\partial x} + v_j \frac{\partial c_j}{\partial y} &= D_j \frac{\partial^2 c_j}{\partial y^2}, \quad j = 1,2. \end{aligned} \quad (1.59)$$

with boundary conditions accounting for the continuity of the velocities distribution and the flows of momentum and mass at the phase interface:

$$x = 0, \quad u_j = u_{j0}, \quad c_j = c_{j0}, \quad j = 1,2;$$

$$\begin{aligned}
y = 0, \quad u_1 = u_2, \quad \mu_1 \frac{\partial u_1}{\partial y} = \mu_2 \frac{\partial u_2}{\partial y}, \\
v_j = -\frac{MD_j}{\rho_{j0}^*} \frac{\partial c_j}{\partial y}, \quad j = 1, 2, \\
c_1 = \chi c_2, \quad \frac{D_1 \rho_1^*}{\rho_{10}} \frac{\partial c_1}{\partial y} = \frac{D_2 \rho_2^*}{\rho_{20}} \frac{\partial c_2}{\partial y}; \\
y \rightarrow \infty, \quad u_1 = u_{10}, \quad c_1 = c_{10}; \\
y \rightarrow \infty, \quad u_2 = u_{20}, \quad c_2 = c_{20}. \tag{1.60}
\end{aligned}$$

The interphase mass transfer rate for a surface of length  $L$  is determined by averaging the local mass fluxes:

$$J = MK_j(c_{10} - \chi c_{20}) = -\frac{1}{L} \int_0^L I_j dx = MK_j \left( \frac{c_{10}}{\chi} - c_{20} \right) = -\frac{1}{L} \int_0^L I_2 dx, \tag{1.61}$$

where  $K_j$  ( $j = 1, 2$ ) are the interphase mass transfer coefficients, while the local mass fluxes are obtained from (1.20):

$$I_j = -\frac{MD_j \rho_j^*}{\rho_{j0}^*} \left( \frac{\partial c_j}{\partial y} \right)_{y=0}, \quad j = 1, 2. \tag{1.62}$$

From (1.61) and (1.62) the Sherwood number is obtained:

$$Sh_j = \frac{K_j L}{D_j} = \frac{\rho_j^*}{\rho_{j0}^*} \frac{\chi^{1-j}}{c_{10} - \chi c_{20}} \int_0^L \left( \frac{\partial c_j}{\partial y} \right)_{y=0} dx, \quad j = 1, 2. \tag{1.63}$$

The equations (1.59) and (1.60) can be solved introducing similarity variables:

$$\begin{aligned}
u_j &= 0.5 j u_{j0} \varepsilon_j \phi_j', \\
v_j &= (-1)^{j-1} 0.5 j \left( \frac{u_{j0} v_j}{\chi} \right)^{0.5} (\xi_j \phi_j' - \phi_j), \\
c_j &= c_{j0} - (-\chi)^{1-j} (c_{10} - \chi c_{20}) \psi_j, \\
\phi_j &= \phi_j(\xi_j), \quad \psi_j = \psi_j(\xi_j)^{0.5}, \\
\varepsilon_j &= Sc_j^{0.5}, \quad Sc_j = \frac{v_j}{D_j}, \quad j = 1, 2. \tag{1.64}
\end{aligned}$$

Thus, as a result is obtained:

$$\begin{aligned}
& \phi_j''' + j\varepsilon_j^{-1}\phi_j\phi_j'' = 0, \\
& \psi_j'' + j\varepsilon_j\phi_j\psi_j' = 0, \\
& \phi_j(0) = (-1)^j\theta_{j+2}\psi_j'(0), \quad \phi_j'(\infty) = \frac{2}{j\varepsilon_j}, \\
& \psi_j(\infty) = 0, \quad j = 1, 2; \\
& \phi_1'(0) = 2\theta_1 \frac{\varepsilon_2}{\varepsilon_1} \phi_2'(0), \\
& \phi_2''(0) = -0.5\theta_2 \left( \frac{\varepsilon_1}{\varepsilon_2} \right)^2 \phi_2''(0), \\
& \psi_2'(0) = \frac{\chi}{\varepsilon_0} \psi_1'(0), \quad \psi_1(0) + \psi_2(0) = 1 \quad , \tag{1.65}
\end{aligned}$$

where

$$\begin{aligned}
& \theta_1 = \frac{u_{20}}{u_{10}}, \quad \theta_2 = \left( \frac{\mu_1}{\mu_2} \right) \left( \frac{V_1}{V_2} \right)^{-0.5} \left( \frac{u_{10}}{u_{20}} \right)^{1.5}, \\
& \theta_3 = \frac{M(c_{10} - \chi c_{20})}{\varepsilon_1 \rho_{10}}, \quad \theta_4 = \frac{M(c_{10} - \chi c_{20})}{2\varepsilon_2 \rho_{20} \chi}, \\
& \varepsilon_0 = \frac{\dot{\rho}_{10} \dot{\rho}_2}{\dot{\rho}_{20} \dot{\rho}_1} \left( \frac{D_2 u_{20}}{D_1 u_{10}} \right)^{0.5} . \tag{1.66}
\end{aligned}$$

It follows from (1.65) that the absorbed material concentration on the phase interface ( $y = 0$ ) is constant. This allows a set of new boundary conditions to be used

$$\psi_1(0) = A, \quad \psi_2(0) = 1 - A, \tag{1.67}$$

where  $A$  is determined from the conditions of the mass flow continuity on the phase interface. Thus (1.67) permits the solution of (1.65) as two independent problems.

The parameters  $\theta_1$  and  $\theta_2$  account for the kinematic and dynamic interactions between the phases, while  $\theta_3$  and  $\theta_4$  - the rate of the non-linear effects in the gas and the liquid phases. For the cases of practical interest  $\theta_k < 1$  ( $k = 1, \dots, 4$ ) is valid and the problem could be solved making use of the perturbation method [45], expressing the unknown functions by an expansion of the following type

$$F = F^{(0)} + \theta_1 F^{(1)} + \theta_2 F^{(2)} + \theta_3 F^{(3)} + \theta_4 F^{(4)} + \dots, \tag{1.68}$$

where  $F$  is a vector function

$$F = F(\phi_1, \phi_2, \psi_1, \psi_2, A). \tag{1.69}$$

The zero-order approximation is obtained from (1.65) when is substituted  $\theta_k = 0$ ,  $k = 1, \dots, 4$ .

The first-order approximations are obtainable from the equations

$$\begin{aligned} \phi_j^{(k)'''} + j\epsilon_j^{-1}(\phi_j^{(k)''}\phi_j^{(0)} + \phi_j^{(0)''}\phi_j^{(k)}) &= 0, \\ \psi_j^{(k)''} + j\epsilon_j(\phi_j^{(k)}\psi_j^{(0)'} + \phi_j^{(0)}\psi_j^{(k)'}) &= 0, \\ k = 1, \dots, 4, \quad j = 1, 2 \end{aligned} \quad (1.70)$$

subject to boundary conditions

$$\begin{aligned} \phi_j^{(0)}(0) &= 0, k = 1, 2, j = 1, 2; \\ \phi_1^{(j)}(0) &= -\psi_1^{(0)'}(0), \quad \phi_2^{(j)}(0) = -\psi_2^{(2)'}(0), \\ \phi_1^{(j)}(0) &= 0, \phi_2^{(j)}(0) = 0; \\ \phi_1^{(k)'}(0) &= 0, \quad k = 2, 3, 4; \\ \phi_1^{(j)'}(0) &= 2\frac{\epsilon_2}{\epsilon_1}\phi_2^{(0)'}(0); \\ \phi_j^{(k)'}(0) &= 0, \quad k = 1, \dots, 4, \quad j = 1, 2; \\ \psi_j^{(k)'}(0) &= A^{(k)}, \\ \psi_j^{(k)}(\infty) &= 0, \quad k = 1, \dots, 4, \quad j = 1, 2; \\ \phi_2^{(k)''}(0) &= 0, \quad k = 1, 3, 4; \\ \phi_2^{(2)''}(0) &= -\frac{1}{2}\left(\frac{\epsilon_1}{\epsilon_2}\right)^2\phi_1^{(0)''}(0); \\ \psi_2^{(k)}(0) &= -A^{(k)}, \quad k = 1, \dots, 4. \end{aligned} \quad (1.71)$$

The values for  $A^{(k)}$  ( $k = 1, \dots, 4$ ) are calculated from the equation

$$\psi_2^{(k)'}(0) = \frac{\chi}{\epsilon_0}\psi_1^{(k)'}(0), \quad k = 1, \dots, 4. \quad (1.72)$$

The solutions of problems of the type (1.65) have been reported in a number of publications [4, 6, 27 - 29, 36, 38 - 40, 45, 63]. Using these solutions could be written:

$$\begin{aligned} \phi_1^{(0)}(\xi_1) &= f(z), \quad z = \frac{2}{\epsilon_1}\xi_1, \\ \psi_1^{(0)}(\xi_1) &= A^{(0)}\left(1 - \frac{1}{\varphi_{10}}\right)\int_0^z E(\epsilon_1, p)dp, \end{aligned}$$

$$\begin{aligned}
E(\varepsilon_1, p) &= \exp \left[ -\frac{\varepsilon_1^2}{2} \int_0^p f(s) ds \right], \\
\phi_2^{(0)}(\xi_2) &= \varepsilon_2^{-1} \xi_2, \quad \psi_2^{(0)}(\xi_2) = (I - A^{(0)}) \operatorname{erfc} \xi_2, \\
A^{(0)} &= \frac{1}{1+a}, \quad a = \frac{\chi \sqrt{\pi}}{\varepsilon_0 \varepsilon_1 \varphi_{10}}, \\
\phi_1^{(1)}(\xi_1) &= \frac{1}{\alpha} f'(z), \quad \phi_2^{(1)}(\xi_2) \equiv 0, \quad \alpha = f''(0), \\
\psi_1^{(1)}(\xi_1) &= A^{(1)} + \frac{A^{(0)}}{\alpha \varphi_{10}} [I - E(\varepsilon_1, z)] - \left( \frac{A^{(1)}}{\varphi_{10}} + \frac{A^{(0)}}{\alpha \varphi_{10}^2} \right) \int_0^z E(\varepsilon_1, p) dp, \\
\psi_1^{(1)}(\xi_2) &= -A^{(1)} \operatorname{erfc} \xi_2, \quad A^{(1)} = -\frac{1}{\alpha \varphi_{10}} \frac{\alpha_0}{(1+a_0)^2}, \\
\phi_1^{(2)}(\xi_1) &\equiv 0, \quad \phi_2^{(2)}(\xi_2) = \alpha \sqrt{\pi} \int_0^{\varepsilon_2/E_2} \operatorname{erfc} p dp, \\
\psi_1^{(2)}(\xi_1) &= A^{(2)} \left[ I - \frac{1}{\varphi_{10}} \int_0^z E(\varepsilon_1, p) dp \right], \\
\psi_2^{(2)}(\xi_2) &= -A^{(2)} + [A^{(2)} - 4\alpha \varepsilon_2 (I - A^{(0)}) \bar{\varphi}_2] \operatorname{erfc} \xi_2 + 4\alpha \varepsilon_2 (I - A^{(0)}) Q(\varepsilon_2, \xi_2), \\
Q(\varepsilon_2, \xi_2) &= \int_0^{\xi_2} \left[ \exp(-q^2) \int_0^q \int_0^{p/\varepsilon_2} \operatorname{erfc} s ds \right] dp dq \approx \\
&\approx \frac{1}{8} \sqrt{\frac{\pi}{Sc_2}} \operatorname{erf} \xi_2 - \frac{1}{4\sqrt{Sc_2}} \xi_2 \exp(-\xi_2^2), \\
A^{(2)} &= 4\alpha \varepsilon_2 \bar{\varphi}_2 \frac{a}{(1+a)^2}, \quad \bar{\varphi}_2 = Q(\varepsilon_2, \infty) = \frac{1}{8} \sqrt{\frac{\pi}{Sc_2}}, \\
\phi_1^{(3)}(\xi_1) &= \frac{2A^{(0)}}{\varepsilon_1 \varphi_{10}} \varphi(z), \quad \phi_2^{(3)}(\xi_2) \equiv 0, \\
\psi_1^{(3)}(\xi_1) &= A^{(3)} - \left( \frac{A^{(3)}}{\varphi_{10}} + \frac{\varepsilon_1 A^{(0)} \varphi_{13}}{\varphi_{10}^3} \right) \int_0^z E(\varepsilon_1, p) dp + \\
&+ \frac{\varepsilon_1 A^{(0)}}{\varphi_{10}^2} \int_0^z \left[ \int_0^p \varphi(s) ds \right] E(\varepsilon_1, p) dp, \\
\psi_2^{(3)}(\xi_2) &= -A^{(3)} \operatorname{erfc} \xi_2, \quad A^{(3)} = -\frac{\varepsilon_1 \varphi_{13}}{\varphi_{10}^2} \frac{a_0}{(1+a_0)^2}, \\
\phi_1^{(4)}(\xi_1) &\equiv 0, \quad \phi_2^{(4)}(\xi_2) = -\frac{2}{\sqrt{\pi}} (1 - A^{(0)}), \\
\psi_1^{(4)}(\xi_1) &= A^{(4)} \left( I - \frac{1}{\varphi_{10}} \int_0^z E(\varepsilon_1, p) dp \right),
\end{aligned}$$

$$\begin{aligned}\psi_2^{(4)}(\xi_2) &= -A^{(4)} - \frac{4\epsilon_2}{\pi} (I - A^{(0)})^2 + \frac{4\epsilon_2}{\pi} (I - A^{(0)})^2 \exp(-\xi_2^2) + \\ &+ \left[ A^{(4)} + \frac{4\epsilon_2}{\pi} (I - A^{(0)})^2 \right] \operatorname{erf} \xi_2, \\ A^{(4)} &= -\frac{4\epsilon_2}{\pi} \frac{a^2}{(1+a)^3},\end{aligned}\quad (1.73)$$

where  $f$  and  $\varphi$  are solutions of (1.29), and  $\varphi_{10}$  and  $\varphi_{13}$  are expressed as:

$$\begin{aligned}\varphi_{10} &= \int_0^\infty E(\epsilon_1, p) dp \approx 3.01 Sc_I^{-0.35}, \\ \varphi_{13} &= \int_0^\infty \left[ \int_0^p \varphi(s) ds \right] E(\epsilon_1, p) dp \approx 6.56 Sc_I^{-0.8},\end{aligned}\quad (1.74)$$

i.e. their values can be obtained from  $\varphi_0$  and  $\varphi_3$  in (1.30) if is substituted  $\epsilon = \epsilon_1$  ( $Sc = Sc_I$ ).

The non-linear interphase mass transfer rate (the Sherwood number), are obtainable from (1.63):

$$Sh_j = -\frac{\rho_i^*}{\rho_{j0}^*} \sqrt{Pe_j} \psi'_j(0), \quad Pe_j = \frac{u_{j0} L}{D_j}, \quad j = 1, 2, \quad (1.75)$$

where  $\psi'_1(0)$  and  $\psi'_2(0)$  can be determined from (1.73) :

$$\begin{aligned}\psi'_1(0) &= -\frac{2}{\epsilon_1 \varphi_{10}} \frac{I}{1+a} - \frac{2\theta_1}{\alpha \varphi_{10}^2 \epsilon_1} \frac{I}{(1+a)^2} - 8\theta_2 \alpha \frac{\epsilon_2}{\epsilon_1} \frac{\bar{\varphi}_2}{\varphi_{10}} \frac{a}{(1+a)^2} - 2\theta_3 \frac{\varphi_{13}}{\varphi_{10}^3} \frac{I}{(1+a)^2} + \\ &+ 8\theta_4 \frac{\epsilon_2}{\pi \varphi_{10} \epsilon_1} \frac{a^2}{(1+a)^3}, \\ \psi'_2(0) &= -\frac{2}{\sqrt{\pi}} \frac{a}{1+a} - \theta_1 \frac{2}{\sqrt{\pi \alpha \varphi_{10}}} \frac{a}{(1+a)^2} - 8\theta_2 \frac{\alpha \epsilon_2 \bar{\varphi}_2}{\sqrt{\pi}} \frac{a^2}{(1+a)^2} - \\ &- 2\theta_3 \frac{\epsilon_1 \varphi_{13}}{\sqrt{\pi \varphi_{10}^2}} \frac{a}{(1+a)^3} + 8\theta_4 \frac{\epsilon_2}{\pi \sqrt{\pi}} \frac{a^3}{(1+a)^3}.\end{aligned}\quad (1.76)$$

In the cases where the rate of the interphase mass transfer is limited by the diffusion resistance in the gas phase, from the last condition in (1.65) it follows that  $\chi/\epsilon_0 \rightarrow 0$ , i.e.  $a \rightarrow 0$ . Thus the Sherwood number can be expressed in the form

$$Sh_i = \frac{\rho_i^*}{\rho_{10}^*} Pe_i^{0.5} \left( \frac{2}{\epsilon_1 \varphi_{10}} + \frac{2\theta_1}{\epsilon_1 \alpha \varphi_{10}^2} + 2\theta_3 \frac{\varphi_{13}}{\varphi_{10}^3} \right). \quad (1.77)$$

When the process is limited by the resistance in the liquid phase,  $\chi/\varepsilon_0 \rightarrow \infty$ ,  $a \rightarrow \infty$ , i.e.

$$Sh_2 = \frac{\dot{\rho}_2}{\dot{\rho}_{20}} Pe_2^{0.5} \left( \frac{2}{\sqrt{\pi}} + 8\theta_2 \frac{\alpha\varepsilon_2 \bar{\varphi}_2}{\sqrt{\pi}} - 8\theta_4 \frac{\varepsilon_2}{\pi\sqrt{\pi}} \right). \quad (1.78)$$

The comparison of the non-linear effects in both the gas and the liquid [63] shows that the ratio of the parameters  $\theta_3$  and  $\theta_4$  takes the form :

$$\frac{\theta_3}{\theta_4} = \frac{2\varepsilon_2 \dot{\rho}_{20} \chi}{\varepsilon_1 \dot{\rho}_{10}} \gg 1 \quad (1.79)$$

and is always greater than unity. The minimum value of this ratio occurs in cases of gases of

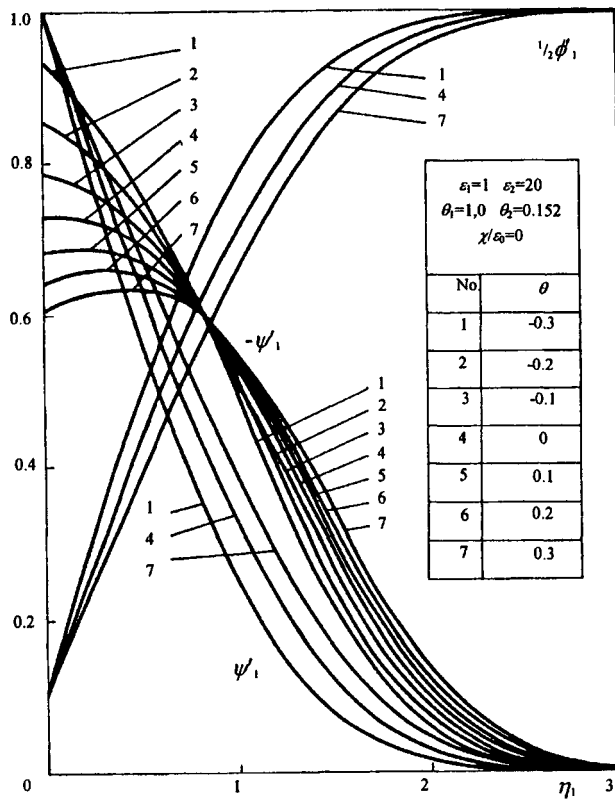


Fig.1.10. Dimensionless velocity and diffusion flux in the gas phase, when the diffusive resistance is in the gas phase.

high solubility, where  $\theta_3$  is greater than  $\theta_4$  by more than two orders of magnitude, i.e. for numerical calculation it is always possible to assume  $\theta_4 = 0$ .

A numerical solution of the equations (1.70,1.71) has been performed as a check of the asymptotic theory, and the results thus obtained [63,64] are shown in figures 1.10-1.12

The analysis of the results (Fig.1.10) demonstrates that the non-linear effects are most significant in cases, where the non-linear interphase mass transfer is limited by the mass transfer in the gas phase ( $\chi/\varepsilon_0 = 0$ ). When the diffusion resistances are commensurable ( $\chi/\varepsilon \approx 1$ ) the non-linear effects are considerably smaller (Fig. 1.11) and their appearance in the liquid phase (Fig. 1.12) is a result from the hydrodynamic influence of the gas phase. These effects are totally absent, however, when the process is limited by the mass transfer in the liquid phase.

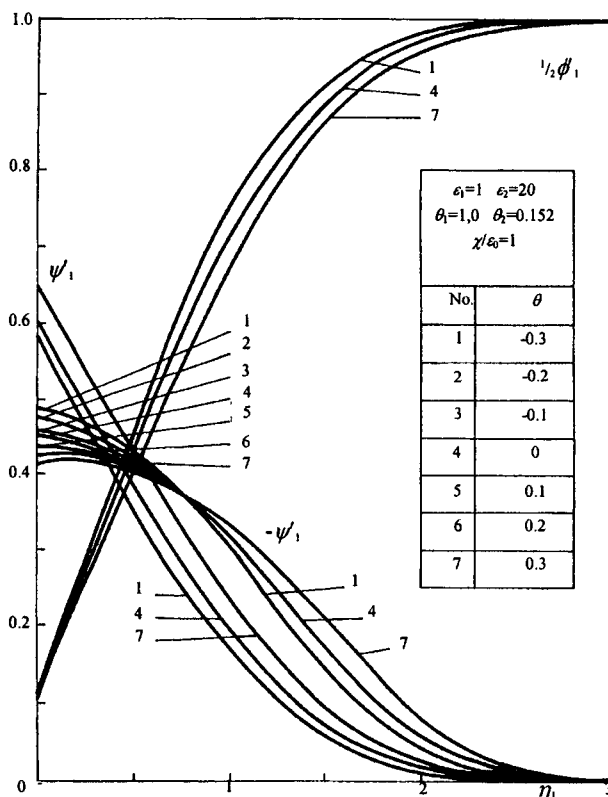


Fig.1.11. Dimensionless velocity and diffusion flux in the gas phase when diffusion resistances in the gas and the liquid are of the same order.

The influence of the direction of the interphase mass transfer on the kinetics of the mass transfer in the gas-liquid systems is similar to that, which has been observed in the systems gas (liquid)-solid surface, i.e. the diffusion transfer in the case of absorption is greater than in the case of desorption.

It is evident from Fig. 1.10 that, when (in the cases of absorption and desorption) the concentration gradients are equal and only their directions change, the deviation of the non-

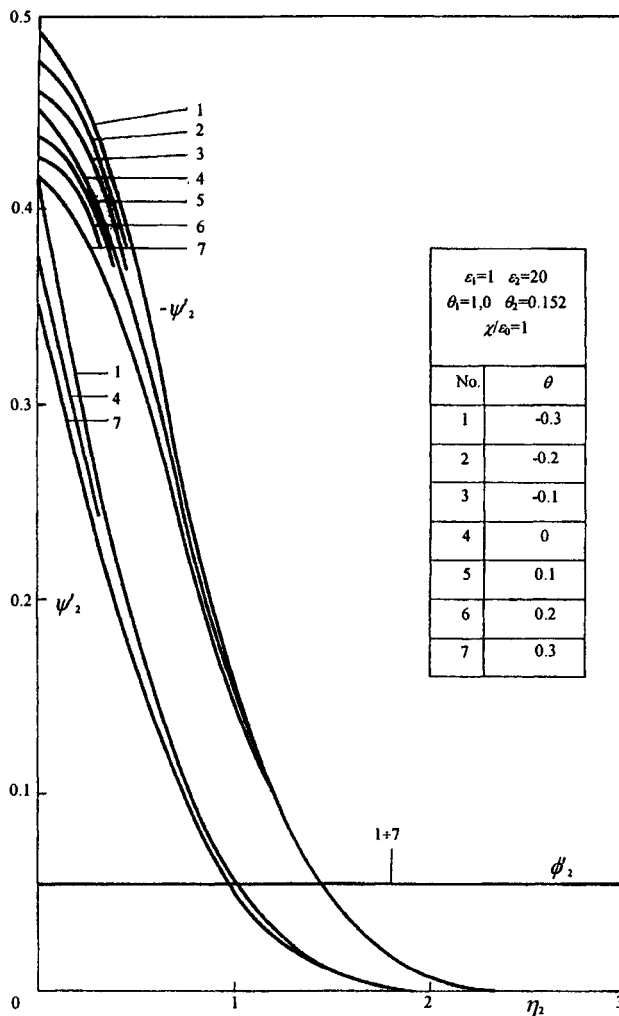


Fig.1.12. Dimensionless velocity and diffusion flux in the liquid phase when diffusion resistances in the gas and the liquid are the same order.

linear mass transfer from linearity ( $\theta_3 = 0$ ) is not symmetrical. This "contradicts" with the asymptotic theory (1.77), which could be explained by the absence of the quadratic terms (proportional to  $\theta_3^2$ ). It is evident that the asymptotic theory has to be made more precise and to include all the quadratic terms. In the cases of a non-linear interphase mass transfer limited by the mass transfer in the gas phase, the equations (1.65) take the form

$$\begin{aligned} \phi''' + \varepsilon^{-1} \phi'_1 \phi''_1 &= 0, \\ \phi_2''' + 2\varepsilon_2^{-1} \phi_2 \phi''_2 &= 0, \\ \psi_1'' + \varepsilon_1 \phi_1 \psi'_1 &= 0; \\ \phi_1(0) &= -\theta_3 \psi'_1(0), \quad \phi_2(0) = 0, \\ \phi'_1(\infty) &= \frac{2}{\varepsilon_1}, \quad \phi'_2(\infty) = \frac{1}{\varepsilon_2}, \\ \phi'_1(0) &= 2\theta_3 \frac{\varepsilon_2}{\varepsilon_1} \phi'_2(0), \\ \phi_2''(0) &= -0.5\theta_2 \left( \frac{\varepsilon_1}{\varepsilon_2} \right)^2 \phi_1''(0), \\ \psi_1(0) &= 1, \quad \psi_1(\infty) = 0. \end{aligned} \tag{1.80}$$

In order to solve the problem (1.80) the expansion (1.68) is used, where the following terms should be added:

$$\theta_1^2 F^{(11)} + \theta_3^2 F^{(33)} + \theta_1 \theta_3 F^{(13)} ,$$

and in the relationships (1.73) to substitute  $a_0 = 0$ .

Approximations proportional to  $\theta_1^2$  have been obtained in [27,28]:

$$\begin{aligned} \phi_1^{(11)}(\xi_1) &= F(z) , \quad \phi_2^{(11)}(\xi_2) \equiv 0 , \\ \psi_1^{(11)}(\xi_1) &= \left( \frac{\varepsilon_1^4 \varphi_{11}}{8\alpha^2 \varphi_{10}^3} - \frac{\varepsilon_1^2 \varphi_{12}}{2\varphi_{10}^2} - \frac{\varepsilon_1}{2\alpha^2 \varphi_{10}^3} \right) \int_0^z E(\varepsilon_1, p) dp + \\ &+ \frac{\varepsilon_1^2}{2\varphi_{10}} \int_0^z \left[ \int_0^p F(s) ds \right] E(\varepsilon_1, p) dp + \frac{\varepsilon_1}{2\alpha^2 \varphi_{10}^2} [I - E(\varepsilon_1, z)] - \\ &- \frac{\varepsilon_1^4}{8\alpha^2 \varphi_{10}} \int_0^z f^2(p) E(\varepsilon_1, p) dp , \end{aligned} \tag{1.81}$$

where the function  $F$  is the solution of

$$2F''' + fF'' + f''F = -\frac{1}{\alpha^2} f' f''' ,$$

$$F(0) = F'(0) = F'(\infty) = 0 \quad (1.82)$$

and has been tabulated in [39], while  $\varphi_{11}$  and  $\varphi_{12}$  have been obtained in [27]:

$$\begin{aligned} \varphi_{11} &= \int_0^\infty f^2(p) E(\varepsilon_1, p) dp \approx 3.01 Sc_1^{-1.608}, \\ \varphi_{12} &= \int_0^\infty \left[ \int_0^p F(s) ds \right] E(\varepsilon_1, p) dp \approx 3.05 Sc_1^{-1.285}. \end{aligned} \quad (1.83)$$

Approximations proportional to  $\theta_3^2$  have been obtained in [33]:

$$\begin{aligned} \psi_1^{(33)}(\xi_1) &= \frac{2\varphi_3}{\varphi_{10}^3} \varphi(z) - \frac{4}{\varepsilon_1^2 \varphi_{10}^2} \bar{\varphi}(z), \quad \psi_2^{(33)} \equiv 0, \\ \psi_1^{(33)}(\xi_1) &= \left( -\frac{\varepsilon_1^2 \varphi_{13}^2}{\varphi_{10}^5} + \frac{\varepsilon_1^2 \varphi_{133}}{2\varphi_{10}^4} + \frac{2\bar{\varphi}_{133}}{\varphi_{10}^4} \right) \int_0^z E(\varepsilon_1, p) + \\ &+ \frac{\varepsilon_1^2 \varphi_{13}}{\varphi_{10}^4} \int_0^z \left[ \int_0^p \varphi(s) ds \right] E(\varepsilon_1, p) dp - \frac{\varepsilon_1^2}{2\varphi_{10}^3} \int_0^z \left[ \int_0^p f(s) ds \right]^2 E(\varepsilon_1, p) dp - \\ &- \frac{2}{\varphi_{10}^3} \int_0^z \left[ \int_0^p \bar{\varphi}(s) ds \right] E(\varepsilon_1, p) dp, \end{aligned} \quad (1.84)$$

where  $\bar{\varphi}$  is the solution of (1.29). Thus  $\varphi_{133}$  and  $\bar{\varphi}_{133}$  take the forms:

$$\begin{aligned} \varphi_{133} &= \int_0^\infty \left[ \int_0^p \varphi(s) ds \right]^2 E(\varepsilon_1, p) dp \approx 24 Sc_1^{-1.3}, \\ \bar{\varphi}_{133} &= \int_0^\infty \left[ \int_0^p \bar{\varphi}(s) ds \right] E(\varepsilon_1, p) dp \approx 0.326 Sc_1^{-1.63}, \end{aligned} \quad (1.85)$$

i.e. they may be obtained from  $\varphi_{33}$  and  $\bar{\varphi}_{33}$  in (1.33) via the substitution  $\varepsilon = \varepsilon_1$  ( $Sc = Sc_1$ ). From (1.28) and (1.84) it is evident that  $\psi_1^{(33)}(\xi_1) \equiv \psi_2^{(33)}(\eta)$ , if  $\varepsilon_1 = \varepsilon$ . Approximations proportional to  $\theta_1 \theta_3$ , have been obtained in [33]:

$$\begin{aligned} \phi_1^{(13)} &= \frac{1}{\alpha \varphi_{10}^2} \varphi(z) - \frac{2}{\varepsilon_1 \alpha \varphi_{10}} \bar{\varphi}(z), \quad \phi_2^{(13)}(\xi_2) \equiv 0, \\ \psi_1^{(13)}(\xi_1) &= \left( -\frac{\varepsilon_1 \varphi_{13}}{2\alpha \varphi_{10}^4} + \frac{\varepsilon_1 \varphi_{113}}{\alpha \varphi_{10}^3} + \frac{\varepsilon_1 \bar{\varphi}_{113}}{\alpha \varphi_{10}^3} - \frac{2\varepsilon_1 \varphi_{13}}{\alpha \varphi_{10}^4} \right) \int_0^z E(\varepsilon_1, p) dp + \end{aligned}$$

$$\begin{aligned}
& + \left( \frac{\varepsilon_1}{\alpha \varphi_{10}^3} + \frac{\varepsilon_1^2}{2\alpha \varphi_{10}^3} \right) \int_0^z \left[ \int_0^p \varphi(s) ds \right] E(\varepsilon_1, p) dp - \frac{\varepsilon_1}{\alpha \varphi_{10}^2} \int_0^z \left[ \int_0^p \bar{\varphi}(s) ds \right] E(\varepsilon_1, p) dp + \\
& + \frac{\varepsilon_1}{\alpha \varphi_{10}^2} E(\varepsilon_1, z) \int_0^z \varphi(p) dp - \frac{\varepsilon_1}{\alpha \varphi_{10}^2} \int_0^z \varphi(p) E(\varepsilon_1, p) dp + \\
& + \frac{\varepsilon_1 \varphi_{13}}{\alpha \varphi_{10}^3} [I - E(\varepsilon_1, z)] \tag{1.86}
\end{aligned}$$

where  $\bar{\varphi}$  is the solution of the problem

$$\begin{aligned}
& 2\bar{\varphi}''' + f''\bar{\varphi}'' + f'''\bar{\varphi} = f'\varphi'' + f'''\varphi, \\
& \bar{\varphi}(0) = \bar{\varphi}'(0) = \bar{\varphi}(\infty) = 0 \tag{1.87}
\end{aligned}$$

and  $\varphi_{113}$  and  $\bar{\varphi}_{113}$  have been obtained in [7]:

$$\varphi_{113} = \int_0^\infty \left[ \int_0^p \bar{\varphi}(s) ds \right] E(\varepsilon_1, p) dp \approx Sc_i^{-1.3}, \tag{1.88}$$

$$\bar{\varphi}_{113} = \int_0^\infty \varphi(p) E(\varepsilon_1, p) dp \approx 4.18 Sc_i^{-0.46}. \tag{1.89}$$

The expressions derived allow to determinate the rate of the non-linear interphase mass transfer in the gas-liquid system when the process is limited by the mass transfer in the gas. From (1.75) is found

$$Sh_i = \frac{K_i L}{D_i} = \frac{\rho_i^*}{\rho_{i0}} \sqrt{Pe_i} \psi'_i(0), \tag{1.90}$$

where  $\psi'_i(0)$  is calculated taking all the quadratic approximations into account

$$\begin{aligned}
& -\psi'_i(0) = \frac{2}{\varepsilon_1 \varphi_{10}} + \theta_1 \frac{2}{\varepsilon_1 \alpha \varphi_{10}^2} + \theta_3 \frac{2\varphi_{13}}{\varphi_{10}^3} + \\
& + \theta_1^2 \left( -\frac{\varepsilon_1^3 \varphi_{11}}{4\alpha^2 \varphi_{10}^2} + \frac{\varepsilon_1 \varphi_{12}}{\varphi_{10}^2} + \frac{2}{\varepsilon_1 \alpha^2 \varphi_{10}^3} \right) + \theta_3^2 \left( \frac{2\varepsilon_1 \varphi_{13}^2}{\varphi_{10}^5} - \frac{\varepsilon_1 \varphi_{133}}{\varphi_{10}^4} - \frac{4\bar{\varphi}_{133}}{\varepsilon_1 \varphi_{10}^4} \right) + \\
& + \theta_1 \theta_3 \left( \frac{\varepsilon_1 \varphi_{13}}{\alpha \varphi_{10}^4} - \frac{2\varphi_{113}}{\alpha \varphi_{10}^3} - \frac{2\bar{\varphi}_{113}}{\alpha \varphi_{10}^3} + \frac{4\varphi_{13}}{\alpha \varphi_{10}^4} \right). \tag{1.91}
\end{aligned}$$

The expression (1.91) is the main result from the asymptotic theory of the non-linear interphase mass transfer in the gas-liquid systems and is in good agreement (see Table 1.5) with the results from the numerical solution  $\psi'_{IN}(\theta)$  of the problem (1.65) obtained in [64].

The kinetics of the linear interphase mass transfer in the gas-liquid systems limited by a non-linear mass transfer in the gas is determined by the expressions (1.61), (1.90) and (1.91). Having in mind that  $c_{10}$  and  $\chi c_{20}$  are the concentrations at the boundaries of the diffusion boundary layer in the gas, it could consider  $(c_{10} - \chi c_{20})$  as the constant value of the concentration difference in the diffusion boundary layer. In order to analyze the influence of the big concentration difference on the interphase mass transfer rate it is necessary to use [44] its dimensionless form:

$$\Delta c_1 = M \frac{|c_{10} - \chi c_{20}|}{\rho_{10}^*} = (-1)^m \varepsilon_1 \theta_{3m} \quad (\theta_{31} = \theta_3 \leq 0, \quad \theta_{32} = \theta_{32} \geq 0).$$

**Table 1.5.**  
**Comparison of the results from the asymptotic and numerical solutions.**

$\varepsilon_1 = 1,$	$\theta_1 = 0.1,$	$\theta_2 = 0.152$
$\theta_3$	$-\psi'_{IN}(\theta)$	$-\psi'_I(\theta)$
0	0.730	0.738
-0.1	0.682	0.689
+0.1	0.785	0.787
-0.2	0.641	0.642
+0.2	0.851	0.837
-0.3	0.605	0.595
+0.3	0.932	0.888

The term  $\rho_1^*/\rho_{10}^*$  in (1.90) accounts for the convective mass transfer as a result of a secondary flow induction. This effect is significant at high concentrations at the phase interface ( $\chi c_{20}$ ) in case of desorption. At small values of  $\Delta c_1$  in absorption or desorption, when  $\chi c_{20} = 0$ , this effect could be neglected.

In the case of desorption ( $\theta_3 < 0$ ) the interphase mass transfer rate depends on the change in  $\Delta c_1$ , i.e. on the change of  $\theta_3$ .

The above considerations indicate that the influence of the big concentration difference is diverse and it is of interest to compare the interphase mass transfer rates at constant value of concentration difference  $\Delta c_1$  and different directions of the mass transfer.

In the linear theory approximations the interphase mass transfer rate  $J_{10}$  is determined from (1.61), if  $\theta_3 = 0$  and  $\rho_1^*/\rho_{10}^* = 1$  are substituted in (1.90) and (1.91).

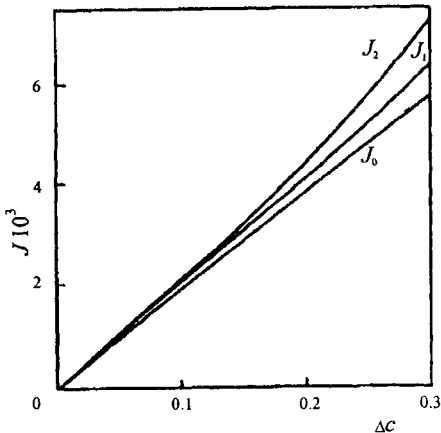


Fig.1.13. Effect of the big concentration difference  $\Delta c_1$  and the direction of the mass transfer on the non-linear interphase mass transfer rate

The non-linear interphase mass transfer rate in the case of desorption  $J_1$  is obtained from (1.61) for values  $\theta_3 < 0$ .

In the absorption cases ( $\theta_3 > 0$ ) and  $\chi c_{20} = 0$ , so  $\rho_1^\bullet / \rho_{10}^\bullet = 1$  has to be substituted in the equation for the interphase mass transfer rate.

The influence of the big concentration difference  $\Delta c_1$  and the direction of the mass transfer on the non-linear interphase mass transfer rate and the different effects of the non-linear mass transfer for  $Pe_1 = 10^4$  and  $\varepsilon = 1$  are presented on Fig. 1.13 and in Table 1.6. It is evident that the increase in the concentration gradient  $\Delta c_1$  in the gas in the cases of desorption ( $\theta_3 < 0$ ) leads to an increase in the ratio  $\rho_1^\bullet / \rho_{10}^\bullet$  and to decrease in  $\psi_1(0)$ , but the interphase mass transfer rate  $J_1$  increases and is always greater than the rate  $J_0$  obtained in linear theory approximations ( $\theta_3 = 0$ ). In desorption ( $\theta_3 > 0$ ) the interphase mass transfer rate  $J_2$  is always greater than the desorption rate  $J_1$ .

The theoretical result thus obtained shows that the direction of the intensive interphase mass transfer in the gas-liquid system influences the transfer kinetics. This is a hydrodynamic effect, i.e. the intensive interphase mass transfer induces a flow at the phase interface, the velocity of which is directed normally to the surface. This gives reasons to expect similar effects in the multicomponent interphase mass transfer for those components, for which the concentration gradient is not very big.

Table 1.6.

Effect of the big concentration difference  $\Delta c_1$  on the convective flow, diffusion flux and Sherwood number.

$\Delta c_1 \cdot 10^2$	$\theta_3$	$\rho_1^* / \rho_{10}^*$	$-\psi'_1(0)$	$Sh_1$
0.00	0.000	1.00	0.730	73.0
0.65	0.113	1.11	0.676	75.0
1.30	0.274	1.27	0.614	78.0
1.95	0.517	1.52	0.535	81.3
0.65	-0.100	1.00	0.785	78.5
1.30	-0.200	1.00	0.851	85.1
1.95	-0.300	1.00	0.932	93.2

### 1.3.2. Multicomponent interphase mass transfer in the case of an intensive mass transfer in the gas

The kinetics of the multicomponent interphase mass transfer in gas-liquid systems is of practical interest in cases of intensive interphase mass transfer of one of the components and the gas and the liquid flows hydrodynamics being dependent on the non-linear mass transfer of this component in the gas phase.

Let  $n$  components are considered, the interphase mass transfer for which is associated with concentration gradients having no practical influence on the flow hydrodynamics [73]. At low concentrations  $c_i$  ( $i = 1, \dots, n$ ) of the diffusing substances and insignificant differences between diffusivity coefficients  $D_i$  ( $i = 1, \dots, n$ ) the theory of the multicomponent interphase mass transfer could be considered in the independent diffusion approximation [22, 59]. For the purpose  $c_2 \equiv c_{20}$  has to be substituted in the equations (1.59) and (1.60) and the transfer equations for the components with small concentration gradients added:

$$\begin{aligned}
 u_j \frac{\partial c_{ij}}{\partial x} + v_j \frac{\partial c_{ij}}{\partial y} &= D_{ij} \frac{\partial^2 c_{ij}}{\partial y^2}; \\
 x = 0, \quad c_{ij} &= c_{ij0}; \\
 y = 0, \quad c_{i1} &= \chi_i c_{i2}, \quad -D_{i1} \frac{\partial c_{i1}}{\partial y} + c_{i1} v_1 = -D_{i2} \frac{\partial c_{i2}}{\partial y}; \\
 y \rightarrow \infty, \quad c_{i1} &= c_{i10}; \\
 y \rightarrow -\infty, \quad c_{i2} &= c_{i20}, \quad i = 1, \dots, n, \quad j = 1, 2. \tag{1.92}
 \end{aligned}$$

In the dimensionless variables of (1.64) must add to the equation (1.80):

$$\psi''_{ij} + j \varepsilon_j \alpha_{ij} \phi_j \psi'_{ij} = 0;$$

$$\psi_{i1}(0) + \psi_{i2}(0) = 1,$$

$$\begin{aligned}\psi'_{ij}(0) &= \frac{\varepsilon_{i0}}{\chi_i} \psi'_{i2}(0) + \varepsilon_i \theta_3 \alpha_{ii} \left[ \psi_{ii}(0) - \frac{c_{i0}}{c_{i0} - \chi_i c_{i20}} \right] \psi'_i(0), \\ \psi_{ij}(\infty) &= 0, \quad i = 1, \dots, n, \quad j = 1, 2,\end{aligned}\tag{1.93}$$

where

$$\begin{aligned}\psi_{ij} &= \psi_{ij}(\xi_j) = -(-\chi_i)^{j-1} \frac{c_{ij} - c_{i0}}{c_{i0} - \chi_i c_{i20}}, \\ \varepsilon_{i0} &= \frac{D_{i2}}{D_{i1}} \left( \frac{u_{20} D_1}{u_{10} D_{i1}} \right)^{0.5}, \quad \alpha_{ij} = \frac{D_j}{D_{ij}},\end{aligned}\tag{1.94}$$

while  $\chi_i (i = 1, \dots, n)$  are the Henry's constants of the individual components.

The equations for the multicomponent interphase mass transfer rate could be obtained in the same manner as the solutions (1.61) and (1.90):

$$\begin{aligned}J_{ij} &= M_i K_{ij} \chi_i^{1-j} (c_{i0} - \chi_i c_{i20}) = -\frac{I^L}{L} \int_0^L I_{ij} dx, \\ I_{ij} &= -M_i D_{ij} \left( \frac{\partial c_{ij}}{\partial y} \right)_{y=0} + (2-j) M_i (v_j c_{ij})_{y=0}, \\ Sh_{ij} &= \frac{K_{ij} L}{D_{ij}} = -\sqrt{Pe} \left\{ \psi'_j(0) + (2-j) \varepsilon_j \theta_3 \alpha_{ij} \psi'_j(0) \left[ \frac{c_{ij0}}{c_{i0} - \chi_i c_{i20}} - \psi_{ij}(0) \right] \right\}, \\ i &= 1, \dots, n, \quad j = 1, 2.\end{aligned}\tag{1.95}$$

In order to solve the problem (1.93), the following boundary conditions should be imposed, as it has been done in (1.67):

$$\psi_{ii}(0) = A_i, \quad \psi_{i2}(0) = 1 - A_i, \quad i = 1, \dots, n.\tag{1.96}$$

In (1.93) the functions  $\phi_j (j = 1, 2)$  can be expressed in the form

$$\phi_j = \phi_j^{(0)} + \theta_1 \phi_j^{(1)} + \theta_2 \phi_j^{(2)} + \theta_3 \phi_j^{(3)} + \dots, \quad j = 1, 2.\tag{1.97}$$

This permits to find  $\psi_{ij} (i = 1, \dots, n; j = 1, 2)$  as an expansion of the powers of the small parameters  $\theta_k (k = 1, \dots, 3)$ :

$$\psi_{ij} = \psi_{ij}^{(0)} + \theta_1 \psi_{ij}^{(1)} + \theta_2 \psi_{ij}^{(2)} + \theta_3 \psi_{ij}^{(3)} + \dots, \quad i = 1, \dots, n, \quad j = 1, 2.\tag{1.98}$$

If is substituted (1.98) in (1.93) and is maken an expansion analogous to (1.96), using the perturbation method a number of boundary problems could be derived for the different approximations. These problems are solved in the same way as (1.73) and the result is:

$$\psi_{ii}^{(0)}(\xi_i) = A_i^{(0)} \left[ I - \frac{1}{\varphi_{10i}} \int_0^z E(\varepsilon_{ii}, p) dp \right],$$

$$E(\varepsilon_{ii}, p) = \exp \left[ -\frac{\bar{\varepsilon}_{ii}^2 p}{2} \int_0^p f(s) ds \right],$$

$$z = \frac{2}{\varepsilon_i} \xi_i, \quad \bar{\varepsilon}_{ij} = \sqrt{\varepsilon_j \varepsilon_{ij}} = \varepsilon_j \sqrt{\alpha_{ij}}, \quad \varepsilon_{ij} = \varepsilon_j \alpha_{ij},$$

$$\varphi_{10i} = \int_0^\infty E(\bar{\varepsilon}_{ii}, p) dp \approx 3.01 \bar{\varepsilon}_{ii}^{-0.7},$$

$$\psi_{i2}^{(0)}(\xi_2) = (I - A_i^{(0)}) erfc \sqrt{\alpha_{i2}} \xi_2,$$

$$A_i^{(0)} = \frac{1}{1 + a_i}, \quad a_i = \frac{\sqrt{\pi} \chi_i}{\varphi_{10} \varepsilon_i \varepsilon_{i0} \sqrt{\alpha_{i2}}},$$

$$\psi_{ii}^{(1)}(\xi_i) = A_i^{(1)} + \frac{A_i^{(0)}}{\alpha \varphi_{10i}} \left[ I - E(\bar{\varepsilon}_{ii}, z) - \left( \frac{A_i^{(1)}}{\varphi_{10i}} + \frac{A_i^{(0)}}{\alpha \varphi_{10i}^2} \right) \int_0^z E(\bar{\varepsilon}_{ii}, p) dp \right],$$

$$\psi_{i2}^{(1)}(\xi_2) = -A_i^{(1)} erfc \sqrt{\alpha_{i2}} \xi_2,$$

$$A_i^{(1)} = -\frac{1}{\alpha \varphi_{10i}} \frac{a_i}{(1 + a_i)^2},$$

$$\psi_{ii}^{(2)}(\xi_i) = A_i^{(2)} \left[ I - \frac{1}{\varphi_{10i}} \int_0^z E(\bar{\varepsilon}_{ii}, p) dp \right],$$

$$\psi_{i2}^{(2)}(\xi_2) = -A_i^{(2)} + \left[ A_i^{(2)} - \frac{4\alpha \varepsilon_{i2} \bar{\varphi}_{i2}}{\sqrt{\alpha_{i2}}} (I - A_i^{(0)}) \right] erfc \sqrt{\alpha_{i2}} \xi_2 +$$

$$+ \frac{4\alpha \varepsilon_{i2}}{\sqrt{\alpha_{i2}}} (I - A_i^{(0)}) Q(\alpha_{i2}, \varepsilon_2, \xi_2)$$

$$Q(\alpha_{i2}, \varepsilon_2, \xi_2) = \int_0^{\sqrt{\alpha_{i2}} \xi_2} \left[ \exp(-q^2) \int_0^{p/\varepsilon_2 \sqrt{\alpha_{i2}}} \exp(-s^2) ds \right] dp dq$$

$$= \frac{\sqrt{\pi}}{8 \varepsilon_2 \sqrt{\alpha_{i2}}} \operatorname{erf} \sqrt{\alpha_{i2}} \xi_2 - \frac{1}{4 \varepsilon_2} \xi_2 \exp(-\alpha_{i2} \xi_2^2) -$$

$$- \frac{2}{\sqrt{\pi}} \sum_{m=0}^{\infty} (-1)^m \frac{\varepsilon_2^{-(2m+2)} \alpha_{i2}^{-(m+1)} J_m}{m! (2m+1)(2m+2)(2m+3)} \approx$$

$$\begin{aligned}
& \approx \frac{\sqrt{\pi}}{8\varepsilon_2\sqrt{\alpha_{i2}}} \operatorname{erf} \sqrt{\alpha_{i2}} \xi_2 - \frac{1}{4\varepsilon_2} \xi_2 \exp(-\alpha_{i2} \xi_2^2), \\
J_m &= \int_0^{\sqrt{\alpha_{i2}} \xi_2} q^{2m+3} \exp(-q^2) dq = -\frac{1}{2} \alpha_{i2}^{m+1} \xi_2^{2m+2} \exp(-\alpha_{i2} \xi_2^2) + (m+1) J_{m-1}, \\
J_{-1} &= \frac{1}{2} [1 - \exp(-\alpha_{i2} \xi_2^2)], \\
\bar{\varphi}_{i2} &= Q(\alpha_{i2}, \varepsilon_2, \infty) \approx \frac{\sqrt{\pi}}{8\varepsilon_2\sqrt{\alpha_{i2}}}, \\
A_i^{(2)} &= \frac{4\alpha\varepsilon_{i2}\bar{\varphi}_{i2}}{\sqrt{\alpha_{i2}}} \frac{a_i}{(1+a_i)^2}, \\
\psi_{i3}^{(3)}(\xi_1) &= A_i^{(3)} - \left( \frac{A_i^{(3)}}{\varphi_{i0i}} + \frac{\varepsilon_{ii} A_i^{(0)} \varphi_{i3i}}{\varphi_{i0} \varphi_{i0i}^2} \right) \int_0^z E(\bar{\varepsilon}_{ii}, p) dp + \\
&+ \frac{\varepsilon_{ii} A_i^{(0)}}{\varphi_{i0} \varphi_{i0i}} \int_0^\infty \left[ \int_0^p \varphi(s) ds \right] E(\bar{\varepsilon}_{ii}, p) dp, \\
\psi_{i2}^{(3)}(\xi_2) &= -A_i^{(3)} \operatorname{erfc} \sqrt{\alpha_{i2}} \xi_2, \\
A_i^{(3)} &= -\frac{\varepsilon_{ii} \varphi_{i3i}}{\varphi_{i0} \varphi_{i0i}} \frac{a_i}{(1+a_i)^2} + \frac{\varepsilon_i \varepsilon_{ii} \varphi_{i0i}}{2} \left( A^{(0)} - \frac{c_{i10}}{c_{i10} - \chi_i c_{i20}} \right) \frac{a_i}{1+a_i}, \\
\varphi_{i3i} &= \int_0^\infty \left[ \int_0^p \varphi(s) ds \right] E(\bar{\varepsilon}_{ii}, p) dp \approx 6.5 \bar{\varepsilon}_{ii}^{-1.6}, \quad i = 1, \dots, n. \tag{1.99}
\end{aligned}$$

From (1.95) and (1.99) can be found an expression of the Sherwood number

$$\begin{aligned}
Sh_{ii} &= -\sqrt{Pe_i} \left\{ \psi'_{ii}(0) + \theta_j \varepsilon_{ii} \psi'_j(0) \left[ \frac{c_{i10}}{c_{i10} - \chi_i c_{i20}} - \psi_{ii}(0) \right] \right\}, \\
Sh_{i2} &= -\sqrt{Pe_2} \psi'_{i2}(0), \quad i = 1, \dots, n, \tag{1.100}
\end{aligned}$$

where for  $\psi'_{ii}(0)$  and  $\psi_{ii}(0)$  can be used as zero-order approximations

$$\psi_i^{(0)}(0) = -\frac{2}{\varepsilon_i \varphi_{i0}}, \quad \psi_{ii}^{(0)} = \frac{1}{1+a_i}, \quad i = 1, \dots, n \tag{1.101}$$

and  $\psi'_{ii}(0)$  and  $\psi'_{i2}(0)$  take the forms:

$$\begin{aligned}
-\psi'_{ii}(0) &= \frac{2}{\varepsilon_i \varphi_{10i}} \frac{1}{1+a_i} + \frac{2\theta_1}{\alpha \varepsilon_i \varphi_{10i}^2} \frac{1}{(1+a_i)^2} + \frac{8\theta_2 \alpha \varepsilon_{i2} \bar{\varphi}_{i2}}{\varepsilon_i \varphi_{10i} \sqrt{\alpha_{i2}}} \frac{a_i}{(1+a_i)^2} + \\
&+ \theta_3 \left[ \frac{2\alpha_{i1} \bar{\varphi}_{i3i}}{\varphi_{10} \varphi_{10i}^2} \frac{1}{(1+a_i)^2} + \frac{\varepsilon_{ii}}{\varphi_{10}} \frac{a_i}{1+a_i} \left( \frac{2}{1+a_i} - \frac{c_{i10}}{c_{i10} - \chi_i c_{i20}} \right) \right] \\
-\psi'_{i2}(0) &= \frac{2\sqrt{\alpha_{i2}}}{\sqrt{\pi}} \frac{a_i}{1+a_i} + \frac{2\theta_1 \sqrt{\alpha_{i2}}}{\alpha \varphi_{10i} \sqrt{\pi}} \frac{a_i}{(1+a_i)^2} + \frac{8\theta_2 \alpha \varepsilon_{i2} \bar{\varphi}_{i2}}{\sqrt{\pi}} \frac{a_i^2}{(1+a_i)^2} + \\
&\theta_3 \left[ \frac{2\varepsilon_{ii} \varphi_{13i} \sqrt{\alpha_{i2}}}{\varphi_{10} \varphi_{10i} \sqrt{\pi}} \frac{a_i}{(1+a_i)^2} - \frac{\varepsilon_i \varepsilon_{ii} \varphi_{10i} \sqrt{\alpha_{i2}}}{\varphi_{10} \sqrt{\pi}} \frac{a_i}{1+a_i} \left( \frac{1}{1+a_i} - \frac{c_{i10}}{c_{i10} - \chi_i c_{i20}} \right) \right], \\
i &= 1, \dots, n. \tag{1.102}
\end{aligned}$$

In the cases when the mass transfer is limited by the mass transfer in the gas phase  $\chi_i \rightarrow 0$  and it may be substituted in (1.102) :

$$\frac{\chi_i}{\varepsilon_{i0}} = 0, \quad a_i = 0, \quad i = 1, \dots, n. \tag{1.103}$$

Thus the expression (1.100) for  $Sh_{ii}$  takes the form:

$$Sh_{ii} = \sqrt{Pe_i} \left( \frac{2}{\varepsilon_i \varphi_{10i}} + \frac{2\theta_1}{\alpha \varepsilon_i \varphi_{10i}^2} + \frac{2\theta_3 \alpha_{ii} \varphi_{13i}}{\varphi_{10} \varphi_{10i}^2} \right), \quad i = 1, \dots, n \tag{1.104}$$

If the interphase mass transfer is limited by the mass transfer in the liquid phase,  $\chi_i \rightarrow \infty$  and it could be substituted  $\frac{\varepsilon_{i0}}{\chi_i} = 0, a_i \rightarrow \infty, i = 1, \dots, n$ , in (1.102), so the expression (1.100) for  $Sh_{i2}$  becomes :

$$Sh_{i2} = \sqrt{Pe_2} \left( \frac{2\sqrt{\alpha_{i2}}}{\sqrt{\pi}} + \frac{8\theta_2 \alpha \varepsilon_{i2} \bar{\varphi}_{i2}}{\sqrt{\pi}} \right), \quad i = 1, \dots, n. \tag{1.105}$$

In cases when the diffusion resistances in both phases are commensurable  $\left( \frac{\chi_i}{\varepsilon_{i0}} \approx 1 \right)$

from (1.99) one is obtained:

$$\psi_{ii}^{(j)}(0) \leq 0, \quad \psi_{i2}^{(j)}(0) \geq 0, \quad i = 1, \dots, n. \tag{1.106}$$

It follows from (1.102) and (1.106) that the increase in the big concentration gradient ( $\theta$ ) leads to an increase of the diffusion transfer in the gas phase and to its decrease in the liquid phase.

As could be seen from (1.105), in the case of a multicomponent interphase mass transfer limited by the mass transfer in the liquid phase the non-linear effects have no impact on the process rate.

### 1.3.3. Non-linear interphase mass transfer between two liquids

The mathematical description of the kinetics of the interphase mass transfer in the liquid-liquid systems is the basis for the extraction processes and equipment design. The intensification of this process by generating big concentration gradients leads to the appearance of non-linear effects in the kinetics of the mass transfer in both phases. In a number of cases these effects are connected with the induction of tangential flows along the phase boundary (Marangoni's effect) as a result of a surface (interphase) tension gradient creation. It has already been shown that great mass fluxes can induce secondary flows, the velocities of which are directed normally to the phase interface. The theoretical analysis of the influence of these secondary flows on the kinetics of the interphase mass transfer in the liquid-liquid systems makes it possible to separate this non-linear effect from that of Marangoni and is a basis for the calculation of the extraction processes with intensive interphase mass transfer.

The extraction processes are realized most frequently in equipment where one of the liquids is dispersed in the form of drops. The small sizes of the drops are the reason why the velocities and the concentrations changes take place in thin layers along the phases interface. This allows the use of the boundary layer approximations for the theoretical analysis of the extraction kinetics under conditions of intensive interphase mass transfer.

In practice both the liquids are moving, one of them being a dispersed phase(drops) and the other - dispersion medium (a continuous phase).

In as much as the kinetics of the interphase mass transfer depends primarily on the drops velocities, in the further discussion would consider the interphase mass transfer between two liquids, one of them being stagnant.

Let the moving phase is assumed as phase 1 and the stagnant phase - as phase 2 [74]. Thus for the interphase mass transfer in both liquids (1.59) and (1.60) are applicable if the substitution takes place

$$u_{20} = 0, \quad \chi = m, \quad (1.107)$$

where  $m$  is the coefficient of distribution of the extracted substance between the liquids 1 and 2.

The interphase mass transfer rate and the Sherwood number are obtained from the equations (1.61)-(1.63):

$$J = MK_j m^{l-j} (c_{10} - mc_{20}) = -\frac{I}{L} \int_0^L I_j dx,$$

$$Sh_j = \frac{K_j L}{D_j} = \frac{\rho_j^*}{\rho_{j0}^*} \frac{m^{j-1}}{c_{j0} - mc_{20}} \int_0^L \left( \frac{\partial c_j}{\partial y} \right)_{y=0} dx, \quad j = 1, 2 \quad . \quad (1.108)$$

It is possible to solve the task (1.59), (1.60) taking (1.107) into consideration, if the following similarity variables are entered:

$$\begin{aligned} u_j &= 0.5 u_{j0} \phi_j', \\ v_j &= (-1)^{j-1} \left( \frac{u_{j0} D_j}{4x} \right)^{0.5} (\xi_j \phi_j' - \phi_j), \\ c_j &= c_{j0} + (-1)^{j-1} \frac{c_{j0} - mc_{20}}{m^{j-1}} \psi_j, \\ \phi_j &= \phi_j(\xi_j), \quad \psi_j = \psi_j(\xi_j), \\ \xi_j &= (-1)^{j-1} y \left( \frac{u_{j0}}{4D_j x} \right)^{0.5}, \quad \varepsilon_j = Sc_j^{0.5}, \\ Sc_j &= \frac{v_j}{D_j}, \quad j = 1, 2 \quad . \end{aligned} \quad (1.109)$$

The result is:

$$\begin{aligned} \psi_j''' + \varepsilon_j^{-2} \phi_j \phi_j'' &= 0, \\ \psi_j'' + \phi_j \psi_j' &= 0, \\ \phi_j(0) &= (-1)^{j-1} \Delta_j \psi_j'(0), \\ \phi_j'(0) &= \phi_2'(0), \quad \phi_1'(0) = -a \phi_2''(0), \\ \psi_1(0) &= 1 - \psi_2(0), \quad \psi_1'(0) = \frac{b}{m} \psi_2'(0), \\ \phi_1'(\infty) &= 2, \quad \phi_2'(\infty) = 0, \quad \psi_j(\infty) = 0, \quad j = 1, 2, \end{aligned} \quad (1.110)$$

where

$$\begin{aligned} \Delta_j &= \frac{M(m c_{20} - c_{j0})}{\rho_j^* m^{j-1}}, \\ a &= \frac{\varepsilon_2 \rho_{20}}{\varepsilon_1 \rho_{j0}} \sqrt{\frac{\nu_2}{\nu_1}}, \quad \nu_j = \frac{\mu_j}{\rho_{j0}}, \\ b &= \frac{\rho_{j0} \rho_2^*}{\rho_1^* \rho_{20}^*} \sqrt{\frac{D_2}{D_1}}, \quad j = 1, 2. \end{aligned} \quad (1.111)$$

Expressed in the new variables the Sherwood number (1.108) takes the form:

$$\begin{aligned} Sh_j &= -\frac{\dot{\rho}_j}{\dot{\rho}_{j0}} Pe_j^{\theta,5} \psi'_j(0), \\ Pe_j &= \frac{u_{10}L}{D_j}, \quad j = 1,2, \end{aligned} \quad (1.112)$$

where  $\psi'_j(0)$  ( $j = 1,2$ ) is the solution of (1.110).

In (1.110)  $\varepsilon_j \ll 1$ , i.e.  $\phi_j$  ( $j = 1,2$ ) could be determined as zero-order approximation with respect to these parameters with accuracy subject to arbitrary constants:

$$\phi_j = \alpha_j \xi_j^2 + \beta_j \xi_j + \gamma_j, \quad j = 1,2, \quad (1.113)$$

which are determined from the boundary conditions. So could be rewritten equation (1.110) as:

$$\begin{aligned} \psi''_j + (\alpha_j \xi_j^2 + \beta_j \xi_j + \gamma_j) \psi'_j &= 0, \\ \psi_j(0) &= 1 - \psi_2(0), \quad \psi'_j(0) = \frac{b}{m} \psi'_2(0) \\ \psi_j(\infty) &= 0, \quad j = 1,2. \end{aligned} \quad (1.114)$$

The solution of these equations will be obtained in the form:

$$\begin{aligned} \psi_j &= \frac{(2-j)b\varphi_1 + (j-1)m\varphi_2}{b\varphi_1 + m\varphi_2} \left( 1 - \varphi_j^{-1} \int_0^{\xi_j} E(p_j) dp_j \right), \\ E(p_j) &= \exp \left( -\frac{\alpha_j}{3} p_j^3 - \frac{\beta_j}{2} p_j^2 - \gamma_j p_j \right), \\ \varphi_j &= \int_0^{\infty} E(p_j) dp_j, \quad j = 1,2. \end{aligned} \quad (1.115)$$

The result allows to determine  $\psi'_j(0)$ :

$$\psi'_j(0) = \frac{(2-j)b\varphi_1 + (j-1)m\varphi_2}{b\varphi_1 + m\varphi_2} \cdot \frac{1}{\varphi_j}, \quad j = 1,2 \quad (1.116)$$

and to make a substitution in (1.112) for the Sherwood number calculation.

It is evident that the integration constants are not determinable in the diffusion boundary layer approximations (1.109). The laminar boundary layer variables can be used for this purpose:

$$\phi_j(\xi_j) = \varepsilon_j f_j(z_j), \quad \varepsilon_j z_j = \xi_j, \quad j = 1,2. \quad (1.117)$$

Thus, from (1.112) it follows:

$$\begin{aligned} f_j''' + f_j f_j'' &= 0, \\ f_2(0) &= (-1)^{j-1} \frac{\Delta_j}{\varepsilon_j} \psi_j'(0) = \frac{\gamma_j}{\varepsilon_j}, \\ f_1'(0) &= f_2'(0) = \beta_1 = \beta_2 = \beta, \quad f_1''(0) = -\alpha_0 f_2''(0) = \alpha, \\ f_1'(\infty) &= 2, \quad f_2'(\infty) = 0, \quad j = 1, 2, \end{aligned} \quad (1.118)$$

where

$$\alpha_0 = \frac{\mu_2}{\mu_1} \left( \frac{\nu_1}{\nu_2} \right)^{0.5}, \quad \psi_j = \psi_j(\xi_j) \quad j = 1, 2. \quad (1.119)$$

The solution of the system (1.114) and (1.118) for  $f_j$  and  $\psi_j$  ( $j = 1, 2$ ) determination could be found by means of an iterative procedure, where the initial guesses are  $f_j^{(0)}$  and  $\psi_j^{(0)}$  ( $j = 1, 2$ ), i.e. the zero-order approximations of the problem solution (1.114) and (1.118) for  $f_j$  and  $\psi_j$  with respect to the small parameters  $\Delta_j$  ( $j = 1, 2$ ). Thus, the following is obtained:

$$\begin{aligned} f_j^{(0)''' + f_j^{(0)} f_j^{(0)''}} &= 0, \\ f_1^{(0)}(0) &= f_2^{(0)}(0) = 0, \quad f_1^{(0)'}(0) = f_2^{(0)'}(0) = b_0, \\ f_1^{(0)''}(0) &= -\alpha_0, \quad f_2^{(0)''}(0) = a_0, \quad f_1^{(0)''}(\infty) = 2, \quad f_2^{(0)''}(\infty) = 0; \end{aligned} \quad (1.120)$$

$$\begin{aligned} \psi_i^{(0)''' + \phi_j^{(0)} \psi_j^{(0)'}} &= 0, \\ \psi_i^{(0)}(0) &= 1 - \psi_2^{(0)}(0), \quad \psi_i^{(0)'} = \frac{b}{m} \psi_2^{(0)'}(0), \\ \psi_j^{(\infty)} &= 0, \quad j = 1, 2, \end{aligned} \quad (1.121)$$

where

$$\begin{aligned} \phi_j^{(0)} &= \alpha_j^{(0)} \xi_j^2 + \beta_j^{(0)} \xi_j = \varepsilon_j f_j^{(0)}(z_j), \quad j = 1, 2, \\ \alpha_1^{(0)} &= \frac{a_0}{2\varepsilon_1}, \quad \alpha_2^{(0)} = -\frac{a_0}{2\alpha_0 \varepsilon_2}, \quad \beta_1^{(0)} = \beta_2^{(0)} = b_0. \end{aligned} \quad (1.122)$$

The parameters  $a_0$  and  $b_0$  can be obtained from the numerical determination of  $f_j^{(0)}$  ( $j = 1, 2$ ). On this basis it is possible to find  $\psi_j^{(0)}$  ( $j = 1, 2$ ):

$$\psi_j^{(0)} = \frac{(2-j)b\varphi_{10} + (j-1)m\varphi_{20}}{b\varphi_{10} + m\varphi_{20}} \left( I - \varphi_{j0}^{-1} \int_0^{\xi_j} E_0(p_j) dp_j \right),$$

$$E_0(p_j) = \exp\left(-\frac{\alpha_j^{(0)}}{3} p_j^3 - \frac{\beta_j^{(0)}}{2} p_j^2\right),$$

$$\varphi_{j0} = \int_0^\infty E_0(p_j) dp_j, \quad j = 1, 2. \quad (1.123)$$

The first iteration starts with the solution of (1.118) via the substitution

$$\psi'_j(0) = \psi_j^{(0)}(0), \quad j = 1, 2. \quad (1.124)$$

The numerical solution of (1.118) allows the determination of  $\alpha$  and  $\beta$  as well as the integration constants (1.113):

$$\alpha_1 = \frac{\alpha}{2\varepsilon_1}, \quad \alpha_2 = -\frac{\alpha}{2\alpha_0\varepsilon_2}, \quad \beta_j = \beta,$$

$$\gamma_j = -(-1)^{j-1} \frac{(2-j)b\varphi_{j0} + (j-1)m\varphi_{20}}{b\varphi_{j0} + m\varphi_{20}} \cdot \frac{\Delta_j}{\varphi_{j0}}, \quad j = 1, 2. \quad (1.125)$$

The first iteration concludes with the solution of the system (1.114) and the determination of the value of the integral in (1.115), which allows to obtain  $\psi'_j(0)$  ( $j = 1, 2$ ) in the Sherwood number (1.118).

The next iterations are executed in the same manner, i.e.  $f_j$ ,  $\phi_j$ ,  $\psi_j$  are consecutively calculated using  $\psi'_j(0)$  from the respective preceding iteration.

This iterative approach has been applied for the solution of the problem (1.110) at  $\varepsilon_1 = \varepsilon_2 = 10$ ,  $\Delta_1 = \Delta_2 = \pm 0.1$ ,  $\pm 0.3$ ,  $\pm 0.5$ ,  $a = b = m = 1$ , as well as in cases when the interphase mass transfer is limited by the mass transfer either in the first ( $m/b = 0$ ) or the second ( $b/m = 0$ ) phase.

The results thus obtained demonstrate the quick convergence of the iterative method. In most of the cases two iterations are sufficient and only as a matter of exception (at  $\Delta_2 = 0.5$ ,  $b/m = 0$ ) a third iterations is required.

The values  $\psi'_j(0)$ ,  $j = 1, 2$ , allowing the determination of the Sherwood number from (1.112) are included in Table 1.7. It is evident that the direction of the interphase mass transfer affects the diffusion mass transfer in a way similar to that demonstrated for the gas-liquid systems.

In cases of commensurable diffusion resistencies ( $b/m \sim 1$ ) the increase in the diffusion mass transfer rate in the one phase is coupled with decrease in the diffusion mass transfer rate in the other phase. In the particular case ( $b/m = 1$ ,  $\Delta_1 = \Delta_2$ ) both effects compensate each other completely and the results from the non-linear theory ( $\Delta_1 = \Delta_2 \neq 0$ ) coincide with those from the linear theory ( $\Delta_1 = \Delta_2 = 0$ ).

Table 1.7.  
Dimensionless diffusion flux.

$\theta_1 = \theta_2$	$a = 1,$	$\varepsilon_1 = \varepsilon_2 = 10$	
	$b/m = 1$	$m/b = 0$	$b/m = 0$
	$\psi_1(0) = \psi_2'(0)$	$\psi_2'(0) = 0$	$\psi_1'(0) = 0$
-	$-\psi_1'(0)$	$-\psi_1'(0)$	$-\psi_2'(0)$
0	0.4319	0.8786	0.8497
0.1	0.4316	0.8261	0.9073
-0.1	0.4316	0.9400	0.8003
0.3	0.4289	0.7398	1.0562
-0.3	0.4289	1.0996	0.7189
0.5	0.4237	0.6689	1.2703
-0.5	0.4238	1.3305	0.6519

## CHAPTER 1.4. GAS – FALLING LIQUID FILM – SOLID SURFACE SYSTEM

The theoretical investigations of the non-linear mass transfer in gas-liquid systems show [45, 63] that practically the non-linear effects are essential in cases when the diffusion resistances in the gas phase limits the mass transfer rate.

The literature review in the area of the theory of kinetics of non-linear mass transfer in two-phase systems with intensive interphase mass transfer indicate the great importance of the creation of a theory of the non-linear mass transfer between a gas and a falling liquid film in the cases where the mass transfer in the gas phase limits the process. Based on this, an attempt to explain the difference in mass transfer rates in absorption and desorption of high soluble gases will be made.

### 1.4.1. Non-linear interphase mass transfer between the gas and the falling liquid film

The non-linear mass transfer between a gas and a falling liquid film in the cases of absorption and desorption of gases may be described with the help of the Navier – Stocks equation, the equation of convective diffusion in the gas and the liquid and the equation of the macroscopic balance of the liquid film, i.e. the condition of “non-leakage flow” through the film surface. In the cases of intensive mass transfer it is necessary to add a condition, allowing to determine a secondary flow depending on the mass flux. Then the condition of “non-leakage flow” turns into a condition of “leakage flow”, considering the secondary flow rate.

The theoretical and experimental studies [5, 35] show that the falling liquid film along a vertical surface may be described with satisfactory precision by the Navier – Stocks equation in the zero – order approximation of the small parameter  $(h_0 / L_\infty)^2$ :

$$\nu \frac{\partial^2 u}{\partial y^2} + g = 0, \quad \frac{\partial u}{\partial x} + \frac{\partial v}{\partial y} = 0, \quad (1.126)$$

where  $h_0$  is the film thickness at a certain distance  $L_\infty$ .

The boundary conditions of the system (1.126) express the “slipping effect” along the solid surface  $y = 0$  and continuity of the stress tensor at the phase boundary  $y = h$ :

$$\begin{aligned} y = 0, \quad u = 0, \quad v = 0; \\ y = h, \quad \mu \frac{\partial u}{\partial y} = \tilde{\mu} \frac{\partial \tilde{u}}{\partial y}. \end{aligned} \quad (1.127)$$

The thickness of the film is determined [5, 35] by the macroscopic balance (the condition of “leakage flow” at the phase boundary), considering the secondary flow in the liquid film [30] as a result of the intensive interphase mass transfer:

$$y = h, \quad h \dot{u} - v = \frac{MD}{\rho_0^*} \frac{\partial c}{\partial y}. \quad (1.128)$$

The change of the film thickness is connected with the change of the liquid velocity along the length of the film. This leads to the necessity to introduce boundary conditions for the velocity and the thickness along the film length. In the theoretical analysis of the film flow [1, 5, 29] it was shown that as a result of the small thickness of the film these effects quickly decrease and at a certain distance ( $L_\infty$ ) from the beginning of the film an asymptotic flow occurs, i.e. the flow velocity does not depend on the length coordinate. This fact gives a reason to use as boundary conditions the following expressions:

$$x \rightarrow L_\infty, \quad \frac{\partial u}{\partial x} \rightarrow 0, \quad h \rightarrow h_0. \quad (1.129)$$

In order to determine the concentration of the absorbed (desorbed) substance in (1.128) it is necessary to solve the equation of convective diffusion in the liquid. Practically, the thickness of the diffusion boundary layer in the liquid is always smaller than the film thickness, and as a result of this fact a boundary layer approximation can be used:

$$u \frac{\partial c}{\partial x} + v \frac{\partial c}{\partial y} = D \frac{\partial^2 c}{\partial y^2}, \quad (1.130)$$

with boundary conditions, taking into account the impermeability of the solid wall and the continuity of the mass flux through the phase boundary:

$$\begin{aligned} x = 0, \quad c = c_0; \\ y = 0, \quad \frac{\partial c}{\partial y} = 0; \\ y = h, \quad \frac{D \rho^*}{\rho_0^*} \frac{\partial c}{\partial y} = \frac{\tilde{D} \tilde{\rho}^*}{\tilde{\rho}_0^*} \frac{\partial \tilde{c}}{\partial y}. \end{aligned} \quad (1.131)$$

In (1.131) the availability of a convective flux of substance is assumed (see 1.3), i.e.  $\rho^* = \rho_0 + Mc^*$  and  $\tilde{\rho}^* = \tilde{\rho}_0^* + M\tilde{c}^*$ , where  $\tilde{c}^*$  and  $c^*(\tilde{c}^* = \chi c^*)$  are the concentrations of the absorbed substance at the interphase boundary. Here has to be born in mind that under normal pressure

$$\frac{\rho^*}{\rho_0^*} \approx 1.$$

The theoretical analysis of the simultaneous movement of the gas and the liquid film [5, 29, 35] shows that the Navier – Stocks equation for the gas may be written in the boundary layer approximations:

$$\tilde{u} \frac{\partial \tilde{u}}{\partial x} + \tilde{v} \frac{\partial \tilde{u}}{\partial y} = \tilde{v} \frac{\partial^2 \tilde{u}}{\partial y^2}, \quad \frac{\partial \tilde{u}}{\partial x} + \frac{\partial \tilde{v}}{\partial x} = 0. \quad (1.132)$$

The boundary conditions of equation (1.119) express the continuity of the velocities at the phase boundaries and the potential gas flow outside the boundary layer:

$$\begin{aligned} x = 0, \quad \tilde{u} &= \tilde{u}_0; \\ y = h, \quad \tilde{u} &= u, \quad \tilde{v} = v; \\ y \rightarrow \infty, \quad \tilde{u} &= \tilde{u}_0. \end{aligned} \quad (1.133)$$

The thickness of the laminar and the diffusion boundary layers in gases are of one and the same order, and for the description of the mass transfer in the gas phase an analogous approximation can be used:

$$\tilde{u} \frac{\partial \tilde{c}}{\partial x} + \tilde{v} \frac{\partial \tilde{c}}{\partial y} = \tilde{v} \frac{\partial^2 \tilde{c}}{\partial y^2}, \quad (1.134)$$

with boundary conditions, expressing the thermodynamical equilibrium at the phase boundary and the constant concentration outside the boundary layer:

$$\begin{aligned} x = 0, \quad \tilde{c} &= \tilde{c}_0; \\ y = h, \quad \tilde{c} &= \chi c; \\ y \rightarrow \infty, \quad \tilde{c} &= \tilde{c}_0. \end{aligned} \quad (1.135)$$

The intensive mass transfer between the gas and the liquid induces a secondary flow [5, 35, 45]. The velocity of this flow  $\tilde{v}_n$  (in the above mentioned approximations) may be expressed by means of the mass flux through the phase boundary:

$$\tilde{v}_n = \tilde{v}(x, h) - h \tilde{u}(x, h) = - \frac{MD}{\tilde{\rho}_0^*} \left( \frac{\partial \tilde{c}}{\partial y} \right)_{y=h}. \quad (1.136)$$

Equation (1.136) makes possible to consider the influence of the mass transfer on the hydrodynamics and introduces non-linearity in the left part of (1.134), i.e. (1.136) is the basis for the calculation of the non-linear mass transfer under conditions of intensive interphase mass transfer.

The interphase mass transfer rate between the gas and the liquid in the discussed case is determined by the kinetics of the non-linear mass transfer in the gas phase. This rate can be obtained finding the average mass flux for the given length of the film  $L$ :

$$J = M\tilde{K}(\tilde{c}_0 - \chi c_0) = \frac{1}{L} \int_0^L \tilde{I} dx, \quad (1.137)$$

where the local mass flux has (as a result of the secondary flow) a diffusive and a convective components:

$$\begin{aligned} \tilde{I} &= -M\tilde{D}\left(\frac{\partial \tilde{c}}{\partial y}\right)_{y=h} + M\chi c_0[\tilde{v}(x, h) - h'\tilde{u}(x, h)] = -\frac{M\tilde{D}\tilde{\rho}^*}{\tilde{\rho}_0^*}\left(\frac{\partial \tilde{c}}{\partial y}\right)_{y=h}, \\ \tilde{\rho}^* &= \tilde{\rho}_0^* + M\chi c^*. \end{aligned} \quad (1.138)$$

Expressions (1.137) and (1.138) allow to determine the Sherwood number after solving equations (1.126) – (1.136):

$$\tilde{Sh} = \frac{\tilde{K}L}{\tilde{D}} = -\frac{\tilde{\rho}^*}{\tilde{\rho}_0^*} \frac{1}{\tilde{c}_0 - \chi c_0} \int_0^L \left(\frac{\partial \tilde{c}}{\partial y}\right)_{y=h} dx. \quad (1.139)$$

In order to solve the system of equations (1.126) – (1.136), it is necessary to introduce the following dimensionless variables:

$$\begin{aligned} X &= \frac{x}{L}, \quad Y = \frac{y}{h_0}, \\ U(X, Y) &= \frac{u}{u_0}, \quad V(X, Y) = \frac{v}{\varepsilon_0 u_0}, \\ H(X) &= \frac{h}{h_0}, \quad \tilde{Y} = \frac{y-h}{\tilde{\delta}}, \\ \tilde{U}(X, \tilde{Y}) &= \frac{\tilde{u}}{\tilde{u}_0}, \quad \tilde{V}(X, \tilde{Y}) = \frac{\tilde{v}}{\tilde{\varepsilon}_0 \tilde{u}_0}, \\ C &= \frac{c - c_0}{\tilde{c}_0 / \chi - c_0}, \quad \tilde{C} = \frac{\tilde{c} - c_0}{\tilde{c}_0 - \chi c_0}, \end{aligned} \quad (1.140)$$

where

$$\varepsilon_0 = \frac{h_0}{L}, \quad u_0 = \frac{gh_0^2}{3\nu}, \quad \tilde{\varepsilon}_0 = \frac{\tilde{\delta}}{L}, \quad \tilde{\delta} = \left( \frac{\tilde{D}L}{\tilde{u}_0} \right)^{0.5}. \quad (1.141)$$

In this way five interconnected boundary problems are obtained:

$$\begin{aligned} \frac{\partial^2 U}{\partial Y^2} &= -3, \quad \frac{\partial U}{\partial X} + \frac{\partial V}{\partial Y} = 0; \\ Y = 0, \quad U &= 0, \quad V = 0; \\ Y = H, \quad \frac{\partial U}{\partial Y} &= \theta_2 \left( \frac{\partial \tilde{U}}{\partial \tilde{Y}} \right)_{\tilde{Y}=0}; \\ X \rightarrow L_\infty / L, \quad \frac{\partial U}{\partial X} &\rightarrow 0. \end{aligned} \quad (1.142)$$

$$\begin{aligned} H'U(X, H) &= V(X, H) + \theta_2 \left( \frac{\partial C}{\partial Y} \right)_{Y=H}; \\ X \rightarrow L_\infty / L, \quad H &\rightarrow l. \end{aligned} \quad (1.143)$$

$$\begin{aligned} U \frac{\partial C}{\partial X} + V \frac{\partial C}{\partial Y} &= Fo \frac{\partial^2 C}{\partial Y^2}; \\ X = 0, \quad C &= 0; \\ Y = 0, \quad \frac{\partial C}{\partial Y} &= 0; \\ Y = H, \quad \frac{\partial C}{\partial Y} &= \beta \left( \frac{\partial \tilde{C}}{\partial \tilde{Y}} \right)_{\tilde{Y}=0}. \end{aligned} \quad (1.144)$$

$$\begin{aligned} \tilde{U} \frac{\partial \tilde{U}}{\partial X} + \tilde{V} \frac{\partial \tilde{U}}{\partial \tilde{Y}} &= S \tilde{C} \frac{\partial^2 \tilde{U}}{\partial \tilde{Y}^2} + \delta_0 H' \tilde{U} \frac{\partial \tilde{U}}{\partial \tilde{Y}}; \\ \frac{\partial \tilde{U}}{\partial X} + \frac{\partial \tilde{V}}{\partial \tilde{Y}} &= \delta_0 H' \frac{\partial \tilde{U}}{\partial \tilde{Y}}; \\ X = 0, \quad \tilde{U} &= l; \\ \tilde{Y} = 0, \quad \tilde{U} &= \theta_1 U(X, H), \quad V = -\theta_2 \frac{\partial \tilde{C}}{\partial \tilde{Y}} + \delta_0 H' \tilde{U}; \\ \tilde{Y} \rightarrow \infty, \quad \tilde{U} &= l. \end{aligned} \quad (1.145)$$

$$\begin{aligned} \tilde{U} \frac{\partial \tilde{C}}{\partial X} + \tilde{V} \frac{\partial \tilde{C}}{\partial \tilde{Y}} &= \frac{\partial^2 \tilde{C}}{\partial \tilde{Y}^2} + \delta_0 H' \tilde{U} \frac{\partial \tilde{C}}{\partial \tilde{Y}}; \\ X = 0, \quad \tilde{C} &= l; \\ \tilde{Y} = 0, \quad \tilde{C} &= C; \end{aligned}$$

$$\tilde{Y} \rightarrow \infty, \quad \tilde{C} = I, \quad (1.146)$$

where

$$\begin{aligned} \delta_0 &= \frac{h_0}{\tilde{\delta}}, \quad S\tilde{c} = \frac{\nu}{\tilde{D}}, \quad Fo = \frac{DL}{u_0 h_0^2}, \\ \theta_1 &= \frac{u_0}{\tilde{u}_0}, \quad \theta_2 = \frac{\tilde{\mu}\delta_0}{\mu\theta_1}, \quad \theta_3 = \frac{M}{\tilde{\rho}_0}(\tilde{c}_0 - \chi c_0), \\ \theta_4 &= \frac{MD(\tilde{c}_0 - \chi c_0)}{\varepsilon_0 u_0 h_0 \rho_0^* \chi}, \quad \beta = \frac{\delta_0 \chi \tilde{D} \tilde{\rho}^*}{D \rho_0^*}. \end{aligned} \quad (1.147)$$

The parameter  $\theta_3$  determines the mass transfer direction [41]. In the cases of absorption  $\theta_3 > 0$ , and for desorption  $\theta_3 < 0$ . In the approximations of the linear theory of mass transfer  $\theta_3 = 0$  [27].

The solution of the problem (1.142) – (1.146) creates the possibility to determine the Sherwood number from (1.139), and having in mind the new variables, it takes the form:

$$Sh = -\frac{\tilde{\rho}^*}{\tilde{\rho}_0} \sqrt{\tilde{P}e} \int_0^1 \left( \frac{\partial \tilde{C}}{\partial \tilde{Y}} \right)_{\tilde{Y}=0} dX, \quad \tilde{P}e = \frac{\tilde{u}_0 L}{\tilde{D}}. \quad (1.148)$$

In the cases of highly soluble gases, when the process is limited by the mass transfer in the gas phase, the parameters  $\beta$  and  $\delta_0$  in equations (1.142) – (1.146) are practically equal to zero. If in (1.142) – (1.146)  $\beta = \delta_0 = 0$  is assumed, from (1.144) it follows that  $C \equiv 0$ , and in (1.143) the following substitution should be made:

$$\theta_4 \left( \frac{\partial C}{\partial Y} \right)_{Y=H} = \theta_0 \theta_3 \left( \frac{\partial \tilde{C}}{\partial \tilde{Y}} \right)_{\tilde{Y}=0}, \quad \theta_0 = \frac{\tilde{\rho}^* \sqrt{\tilde{u}_0 \tilde{D} L}}{h_0 u_0 \rho_0^*}, \quad (1.149)$$

using the condition of continuity of the mass flux through the phase boundary. In these approximations it is possible to solve (1.142) – (1.143) and (1.145) – (1.146) as two conditionally independent problems in the liquid and the gas.

The velocity distribution in the film is determined by (1.142):

$$\begin{aligned} U &= -\frac{3}{2} Y^2 + \left[ 3H + \theta_2 \left( \frac{\partial \tilde{U}}{\partial \tilde{Y}} \right)_{\tilde{Y}=0} \right] Y, \\ V &= -\frac{1}{2} \left[ 3H' + \theta_2 \frac{d}{dX} \left( \frac{\partial \tilde{U}}{\partial \tilde{Y}} \right)_{\tilde{Y}=0} \right] Y^2. \end{aligned} \quad (1.150)$$

Substituting the expressions (1.150) in equation (1.143), the film thickness can be found:

$$H^3 = 1 - \frac{1}{2} \theta_2 \left( \frac{\partial \tilde{U}}{\partial \tilde{Y}} \right)_{\tilde{Y}=0} H^2 - \theta_2 \theta_3 \int_X^{L_\infty/L} \left( \frac{\partial \tilde{C}}{\partial \tilde{Y}} \right)_{\tilde{Y}=0} dX. \quad (1.151)$$

The equations of velocity distribution (1.150) and the film thickness (1.151) obtain their final form after the solution of (1.145), (1.146).

In the expressions (1.150)  $\theta_2$  is a small parameter, i.e. it is possible to assume  $\tilde{U}$  as a zero-th order approximation concerning  $\theta_2$ . This allows us to solve (1.145) in the zero-th order approximation regarding  $\theta_2$ . Thus it is necessary to substitute  $U(X, H)$  in a zero-th order approximation regarding the small parameter  $\theta_2$ , i.e.

$$U(X, H) = \frac{3}{2}. \quad (1.152)$$

The velocity and concentration distribution in a gas can be determined from (1.145) and (1.146), utilising the similarity variables as following:

$$\begin{aligned} \tilde{U} &= 0.5\tilde{\varepsilon}\phi', & \tilde{V} &= 0.5\tilde{\varepsilon} \frac{1}{\sqrt{X}}(\eta\phi' - \phi), & \tilde{C} &= 1 - \psi, \\ \phi &= \phi(\eta), & \psi &= \psi(\eta), & \eta &= \frac{\tilde{Y}}{2\sqrt{X}}, & \tilde{\varepsilon} &= S\tilde{c}^{0.5}. \end{aligned} \quad (1.153)$$

The result is directly obtained:

$$\begin{aligned} \phi''' + \tilde{\varepsilon}^{-1}\phi\phi'' &= 0, & \psi'' + \tilde{\varepsilon}\phi\psi' &= 0, \\ \phi(0) &= -\theta_2\tilde{\varepsilon}^{-1}\psi'(0), & \phi'(0) &= 3\theta_2\tilde{\varepsilon}^{-1}, & \phi'(\infty) &= 2\tilde{\varepsilon}^{-1}, \\ \psi(0) &= 1, & \psi(\infty) &= 0. \end{aligned} \quad (1.154)$$

The mass transfer rate is determined by the Sherwood number from (1.148). In the new variables this relation takes the following form:

$$Sh = \frac{\tilde{\rho}^*}{\rho_0} P \tilde{\varepsilon}^{0.5} \psi'(0), \quad (1.155)$$

where  $\psi'(0)$  is obtained after solving the problem (1.154). In the cases of practical interest the parameters  $\theta_1$  and  $\theta_3$  in (1.154) are small, which provides the opportunity to apply the perturbation method, i.e. to substitute

$$A = A_0 + \theta_1 A_1 + \theta_3 A_3 + \theta_1^2 A_{11} + \theta_3^2 A_{33} + \theta_1 \theta_3 A_{13} + \dots, \quad (1.156)$$

where  $A$  is a vector function:

$$A = (\phi, \psi). \quad (1.157)$$

In (1.154) it is possible to substitute:

$$-\frac{\theta_3}{\tilde{\varepsilon}} = \theta \quad (1.158)$$

and to compare with (1.23). It is obvious that some of the functions in (1.156) may be determined from (1.28). If equation (1.156) is substituted in (1.154), a series of finite problems can be obtained, which have been solved for different approximations [7]:

$$\begin{aligned} \phi_0(\eta) &= f(z), \quad \psi_0(\eta) = 1 - \frac{1}{\varphi_0} \int_0^z E(\tilde{\varepsilon}, p) dp, \quad z = \frac{2}{\tilde{\varepsilon}} \eta, \\ \varphi_0 &= \int_0^\infty E(\tilde{\varepsilon}, p) dp \approx 3.01 \tilde{S} c^{-0.35}, \quad E(\tilde{\varepsilon}, p) = \exp \left[ -\frac{\tilde{\varepsilon}^2}{2} \int_0^p f(s) ds \right], \\ \phi_1(\eta) &= \frac{3}{2\alpha} f'(z), \quad \psi_1(\eta) = \frac{3}{2\alpha_0 \varphi_0} \left[ 1 - E(\tilde{\varepsilon}, z) - \frac{1}{\varphi_0} \int_0^z E(\tilde{\varepsilon}, p) dp \right], \\ \phi_{11}(\eta) &= \frac{9}{4} F(z), \\ \psi_{11}(\eta) &= \left( -\frac{9\tilde{\varepsilon}^2 \varphi_2}{8\varphi_0^2} - \frac{9}{4\alpha^2 \varphi_0^3} + \frac{9\tilde{\varepsilon}^4 \varphi_1}{32\alpha^2 \varphi_0^2} \right) \int_0^z E(\tilde{\varepsilon}, p) dp + \right. \\ &\quad \left. + \frac{9\tilde{\varepsilon}^2}{8\varphi_0} \int_0^z \left[ \int_0^p F(s) ds \right] E(\tilde{\varepsilon}, p) dp + \frac{9}{4\alpha^2 \varphi_0^2} [1 - E(\tilde{\varepsilon}, z)] - \right. \\ &\quad \left. - \frac{9\tilde{\varepsilon}^4}{32\alpha^2 \varphi_0} \int_0^z f^2(p) E(\tilde{\varepsilon}, p) dp, \right. \\ \varphi_1 &= \int_0^\infty f^2(p) E(\tilde{\varepsilon}, p) dp \approx 3.011 \tilde{S} c^{-1.608}, \\ \varphi_2 &= \int_0^\infty \left[ \int_0^p F(s) ds \right] E(\tilde{\varepsilon}, p) dp \approx 3.052 \tilde{S} c^{-1.283}, \\ \phi_3(\eta) &= \frac{2}{\tilde{\varepsilon}^2 \varphi_0} \varphi(z), \\ \psi_3(\eta) &= \frac{1}{\varphi_0^2} \int_0^z \left[ \int_0^p \varphi(s) ds \right] E(\tilde{\varepsilon}, p) dp - \frac{\varphi_3}{\varphi_0^3} \int_0^z E(\tilde{\varepsilon}, p) dp, \\ \varphi_3 &= \int_0^\infty \left[ \int_0^p \varphi(s) ds \right] E(\tilde{\varepsilon}, p) dp \approx 6.56 \tilde{S} c^{-0.8}, \end{aligned}$$

$$\begin{aligned}
\phi_{33}(\eta) &= \frac{2\varphi_3}{\tilde{\varepsilon}^2 \varphi_0^3} \varphi(z) - \frac{4}{\tilde{\varepsilon}^4 \varphi_0^2} \bar{\varphi}(z), \\
\psi_{33}(\eta) &= \left( -\frac{2\varphi_3^2}{\varphi_0^5} - \frac{\varphi_{33}}{2\varphi_0^4} + \frac{2\bar{\varphi}_{33}}{\tilde{\varepsilon} \varphi_0^4} \right)_0^z E(\tilde{\varepsilon}, p) dp + \\
&+ \frac{2\varphi_3}{\varphi_0^4} \int_0^z \left[ \int_0^p \varphi(s) ds \right] E(\tilde{\varepsilon}, p) dp - \frac{1}{2\varphi_0^3} \int_0^z \left[ \int_0^p \varphi(s) ds \right]^2 E(\tilde{\varepsilon}, p) dp - \\
&- \frac{2}{\tilde{\varepsilon}^2 \varphi_0^3} \int_0^z \left[ \int_0^p \bar{\varphi}(s) ds \right] E(\tilde{\varepsilon}, p) dp, \\
\varphi_{33} &= \int_0^\infty \left[ \int_0^p \varphi(s) ds \right]^2 E(\tilde{\varepsilon}, p) dp \approx 24 \tilde{S} c^{-1.3}, \\
\bar{\varphi}_{33} &= \int_0^\infty \left[ \int_0^p \bar{\varphi}(s) ds \right] E(\tilde{\varepsilon}, p) dp \approx 0.326 \tilde{S} c^{-1.63}, \\
\phi_{13}(\eta) &= \frac{3}{\alpha \tilde{\varepsilon}^2 \varphi_0^2} \varphi(z) - \frac{3}{\alpha \tilde{\varepsilon}^2 \varphi_0} \bar{\varphi}(z), \\
\psi_{13}(\eta) &= \left( -\frac{9\varphi_3}{2\alpha \varphi_0^4} + \frac{3\varphi_{13}}{2\alpha \varphi_0^3} + \frac{3\bar{\varphi}_{13}}{2\alpha \varphi_0^3} \right)_0^z E(\tilde{\varepsilon}, p) dp + \\
&+ \frac{3}{\alpha \varphi_0^3} \int_0^z \left[ \int_0^p \varphi(s) ds \right] E(\tilde{\varepsilon}, p) dp - \frac{3}{2\alpha \varphi_0^2} \int_0^z \left[ \int_0^p \bar{\varphi}(s) ds \right]^2 E(\tilde{\varepsilon}, p) dp + \\
&+ \frac{3}{2\alpha \varphi_0^2} E(\tilde{\varepsilon}, z) \int_0^z \varphi(s) ds - \frac{3}{2\alpha \varphi_0^2} \int_0^z \varphi(p) E(\tilde{\varepsilon}, p) dp + \frac{3\varphi_3}{2\alpha \varphi_0^3} [l - E(\tilde{\varepsilon}, z)], \\
\varphi_{13} &= \int_0^\infty \left[ \int_0^p \bar{\varphi}(s) ds \right] E(\tilde{\varepsilon}, p) dp \approx \tilde{S} c^{-1.3}, \\
\bar{\varphi}_{13} &= \int_0^\infty \varphi(p) E(\tilde{\varepsilon}, p) dp \approx 4.18 \tilde{S} c^{-0.46}. \tag{1.159}
\end{aligned}$$

In these expressions the functions  $f, F, \varphi, \bar{\varphi}, \bar{\bar{\varphi}}$  are obtained by means of solving the system (1.29), adding the following relationships:

$$\begin{aligned}
2F''' + fF'' + f''F &= -\frac{l}{\alpha^2} f' f'', \\
2\bar{\varphi}'' + f\bar{\varphi}'' + f''\bar{\varphi} &= f' \varphi'' + f''' \varphi, \\
F(0) = F'(0) = F'(\infty) &= 0, \\
\bar{\varphi}(0) = \bar{\varphi}'(0) = \bar{\varphi}'(\infty) &= 0. \tag{1.160}
\end{aligned}$$

The non-linear effects in the gas influence the hydrodynamics of the film as it was already shown in (1.150) and (1.151), i.e. the velocity distributions and the film thickness depend on the velocity and concentration gradient in the gas. The film hydrodynamics depends on the small parameter  $\theta_2$ , which is determined as in (1.147) from the condition for stress tensor continuity at the phase boundary and accounts for the dynamic interaction of the gas and the liquid. Keeping the order of precision of the approximations obtained up to this moment, the velocity distribution in the liquid may be obtained in the first order approximation of the small parameter  $\theta_2$ :

$$\begin{aligned} U &= -\frac{3}{2}Y^2 + \left[ 3H + \theta_2 \frac{\tilde{\varepsilon}}{4\sqrt{X}} \phi_0''(0) \right] Y, \\ V &= -\frac{1}{2} \left[ 3H' + \theta_2 \frac{\tilde{\varepsilon}}{8X\sqrt{X}} \phi_0''(0) \right] Y^2, \end{aligned} \quad (1.161)$$

where  $H$  is determined from the expression:

$$H^3 = 1 - \theta_2 \frac{\tilde{\varepsilon}}{8\sqrt{X}} \phi_0''(0) H^2 + \theta_0 \theta_3 [\psi_0'(0) + \theta_1 \psi_1'(0) + \theta_3 \psi_3'(0)] (\sqrt{L_\infty/L} - \sqrt{X}). \quad (1.162)$$

In order to determine  $H$ , it is convenient to use the following series:

$$H = 1 + \theta_2 H_2 + \theta_3 H_3 + \theta_3^2 H_{33} + \theta_1 \theta_3 H_{13} + \dots \quad (1.163)$$

If (1.149) is substituted in (1.148) and the terms of the same orders of  $\theta_2, \theta_3, \theta_3^2$  and  $\theta_1 \theta_3$  are equalized, taking into consideration (1.159), one is obtained:

$$\begin{aligned} H_2 &= -\frac{\alpha}{6\tilde{\varepsilon}\sqrt{X}}, \quad H_3 = -\frac{2\theta_0}{3\tilde{\varepsilon}\phi_0} (\sqrt{L_\infty/L} - \sqrt{X}), \\ H_{33} &= \frac{4\theta_0^2}{9\tilde{\varepsilon}^2\phi_0^2} (\sqrt{L_\infty/L} - \sqrt{X})^2 - \frac{2\theta_0\phi_3}{3\tilde{\varepsilon}\phi_0^3} (\sqrt{L_\infty/L} - \sqrt{X}), \\ H_{13} &= -\frac{\theta_0}{\alpha\tilde{\varepsilon}\phi_0^2} (\sqrt{L_\infty/L} - \sqrt{X}). \end{aligned} \quad (1.164)$$

Substituting  $\phi_0''(0)$  from (1.159) into (1.161) and (1.164) into (1.163), the final result is obtained:

$$\begin{aligned} U &= -\frac{3}{2}Y^2 + \left[ 3H + \frac{\alpha\theta_2}{\tilde{\varepsilon}\sqrt{X}} \right] Y, \\ V &= -\frac{1}{2} \left[ 3H' + \frac{\alpha\theta_2}{2\tilde{\varepsilon}X\sqrt{X}} \right] Y^2, \end{aligned} \quad (1.165)$$

where  $H$  is determined by the expression:

$$\begin{aligned} H = & 1 - \frac{\alpha\theta_2}{6\tilde{\varepsilon}\sqrt{X}} - \frac{2\theta_0\theta_3}{2\tilde{\varepsilon}\varphi_0}(\sqrt{L_\infty/L} - \sqrt{X}) - \\ & - \theta_3^2 \left[ \frac{4\theta_0^2}{9\tilde{\varepsilon}^2\varphi_0^2} (\sqrt{L_\infty/L} - \sqrt{X})^2 + \frac{2\theta_0\theta_3}{3\tilde{\varepsilon}\varphi_0^3} (\sqrt{L_\infty/L} - \sqrt{X}) \right] - \\ & - \theta_1\theta_3 \frac{\theta_0}{\alpha\tilde{\varepsilon}\varphi_0^2} (\sqrt{L_\infty/L} - \sqrt{X}). \end{aligned} \quad (1.166)$$

The mass transfer rate in the discussed case is determined by the Sherwood number from (1.155), where  $\psi'(0)$  may be obtained from (1.159):

$$\begin{aligned} \psi'(0) = & - \left[ \frac{2}{\tilde{\varepsilon}\varphi_0} + \frac{3\theta_1}{\alpha\tilde{\varepsilon}\varphi_0^2} + \frac{2\theta_3\varphi_3}{\tilde{\varepsilon}\varphi_0^3} + \theta_1^2 \left( \frac{9\tilde{\varepsilon}\varphi_2}{4\varphi_0^2} + \frac{9}{2\alpha^2\tilde{\varepsilon}\varphi_0^3} - \frac{9\tilde{\varepsilon}^3\varphi_1}{16\alpha^2\varphi_0^2} \right) + \right. \\ & \left. + \theta_3^2 \left( \frac{4\varphi_3^2}{\tilde{\varepsilon}\varphi_0^5} - \frac{\varphi_{33}}{\tilde{\varepsilon}\varphi_0^4} - \frac{4\bar{\varphi}_{33}}{\tilde{\varepsilon}^3\varphi_0^4} \right) + \theta_1\theta_3 \left( \frac{9\varphi_3}{\alpha\tilde{\varepsilon}\varphi_0^4} - \frac{3\varphi_{13}}{\alpha\tilde{\varepsilon}\varphi_0^3} - \frac{3\bar{\varphi}_{13}}{\alpha\tilde{\varepsilon}\varphi_0^3} \right) \right]. \end{aligned} \quad (1.167)$$

From (1.167) it is obvious that the non-linear effects increase the diffusion transfer during absorption ( $\theta_3 > 0$ ) and decrease it during desorption ( $\theta_3 < 0$ ), compared to the transfer, obtained according to the linear theory ( $\theta_3 = 0$ ). If  $\psi'(0)$  is expressed through  $\psi'_+$ ,  $\psi'_-$ ,  $\psi'_0$  for the cases of absorption, desorption and small concentration gradients (when the absorption and desorption rates are practically equal) correspondingly, then from (1.155) and (1.167) one is obtained:

$$\frac{\psi'_+ - \psi'_0}{\psi'_+ - \psi'_-} = \frac{1}{2} + \theta_3 \frac{\frac{1}{\tilde{\varepsilon}^2\varphi_0^2} (4\tilde{\varepsilon}^2\varphi_3^2 - \tilde{\varepsilon}^2\varphi_0\varphi_{33} - 4\varphi_0\bar{\varphi}_{33})}{4\varphi_3 + \frac{6\theta_1}{\alpha\varphi_0} (3\varphi_3 - \varphi_0\varphi_{13} - \varphi_0\bar{\varphi}_{13})}. \quad (1.168)$$

The expression (1.168), which follows directly from the non-linear theory of mass transfer, may be verified on the basis of experimental data for the mass transfer coefficient for absorption and desorption of a highly soluble gas at high and low concentration gradients.

The accuracy of the asymptotic theory was determined [2] by means of the numerical solution of the problem (1.154). The numerical results (Fig. 1.14) show that in cases of absorption of highly soluble gases and at high concentration gradients the diffusion mass transfer is greater than in cases of desorption.

Table 1.8 displays the theoretical results for the secondary flow velocity  $\phi_N(0)$  and the diffusion mass transfer rate  $\psi'_N(0)$ , obtained through a numerical method, and the results of the asymptotic theory  $\phi(0)$  and  $\psi'(0)$ . It can be seen from the table that the

approximation accuracy of the asymptotic theory is high enough for the practical calculations of the mass transfer kinetics.

The difference in the mass transfer rates for the absorption and desorption processes of highly soluble gases was noticed experimentally by several authors [18, 23, 47, 52]. In all cases it was explained with the help of Marangoni effect, i.e. a hydrodynamic effect induced from a secondary flow whose rate is tangential to the interphase surface. This flow is attributed to the appearance of a surface tension gradient due to the non-uniform temperature and/or concentration distribution at the interphase boundary. The present study proposes a theory, which explains these experimental results using non-linear effects due to induced secondary flows, which rate is normally directed to the phase boundary. The secondary flows are induced by high mass fluxes.

Clarification of the mass transfer mechanism in the cases of intensive interphase mass transfer requires experimental data for the absorption and the desorption and a comparative analysis of these data with the help of the theory of non-linear mass transfer, and the Marangoni effect. Considering this matter it is very interesting to define normal secondary flows and to explain their influences (as a result of intensive interphase mass transfer) on the hydrodynamic stability of the flows at the interphase boundary.

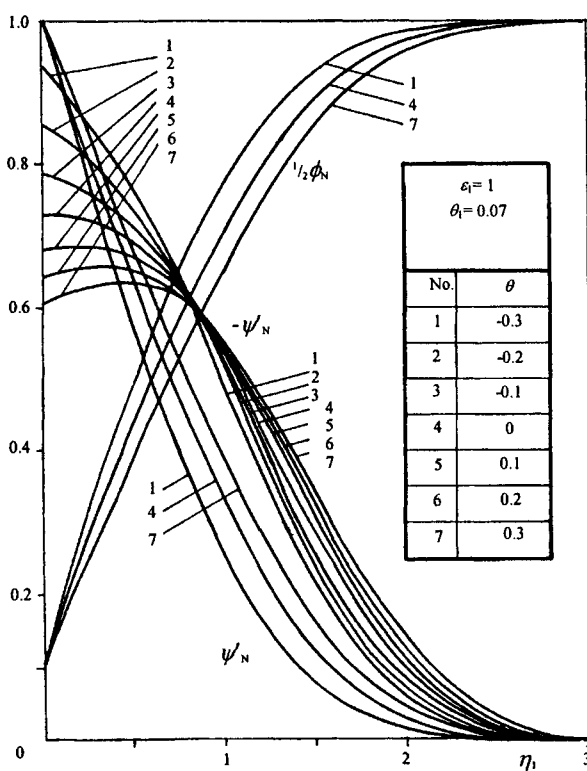


Fig. 1.14. Numerical solutions in gas phase.

**Table 1.8.**  
Compression between the numerical and asymptotic solutions

$\theta_3$	$\theta_1$	$\phi_N(0)$	$\phi(0)$	$-\psi'_N(0)$	$-\psi'(0)$
0	0.0720	0	0	0.730	0.733
0.1	0.0723	0.0785	0.0784	0.785	0.794
-0.1	0.0718	-0.0682	-0.0687	0.682	0.690
0.2	0.0725	0.1700	0.1660	0.851	0.857
-0.2	0.0716	-0.1280	-0.1280	0.641	0.650
0.3	0.0730	0.2800	0.2640	0.932	0.929
-0.3	0.0714	-0.1820	-0.1770	0.605	0.618

#### 1.4.2. Non-linear effects in the case of a multicomponent interphase mass transfer between the gas and the liquid film

Earlier in this book it was shown that the non-linear mass transfer (as a result of the intensive mass transfer in the gas phase) leads to a significant change in the velocity distribution in the liquid and the gas. In the cases of a multicomponent mass transfer it leads not only to a change in the mass transfer rate of the component with the higher concentration gradient, but also to a change in the mass transfer rate of the components, which concentration gradients do not influence the hydrodynamics of the flow.

There are numerous experimental works [10, 11, 23], in which the mass transfer of one of the components is considered as a cause of the change of the mass transfer of other components as a result of a parallel interphase mass transfer in gas-liquid and liquid-liquid systems. In these cases a rise in the mass transfer rate is observed, which is explained with the Marangoni effect, since this cannot be done within the linear theory of mass transfer [5].

This effect has been considered as a multicomponent interphase mass transfer in the cases when the concentration of one of the components in the gas phase influences the hydrodynamics of the flow, i.e. as a non-linear effect.

Let  $\tilde{c}_i$  and  $c_i$  ( $i = 1, \dots, n$ ) are the concentrations of the components in the gas and in the liquid respectively, mass transfer of which does not affect the hydrodynamics of the flow. The distributions of the concentrations are determined from:

$$\tilde{u} \frac{\partial \tilde{c}_i}{\partial x} + \tilde{v} \frac{\partial \tilde{c}_i}{\partial y} = \tilde{D}_i \frac{\partial^2 \tilde{c}_i}{\partial y^2};$$

$$x = 0, \quad \tilde{c}_i = \tilde{c}_{0i};$$

$$y = h, \quad \tilde{c}_i = \chi c_i;$$

$$y \rightarrow \infty, \quad \tilde{c}_i = \tilde{c}_{0i};$$

$$u \frac{\partial c_i}{\partial x} + v \frac{\partial c_i}{\partial y} = D_i \frac{\partial^2 c_i}{\partial y^2};$$

$$x = 0, \quad c_i = c_{0i};$$

$$y = 0, \quad \frac{\partial c_i}{\partial y} = 0;$$

$$y = h, \quad I_i = \tilde{I}_i, \quad i = 1, \dots, n, \quad (1.169)$$

where the mass fluxes  $I_i$  and  $\tilde{I}_i$  have diffusive and convective components because of the non-linear mass transfer of the component with the highest concentration gradient:

$$\begin{aligned} \tilde{I}_i &= -M_i \tilde{D}_i \left( \frac{\partial \tilde{c}_i}{\partial y} \right)_{y=h} + M_i \tilde{v}_n (\tilde{c}_i)_{y=h}, \\ I_i &= -M_i D_i \left( \frac{\partial c_i}{\partial y} \right)_{y=h} + M_i v_n (c_i)_{y=h}, \quad i = 1, \dots, n, \\ \tilde{v}_n &= -\frac{M \tilde{D}}{\tilde{\rho}_0} \left( \frac{\partial \tilde{c}}{\partial y} \right)_{y=h}, \quad v_n = -\frac{MD}{\rho_0} \left( \frac{\partial c}{\partial y} \right)_{y=h}. \end{aligned} \quad (1.170)$$

In (1.169) and (1.170) the velocity distribution is determined (see 1.4.1.) considering the non-linear mass transfer of one of the components in the gas phase.

The solution of the problem (1.169) allows to find the mass transfer rate:

$$\begin{aligned} J_i &= M_i \tilde{K}_i (\tilde{c}_{0i} - \chi_i c_{0i}) = \frac{1}{L} \int_0^L \tilde{I}_i dx = \\ &= M_i \tilde{K}_i (\tilde{c}_{0i} / \chi_i - c_{0i}) = \frac{1}{L} \int_0^L I_i dx, \quad i = 1, \dots, n. \end{aligned} \quad (1.171)$$

Here a mathematical description in a zero-th order approximation of the small parameter  $(h_0 / L)^2$  is used, as it has been done in (1.51).

The Sherwood number for the gas and the liquid is obtained from (1.170):

$$\begin{aligned} S\tilde{h}_i &= \frac{\tilde{K}_i L}{\tilde{D}_i} = \frac{1}{M_i \tilde{D}_i (\tilde{c}_{0i} - \chi_i c_{0i})} \int_0^L \tilde{I}_i dx, \\ Sh_i &= \frac{K_i L}{D_i} = \frac{\chi_i}{M_i D_i (\tilde{c}_{0i} - \chi_i c_{0i})} \int_0^L I_i dx, \quad i = 1, \dots, n. \end{aligned} \quad (1.172)$$

In order to solve (1.169) it is necessary to introduce the dimensionless variables (1.140) and

$$\tilde{C}_i = \frac{\tilde{c}_i - \chi_i c_{0i}}{\tilde{c}_{0i} - \chi_i c_{0i}}, \quad C_i = \frac{c_i - c_{0i}}{\tilde{c}_{0i} / \chi_i - c_{0i}}, \quad i = 1, \dots, n. \quad (1.173)$$

In the new variables the problem (1.169) has the form:

$$\begin{aligned}
& \tilde{U} \frac{\partial \tilde{C}_i}{\partial X} + \tilde{V} \frac{\partial \tilde{C}_i}{\partial \tilde{Y}} = \left( \frac{\tilde{\varepsilon}}{\varepsilon_i} \right)^2 \frac{\partial^2 \tilde{C}_i}{\partial \tilde{Y}^2} + \delta_0 H' \tilde{U} \frac{\partial \tilde{C}_i}{\partial \tilde{Y}} ; \\
& X = 0, \quad \tilde{C}_i = I ; \\
& \tilde{Y} = 0, \quad \tilde{C}_i = (C_i)_{Y=H} ; \\
& \tilde{Y} \rightarrow \infty, \quad \tilde{C}_i = 1 ; \quad i = 1, \dots, n . \tag{1.174}
\end{aligned}$$

$$\begin{aligned}
& U \frac{\partial C_i}{\partial X} + V \frac{\partial C_i}{\partial Y} = F o_i \frac{\partial^2 C_i}{\partial Y^2} ; \\
& X = 0, \quad C_i = 0 ; \\
& Y = 0, \quad \frac{\partial C_i}{\partial Y} = 0 ; \\
& Y = H, \quad \frac{\partial C_i}{\partial Y} = \beta_i \left( \frac{\partial \tilde{C}_i}{\partial \tilde{Y}} \right)_{\tilde{Y}=0} + \\
& + \theta_3 \beta_i \frac{\tilde{D}_i}{\tilde{D}_i} \left[ \frac{\chi_i c_{0i}}{\tilde{c}_{0i} - \chi_i c_{0i}} + (\tilde{C}_i)_{\tilde{Y}=0} \right] \left( \frac{\partial \tilde{C}_i}{\partial \tilde{Y}} \right)_{\tilde{Y}=0} - \\
& - \varepsilon_0 \theta_3 \frac{\tilde{D}_i \tilde{\rho}^*}{D_i \rho_0} \left[ \frac{\chi_i c_{0i}}{\tilde{c}_{0i} - \chi_i c_{0i}} + (C_i)_{Y=H} \right] \left( \frac{\partial \tilde{C}_i}{\partial \tilde{Y}} \right)_{\tilde{Y}=0}, \quad i = 1, \dots, n , \tag{1.175}
\end{aligned}$$

where

$$\tilde{\varepsilon}_i = \tilde{S} c_i^2, \quad \tilde{S} c_i = \frac{\tilde{V}}{\tilde{D}_i}, \quad \beta_i = \frac{\delta_0 \chi_i \tilde{D}_i}{D_i}, \quad F o_i = \frac{D_i L}{u_0 h_0^2}, \quad i = 1, \dots, n . \tag{1.176}$$

In references [3,7] it was shown that in cases of non-linear mass transfer of highly soluble gases  $\delta_0 \rightarrow 0$ , i.e. in (1.174) and (1.175) the terms, proportional to  $\delta_0$ , can be ignored.

The mass transfer in the gas phase limits the mass transfer rate, when  $\beta_i \ll 1$ . In this case from (1.176) it follows:

$$\beta_i = 0, \quad \left( \frac{\partial C_i}{\partial Y} \right)_{Y=H} = 0, \quad C_i = 0, \quad i = 1, \dots, n , \tag{1.177}$$

$$\begin{aligned}
& \tilde{U} = \frac{1}{2} \tilde{\varepsilon} \phi', \quad \tilde{V} = \frac{\tilde{\varepsilon}}{2\sqrt{X}} (\eta \phi' - \phi), \quad \tilde{C}_i = 1 - \tilde{\psi}_i, \\
& \phi = \phi(\eta), \quad \tilde{\psi}_i = \tilde{\psi}_i(\eta), \quad \eta = \frac{\tilde{Y}}{2\sqrt{X}}, \quad i = 1, \dots, n . \tag{1.178}
\end{aligned}$$

In this way (1.175) takes the form:

$$\begin{aligned} \psi_i'' + \bar{a}_i \phi \psi_i' &= 0, \\ \psi_i(0) = 1, \quad \psi_i(\infty) = 0, \quad i = 1, \dots, n, \end{aligned} \quad (1.179)$$

where  $\bar{a}_i = \varepsilon_i^2 / \tilde{\varepsilon}$  and  $\phi(\eta)$  denotes the non-linear mass transfer in the gas and is determined asymptotically in 1.4.1. Having in mind that  $\phi$  depends on two small parameters  $\theta_1$  and  $\theta_3$ , for the solution of (1.179) the following series can be used:

$$A = A_0 + \theta_1 A_1 + \theta_3 A_3 + \theta_1^2 A_{11} + \theta_3^2 A_{33} + \theta_1 \theta_3 A_{13} + \dots, \quad (1.180)$$

where  $A$  is a vector function:

$$A = (\phi \tilde{\psi}_i), \quad i = 1, \dots, n. \quad (1.181)$$

Using the approximation for  $\phi$  from 1.4.1., a number of finite problems for  $\tilde{\psi}_i$  is obtained [44], that are solved through the methods used to obtain (1.159):

$$\begin{aligned} \tilde{\psi}_{0i}(\eta) &= 1 - \frac{1}{\varphi_{0i}} \int_0^z E(\varepsilon_i, p) dp, \quad z = \frac{2}{\tilde{\varepsilon}} \eta, \\ \varphi_{0i} &= \int_0^\infty E(\varepsilon_i, p) dp \approx 3.01 \tilde{S} c_i^{-0.35}, \quad E(\varepsilon_i, p) = \exp \left[ -\frac{\varepsilon_i^2}{2} \int_0^p f(s) ds \right], \\ \tilde{\psi}_{1i}(\eta) &= \frac{3}{2\alpha \varphi_{0i}} - \frac{3}{2\alpha \varphi_{0i}^2} \int_0^z E(\varepsilon_i, p) dp - \frac{3}{2\alpha \varphi_{0i}} E(\varepsilon_i, z), \\ \tilde{\psi}_{3i}(\eta) &= \frac{\bar{a}_i}{\tilde{\varepsilon} \varphi_0 \varphi_{0i}} \int_0^z \left[ \int_0^p \varphi(s) ds \right] E(\varepsilon_i, p) dp - \frac{\bar{a}_i \varphi_{3i}}{\tilde{\varepsilon} \varphi_0 \varphi_{0i}^2} \int_0^z E(\varepsilon_i, p) dp, \\ \varphi_{3i} &= \int_0^\infty \left[ \int_0^p \varphi(s) ds \right] E(\varepsilon_i, p) dp \approx 6.56 \tilde{S} c_i^{-0.8}, \\ \tilde{\psi}_{11i}(\eta) &= \left( -\frac{9\bar{a}_i \tilde{\varepsilon} \varphi_{2i}}{8\varphi_{0i}^2} - \frac{9}{4\alpha^2 \varphi_{0i}^3} + \frac{9\bar{a}_i^2 \tilde{\varepsilon}^2 \varphi_{1i}}{32\alpha^2 \varphi_{0i}^2} \right) \int_0^z E(\varepsilon_i, p) dp + \\ &+ \frac{9\bar{a}_i \tilde{\varepsilon}}{8\varphi_{0i}} \int_0^z \left[ \int_0^p F(s) ds \right] E(\varepsilon_i, p) dp + \frac{9}{4\alpha^2 \varphi_{0i}^2} [1 - E(\varepsilon_i, z)] - \\ &- \frac{9\bar{a}_i^2 \tilde{\varepsilon}^2}{32\alpha^2 \varphi_{0i}} \int_0^z f^2(p) E(\varepsilon_i, p) dp, \\ \varphi_{1i} &= \int_0^\infty f^2(p) E(\varepsilon_i, p) dp \approx 3.01 \tilde{S} c_i^{-1.608}, \end{aligned}$$

$$\begin{aligned}
\varphi_{2i} &= \int_0^\infty \left[ \int_0^p F(s) ds \right] E(\varepsilon_i, p) dp \approx 3.052 \tilde{S} c_i^{-1.283}, \\
\psi_{33i}(\eta) &= \left( -\frac{\bar{a}_i \varphi_3 \varphi_{3i}}{\tilde{\varepsilon} \varphi_0^3 \varphi_{0i}^2} - \frac{\bar{a}_i^2 \varphi_{3i}^2}{\tilde{\varepsilon}^2 \varphi_0^2 \varphi_{0i}^3} + \frac{\bar{a}_i^2 \varphi_{33i}}{2\tilde{\varepsilon}^2 \varphi_0^2 \varphi_{0i}^2} + \frac{2\bar{a}_i \varphi_{33i}}{\tilde{\varepsilon}^3 \varphi_0^2 \varphi_{0i}^2} \right) \int_0^z E(\varepsilon_i, p) dp + \\
&+ \left( \frac{\bar{a}_i \varphi_3}{\varepsilon \varphi_0^3 \varphi_{0i}} + \frac{\bar{a}_i^2 \varphi_{3i}^2}{\tilde{\varepsilon}^2 \varphi_0^2 \varphi_{0i}^2} \right) \int_0^z \left[ \int_0^p \varphi(s) ds \right] E(\varepsilon_i, p) dp - \frac{\bar{a}_i^2}{2\tilde{\varepsilon}^2 \varphi_0^2 \varphi_{0i}} \int_0^z \left[ \int_0^p \varphi(s) ds \right]^2 E(\varepsilon_i, p) dp \\
&- \frac{2\bar{a}_i}{\tilde{\varepsilon}^3 \varphi_0 \varphi_{0i}} \int_0^z \left[ \int_0^p \bar{\varphi}(s) ds \right] E(\varepsilon_i, p) dp, \\
\varphi_{33i} &= \int_0^\infty \left[ \int_0^p \varphi(s) ds \right]^2 E(\varepsilon_i, p) dp \approx 24 \tilde{S} c_i^{-1.3}, \\
\bar{\varphi}_{33i} &= \int_0^\infty \left[ \int_0^p \bar{\varphi}(s) ds \right] E(\varepsilon_i, p) dp \approx 0.326 \tilde{S} c_i^{-1.63}, \\
\tilde{\psi}_{13i}(\eta) &= \left( -\frac{3\bar{a}_i \varphi_{3i}(\varphi_{0i} + \varphi_0)}{2\alpha\tilde{\varepsilon} \varphi_0^2 \varphi_{0i}^2} + \frac{3\bar{a}_i \varphi_{13i}}{2\alpha\tilde{\varepsilon} \varphi_0 \varphi_{0i}^2} + \frac{3\bar{a}_i \bar{\varphi}_{13i}}{2\alpha\tilde{\varepsilon} \varphi_0 \varphi_{0i}^2} \right) \int_0^z E(\varepsilon_i, p) dp + \\
&+ \frac{3\bar{a}_i(\varphi_{0i} + \varphi_0)}{2\alpha\tilde{\varepsilon} \varphi_0^2 \varphi_{0i}^2} \int_0^z \left[ \int_0^p \varphi(s) ds \right] E(\varepsilon_i, p) dp - \frac{3\bar{a}_i}{2\alpha\tilde{\varepsilon} \varphi_0 \varphi_{0i}} \int_0^z \left[ \int_0^p \bar{\varphi}(s) ds \right] E(\varepsilon_i, p) dp + \\
&+ \frac{3\bar{a}_i}{2\alpha\tilde{\varepsilon} \varphi_0 \varphi_{0i}} E(\varepsilon_i, z) \int_0^z \varphi(s) ds - \frac{3\bar{a}_i}{2\alpha\tilde{\varepsilon} \varphi_0 \varphi_{0i}} \int_0^z \varphi(p) E(\varepsilon_i, p) dp + \frac{3\bar{a}_i \varphi_{3i}}{2\alpha\tilde{\varepsilon} \varphi_0 \varphi_{0i}^2} [l - E(\varepsilon_i, z)], \\
\varphi_{13i} &= \int_0^\infty \left[ \int_0^p \bar{\varphi}(s) ds \right] E(\varepsilon_i, p) dp \approx \tilde{S} c_i^{-1.3}, \\
\bar{\varphi}_{13i} &= \int_0^\infty \varphi(p) E(\varepsilon_i, p) dp \approx 4.18 \tilde{S} c_i^{-0.46}, \quad i = 1, \dots, n. \tag{1.182}
\end{aligned}$$

The determination of expressions (1.182) makes it possible to find the Sherwood number. That is why (1.170) and (1.173) are substituted in (1.172):

$$\begin{aligned}
\tilde{S} h_i &= \sqrt{\tilde{P} e} \left[ - \int_0^1 \left( \frac{\partial \tilde{C}_i}{\partial \tilde{Y}} \right)_{\tilde{Y}=0} dX - \theta_3 \frac{\tilde{D}_i c_{0i}}{\tilde{D}_i (\tilde{c}_{0i} - \chi_i c_{0i})} \int_0^1 \left( \frac{\partial \tilde{C}}{\partial \tilde{Y}} \right)_{\tilde{Y}=0} dX \right], \\
i &= 1, \dots, n. \tag{1.183}
\end{aligned}$$

In the cases of highly soluble gases  $\chi_i \rightarrow 0$ , i.e. the second term is insignificant. Using this condition and (1.179), the relationship takes the following form:

$$\tilde{S}h_i = -\sqrt{\tilde{P}e} \int_0^1 \left( \frac{\partial \tilde{C}_i}{\partial \tilde{Y}} \right)_{\tilde{Y}=0} dX = \sqrt{\tilde{P}e} \psi'_i(0), \quad i = 1, \dots, n, \quad (1.184)$$

where  $\psi'_i(0)$  is defined from the expression:

$$\begin{aligned} \psi'_i(0) = & -\frac{2}{\tilde{\varepsilon}\varphi_{0i}} - \theta_1 \frac{3}{\alpha\tilde{\varepsilon}\varphi_{0i}^2} - \theta_3 \frac{2\bar{a}_i\varphi_{3i}}{\tilde{\varepsilon}^2\varphi_0\varphi_{0i}^2} - \\ & - \theta_1^2 \left( \frac{9\bar{a}_i\varphi_{2i}}{4\varphi_{0i}^2} + \frac{9}{2\alpha^2\tilde{\varepsilon}\varphi_{0i}^3} - \frac{9\bar{a}_i^2\tilde{\varepsilon}\varphi_{2i}}{16\alpha^2\varphi_{0i}^2} \right) - \\ & - \theta_3^2 \left( \frac{2\bar{a}_i\varphi_3\varphi_{3i}}{\tilde{\varepsilon}^2\varphi_0^2\varphi_{0i}^2} + \frac{2\bar{a}_i^2\varphi_{3i}^2}{\tilde{\varepsilon}^3\varphi_0^2\varphi_{0i}^3} - \frac{\bar{a}_i^2\varphi_{33i}}{\tilde{\varepsilon}^3\varphi_0^2\varphi_{0i}^2} - \frac{4\bar{a}_i\bar{\varphi}_{33i}}{\tilde{\varepsilon}^4\varphi_0^2\varphi_{0i}^2} \right) - \\ & - \theta_1\theta_3 \frac{3\bar{a}_i}{\alpha\tilde{\varepsilon}^2\varphi_0\varphi_{0i}^2} \left[ \varphi_{3i} \left( 1 + \frac{\varphi_{0i}}{\varphi_0} \right) + \varphi_{13i} + \bar{\varphi}_{13i} \right], \quad i = 1, \dots, n. \end{aligned} \quad (1.185)$$

The comparison of  $\psi'_i(0)$  and  $\tilde{\psi}'_i(0)$ , carried out in 1.4.1., shows that they are very close, with an insignificant difference in the values of  $\tilde{\varepsilon}_i$  and  $\tilde{\varepsilon}$ . From here it follows that in cases of multicomponent mass transfer, when the mass transfer of one of the components is non-linear due to a high concentration gradient, the mass transfer coefficients of all components have close values. In this way, the non-linear effects are the same for the mass transfer coefficients of all components.

The mass transfer rate is limited by the mass transfer in the liquid phase, when  $\beta_i \gg 1$ . In this case from (1.175) it follows:

$$\begin{aligned} \beta_i^{-1} = 0, \quad \left( \frac{\partial \tilde{C}_i}{\partial \tilde{Y}} \right)_{\tilde{Y}=0} = 0, \quad \tilde{C}_i \equiv 1, \quad (C_i)_{Y=H} = (\tilde{C}_i)_{\tilde{Y}=0} = 1, \\ i = 1, \dots, n. \end{aligned} \quad (1.186)$$

and the problem is diminished to the solution of (1.175), considering (1.186), and  $U$ ,  $V$  and  $H$  are defined in 1.4.1. For this aim the variables of the diffusive boundary layer are introduced:

$$Y_i = \frac{H - Y}{\sqrt{Fo_i}}, \quad i = 1, \dots, n. \quad (1.187)$$

In this way, the problem (1.175) takes the form:

$$\begin{aligned} U \frac{\partial C_i}{\partial X} + \frac{H'U - V}{\sqrt{Fo_i}} \frac{\partial C_i}{\partial Y_i} = \frac{\partial^2 C_i}{\partial Y_i^2}, \\ X = 0, \quad C_i = 0; \end{aligned}$$

$$\begin{aligned} Y_i &= 0, \quad C_i = I; \\ Y_i &\rightarrow \infty, \quad C_i = 0, \quad i = 1, \dots, n. \end{aligned} \tag{1.188}$$

If the following substitutions are made:

$$\delta_1 = Fo_i, \quad \delta_2 = \theta_2, \quad \delta_3 = \theta_0\theta_3, \quad \delta_4 = \frac{\theta_0\theta_3}{\sqrt{Fo_i}}, \quad i = 1, \dots, n, \tag{1.189}$$

then the problem (1.188) takes the following form in the first order approximation of the small variables  $\delta_1, \delta_2, \delta_3, \delta_4$  ( $i = 1, \dots, n$ ):

$$\begin{aligned} &\left[ \frac{3}{2}(1 - \delta_{1i}Y_i^2) + \delta_2 \frac{\alpha}{2\tilde{\varepsilon}\sqrt{X}} - \delta_3 \frac{2}{\tilde{\varepsilon}\varphi_0} (\sqrt{L_\infty/L} - \sqrt{X}) \right] \frac{\partial C_i}{\partial X} + \\ &+ \left[ \delta_2 \frac{\alpha Y_i}{4\tilde{\varepsilon}X\sqrt{X}} - \delta_3 \frac{Y_i}{\tilde{\varepsilon}\varphi_0\sqrt{X}} + \delta_4 \frac{1}{\tilde{\varepsilon}\varphi_0\sqrt{X}} \right] \frac{\partial C_i}{\partial Y_i} = \frac{\partial^2 C_i}{\partial Y_i^2}; \\ &X = 0, \quad C_i = 0; \\ &Y_i = 0, \quad C_i = I; \\ &Y_i \rightarrow \infty, \quad C_i = 0, \quad i = 1, \dots, n. \end{aligned} \tag{1.190}$$

From (1.190) it follows that for the solution of the problem the following series may be used:

$$C_i = C_{0i} + \delta_{1i}C_{1i} + \delta_2C_{2i} + \delta_3C_{3i} + \delta_4C_{4i} + \dots, \tag{1.191}$$

In this way with the help of the perturbation method finite problems are obtained. In a zero-th order approximation it may be written:

$$\begin{aligned} &\frac{3}{2} \frac{\partial C_{0i}}{\partial X} = \frac{\partial^2 C_{0i}}{\partial Y_i^2}; \\ &X = 0, \quad C_{0i} = 0; \\ &Y_i = 0, \quad C_{0i} = I; \\ &Y_i \rightarrow \infty, \quad C_{0i} = 0, \quad i = 1, \dots, n, \end{aligned} \tag{1.192}$$

where for  $C_{0i}$  it was obtained [5]:

$$C_{0i} = erfc\zeta_i, \quad \zeta_i = \left( \frac{3Y_i^2}{8X} \right)^{1/2}, \quad i = 1, \dots, n. \tag{1.193}$$

In the first order approximation of  $\delta_{1i}$  the following relations can be written:

$$\begin{aligned} \frac{3}{2} \frac{\partial C_{ii}}{\partial X} &= \frac{\partial^2 C_{ii}}{\partial Y_i^2} + \frac{3}{2} Y_i^2 \frac{\partial C_{0i}}{\partial X}; \\ X = 0, \quad C_{ii} &= 0; \\ Y_i = 0, \quad C_{ii} &= I; \\ Y_i \rightarrow \infty, \quad C_{ii} &= 0, \quad i = 1, \dots, n, \end{aligned} \tag{1.194}$$

where  $C_{ii}$  is determined [5] with the help of the Green function:

$$C_{ii} = \frac{1}{\sqrt{6\pi}} \left( Y_i \sqrt{X} + \frac{Y_i^3}{2\sqrt{X}} \right) \exp\left(-\frac{3Y_i^2}{8X}\right), \quad i = 1, \dots, n. \tag{1.195}$$

In the first order approximation of  $\delta_2$ , the following relations can be written:

$$\begin{aligned} \frac{3}{2} \frac{\partial C_{2i}}{\partial X} - \frac{\partial^2 C_{2i}}{\partial Y_i^2} &= \frac{\alpha}{2\tilde{\varepsilon}\sqrt{X}} \left( \frac{\partial C_{0i}}{\partial X} + \frac{Y_i}{2\sqrt{X}} \frac{\partial C_{0i}}{\partial Y_i} \right); \\ X = 0, \quad C_{2i} &= 0; \\ Y_i = 0, \quad C_{2i} &= I; \\ Y_i \rightarrow \infty, \quad C_{2i} &= 0, \quad i = 1, \dots, n, \end{aligned} \tag{1.196}$$

where the right part is equal to zero, i.e.  $C_{2i} \equiv 0$ .

In the first order approximation of  $\delta_3$ , the following relations can be written:

$$\begin{aligned} \frac{3}{2} \frac{\partial C_{3i}}{\partial X} &= \frac{\partial^2 C_{3i}}{\partial Y_i^2} + \frac{2}{\tilde{\varepsilon}_0 \varphi} \left( \sqrt{L_\infty/L} - \sqrt{X} \right) \frac{\partial C_{0i}}{\partial X} + \frac{Y_i}{\tilde{\varepsilon} \varphi_0 \sqrt{X}} \frac{\partial C_{0i}}{\partial Y_i}; \\ X = 0, \quad C_{3i} &= 0; \\ Y_i = 0, \quad C_{3i} &= 0; \\ Y_i \rightarrow \infty, \quad C_{3i} &= 0, \quad i = 1, \dots, n, \end{aligned} \tag{1.197}$$

where  $C_{3i}$  is determined with the help of the Green function:

$$C_{3i} = \sqrt{\frac{2}{3\pi}} \frac{1}{\tilde{\varepsilon} \varphi_0} \left( \sqrt{L_\infty/L} \frac{Y_i}{\sqrt{X}} - \frac{4}{3} Y_i \right) \exp\left(-\frac{3Y_i^2}{8X}\right), \quad i = 1, \dots, n. \tag{1.198}$$

In the first order approximation of  $\delta_4$ , the following relations can be written:

$$\frac{3}{2} \frac{\partial C_{4i}}{\partial X} = \frac{\partial^2 C_{4i}}{\partial Y_i^2} - \frac{1}{\tilde{\varepsilon} \varphi_0 \sqrt{X}} \frac{\partial C_{0i}}{\partial Y_i};$$

$$\begin{aligned} X &= 0, \quad C_{4i} = 0; \\ Y_i &= 0, \quad C_{4i} = 0; \\ Y_i &\rightarrow \infty, \quad C_{4i} = 0, \quad i = 1, \dots, n, \end{aligned} \quad (1.199)$$

where  $C_{4i}$  is determined with the help of the Greene function:

$$C_{4i} = \frac{2}{\tilde{\varepsilon}\varphi_0} \sqrt{\frac{2}{3\pi}} \left[ \exp\left(-\frac{3Y_i^2}{8X}\right) - \operatorname{erfc}\left(-\frac{3Y_i^2}{8X}\right)^{1/2} \right], \quad i = 1, \dots, n. \quad (1.200)$$

The expressions obtained for  $C_{ii}, \dots, C_{4i}$ ,  $i = 1, \dots, n$ , allow to determine the Sherwood number. For this purpose from (1.170) – (1.173) and (1.187) the following relation is found:

$$\begin{aligned} Sh_i &= \sqrt{Pe_i} \int_0^1 \left( \frac{\partial C_i}{\partial Y_i} \right)_{Y_i=0} dX - \\ &- \frac{\tilde{c}_0 - \chi c_0}{\chi} \frac{MDL\beta}{\rho_0^* D_i h_0} \left[ \frac{\chi_i c_{10}}{\tilde{c}_{0i} - \chi_i c_{0i}} \int_0^1 \left( \frac{\partial \tilde{C}}{\partial \tilde{Y}} \right)_{\tilde{Y}=0} dX + \right. \\ &+ \left. \int_0^1 (C_i)_{Y_i=0} \left( \frac{\partial \tilde{C}}{\partial \tilde{Y}} \right)_{\tilde{Y}=0} dX \right] \approx \sqrt{Pe_i} \int_0^1 \left( \frac{\partial C_i}{\partial Y_i} \right)_{Y_i=0} dX, \\ i &= 1, \dots, n, \end{aligned} \quad (1.201)$$

where  $Pe_i = u_0 L / D_i$ . From (1.179) – (1.188) it is finally obtained:

$$\begin{aligned} Sh_i &= -\sqrt{\frac{6Pe_i}{\pi}} \left[ 1 - \frac{\delta_{ii}}{9} - \frac{2\delta_3}{3\tilde{\varepsilon}\varphi_0} \left( \sqrt{L_\infty / L} - \frac{2}{3} \right) - \right. \\ &\left. - \frac{2\delta_{4i}}{\tilde{\varepsilon}\varphi_0} \sqrt{\frac{2}{3\pi}} \right], \quad i = 1, \dots, n. \end{aligned} \quad (1.202)$$

From (1.189) it can be seen that parameters  $\delta_3$  and  $\delta_{4i}$  have the form:

$$\begin{aligned} \delta_3 &= \frac{\tilde{\rho}^*}{\tilde{\rho}_0^*} \frac{\sqrt{\tilde{D}\tilde{u}_0 L}}{u_0 h_0} \frac{M(\tilde{c}_0 - \chi c_0)}{\rho_0^*}, \\ \delta_{4i} &= \frac{\tilde{\rho}^*}{\tilde{\rho}_0^*} \frac{\sqrt{\tilde{D}\tilde{u}_0 h_0}}{D_i u_0} \frac{M(\tilde{c}_0 - \chi c_0)}{\rho_0^*}, \quad i = 1, \dots, n \end{aligned} \quad (1.203)$$

and depend on the concentration gradient of the component with the intensive mass transfer, i.e. the mass transfer rate of the components in the liquid is determined by the concentration

gradient of the component with the intensive mass transfer and depends on the mass transfer direction.

Absorption (desorption) of the component with the intensive mass transfer leads to a decrease (increase) in the diffusive mass transfer of the rest of the components in the liquid. Comparing (1.186) and (1.203), it becomes clear that the effect of the intensive mass transfer direction is opposite to the cases when the mass transfer in the gas or the liquid limits the mass transfer in the components with low concentration gradients.

## CHAPTER 1.5. EFFECTS OF CONCENTRATION AND TEMPERATURE ON THE NON- LINEAR MASS TRANSFER

The theoretical analysis of non-linear the mass transfer and the hydrodynamic stability of the systems with intensive interphase mass transfer which has been done so far considers the “pure“ effect of large concentration gradients. Under these conditions, however, the concentrations themselves are high and their influence is manifested by the concentration dependencies of density, viscosity and diffusivity. In order to determine these effects the use of the basic model of non-linear mass transfer is needed.

### 1.5.1. Concentration effects

The theoretical analysis of the dependence of the velocity of induced flow from the concentration gradient will be developed in the case of laminar gas flow flowing over solid surface. Consider a binary gas mixture, where the gas 2 has a partial density  $\rho_2$  and flows over the surface with an average mass velocity of  $w_2$ , while the gas 1 is injected through the solid surface with an average mass velocity of  $w_1$  and has a partial density  $\rho_1$ , i. e.

$$\rho = \sum_{i=1}^2 \rho_i, \quad w = \frac{\sum_{i=1}^2 \rho_i w_i}{\rho}. \quad (1.204)$$

The diffusion velocity  $W_i$  is the deviation of the velocity  $w_i$  from the gas mixture velocity  $w$ :

$$W_i = w_i - w, \quad i = 1, 2. \quad (1.205)$$

From (1.205) it directly follows that

$$\sum_{i=1}^2 \rho_i w_i = w \sum_{i=1}^2 \rho_i - \sum_{i=1}^2 \rho_i W_i = w\rho + \sum_{i=1}^2 \rho_i W_i. \quad (1.206)$$

Hence, from (1.204) and (1.205) is obtained

$$\sum_{i=1}^2 \rho_i W_i = 0. \quad (1.207)$$

The law of conservation of mass holds for each component:

$$\operatorname{div}(\rho_i \mathbf{w}_i) = \operatorname{div}[\rho_i (\mathbf{w}_i + \mathbf{W}_i)] = 0, \quad i = 1, 2, \quad (1.208)$$

accepting  $i$  as a summation index for the mixture one will be found:

$$\operatorname{div}(\rho \mathbf{w}) = 0. \quad (1.209)$$

Consider isothermal diffusion of gas 1 into gas 2. The mass flux of gas 1 as a result of the diffusion is defined from the mass concentration gradient:

$$\mathbf{J}_1 = c_1 \mathbf{W}_1 = -D_{12} \mathbf{grad} c_1, \quad c_1 = \rho_1 / \rho, \quad (1.210)$$

where  $D_{12}$  is the diffusivity,  $c_i$  - mass concentration of gas 1 (weight factors).

From (1.205), (1.208), and (1.210) is obtained:

$$\operatorname{div} \rho_i \mathbf{w} = \operatorname{div}(\rho D_{12} \mathbf{grad} c_1). \quad (1.211)$$

Using the formula

$$\operatorname{div}(ab) = b \mathbf{grad} a + a \operatorname{div} b \quad (1.212)$$

the following expression is directly obtained:

$$\operatorname{div}(c_1 \rho \mathbf{w}) = \rho \mathbf{w} \cdot \mathbf{grad} c_1 + c_1 \operatorname{div} \rho \mathbf{w}. \quad (1.213)$$

Taking into account (1.209) is obtained from (1.213) that

$$\rho \mathbf{w} \cdot \mathbf{grad} c_1 = \operatorname{div}(\rho D_{12} \mathbf{grad} c_1). \quad (1.214)$$

Having denoted with  $u$  and  $v$  the components of the velocity  $\mathbf{w}$  and applying the boundary layer approximation ( $\partial^2/\partial x^2 \ll \partial^2/\partial y^2$ ) from (1.214) one can be reached to the following:

$$\rho \left( u \frac{\partial c_1}{\partial x} + v \frac{\partial c_1}{\partial y} \right) = \frac{\partial}{\partial y} \left( \rho D_{12} \frac{\partial c_1}{\partial y} \right), \quad (1.215)$$

where  $u$  and  $v$  satisfy the equations of the gas mixture motion.

Only one limitation is applied while obtaining the above results - the processes are supported to be isothermal. Further, for definiteness one will be considered a potential gas flow with a constant velocity  $u_0$  over a semi-infinite flat plate. Thus, the equations of motion of the gas mixture assume the following form:

$$\rho \left( u \frac{\partial u}{\partial x} + v \frac{\partial u}{\partial y} \right) = \frac{\partial}{\partial y} \left( \mu \frac{\partial u}{\partial y} \right), \quad \operatorname{div} \rho w = 0; \\ x = 0, \quad u = u_0; \quad y = 0, \quad u = 0, \quad v = v_n; \quad y \rightarrow \infty, \quad u = u_0, \quad (1.216)$$

where  $v_n$  is the velocity of the induced by the intensive interphase mass transfer. This velocity is a normal component of the velocity  $w$  to the solid surface. If one is accepted that the second component of the gas does not go through the solid surface  $w_2$ , so from (1.205) could be directly obtained:

$$y = 0, \quad w = -W_2. \quad (1.217)$$

From (1.207) and (1.210) is found

$$-c_1 W_1 = c_2 W_2 = (1 - c_1) W_2 = D_{12} \operatorname{grad} c_1 \quad (1.218)$$

and (1.308) has the following form:

$$w = - \left( \frac{D_{12}}{1 - c_1} \operatorname{grad} c_1 \right)_{y=0} = - \left( \frac{D_{12} \rho}{\rho_2} \operatorname{grad} c_1 \right)_{y=0}. \quad (1.219)$$

Express the gas 1 concentration in (1.219) as moles per a unit volume, while for  $D_{12}$ ,  $\rho$  and  $\rho_2$  on the solid surface ( $y = 0$ ) the denotations  $D$ ,  $\rho^*$  and  $\rho_0^*$  can be used:

$$c = \rho_1/M, \quad D = D_{12}, \quad \rho^* = \rho, \quad \rho_0^* = \rho_2 (y = 0). \quad (1.220)$$

Thus, from (1.219) it could be obtained the normal component of the velocity on the phase boundary:

$$v_n = - \frac{MD\rho^*}{\rho_0^*} \left[ \frac{\partial}{\partial y} \left( \frac{c}{\rho} \right) \right]_{y=0}. \quad (1.221)$$

The results obtained so far (1.215), (1.216), (1.220), (1.221) allow to formulate in general the mass transfer in the diffusion boundary layer in the case of gas or liquid flow over semi-infinite flat plate at the boundary layer approximations:

$$\rho \left( u \frac{\partial u}{\partial x} + v \frac{\partial u}{\partial y} \right) = \frac{\partial}{\partial y} \left( \mu \frac{\partial u}{\partial y} \right),$$

$$u \frac{\partial \rho}{\partial x} + v \frac{\partial \rho}{\partial y} + \rho \left( \frac{\partial u}{\partial x} + \frac{\partial u}{\partial y} \right) = 0,$$

$$\rho \left( u \frac{\partial c}{\partial x} + v \frac{\partial c}{\partial y} \right) = \frac{\partial}{\partial y} \left( \rho D \frac{\partial c}{\partial y} \right); \quad (1.222)$$

$$\begin{aligned} x = 0, \quad u = u_0, \quad c = c_0; \\ y = 0, \quad u = 0, \quad v = - \frac{MD}{\rho_0^*} \left( \frac{\partial c}{\partial y} \right)_{y=0} - \frac{D(\rho^* - \rho_0^*)}{\rho^* \rho_0^*} \left( \frac{\partial \rho}{\partial y} \right)_{y=0}, \quad c = c^*; \\ y \rightarrow \infty, \quad u = u_0, \quad c = c_0, \end{aligned} \quad (1.223)$$

where

$$\rho^* = \rho_0^* + Mc^*. \quad (1.224)$$

Equation determining  $\rho$  should be added into (1.222) and (1.223). At constant pressure and temperature  $\rho$  cannot be obtained from the equation of state. According to (1.204)  $\rho$  depends only on the concentration of the components:

$$\rho = \rho_2 + Mc. \quad (1.225)$$

The comparison of (1.222-1.225) with the models (1.18) shows that the results of the asymptotic theory of non-linear mass transfer in systems with intensive interphase mass transfer have been obtained in the following approximations:

$$\rho = const, \quad \mu = const, \quad D = const. \quad (1.226)$$

The theoretical analysis of the influence of the diffused substance concentration on the density, viscosity and diffusivity shows that in a number of cases these effects can be considered as small [31] (first order approximation):

$$\begin{aligned} \rho = \rho_0(1 + \bar{\rho}C), \quad \mu = \mu_0(1 + \bar{\mu}C), \\ D = D_0(1 + \bar{D}C), \quad C = \frac{c - c_0}{c^* - c_0}, \end{aligned} \quad (1.227)$$

where  $\bar{\rho}$ ,  $\bar{\mu}$  and  $\bar{D}$  are small parameters defined from the experimental data for the dependence of  $\rho$ ,  $\mu$  and  $D$  from  $c$ .

The introduction of (1.226) and (1.227) into (1.223) leads to complete mathematical description of the hydrodynamics and the mass transfer in systems with intensive interphase mass transfer. These are practically simplified Oberbeck-Boussinesq equations, where the gravitational effect is negligible at the boundary layer approximations in the case of horizontal flat plate if the following condition is valid:

$$\frac{g}{u_0^2} \sqrt{\frac{\nu_0 l}{u_0}} < 10^{-2}, \quad \nu_0 = \frac{\mu_0}{\rho_0}, \quad (1.228)$$

i.e. the second Navier-Stokes equation reaches the usual form in the boundary layer approximations:

$$\frac{\partial p}{\partial y} = 0. \quad (1.229)$$

The concentration effects were investigated within the concentration range  $0 \div c_{max}$  where there is a significant effect of non-linear mass transfer ( $\theta = 0.3$ ). The concentration difference  $\Delta c$  can be determined by:

$$\Delta c = \frac{M(c^* - c_0)}{\rho_0} \quad (1.230)$$

and used to a normalize scale of concentrations:

$$C = c / \Delta c, \quad C^* = c^* / \Delta c, \quad C_{max} = c_{max} / \Delta c. \quad (1.231)$$

From Table 1.9 it is evident that for the diffusion of ammonia into air, the influence of the ammonia concentration on the density ( $\bar{\rho} C_{max}$ ) and viscosity ( $\bar{\mu} C_{max}$ ) is effected about 15-16%. For more precise analysis these effects must be taken into account. For gas mixtures the concentration effect on the diffusivity is negligible.

Table 1.9  
Maximum concentration effect on the density, viscosity and diffusivity.

system	ammonia air	acetic acid water	acetic acid toluen	acetone water	water acetone
$c_{max} \text{ kmol / m}^3$	0.0134	3.80	3.40	3.68	10.60
$\theta$	0.3	0.3	0.3	0.3	0.3
$\Delta c \text{ kmol / m}^3$	0.0160	3.92	3.52	3.81	10.9
$C_{max}$	0.837	0.969	0.967	0.967	0.968
$\bar{\rho}$	-0.149	0.0134	0.0420	-0.518	0.0461
$\bar{\rho} C_{max}$	-0.125	0.0130	0.0420	-0.050	0.0450
$\bar{\mu}$	-0.190	0.0208	0.263	-0.0854	0.746
$\bar{\mu} C_{max}$	-0.159	0.0200	0.254	-0.0830	0.722
$\bar{D}$	0	0	0	-0.336	-0.843
$\bar{D} C_{max}$	0	0	0	-0.325	-0.816

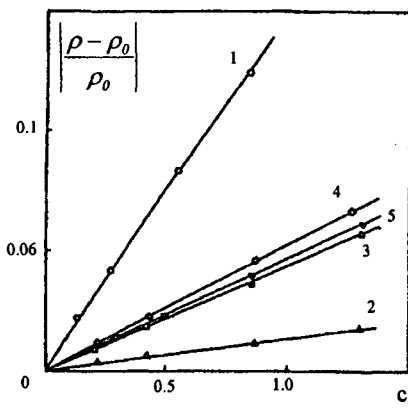


Fig. 1.15. Linear approximation of the dependence of the density on the concentration for different systems: (1) ammonia-air; (2) acetic acid -water; (3) acetic acid-toluene; (4) acetone-water; (5) water-acetone

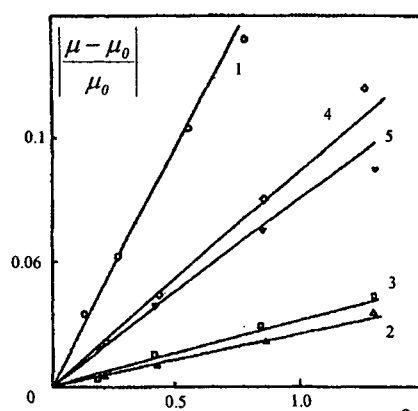


Fig. 1.16. Linear approximation of the dependence of the viscosity on the concentration for different systems: (1) ammonia-air; (2) acetic acid -water; (3) acetic acid-toluene; (4) acetone-water; (5) water-acetone

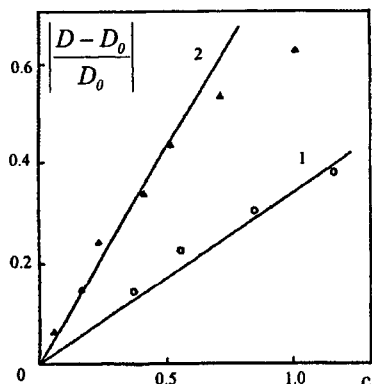


Fig. 1.17. Linear approximation of the dependence of the diffusivity on the concentration for different systems: (4) acetone in water; (5) water in acetone

For liquid mixtures the effect of the concentration on the density (Table 1.9) is a few percents (under 5%), which is valid for a great number of completely mixing pairs of liquids. There is a similar effect of the viscosity but with many exceptions (acetic acid - toluen, water - acetone).

The effect of the concentration on the diffusivity for a liquid diffused in another one is often significant [59]. For acetone - water (Table 1.9) the dependence deviates from the linear. In cases of the parameters  $\bar{\rho}$ ,  $\bar{\mu}$  and  $\bar{D}$  exceeding 0.3 the linear approximation (1.227) is not accurate enough, since neglecting the second order approximations leads to error of more than 10%.

The approximation accuracy (1.227) is shown on Figures 1.15-1.17. The accuracy is acceptable for relatively high concentration.

The analysis of the approximations of non-linear mass transfer theory [75], which is developed for  $\bar{\rho} = \bar{\mu} = \bar{D} = 0$  shows that the results are valid in the cases, where these parameters are small enough (for instance  $< 0.05$ ). It is valid for different systems gas (liquid) - solid, gas - liquid, liquid - liquid. At these conditions the hydrodynamics and the mass transfer depend on the concentration gradient ( $\theta$ ). When the parameters  $\bar{\rho}$ ,  $\bar{\mu}$  and  $\bar{D}$  are within the interval (0.1÷0.3) the concentration affects the mass transfer and this effect can be considered by introducing the linear approximation (1.227). For systems in which these parameters assume values greater than 0.3 the non-linear terms should be added into (1.227).

### 1.5.2. Influence of the high concentration on the mass transfer rate

The mass transfer rate can be expressed by the mass transfer coefficient. It will be defined from the average diffusion flux through a surface with a specific length  $L$ :

$$J = Mk(c^* - c_0) = \frac{M}{L} \frac{\rho^*}{\rho_0} \int_0^L D \left( \frac{\partial c}{\partial y} \right)_{y=0} dx. \quad (1.231)$$

The thickness of the diffusion boundary layer in gases and liquids is of different order of magnitude. That is why the different numerical algorithms [76] is used.

The thickness of laminar and diffusion boundary layers in gases is of the same order of magnitude, so one characteristic scale can be applied:

$$\delta_0 = \sqrt{\frac{D_0 L}{u_0}}. \quad (1.232)$$

The problem (1.222) can be expressed in the terms of the following dimensionless variables:

$$\begin{aligned} x &= LX, \quad y = \delta_0 Y, \\ u &= u_0 U, \quad v = v_0 \frac{\delta_0}{L} V, \quad c = c_0 + (c^* - c_0) C. \end{aligned} \quad (1.233)$$

Introducing (1.233) into (1.222) leads to the following equations

$$\begin{aligned}
& \varphi \left( U \frac{\partial U}{\partial X} + V \frac{\partial U}{\partial Y} \right) = Sc \frac{\partial}{\partial Y} \left( \psi \frac{\partial U}{\partial Y} \right), \\
& \frac{\partial}{\partial X} (\varphi U) + \frac{\partial}{\partial Y} (\varphi V) = 0, \\
& \varphi \left( U \frac{\partial C}{\partial X} + V \frac{\partial C}{\partial Y} \right) = \frac{\partial}{\partial Y} \left( \varphi \omega \frac{\partial C}{\partial Y} \right) \\
& X = 0, \quad U = 1, \quad C = 0; \\
& Y = 0, \quad U = 0, \quad V = -\theta \frac{\partial}{\partial Y} \left( \frac{\frac{c_0}{\Delta c} + C}{\varphi} \right), \quad C = 1; \\
& Y \rightarrow \infty, \quad U = 1, \quad C = 0,
\end{aligned} \tag{1.234}$$

where

$$\begin{aligned}
\theta_0 &= \frac{M \Delta c_0}{\rho_0^*} \varphi(1) \omega(1), \quad \rho^* = \rho_0 \varphi(1), \quad \rho_0^* = \rho_0 \varphi(1) - M c^*, \\
\Delta c_0 &= c^* - c_0, \quad Sc = \frac{\mu_0}{\rho_0 D_0}, \\
\varphi &= \varphi(C) = \rho / \rho_0, \quad \psi = \psi(C) = \mu / \mu_0, \quad \omega = \omega(C) = D / D_0, \\
\varphi(0) &= 1, \quad \psi(0) = 1, \quad \omega(0) = 1.
\end{aligned} \tag{1.235}$$

The solution of the problem (1.234) can be obtained after introducing the similarity variables:

$$\begin{aligned}
\varphi U &= \Phi', \quad \varphi V = \frac{1}{2\sqrt{X}} (\Phi' \eta - \Phi), \quad C = F, \\
\Phi &= \Phi(\eta), \quad F = F(\eta), \quad \eta = \frac{Y}{\sqrt{X}}, \quad \Phi' = \frac{d\Phi}{d\eta}.
\end{aligned} \tag{1.236}$$

Hence, directly from (1.234) is obtained the following:

$$\begin{aligned}
& 2Sc\varphi^2\psi\Phi'' + \varphi^2\Phi\Phi'' - \varphi\varphi'\Phi\Phi'F' + \\
& + 2Sc\varphi(\varphi\psi' - \varphi'\psi)\Phi''F' - 2Sc\varphi'(\varphi\psi' - 2\varphi'\psi)\Phi'F'^2 = 0, \\
& 2\varphi\omega F'' + 2(\varphi'\omega + \varphi'\psi)F'^2 + \Phi F' = 0, \\
& \Phi(0) = -\theta F'(0), \quad \Phi'(0) = 0, \quad \Phi'(\infty) = 1, \\
& F(0) = 1, \quad F(\infty) = 0, \quad \theta = 2\theta_0 \frac{\Delta c_0 \varphi(1) - c^* \varphi'(1)}{\Delta c_0 \varphi(1)}.
\end{aligned} \tag{1.237}$$

The functions  $\varphi, \psi$  and  $\omega$  in (1.237) are set outwardly by spline approximations of the experimental dependencies of  $\rho, \mu$  and  $D$  on  $c$ . For a wide range of gas mixtures these functions can be obtained with enough accuracy through the linear approximation

$$\varphi = I + \bar{\rho}C, \quad \psi = I + \bar{\mu}C, \quad \omega = I + \bar{D}C. \quad (1.238)$$

The introduction of (1.238) into (1.237) leads to the following equations:

$$\begin{aligned} & 2Sc(I + \bar{\rho}F)^2(I + \bar{\mu}F)\Phi'' + (I + \bar{\rho}F)^2\Phi\Phi'' - \bar{\rho}(I + \bar{\rho}F)\Phi\Phi'F' + \\ & + 2Sc(I + \bar{\rho}F)[\bar{\mu}(I + \bar{\rho}F) - \bar{\rho}(I + \bar{\mu}F)]\Phi''F' - 2Sc\bar{\rho}[\bar{\mu}(I + \bar{\rho}F) - \\ & - 2\bar{\rho}(I + \bar{\mu}F)]\Phi'F'^2 = 0, \\ & 2(I + \bar{\rho}F)(I + \bar{D}F)F'' + 2[\bar{\rho}(I + \bar{D}F) + \bar{D}(I + \bar{\rho}F)]F'^2 + \Phi F' = 0, \\ & \theta = 2\theta_0 \frac{1 - \frac{c_0}{\Delta c_0} \bar{\rho}}{I + \bar{\rho}}. \end{aligned} \quad (1.239)$$

The parameters  $\bar{\rho}$  and  $\bar{\mu}$  in (1.239) are small, while  $\bar{D} = 0$ . Omitting the square terms regarding the small parameters  $\bar{\rho}$  and  $\bar{\mu}$  leads to:

$$\begin{aligned} & 2Sc(I + 2\bar{\rho}F + \bar{\mu}F)\Phi''' + (I + 2\bar{\rho}F)\Phi\Phi'' - \\ & - \bar{\rho}\Phi\Phi'F' + 2Sc(\bar{\mu} - \bar{\rho})\Phi''F' = 0, \\ & 2(I + \bar{\rho}F)F'' + 2\bar{\rho}F'^2 + \Phi F' = 0, \\ & \Phi(0) = -\theta F'(0), \quad \Phi'(0) = 0, \quad \Phi'(\infty) = 1, \\ & F(0) = 1, \quad F(\infty) = 0. \end{aligned} \quad (1.240)$$

The problem (1.240) can be solved conveniently using the following algorithm:

1. Determination of the zero-th approximations of  $\Phi$  and  $F$  by solving the boundary problem:

$$\begin{aligned} & 2\Phi^{(0)} + \Phi^{(0)}\Phi''^{(0)} = 0, \\ & \Phi^{(0)}(0) = 0, \quad \Phi'^{(0)}(0) = 0, \quad \Phi''^{(0)}(0) = 0.33206, \quad (\Phi'^{(0)}(\infty) = 1), \\ & 2F''^{(0)} + \Phi^{(0)}F'^{(0)} = 0, \\ & F^{(0)}(0) = 1, \quad F'^{(0)}(0) = 0.33205, \quad (F^{(0)}(\infty) = 0). \end{aligned} \quad (1.241)$$

2. Determining  $\Phi$  at the  $k$ -th iteration:

$$\begin{aligned} & 2Sc(I + 2\bar{\rho}F^{(k-1)} + \bar{\mu}F^{(k-1)})\Phi''^{(k)} + (I + 2\bar{\rho}F^{(k-1)})\Phi^{(k)}\Phi''^{(k)} - \\ & - \bar{\rho}\Phi^{(k-1)}\Phi'^{(k-1)}F'^{(k-1)} + 2Sc(\bar{\mu} - \bar{\rho})\Phi''^{(k-1)}F'^{(k-1)} = 0, \\ & \Phi^{(k)}(0) = -\theta F'^{(k-1)}(0), \quad \Phi'^{(k)}(0) = 0, \quad \Phi'(\infty) = 1, \end{aligned} \quad (1.242)$$

while the value of  $\Phi'(k)(0)$  is varied till the condition  $\Phi'(k)(6) = 1$  is reached with accuracy  $10^{-3}$ .

### 3. Determining $F$ at the k-th iteration

$$\begin{aligned} 2\left(1 + \bar{\rho}F^{(k-1)}\right)F''^{(k)} + 2(\bar{\rho}F'^{(k-1)})^2 + \Phi^{(k)}F'^{(k)} &= 0, \\ F^{(k)}(0) = 1, \quad F^{(k)}(\infty) = 0, \end{aligned} \quad (1.243)$$

while  $F'(k)(0)$  is varied till  $F'(k)(\infty) = 0$  with the accuracy  $10^{-3}$ .

4. The calculation procedure (from step 2 of the algorithm) is repeated until result confirming:

$$|\Phi''^{(k)}(0) - \Phi''^{(k-1)}(0)| \leq 10^{-3}, |F'^{(k)}(0) - F'^{(k-1)}(0)| \leq 10^{-3} \quad (1.244)$$

is obtained.

The integration of (1.241-1.243) is performed numerically with a step  $h = 10^{-2}$  in the interval  $0 \leq \eta \leq 6$ .

The results for  $\Phi''(0)$  and  $F'(0)$  in the case of  $Sc = 1$  are shown in Table 1.10 for different values of  $\theta$ ,  $\bar{\rho}$  and  $\bar{\mu}$ . They are obtained with 3-4 iterations

Table 1.10.

Comparative data for the momentum transfer ( $\Phi''(0)$ ) and the mass transfer ( $F'(0)$ ) at high concentrations (effect due to density ( $\bar{\rho} \neq 0$ ), viscosity ( $\bar{\mu} \neq 0$ ) and large concentration gradients ( $\theta \neq 0$ ) in gases.

No.	$Sc = 1$				
	$\theta$	$\bar{\rho}$	$\bar{\mu}$	$\Phi''(0)$	$-F'(0)$
1	0	0	0	0.332	0.332
2	0.3	0	0	0.301	0.299
3	-0.3	0	0	0.373	0.372
4	0.3	0.15	0	0.356	0.187
5	0	0.15	0	0.379	0.198
6	-0.3	-0.15	0	0.329	0.531
7	0.3	0	0.2	0.264	0.292
8	0	0	0.2	0.290	0.322
9	-0.3	0	-0.2	0.447	0.386
10	0.3	0.15	0.2	0.320	0.187
11	0	0.15	0.2	0.340	0.198
12	-0.3	0.15	0.2	0.362	0.211
13	0	-0.15	0	0.280	0.446
14	0	0	-0.2	0.394	0.343
15	0	-0.15	-0.2	0.347	0.469
16	-0.3	-0.15	-0.2	0.417	0.558

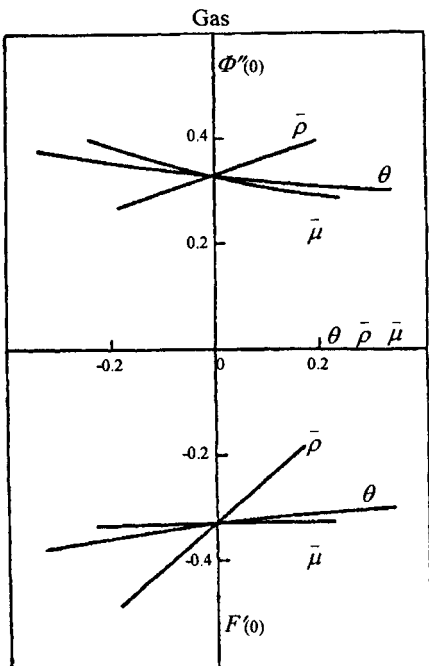


Fig. 1.18. Influence of high concentrations through the viscosity ( $\bar{\mu}$ ), density ( $\bar{\rho}$ ) and large concentration gradients ( $\theta$ ) on the hydrodynamics ( $\Phi''(0)$ ) and the mass transfer ( $F'(0)$ ) in gases.

The mass transfer rate in gases can be determined from data in Table 1.10. In order to do this (1.237) and (1.240) are introduced into (1.235):

$$Sh = \frac{kL}{D_0} = -2 \frac{\rho^*}{\rho_0} Pe^{1/2} F'(0), \quad Pe = \frac{u_0 L}{D_0}. \quad (1.245)$$

The results obtained in Table 1.10 show that (Fig. 1.18) the dependence of  $\Phi''(0)$  and  $F'(0)$  on  $\theta$ ,  $\bar{\rho}$  and  $\bar{\mu}$  is monotone. The change in viscosity  $\bar{\mu}$  has no effect of practical importance on the mass transfer rate ( $F'(0)$ ), while the effect of the density  $\bar{\rho}$  is 6-7 times greater than that of the non-linear mass transfer ( $\theta$ ).

The thickness of the laminar and diffusion boundary layers in liquids are of different order of magnitude, so two specific scales should be applied:

$$\delta_1 = \sqrt{\frac{\mu_0 L}{\rho_0 u_0}}, \quad \delta_2 = \sqrt{\frac{D_0 L}{u_0}}, \quad \frac{\delta_1}{\delta_2} = \varepsilon = Sc^{1/2}. \quad (1.246)$$

Considering these two scales the following dimensionless variables should be introduced:

$$\begin{aligned} x &= LX, \quad y = \delta_1 Y_1 = \delta_2 Y_2, \\ u &= u_0 U_1(X, Y_1) = u_0 U_2(X, Y_2), \\ v &= u_0 \frac{\delta_1}{L} V_1(X, Y_1) = u_0 \frac{\delta_2}{L} V_2(X, Y_2), \\ c &= c_0 + \Delta c_0 C_1(X, Y_1) = c_0 + \Delta c_0 C_2(X, Y_2), \end{aligned} \quad (1.247)$$

where

$$\begin{aligned} Y_2 &= \varepsilon Y_1, \\ U_2(X, Y_2) &= U_1(X, \varepsilon^{-1} Y_2), \quad U_1(X, Y_1) = U_2(X, \varepsilon Y_1), \\ V_2(X, Y_2) &= \varepsilon V_1(X, \varepsilon^{-1} Y_2), \quad V_1(X, Y_1) = \varepsilon^{-1} V_2(X, \varepsilon Y_1), \\ C_2(X, Y_2) &= C_1(X, \varepsilon^{-1} Y_2), \quad C_1(X, Y_1) = C_2(X, \varepsilon Y_1). \end{aligned} \quad (1.248)$$

In the new variables the problem obtains the following form:

$$\begin{aligned} \varphi_1 \left( U_1 \frac{\partial U_1}{\partial X} + V_1 \frac{\partial U_1}{\partial Y_1} \right) &= \frac{\partial}{\partial Y_1} \left( \varphi_1 \frac{\partial U_1}{\partial Y_1} \right), \\ \frac{\partial}{\partial X} (\varphi_1 U_1) + \frac{\partial}{\partial Y_1} (\varphi_1 V_1) &= 0, \\ \varphi_2 \left( U_2 \frac{\partial C_2}{\partial X} + V_2 \frac{\partial C_2}{\partial Y_2} \right) &= \frac{\partial}{\partial Y_2} \left( \varphi_2 \omega_2 \frac{\partial C_2}{\partial Y_2} \right); \\ X_1 &= 0, \quad U_1 = U_2 = 1, \quad C_1 = C_2 = 0; \\ Y_1 = Y_2 &= 0, \quad U_1 = U_2 = 0, \quad C_1 = C_2 = 0, \quad V_2 = -\theta_0 \frac{\partial}{\partial Y_2} \left( \frac{\frac{c_0}{\Delta c} + C_2}{\varphi_2} \right); \\ Y_1 = Y_2 &\rightarrow \infty, \quad U_1 = U_2 = 1, \quad C_1 = C_2 = 0. \end{aligned} \quad (1.249)$$

The boundary problem can be expressed by the following similarity variables:

$$\begin{aligned} \varphi_1 U_1 &= \Phi'_1(\eta_1), \quad \varphi_2 U_2 = \Phi'_2(\eta_2), \quad \eta_1 = \frac{Y_1}{\sqrt{X}}, \quad \eta_2 = \frac{Y_2}{\sqrt{X}}, \\ \varphi_1 V_1 &= \frac{1}{2\sqrt{X}} (\Phi'_1 \eta_1 - \Phi_1), \quad \varphi_2 V_2 = \frac{1}{2\sqrt{X}} (\Phi'_2 \eta_2 - \Phi_2), \\ C_1 &= F_1(\eta_1), \quad C_2 = F_2(\eta_2), \quad \eta_2 = \varepsilon \eta_1, \end{aligned} \quad (1.250)$$

while for  $\varphi, \psi$  and  $\omega$  linear approximations could be used:

$$\varphi_i = I + \bar{\rho}F_i, \quad \psi_i = I + \bar{\mu}F_i, \quad \omega_i = I + \bar{D}F_i, \quad i = 1, 2. \quad (1.251)$$

In the new variables (1.249) gets the following form

$$\begin{aligned} & 2(I + 2\bar{\rho}F_1 + \bar{\mu}F_1)\Phi''_i + (I + 2\bar{\rho}F_1)\Phi'_i\Phi''_i - \bar{\rho}\Phi_i\Phi'_iF'_i + 2(\bar{\mu} - \bar{\rho})\Phi''_iF'_i = 0, \\ & 2(I + \bar{\rho}F_2 + \bar{D}F_2)\Phi''_2 + 2(\bar{\rho} + \bar{D})F'^2_2 + \Phi'_2F'_2 = 0, \\ & \Phi_2(0) = -\theta F'_2(0), \quad \Phi'_i(0) = 0, \quad \Phi'_i(\infty) = 1, \quad F_2(0) = I, \quad F_2(\infty) = 0, \end{aligned} \quad (1.252)$$

where

$$\begin{aligned} F_1(\eta_1) &= F_2(\eta_2) = F_2(\varepsilon\eta_1), \quad F'_1(\eta_1) = \varepsilon F'_2(\varepsilon\eta_1), \\ \Phi_2(\eta_2) &= \varepsilon\Phi_1(\eta_1) = \varepsilon\Phi_1(\varepsilon^{-1}\eta_2), \quad \Phi_2(0) = \varepsilon\Phi_1(0) = -\theta F'_2(0). \end{aligned} \quad (1.253)$$

The problem (1.252) can be directly solved using the following algorithm:

1. Determination of the zero-th approximations of  $\Phi_i(\eta_i)$  by integration of the equation:

$$\begin{aligned} & \Phi''_i^{(0)} + \Phi'^{(0)}_i\Phi''_i^{(0)} = 0, \\ & \Phi'^{(0)}_i(0) = 0, \quad \Phi'^{(0)}_i(0) = 0, \quad \Phi'^{(0)}_i(\infty) = 1, \end{aligned} \quad (1.254)$$

with a step  $h_i = 0.06/\varepsilon$  in the interval  $0 \leq \eta_i \leq 6$ .  $\Phi'^{(0)}_i$  is varied until the condition  $\Phi'^{(0)}_i(6) \geq 0.999$  is satisfied.

2. Determination of the zero-th approximations of  $\Phi_2(\eta_2)$ :

$$\Phi_2^{(0)}(\eta_2) = \varepsilon\Phi_1^{(0)}(\eta_1), \quad \eta_2 = \varepsilon\eta_1, \quad 0 \leq \eta_1 \leq 6. \quad (1.255)$$

3. Determination of the zero-th approximations of  $F_2(\eta_2)$  by integration of the equation:

$$\begin{aligned} & F''_2^{(0)} + \Phi_2^{(0)}F'_2^{(0)} = 0, \\ & F_2^{(0)}(0) = I, \quad F_2^{(0)}(\infty) = 0, \end{aligned} \quad (1.256)$$

with a step  $h_2 = 0.06$  in the interval  $0 \leq \eta_2 \leq 60$ . In order to do this  $F_2^{(0)}(0)$  is varied until the condition  $F_2^{(0)}(60) \leq 0.001$  is satisfied.

4. Determination of the zero-th approximations of  $F_i(\eta_i)$  and  $F'_i(\eta_i)$ :

$$F_i^{(0)}(\eta_i) = F_2^{(0)}(\eta_2) = F_2^{(0)}(\varepsilon\eta_1), \quad F'_i^{(0)}(\eta_i) = \varepsilon F'_2^{(0)}(\eta_2) = \varepsilon F'_2^{(0)}(\varepsilon\eta_1) \quad (1.257)$$

5. Determining  $\Phi_i(\eta_i)$  at the k-th iteration:

$$\begin{aligned}
& 2\left(1 + 2\bar{\rho}F_i^{(k-1)} + \bar{\mu}F_i^{(k-1)}\right)\Phi_i''^{(k)} + \left(1 + 2\bar{\rho}F_i^{(k-1)}\right)\Phi_i'^{(k)}\Phi_i''^{(k)} - \\
& - \bar{\rho}\Phi_i'^{(k-1)}\Phi_i''^{(k-1)}F_i'^{(k-1)} + 2(\bar{\mu} - \bar{\rho})\Phi_i''^{(k-1)}F_i'^{(k-1)} = 0, \\
& \Phi_i^{(k)}(0) = -\frac{\theta}{\varepsilon}F_2'^{(k-1)}(0), \quad \Phi_i'^{(k)}(0) = 0, \quad \Phi_i''^{(k)}(\infty) = 1,
\end{aligned} \tag{1.258}$$

while the value of  $\Phi_i''^{(k)}(0)$  is varied till the condition  $\Phi_i''^{(k)}(6) \geq 0.999$  is reached.

6. Determining  $\Phi_2(\eta_2)$  at the k-th iteration:

$$\Phi_2^{(k)}(\eta_2) = \varepsilon\Phi_i^{(k)}(\eta_1) = \varepsilon\Phi_i^{(k)}(\varepsilon^{-1}\eta_2), \quad 0 \leq \eta_2 \leq 60. \tag{1.259}$$

7. Determining  $F_2(\eta_2)$  at the k-th iteration with a step  $h_2$  in the interval  $0 \leq \eta_2 \leq 60$ :

$$\begin{aligned}
& 2\left(1 + \bar{\rho}F_2^{(k-1)} + \bar{D}F_2^{(k-1)}\right)F_2''^{(k)} + 2(\bar{\rho} + \bar{D})(F_2'^{(k-1)})^2 + \Phi_2^{(k)}F_2''^{(k)} = 0, \\
& F_2^{(k)}(0) = 1, \quad F_2^{(k)}(\infty) = 0,
\end{aligned} \tag{1.260}$$

while the value of  $F_2''^{(k)}(0)$  is varied till the condition  $F_2''^{(k)}(60) \leq 0.001$  is satisfied.

8. Determining  $F_i(\eta_1)$  and  $F'_i(\eta_1)$  at the k-th iteration:

$$F_i^{(k)}(\eta_1) = F_2^{(k)}(\eta_2) = F_2^{(k)}(\varepsilon\eta_1), \quad F_i'^{(k)}(\eta_1) = \varepsilon F_2'^{(k)}(\eta_2) = \varepsilon F_2'^{(k)}(\varepsilon\eta_1), \quad 0 \leq \eta_1 \leq 6. \tag{1.261}$$

9. The calculation procedure (from step 5 of the algorithm on) is repeated until convergence is reached:

$$|\Phi_i''^{(k)}(0) - \Phi_i''^{(k-1)}(0)| \leq 10^{-3}, \quad |F_2''^{(k)}(0) - F_2''^{(k-1)}(0)| \leq 10^{-3}, \tag{1.262}$$

The results obtained for  $\Phi_i''(0)$  and  $F_2''(0)$  at  $\varepsilon = 10$  and for different values of  $\theta, \bar{\rho}, \bar{\mu}$  and  $\bar{D}$  are shown in Table 1.11. They are obtained with 3-4 iterations. The mass transfer rate in liquids can be determined from the data in Table 1.11. In order to do this (1.247) and (1.250) are introduced into (1.231):

$$Sh = -2 \frac{\rho^*}{\rho_0} (1 + \bar{D}) P e^{1/2} F_2'(0). \tag{1.263}$$

The results obtained in Table 1.11 show (Fig. 1.19) that the influence of density  $\bar{\rho}$  and viscosity  $\bar{\mu}$  on the hydrodynamics ( $\Phi_i''(0)$ ) is similar to that observed in the case of gases, while this influence on the mass transfer rate ( $F_2'(0)$ ) is practically insignificant. The change in diffusivity  $\bar{D}$  does not affect  $\Phi_i''(0)$  as well as  $F_2'(0)$ .

The theoretical analysis of the influence of high concentration gradients of transferred substance on the hydrodynamics ( $\Phi''(0)$ ) and mass transfer ( $F'(0)$ ) through the concentration dependencies of density ( $\bar{\rho}$ ), viscosity ( $\bar{\mu}$ ) and diffusivity ( $\bar{D}$ ) shows that the

Table 1.11

Comparative data for the momentum transfer ( $\Phi''(0)$ ) and the mass transfer ( $F'(0)$ ) at high concentrations(effect due to density ( $\bar{\rho} \neq 0$ ), viscosity ( $\bar{\mu} \neq 0$ ) and large concentration gradients ( $\theta \neq 0$ ) in liquids.

No	$Sc = 100$					
	$\theta$	$\bar{\rho}$	$\bar{\mu}$	$\bar{D}$	$\Phi''(0)$	$-F'(0)$
1	0	0	0	0	0.332	0.332
2	0.03	0	0	0	0.330	0.176
3	-0.03	0	0	0	0.334	0.206
4	0	0.15	0	0	0.397	0.194
5	0	-0.15	0	0	0.201	0.181
6	0	0	0.2	0	0.272	0.186
7	0	0	-0.2	0	0.418	0.194
8	0	0	0	0.30	0.332	0.192
9	0	0	0	-0.30	0.332	0.186
10	0.03	0.15	0.2	0.30	0.272	0.177
11	-0.03	0.15	0.2	0.30	0.275	0.200
12	0.03	-0.15	-0.2	-0.30	0.243	0.164
13	-0.03	-0.15	-0.2	-0.30	0.247	0.206
14	0.3	0	0	0	0.318	0.135
15	-0.1	0	0	0	0.342	0.268

change of the density with the concentration affects the hydrodynamics in gases and liquids but does not influence the mass transfer in gases. The change in the viscosity with the concentration affects the hydrodynamics in gases and liquids and the mass transfer. The change in the diffusivity with the concentration does not influence the hydrodynamics and the mass transfer.

These results show that the predictions of the non-linear theory of mass transfer at constant values of density, viscosity and diffusivity [76] are of acceptable accuracy for gases and liquids if the density of the transferred substance is not sufficiently different from the density of the gas mixture. That is why, the models of mass transfer in systems with intensive interphase mass transfer could be considerably simplified.

### 1.5.3. Non-linear mass transfer and Marangoni effect

Intensification of the mass transfer in the industrial gas-liquid systems is obtained quite often by creation of large concentration gradients. This can be reached in a number of cases as a result of a chemical reaction of the transferred substance in the liquid phase. The thermal effect of the chemical reactions creates significantly high temperature gradients. The temperature and concentration gradients created can affect considerably the mass transfer kinetics in gas-liquid systems. Hence, the experimentally obtained mass transfer coefficients differ significantly from those predicted by the linear theory of mass transfer.

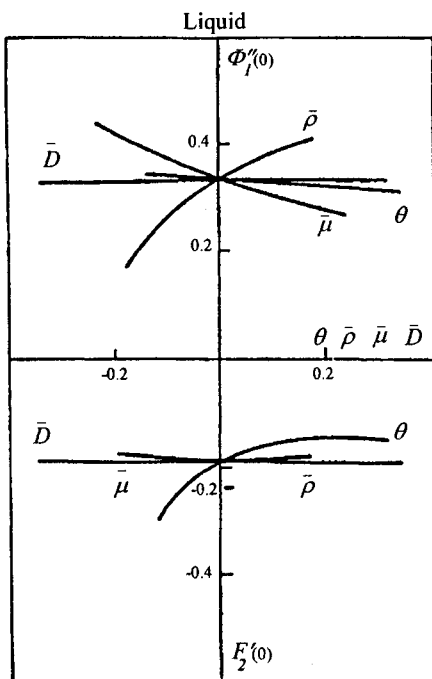


Fig. 1.19. Influence of high concentrations through the viscosity ( $\bar{\mu}$ ), density ( $\bar{\rho}$ ) and large concentration gradients ( $\theta$ ) on the hydrodynamics ( $\Phi'_I(0)$ ) and the mass transfer ( $F'_2(0)$ ) in liquids.

As it was shown in a number of papers [67-72, 77-83] the temperature and concentration gradients on the gas-liquid or liquid-liquid interphase surface can create a interfacial tension gradient. As a result of this a secondary flow is induced. The velocity of the induced flow is directed tangentially to the interface. It leads to a change in the velocity distribution in the boundary layer and therefor to a change in the mass transfer kinetics. These effects are thought to be of the Marangoni type and provide an explanation to all experimental deviations from the prediction of the linear theory of the mass transfer, where the hydrodynamic of the flow does not depend on the mass transfer.

The studies of gas-liquid and liquid – liquid systems with intensive interphase mass transfer as a result of large concentration gradients show (see Chapter 1.3) that under these conditions the induced secondary flow is directed normally to the interface. It leads to “injection” or “suction” of a substance in the boundary layer, therefore to a change in the velocity distribution in the layer and the in mass transfer kinetics. This effect of non-linear mass transfer can explain a number of experimental deviations from the linear theory of mass transfer [84] which have been explained with the Marangoni effect.

The above mentioned two effects (the Marangoni effect and the effect of the non-linear mass transfer) can manifest themselves separately as well as in combination. That is why their influence on the mass transfer kinetics has to be assessed.

Co-current gas and liquid flows in the laminar boundary layer along the flat phase surface will be considered. One of the gas components is absorbed by the liquid and reacts with a component in the liquid phase. The chemical reaction rate is of first order. The thermal effect of the chemical reaction creates a temperature gradient, i. e. the mass transfer together with a heat transfer can be observed. Under these conditions the mathematical model takes the following form:

$$\begin{aligned} u_j \frac{\partial u_j}{\partial x} + v_j \frac{\partial u_j}{\partial y} &= v_j \frac{\partial^2 u_j}{\partial y^2}, & \frac{\partial u_j}{\partial x} + \frac{\partial v_j}{\partial y} &= 0, \\ u_j \frac{\partial c_j}{\partial x} + v_j \frac{\partial c_j}{\partial y} &= D_j \frac{\partial^2 c_j}{\partial y^2} - (j-1)k c_j, \\ u_j \frac{\partial t_j}{\partial x} + v_j \frac{\partial t_j}{\partial y} &= \alpha_j \frac{\partial^2 t_j}{\partial y^2} + (j-1) \frac{q}{\rho_j c_{p_j}} k c_j; & j &= 1, 2, \end{aligned} \quad (1.264)$$

where the indexes 1 and 2 are referred to the gas and the liquid respectively. The influence of the temperature on the chemical reaction rate is not included in (1.264) because it has no considerable affect in the comparative analysis of these two effects.

The boundary conditions of (1.264) determine the potential two-phase flows far from the phase boundary. Thermodynamic equilibrium and continuity of velocity and momentum, mass and heat fluxes can be detected on the phase boundary. It has been shown in [84] that in the gas-liquid systems the effect of non-linear mass transfer is confined into the gas phase. Taking into account these considerations the boundary conditions assume the following form:

$$\begin{aligned} x = 0, \quad u_j &= u_{j0}, \quad c_1 = c_{10}, \quad c_2 = 0, \quad t_j = t_0; \\ y \rightarrow \infty, \quad u_1 &= u_{10}, \quad c_1 = c_{10}, \quad t_1 = t_0; \\ y \rightarrow -\infty, \quad u_2 &= u_{20}, \quad c_2 = 0, \quad t_2 = t_0; \\ y = 0, \quad u_1 &= u_2, \quad \mu_1 \frac{\partial u_1}{\partial y} = \mu_2 \frac{\partial u_2}{\partial y} - \frac{\partial \sigma}{\partial x}, \\ v_1 &= -\frac{MD_1}{\rho_{10}^*} \frac{\partial c_1}{\partial y}, \quad v_2 = 0, \\ c_1 &= \chi c_2, \quad D_1 \frac{\rho_1^*}{\rho_{10}^*} \frac{\partial c_1}{\partial y} = D_2 \frac{\partial c_2}{\partial y}, \quad \rho_1^* = \rho_{10}^* + M c_1^*, \\ t_1 &= t_2, \quad \lambda_1 \frac{\partial t_1}{\partial y} + \rho_1 c_{p1} v_1 t_1 = \lambda_2 \frac{\partial t_2}{\partial y}, \quad j = 1, 2. \end{aligned} \quad (1.265)$$

At high enough values of  $c_0$  a large concentration gradient directed normally to the interface  $(\partial c_1 / \partial y)_{y=0}$ , can be observed, which induces a secondary flow with the rate  $v_1$ .

The tangential concentration and temperature gradients along the phase boundary create surface tension gradient:

$$\frac{\partial \sigma}{\partial x} = \frac{\partial \sigma}{\partial c_2} \frac{\partial c_2}{\partial x} + \frac{\partial \sigma}{\partial t_2} \frac{\partial t_2}{\partial x}, \quad (1.266)$$

which induces a tangential secondary flow, which rate is proportional to  $\partial \sigma / \partial x$ . Later the use of substance, which is not surface active, i. e.  $\partial \sigma / \partial c_2 \approx 0$ , will be examined.

The mass transfer rate ( $J_c$ ) and the heat transfer rate ( $J_t$ ) can be determined from the local mass ( $I_c$ ) and heat ( $I_t$ ) fluxes after taking the average of these fluxes along a length ( $L$ ) of the interface:

$$\begin{aligned} J_c &= k_c c_0 = \frac{1}{L} \int_0^L I_c dx, & I_c &= \frac{MD_I \rho_I^*}{\rho_{I0}} \left( \frac{\partial c_I}{\partial y} \right)_{y=0}, \\ J_t &= k_t t_0 = \frac{1}{L} \int_0^L I_t dx, & I_t &= -\lambda_I \left( \frac{\partial t_I}{\partial y} \right)_{y=0} + \rho_I c_{pI} (v_I t_I)_{y=0}, \end{aligned} \quad (1.267)$$

where  $c_I$  and  $t_I$  are determined upon solving the problems (1.264)-(1.265). In order to do this the following dimensionless variables are introduced:

$$\begin{aligned} x &= LX, & y &= (-1)^{j+1} \delta_j Y_j, & \delta_j &= \sqrt{\frac{v_j L}{u_{j0}}}, \\ u_j &= u_{j0} U_j(X, Y_j), & v_j &= (-1)^{j+1} u_{j0} \frac{\delta_j}{L} V_j(X, Y_j), \\ c_j &= (-\chi)^{l-j} c_0 C_j(X, Y_j), & t_j &= t_0 + (-1)^{j+1} t_0 T_j(X, Y_j), & j &= 1, 2. \end{aligned} \quad (1.268)$$

The introduction of (5) into (1) and (2) leads to the following equations:

$$\begin{aligned} U_j \frac{\partial U_j}{\partial X} + V_j \frac{\partial U_j}{\partial Y_j} &= \frac{\partial^2 U_j}{\partial Y_j^2}, & \frac{\partial U_j}{\partial X} + \frac{\partial V_j}{\partial Y_j} &= 0, \\ U_j \frac{\partial C_j}{\partial X} + V_j \frac{\partial C_j}{\partial Y_j} &= \frac{1}{Sc_j} \frac{\partial^2 C_j}{\partial Y_j^2} - (j-1) Da C_j, \\ U_j \frac{\partial T_j}{\partial X} + V_j \frac{\partial T_j}{\partial Y_j} &= \frac{1}{Pr_j} \frac{\partial^2 T_j}{\partial Y_j^2} + (j-1) Q Da C_j, & j &= 1, 2, \end{aligned} \quad (1.269)$$

where

$$Da = \frac{kl}{u_{20}}, \quad Q = \frac{qc_0}{\chi \rho_2 c_{p2} t_0}, \quad Sc_j = \frac{\nu_j}{D_j}, \quad Pr_j = \frac{\nu_j}{a_j}, \quad j = 1, 2. \quad (1.270)$$

The boundary conditions of (1.268) have the following form:

$$\begin{aligned} X = 0, \quad U_j = 1, \quad C_j = 1, \quad C_2 = 0, \quad T_j = 0, \quad j = 1, 2; \\ Y_1 \rightarrow \infty, \quad U_1 = 1, \quad C_1 = 1, \quad T_1 = 0; \\ Y_2 \rightarrow \infty, \quad U_2 = 1, \quad C_2 = 0, \quad T_2 = 0; \\ Y_1 = Y_2 = 0, \quad U_1 = \theta_1 U_2, \quad \theta_2 \frac{\partial U_1}{\partial Y_1} = -\frac{\partial U_2}{\partial Y_2} + \theta_4 \frac{\partial T_2}{\partial X}, \\ V_1 = -\theta_3 \frac{\partial C_1}{\partial Y_1}, \quad V_2 = 0, \quad C_1 + C_2 = 0, \quad T_1 + T_2 = 0, \\ \theta_5 \frac{\partial C_1}{\partial Y_1} = \frac{\partial C_2}{\partial Y_2}, \quad \theta_6 \frac{\partial T_1}{\partial Y_1} = \frac{\partial T_2}{\partial Y_2}. \end{aligned} \quad (1.271)$$

The effect of convective transfer in (1.271) is omitted as a small of higher order, while the parameters  $\theta$  have the following form:

$$\begin{aligned} \theta_1 = \frac{u_{20}}{u_{10}}, \quad \theta_2 = \frac{\mu_1}{\mu_2} \sqrt{\frac{\nu_2}{\nu_1}} \left( \frac{u_{20}}{u_{10}} \right)^{3/2}, \quad \theta_3 = \frac{Mc_0}{\rho_{10}^* Sc_1}, \\ \theta_4 = \frac{\partial \sigma}{\partial t_2} \frac{t_0}{u_{20} \mu_2} \sqrt{\frac{\nu_2}{u_{20} l}}, \quad \theta_5 = \chi \frac{D_1}{D_2} \frac{\rho_1^*}{\rho_{10}^*} \sqrt{\frac{u_{10} \nu_2}{u_{20} \nu_1}}, \quad \theta_6 = \frac{\lambda_1}{\lambda_2} \sqrt{\frac{u_{10} \nu_2}{u_{20} \nu_1}}. \end{aligned} \quad (1.272)$$

From (1.267) and (1.268) are directly obtained the expressions for the Sherwood and Nusselt numbers:

$$\begin{aligned} Sh = \frac{k_c L}{D_1} = M \sqrt{Re_1} \int_0^L \left( I + \theta_3 Sc_1 C_1^* \left( \frac{\partial C_1}{\partial Y_1} \right)_{Y_1=0} \right) dX, \\ Nu = \frac{k_c L}{\lambda_1} = -Re_1 \left[ \int_0^L \left( \frac{\partial T_1}{\partial Y_1} \right)_{Y_1=0} dX + \theta_3 Pr_1 \int_0^L \left( I + T_1^* \right) \left( \frac{\partial C_1}{\partial Y_1} \right)_{Y_1=0} dX \right], \\ C_1^* = C_1(X, 0), \quad T_1^* = T_1(X, 0), \quad Re_1 = \frac{u_{10} L}{\nu_1}. \end{aligned} \quad (1.273)$$

The problem (1.269) with the appropriate set of boundary conditions can be solved conveniently using the iterative algorithm, where 6 problems are solved consecutively, until a convergence with respect to the integral  $J_i$  in (1.280) is reached.

$$\begin{aligned}
& U_1^{(k)} \frac{\partial U_1^{(k)}}{\partial X} + V_1^{(k)} \frac{\partial U_1^{(k)}}{\partial Y_1} = \frac{\partial^2 U_1^{(k)}}{\partial Y_1^2}, \quad \frac{\partial U_1^{(k)}}{\partial X} + \frac{\partial V_1^{(k)}}{\partial Y_1} = 0; \\
& X = 0, \quad U_1^{(k)} = 1; \\
& Y_1 = 0, \quad U_1^{(k)} = \theta_1 U_2^{(k-1)}, \quad V_1^{(k)} = -\theta_3 \frac{\partial C_1^{(k-1)}}{\partial Y_1}; \\
& Y_1 \rightarrow \infty, \quad (Y_1 \geq Y_{1\infty}), \quad U_1^{(k)} = 1; \\
& 0 \leq X \leq I, \quad 0 \leq Y_1 \leq Y_{1\infty}; \\
& \theta_1 = 0.1, \quad Y_{1\infty} = 6, \quad (\text{at the first iteration } \theta_1 = \theta_3 = 0). \tag{1.274}
\end{aligned}$$

$$\begin{aligned}
& U_2^{(k)} \frac{\partial U_2^{(k)}}{\partial X} + V_2^{(k)} \frac{\partial U_2^{(k)}}{\partial Y_2} = \frac{\partial^2 U_2^{(k)}}{\partial Y_2^2}, \quad \frac{\partial U_2^{(k)}}{\partial X} + \frac{\partial V_2^{(k)}}{\partial Y_2} = 0; \\
& X = 0, \quad U_2^{(k)} = 1; \\
& Y_2 = 0, \quad \frac{\partial U_2^{(k)}}{\partial Y_2} = -\theta_2 \left( \frac{\partial U_1^{(k)}}{\partial Y_1} \right)_{Y_1=0} + \theta_4 \left( \frac{\partial T_2^{(k-1)}}{\partial X} \right)_{Y_2=0}, \quad V_2^{(k)} = 0; \\
& Y_2 \rightarrow \infty, \quad (Y_2 \geq Y_{2\infty}), \quad U_2^{(k)} = 1; \\
& 0 \leq X \leq I, \quad 0 \leq Y_2 \leq Y_{2\infty}; \\
& \theta_2 = 0.145, \quad Y_{2\infty} = 6, \quad (\text{at the first iteration } \theta_4 = 0). \tag{1.275}
\end{aligned}$$

$$\begin{aligned}
& U_1^{(k)} \frac{\partial C_1^{(k)}}{\partial X} + V_1^{(k)} \frac{\partial C_1^{(k)}}{\partial Y_1} = \frac{1}{Sc_1} \frac{\partial^2 C_1^{(k)}}{\partial Y_1^2}; \\
& X = 0, \quad C_1^{(k)} = 1; \\
& Y_1 = 0, \quad C_1^{(k)} = -C_2^{(k-1)}(X, 0); \\
& Y_1 \rightarrow \infty (Y_1 \geq \bar{Y}_1), \quad C_1^{(k)} = 1; \\
& 0 \leq X \leq I, \quad 0 \leq Y_1 \leq \bar{Y}_1; \\
& Sc_1 = 0.735, \quad \bar{Y}_1 = 7 \quad (\text{at the first iteration } C_2^{(k)}(X, 0) = 0). \tag{1.276}
\end{aligned}$$

$$\begin{aligned}
& U_2^{(k)} \frac{\partial C_2^{(k)}}{\partial X} + V_2^{(k)} \frac{\partial C_2^{(k)}}{\partial Y_2} = \frac{1}{Sc_2} \frac{\partial^2 C_2^{(k)}}{\partial Y_2^2} - Da C_2^{(k)}; \\
& X = 0, \quad C_2^{(k)} = 0; \\
& Y_2 = 0, \quad \frac{\partial C_2^{(k)}}{\partial Y_2} = \theta_5 \left( \frac{\partial C_1^{(k)}}{\partial Y_1} \right)_{Y_1=0}; \\
& Y_2 \rightarrow \infty (Y_2 \geq \bar{Y}_2), \quad C_2^{(k)} = 0; \\
& 0 \leq X \leq I, \quad 0 \leq Y_2 \leq \bar{Y}_2;
\end{aligned}$$

$$Sc_2 = 564, \quad \theta_5 = 18.3, \quad \bar{Y}_2 = 0.26, \quad Da = 10. \quad (1.277)$$

$$\begin{aligned} U_l^{(k)} \frac{\partial T_l^{(k)}}{\partial X} + V_l^{(k)} \frac{\partial T_l^{(k)}}{\partial Y_l} &= \frac{1}{Pr_l} \frac{\partial^2 T_l^{(k)}}{\partial Y_l^2}; \\ X = 0, \quad T_l^{(k)} &= 0; \\ Y_l = 0, \quad T_l^{(k)} &= -T_2^{(k-1)}(X, 0); \\ Y_l \rightarrow \infty (Y_l \geq \bar{\bar{Y}}_l), \quad T_l^{(k)} &= 0; \\ 0 \leq X \leq l, \quad 0 \leq Y_l \leq \bar{\bar{Y}}_l; \\ Pr_l = 0.666, \quad \bar{\bar{Y}}_l &= 7.4 \quad (\text{at the first iteration } T_2^{(k)}(X, 0) = 0). \end{aligned} \quad (1.278)$$

$$\begin{aligned} U_2^{(k)} \frac{\partial T_2^{(k)}}{\partial X} + V_2^{(k)} \frac{\partial T_2^{(k)}}{\partial Y_2} &= \frac{1}{Pr_2} \frac{\partial^2 T_2^{(k)}}{\partial Y_2^2} + QDaC_2^{(k)}; \\ X = 0, \quad T_2^{(k)} &= 0; \\ Y_2 = 0, \quad \frac{\partial T_2^{(k)}}{\partial Y_2} &= \theta_6 \left( \frac{\partial T_l^{(k)}}{\partial Y_l} \right)_{Y_l=0}; \\ Y_2 \rightarrow \infty (Y_2 \geq \bar{\bar{Y}}_2), \quad T_2^{(k)} &= 0; \\ Pr_2 = 6.54, \quad \theta_6 &= 0.034, \quad \bar{\bar{Y}}_2 = 2.4, \quad QDa = 8.6. \end{aligned} \quad (1.279)$$

The values of the parameters in (1.274)-(1.279) are calculated for the process of absorption of NH<sub>3</sub> in water or water solutions of strong acids.

The solution of (1.274)-(1.279) allows the determination of

$$\begin{aligned} J_1 &= \int_0^l \left( \frac{\partial C_1}{\partial Y_l} \right)_{Y_l=0} dX, & J_2 &= \int_0^l C_1(X, 0) \left( \frac{\partial C_1}{\partial Y_l} \right)_{Y_l=0} dX, \\ J_3 &= \int_0^l \left( \frac{\partial T_l}{\partial Y_l} \right)_{Y_l=0} dX, & J_4 &= \int_0^l T_l(X, 0) \left( \frac{\partial C_1}{\partial Y_l} \right)_{Y_l=0} dX. \end{aligned} \quad (1.280)$$

The introduction of (1.280) into (1.273) allows the determination of the Sherwood and Nusselt numbers:

$$Sh = M \sqrt{Re_l} (J_1 + \theta_3 Sc_1 J_2), \quad Nu = -\sqrt{Re_l} [J_3 + \theta_3 Pr_l (J_1 + J_4)]. \quad (1.281)$$

The results obtained by solving of these problems are shown in Tables 1.12 – 1.14.

The comparative analysis of the non-linear mass transfer effect and the Marangoni effect in gas-liquid and liquid-liquid systems show, (Tables 1.12, 1.13), that the Marangoni

effect does not affect on the heat and mass transfer kinetics, because in real systems the parameter  $\theta_4$  is very small.

However, in cases where the velocity of the second phase is very low the occurrence of the Marangoni effect to be expected because of its velocity dependence from  $(u_{20})^{-3/2}$ . In order to evaluate the above case systems with the velocity in the volume of the second phase equals to zero ( $u_{20}=0$ ) have been investigated. The numerical results (Table 1.14) show that under these conditions the Marangoni effect is negligible too.

The results obtained show that the Marangoni effect is negligible in two phase systems with movable phase boundary and absence of surface active agents. The deviations from the linear mass transfer theory have to be explained by the non-linear mass transfer effect in conditions of the large concentration gradients.

Table 1.12

Influence of the non-linear mass transfer effect and Marangoni effect on the heat and mass transfer kinetics in gas-liquid systems.

No	$\theta_3$	$\theta_4$	Gas-liquid			
			$\theta_1=0.1$	$\theta_2=0.145$	$J_1$	$J_2$
1	0	0	0.5671	0.09721	0.01855	-0.01337
2	0.2	0	0.6129	0.01155	0.02143	-0.01554
3	-0.2	0	0.5274	0.08542	0.01623	-0.01162
4	0	$10^{-4}$	0.5671	0.09721	0.01855	-0.01338
5	0	$10^{-3}$	0.5671	0.09721	0.01855	-0.01337
6	0	$10^{-2}$	0.5670	0.09718	0.01857	-0.01339
7	0	$10^{-1}$	0.5658	0.09696	0.01879	-0.01364
8	0	1	0.5658	0.09696	0.01879	-0.01364
9	0	5	0.5660	0.09696	0.01854	-0.01345

Table 1.13

Influence of the non-linear mass transfer effect and Marangoni effect on the heat and mass transfer kinetics in liquid-liquid systems.

No	$\theta_{31}$	$\theta_{32}$	$\theta_4$	Liquid-liquid			
				$\theta_1=0.9$	$\theta_2=3$	$(u_2(X, Y_2)=1)$	$J_4$
1	0	0	0	21.1000	4.8778	0.3320	-0.0524
2	$4.10^{-4}$	$-8.10^{-4}$	0	22.5419	5.7854	0.4288	-0.0628
3	0	0	$2.10^{-4}$	21.1000	4.8778	0.3320	-0.0524
4	0	0	$1.10^{-3}$	21.0999	4.8778	0.3320	-0.0524
5	0	0	$1.10^{-2}$	21.0990	4.8774	0.3320	-0.0524
6	0	0	$1.10^{-1}$	21.0899	4.8736	0.3319	-0.0524
7	0	0	5	20.5698	4.6527	0.3291	-0.0513

Table 1.14

Influence of the non-linear mass transfer effect and Marangoni effect on the heat and mass transfer kinetics in liquid-liquid systems when the second liquid is immobile.

No	Liquid-liquid $\theta_1=1$ $\theta_2=1$ ( $u_2(X, Y_2)=10^{-4}$ )							
	$\theta_{31}$	$\theta_{32}$	$\theta_4$	$J_1$	$J_2$	$J_3$	$J_4$	
1	0	0	0	16.9333	3.3960	0.3041	-0.0460	
2	$4.10^{-4}$	$-8.10^{-4}$	0	18.3164	4.0715	0.3967	-0.0551	
3	0	0	$2.10^{-4}$	16.9333	3.3960	0.3041	-0.0460	
4	0	0	$1.10^{-3}$	16.9331	3.3959	0.3042	-0.0460	
5	0	0	$1.10^{-2}$	16.9314	3.3952	0.3041	-0.0596	
6	0	0	$1.10^{-1}$	16.9145	3.3885	0.3040	-0.0592	
7	0	0	1	16.7421	3.3201	0.3026	-0.0456	
8	0	0	5	15.8955	2.9669	0.2968	-0.0437	

♦

In Part 1 of the book the effect of non-linear mass transfer induced by high concentration gradients has been discussed. This effect can explain many disagreements between the experimental data and the predictions of the linear mass transfer theory. Earlier most of these effects were considered as Marangoni effects. However, in many cases the deviations from the linear theory are significantly greater than those predicted by the non-linear mass transfer theory. This may be attributed to the loss of hydrodynamic stability as a result of secondary flows induced by the large concentration gradients. These effects will be discussed in the fifth part.

## References

- Chr. Boyadjiev and V. Beshkov, J. Eng. Physics (Russia), 27 (1974) 702 (in Russian).
- Chr. Boyadjiev, J. Eng. Physics (Russia), 59 (1990) 92 (in Russian).
- Chr. Boyadjiev, J. Eng. Physics (Russia), 59 (1990) 593 (in Russian).
- Chr. Boyadjiev, Theoretical Fundamentals of Chemical Technology (Russia), 6 (1972) 118.
- Chr. Boyadjiev and V. Beshkov, Mass Transfer in Falling Liquid Films, Mir, Moscow, 1988 (in Russian).
- Chr. Boyadjiev and L. Velchev, Theoretical Fundamentals of Chemical Technology (Russia), 5 (1971) 912.
- Chr. Boyadjiev and E. Toshev, J. Eng. Physics (Russia), 59 (1990) 277.
- B. I. Brounstein and G. A. Fishbain, Hydrodynamics, Mass and Heat Transfer in Disperse Systems, Himia, Leningrad, 1977 (in Russian).

9. A. M. Golovin, N. M. Rubinina and V. M. Hohrin, Theoretical Fundamentals of Chemical Technology (Russia), 5 (1971) 651.
10. V. I. Kosorotov at all., Theoretical Fundamentals of Chemical Technology (Russia), 5 (1971) 239.
11. V. I. Kosorotov at all., Theoretical Fundamentals of Chemical Technology (Russia), 5 (1971) 474.
12. V. S. Krylov, Advances of Chemistry (Russia), 49 (1980) 118.
13. V. S. Krylov, V. E. Bogoslovsky and N. N. Mihnev, J. Applied Chemistry (Russia), 49 (1976) 1769.
14. V. S. Krylov and A. D. Davidov, Proc. "Advanced Methods in Electrochemical Machining" - Shtiinca, Kishinev, (1972) 13 (in Russian).
15. V. S. Krylov and V. N. Malienko, Thermodynamics of Irreversible Processes and its Applications, Proc. 1<sup>st</sup> USSR Conf., Chernovcy (1972), 69 (in Russian).
16. V. S. Krylov and V. N. Malienko, Electrochemistry (Russia), 9 (1973) 3.
17. V. G. Levich, Physico-Chemical Hydrodynamics, Prentice Hall, Saglewood Cliffs. W. J. 1962.
18. V. M. Ram, Gas Absorption, Himia, Moscow, 1976 (in Russian)..
19. A. A. Samarsky, Introduction to the Theory of Difference Schemes, Nauka, Moscow, 1976 (in Russian).
20. J. Hirshfelder, E. Kertis and R. Berd, Molecular Theory of Gases and Liquids, Inostrannaja Literatura, Moscow, 1961 (in Russian).
21. A. Tom and K. Aplt, Numerical Calculations of Fields in Technics and Physics, Energia, Moscow, 1964 (in Russian).
22. D. A. Frank – Kamenecky, Diffusion and Heat Transfer in Chemical Kinetics, Mir, Moscow, 1987 (in Russian).
23. U. V. Fumer, U. V. Axelrod, U. V. Dilman and A. L. Lashkov, Theoretical Fundamentals of Chemical Technology (Russia), 5 (1971) 134.
24. S. U. Uan, Cooling by Means of Liquid Films – Turbulence Flows and Heat Transfer, Edited by Lic Czja-Czjao, Inostrannaja Literatura, Moscow, 1963 (in Russian).
25. N. N. Janenko, Method of Partial Steps for Solution of Multidimensional Problems of Mathematical Physics, Nauka, Novosibirsk, 1976 (in Russian).
26. R. B. Bird, W. E. Stewart and E. N. Lightfoot, Transport Phenomena, Willey, New York, 1960.
27. Chr. Boyadjiev, Int. Chem. Eng., 11 (1971) 459.
28. Chr. Boyadjiev, Int. Chem. Eng., 11 (1971) 464.
29. Chr. Boyadjiev, Int. Chem. Eng., 11 (1971) 470.
30. Chr. Boyadjiev, Int. J. Heat Mass Transfer, 25 (1982) 535.
31. Chr. Boyadjiev, Int. J. Heat Mass Transfer, 27 (1984) 1277.
32. Chr. Boyadjiev, Hung. J. Ind. Chem., 18 (1990) 1.
33. Chr. Boyadjiev, Hung. J. Ind. Chem., 26 (1998) 181.
34. Chr. Boyadjiev, Hung. J. Ind. Chem., 18 (1990) 7.
35. Chr. Boyadjiev and V. Beshkov, Mass Transfer in Liquid Film Flows, Bulg. Acad. Sci., Sofia, 1984.
36. Chr. Boyadjiev and D. Elenkov, Int. Chem. Eng., 11 (1971) 474.
37. Chr. Boyadjiev, Pl. Mitev and Tsv. Sapundjiev, Int. J. Multiphase Flow, 3 (1976) 51.
38. Chr. Boyadjiev and Pl. Mitev, Chem. Eng. J., 14 (1977) 225.

39. Chr. Boyadjiev and M. Piperova, Int. Chem. Eng., 11 (1971) 479.
40. Chr. Boyadjiev and E. Toshev, Hung. J. Ind. Chem., 17 (1989) 457.
41. Chr. Boyadjiev and N. Vulchanov, C. r. Acad. Bulg. Sci., 40, No 11 (1987) 35.
42. Chr. Boyadjiev and N. Vulchanov, C. r. Acad. Bulg. Sci., 41, No 10 (1988) 49.
43. Chr. Boyadjiev, J. Eng. Physics (Russia), 60 (1991) 845.
44. Chr. Boyadjiev, Russ. J. Eng. Thermophys., 2 (1992) 289.
45. Chr. Boyadjiev and N. Vulchanov, Int. J. Heat Mass Transfer, 31 (1988) 795.
46. Chr. Boyadjiev and N. Vulchanov, Int. J. Heat Mass Transfer, 33 (1990) 2039.
47. P. L. Brian, J. E. Vivian and D. C. Matiatos, AIChE J., 13 (1967) 28.
48. W. S. Chang, Int. J. Heat Mass Transfer, 16 (1973) 811.
49. J. Douylas and H. H. Rachford, Trans. Am. Math. Soc., 82 (1956) 421.
50. J. L. Duda and J. S. Vrentas, Int. J. Heat Mass Transfer, 14 (1971) 395.
51. A. S. Emanuel and D. R. Olander, Int. J. Heat Mass Transfer, 7 (1964) 539.
52. P. Grassman and G. Andres, Chem. Eng. Techn., Bd. 31 No.3 (1959) 154.
53. A. W. Nienow, R. Unahabkhokha and J. W. Mullin, Chem. Eng. Sci., 24 (1968) 1655.
54. D. R. Olander, Int. J. Heat Mass Transfer, 5 (1962) 765.
55. D. R. Olander, J. Heat Transfer, Trans. ASME, Ser. C, 84 (1962) 185.
56. J. Y. Parlange, Acta Mech., 18 (1973), 157.
57. W. E. Ranz and P. F. Dickinson, Ind. Eng. Chem. Funds, 4 (1965) 345.
58. S. M. Ross, J. Fluid Mech., 63 (1974) 157.
59. T. K. Sherwood, R. L. Pigford, C. R. Wilke, *Mass Transfer*, McGraw-Hill, New York, 1975.
60. E. W. Sparrow and J. L. Gregg, J. Heat Transfer, Trans. ASME, Ser. C, 82 (1960) 294.
61. E. Toshev and Chr. Boyadjiev, Hung. J. Ind. Chem. 22 (1994) 81.
62. R. Unahabkhokha, A. W. Nienow and J. W. Mullin, Chem. Eng. Sci., 26 (1972) 357.
63. N. Vulchanov and Chr. Boyadjiev, Int. J. Heat Mass Transfer, 31 (1988) 801.
64. N. Vulchanov and Chr. Boyadjiev, Int. J. Heat Mass Transfer, 33 (1990) 2045.
65. N. Vulchanov and Chr. Boyadjiev, Theor. Appl. Mech., 19, No. 4 (1988) 74.
66. S. W. Yuan and A. B. Finkelstein, J. Heat Transfer, Trans. ASME, Ser. C, 78 (1956) 719.
67. C. V. Sternling and L. E. Scriven, AIChEJ, 5 (1959) 514.
68. H. Linde, E. Schwarz and K. Groger, Chem. Eng. Sci., 22 (1967) 823.
69. E. Ruckenstein and C. Berbente, Chem. Eng. Sci., 19 (1964) 329.
70. W. J. Thomas and E. Mc. K. Nicholl, Trans. Inst. Chem. Eng., 47 No. 10 (1969) 325.
71. V. V. Dilman, N. N. Kulov, V. A. Lothov, V. A. Kaminski and V.I. Najdenov, *Theoretical Fundamentals of Chemical Technology* (Russia), 32 (1998) 377.
72. K. E. Porter, A. D. C. Cantwell, and C. Mc. Dermott, AIChEJ, 17 (1971) 536.
73. Chr. Boyadjiev, Hung. J. Ind. Chem., 26 (1998) 245.
74. Tsv. Sapundjiev and Chr. Boyadjiev, Russ. J. Eng. Thermophysics (Russia), 3 (1993) 185.
75. Chr. Boyadjiev, Bulgarian Chemical Communications, 26 (1993) 33.
76. Chr. Boyadjiev and I. Halatchev, Int. J. Heat Mass Transfer, 41 (1998) 939.
77. M. Hennenberg, P. M. Bisch, M. Vignes-Adler and A. Sanfeld, *Interfacial Instability and Longitudinal Waves in Liquid-Liquid Systems* Lecture Note in Physics, Springer-Verlag, Berlin, No. 105 (1979) 229.
78. H. Linde, P. Schwartz, H. Wilke, *Dissipative Structures and Nonlinear Kinetics of the Marangoni – Instability*, Lecture Note in Physics, Springer-Verlag, Berlin, No. 105 (1979) 75.

79. A. Sanfeld, A. Steinchen, M. Hennenberg, P. M. Bisch, D. Van Lamswerde-Galle and W. Dall-Vedove, "Mechanical and Electrical Constraints and Hydrodynamic Interfacial Instability" Lecture Note in Physics, Springer-Verlag, Berlin, No. 105 (1979) 168.
80. H. Savistowski, Interfacial Convection. Ber. Bunsenges Phys. Chem., 85 (1981) 905.
81. T. S. Sorensen and M. Hennenberg, Instability of a Spherical Drop with Surface Chemical Reaction and Transfer of Surfactants, Lecture Note in Physics, Springer-Verlag, Berlin, No. 105 (1979) 276.
82. L. E. Scriven and C. V. Sterling, Nature (London) 127, No. 4733 (1960) 186.
83. J. Velarde, and L. Castillo, Transport and Reactive Phenomena Leading to Interfacial Instability, Convective Transport and Instability Phenomena, edited by J. Zierep, H. Oertel, Verlag G. Braun, Kalsruhe, 1981.
84. H. Schlichting, Grenzschicht-Theorie, Verlag G. Braun, Karsruhe, 1965.

## PART 2

### Electrochemical Systems With High Intensity Electric Currents

The analysis of the mechanism of the convective transport of a mass and a charge in electrochemical systems in many cases is possible if the hydrodynamic field is preliminary known. By a substitution of the velocity field in the equations of the convective transport it is possible to determine the rate of exchange between the phases. However, in the case of systems where the transport of both the mass and the charge occur due to high gradients of the ion concentrations and the electric potential, this procedure of problem solution is incorrect. The incorrect situation follows from the fact that intensive mass transfer induces a secondary flow. As shown in Chapter 1.1, the velocity of that induced flow is normal to the interphase boundary and directed toward the mass flux. The particular form of the relationship depends on the solution of a coupled system of equations of momentum, mass and charge as well as the boundary conditions for the momentum and mass transfer at the interphase boundary. These effects will be considered in the case of electrodissolution and electrorecovery of metals under non-isothermal conditions and gas desorption.

#### CHAPTER 2.1. FUNDAMENTALS OF THE KINETIC THEORY OF TRANSPORT OF MASS AND CHARGE IN ELECTRIC SYSTEMS

The investigation of interphase exchange in systems with relatively high rate of the electrochemical reactions needs of quantitative fundamental description of the kinetics of transport of both the ionic and the dipole reagents from the solution depth toward the interphase boundary. Near to the charged interphase boundaries the resulting rate of both the ionic and the dipole reagent has a migration component due to the reagent migration in an electric field. If particle charges or particle dipole moments under the migration are significant, thus the particle-particle and particle-field (at the polarized interphase boundary) interactions take important roles. Moreover, the correct description of ion-ion interactions in solutions with moderate and high concentrations is an important problem of mass transfer in electrical systems. The complexity of the problem follows from the fact that the solution must take into account both the long-time and short time interactions from the point of view of irreversible statistical mechanics. In most of electrical systems occurring in the practice solution concentrations (where an ionic transport exists) are greater than those allowing simplifications of the model equations.

There are three approaches for obtaining solution of mass transfer problems in electrolyte solutions. These approaches are based on different physical assumptions and mathematical simplifications. Because of that the efficiency of their applications depends on the adequacy of the models and the physicochemical characteristics of the systems described. Here these approaches will be described separately as well as their physicochemical bases and applicability.

### 2.1.1. Method of the self-consistent field

Under the assumptions of the method the electric field that is the reason for particle migration is considered as quasi-stationary with respect of the moving particles. Let swarm of type  $i$  particles diffuse due the force applied by an external physical field (the force  $F_i$  of the external field does not depend on the particle concentration  $c_i$ ). In this case the mass particle flux  $j_i$  is a sum of the diffusional and the migration fluxes:

$$j_i = M_i (D_i \mathbf{grad} c_i - c_i u_i F_i), \quad (2.1)$$

where  $M_i$ ,  $D_i$  and  $u_i$  are the molecular mass, diffusion coefficient and particle mobility. Using Nernst-Einstein relationship  $D_i = u_i kT$  equation (2.1) may be expressed as

$$j_i = -D_i M_i \left( \mathbf{grad} c_i - \frac{c_i}{kT} F_i \right). \quad (2.2)$$

The transport of ions with a charge  $ez_i$  ( $e$  – elementary charge,  $z_i$  - valence) in an external electric field with intensity of  $\mathbf{E}$  is due to a force  $F_i = ez_i \mathbf{E}$ . Hence, the equation (2.2) takes the form

$$j_i = -D_i M_i \left( \mathbf{grad} c_i - \frac{ez_i c_i}{kT} \mathbf{E} \right). \quad (2.3)$$

The system of equations (2.3) has been conceived by Nernst [113]. If the field  $\mathbf{E}$  can be considered as preliminary known then the following equation describing adequately the mass transfer could be derived:

$$M_i \frac{\partial c_i}{\partial t} + \operatorname{div} j_i = Q_i, \quad (2.4)$$

where  $Q_i$  - the source producing the transported particles. The application of equation. (2.3) for describing of real processes depends on the adequate description of the diffusion flux as a linear function of the concentration gradient.

The method of the self-consistent field postulates that (2.3) may be applied in the case of ionic mass transfer. In this case the force  $F_i$  is due to the self-consistent field while the field intensity  $\mathbf{E}$  depends on the concentration of ionic components in the solution. The main property of the self-consistent field is that its space distributions, together with the concentration field  $c_i$ , satisfies the following system of equations:

$$\frac{\partial c_i}{\partial t} - \operatorname{div} \left\{ D_i \mathbf{grad} c_i - \frac{ez_i D_i c_i}{kT} \mathbf{E} \right\} = \frac{Q_i}{M_i}, \quad (2.5)$$

$$\operatorname{div}(\varepsilon_o \mathbf{E}) = 4\pi\varepsilon \sum_i z_i c_i, \quad (2.6)$$

where  $\varepsilon_o$  is the dielectric permeability of the medium.

In the case of a thermodynamic equilibrium of all the ionic species in the solution ( $j_i = 0$  for all  $i$ ) and in the absence of volumetric chemical reactions ( $Q_i = 0$ ) the system (2.5)-(2.6) may be reduced to Poisson-Boltzmann's equation

$$\operatorname{div}(\varepsilon_o \mathbf{grad}\varphi) + 4\pi\varepsilon \sum_i z_i c_{io} \exp\left[-\frac{\varepsilon z_i \varphi}{kT}\right] = 0 \quad (2.7)$$

for the potential  $\varphi$  of the self-consistent field, where  $\mathbf{E} = -\mathbf{grad}\varphi$  and  $c_{io}$  are the volumetric ionic concentrations. The equation (2.7) is the base of the theory of Guy-Chapman's double diffusion electric layer. If  $L$  is the length scale, i.e. the distance where there are changes of the profiles  $c_i(r, t)$  and  $\mathbf{E}(r, t)$ , the system (2.5)-(2.6) may be expressed in a dimensionless form

$$\begin{aligned} \frac{\partial C_i}{\partial \tau_i} - \operatorname{div}^* \{ \mathbf{grad}^* C_i - e z_i C_i \varepsilon \} &= \frac{L^2 Q_i}{D_i M_i c_{io}}, \\ (kL)^{-2} \operatorname{div}^*(\varepsilon_o \varepsilon) &= A \sum_i z_i C_i, \\ \tau_i &= \frac{D_i t}{L^2}, \quad C_i = \frac{c_i}{c_{io}}, \quad \varepsilon = \frac{kTE}{L}, \\ k &= \left[ 4\pi e^2 \sum_i \frac{z_i^2 c_{io}}{\varepsilon_o k T} \right]^{\frac{1}{2}}, \end{aligned} \quad (2.8)$$

where  $A$  is a coefficient of order of 1. The value  $k^{-1}$ , the so-called Guy's length, is of order of  $\frac{\varepsilon_o}{c_o^{1/2}} \cdot 10^{-8}$  cm;  $c_o$  is the characteristic concentration (molls per liter). The length  $L$  depends on the mixing in the solution, so for real system it has a magnitude in the range  $10^{-4} - 10^{-3}$  cm. Thus, the parameter  $(kL)^{-2}$  is sufficiently small than 1 and the zero-order approximation of the equation (2.6) may be replaced by the equation of the local electrical neutrality of the solution:

$$\sum_i z_i c_i = 0. \quad (2.9)$$

The systems (2.3) and (2.9) have been created and applied for a description of a steady-state ionic mass transfer in several simple cases. It has been demonstrated that the condition (2.9) has been satisfied only for in the area outside the boundaries of a double diffusional electric layer with a thickness  $k^{-1}$ . Inside the double electric layer the kinetics of ionic mass transfer may be described by the complete system (2.5)-(2.6).

Statistical and mechanical analysis' of the applicability of the method of self-consistent field has been performed in [21]. This analysis demonstrates that the system of equations (2.5)-(2.6) could be derived from the complete system for a chain of correlative functions. The system describes the spacio-temporal distribution of the charged particles (considered as points) near the polarized interphase boundary under non-equilibrium conditions and zero-order approximation with respect to the parameter  $k^3V$ , where  $V$  - the mean volume associated with one particle in the solution. For aqueous electrolyte solutions of one and two valences at ambient temperature this parameter is

$$k^3V \approx 54\sqrt{c_o}, \quad (2.10)$$

where  $c_o$  is the volumetric concentration (molls per liter).

From the point of view of the statistical mechanics the system of equations describing the ionic mass transfer, based on the concept of the self-consistent field, is valid only under small (in order of  $10^{-3} M$ ) volumetric concentrations of the electrolyte.

### 2.1.2. Transport of neutral molecules in the self-consistent field of the double electric layer

Equation (2.2) can be used for the description of the transport mechanism of neutral particles having dipole moments under the action of a non-homogeneous electric field. The field is generated simultaneously by the charged interphase boundary and the ions in a solution of electrolyte excessive content. In this case and if the volumetric electrolyte concentration satisfies the condition  $k^3V \ll 1$ , the distribution of the potential in the proximity of the interphase boundary is described by equation (2.7). The self-consistent field intensity  $E$  is the solution of equation (2.7), but it, does not depend on the local particle concentration  $c_i(x)$ , because it is assumed as a quasi-external with respect to them. The mass transfer problem in such systems calls for an explicit form of the solution for the force  $F$  (see equation 2.2) expressed as a function of the parameters of the double electric layer.

In accordance with the general definition, the projection of the force  $F$  on  $i^{th}$ -axis of a fixed co-ordinate system is

$$F_i = \sum_{k=1}^3 \int_S \sigma_{ik} n_k dS, \quad (2.11)$$

where  $\sigma_{ik}$  is the stress tensor and  $n_k (k = 1, 2, 3)$  - a projection of the unit normal vector  $n$  on the surface  $dS$ , where the force  $F$  is applied. In the mass transfer situation discussed here the stress tensor  $\sigma_{ik}$  considers both the electric and the osmotic forces:

$$\sigma_{ik} = \frac{\epsilon_o}{4\pi} \left( E_i E_k - \frac{1}{2} \delta_{ik} E^2 \right) + kT \sum_a \{ c_a(x) - c_{ao} \}, \quad (2.12)$$

where  $\delta_{ik}$  - Kroneker delta,  $c_a(x)$  and  $c_{ao}$  - concentrations of ions of type  $a$  at the point  $x$ .

The first term of the right-hand part of Eq.(2.12) is Maxwell's stress tensor , while the second one characterizes the osmotic pressure connected with the non-uniformity space distribution of the particle (in the present case the particles are the electrolyte ions) generating the external field.

Within the frame of the theory of Guy-Chapman for a co-planar double electric layer (with parallel flat boundaries) generated by a binary z-z valence electrolyte with a volumetric concentration  $c_\phi$  the following relationships are valid:

$$E_x = \left( \frac{32\pi c_\phi kT}{\epsilon_o} \right)^{\frac{l}{2}} \operatorname{sh} \left( \frac{ez\varphi(x)}{2kT} \right), \quad E_y = E_z = 0,$$

$$\sum_a \{c_a(x) - c_{ao}\} = \frac{\epsilon_o E_x^2}{8\pi kT} = 4 c_\phi \operatorname{sh}^2 \left( \frac{ez\varphi(x)}{2kT} \right), \quad (2.13)$$

where  $\varphi(x)$  is the potential distribution in the diffusion part of the double electric layer. From the above relationships in the particular case it follows that the tensor  $\sigma_{ik}$  has a non-zero component  $\sigma_{xx}$ :

$$\sigma_{xx} = \frac{\epsilon_o}{4\pi} E_x^2. \quad (2.14)$$

The equation presented above indicates that the contribution of the osmotic pressure in the stress tensor  $\sigma_{xx}$  is of the same order as the contribution of the electric force generated by the double electric layer. This fact has been reported originally by Frumkin [56] as a part of the problem concerning the surface tension of electrolyte solutions. It has been shown in [56] that the osmotic pressure leads to two-time lower values of the calculated surface tension.

Equations (2.11) and (2.14) allow the calculation of a force action on a single particle originated by a self-consistent field. Consider the particle as a thin (with respect to Guy's length) flat disk with an area  $S$  and a thickness  $l$  and a symmetry axis parallel with the  $x$ -axis. The disk will be subjected to a force acting in the opposite direction and with a magnitude:

$$F_x = -ezE_x^2 Sl \sqrt{\frac{2c_\phi \epsilon_o}{\pi kT} \left( 1 + \frac{\epsilon_o E_x^2}{32\pi c_\phi kT} \right)}. \quad (2.15)$$

The force characterizes the rate of migration transport determined by the second term of right-hand part of the equation (2.2).

The example commented above demonstrates a mass transfer phenomenon in a non-homogeneous external electric field. The problem is related to the mathematical theory of several technological processes such as flotation of charged colloidal particles, metal extraction from solutions in an electric field by means of liquid ion-selective membranes, separation of solutes by electro-osmosis etc.

### 2.1.3. Method of the local thermodynamic equilibrium

From general point of view the mass transfer equation for heterogeneous systems, (with respect the problems discussed in the previous point) may be derived by means of the local thermodynamic equilibrium as a basic assumption of the irreversible thermodynamics. Taking into account the assumptions of the method the mass transfer driving force for each of solution components can be expressed as a linear combination of the chemical gradients (in the case of ions this is the electrochemical gradient) of all the species in the solution. The next assumption is that in every point of the space at a given time, the local chemical potential is dependent on both the local concentrations and the local characteristics of the electric field. The relations are the equilibrium thermodynamic relations in the absence of a mass transfer. The principle of the local thermodynamic equilibrium is applicable to such relatively slow processes as diffusion and migration. In these cases the characteristic time scales are significantly greater than the correlation time, i.e. the time for the establishment of the equilibrium value of the energy exchanged between the particles.

In the work [124] a relationship between the gradient of the chemical potential of an arbitrary ( $i^{th}$ ) solution component  $\mathbf{grad}\mu_i$  and the diffusion-migration fluxes of all  $j_k$  components was established. The relationship follows from the equation

$$\sum_{k=1}^n \left\{ M_i c_i c_k \mathbf{grad}\mu_i + \frac{kT}{M_k D_{ik}} (M_k c_k j_i - M_i c_i j_k) \right\} = 0 \quad (i = 1, 2, \dots, n), \quad (2.16)$$

where  $n$  is the number of components of the solution (including the solvent),  $D_{ik}$  - binary diffusional coefficient. These coefficients satisfy the reciprocal relation  $D_{ik} = D_{ki}$ . If  $\mu_i = \mu_i(c_1, c_2, \dots, c_n, \varphi)$  are known (from the equilibrium thermodynamics) functions of the local concentrations and electric potential, thus the solution of (2.16), together with the continuity equations (2.5) as well as Maxwell's (2.6) and Gibbs-Duhham's relations, in the form :

$$\sum_{k=1}^n c_k \mathbf{grad}\mu_k = 0 \quad (2.17)$$

completely determines the mass transfer kinetics.

The main problem in the description of ionic mass transfer by means of the equations mentioned above is that there are strong correlation effects with the Coulomb interaction between the ions. Because of that the coefficients of binary diffusion of ions  $D_{ik}$  could neither experimentally nor theoretically be determined [38,110,111,116,117] in the general case. The problem may be solved satisfactory in the particular case of binary solution and a stationary electric current only [35]. In this case, the solution of (2.16)- (2.17) with respect to the fluxes  $j_1, j_2, j_3$  of the cations, the anions and the solvent molecules respectively is:

$$\frac{(z_1 - z_2)}{M_1 D_{eff}} j_1 = \frac{M_3 z_2 c}{\rho k T} (c_1 \mathbf{grad}\mu_1 + c_2 \mathbf{grad}\mu_2) - \frac{i}{e D_{23}} \left[ \frac{c_1}{\rho D_{13}} (M_1 D_{13} - M_2 D_{23}) - 1 \right], \quad (2.18)$$

$$\frac{z_1 - z_2}{M_2 D_{eff}} \mathbf{j}_2 = \frac{M_3 z_2 c}{\rho kT} (c_1 \mathbf{grad} \mu_1 + c_2 \mathbf{grad} \mu_2) - \frac{\mathbf{i}}{e D_{13}} \left[ \frac{c_2}{\rho D_{23}} (M_1 D_{13} - M_2 D_{23}) + I \right], \quad (2.19)$$

$$\frac{(z_1 - z_2)}{M_3 D_{eff}} \mathbf{j}_3 = \frac{(z_2 M_1 - z_1 M_2) c}{\rho kT} (c_1 \mathbf{grad} \mu_1 + c_2 \mathbf{grad} \mu_2) - \frac{(M_1 D_{13} - M_2 D_{23}) c_3 \mathbf{i}}{e \rho D_{13} D_{23}}. \quad (2.20)$$

Here  $\mathbf{i} = e \left[ \left( \frac{z_1 \mathbf{j}_1}{M_1} \right) + \left( \frac{z_2 \mathbf{j}_2}{M_2} \right) \right]$  is the vector of electric current density,

$\rho = M_1 c_1 + M_2 c_2 + M_3 c_3$  is the local density of the solution,  $c_3$  - the solvent concentration,  $c = c_1 + c_2 + c_3$  is the total concentration of the liquid phase, while the effective coefficient of ion transport  $D_{eff}$  can be determined by the relation:

$$D_{eff} = \frac{\rho (z_2 - z_1) D_{13} D_{23}}{(z_1 c_1 + z_2 c_2) (M_1 D_{13} - M_2 D_{23}) + \rho (z_2 D_{23} - z_1 D_{13})}. \quad (2.21)$$

From the relations (2.18)-(2.21) it is clear that the system of equations describing the ionic mass transfer does not contain the diffusion coefficient  $D_{12}$  which cannot be experimentally established. In the cases of solution with two or more types of ions the excluding of the coefficients of binary diffusion from the equations becomes impossible [37,38].

The electrochemical potentials of the ions can be expressed in the form:

$$\mu_i = \mu_i^{(0)} + e z_i \varphi + k T \ln \left( \frac{c_i \gamma_i}{c_o} \right), \quad (2.22)$$

where  $\mu_i^{(0)}$  is a standard value depending both on the temperature and the pressure in the solution,  $\gamma_i$  is the activity coefficient,  $c_o$  - the characteristic concentration. If the condition of a local electroneutrality (2.9) is satisfied, thus it follows from (2.18)-(2.20) that the relationships for the mass fluxes for a binary electrolyte are:

$$\mathbf{j}_1 = - \frac{D_{eff} M_1 M_3 c}{\rho} g(c_1, c_2) \mathbf{grad} c_1 + \frac{M_1 D_{13} \mathbf{i}}{e(z_2 D_{23} - z_1 D_{13})} \left[ \frac{c_1}{\rho D_{13}} (M_1 D_{13} - M_2 D_{23}) - I \right], \quad (2.23)$$

$$\mathbf{j}_2 = - \frac{D_{eff} M_2 M_3 c}{\rho} g(c_1, c_2) \mathbf{grad} c_2 + \frac{M_2 D_{23} \mathbf{i}}{e(z_2 D_{23} - z_1 D_{13})} \left[ \frac{c_2}{\rho D_{23}} (M_1 D_{13} - M_2 D_{23}) + I \right], \quad (2.24)$$

$$g(c_1, c_2) = 1 + \frac{d \ln \gamma_{12}}{d \ln \left( \frac{c_1}{c_o} \right)}, \quad \ln \gamma_{12} = \frac{\nu_1 \ln \gamma_1 + \nu_2 \ln \gamma_2}{\nu_1 + \nu_2}, \quad (2.25)$$

where  $\nu_1$  and  $\nu_2$  are the number of cations and anions after a molecule disassociation in the electrolyte,  $\gamma_{12}$  is the mean coefficient of electrolyte activity.

## CHAPTER 2.2. ANODIC METAL DISSOLUTION IN AN ELECTROLYTE FLOW

The mathematical description of the process microkinetics in case of intensive anodic dissolution, applied for a fine treatment of metal details is usually based on the so-called "ideal process" [5,104]. The model supposes that: 1) Ohm's law is valid over the whole space occupied by the solution till the electrode surfaces; 2) the potential distribution is described by the Laplace equation; 3) The current density during the reaction of the anodic metal dissolution is steady state, i.e. 100 % current output. This means, that the calculations following from the application of the "ideal" model may give satisfactory results only for a system where the effects of both the chemical and the concentration overpotentials do not play significant roles. Moreover, the main electric resistance depends of the volumetric properties of the solution which remain constant in all the points of the gap between the electrodes. From a mathematical point of view the problem of "ideal" process of anodic dissolution is similar to the process of fluid filtration through porous media described by Darcy's law [15]. The principal difficulty comes from the solution of the Laplace equation for the area occupied by the electrolyte. Even in this simple mathematical model the problem for the determination of the shape of the gap between the electrodes becomes very complicated and its solution needs numerical methods. The analytical solution of the problem may be found for special cases only, mainly for systems with bidimensional geometry allowing the application of the theory of the complex functions [24, 32,42,82,119,121]. An elegant analytical method based on relations between the components of complex potential and the solutions of characteristic hypergeometric equation has been developed by Polubarinova-Kochina [51] for the cases of the filtration theory. The method, without any modifications, can be applied to the problems for stationary electrochemical machining problems upon the conditions of the "ideal" process model. The values of the current functions at the filtration boundaries (while the shape of the boundary is determined from the solution) are direct analogues of those with known potentials at electrodes of the electrochemical cell.

However, the practical situations are considerably different for the non-ideal processes. Thus, the calculations based on the "ideal" process do not satisfy the requirements. The next example illustrates the incorrectness of the extrapolation of Ohm's law inside the zone near the electrodes under high densities of anodic current of dissolution. In [33,86,125] it has been shown that solutions for ionic mass transfer may be obtained under the assumptions of the diffusional model of Nernst. These solutions are valid for some situations of anodic metal dissolution in indifferent electrolytes. These solutions demonstrate that in the case of one-one-valence electrolyte the field intensity  $E$  close to the electrode surface and the density of the anodic current are related as follows:

$$E = \frac{iRT}{2D_m F^2 c_o} \left( 1 + \frac{i\delta}{2D_m F c_o} \right)^{-1}, \quad (2.26)$$

where  $D_m$  is the diffusivity of the metal ions in the solution;  $F$  - Faraday's constant;  $R$  - the universal gas constant;  $c_o$  - volumetric concentration of the indifferent electrolyte;  $\delta$  - the

effective thickness of the diffusional Nernst's layer. The evaluations indicate that for highly concentrated solutions ( $c_o > 1$  mole/liter) and current density about  $100 \text{ A/cm}^2$  the second term in the brackets of (2.26) remains greater than unity even under an intensive mixing of the solution ( $\delta < 10^{-4} \text{ cm}$ ). This means that the relationship of Ohm's law

$$E = \frac{iRT}{(D_A + D_k)F^2 c_o}, \quad (2.27)$$

already employed in [88,89,109] for solutions of shape formation problems is inapplicable in the area located very close to the anode surface. Here,  $D_A$  and  $D_k$  are the coefficients of binary diffusion of anions and cations of the indifferent electrolyte respectively. The extrapolation of Ohm's law into the zone near the anode leads to significant errors. The correct description of process kinetics during an anodic dissolution of metals may be made by means of the system (2.5), (2.6), (2.16) and (2.17). Taking into account the specific hydrodynamic situations mentioned above, the boundary conditions of these systems differs significantly from those employed at low rate mass transfer. It is better to define the boundary conditions from the qualitative description of the potential distribution established in the electrolyte solution flowing in the gap under conditions corresponding to Reynolds numbers higher than unity.

Figure 2.1 shows schematically the potential distribution in an electrochemical cell. The zones I and VII are Helmholtz double electric layers, II and VI – diffusion double electric layers, III and V – diffusion boundary layers and IV- a zone of the ohmic potential drop. The potential drop inside the diffusional boundary layers (concentration overpotentials) may be expressed as:

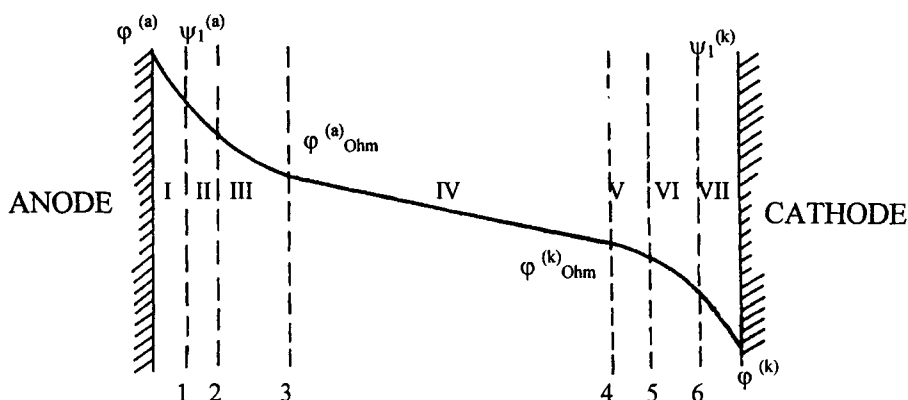


Fig.2.1 Potential distribution in an electrolyte cell.

$$\begin{aligned}\eta_{conc.}^{(a)} &= \psi_i^{(a)} - \psi_{ip}^{(a)} - \varphi_{Ohm}^{(a)}, \\ \eta_{conc.}^{(k)} &= \varphi_{Ohm}^{(k)} - \psi_i^{(k)} + \psi_{ip}^{(k)},\end{aligned}\quad (2.28)$$

where  $\psi_{ip}^{(a)}$  and  $\psi_{ip}^{(k)}$  are the potential drops in anodic and cathodic diffusional double electric layers in the absence of an electric current through the cell. The electrochemical overpotential is

$$\eta_{chem.}^{(a)} = \varphi^{(a)} - \psi_i^{(a)} - (\varphi_p^{(a)} - \psi_{ip}^{(a)}). \quad (2.29)$$

It is related with the local current density  $i_a$  through the relation [57]:

$$i_a = i_a^{(0)} \left\{ \exp \left[ \frac{\alpha z_m F}{RT} \eta_{chem.}^{(a)} \right] - k_a c_m^{(S_a)} \exp \left[ - \frac{(1-\alpha) z_m F}{RT} \eta_{chem.}^{(a)} \right] \right\}. \quad (2.30)$$

Here  $i_a^{(0)}$  - exchange anodic current density,  $\alpha$  - macroscopic transfer coefficient,  $k_a$  - rate constant of the electrochemical cations' renewal at the anode.

Cathodic electrochemical overpotential, in the case of electrochemical machining, usually is related with water disassociation



If  $i_k^{(0)}$  is the exchange current density of the above reaction and  $c_H^{(S_k)}$  is the concentration of hydroxyl ions at the cathode surface the respective cathodic chemical overpotential is

$$\eta_{chem.}^{(k)} = \varphi_p^{(k)} - \psi_{ip}^{(k)} - (\varphi^{(k)} - \psi_i^{(k)}). \quad (2.32)$$

It is related with the cathode density current  $i_k$  through the relationship

$$i_k = i_k^{(0)} \left\{ \exp \left[ \frac{\beta F}{RT} \eta_{chem.}^{(k)} \right] - k_k c_H^{(S_k)} \exp \left[ - \frac{(1-\beta) F}{RT} \eta_{chem.}^{(k)} \right] \right\}, \quad (2.33)$$

where  $\beta$  is a macroscopic cathodic transfer coefficient.

In zone IV all the ionic concentrations are homogeneously distributed with respect to the field intensity. The relation between the electric current density and the potential is Ohm's law

$$i = F \sum_k \frac{z_k}{M_k} j_k = -\sigma \text{grad} \varphi . \quad (2.34)$$

In a gap with flat parallel poles at a distance  $h$  the equation (2.34) has only one component in a direction normal to the electrode surface and can be expressed in a scalar form

$$\Delta\varphi_{Ohm} = \varphi_{Ohm}^{(a)} - \varphi_{Ohm}^{(k)} = \frac{hi}{\sigma}. \quad (2.35)$$

The quantities  $i_a$  and  $i_k$  are related with the total mass fluxes of ions existing in the solution

$$\begin{aligned} -\frac{i_a}{F} &= \sum_i z_i \left\{ \frac{\mathbf{j}_i^{(S_a)}, \mathbf{n}^{(a)}}{M_i} + c_i \left( \left[ \mathbf{v}^{(S_a)} - \frac{d\mathbf{r}^{(a)}}{dt} \right], \mathbf{n}^{(a)} \right) \right\}, \\ -\frac{i_k}{F} &= \sum_k z_k \left\{ \frac{\mathbf{j}_i^{(S_k)}, \mathbf{n}^{(k)}}{M_i} + c_i \left( \left[ \mathbf{v}^{(S_k)} - \frac{d\mathbf{r}^{(k)}}{dt} \right], \mathbf{n}^{(k)} \right) \right\}. \end{aligned} \quad (2.36)$$

Here,  $\mathbf{n}^{(a)}$  and  $\mathbf{n}^{(k)}$  are unit normal vectors with respect the surfaces of the anode and the cathode. They are external with respect the solution. Assuming that the only electrochemical reaction at the anode is the ionization of metal atoms and under the effect of the boundary conditions (2.30) and (2.36) the result is

$$\begin{aligned} \frac{(\mathbf{j}_m^{(S_a)}, \mathbf{n}^{(a)})}{\rho^{(S_a)} - M_m c_m^{(S_a)}} &= -\frac{M_m i_a}{\rho^{(S_a)} z_m F}, \\ (\mathbf{j}_i^{(S_a)}, \mathbf{n}^{(a)}) &= \frac{M_i M_m c_i^{(S_a)} i_a}{\rho^{(S_a)} z_m F}, \quad (i \neq m). \end{aligned} \quad (2.37)$$

When the mass transfer effects on ionic fluxes at the cathode are negligible the corresponding boundary conditions for these fluxes are:

$$\begin{aligned} (\mathbf{j}_{\Gamma}^{(S_k)}, \mathbf{n}^{(k)}) &= -\frac{M_{\Gamma} i_k}{F}, \\ (\mathbf{j}_i^{(S_k)}, \mathbf{n}^{(k)}) &= 0, \quad (i \neq \Gamma). \end{aligned} \quad (2.38)$$

From the conditions of ionic charge conservation it follows that the quantities  $i_a$  and  $i_k$  are interrelated. The relation may be established from the general equation of mass conservation for an arbitrary  $i^{\text{th}}$  ionic solution component. The equation applied to the whole gap between the electrodes is

$$\int_{S_a} \left\{ c_i \left( \left[ \mathbf{v}^{(S_a)} - \frac{d\mathbf{r}^{(a)}}{dt} \right], \mathbf{n}^{(a)} \right) + \frac{I}{M_i} (\mathbf{j}^{(S_a)}, \mathbf{n}^{(a)}) \right\} dS_a +$$

$$\int_{S_a} \left\{ c_i \left( \left[ v^{(S_k)} - \frac{dr^{(k)}}{dt} \right], n^{(k)} \right) + \frac{I}{M_i} (j^{(S_k)}, n^{(k)}) \right\} dS_k = 0, \quad (2.39)$$

where  $S_a$  and  $S_k$  are the surface areas of the anode and the cathode, respectively. A multiplication of all the terms of (2.39) with  $z_i F$  followed with a summation for all kinds of ions and obeying also (2.36) gives the total current  $I$  through the cell:

$$\int_{S_a} i_a dS_a = \int_{S_k} i_k dS_k = I. \quad (2.40)$$

In accordance with the comments made above, the electrode potentials  $\phi^{(a)}$  and  $\phi^{(k)}$  satisfy the relationships:

$$\begin{aligned} \phi^{(a)} &= \varphi^{(a)} - \varphi_{\text{Ohm}}^{(a)} = \varphi_p^{(a)} - \eta_{\text{conc.}}^{(a)} - \eta_{\text{chem.}}^{(a)}, \\ \phi^{(k)} &= \varphi^{(k)} - \varphi_{\text{Ohm}}^{(k)} = \varphi_p^{(k)} + \eta_{\text{conc.}}^{(k)} + \eta_{\text{chem.}}^{(k)}. \end{aligned} \quad (2.41)$$

The solutions for ionic concentration distributions in connection with the relations (2.30), (2.40) and (2.41) allow a determination of  $(j_m^{(S_a)}, n_a)$  as a function of the cell geometry and the current  $I$  at given values of  $\phi^{(a)}$  and  $\phi^{(k)}$ .

### 2.2.1. Dissolution of surfaces equi-accessible with respect the ionic mass transfer

The problem of anodic metal dissolution in a solution of its own salt, e.g. dissolution of iron in a ferric chloride for example, will be discussed as an example of application of the equations and boundary conditions discussed in the previous point. In order to obtain an analytical solution of the problem several simplifications will be made. Let's suggest that the system satisfies the following conditions [26,28-30]:

1. The surface subjected to anodic dissolution is equi-accessible from a diffusional point of view.
2. The process is steady state, i.e. the concentration of each of the components at any distance from the anode is time independent.
3. The ionic mass transfer occurs at very high Schmidt numbers and the velocity profile inside the diffusion boundary layer may be approximated by a homogeneous velocity distribution assuming the velocity equal to that at the anode ( $V = V_s$ ).
4. The ratio of the effective diffusion boundary layer thickness to the one of diffusion near-anode layer is negligible, so the solution may be assumed as electrically neutral in all the point as well as at the points at the interphase boundary. Thus equation (2.6) may be replaced by (2.9).

The condition of an equi-accessible surface for the mass transfer seems that the local component concentrations are simultaneously space and time independent:

$$c_i = c_c \{ [r - r^{(a)}], n \} t \}. \quad (2.42)$$

Introducing in (2.5) a new variable  $x = (\mathbf{r}, \mathbf{n}) - (\mathbf{r}^{(a)}, \mathbf{n})$  instead of  $\mathbf{r}$  it follows that

$$\frac{\partial c_i}{\partial t} + \left\{ (\mathbf{v}, \mathbf{n}) - \left( \frac{d\mathbf{r}^{(a)}}{dt}, \mathbf{n} \right) \right\} \frac{\partial c_i}{\partial x} + \frac{i}{M_i} (\mathbf{j}_i, \mathbf{n}) = 0, \quad i = 1, 2, 3. \quad (2.43)$$

The assumptions for the steady state mass transfer process and the homogeneity of the velocity profile allow time derivative elimination and the replacement of the term in the curly brackets with the right side of equation (1.4):

$$\frac{M_i(\mathbf{j}_{is}, \mathbf{n})}{\rho_s - M_i c_{is}} \frac{dc_i}{dx} + \frac{d}{dx} (\mathbf{j}_i, \mathbf{n}) = 0, \quad i = 1, 2, 3. \quad (2.44)$$

Integrating the above equations with the boundary conditions (2.37) yields:

$$(\mathbf{j}_i, \mathbf{n}) = \frac{M_i i}{z_i F} \left( \frac{M_i c_i}{\rho_s} - \delta_{ii} \right), \quad (2.45)$$

where  $\delta_{ii}$  is Kronecker delta.

By substitution the fluxes  $\mathbf{j}_i$  in the left part of (2.45) with their forms expressed by means of the electrochemical potentials (see equations (2.18)-(2.20)) and with the help of (2.9) two independent equations may be obtained:

$$\begin{aligned} & \left( 1 + \frac{d \ln \gamma_{12}}{d \ln c_1} \right) \frac{dc_1}{dx} + \frac{i}{(z_1 - z_2) F M_3 D_{23} c} \times \\ & \times \left\{ \frac{M_1 D_{13} - M_2 D_{23}}{D_{13}} c_1 - \rho \left[ 1 - \frac{(z_1 - z_2) D_{23}}{z_1 D_{eff}} \left( 1 - \frac{M_1 c_{1s}}{\rho_s} \right) \right] \right\} = 0, \\ & \left( 1 + \frac{d \ln \gamma_{12}}{dc_1} \right) \frac{dc_1}{dx} - \frac{z_2 i}{(z_2 M_1 - z_1 M_2) F c} \left\{ \frac{M_1 D_{13} - M_2 D_{23}}{(z_1 - z_2) D_{13} D_{23}} c_3 - \frac{\rho M_1 c_{3s}}{z_1 \rho_s D_{eff}} \right\} = 0. \end{aligned} \quad (2.46)$$

Here the quantity  $\gamma_{12}$  presents the mean coefficient of electrolyte activity.

If the function  $\gamma_{12} = \gamma_{12}(c_1, c_2, c_3)$  is known, thus the equations (2.9) and (2.46) form a closed system of equations allowing determination of the local concentrations  $c_1, c_2, c_3$ . However, the system is non-linear, so the estimation of the analytical solution is impossible without further simplifications. Consider a particular example of the solution content where the local ion concentrations are low with respect to the one of the solvent ( $c \approx c_3$ ), but due to high molar mass of the dissolving metal the local cation density  $M_1 c_1$  is comparable with the local solution density. Substituting  $c = c_3 = const.$  and using (2.46) the following equation about the concentration  $c_1$  is available:

$$\left(1 + \frac{d \ln \gamma_{12}}{d \ln c_1}\right) \frac{dc_1}{dx} - \frac{i M c_1}{z_1 F D_{\text{eff}} \rho_s} = \frac{i}{(z_1 - z_2) F D_{23}} \left[ 1 - \frac{(z_1 - z_2) D_{23}}{z_1 D_{\text{eff}}} \left( 1 - \frac{M_1 c_{1s}}{\rho_s} \right) \right]. \quad (2.47)$$

The existing empirical correlations for activity coefficients of electrolytes [54] have very complicated forms. Because of that the integration of (2.47) is impossible without applications of numerical methods. However, the quantitative investigation of the specific behaviour of ionic mass transfer with a high anodic dissolution may be performed by means of the equation (2.47) in an analytical form. In fact, if the interaction of the momentum transfer and the mass transfer (described by the boundary conditions (1.4) and (2.37)) is not taken into account, the cation transport may be described by the folding equation

$$\left(1 + \frac{d \ln \gamma_{12}}{d \ln c_1}\right) \frac{dc_1}{dx} = \frac{z_2 i}{z_1 (z_1 - z_2) F D_{13}}. \quad (2.48)$$

The comparison of (2.47) and (2.48) shows that the effect of mutual interaction of the interphase exchange of mass and momentum becomes significant under the conditions of an anodic dissolution. In this case the partial cation density  $M_1 c_{1s}$  in near-anode zone is comparable to the solution density  $\rho_s$ . The quantitative assessment of the contribution of this effect, without lack of generality, may be performed with the following example. Consider a limited area of concentration near the minimum of the curve  $\ln \gamma_{12} = f(c_1)$ . For many aqueous electrolyte solutions this minimum is located at concentrations about 1 mol/l per liter [54], i.e. in the area where the ratio  $\frac{M_1 c_{1s}}{\rho_s}$  may reach a value of several decades of percents.

In this case substituting  $\frac{d \ln \gamma_{12}}{d \ln c_1} = 0$  in (2.48) and assuming that at a distance  $x = \delta$  from the anode the concentration  $c_1$  reaches its volumetric value,  $c_{10}$  upon integration the final relationship is

$$\begin{aligned} c_1 &= (c_{10} + A) \exp \left[ - \frac{i M_1 (\sigma - x)}{z_1 F D_{\text{eff}} \rho_s} \right] - A, \\ A &= c_{1s} + \frac{z_2 D_{23} \rho_s}{M_1 (z_1 D_{13} - z_2 D_{23})}. \end{aligned} \quad (2.49)$$

The value of  $\delta$  may be considered as an effective thickness of the diffusion boundary layer.

The relation (2.49) allows the evaluation of the equation for near-cathode concentration of the cations  $c_{1s}$ :

$$\left\{ 2 - \exp \left[ - \frac{i M_1 \delta}{z_1 F D_{\text{eff}} \rho_s} \right] \right\} c_{1s} = \left[ c_{10} + \frac{z_2 D_{23} \rho_s}{M_1 (z_1 D_{13} - z_2 D_{23})} \right] \exp \left[ - \frac{i M_1 \delta}{z_1 F D_{\text{eff}} \rho_s} \right] -$$

$$-\frac{z_2 D_{23} \rho_s}{M_1 (z_1 D_{23} - z_2 D_{23})}. \quad (2.50)$$

If the effect of the diffusion flux on the convective ionic mass transfer from anode surface is negligible, taking into account (2.48) the equation for  $c_{1s}$  may be expressed as:

$$c_{1s} = c_{10} - \frac{z_2 i \delta}{z_1 (z_1 - z_2) F D_{13}}. \quad (2.51)$$

The analysis of (2.50) shows that the determined value of  $c_{1s}$  under an arbitrary current density  $i$  is lower than the evaluated from equation (2.51).

The relationship (2.50) for  $c_{1s} = c_{1s}(i)$  has a monotonous character and at high currents has asymptotic values  $c_{1s}^{\max}$ :

$$c_{1s}^{\max} = -\frac{z_2 D_{23} \rho_s}{2 M_1 (z_1 D_{13} - z_2 D_{23})}. \quad (2.52)$$

The results show that at a fixed density of anodic current the real cation concentration in near-anode layer is always lower than that calculated under the assumption of an absence of mutual effects of both the momentum and mass transfer. An important conclusion following from the above result is that it is possible to reach higher current densities at "critical" metal anion concentration. The current densities are higher with respect to those calculated in accordance with the classical theory of the convective diffusion at low rate of the interphase mass transfer. The existence of a "critical" anion concentration in a real situation may be attributed to the solution saturation or to other constraints, e.g. reactions of complex formation or metal passivation etc.

The analysis carried out here shows that the reciprocal action of momentum and mass transfer must be taken into account. The assessments show that this interaction affects significantly the calculation accuracy at current densities about  $10 \text{ A/cm}^2$  and higher in solutions of the concentration of one mol/l.

Figure 2.2 shows the variations of dimensionless cation concentration  $c_{1s} = \frac{c_{1s}}{c_{10}}$  (line

- 1) in the near-anode zone ( $\delta=10^{-3}$ ) with the dimensionless anodic current density  $I = \frac{i|z_2|\delta}{z_1(z_1 - z_2)FD_{13}c_{10}}$  and the case of Fe(II) dissolution in 1N aqueous solution of  $\text{FeCl}_2$ .

The linear relationship (line 2) corresponds to the case of absence of mass flux from the anode surface. The lines indicate that at a fixed anodic current density the real cation concentration in the near-anode zone is always lower than that calculated under the assumption that the reciprocal actions of momentum and mass transfer are absent.

The analysis of the macrokinetics of anodic dissolution done here for the example of a binary electrolyte may be developed for the cases of solutions containing three kinds of ions: cations, anions and ions of electrically neutral electrolyte. Such analysis has been performed in papers [28,30,31,33,34].

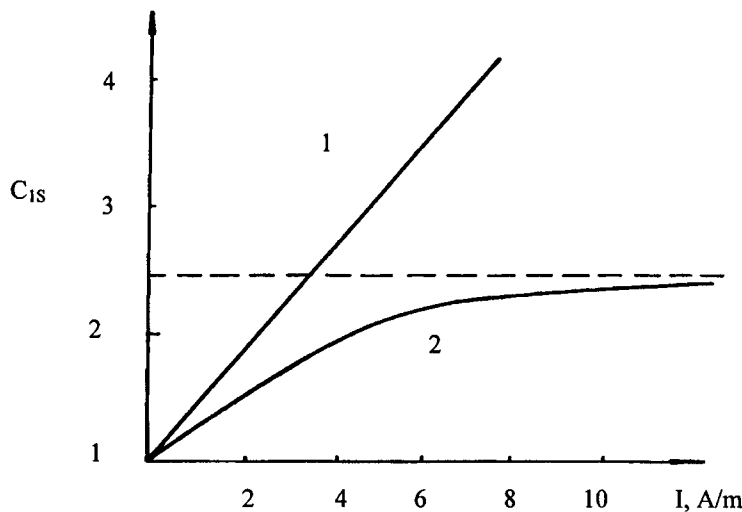


Fig.2.2. Variations of ion concentrations near the anode with the electric current intensity,  $I$ ,  
System :  $\text{Fe}^{2+}/\text{FeCl}_2$ .

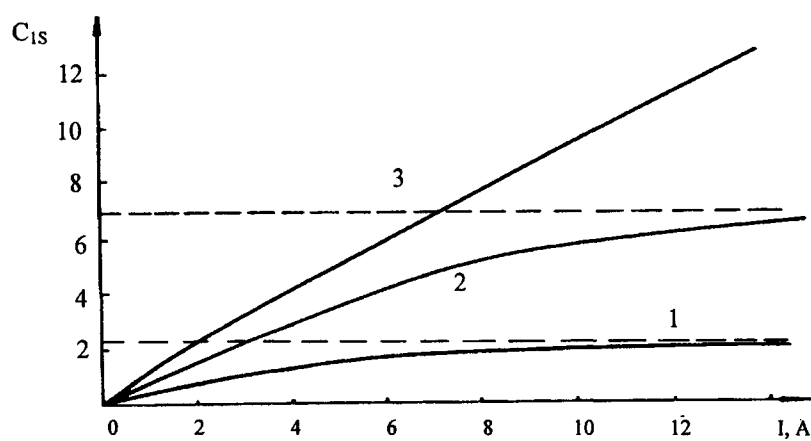


Fig. 2.3 Variations of ion concentrations near the anode with the electric current intensity,  $I$ .  
System:  $\text{Fe}^{2+}/\text{FeCl}_2$ .

Figure 2.3 shows the curves of variation of the dimensionless anodic concentration of the cations of dissolving metal  $C_{1s} = \frac{c_{1s}}{c_0}$  with dimensionless anodic current density  $I$  in the case of the system  $\text{Ni}^{2+}/\text{CuSO}_4$ . Curve 3 is calculated with the assumption that the effect of the mass transfer on the hydrodynamics is negligible.

As in the case of binary electrolyte (see Fig.2.2) the lines 1 and 2 demonstrate asymptotic behaviour. The asymptotic concentrations of an electrically neutral electrolyte and Ni are about 9 molles per liter. The calculations show that at  $\delta = 10^{-3}$  cm the limit concentration of cations may be reached at current densities higher than  $100 \text{ A/cm}^2$ . At current densities lower than  $10 \text{ A/cm}^2$  the nickel cation concentration near the anode does not exceed 0.8 M (at  $c_0 = 1\text{M}$ ) and 3.6 M (at  $c_0 = 5\text{M}$ ).

The physical explanation of the "saturation" effect on the anodic layer is that at high current densities the mass transfer affects the hydrodynamics. Under such conditions the rate of cation removal from the near-anode layer by convection is practically equal to the rate of cation accumulation due to the metal dissolution.

## 2.2.2. Ionic mass transfer due to an anodic dissolution complicated with a reaction of complex formation

In many processes of anodic dissolution there is an important contribution of the solution anions [19,20]. In this case the rate of metal ionization increases in parallel with the increase of the anion concentration. In some cases (anodic dissolution of tungsten in alkali [95] or palladium in sodium chloride for example [201]) there are "limiting" anodic currents proportional of the anion concentration. They may be attributed to the hindered removal of the reaction products from the electrode surface [12,106] as well as to the formation of films of salts [13] or oxides [74,75] on it. An analysis of the relationship between the limiting current density and the solution content has been carried out in a number of works [11,14,105]. It was conceived as explanation that in the regime of the limiting current the concentration near the anode is close to that reached at the solution saturation by the reaction products. The difficulties hindering the elucidation of the mechanism of this phenomenon is related mainly to the fact that the metal dissolution is accompanied with electrode passivation. Usually the passivation phenomenon is under a diffusion control near the electrode surface [18,99]. This hinders the detection of the mechanism clarification for the rate of the anodic metal dissolution.

In order to solve some of the problems mentioned above it is important to calculate the distributions of both the ionic concentrations and the electric potential in the near-anode layer. Such calculations may predict the occurrence of a limiting current of dissolution as well as set up the conditions of the regimes and establish current values. The rates of ionic mass transfer during anodic dissolution of metals have been calculated in [1,2,53] under conditions allowing formation of complexes between metal cations and the solution anions. In these studies the charge densities of all the ions in the solution have been assumed as equal. Further, the results of the above investigations have been generalized for the case of arbitrary ion charges [36].

In a steady state the anodic dissolution of a metal  $M$  in an electrolyte solution consisting of cations  $K^{z_1}$  and anions  $A^{z_2}$  accompanied with a formation of an ionic complex  $B^{z_1}$  is described by the following electrochemical reaction:



where  $n = bz_3 - az_2$ . The assumption that the mixing conditions in the solution allow formation of diffusion layers with a thickness  $\delta$  equal for all the ions leads to the validity of Nernst's model. Moreover, the potential drop across the diffusion boundary layer may be neglected if the solution concentration is big enough. The diffusion Nernst's model allows a description of the ionic mass transfer equations in the form:

$$\begin{aligned} j_i &= -D_i \frac{dc_i}{dx} - \frac{z_i D_i c_i F}{RT} \frac{d\varphi}{dx}, \\ \sum_{i=1}^3 z_i c_i &= 0. \end{aligned} \quad (2.54)$$

Here  $j_i (i = 1, 2, 3)$  are the diffusion fluxes of the ions  $K^{z_1}, A^{z_2}, B^{z_3}$ ;  $c_i$  and  $D_i$  are the local concentrations and the diffusion coefficients of these ions;  $\varphi$  is the electric potential depending on the depth inside the solution. Assume  $i$  as a designation of the anodic current density and suppose that the cations  $K^{z_1}$  do not act in the electrode reaction. The assumptions allow the writing of the following relationships:

$$j_1 = 0, \quad j_2 = -\frac{ai}{nF}, \quad j_3 = -\frac{bi}{nF}. \quad (2.55)$$

The decelerating charge theory gives a relationship between the current density  $i$  and the electrode potential  $\varphi_0$  as follows:

$$i = Knc_{2s}^a \exp\left[\frac{\alpha nF(\varphi_0 - \varphi_s)}{RT}\right], \quad (2.56)$$

where  $K$  and  $\alpha$  are constants. The subscript  $s$  designates that the respective quantity must be calculated at  $x = 0$ .

The boundary conditions of (2.54) are:

$$c_1 = c_{10}, \quad c_2 = c_{20}, \quad c_3 = 0, \quad \varphi = 0 \text{ at } x = \delta. \quad (2.57)$$

The introduction of the dimensionless variables:

$$y = \frac{x}{\delta}, \quad C_i = \frac{c_i}{c_{20}}, \quad \phi = \frac{F\varphi}{RT}, \quad J_i = \frac{j_i \delta}{D_i c_{20}}, \quad I = \frac{i \delta}{nFD_2 c_{20}} \quad (2.58)$$

leads to the dimensionless form of the system (2.54):

$$\frac{dC_i}{dy} + z_i C_i \frac{d\phi}{dy} + J_i = 0, \quad i = 1, 2, 3, \quad (2.59)$$

$$\sum_{i=1}^3 z_i C_i = 0, \quad (2.60)$$

$$y = l, \quad C_1 = -\frac{z_2}{z_l}, \quad C_2 = l, \quad C_3 = 0, \quad \phi = 0. \quad (2.61)$$

The multiplication of all the terms of (2.59) with  $z_i$  and the consequent summation along all induces  $i$  as well as taking into account the conditions (2.60) give:

$$\frac{d\phi}{dy} = -\frac{a(z_3 - \lambda z_2)}{\lambda} I \left( \sum_{i=1}^3 z_i^2 C_i \right)^{-l}, \quad (2.62)$$

where  $\lambda = \frac{aD_3}{bD_2}$ . The use of the dimensionless potential  $\phi$  as an independent variable allows to obtain from (2.59)-(2.62) the following system of equations:

$$\begin{aligned} \frac{dC_i}{d\phi} + z_i C_i - \frac{\lambda J_i}{aI(z_3 - \lambda z_2)} \sum_{k=1}^3 z_k^2 C_k &= 0, \quad i = 1, 2, 3; \\ \phi = 0, \quad C_1 = -\frac{z_2}{z_l}, \quad C_2 = l, \quad C_3 = 0. \end{aligned} \quad (2.63)$$

The solution of (2.63) has the form

$$\begin{aligned} C_1 &= -\left(\frac{z_2}{z_l}\right) \exp(-z_l \phi), \\ C_2 &= \frac{l}{1 - \lambda z^*} \left\{ \exp\left[\frac{z_2 z_3 (\lambda - l)}{z_3 - \lambda z_2}\right] - \lambda z^* \exp(-z_l \phi) \right\}, \\ C_3 &= \frac{z_2}{z_3 (1 - \lambda z^*)} \left\{ \exp(-z_l \phi) - \exp\left[\frac{z_2 z_3 (\lambda - l)}{z_3 - \lambda z_2}\right] \phi \right\}, \end{aligned} \quad (2.64)$$

where  $z^* = \frac{z_2(z_1 - z_3)}{z_3(z_1 - z_2)}$ . The substitution of (2.64) in (2.62) and the subsequent integration gives a relationship describing the space potential distribution in an implicit form

$$\frac{az_l z_3 (l - \lambda z^*)}{\lambda} I(l - y) = \frac{z_l (z_3 - z_2)}{\lambda - l} \left\{ 1 - \exp\left[\frac{z_2 z_3 (\lambda - l)}{z_3 - \lambda z_2} \phi\right] \right\} -$$

$$-z_2(z_1 - z_3)\{I - \exp(-z_1\phi)\}. \quad (2.65)$$

At  $z_1 = z_3 = I$ ,  $z_2 = -I$ ,  $a = b = I$  the relationships (2.64) coincide with those obtained in [1]. At  $z_2 = z_3 = -z_1 = -z$ ,  $b = I$  the result from (2.64) is the same as the one derived in [2].

If the distributions of both the ionic concentration and the potential are known, thus it is possible to determine the current-potential relationship of the anodic dissolution process. Because of that, express the kinetic equation (2.56) in a new dimensionless form by the help of (2.64):

$$I = I_0 \left[ \frac{\eta}{z_2 z_3 (\lambda - I)} \right]^a \exp(\alpha n \phi_0) \left\{ z_3(z_1 - z_2) \exp \left[ \left( \frac{z_2 z_3 (\lambda - I)}{z_3 - \lambda z_2} - \frac{\alpha n}{a} \right) \phi_s \right] - \right. \\ \left. - \lambda z_2(z_1 - z_3) \exp \left[ - \left( z_1 + \frac{\alpha n}{a} \right) \phi_s \right] \right\}, \quad (2.66)$$

$$\text{where } I_0 = \frac{K \delta c_{20}^{a-1}}{FD_2}, \quad \eta = \frac{z_2 z_3 (\lambda - I)}{[z_3(z_1 - z_2) - \lambda z_2(z_1 - z_3)]}.$$

The potential of the external Helmholtz plane  $\phi_3$  may be obtained as function of the electrode potential  $\phi_0$  by means of equation (2.65) at  $y = 0$  and by a substitution of the result for  $I$  in (2.66). The final relationship is

$$I_0 \exp[\alpha n(\phi_0 - \phi_s)] \left\{ z_3(z_1 - z_2) \exp \left[ \frac{z_2 z_3 (\lambda - I)}{z_3 - \lambda z_2} \right] - \lambda z_2(z_1 - z_3) \exp(-z_1 \phi_s) \right\}^a = \\ = \frac{\lambda(z_1 - z_2)}{az_1} \left[ \frac{z_2 z_3 (\lambda - I)}{\eta} \right]^{a-1} \left\{ \begin{array}{l} \left. \frac{z_2 z_3}{\eta} - \frac{z_1(z_3 - z_2)}{\lambda - I} \exp \left[ \frac{z_2 z_3 (\lambda - I)}{z_3 - \lambda z_2} \phi_s \right] \right. \\ + z_2(z_1 - z_3) \exp(-z_1 \phi_s) \end{array} \right\}. \quad (2.67)$$

The equations (2.66)-(2.67) describe the function  $I(\phi_0)$  in a parametric form, i.e. the current-potential characteristic of the process.

The relationships obtained above permit to study the important problem of the existence the limiting current of the anodic dissolution accompanied by a complex formation. The analysis of (2.66)-(2.67) shows that at  $z_3 > 0$  the limiting current may exist at  $\lambda > 1$  only.

Under such conditions

$$I_{lim} = \frac{\lambda(z_1 - z_2)}{az_1(\lambda - 1)} . \quad (2.68)$$

In the regime of a limiting diffusion current (related to anion consumption at the electrode) the reaction is limited by the delivery of anions  $A^{z_1}$  towards the electrode surface and  $I_{lim} = I$  is valid. The right side of equation (2.68) may be significantly greater than unity. This means that during the migration transport there is an interaction of the reagent (anion  $A^{z_1}$ ) and the reaction yield (cation  $B^{z_1}$ ). If the value of the diffusion coefficient of the ions  $B^{z_1}$  is moderate (i.e. the quantity  $\lambda$  is slightly greater than unity) it follows that the excess of these ions (with respect to the solution volume) in the near-electrode layer leads to an increase of the anion  $A^z$  concentration in that zone. The latter is attributed to the electrostatic attraction. Thus, the existence of a limiting current at a zero concentration  $c_2$  at  $y = 0$  requires high current densities ( $I_{lim} > I$ ). So, the significant increase of the density of the limiting diffusion current is a result of the interaction between the charged ionic reagents and the reaction products during their migration. The phenomenon has the same physical nature as the so-called exaltation currents described in the literature [8,15,58,97]. The exaltation current is a result of the fact that the resulting current of two parallel processes at the electrodes (e.g. redox reactions) exceeds the algebraic sum of the partial diffusion limiting current of the separate processes.

At  $z_3 = 0$  the limiting current is independent of  $\lambda$ :

$$I_{lim} = \frac{z_1 - z_2}{az_1} . \quad (2.69)$$

In the case of  $z_3 < 0$  the limiting current exists at all values of the parameter  $\lambda$ . Under these conditions  $I_{lim}$  is

$$I_{lim} = \frac{z_1 - z_2}{az_1(\lambda - 1)} \left[ \lambda - (\lambda z^*)^\eta \right] . \quad (2.70)$$

At  $\lambda \rightarrow \infty$  and a limited value of  $a$  the equation (2.70) gives the asymptotic value of the limiting current

$$I_{lim} = \frac{z_1 - z_2}{az_1} . \quad (2.71)$$

The equation (2.71) allows the expression of simple relationships for the limiting current in particular cases:

$$\lambda = 1, \quad I_{lim} = \frac{z_1 - z_2}{az_1} \left\{ 1 + \frac{z_2 z_3}{z_1(z_3 - z_2)} \ln \left[ \frac{z_3(z_1 - z_2)}{z_2(z_1 - z_3)} \right] \right\};$$

$$\lambda = \frac{z_3(z_1 - z_2)}{z_2(z_1 - z_3)},$$

$$I_{lim} = \frac{z_3(z_1 - z)^2}{az_1^2(z_3 - z_2)} \left\{ I - \frac{z_2(z_1 - z_3)}{z_3(z_1 - z_2)} \exp \left[ \frac{z_1(z_2 - z_3)}{(z_1 - z_2)(z_1 - z_3)} \right] \right\}. \quad (2.72)$$

The results obtained in this part may be generalized for the cases where the volumetric ion concentration  $B^{z_i}$  is not zero. The general relationship may be found elsewhere [39].

### 2.2.3. Comparison between the theoretical predictions and the experimental data

The effect of the limiting current may be detected on the polarization curves of tungsten [74,95]. The explanation made in [74] is based on the assumption that a solid film of tungsten oxide exists on the anode surface. Moreover, the removal of the products of the film dissolution is the process limiting stage. The additional experiments performed [25] on tungsten oxide dissolution did permit to establish that the probable reason of the occurrence of anodic limiting currents is the consumption of hydroxyl ions during the process. Some of the experimental polarization curves have been obtained in solution of KOH by a potentiometric method and a rotating disk electrode. The results are shown on Fig. 2.4. . The data of anodic tungsten dissolution have been obtained with 1N solution of KOH and at tree rotational speeds of the disk (turns/min): 3500, 2100 and 1200 (curves 1, 2 and 3 respectively). The dotted lines correspond to the equations described in 2.2.2.

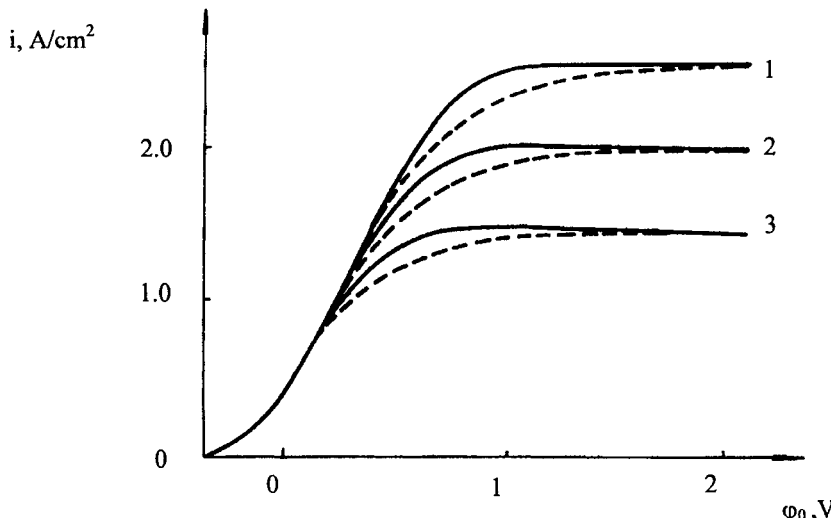


Fig. 2.4 Polarization curves at an anodic dissolution of tungsten.

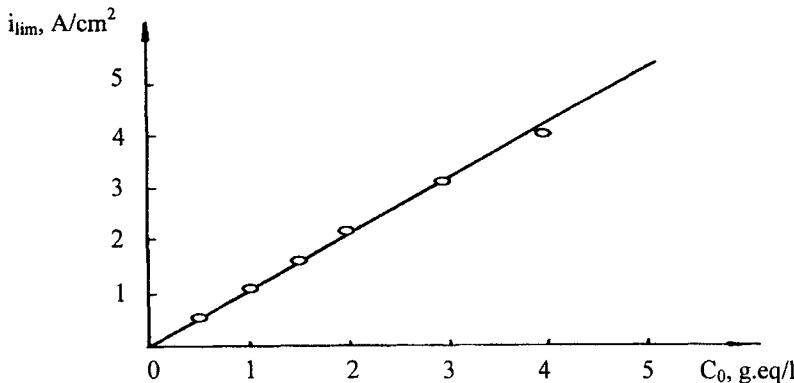


Fig.2.5 The density of the anodic current during a dissolution of tungsten.

Figure 2.5 demonstrates the variations of the limiting current density  $i_{lim}$  with the alkali concentration  $c_0$  under conditions of anodic dissolution in an aqueous solution of KOH. The calculated data (solid line) and those obtained experimentally (the data points) correspond to the limiting currents of a rotating tungsten disk (750 turns/min).

The interpretation of the data has been carried out on the basis of the equation describing the total electrochemical reaction of atom ionization in an alkali solution:



In accordance with the discussion in 2.2.2 a limiting current should exist as a result of the delivery of  $\text{OH}^-$  ions towards the electrode surface. The current density is determined by the equation (2.70) having a dimension form:

$$i_{lim} = \frac{3FD_2c_0}{2\delta(\lambda-1)} \left[ \lambda - \left( \frac{3}{4}\lambda \right)^{\frac{2(\lambda-1)}{(3\lambda-4)}} \right]. \quad (2.74)$$

Here  $\lambda = \frac{8D_3}{D_2}$ ,  $D_2$  is the diffusivity of the hydroxyl ions,  $D_3$  - diffusivity of  $\text{WO}_4^{2-}$  ions.

The calculations have been carried under the assumption that  $D_2 = 5.26 \cdot 10^{-5} \text{ cm}^2 \cdot \text{s}^{-1}$ , while  $D_3$  has been evaluated by means of Nernst-Einstein's relationship [47] relating the limiting electrical conductivity of ions (published data). The diffusion layer thickness  $\delta$  has been established with the help of the rotating disk electrode theory [50]. The calculations of the

polarization curves have been made using the equation (2.66) under the assumption that  $I_0 = 5 \cdot 10^{-3}$  and  $\alpha = 0.5$ .

It is clear that there is a good agreement between the theory and the experimental data. It is important to note that the analysis performed allows a prediction of the limiting current density. In contrast to the currents depending on the potential, the prediction of the limiting current does not require detailed knowledge of the dissolution mechanism. In this respect no data about the kinetic parameters corresponding to the limiting process stage ( $I_0$  and  $\alpha$ ) are needed. The importance of the information given by the value of  $i_{lim}$  due to the fact that during the limiting current "stage" an electrochemical polishing of the tungsten is done [95]. Moreover, the limiting current limits the rate of the electrochemical machining of tungsten metal bodies.

#### 2.2.4. Ionic mass transfer effects on the hydrodynamics during dissolution of a rotating disk electrode surface

The diffusion model of Nernst allows simple rate equations of the ionic mass transfer. In many cases Nernst's model has no ability to express the quantitative side of the phenomenon as well as the interaction of mass and momentum transfer. In the Nernst's model the convective mass transfer is omitted. However, the convective transport affects the thickness of the diffusion layer  $\delta$  as well as the form of the complete equations describing the mass transfer. Because of that an attempt was made to create a method with two main purposes: a creation of a model with a correct contribution of the convective mass transfer and an assessment of the Nernst's model accuracy.

As an object illustrating the method applied a rotating disk was chosen. The flow regime is laminar. Hydrodynamic equations of similar situations taking into account the variable transport properties have been conceived and solved in some particular cases [6,118,122,136]. Below a general approach is discussed. The method applied is based on the "joining" of the asymptotic solutions of the velocity fields.

Let the Navier-Stokes equations be expressed in a cylindrical co-ordinate system with a polar axis  $x$  passing through the center of the disk. The equi-accessibility of the disk surface allows the description of the density ( $\rho$ ) and the kinematic viscosity ( $\nu$ ) of the solution as a function of the concentrations of the dissolved matter and the co-ordinate  $x$ . The introduction of a new variable  $\zeta$  by the relation

$$\zeta = \sqrt{\omega} \int_0^x \frac{dx'}{\sqrt{\nu(x')}}, \quad (2.75)$$

( $\omega$  is the angular velocity of the rotating disk) permits to express the velocity profiles  $v_r$ ,  $v_\theta$  and  $v_x$  in the forms

$$v_r = r\omega F(\zeta), \quad v_\theta = r\omega G(\zeta), \quad v_x = \sqrt{v\omega} H(\zeta). \quad (2.76)$$

The substitution of (2.76) in the Navier-Stokes equations (and after some rearrangements) gives:

$$\begin{aligned}
 F^2 - G^2 + HF' - F'' &= F' \left( \ln \sqrt{\frac{\rho^2 \nu}{\rho_0^2 \nu_0}} \right), \\
 2FG + HG' - G'' &= G' \left( \ln \sqrt{\frac{\rho^2 \nu}{\rho_0^2 \nu_0}} \right), \\
 2F + H' &= -H \left( \ln \sqrt{\frac{\rho^2 \nu}{\rho_0^2 \nu_0}} \right),
 \end{aligned} \tag{2.77}$$

where  $\rho_0$  and  $\nu_0$  are the values of the density and the kinematic viscosity far away from the disk (at  $x \rightarrow \infty$ ). The strokes denote the derivatives with respect to  $\zeta$ . The transport equations consist of the first order derivatives with respect to the function  $H(\zeta)$  only. The determination of this function requires one boundary condition only. Taking into account the mass flux of the solution at  $x = 0$  provoked by the moving center of the liquid phase as a result of the dissolution process (see (1.4)) the boundary conditions are:

$$\begin{aligned}
 F(0) &= 0, \quad G(0) = 1, \quad H(0) = c_0 \lambda_0 I \sqrt{\frac{\nu_0}{\nu_s} \left( \frac{\rho_s}{M_s} - c_{ls} \right)^{-1}}, \\
 F(\infty) &= 0, \quad G(\infty) = 0.
 \end{aligned} \tag{2.78}$$

Here  $\lambda_0 = \left( \frac{D_1}{\nu_0} \right)^{\frac{1}{3}}$ ,  $I = \frac{i \nu_0^{\frac{1}{2}} D_1^{-\frac{2}{3}}}{z_i F c_0 \sqrt{\omega}}$ ,  $D_1$  - the diffusivity of the dissolving metal cations (with a charge  $z_1$ ),  $i$  - the anodic current density,  $c_0$  - the local cation concentration in the solution depth,  $c_{ls}$  - the local cation concentration at the disk surface (subscript  $s$  denotes the conditions at the surface).

For liquids  $\lambda_0 \ll 1$  due to the small values of the diffusivity. If the rotation velocity  $\omega$  and the concentration  $c_0$  are enough to assure an intensive mass transfer in all the range of variations of  $i$ , the condition  $\lambda_0^2 I \ll 1$  is satisfied. This allows a solution of the hydrodynamic problem by means of the "joining" of the asymptotic expansions [4]. Because of that the functions  $F, G$  and  $H$  may be expressed in the following expansions:

$$\begin{aligned}
 F &= F_0(\zeta) + \lambda_0 f(y) + \dots, \\
 G &= G_0(\zeta) + \lambda_0 g(y) + \dots, \\
 H &= H_0(\zeta) + \lambda_0^2 h(y) + \dots.
 \end{aligned} \tag{2.79}$$

The functions  $y = \frac{\zeta}{\lambda_0}, F_0, G_0$  and  $H_0$  are solutions of Karman's problem [101]. They are valid in the case of constant properties ( $\rho = \rho_0, \nu = \nu_0$ ) and in the absence of a mass transfer ( $I = 0$ ). At  $\zeta \ll 1$  the functions  $F_0, G_0$  and  $H_0$  take the forms

$$F_0 = a\zeta, \quad G_0 = 1 - b\zeta, \quad H_0 = -a\zeta^2 \quad (a = 0.51; \quad b = 0.62). \quad (2.80)$$

A substitution of the expansions (2.79) into the transport equation and a consequent equalization of the terms with equal powers of  $\lambda_0$  give the following system equations for  $f, g$  and  $h$

$$\begin{aligned} \frac{d^2 f}{dy^2} + \left( \frac{df}{dy} + a \right) \frac{d}{dy} \left( \ln \sqrt{\frac{\rho^2 v}{\rho_0^2 v_0}} \right) &= 0, \\ \frac{d^2 g}{dy^2} + \left( \frac{dg}{dy} - b \right) \frac{d}{dy} \left( \ln \sqrt{\frac{\rho^2 v}{\rho_0^2 v_0}} \right) &= 0, \\ \frac{dh}{dy} + (h - ay^2) \frac{d}{dy} \left( \ln \sqrt{\frac{\rho v^2}{\rho_0^2 v_0}} \right) + 2f &= 0. \end{aligned} \quad (2.81)$$

The boundary conditions at  $y = 0$  are:

$$f(0) = 0, \quad g(0) = 0, \quad h(0) = c_0 I \sqrt{\frac{v_0}{v}} \left( \frac{\rho_s}{M_1} - c_{1s} \right)^{-1}. \quad (2.82)$$

The solution of the first equation for  $f$  is:

$$f(y) = -ay + B \sqrt{\rho_0^2 v_0} \int_0^y \frac{dy'}{\sqrt{\rho^2 v}}. \quad (2.83)$$

The determination of the constant  $B$  may be carried out by obtaining the "internal" solution  $F(y)$  as function of the "external" independent variable  $\zeta = \lambda_0 y$ . At  $y \rightarrow \infty$  and finite values of  $\zeta$  the "internal" solution must approach the "external" solution  $F = a\zeta$ . The condition of "joining" may be formulated as:

$$a\zeta = B \sqrt{\rho_0^2 v_0} \lim_{\lambda_0 \rightarrow 0} \left\{ \lambda_0 \int_0^{\frac{\zeta}{\lambda_0}} \frac{dy'}{\sqrt{\rho^2 v}} \right\}. \quad (2.84)$$

From this condition the value of  $B$  is  $B = a$ . In a similar way the solution for  $g(y)$  may be obtained. The knowledge of the explicit form of the function  $f(y)$  allows the determination of  $h(y)$ :

$$h(y) = c_0 I \frac{\rho_s}{\rho_0} \sqrt{\frac{\rho_0^2 v_0}{\rho^2 v}} \left( \frac{\rho_s}{M_I} - c_{Is} \right)^{-1} + a y^2 - 2a \sqrt{\frac{\rho_0^2 v_0}{\rho^2 v}} \int_0^y dy' \sqrt{\rho^2 v} \int_0^{y'} \frac{dy''}{\sqrt{\rho^2 v}}. \quad (2.85)$$

Thus, with accuracy determined by the terms of the order of  $\lambda_0^2$  (in the area of the diffusion boundary layer) the function  $H(y)$  may be expressed as

$$H(y) = \frac{\lambda_0^2}{\rho} \sqrt{\frac{v_0}{v}} \left\{ \frac{c_0 \rho_s M_I I}{\rho_s - M_I c_{Is}} - 2a \rho_0 \int_0^y \int_0^{y'} \frac{\rho(y') \sqrt{v(y')} dy'' dy'}{\rho(y'') \sqrt{v(y'')}} \right\}. \quad (2.86)$$

At constant  $\rho$  and  $v$  as well as in the absence of a mass transfer the function takes the simple form:

$$H(y) = -a \lambda_0^2 y^2. \quad (2.87)$$

The quantitative assessments of the effect of both the mass flux and the variable transport properties on the rate of the anodic dissolution will be performed in 2.2.5.

## 2.2.5. Anodic dissolution of metals in concentrated solutions with variable physical properties

One of the principle difficulties emerging in the theoretical description of the macroscopic kinetics is related to the fact that the effective transport coefficients of both the mass and the momentum transport depend on the ion concentrations in the electrolyte. This is very important for the transport phenomena in the near-anode area where the local concentrations are significantly greater than the volumetric ones. The experimental methods do not provide satisfactory data about the near-electrode ion concentrations and the local transport liquid properties under the conditions of an intensive mass transfer. Because of that there is a lack of analysis of the ionic mass transfer in concentrated electrolytes as well as estimations of the contributions of the molecular viscosity and the convective-migration diffusivity to the anodic dissolution. In some earlier works [6,84,120,122,136] mathematical models of the intensive interphase mass transfer and the heat exchange have been developed. They have been applied to purely physical processes without taking into account the charge transport and the electric field effects. The variable physical properties and the concentrations effects of the diffusion coefficients during an electrical deposition of metals from concentrated solutions have been analyzed in [118]. The current-potential curves of an anodic dissolution have been calculated numerically in [38]. The description of the local coefficients of ion activities described by Debay-Hukel theory as well as constant values of both the density and the viscosity of the solution have been assumed. The effects of the variations of both the solution viscosity and ion activity coefficients on the dissolution of a rotating metal disk under laminar flow of a binary electrolyte has been analyzed in a number of works [40,41,43,71,72].

In the case of an equi-accessible dissolving surface in a concentrated solution the equation describing the cation concentration profiles in the near-anode area of a binary electrolyte is

$$\operatorname{div}(\mathbf{j}_i + c_i \mathbf{v}) = 0, \quad (2.88)$$

where  $\mathbf{j}_i$  is determined from (2.23). Equation (2.88) is valid if the mass resistance of the diffusion part of the double-electric layer is negligible. The substitution of the explicit form of  $\mathbf{j}_i$  into (2.88) and under the assumption of incompressibility of the solution

$$\operatorname{div}(\rho \mathbf{v}) = 0 \quad (2.89)$$

gives

$$\nu \left[ 1 - \frac{d\rho}{dc_1} \frac{c_1}{\rho} \right] \frac{dc_1}{dy} - \frac{D_{eff} i (M_1 D_1 - M_2 D_2)}{F(z_1 - z_2) D_1 D_2} \frac{d}{dy} \left( \frac{c_1}{\rho} \right) = \frac{D_{eff} M_3 v_0^{\frac{1}{3}} \sqrt{\omega}}{D_1^{\frac{1}{3}}} \frac{d}{dy} \left( \frac{cg}{\rho \sqrt{v}} \frac{dc_1}{dy} \right). \quad (2.90)$$

Here all the values are like those described in 2.2.4. The boundary conditions applicable to (2.90) follow from (2.23):

$$\begin{aligned} y = 0, \\ \frac{(z_2 - z_1) D_2 \sqrt{v_0} M_3 c g}{z_1 D_1 \sqrt{v_s} \rho_s c_{20} I} \left( \frac{dc_1}{dy} \right)_s + \left\{ \frac{D_2}{D_1} \left( M_2 + \frac{z_2 M_1}{z_1} \right) - 2 M_1 \right\} \frac{c_{1s}}{\rho_s} = \frac{z_2 D_2}{z_1 D_1} - 2; \\ y \rightarrow \infty, \quad c_1 = c_{10}. \end{aligned} \quad (2.91)$$

The condition (2.91) may be obtained if the component of the flux  $\mathbf{j}_i$  oriented normally to the electrode surface is set equal to the quantity  $\frac{M_1 i}{z_1 \rho_s F}$  (see equation. (2.37)).

The determination of the velocity profile  $v = v(y)$  requires the solution of the Navier-Stokes equations with boundary conditions taking into account the effect of the mass transfer on the hydrodynamics. Imposing conditions of intensive dissolution the shape of the velocity profile (near-electrode zone) is significantly affected by a mechanical impulse transferred to the solution by the ions of dissolving metal. A similar solution (see equation (2.86)) with an accuracy of second order terms with respect to the parameter  $\lambda_0 = \left( \frac{D_1}{v_0} \right)^{\frac{1}{3}}$  has been developed in 2.2.4. This solution is:

$$v(y) = \frac{\lambda_0^2 \sqrt{v_0 \omega}}{\rho} \left\{ \frac{M_1 \rho_s c_{10} i}{\rho_s - M_1 c_{1s}} - 2 a \rho_0 \int_0^y \int_0^{y'} \frac{\rho(y') \sqrt{v(y')} dy'' dy'}{\rho(y'') \sqrt{v(y'')}} \right\}. \quad (2.92)$$

In order to create a closed system of equations describing the ion concentration distributions near the electrode the knowledge of the space distribution of both the solution viscosity and the density is required. The experimental data existing in the literature

[6,52,85,87,94,108] indicate that under an intensive mass transfer these distributions as well as the ion coefficients of activity near the mass transfer surface may be expressed by means of exponential functions:

$$\begin{aligned} g &= g_s \exp\left[-\frac{k}{c_{20}}(c_1 - c_{1s})\right], \\ \rho &= \rho_s \exp\left[\frac{m}{c_{20}}(c_1 - c_{1s})\right], \\ \nu &= \nu_s \exp\left[\frac{n}{c_{20}}(c_1 - c_{1s})\right], \end{aligned} \quad (2.93)$$

where  $k, m$  and  $n$  are empirical positive constants.

The introduction of dimensionless variables by means of volumetric anion concentration  $c_{20}$ :

$$C = \frac{c}{c_{20}}, \quad C_1 = \frac{c_1}{c_{20}}, \quad C_{1s} = \frac{c_{1s}}{c_{20}}, \quad I = \frac{i \nu_0^{\frac{1}{6}} D_1^{-\frac{2}{3}}}{z_1 F_1 c_{20} \sqrt{\omega}}, \quad (2.94)$$

allows the expressions of (2.90) and the boundary conditions (2.91) in the forms:

$$\begin{aligned} &\frac{d}{dy} \left\{ g_s C \exp\left[-\left(m + \frac{n}{2} + k\right)(C_1 - C_{1s})\right] \frac{dC_1}{dy} \right\} + \\ &+ A \exp[-m(C_1 - C_{1s})] (I - mC_{1s}) \frac{dC_1}{dy} \int_0^y \int_0^{y'} \exp\left\{\left(m + \frac{n}{2}\right)[C_1(y') - C_1(y'')]\right\} dy'' dy' + \\ &+ B \frac{d}{dy} \left\{ \exp[-m(C_1 - C_{1s})] C_1 \right\} - M \exp[-m(C_1 - C_{1s})] \frac{dC_1}{dy} = 0; \\ &y = 0, \quad \frac{dC_1}{dy} = N; \quad y \rightarrow \infty, \quad C_1 = -\frac{z_2}{z_1}. \end{aligned} \quad (2.95)$$

In the above equations the following designations have been used

$$\begin{aligned} A &= \frac{2a\rho_0(z_1 D_1 - z_2 D_2)}{(z_1 - z_2) D_2 M_3 c_{20}} \sqrt{\frac{\nu_s}{\nu_0}}, \\ B &= \frac{z_1 I (M_1 D_1 - M_2 D_2)}{(z_1 - z_2) D_2 M_3} \sqrt{\frac{\nu_s}{\nu_0}}, \end{aligned}$$

$$M = \frac{M_1 I (z_1 D_1 - z_2 D_2)}{(z_1 - z_2) D_2 M_3} \sqrt{\frac{v_s}{v_0}},$$

$$N = \frac{z_2 \rho_s I}{(z_1 - z_2) g_s C_s M_3 c_{20}} \left[ 1 + \frac{c_{1s} (z_1 M_2 - z_2 M_1)}{z_2 \rho_s} \right] \sqrt{\frac{v_s}{v_0}}. \quad (2.96)$$

Suppose that modules of all the powers in the exponential functions in (2.93) are small with respect to the unity, thus the equation (2.95) may be expressed in a linearized form. The solution of the linearized equation with boundary conditions  $C_1 = C_{1s}$  at  $y = 0$  and  $C_1 = -\frac{z_2}{z_1}$  at  $y \rightarrow \infty$  determines the profile of the cation concentration as a function of  $C_{1s}$ . The calculation of the derivative  $\frac{dC_1}{dy}$  at  $y = 0$  and its substitution in the boundary conditions (2.95) give a relationship between  $I$  and  $C_{1s}$  [71,72]:

$$I = I_0 \begin{cases} 1 + A_1 + A_2 + 0.562(B_1 + B_2)\Delta C_1 + \left( \frac{2z_2}{3z_1} - 0.408\Delta C_1 \right)k + \\ + \left( \frac{z_2}{z_1} - 0.674\Delta C_1 \right)m + \left( \frac{z_2}{6z_1} - 0.244\Delta C_1 \right)n \end{cases} \left( \frac{v_0}{\bar{v}} \right)^{\frac{1}{6}}. \quad (2.97)$$

Here  $I_0$  is the dimensionless current density corresponding to the theory of a mass transfer from an infinite and diluted solution toward a rotating disk [50]:

$$I_0 = 0.62 \left( 1 - \frac{z_1}{z_2} \right) \left( \frac{D_1}{D_{eff}} \right)^{\frac{1}{3}} \Delta C_1. \quad (2.98)$$

The quantity  $\bar{v}$  corresponds to an infinitely diluted solution,  $\Delta C_1 = \frac{(c_{1s} - c_{10})}{c_{20}}$  is the dimensionless driving force of the dissolution process. The other parameters are described by the following relationships:

$$A_1 = \frac{(M_1 D_1 - M_2 D_2) z_1 c_{1s}}{z_2 D_2 \rho_s}, \quad A_2 = \frac{(z_2 D_2 - z_1 D_1) M_1 c_{1s}}{z_2 D_2 \rho_s},$$

$$B_1 = \frac{(M_1 D_1 - M_2 D_2) z_1 c_{10}}{z_2 D_2 \rho_s}, \quad B_2 = \frac{(z_2 D_2 - z_1 D_1) M_1 c_{10}}{z_2 D_2 \rho_s}. \quad (2.99)$$

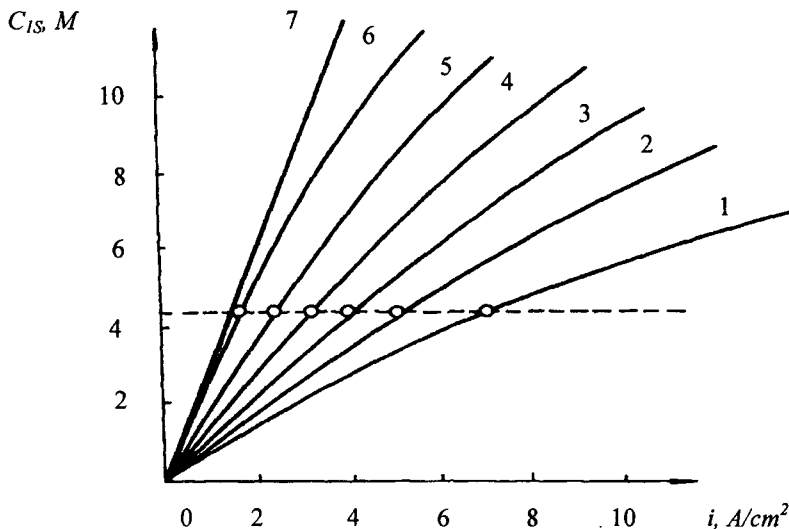


Fig.2.6 Variation of the anodic concentration with the current density. Nickel dissolution.

The parameters  $A_1$  and  $B_1$  contribute to the mutual effect of the migration and the diffusion fluxes of the ionic components of the solution, while  $A_2$  and  $B_2$  present the effect of the normal component of the fluid velocity at the disk surface. The values of  $A_1$  and  $A_2$  show the contribution of the above effects at the disk surface, while  $B_1$  and  $B_2$  present the same phenomena in the bulk of the solution.

#### 2.2.6. Effect of saturation of near-anode layer by electrode reaction products

The equation (2.97) may apply for calculations of the cation concentrations of the dissolving metal in the near-anode zone. This assumes that the values of  $k, m$  and  $n$  are known from separate experiments. These calculations are important from a practical point of view because they allow the tests of some theoretical hypotheses about the anodic dissolution mechanism. Moreover, they permit to predict the critical regimes related to critical solution concentrations. As mentioned (see 2.2.2) some authors interpreting "the limiting" anodic currents came up with the hypothesis that with this regime the solution concentration at the anode surface is equal to that corresponding to the saturation with electrode reaction products. In order to verify the above hypothesis the relationship between the limiting anodic current and the concentration (a nickel rotating electrode in a solution of  $NiCl_2$  at 1540 turns/min) has been investigated [10]. The experimental data have been treated in accordance with equation (2.97). The values of  $m$  and  $n$  have been obtained in the literature, while the value of  $k$  has been determined as  $k = 0.18$ . It was found that the determined value of  $k$  is

independent of the solution concentration  $c_{20}$  in the range of 0.5 to 4.0 M. Using these data and by means of equation (2.97) the relationships  $c_{1s} = c_{1s}(i)$  have been calculated at various solution concentrations. The curves are shown on Fig. 2.6.

The circles show the experimental data obtained in [10] and corresponding to the density of the limiting anodic current at a given concentration. All the experimental points lie on a horizontal line corresponding to a saturated solution of nickel chloride ( $c_{1s} = 4.36\text{M}$ ). This fact confirms the results obtained in [11,14,105] under the assumption that the solution is saturated within the regime of the limiting current. A similar result has been obtained [10] upon anodic dissolution of copper disk electrode rotating in a solution of copper sulphate. These experiments have been carried out with a volumetric salt concentration of 0.5M. The constant  $k$  has been determined in separate experiments on cathodic copper deposition from a solution of CuSO<sub>4</sub>. The experimental data indicate that the observed density of the limiting anodic current corresponds to the concentration of a saturated solution of CuSO<sub>4</sub>.

The analysis of the curves in Fig.2.6 shows that the convective transport mechanism together with the mechanical impulse of the intensive dissolution lead to a significant decrease of the cation concentration in the zone close to the anode. This decrease is important from a practical point of view because it allows applications of higher current densities in the cases where the cation concentrations in that zone are limited. The limitation is related to the solution saturation as well as the formation of complexes at the anode.

### 2.2.7 Electrochemical dissolution of metal inclusions in channels

A solution of a simple problem of the electrochemical machining, i.e. an anodic dissolution of a metal inclusion in a channel is discussed here. The electrolyte fills up a semi-infinite channel with insulating walls. The problem is related to a number of applications, e.g. local metal corrosion, processes in electrochemical transducers, polygraphic processes etc. Here one-dimensional model of a channel ( $0 \leq x \leq \infty$ ) with a flowing boundary metal-solution will be discussed. The area  $0 \leq x \leq L(t)$  is filled with a salt solution of the dissolving metal (a binary electrolyte). The area  $L < x < \infty$  corresponds to the metal phase. The rate of channel depth increase will be calculated with the assumption of steady-state concentrations simultaneously at the channel inlet and ( $x = 0$ ) and at the metal-solution interphase boundary  $x = L$ . The salt concentration at  $x = 0$  depends on the initial experimental condition, while at  $x = L$  it is equal to the concentration at saturation. The first condition is assumed for a simplification, while the second one exist in many real electrochemical systems. For example, the second condition corresponds to the pitting corrosion of metals. The rate of dissolution at the bottom of the pitting is some times is quite significant, so the cation concentration at  $x = L$  reaches the concentration of saturation. In many technological processes of electrochemical recovery of metals from channels the condition of a saturated solution at the dissolving surface corresponds to the maximum output.

Here the problem will be solved by a simultaneous consideration of the equations of the hydrodynamics and the ionic mass transfer taking into account the movement of the interphase boundary. The physical and the transport properties are concentration dependent.

The mathematical formulation of the one-dimensional channel model [63] is:

$$\frac{\partial \rho}{\partial t} + \frac{\partial(\rho v)}{\partial x} = 0, \quad 0 \leq x \leq L(t);$$

$$\begin{aligned}
& \frac{\partial c_I}{\partial t} + \frac{\partial}{\partial x}(j_I + c_I v) = 0, \quad 0 \leq x \leq L(t); \\
& \frac{\partial L}{\partial t} = \frac{iM_I}{z_I F \rho_m}; \\
& x = L(t), \quad \rho_s v = \frac{iM_I}{z_I F}, \quad j_I + c_{Is} v = \frac{i}{z_I F}, \quad c_I = c_{Is}; \\
& x = 0, \quad c_I = c_{I0}; \quad t = 0, \quad L = 0. \tag{2.100}
\end{aligned}$$

Here  $v = v(x, t)$  is the local solution velocity induced by the interphase mass transfer and  $i = i(t)$  is the anodic current density. The density of the solution  $\rho$  depends on the local cation concentration of the dissolving metal, i.e. it is a function of the co-ordinate  $x$  and the time  $t$ . The quantity  $\rho_m$  represents the metal phase density,  $z_I$ -the charge of metal cations,  $M_I$ -the cation atomic mass,  $j_I$ -the diffusion-migration cation flux determined by (2.23). The equation (2.23) may be expressed in the following form

$$j_I = -\frac{D_{eff} M_I c g(c_I)}{\rho(c)} \frac{\partial c_I}{\partial x} + \frac{D_I i}{F(z_2 D_2 - z_I D_I)} \left[ \frac{c_I}{\rho(c_I) D_I} (M_I D_I - M_2 D_2) - 1 \right], \tag{2.101}$$

where  $D_I$  and  $D_2$  are the diffusivities of both the cations and the anions respectively in an infinitely diluted solution.

The problem defined by (2.100) is Stephan's problem [17, 90]. A closed form solution may be obtained in particular cases only.

In a simplified case when both the solution density  $\rho$  and the function  $g$  are independent of the concentration  $c_I$  (this case corresponds to the situation of a diluted solution) from equation (2.100) it follows that:

$$v = \frac{iM_I}{z_I F \rho_0}, \tag{2.102}$$

where  $\rho_0$ -solution density at an infinite dilution.

The solution  $L(t)$  will be expressed in the form

$$L(t) = 2\bar{\lambda} \sqrt{D_{eff} t} \tag{2.103}$$

with an unknown constant  $\bar{\lambda}$ . The dimensionless variables introduced are:

$$C = \frac{c_I - c_{Is}}{c_{I0} - c_{Is}}, \quad y = \frac{x}{2\sqrt{D_{eff} t}}, \quad A = \frac{\rho_m}{\rho} (1 + \zeta),$$

$$B = \frac{2z_2 D_2 \rho_m}{M_I (c_{Is} - c_{I0}) (z_2 D_2 - z_I D_I)},$$

$$N = \frac{2\rho_m c_{ls}(1+\varsigma)}{\rho_0(c_{ls} - c_{l0})},$$

$$\varsigma = \frac{z_1(M_1 D_1 - M_2 D_2)}{M_1(z_2 D_2 - z_1 D_1)}. \quad (2.104)$$

Thus, under the above assumptions the dimensionless form of Stephan's problem is:

$$\frac{d^2C}{dy^2} + 2(y + \bar{\lambda}A) \frac{dC}{dy} = 0, \quad 0 \leq y \leq \bar{\lambda};$$

$$y = 0, \quad C = 0; \quad y = \bar{\lambda}, \quad C = 1, \quad \frac{dC}{dy} = \bar{\lambda}(B - 2A - N). \quad (2.105)$$

The last boundary condition determines the value of the parameter  $\bar{\lambda}$ .

The parameters  $A$  and  $N$  represent the normal component of the velocity at the interphase boundary and the mutual interaction of both the cation and anion diffusion fluxes respectively. The second effect is described by the parameter  $\varsigma$ . In the case of infinite diluted solution the parameters  $B$  and  $N$  vanish. The first term in the brackets in (2.105) is due to the term  $\partial c_l / \partial t$  in the original equation (2.100) and his maximum is equal to  $\lambda$ . Taking into account that in most of the practical cases the value of  $A$  is significantly greater than unity the condition  $y \ll \bar{\lambda}A$  is satisfied. Thus, the Stephan problem formulation with the term  $\partial c_l / \partial t$  together with the omitted term of  $\bar{\lambda}A$  is physically incorrect.

The solution of (2.105) has the form:

$$C = \frac{\varphi(y + \bar{\lambda}A) - \varphi(\bar{\lambda}A)}{\varphi(\bar{\lambda} + \bar{\lambda}A) - \varphi(\bar{\lambda}A)}, \quad (2.106)$$

where  $\varphi(x)$  - is the error-function.

The substitution of (2.106) into the last boundary condition of (2.105) gives:

$$\frac{2}{\sqrt{\pi}} \frac{\exp[-\bar{\lambda}^2(1+A)^2]}{\varphi(\bar{\lambda} + \bar{\lambda}A) - \varphi(\bar{\lambda}A)} = \bar{\lambda}(B - 2A - N). \quad (2.107)$$

If in the basic equation (2.100) the term  $\partial c_l / \partial t$  is neglected with corresponds to the absence of the first term inside the brackets in (2.105), the relationships for  $C$  and  $\bar{\lambda}$  are:

$$C = \frac{1 - \exp(-2\bar{\lambda}Ay)}{1 - \exp(-2\bar{\lambda}^2A)}, \quad \frac{2\bar{\lambda}A \exp(-2\bar{\lambda}^2A)}{1 - \exp(-2\bar{\lambda}^2A)} = \bar{\lambda}(B - 2A - N). \quad (2.108)$$

It is evident that at  $\bar{\lambda} \ll 1$  the lefts sides of (2.107) and (2.108) coincide and the corresponding relationship for  $\bar{\lambda}$  is:

$$\bar{\lambda} = \frac{I}{\sqrt{B - N}}. \quad (2.109)$$

The difference between the value of  $\bar{\lambda}$  determined by (2.109) and the roots of the equations (2.107) and (2.108) does not exceed 1% at  $\bar{\lambda} \leq 0.1$ . The latter condition is satisfied for many substances of low solubility. It is clear that at sufficiently low volumetric concentrations of the electrolyte the differences between the roots of (2.107), (2.108) and (2.109) do not exceed several percents even in the case of metals with high solubility. Thus, it may be concluded that in physical systems with constant properties ( $\rho = \text{const.}$ ,  $g = 1$ ) the dissolution rate is so low, that the cation distribution near the surface determined by  $L(t)$  practically coincides with the stationary distribution existing at  $L = \text{const.}$  The conclusion is valid also for systems with variable physical properties because the incorporation of the latter in the equations leads to a decrease of the calculated dissolution rate.

Now, consider the general case of metal dissolution in a solution with variable physical properties:  $\rho = \rho(c_i)$ ,  $g = g(c_i)$ . In accordance with the above conclusions about a quasi-stationary process let the terms  $\partial \rho / \partial t$  and  $\partial c_i / \partial t$  be omitted in the equations (2.100). Using the boundary conditions of (2.100) the first integrals of the transport equations are

$$v = \frac{iM_1}{z_1 F \rho}, \quad j_1 + c_1 v = \frac{i}{z_1 F}. \quad (2.110)$$

The relationship for  $i(L)$  may be obtained from (2.110) under the boundary conditions (2.100). The substitution of  $i(L)$  in (2.100) leads to the following expressions of  $L$  as a time-dependent function:

$$\begin{aligned} L(t) &= \sqrt{L_{\text{crit}}^2 + 4\bar{\lambda}^2 D_{\text{eff}}(t - t_{\text{crit}})}, \\ \bar{\lambda}^2 &= \frac{M_3 c_{30}}{2\rho_m} \int_{c_{10}}^{c_{1s}} \frac{g(c_1) dc_1}{P c_1 + Q \rho(c_1)}, \\ P &= \frac{\left(\frac{M_2}{M_1}\right) z_1 D_2 - z_2 D_1}{z_2 D_2 - z_1 D_1}, \\ Q &= \frac{z_2 D_2}{M_1(z_2 D_2 - z_1 D_1)}. \end{aligned} \quad (2.111)$$

The value of  $L_{\text{crit}}$  determines the maximum channel length that is available at a fixed current density  $\bar{i}$  without a transition into a "limiting regime", i.e. a regime with critical concentrations  $c_{1s}$ . The values of  $L_{\text{crit}}$  may be reached at the time  $t_{\text{crit}}$  determined by

$$t_{crit} = \frac{L_{crit}}{\bar{v}},$$

where  $\bar{v} = -\frac{iM_1}{z_1 F \rho_m}$ .

The critical length  $L_{crit}$  may be obtained from (2.111) under the conditions

$$\frac{dL}{dt} = \bar{v} \text{ at } t = t_{crit}. \quad (2.112)$$

Thus,

$$L_{crit} = \frac{2\bar{\lambda}^2 D_{eff}}{\bar{v}}. \quad (2.113)$$

If the value of  $i = i_{crit}$  than the process reaches the “limiting regime” immediately after the switching on the current, the critical length is zero and the channel length as a function of the time is determined by

$$L = 2\bar{\lambda} \sqrt{D_{eff} t},$$

where the parameter  $\bar{\lambda}$  follows from (2.111).

At  $i < i_{crit}$  the channel length may be expressed as:

$$L(t) = \bar{v}t \text{ at } t \leq t_{crit};$$

and

$$L(t) = \sqrt{L_{crit}^2 + 4\bar{\lambda}^2 D_{eff}(t - t_{crit})} \text{ at } t \geq t_{crit}. \quad (2.114)$$

At very low current densities  $i$  the process does not reach the “limiting regime” and is described by (2.114) at  $t \leq t_{crit}$ .

In this part of the book a solution of the dissolution rate was obtained under the conditions of the “limiting regime”. The solution derived gives slightly overestimated values because the hindering effect of the channel walls on the normal component of the solution velocity (with respect the surface of dissolution) is not taken into account.

### 2.2.8. Dissolution of rectangular channel walls

The problem of an intensive interphase mass transfer between the wall of a tube or a rectangular channel and a liquid flow is interesting from a practical point of view. The quantitative description of the elementary acts of the dissolution and the sedimentation are widely applied in the chemical and electrochemical technology. As already mentioned, in

systems with an intensive mass transfer the additional contribution of the convective transport due to mechanical impulse transferred to the liquid by the dissolving (or sedimenting) metal particles is important. The transferred impulse is proportional to the diffusion particle flux contributing to the mass transfer. Because of that the velocity field near the surfaces is concentration dependent. From this point of view the systems with an intensive mass transfer are similar to the heat transfer problems of a gas injection or suction through a porous channel wall [123, 134]. In both cases the normal component of the velocity is related either to the pressure drop across the porous wall or the surface concentration of the transported substance and to the normal component of its gradient. In the chemical technology there are systems with semitransparent membranes with liquid flows normal to them. [91, 127, 128]. The hydrodynamic conditions as well as the mass transfer rates in channels with such membranes differ significantly from those in channels with impermeable walls. A typical example of a system with a significant mutual interaction of both the hydrodynamics and the mass transfer is the dissolution of a flat metallic anode in a concentrated electrolyte flowing in a narrow gap between the electrodes. Such systems exist in the practice of the electrochemical shape formation of metals and alloys [76, 77, 81, 102, 103, 108, 109, 130].

The analysis of the mass transfer kinetics under an intensive anodic dissolution in a rectangular channel and its effects on the hydrodynamics is an interesting problem for the practice [66, 67, 69, 70].

In the practice of the electrochemical shape formation of metals the knowledge of the ionic mass transfer near the metal surface streamlined by the electrolyte is important. An example is the calculation of the inlet region length of the mass transfer section of a rectangular channel with one soluble wall in a high-density current regime. The existing published data on the heat transfer in the laminar flows in a tube [48, 49], indicate that in a system with high Peclet numbers the inlet channel section may occupy a significant part of the required mass transfer area. It was shown in [69] that under an anodic dissolution at a fixed surface ionic concentration of the dissolving metal the inlet section (in a laminar flow regime) occupies practically the total area available for dissolution

In the laminar flow regime under an excess of an indifferent electrolyte the inlet length of a rectangular channel with one dissolvable wall ( $y = 0$ ) the velocity distribution has the following form [25]:

$$V_x = 6(Y - Y^2) \left\{ I + \sigma \int_0^X I(X') dX' \right\}, \quad V_y = \sigma I(X)(1 - 3Y^2 + 2Y^3). \quad (2.115)$$

$V_x$  and  $V_y$  are dimensionless velocity components corresponding to the dimension velocities  $v_x$  and  $v_y$  through the relationships:

$$V_x = \frac{v_x}{\bar{v}_x}, \quad V_y = \frac{hv_y}{D}.$$

$\bar{v}_x$  is the average (with respect to the channel cross-section) velocity at  $x = 0$  (channel inlet) and  $h$  is the distance between the walls,  $D$  - the cation diffusivity of the dissolving metal. The dimensionless independent variables  $X$  and  $Y$  are

$$X = \frac{Dx}{h^2 \bar{U}}, \quad Y = \frac{y}{h}.$$

The function  $I = \frac{hi}{zDFc_0}$  represents the dimensionless density of the anodic current. Here  $z$  is the charge of the cations,  $c_0$  - the volumetric concentration of the indifferent electrolyte. The small dimensionless parameter is introduced by the atomic mass  $M$  and the solution density (near the anode surface) as follows:

$$\sigma = \frac{Mc_0}{\rho_s}.$$

The convective mass transfer problem at high Peclet number under the hydrodynamic conditions imposed by the velocity distribution (2.115) is formulated as follows:

$$\begin{aligned} V_x \frac{\partial C}{\partial X} + V_y \frac{\partial C}{\partial Y} &= \frac{\partial^2 C}{\partial Y^2}, \\ X = 0, \quad C &= 0; \\ Y = 0, \quad \frac{\partial C}{\partial Y} &= -I(1 - \sigma C), \\ Y = I, \quad C &= 0. \end{aligned} \tag{2.116}$$

The boundary condition at  $Y = 0$  represents the effect of the mechanical impulse transferred to the solution by the cations of the dissolving metal. The condition at  $y = I$  should be interpreted as a condition requiring the existence of a physical mechanism explaining the cation removal from the gap between the electrodes. The dimensionless concentration  $C$  is expressed by the concentration  $c_0$ . The value of  $I$  in (2.116) will be considered as constant and independent of the co-ordinate  $X$ .

In the paper [25] it was reported that if the channel lengths  $L$  satisfies the condition  $\frac{DL}{h^2 \bar{U}_x} < 10^{-4}$ , the terms of (2.116) containing  $Y$  in powers greater than unity may be neglected. Moreover, this allows the contribution of the integral term of  $V_x$  to be eliminated.

As a result of these simplifications the solution of the problem may be expressed as a solution of the following equation

$$6Y \frac{\partial C}{\partial X} + \sigma I \frac{\partial C}{\partial Y} = \frac{\partial^2 C}{\partial Y^2} \tag{2.117}$$

with the boundary conditions (2.116).

The problem will be solved by replacing the boundary condition at the rigid surface by  $C = C_s(X)$  at  $Y = 0$ . The function  $C_s(X)$  may be obtained from the boundary conditions at  $Y = 0$  after the solution of the problem. Taking into consideration that Dughamel's theorem

allows the problem solution with an arbitrary  $C_s(X)$  through the solution at  $C_s = \text{const.}$ , the introduction of new independent variables is possible:

$$\eta = Y \left( \frac{2}{3X} \right)^{1/3}, \quad \zeta = X^{1/3}. \quad (2.118)$$

Thus, the equation (2.117) may be expressed for the function  $U(\eta, \zeta)$ :

$$\frac{\partial^2 U}{\partial \eta^2} + \left[ 3\eta^2 - \left( \frac{3}{2} \right)^{\frac{1}{3}} \sigma \zeta I \right] \frac{\partial U}{\partial \eta} - 3\eta \zeta \frac{\partial U}{\partial \zeta} = 0. \quad (2.119)$$

The function  $U(\eta, \zeta)$  must satisfy the following boundary conditions:

$$\zeta = 0, \quad U = 0; \quad \eta = 0, \quad U = 1; \quad \eta \rightarrow \infty, \quad U \rightarrow 0. \quad (2.120)$$

Taking into account the assumed restriction of the channel length, the values of  $X$ , as well as  $\zeta$  are significantly lower than unity. Thus, the solution of (2.119) may be expressed as an expansion

$$U(\eta, \zeta) = U_0(\eta) + \zeta U_1(\eta) + \dots \quad (2.121)$$

By substituting of the expansion (2.121) and the boundary conditions (2.120) in the equation (2.119) the solution may be obtained by the well-known methods for ordinary differential equations:

$$U_0 = I - \frac{1}{\Gamma\left(\frac{4}{3}\right)} \int_0^\eta e^{-t'} dt,$$

$$U_1 = \frac{\left(\frac{3}{2}\right)^{\frac{1}{3}} \sigma \eta I}{2\Gamma\left(\frac{4}{3}\right)} \left\{ \Gamma\left(\frac{4}{3}\right) - \int_0^\eta e^{-t'} dt \right\}. \quad (2.122)$$

Note that the zero-order approximation with respect to the parameter  $\zeta$  corresponds to the well-known solution of Leveque [107]. The accuracy of this approximation depends on the value of the dimensionless distance  $X$ . It was demonstrated in [115] that in the case of circular tube the relative error introduced by the change of the exact solution by Leveque's solution is about 15% at  $X = 0,01$  and 6,5% at  $X = 0,001$ .

Let the old variables  $X$  and  $Y$  be used in the relationships for  $U_0$  and  $U_1$ . With the help of the Dughamel's theorem may be found the solution for an arbitrary function  $C_s(X)$ :

$$C_s = \int_0^x \left\{ U_0(X - \bar{\lambda}, Y) + (X - \bar{\lambda})^{\frac{1}{3}} U_1(X - \bar{\lambda}, Y) \right\} dC_s(\bar{\lambda}), \quad (2.123)$$

where the integral must be considered in the Stilless sense.

The substitution of the relationship for  $C$  in the old boundary condition (2.116) allows the expression of an integral equation with respect to the function  $C_s(X)$ :

$$\int_0^x \left\{ \frac{1}{\Gamma\left(\frac{4}{3}\right)} \left[ \frac{2}{3(X - \bar{\lambda})} \right]^{\frac{1}{3}} - \frac{1}{2} \sigma I \right\} dC_s(\bar{\lambda}) = \{I - \sigma C_s(X)\} I. \quad (2.124)$$

The function  $C_s(X)$  will be expressed with respect to the small parameter  $\sigma$ :

$$C_s(X) = C_s^{(0)}(X) + \sigma C_s^{(1)}(X) + \dots . \quad (2.125)$$

At the zero-order approximation the results is:

$$I = \frac{\left(\frac{2}{3}\right)^{\frac{1}{3}}}{\Gamma\left(\frac{4}{3}\right)} \int_0^x (X - \bar{\lambda})^{-\frac{1}{3}} dC_s^{(0)}(\bar{\lambda}). \quad (2.126)$$

The Laplace transformation of both parts of the equation gives:

$$I = \left(\frac{2}{3}\right)^{\frac{1}{3}} \frac{\Gamma\left(\frac{2}{3}\right)}{\Gamma\left(\frac{4}{3}\right)} s^{\frac{1}{3}} L\left(\frac{\partial C_s^{(0)}}{\partial X}\right), \quad (2.127)$$

where  $L$  is Laplace operator

$$L(f) = \int_0^\infty e^{-st} f(t) dt. \quad (2.128)$$

The inverse Laplace transformation gives the following result:

$$C_s^{(0)} = \frac{\left(\frac{2}{3}\right)^{\frac{2}{3}} I X^{\frac{l}{3}}}{\Gamma\left(\frac{5}{3}\right)}. \quad (2.129)$$

The first-order approximation of the problem solution may be found in an analogous way with repeat to the parameter  $\sigma$ . In this case the equation should be considered

$$\int_0^X \frac{dC_s^{(1)}(\bar{\lambda})}{(X - \bar{\lambda})^{\frac{1}{3}}} = - \frac{\left(\frac{2}{3}\right)^{\frac{1}{3}} \Gamma\left(\frac{4}{3}\right)}{2 \Gamma\left(\frac{5}{3}\right)} I^2 X^{\frac{l}{3}}. \quad (2.130)$$

The solution by the Laplace transformation is:

$$C_s^{(1)} = \frac{\left(\frac{2}{3}\right)^{\frac{4}{3}} \left[ \Gamma\left(\frac{4}{3}\right) \right]^2}{2 \left[ \Gamma\left(\frac{5}{3}\right) \right]^2} I^2 X^{\frac{2}{3}}. \quad (2.131)$$

The value of  $C_s^{(1)}$  is negative, so the result obtained indicates that the existence of an induced mass transfer flux in the solution at the anode surface reduces the cation concentration in the zone. Moreover, this induced flux leads to the existence of a normal velocity component  $V_y$ . Thus, it follows that at a fixed current density the length  $l$ , in which the concentration  $C_s$  changes from zero (channel inlet) to 1 (at maximum the solution of the near-anode layer by cations), may exceed significantly the value of  $l_0$ . The value of  $l_0$  may be calculated without consideration of the mass transfer effects on the hydrodynamics. In fact, the solution of the equation  $C_s(l) = 1$  with respect to the length  $l$ , together with the already obtained relationships for  $C_s^{(0)}$  and  $C_s^{(1)}$ , leads to:

$$l = l_0 \left\{ I + \frac{3\sigma \left[ \Gamma\left(\frac{4}{3}\right) \right]^2}{2 \Gamma\left(\frac{5}{3}\right)} \right\}.$$

Here the value of  $l_0$  is

$$l_0 = \frac{9 \left[ \Gamma\left(\frac{5}{3}\right) \right]^3}{4I^3} \frac{h^2 \bar{v}_x}{D}, \quad (2.132)$$

The relationship (2.132) is a solution of  $C_s^{(0)}(l_0) = 1$ . It determines the length in which the concentration  $C_s$  increases from 0 to 1 in the absence of a normal velocity component.

A quantitative assessment of the accuracy of the calculation procedure affected by the diffusion inlet section of the rectangular channel as well as without the effects of the normal velocity component  $V_y$ , may be performed. The comparison of  $C_s^{(0)}$  and  $\sigma C_s^{(1)}$ , defined by (2.129) and (2.131) allows the relative error  $\Delta$  to be expressed as

$$\Delta = \frac{|\sigma C_s^{(1)}(X)|}{C_s^{(0)}(X)} = 0,37\sigma IX^{\frac{l}{3}}. \quad (2.133)$$

The analysis of (2.133) made in [69] shows that at current densities about  $0,5\text{-}2 \text{ A/cm}^2$  the error  $\Delta$  may reach a value of 30%. For more accurate calculations the terms of higher orders with respect to the parameter  $\zeta$  have to be taken into account.

The problem of electrochemical dissolution of the channel wall in a turbulent flow regime of the electrolyte is related to theory of the process of metal shape formation [66, 70]. As in the case of a laminar flow the effect of the normal velocity in the near-anode zone component induced by the mass transfer is significant. The main difference from the laminar flow situation is that there is an additional convective transport due to the turbulent velocity pulsations. Another difference is connected with the lengths of the channel inlet mass transfer sections. Taking into consideration the published information about the turbulent wall flows an assessment of the effect is made below. The assessment takes into account the specific boundary conditions and the mass transfer effects on the hydrodynamics. The latter are due to the mutual interaction of both the mass transfer and the solution hydrodynamics as well as the near-anode cation concentration of the dissolving metal.

In a laminar flow regime the length of the mass transfer inlet section  $l_0$  is determined by the relation  $l_0/h = 0,05Pe$ , where  $h$  is the mean hydraulic diameter of the channel [48]. In most of the real electrochemical systems with a laminarly flowing electrolyte the ratio  $l_0/h$  is grater than  $10^4$ , while the channel length is about  $10^2\text{-}10^3$  time greater than the value of  $h$ . This means that in laminar flow conditions the inlet section hold all the channel length. In a turbulent flow regime the ratio  $l_0/d$  does not exceed 10 and decreases in parallel with the increase of Schmidt number,  $Sc$  (or the Prandtl number in the case of heat transfer). According to the data published in [137] the variations of Reynolds number from 5000 to

75000 (circular cross-section tube and  $Sc = 10^3$ ) the ratio  $\frac{l_0}{d}$  increases from 0.5 to 2.0. The

numerical solution of the heat transfer problem in a turbulent flow regime between two parallel plates at constant temperatures of the one of the plate and heat insulation of the other as well as constant flux densities has been demonstrated in [93]. The solution has been carried out at several values of the Prandtl number. The calculation indicates that the variations of  $Pr$

from 1 to 10 lead to a twofold decrease in the ratio  $\frac{l_0}{d}$  (from 20 to 10). It has been demonstrated earlier [131] that at  $Pr \geq 10$  the near-wall temperature profile is independent of the type of the boundary condition (the boundary condition of a first and a second-order give

similar temperature profiles near the wall). The profiles obtained practically coincide with those obtained analytically [83].

The results obtained in [93, 137] allow to make the assumption that at Schmidt number values of order about  $10^3$  and greater (these values are important for the electrochemical metal dissolution) the cation concentration drops from the value  $c_{1s}$  (at the anode) to the mean volumetric value of  $c_{10}$  (at a distance  $y = \delta$  from the anode surface). The value of  $\delta$  is independent of the co-ordinate  $x$  along the channel length. It is so small, that the longitudinal convective mass transfer in the section  $0 \leq y \leq \delta$  may be neglected. This allows the assumption that the total convective transport in the transverse direction (along the co-ordinate  $y$ ) occurs with a constant velocity equals to the solution velocity  $v_s$  at the anode surface. Further, the axis  $y$  is oriented from the anode ( $y = 0$ ) toward the cathode ( $y = h$ ). The value of  $c_{10}$  is assumed zero for the sake of simplicity.

Thus the following simplification will be used further:

1. The convective transport along the longitudinal channel axis does not affect the profiles of the ionic concentrations in the diffusion boundary layer;
2. The effective thickness of the boundary layer  $\delta$  may be assumed as constant because  $\delta \ll x$ ;
3. The convective mass transport along the co-ordinate  $y$  (transverse to the dissolving surface) occurs at constant velocity equal to that of the solution velocity  $v_s$  in the zone just at the anode surface ( $v_s = \frac{M_i i}{\rho_s z_i F}$ ).

Consider the mass transfer of ions in a solution containing metal cations of local concentration  $c_1$  together with cations and anions of a supporting electrolyte (with the respective concentrations  $c_2$  and  $c_3$ ). Far away from the anode surface,  $y \geq \delta$ , the concentration  $c_1$  is assumed zero, while the concentrations  $c_2$  and  $c_3$  will be assumed equal to their volumetric values -  $c_{20}$  and  $c_{30}$  respectively. If the effect of the double-electric layer is neglected, the transport equations in the diffusion boundary layer are:

$$\begin{aligned} -(D_k + D_t) \frac{dc_k}{dy} + \frac{z_k D_k F c_k}{RT} \varepsilon + v_s c_k &= \frac{j_k}{M_k} \quad k = 1, 2, 3, \\ \sum_{k=1}^3 z_k c_k &= 0. \end{aligned} \quad (2.134)$$

Here  $D_k$  and  $z_k$  are the diffusivity and the valence of the respective ions,  $D_t = D_t(y)$  is the effective coefficient of a turbulent diffusion,  $\varepsilon$  - the local electric field intensity,  $M_k$  - the molecular mass of the ions of a type  $k$ .

The complete mass fluxes of ions  $j_k$  are

$$j_1 = \frac{M_i i}{z_i F}, j_2 = j_3 = 0. \quad (2.135)$$

The boundary conditions in accordance with the above simplifications are:

$$y = \delta, \quad c_1 = 0, \quad c_2 = c_{20}, \quad c_3 = c_{30}. \quad (2.136)$$

Let assume that the following conditions are satisfied

$$D_1 = D_2 = D_3 = D, \quad z_1 = z_2 = -z_3 = z, \quad c_{20} = c_{30} = c_0. \quad (2.137)$$

The dimensionless variables are:

$$\begin{aligned} y^+ &= y \frac{v^*}{\nu}, \quad C_k = \frac{c_k}{c_0}, \quad E = \frac{zFD\varepsilon}{RTv^*}, \quad \delta^+ = \frac{\delta v^*}{\nu}, \\ I &= \frac{i}{zFv^*c_0}, \quad \sigma = \frac{M_1 c_0}{\rho_s}, \quad v^* = \sqrt{\frac{\tau_0}{\rho_s}}, \quad \lambda^* = \frac{D + D_t}{\nu}. \end{aligned} \quad (2.138)$$

The value  $\tau_0$  is the shear stress at the anode (at  $y = 0$ ).

In a dimensionless form the transport equations are:

$$\begin{aligned} \lambda^* \frac{dC_1}{dy^+} - EC_1 - \sigma IC_1 + I &= 0, \\ \lambda^* \frac{dC_2}{dy^+} - EC_2 - \sigma IC_2 &= 0, \\ \lambda^* \frac{dC_3}{dy^+} + EC_3 - \sigma IC_3 &= 0, \\ C_1 + C_2 - C_3 &= 0. \end{aligned} \quad (2.139)$$

The above equations must satisfy the following boundary conditions

$$y^+ = \sigma^+, \quad C_1 = 0, \quad C_2 = I, \quad C_3 = I. \quad (2.140)$$

The solution has the form:

$$\begin{aligned} C_1 &= \frac{I}{2}u - \frac{2}{u} \exp[-2\sigma I \psi(y^+)] \\ C_2 &= \frac{2}{u} \exp[-2\sigma I \psi(y^+)] \\ C_3 &= \frac{I}{2}u, \\ E &= \frac{I}{u}, \end{aligned}$$

$$u(y^+) = \frac{I}{\sigma} + \left(2 - \frac{I}{\sigma}\right) \exp[-\sigma I \psi(y^+)] \psi(y^+) = \int_{y^+}^{\delta^*} \frac{dy}{\lambda^*(y)}. \quad (2.141)$$

The role of the migration mechanism in the ionic mass transport is easy to elucidate by a comparison of the values of the cation concentration near the anode in two cases: under the migration flux effect,  $C_l = C_{ls}$  and its corresponding value in the absence of migration motions  $C_l = C_{ls}^*$ . From the derived relationships it follows that

$$\begin{aligned} C_{ls} &= \frac{I}{2} u_0 - \frac{2}{u} \exp(-2\sigma I \psi_0), \\ u_0 &= \frac{I}{\sigma} + \left(2 - \frac{I}{\sigma}\right) \exp(-\sigma I \psi_0), \\ \psi_0 &= \int_0^{\delta^*} \frac{dy}{\lambda^*(y)}. \end{aligned} \quad (2.142)$$

Thus, the evaluation of  $C_{ls}$  requires the knowledge of the relationship between the ratio  $\frac{D_t}{\nu}$  and the dimensionless distance  $y^+$ . The information required may be obtained by mean of an analysis of the experimental data on turbulent mass transport at high values of the Schmidt number [100], or from the universal velocity profile [62]. At present, the power law relationship about the turbulent attenuation near the wall is wide by used [9, 22, 83, 92, 96, 112, 132, 133, 137]:

$$\left(\frac{D_t}{\nu}\right) = b(y^+)^n, \quad (2.143)$$

where  $n = 3$  or  $4$ .

It has been demonstrated in [66], that at high values of the Schmidt number and greater values of  $y^+$  the value of  $\psi_0$  slightly depends on  $\delta^+$ . In the case of  $Sc \geq 1000$  the condition  $\delta^+ = \infty$  exist at  $y^+ \geq 4$ . In this case

$$\psi_0 = \frac{\pi b^{\frac{1}{n}}}{n \sin(\frac{\pi}{n})} Sc^{\frac{(n-1)}{n}}. \quad (2.144)$$

The calculation in accordance with (2.144) and with the help of experimental data about  $b$  and  $n$ , leads to practically similar results. The numerical results about  $\psi_0$  may be obtained also by means of more complicated relationships  $\left(\frac{D_t}{\nu}\right) = f(y^+)$ , (see for example [138]):

$$\frac{D_t}{\nu} = \frac{a_1(y^+)^3 + a_2(y^+)^4}{I - a_1(y^+)^3 + a_2(y^+)^4}. \quad (2.145)$$

If the effect of the migration mechanism is not taken into consideration, i.e.  $E \equiv 0$  in the basic equations, the relationship for the near-anode concentration obtains the form:

$$C_{ls}^* = \frac{1}{\sigma} (1 - e^{-\sigma I \psi_0}). \quad (2.146)$$

The ratio of the values determined by (2.142) and (2.146) is

$$\frac{C_{ls}}{C_{ls}^*} = \frac{1 + 2(2\sigma - 1)e^{-\sigma I \psi_0} - (4\sigma - 1)e^{-2\sigma I \psi_0}}{2[1 + 2(\sigma - 1)e^{-\sigma I \psi_0} - (2\sigma - 1)e^{-2\sigma I \psi_0}]} \quad (2.147)$$

The numerical evaluations of this ratio show that the increase of the dimensionless current density  $I$ , at a fixed value of  $\sigma$  leads to an increased difference between  $C_{ls}$  and  $C_{ls}^*$ .

At  $\sigma \rightarrow 0$  the ratio (2.147) has a limit

$$\lim_{\sigma \rightarrow 0} (C_{ls} / C_{ls}^*) = \frac{1 + \frac{1}{4} I \psi_0}{1 + \frac{1}{2} I \psi_0}. \quad (2.148)$$

The results discussed above indicate that at excess concentrations of an indifferent electrolyte the local electric field near the anode reduces the concentrations of the ions of the dissolved metal. The effect has been evaluated for the first time by means of the Nernst's diffusion model [28]. The effect is similar to that induced by the normal velocity component  $v_s$  as a result of the interphase mass transfer [29, 31].

The analysis done is related to the simple case of ions with equal charges. The numerical methods for the solution of the differential equation allows to solve the problem of the mass transport under conditions of mutual interaction of the turbulence diffusion and the particle migration at arbitrary charges of the ions. Figure 2.7 shows the variations of  $c_{ls}$  with the current density.

An example of anodic dissolution of the two-valence iron is illustrated at different volumetric concentrations of NaNO<sub>3</sub>: 1, 2 and 4 M. The calculation has been performed at  $Re = 7000$  and  $Sc = 1000$ . The power in (2.143) is assumed to be  $n = 4$ . The data plotted indicate that the increase in the concentration of the indifferent electrolyte at a fixed value of  $c_{ls}$  leads to reduced densities of the anodic currents.

The effect is well known in the field of the electrochemistry as a phenomenon related to the migration cation transport by the electric field of the indifferent electrolyte. The second characteristic of the theoretical curves drawn in Fig. 2.7 is that the intersections of all the curves with the vertical lines, corresponding to the experimentally detected [81] "passivation" attenuation of the anodic process (analogues of the limiting anodic currents)

have projection on the co-ordinate axes at the point coinciding with that of the saturation of the solution of  $\text{NaNO}_3$  by the iron ions.

### CHAPTER 2.3. ELECTROCHEMICAL RECOVERY OF METALS FROM CONCENTRATED SOLUTIONS

In the practice of cathode removal of metals (e.g. galvanization, electroplating, electrochemical transducers of the information, etc.) there is a need to predict the value of the limiting diffusion current with respect to the metal cations. Moreover, such a calculation is interesting from the point of view of better understanding the mechanism of metal recovery. In this case the measured and the predicted values of the limiting current must be compared in accordance with the assumed mechanism of the process. Similar calculations are needed also for diffusion coefficient determination taking into account both the reaction mechanism and the concentration effects.

At diffusion current densities close to the limiting values, the local values of the solution viscosity and density as well as the ionic diffusion coefficients near the cathode (diffusion boundary layer) correspond to the conditions of a ionic mass transfer in an infinitely diluted solution.

As the distance from the cathode surface increases the differences between the local transport coefficients and the solution physical properties and those existing near its surface become significant. This is very important in concentrated solutions where there are significant differences in the ionic concentration profiles and potential distribution as well as the value of the limiting diffusion current.

Numerical experiments have been performed [118] in order to predict the value of the limiting current in the case of copper deposition from a copper sulphate solution. An empirical relationship describing the concentration effect on the diffusion coefficient has been

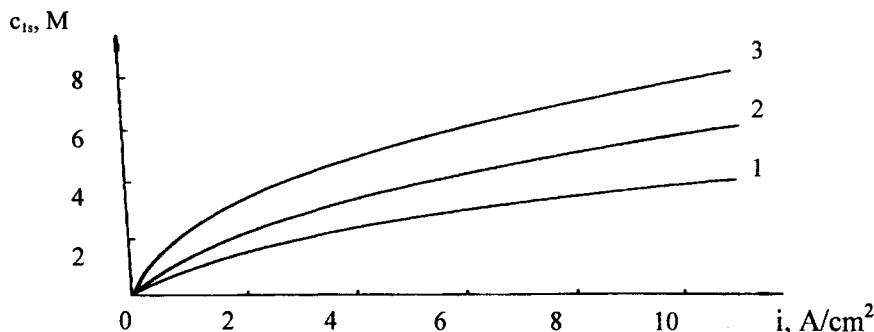


Fig. 2.7 Variations of the anodic concentrations with the current density during a dissolution of iron

employed. The theoretical description of the process [87] under non-stationary conditions postulates a linear relationship between the diffusivity and concentration. The calculations carried out indicate that the theoretical concentration profiles are in a better agreement with those obtained experimentally (by an optical technique), rather than those predicted by the well-known Sand's equation [129].

In order to obtain an analytical relationship allowing a comparison between the theory and the experiments as well as to obtain an information about the effective transport coefficients, a simple one-dimensional system may be considered. The deposition of ions from a concentrated solution on a rotating electrode was chosen to this purpose. The system is considered together with an analytical relationship describing the concentration effects on the effective transport coefficients expressed in a general form. As mentioned in 2.2.5, the experimental data available for the viscosity  $\nu$ , the density  $\rho$  and the local activity coefficient of the salt allow expressions in the forms of (2.93). The use of these relationships in the situation of an anodic dissolution has allowed the expression the kinetic equation (2.97). This kinetic equation relates both the variable physical and transport properties and the solution flow induced by the mass transfer. The relationship (2.97) is valid also in the case of a cathode deposition of metals from solution of their own salts. However, in this situation the current density must be assumed as negative.

Let the equation (2.97) be considered under the condition imposed by a limiting cathodic current where a cation concentration at the cathode surface is zero ( $c_{is} = 0$ ). The substitution  $\Delta C_i = -z_2 / z_1$  in (2.97) leads to

$$i_{lim} = \frac{0,62F(z_2 - z_1)D_1c_{20}\sqrt{\omega}}{D_{eff}^{\frac{1}{3}}\bar{V}^{\frac{1}{6}}} \left\{ 1 + [0,562(B_1 + B_2) + 0,258k + 0,326m - 0,077n]\frac{z_2}{z_1} \right\}. \quad (2.149)$$

The equation (2.149) may be employed for calculation of the limiting currents of a cathodic metal deposition. Moreover, the relationship allows the establishment of a concentration dependence of the limiting diffusion current. However, its correct use requires the knowledge of the values of  $k, m$  and  $n$ . They must be obtained from separate experiments.

### 2.3.1. Method for the establishment of the effects of the apparent diffusion coefficient of the salt

An analysis of the cathodic copper deposition [10] has been carried out, by using published literature data. The results indicated that the effect of the volumetric concentration ( $c_{10}$ ) on the limiting deposition current was not in agreement with the well-known theory of the convective diffusion toward a rotating disk electrode [50]. Further, the concentration effect on the apparent diffusivity  $D^*$  of the salt has been expressed by a linear function

$$D^* = \frac{M_3cg}{\rho} D_{eff} \quad (2.150)$$

in contrast to the well-known exponential relationships. The first result is illustrated on Fig. 2.8. by the variations of the limiting cathodic current with the salt concentration. The system of a copper deposition from solution of  $CuSO_4$  on a rotating copper disk electrode is shown as

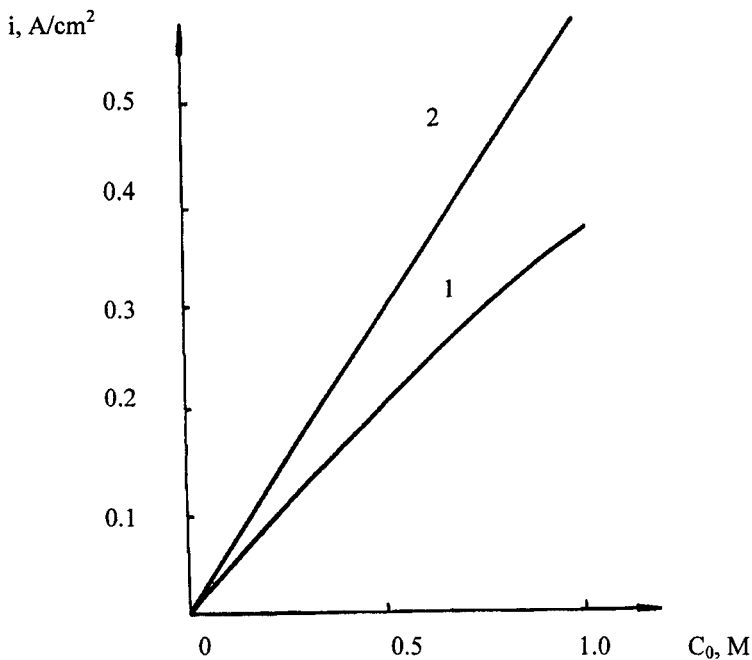


Fig.2.8 Limiting current at the cathode during copper recovery from CuSO<sub>4</sub> solution.  
Effect of the concentration

an example. The line 1 shows the experimental results obtained at 100 r.p.m. rotation speed. The line 2 presents predictions of the traditional theory (2.149) (at  $B_1 = B_2 = k = m = n = 0$ ) considering neither the variations in the physical properties, and nor the transport coefficients, nor the mass flux induced by the mass transport. The second results require an estimation of the equation about  $g$  incorporating the relationship between  $k(c_0)$  and the salt volumetric concentration ( $c_0$ ) as follows:

$$g = g_s \exp \left[ -\frac{k(c_1 - c_{1s})}{c_0} \right]. \quad (2.151)$$

For the comparison of both the experimental and the calculated values of  $i_{lim}$  the choice of a model curve  $g(k, c)$  requires in the cases when the exponential law (2.151) does

not describe well the function  $g(c)$ . The chosen function must coincide with the mean of the real curve  $g(c)$ . The selection of the model function must be performed on the basis of the criterion of the integral

$$J = \int_0^{c_0} |g(c) - g(k, c)| dc. \quad (2.152)$$

The integral may be evaluated by means of a Gauss formula in a single point:

$$J \approx |g(c_0/2) - g(k, c_0/2)|. \quad (2.153)$$

Thus, it follows that:

$$g(k, \frac{c_0}{2}) \approx g(\frac{c_0}{2}). \quad (2.154)$$

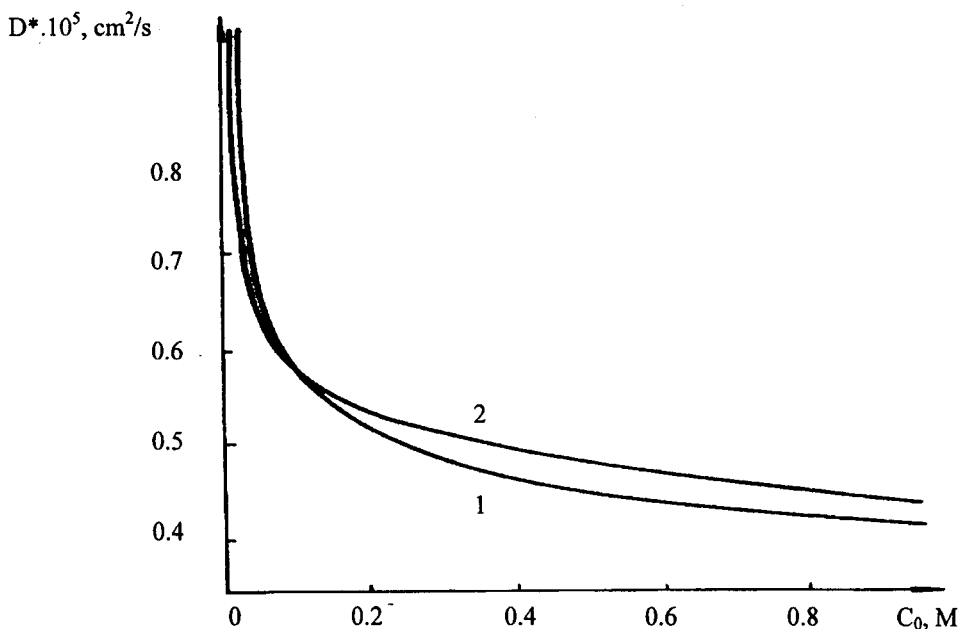


Fig.2.9 Variations of the diffusivity with the concentration

The condition means, that at an arbitrary concentration  $c_0$  the experimental value of  $k$  describes in a best way the concentration effect on the diffusion coefficient described at  $c = 0.5c_0$ . As a result of incremental determination of  $k$  at various points  $c_0$  the relationship describing the above effect should be obtained. Obviously, the form of the obtained function will be more complicated than the exponential one.

Figure 2.9 demonstrates the variations of the apparent diffusion coefficient with the concentration (curve 1) in the case of a copper sulphate in accordance with the above method. The experimental data  $i_{lm}(c_0)$  were found in [94]. The second curve (2) has been obtained in [85] for the same solution, by a non-electrochemical method. The agreement between both curves allows the recommendation of (2.97) and (2.149) for calculations of mass transfer kinetics in concentrated solutions.

## CHAPTER 2.4. EFFECT OF THE NON-ISOTHERMAL CONDITIONS AND THE GAS EVOLUTION

The specific non-isothermal conditions of momentum transfer are related mainly to the thermal effects on the transport coefficients and the physical properties of the medium [55, 73, 135]. The effects of the variable physical properties on the non-isothermal transport lead to complicated relationships about the friction factors of pipes [45, 46, 139] and drag coefficients of rigid bodies [61]. The general analysis of momentum transfer equations shows that the velocity profiles of channel flows in both the laminar and turbulent regimes under non-isothermal conditions have components oriented normally to the channel axis. These components do not exist in the case of an isothermal flow. The existence of a normal velocity component leads to a significant deformation of the corresponding longitudinal component. The electrolyte flow in a narrow gap between the electrodes at high current densities is a typical example of a non-isothermal flow. In fact, such flows are commonly used for the removal of the anode dissolution products as well as for a control of the local surface dissolution of the metal body (in the case of electrochemical shape formation) [11]. The Joule heating leads to an intensive convective heat transfer and non-uniform temperature profiles across the gap. The calculations carried out in [65, 68] demonstrated that the convective heat transfer together with the temperature effects on both the viscosity and the electric conductivity of the solution lead to an increased anode current density. At Reynolds numbers in the range of 100 - 1000 this increase is from 10 to 30 % and strongly depends on the current intensity and the solution content. A situation in which the convective heat transfer and the thermal effects on the electrical conductivity have to be taken into consideration following an intensive mass transfer in electrochemical systems is discussed in the next subchapter (2.4.1).

### 2.4.1. Non-isothermal effects on potential distributions in an injection flow electrochemical cell

The contribution of the thermal effects in the electrochemical metal dissolution has been evaluated in [104] by a numerical solution of the convective heat transfer equations in a stationary laminar flow. A rectangular channel with a laminar flow and fixed temperature values at the walls and the channel inlet has been chosen as an example. The Poiseuille velocity profile has been employed under constant solution heat conductivity. The following empirical relationship [5] of the electrical conductivity  $\sigma(T)$  has been assumed:

$$\sigma(T) = \sigma_0 [1 + \beta(T - T_0)]. \quad (2.155)$$

Here  $\beta$  is an empirical constant,  $T_0$  - the temperature at the channel inlet and  $\sigma_0 = \sigma(T_0)$ . The current density has been assumed as temperature independent. However, the local current density is temperature dependent and varies along the channel length. The current density distribution may be obtained from the solution of the coupled set of equations describing the temperature and the potential distribution in the solution.

Let a rectangular channel with a positive axis  $z$  along the laminar electrolyte flow with constant temperature at the channel inlet be considered. A parabolic velocity profile is assumed. Let the wall at  $x = -a$  be the metallic anode, while the opposite wall at  $x = a$  is the corresponding cathode.

The systems of equations for  $T$  and the potential  $\varphi$  are:

$$\begin{aligned} \frac{\partial}{\partial x} \left( \sigma \frac{\partial \varphi}{\partial x} \right) + \frac{\partial}{\partial z} \left( \sigma \frac{\partial \varphi}{\partial z} \right) &= 0, \\ \lambda \frac{\partial^2 T}{\partial x^2} + \sigma \left[ \left( \frac{\partial \varphi}{\partial x} \right)^2 + \left( \frac{\partial \varphi}{\partial z} \right)^2 \right] &= \rho C_p v_0 \left( I - \frac{x^2}{a^2} \right) \frac{\partial T}{\partial z}, \end{aligned} \quad (2.156)$$

where  $\rho, C_p, \lambda$  are the density, the heat capacity and the thermal conductivity of the medium respectively;  $v_0$  is the maximum liquid velocity at the channel inlet.

In order to simplify the explanation the hydrogen generation is assumed as the only electrochemical reaction at the cathode, so the corresponding boundary condition at  $x = a$  [16] is:

$$i = -\sigma \left[ \frac{\partial \varphi}{\partial x} \right]_{x=a} = A \exp \left( -\frac{W_0 - \alpha F \eta}{RT} \right). \quad (2.157)$$

Here  $i$  is the current density at the cathode;  $A$  is a coefficient depending on the hydrogen concentration but temperature independent (in the case of concentrated solutions the coefficient  $A$  may be assumed as independent of the longitudinal co-ordinate);  $W_0$  - the activation energy at a zero overpotential;  $\eta$  - the hydrogen overpotential;  $\alpha$  - a transport coefficient. The overpotential may be expressed through the electric tension  $V$  applied to the cell, the equilibrium cell potential drop  $\Delta V$  and the Ohmic potential drop  $\Delta \varphi$  (as a function of  $z$ ) as follows:

$$\eta = V - \Delta V - \Delta \varphi. \quad (2.158)$$

The electrode heating effects on the current density will be considered under the assumptions that the heat fluxes at the walls are so small that they do not affect the temperature profiles in the cell. Thus, the following conditions are satisfied:

$$z = 0, \quad T = T_0; \quad x = \pm a, \quad \frac{\partial T}{\partial x} = 0. \quad (2.159)$$

The initial set of equations may be written using the following dimensionless variables:

$$\begin{aligned} X &= \frac{x}{a}, \quad Z = \frac{\bar{\lambda}z}{\rho C_p v_0 a^2}, \quad \psi = \frac{\varphi}{\Delta\varphi_0}, \quad \theta = \frac{T - T_0}{a^2 i_0^2 / \sigma_0 \bar{\lambda}}, \\ \beta^* &= \frac{\beta a^2 i_0^2}{\sigma_0 \bar{\lambda}}, \quad \bar{\lambda}^* = \frac{\bar{\lambda}}{\rho C_p v_0 a}, \quad i_0 = \sigma_0 \frac{\Delta\varphi_0}{2a}. \end{aligned} \quad (2.160)$$

Here  $\Delta\varphi_0$  is the Ohmic potential drop in the cell at  $T = T_0 = \text{const}$ .

$$\sigma_0 \frac{\Delta\varphi_0}{2a} = A \exp \left[ -\frac{W_0 - \alpha F(V - \Delta V - \Delta\varphi_0)}{RT_0} \right]. \quad (2.161)$$

If the parameter  $\beta^*$  is assumed  $\beta^* \ll 1$ , thus the problem may be solved by the successive approximation method. The zero-order approximation at  $\beta^* = 0$  is

$$\psi^{(0)} = -\frac{1}{2}(I + X). \quad (2.162)$$

At the next approximation the function  $\psi$  can be determined from the following system of equations:

$$\begin{aligned} \frac{\partial}{\partial X} \left[ (I + \beta^* \theta^{(0)}) \frac{\partial \psi}{\partial X} \right] &= 0, \\ \frac{\partial^2 \theta^{(0)}}{\partial X^2} - (1 - X^2) \frac{\partial \theta^{(0)}}{\partial Z} &= -4 \left( \frac{\partial \psi^{(0)}}{\partial X} \right)^2. \end{aligned} \quad (2.163)$$

By applying the well-known methods of the mathematical physics and those already used for solving some particular problems [80] the exact solution of the above system may be found. As shown in [68] the solution may be performed by the expression of the function  $\theta^{(0)}$  in the form

$$\theta^{(0)} = MZ + P(X), \quad (2.164)$$

where the constant  $M$  and the function  $P(X)$  are unknown.

The result is an explicit function of the current density from the distance  $z$ :

$$i = \frac{\sigma_0 \Delta \varphi_0}{a} \zeta \left( \frac{\bar{\lambda} z}{\rho C_p v_0 a^2} \right). \quad (2.165)$$

The functions  $\zeta(Z)$  is determined from the transcendent equation

$$\zeta(Z) = B \exp \left\{ - \frac{\tau + \alpha^* \phi(I, Z) \zeta(Z)}{1 + \gamma \theta_s} \right\}. \quad (2.166)$$

$$\text{Here } B = \frac{aA}{\sigma_0 \Delta \varphi_0}, \quad \tau = \frac{[W_0 - \alpha F(V - \Delta V)]}{RT_0}, \quad \alpha^* = \frac{\alpha F \Delta \varphi_0}{RT_0}, \quad \gamma = \frac{a^2 i_0^2}{\sigma_0 \bar{\lambda} T}.$$

The dimensionless temperature at the cathode surface as a function of the co-ordinate  $Z$  is:

$$\theta_s = \frac{3Z}{2} + \frac{3}{35}.$$

The function  $\phi(X, Z)$  may be expressed as

$$\phi(X, Z) = I + X + \alpha^* \left[ -\frac{3}{2} Z(I + X) - \frac{2}{105} + \frac{11}{280} X - \frac{1}{12} X^3 + \frac{1}{40} X^5 \right]. \quad (2.167)$$

In the case of hydrogen generation from acid solutions at a tungsten cathode the following values of the above parameters may be assumed:  $W_0 = 16$  cal/mol,  $A = 10^8$  A/cm<sup>2</sup>,  $i_0 = 10$  A/cm<sup>2</sup>,  $a = 0.5$  mm,  $\sigma_0 = 0.7$  Ohm<sup>-1</sup>·cm<sup>-1</sup> and  $\beta = 0.01$  deg<sup>-1</sup>. The calculation carried out with the above data in [68] indicates that the cathodic current density determined by (2.165) increases monotonously along the channel length. This increase is about 30% at  $Z = 1$ . This indicates that the convective mass transfer should be taken into consideration in the quantitative description of the electrode kinetics at high current densities.

#### 2.4.2. Gas evolution

The electrode processes are associated with a gas evolution. The gas bubbles enhance the mass transfer and the charge transport in the solution. Moreover, the gas phase in the gap between the electrodes decreases the effective electrical conductivity of the solution [76, 102, 103]. The bubbles formation and their subsequent growth blocks some parts of the electrode surface. This hinders the delivery of the reagents and the removal of the reaction products [11, 35]. On the other hand the bubbles induce an additional mixing of the solution that enhance the ionic mass transfer [11, 35].

It was pointed out in [98] that the mass transfer rate may be raised due to the increase of the longitudinal electrolyte velocity. The augmentation is due the reduced channel cross-section area a result of the gas bubble evolution.

Methods for calculation of both the cathodic and the anodic processes with the contribution of the liquid mixing induced by the gas bubbles produced at the electrodes have been developed in various particular situations [3, 35, 44, 64]. The basic assumption of these

methods is the model of the continuous gas film covering the electrode surface. The film surface moves with the time toward the solution depth and "compresses" the diffusion boundary layer. The latter increases the mass transfer rate.



One of the significant trends in the contemporary chemical and electrochemical technologies is the increase of the mass transfer efficiency at the interphase boundaries. In such systems the relationships between the mass fluxes and the driving forces are essentially non-linear. Thus, the development of the fundamentals of the transport phenomena in strongly non-equilibrium systems is needed [27].

The problems discussed in this part allow the electrochemical systems with mutual interaction of the mass, the momentum and the electrical charge transports as well the related effects to be elucidated. In contrast to the systems with low mass transfer rates described by the conventional convective diffusion in liquids, in the systems with an intensive mass transfer the contribution of the momentum transfer is important. The later is not an external-controlling factor of the processes, but is a result of the intensive interphase mass transfer imposed by the particular technological regime. The theory developed here assures the ability to evaluate quantitatively the contribution of the mutual effects of the transport phenomena interactions. These phenomena are described by non-linear relationships between mass fluxes of the ionic reagents and the corresponding concentration driving forces.

## References

1. S. K. Ait'ian , A. D. Davidov and B. N.Kabanov, Electrochemistry (Russia), 8 (1972) 620.
2. S. K. Ait'ian, A. D. Davidov and B. N. Kabanov, Electrochemistry (Russia), 8 (1972) 1391.
3. A. G. Butman, V. S.Krylov and L. I.Heifetz, Theor. Fund. Chem. Technol.(Russia), 9 (1975) 657.
4. M. Van Dyke, Perturbation Methods in Fluid Mechanics, Mir, Moscow, 1967 (in Russian).
5. Yu. S. Volkov and I.I.Moroz, Electron. Treatment. Materials (Russia), № 5-6 (1965) 59.
6. A. M. Golovin, N. M. Rubinina and V. M. Khokhrin, Theor. Fund. Chem. Technol.(Russia), 5 (1971) 651.
7. B. M. Grafov and A. A. Chernenko, Dokl., AN USSR, 146 (1962)135.
8. Yu. Y. Gurevich and Yu. I. Kharkatz , Electrochemistry (Russia), 15 (1979) 94.
9. A. A. Gukhman and B. A. Kader, Theor. Fund. Chem. Technol. (Russia), 3 (1969) 216.
10. A. D. Davidov, G. R. Engelgard, A. H. Malofeeva and V. S. Krylov, Electrochemistry (Russia), 15 (1979) 841.
11. A. D. Davidov and V. D. Kastheev, Itogi nauki i techniki (Advances in sciences and techniques), Electrochemistry (Russia), Proc., VINITI, Moskow, 9 (1974) 154.
12. A. D. Davidov, V. D. Kastheev and B. N. Kabanov, Electrochemistry (Russia), 5(1969) 221.

13. A. D. Davidov, V. D. Kastheev and B. N. Kabanov., *Electrochemistry (Russia)*, 6 (1970) 1760.
14. A. D. Davidov., A. D. Romashkan, M. A. Monina, and V. D. Kastheev., *Electrochemistry (Russia)*, 10 (1974) 1681.
15. B. B. Damaskin and O. A. Petrii, *Introduction in Electrochemical Kinetics*, Visha Shkola, Moscow, 1975 (in Russian).
16. R. R. Dogonadze and A. M. Kuznetsov, *Itogi Nauki (Advances in Sciences) Electrochemistry (Russia)*, 1967, Proc., VINITI, Moscow, (1969) 5.
17. V. M. Zatzepin and L. V. Godulyan, *Dokl. AN USSR*, 238 (1977) 1136.
18. B. N. Kabanov, *Electrochemistry of metals and adsorption*, Nauka, Moscow, 1966 (in Russian).
19. B. N. Kabanov, V. D. Kastheev and A. D. Davidov, *J. Mendelev Society (Russia)*, 16 (1971) 669.
20. L. I. Kadaner and T. V. Slusarskaya, *Anodic oxidation of metals (Russia)*, Proc., Kazan, (1968) 21.
21. V. A. Kiryanov and V. S. Krylov, *Electrochemistry (Russia)*, 10 (1974) 1839.
22. M. Kh. Kishinevskii, T. S. Kornienko and V. A. Parmenov, *Theor. Fund. Chem. Technol. (Russia)* 4 (1970) 489.
23. V. I. Kravtzov, *Electrode Processes in complex Metal Solutions*, Leningrad Univ. Publ., Leningrad, 1969 (in Russian).
24. V. S. Krylov, *Dokl. AN USSR*, 178 (1968) 321.
25. V. S. Krylov, *Macrokinetics of Transport Processes and Interphase Mass Transfer in Electrochemical Systems*, D.Sc. Thesis, Inst. Electrochemistry, AN USSR, Moscow, 1979 (in Russian).
26. V. S. Krylov, *Electrochemical machining of details, Part 1*, Proc. Tula Politechn. Inst. Publ., Tula (1975) 15.
27. V. S. Krylov, *Chemical Industry (Russia)*, 12 (1979) 26.
28. V. S. Krylov, *Electron. Treatment. Materials (Russia)*, 4(1976) 10.
29. V. S. Krylov, *Electrochemistry (Russia)*, 12 (1976) 843.
30. V. S. Krylov, *Electrochemistry (Russia)*, 12 (1976) 1342.
31. V. S. Krylov, *Electrochemistry (Russia)*, 13 (1977) 103.
32. V. S. Krylov and N.I.Gavrilenko, *Electron. Treatment. Materials (Russia)*, 6 (1972) 13.
33. V. S. Krylov and A.D.Davidov, *Metal protection (Russia)*, 13 (1977) 90.
34. V. S. Krylov and A.D.Davidov, *Fifth All Union Meeting on Electrochemistry (Russia)*, VINITI, 2 (1974) 216.
35. V. S. Krylov, A. D. Davidov and E. Kozak, *Electrochemistry (Russia)*, 11 (1975) 1155.
36. V. S. Krylov, A. D. Davidov and V.N.Malinienko, *Electrochemistry (Russia)*, 8(1972) 1461.
37. V. S. Krylov and V. N. Malinienko, *Proc. First. All Union Conf. on Thermodynamics of Irreversible Processes and Applications (Russia)*, Chernovtzi, (1972) 69.
38. V. S. Krylov and V. N. Malinienko, *Electrochemistry (Russia)*, 9 (1973) 3.
39. V. S. Krylov and V. N. Malinienko, *Electrochemistry (Russia)*, 9 (1973) 1073.
40. V. S. Krylov and V. N. Malinienko, *Electrochemistry (Russia)*, 13 (1977) 1653.
41. V. S. Krylov and V. N. Malinienko, *Electron. Treatment. Materials (Russia)*, 6 (1976) 13.
42. A. L. Krylov., V. P. Schuster and R. D. Eidelmann, *Electron. Treatment. Materials (Russia)*, 3 (1969) 21.

43. V. S. Krylov, G. R. Engelgard and A. D. Davidov, Proc. Electrode processes and electrochemical machining technology , Shtiinitza, Kishineu, 1980.
44. V. S. Kublanovskii and V. S. Krylov, Electrochemistry (Russia), 14 (1978) 315.
45. V. L. Leleshuk, B. V. Dyadyakin, Problems of the heat transfer, AN USSR (1959) 123.
46. N. S. Lutikas and A. A., Zhukauskas, Trudii AN Lit. AN SSR, Ser. B, 2 (1966) 143.
47. J. S. Newman, Electrochemical Systems, Prentice-Hall, New Jersey, 1973.
48. B. S. Petukhov, Heat transfer and flow resistance in laminar flow in pipes, Energia, Moscow, 1967 (in Russian).
49. B. S. Petukhov, Thermoenergetics (Russia), 7 (1954) 3.
50. Yu. V. Pleskov and V. Yu. Filinovskii, Rotating Disk Electrode, Nauka, Moscow, 1972 (in Russian).
51. P. Ya. Polubarinova-Kochina, Theory of underground water flow, Gostechizdat, Moscow, 1952 (in Russian).
52. L. N. Rashkovich, V. A. Koptzik, E. N. Volkova, A. N. Israilenko and D. M. Plax, J. Inorg. Chem. (Russia), 12 (1967) 62.
53. V. A. Reshetov, G. N. Reshetova and Z. V. Arkhangelskaya, Electrochemistry (Russia), 8 (1972) 1345.
54. R. Robinson and R. Stokes, Electrolyte Solutions, Inostrannaya Literatura, Moscow, 1963 (in Russian).
55. S. M. Targ, Theory of laminar flows, Gostechizdat, Moscow-Leningrad, 1951 (in Russian)
56. A. N. Frumkin, J. Pure and Appl. Knowledge, Sec. Phys. Math. Sci. (Russia), 1 (1931) 1.
57. A. N. Frumkin, V. S. Bagotzkii, Z. A. Yoffa and B. N. Kabanov, Kinetics of Electrode Processes, Moscow Univ. Publ., Moscow, 1952 (in Russian).
58. Yu. I. Kharkatz, Electrochemistry (Russia), 15 (1979) 246.
59. A. A. Chernenko, Dokl. AN USSR, 153 (1963) 1129.
60. A. A. Chernenko, Electrochemistry (Russia), 7 (1971) 1737.
61. A. A. Shlanchauskas, P.P. Vaitekunas and A.A. Zhukauskas, Trudii Lit. AN SSR, Ser.B, 6 (1965) 139.
62. G. Schlinting, Grätzschicht-Theorie., Verlag G. Broun, Karlsruhe, 1965.
63. G. R. Engelhard, A. D. Davidov and V. S. Krylov, Electrochemistry (Russia), 15 (1979) 1274.
64. G. R. Engelhard and V. S. Krylov, Metal Protection (Russia), 14 (1978) 426.
65. G. R. Engelhard and V. S. Krylov, Electron. Treatment. Materials (Russia), 5 (1978) 55.
66. G. R. Engelhard and V. S. Krylov, Electron. Treatment. Materials (Russia), 6 (1978) 13.
67. G. R. Engelhard and V. S. Krylov, Electron. Treatment. Materials (Russia), 2 (1980) 13.
68. G. R. Engelhard and V. S. Krylov, Electrochemistry (Russia), 14 (1978) 1795.
69. G. R. Engelhard and V. S. Krylov, Electrochemistry (Russia), 15 (1979) 1168.
70. G. R. Engelhard and V. S. Krylov, Electrochemistry (Russia), 15 (1979) 1172.
71. G. R. Engelhard, V. S. Krylov and A. D. Davidov, Metal Protection (Russia), 13 (1977) 606.
72. G. R. Engelhard, A. D. Davidov and V. S. Krylov, Electrochemistry (Russia), 14 (1978) 812.
73. Yang Zan-Tzu, Heat Transfer, 4 (1962) 95 (in Russian).
74. R. D. Armstrong, K. Edmondson and R.F. Firman, J. Electroanalyst. Chem., 40 (1972) 19.

75. R. D. Armstrong, J. A. Harrison, *J. Electroanalyt. Chem.*, 36 (1972) 79.
76. D. Bennion and C.W Tobias, *J. Electrochem. Soc.*, 113 (1966) 593.
77. J. Bannard, *J. Appl. Electrochemistry*, 7 (1977) 1.
78. E. Brunner, *Z. Phys. Chem.*, 47 (1904) 56.
79. E. Brunner, *Z. Phys. Chem.*, 58 (1907) 1.
80. R. D. Cess and E.S. Shuffen, *Appl. Sci. Res.*, A-8 (1959) 339.
81. B. T. Chin and K.-W. Mao, *J. Appl. Electrochem.*, 4 (1974) 155.
82. D. E. Collett, R. C. Hewson-Browne and D. W. Windle, *J. Eng. Math.*, 4 (1970) 29.
83. R. G. Deissler, Analysis of Turbulent Heat Transfer, Mass Transfer and Friction in Smooth Tubes at High Prandtl and Schmidt Numbers. - NACA Rept. 1955, № 1210.
84. A. S. Emanuel and D. R. Olander, *Int. J. Heat Mass Transfer*, 7 (1964) 539.
85. A. S. Emanuel and D. R. Olander, *J. Chem. Engng. Data*, 8 (1963) 31.
86. A. Eucken, *Z. Phys. Chem.*, (1907) 72.
87. W. G. Eversole, H. M. Kinderwater and J.D. Peterson, *J. Phys. Chem.*, 46 (1942) 370.
88. J. M. Fitz-Gerald and J. A. McGeough, *J. Inst. Math. & Appl.*, 5 (1969) 387.
89. J. M. Fitz-Gerald, J. A. McGeough and L. Mc L Marsh, *J. Inst. Math. & Appl.*, 5(1969) 409.
90. B. M Grafov, Extended Abstracts, 28<sup>th</sup> I. S. E. Meeting, Sofia, (1977) 363.
91. L. Grimsrud and A. G. Budd, *Chem. Eng. Prog. Series*, 62 (1966) 20.
92. P. Harriott and R. M. Hamilton, *Chem Eng. Sci.*, 20 (1963) 1073.
93. A. P. Hatton and A. Quarmby, *Int. J. Heat Mass Transfer*, 6 (1963) 903.
94. L. Hsulh and J. Newman, *Electrochim. Acta*, 12 (1967) 429.
95. T., Heumann and N. Stolica, *Electrochim. Acta*, 16 (1971) 1635.
96. D. W. Hubbard and E. N. Lightfoot, *Ind. Eng. Chem., Fundamentals*, 8 (1966) 370.
97. D. Ilkovic, *Coll. Czech. Chem. Commun.*, 6 (1934) 498.
98. D. Jennings, A. T. Kahn, T. B. Stepanek and R. A Whitehead, *Electrochim. Acta*, 20 (1975) 903.
99. B. N. Kabanov, *Electrochim. Acta*, 16 (1971) 321.
100. B. A. Kader and A. M. Yaglom, *Int. J. Heat Mass Transfer*, 15 (1972) 2329.
101. T. Karman, *Z. Angew. Math. Mech.*, 1 (1921) 233.
102. K. Kawafune, T. Mikoshiba and K Noto, *Ann. CIRP*, 16 (1968) 345.
103. K.Kawafune, T. Mikoshiba and K Noto, *Ann. CIRP*, 18 (1970) 303.
104. J. Kozak, *Arch. Budowy Maszyn*, 19 (1972) 43.
105. H. C. Kuo and D. Landolt, *Electrochim. Acta*, 20 (1975) 393.
106. D. Landolt, R. H. Muller and C. W. Tobias, *J. Electrochem. Soc.*, 116 (1969) 1384.
107. M. A. Leveque, *Ann. Mines*, 13 (1928) 201.
108. F.R., McBarnon, R.H. Muller and C.W. Tobias, *Electrochim. Acta*, 21 (1976) 101.
109. J. A. McGeough, *Principles of Electrochemical Machining*. Chapman and Hall, London, 1974.
110. K. Micka, *Ber. Bunsenges. Phys. Chem.*, 72 (1968) 60.
111. D. G. Miller, *J. Phys. Chem.*, 70 (1966) 2639.
112. T. Mizushima, F. Ogino, Y. Oka and N. Fukudo, *Int. J. Heat Mass Transfer*, 14 (1971) 1708.
113. W. Nernst, *Z. Phys. Chem.*, 2 (1888) 613.
114. W. Nernst, *Z. Phys. Chem.*, 17 (1904) 52.
115. J. Newman, *Trans. ASME. J. Heat. Transfer, Ser. C*, 91 (1969) 177.

116. J. Newman, In: P. Delahay, C.W. Tobias (Eds.) *Advances in Electrochemistry and Electrochemical Engineering*, Interscience Publ., New York - London 5 (1967) 87.
117. J. Newman, D. Bennion and C. W. Tobias, *Ber. Bunsenges. Phys. Chem.*, 69 (1965) 608.
118. J. Newman and L. Hsulh, *Electrochim. Acta*, 12 (1967) 117.
119. R. C. Newson-Browne, *J. Eng. Math.*, 5 (1971) 233.
120. A. W. Nienow, R. Unahabkhokha and J. W. Mullin, *Chem. Eng. Sci.*, 24 (1968) 1655.
121. R. H. Nilson and V. G. Tsuei, *Trans. ASME. J. Appl. Mech., Ser. E*, 43 (1976) 55.
122. D. R. Olander, *Int. J. Heat Mass Transfer*, 5 (1962) 765.
123. D. R. Olander, *Trans. ASME. J. Heat Transfer, Ser. C*, 84 (1962) 185.
124. L. Onsager, *Ann. New York Acad. Sci.*, 46 (1945) 241.
125. H. W. Pickering and R. P. Frankenthal, *Electrochim. Soc.*, 119 (1972) 1297.
126. H. W. Pickering and R. P. Frankenthal, *Electrochim. Soc.*, 119 (1972) 1972.
127. R. Popovich, G. Christofor and A.G. Bubb, *Chem. Eng. Progr. Symp. Series*, 67 (1971) 105.
128. S. M. Ross, *J. Fluid Mech.*, 63 (1974) 157.
129. H. J. S. Sand, *J. Phys. Chem.*, 35 (1900) 641.
130. K. Seimiya and K. Kikuchi, *J. Mech. Eng. Lab. (Japan)*, 32 (1978) 20.
131. R. Siegel and E. M. Sparrow, *Trans. ASME. J. Heat Transfer, Ser. C*, 82 (1968) 152.
132. K. K. Sirkar and T. J. Hanratty, *Industr. Eng. Chem., Fundamentals*, 8 (1969) 189.
133. I. S. Son and T. J. Hanratty, *AIChEJ.*, 13 (1967) 689.
134. E. M. Sparrow and J. L. Gregg, *Trans. ASME.J. Heat Transfer, Ser. C*, 82 (1960) 294.
135. M. Tribus and J. Klein, *J. Heat Transfer Symposium, University of Michigan*, (1952) 211.
136. R. Unahabkhokha, A. W. Nienow and J. W. Mullin, *Chem. Eng. Sci.*, 26 (1971) 357.
137. P. Van Shaw, L. R. Reiss and T. J. Hanratty, *AIChEJ.*, 9 (1963) 362.
138. D. T. Wasan, C. L. Tien and C. R. Wilke, *AIChEJ.*, 9 (1963) 567.
139. P. M. Worse-Schmidt and G. Leppert, *Int. J. Heat Mass Transfer*, 8 (1966) 1281.

This Page Intentionally Left Blank

## PART 3

### Chemically Reacting Gas-Liquid Systems

The chemical processes in gas-liquid systems are widely employed in the chemical, power, and food processing industries. The interphase mass transfer processes between the gas and the liquid phases together with chemical transformations are applied for syntheses of new materials [2], separations of gas mixtures by absorption [3] and for heat potential augmentation in the heat pumps. Generally, these processes cover a wide range of situations where one or several components of the gas phase are absorbed by a liquid together with chemical reactions between either the gaseous component themselves or some of them and the liquid phase.

The chemical reactions in the liquid phase affect significantly the gas-liquid interphase mass transfer. Depending on the reaction rate the interphase mass transfer mechanism may be changed and in many cases this affects the limiting stage of the process. The increase of the reaction rate leads to consequent augmentation of the interphase mass transfer rate. This generates high concentration gradients and resulting secondary flows [4] at the face interphase.

The processes of chemical transformations in the liquid affect the interphase mass transfer so it may be linear or non-linear as well as reversible or irreversible.

The heat effects of the chemical transformations could originate temperature gradients at the gas-liquid interphase boundary. The result of this is a gradient of the surface tension that leads to secondary flows at the boundary, which affects the interphase mass transfer kinetics.

In Part 3 the effect of the kinetics of the reaction in the liquid phase on both the mechanism and the kinetics of the interphase mass transfer will be elaborated. The cases of linear and non-linear kinetic laws of chemical reactions, reversible and irreversible chemical transformations and homogenous catalytic reactions will be discussed.

The macrokinetics of the chemical transformations in gas-liquid systems will be considered in the cases of chemosorption in falling liquid films and a sulfuric acid alkylation in a film flow reactor.

The effect of chemical transformations on the interphase mass transfer intensification will be determined by a consideration into account of non-linear and thermo-capillary effects.

From both the practical and theoretical points of view the main problem in the chemically reacting gas-liquid systems is the quantitative description of the interphase mass transfer kinetics with the contribution of the chemical transformations in the liquid phase. The problem requires a detailed mathematical model of the process based on its mechanism. Thus, the first step towards describing the interphase mass transfer kinetics in a gas-liquid system is to evaluate the effect of the chemical reaction rate on its mechanism.

## CHAPTER 3.1. INTERPHASE MASS TRANSFER MECHANISM

The interphase mass transfer of a particular substance between a gas and a liquid complicated with a chemical reaction in the liquid phase is strongly affected by the rate of the chemical transformations. In this case the interphase mass transfer process is a result of the balance between convective and diffusion transports in both phases. Moreover, the balance should consider all the inputs and outputs of a mass resulting from the chemical reaction (for arbitrary volumes in both phases) taking into account that the mass conservation law is satisfied for every arbitrary volume in the liquid and the gaseous phase. Small changes in the rate of the chemical reaction may lead to changes in the mass transfer rates during the subsequent process stages. The large deviations of the chemical reaction rate may affect the limiting stage of the process and significantly change of the interphase mass transfer mechanism.

The gas absorption complicated with a chemical reaction in the liquid phase is widely used for fine separations of gas mixtures in packed bed columns. Taking into account the small dimensions of the packing elements the mass transfer occurs in a thin liquid layers near the face interphase. Because of that the diffusion boundary layer theory [1] is widely used for the analysis of the chemical reaction effects in the liquid phase on the interphase mass transfer mechanism.

Let a gas absorption in a liquid with an irreversible chemical reaction in the liquid phase be considered. The evaluation of the effect of the chemical reaction rate on the mass transfer mechanism will be described by a first-order reaction:

$$\begin{aligned} \tilde{u} \frac{\partial \tilde{c}}{\partial x} + \frac{\partial \tilde{c}}{\partial y} &= \tilde{D} \frac{\partial^2 \tilde{c}}{\partial y^2}, \\ u \frac{\partial c}{\partial x} + v \frac{\partial c}{\partial y} &= D \frac{\partial^2 c}{\partial y^2} - kc. \end{aligned} \quad (3.1)$$

If a potential co-current flow of both phases is assumed and the interphase surface is flat, the boundary conditions of the equations (3.1) are:

$$\begin{aligned} x = 0, \quad \tilde{c} &= \tilde{c}_0, \quad c = 0; \\ y = 0, \quad \tilde{c} &= \chi c, \quad \tilde{D} \frac{\partial \tilde{c}}{\partial y} = D \frac{\partial c}{\partial y}; \\ y \rightarrow \infty, \quad \tilde{c} &= \tilde{c}_0; \quad y \rightarrow -\infty, \quad c = 0. \end{aligned} \quad (3.2)$$

Here a constant concentration of the absorbed substance at the flow inlet as well as in the bulk of liquid flow is assumed. The thermodynamic equilibrium and the mass flow continuity are satisfied at the phase interface.

The analysis of the equations (3.1) and (3.2) requires the following dimensionless variables:

$$X = \frac{x}{L}, \quad Y = \frac{y}{\delta}, \quad \tilde{Y} = \frac{y}{\delta},$$

$$\begin{aligned}\tilde{U} &= \frac{\tilde{u}}{\tilde{u}_0}, & \tilde{V} &= \frac{\tilde{v}}{\varepsilon \tilde{u}_0}, & \tilde{C} &= \frac{\tilde{c}}{\tilde{c}_0}, \\ U &= \frac{u}{u_0}, & V &= \frac{v}{\varepsilon u_0}, & C &= \frac{c}{c_0}, \\ \varepsilon &= \frac{\delta}{L}, & \tilde{\varepsilon} &= \frac{\tilde{\delta}}{L}, & c_0 &= \frac{\tilde{c}_0}{\chi},\end{aligned}\tag{3.3}$$

where  $L$  - the length of the gas-liquid interface,  $\delta$  and  $\tilde{\delta}$  are the thicknesses of the diffusion boundary layers in the liquid and the gas,  $u_0$  and  $\tilde{u}_0$  are the velocities of the potential flows in the bulk of the gas and the liquid respectively,  $\chi$  is the Henry's constant. The scale bases chosen for (3.3) allow the magnitude of all the dimensionless functions and their derivatives to be in order of unity. In this way from (3.1)-(3.2) yields:

$$\begin{aligned}\tilde{U} \frac{\partial \tilde{C}}{\partial X} + \tilde{V} \frac{\partial \tilde{C}}{\partial \tilde{Y}} &= \tilde{F}o \frac{\partial^2 \tilde{C}}{\partial \tilde{Y}^2}, \\ U \frac{\partial C}{\partial X} + V \frac{\partial^2 C}{\partial Y^2} &= Fo \frac{\partial^2 C}{\partial Y^2} - KC; \\ X = 0, \quad \tilde{C} &= 1, \quad C = 0; \\ Y = \tilde{Y} = 0, \quad \tilde{C} &= C, \quad \frac{\chi}{\varepsilon_0} \frac{\partial \tilde{C}}{\partial \tilde{Y}} = \frac{\partial C}{\partial Y}; \\ \tilde{Y} \rightarrow \infty, \quad \tilde{C} &= 1; \quad Y \rightarrow -\infty, \quad C = 0,\end{aligned}\tag{3.4}$$

where

$$\begin{aligned}Fo &= \frac{DL}{u_0 \delta^2}, & \tilde{F}o &= \frac{\tilde{D}L}{\tilde{u}_0 \tilde{\delta}^2}, \\ \varepsilon_0 &= \frac{D\tilde{\delta}}{\tilde{D}\delta}, & K &= \frac{kL}{u_0}.\end{aligned}\tag{3.5}$$

In equations (3.4) all the functions and their derivatives are of the order of unity and the contribution of the terms, i.e. the effect of the physical and chemical phenomena, is determined by the order of the dimensionless parameters.

The mass transfer in the gas is a result of the balance between the convective and the diffusion transport, thus in the first equation of (3.4) the left and the right sides must have equal orders. Taking into account that the order of the left side is unity, the order of the Fourier number must also be unity:

$$\tilde{F}o \sim 1.\tag{3.6}$$

The equations (3.5) and (3.6) allow the determination of the order of the diffusion boundary layer thickness in the gas phase:

$$\tilde{\delta} = \sqrt{\frac{\tilde{D}L}{\tilde{u}_0}} . \quad (3.7)$$

From (3.8) it follows that the thickness of the diffusion boundary layer is a result of the mass transfer conservation law in an arbitrary volume.

The second equation of (3.4) shows that at slow chemical reactions, where  $K < 10^{-2}$ , the term  $KC$  may be omitted. Thus, in the equation of the convective diffusion in the liquid phase  $K = 0$  may be assumed and (3.4) becomes a mathematical description of the physical absorption (in accordance with the approximation of the boundary layer). From the above considerations it follows that at

$$\frac{kL}{u_2} < 10^{-2} \quad (3.8)$$

the change of the chemical reaction rate has no practical effect on the mass transfer rate in the liquid phase.

It follows from (3.8) that  $K = 0$  may be substituted in (3.4), i.e.

$$Fo \sim 1. \quad (3.9)$$

Thus, the thickness of the diffusion boundary layer in liquid phase becomes

$$\delta = \sqrt{\frac{DL}{u_0}} . \quad (3.10)$$

$$\begin{aligned} &\text{The chemical reaction rate affects the mass transfer rate when } K > 10^{-2} . \text{ In the range} \\ &10^{-2} < K < 1 \end{aligned} \quad (3.11)$$

the effect of the chemical reaction rate in the liquid is always lower than that of the convective transport if both the convective and the diffusion transport are of equal orders. In cases when the condition (3.11) is satisfied, the order of Fourier number and the boundary layer thickness could be evaluated from (3.9) and (3.10). Thus the order of the boundary layer thickness in the liquid must be determined from (3.10) in the cases at  $K < 1$ , i.e.

$$\frac{kL}{u_0} < 1. \quad (3.12)$$

The influence of the chemical reaction rate on the mass transfer when  $K > 1$  may be analysed if the second equation of (3.4) is expressed in the form

$$\frac{1}{K} \left( U \frac{\partial C}{\partial X} + V \frac{\partial C}{\partial Y} \right) = \frac{Fo}{K} \frac{\partial^2 C}{\partial Y^2} - C . \quad (3.13)$$

From (3.13) it follows that the increase of the rate of the chemical reaction leads a decrease in the convective transport, while the other two effects (the diffusion transport and the chemical reaction) must have equal orders if  $K > 1$ , i.e.

$$K^{-1} < 1, \quad \frac{Fo}{K} \sim 1. \quad (3.14)$$

From (3.5) and (3.14) it follows also that in the cases when

$$\frac{kL}{u_0} > 1, \quad (3.15)$$

the order of the boundary layer thickness may be determined from (3.14), i.e.

$$\delta = \sqrt{\frac{D}{k}}. \quad (3.16)$$

The analysis of (3.13) shows that at high rates of the chemical reaction ( $K > 10^2$ ), the convective transport may be neglected with respect to the chemical reaction effect. In this case the hydrodynamics does not affect the mass transport if

$$\frac{kL}{u_0} > 10^2, \quad (3.17)$$

then  $K^{-1} = 0$  may be substituted in (3.13) and the boundary layer thickness could be determined from (3.16).

It is evident from (3.4) that the parameter  $\frac{\chi}{\varepsilon_0}$  determines the distribution of the diffusional resistance in the liquid and the gas phases. In a situation where

$$\chi/\varepsilon_0 > 10^2, \quad (3.18)$$

the interphase mass transfer is limited by the transport in the liquid, while if

$$\chi/\varepsilon_0 < 10^{-2} \quad (3.19)$$

the mass transfer in the gaseous phase is the limiting one. In the range

$$10^{-2} < \chi/\varepsilon_0 < 10^2 \quad (3.20)$$

both diffusional resistances are comparable.

Equation (3.5) indicates that  $\varepsilon_0$  depends on  $\delta$ , i.e. on the chemical reaction rate:

$$\begin{aligned} K < 1, \quad \varepsilon_0 &= \sqrt{\frac{Du_0}{\tilde{D}\tilde{u}_0}}; \\ K > 1 \quad \varepsilon_0 &= \sqrt{\frac{Du_0 K}{\tilde{D}\tilde{u}_0}}. \end{aligned} \quad (3.21)$$

In the cases interesting from a practical point of view

$$\frac{D}{\tilde{D}} \sim 10^{-4}, \quad \frac{u_0}{\tilde{u}_0} \sim 10^{-1} \quad (3.22)$$

and from (3.21) it follows that  $\varepsilon_0 \sim 10^{-1}$  when  $K < 1$ .

The distribution of the diffusional resistances strongly depends on the physical solubility of the gas, i.e. from Henry's constant ( $\chi$ ). For low-solubility gases ( $N_2, O_2, CH_4$ ) the value of  $\chi$  is between  $20 \div 60$ . For gases with a medium solubility ( $CO_2, C_2H_2, Cl_2, H_2S, Br_2, SO_2$ ) the Henry's constant is in the range of  $0.02 \div 2$ . For the highly soluble gases ( $HCl, NH_3$ ) the values of  $\chi$  are in the range of  $(1 \div 2)10^{-3}$ .

The analysis of the mutual effects of the physical solubility of the gas ( $\chi$ ) and the chemical reaction rate ( $K$ ) on the distribution of the diffusion resistance between the gas and the liquid shows that for highly soluble gases  $\frac{\chi}{\varepsilon_0} \sim 1$  if  $K < 1$ . This contradicts to the experimental data [3] showing that the interphase mass transfer during absorption of  $HCl$  and  $NH_3$  is limited by the mass transfer in the gaseous phase. Thus, the process in the gas may limit the interphase mass transfer only in the cases when the reaction rate in the liquid phase is high ( $K > 1$ ). From (3.19), (3.21) and (3.22) it follows that in the case of highly soluble gases the interphase mass transfer is limited by the process in the gas if  $K > 10^3$ .

When  $K > 1$  and  $10^{-3} < \chi < 10^2$  the ratio  $\frac{\chi}{\varepsilon_0}$  depends on  $K$ , i.e. the increase of the chemical reaction rate may lead to a change of the limiting stage of the process. In this way it is evident from (3.15) and (3.19) that at

$$K > 1, \quad \chi \sqrt{\frac{\tilde{D}\tilde{u}_0}{Du_0 K}} < 10^{-2}$$

the interphase mass transfer is limited by the process in the gas phase and its rate is independent of the chemical reaction rate.

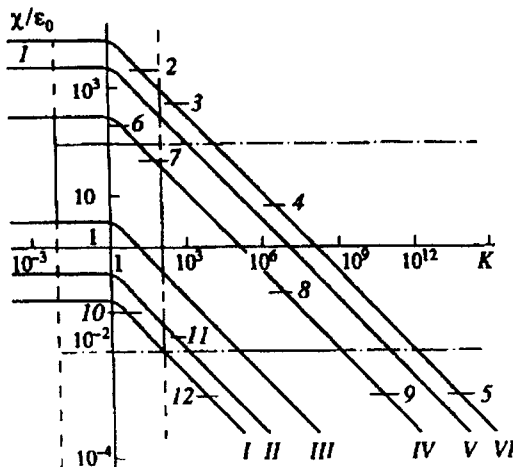


Fig.3.1. Distribution of the diffusion resistance in the gaseous and in the liquid phases under various chemical reaction rates (in the liquid phase).

Figure 3.1 shows the variations of  $\frac{\chi}{\epsilon_0}$  with the changes of  $K$  for several cases of practical interest (3.22) and various values of  $\chi$ . The data plotted allow to determine 12 areas characterized by different interphase mass transfer mechanisms:

1. The chemical reaction rate does not affect the mass transfer and the limiting stage is the process in the liquid.
2. Absorption of low-solubility gas limited by the mass transfer in the liquid and strongly dependent on the chemical reaction rate.
3. The same case like in point 2, but the mass transfer rate is independent of the liquid hydrodynamics.
4. The same like in point 3, but the diffusion resistances in both phases are comparable.
5. Absorption of low-solubility gas limited by the mass transfer in the gaseous phase and independent of the chemical reaction rate.
6. Absorption of gases of medium solubility limited by the mass transfer in the liquid and affected by the chemical reaction rate.
7. The same like in point 6, but the diffusion resistances in both phases are comparable.
8. The same like in point 8, but the mass transfer is independent of the liquid hydrodynamics.
9. Absorption of gases of medium solubility limited by the mass transfer in the gaseous phase and independent of the chemical reaction rate.

10. Absorption of highly soluble gas with comparable diffusion resistances in both phases and a significant effect of the chemical reaction rate.
11. The same like in point 10, but the liquid hydrodynamics does not affect the mass transfer.
12. Absorption of highly soluble gases limited by the mass transfer in the gaseous phase and without effects of the chemical reaction rate in the liquid phase.

It is clear that the chemical reaction rate affect the mass transfer rate. The lower boundary of the range of variations is the rate of the physical absorption limited by the mass transfer in the liquid phase. The upper boundary is the rate of the physical absorption limited by the mass transfer in the gaseous phase. The lower boundary of the range in the case of well soluble gases is a special situation.

The situations listed above have mathematical descriptions following from (3.4) with suitable substitutions of the parameters and functions listed in Table 3.1.

The effect of the chemical reaction rate on the interphase mass transfer mechanism becomes more complicated if irreversible chemical reactions (of arbitrary order) occur.

**Table 3.1**  
The values of the parameters in the model (3.4)

$K < 10^{-2}$	$Fo = 1, \quad K = 0$
$K < 1$	$Fo = 1$
$K > 1$	$\frac{Fo}{K} = 1$
$K > 10^2$	$\frac{Fo}{K} = 1, \quad K^{-1} = 0$
$\frac{\chi}{\varepsilon_0} < 10^{-2}$	$\frac{\chi}{\varepsilon_0} = 0, \quad C = 0$
$\frac{\chi}{\varepsilon_0} > 10^{-2}$	$\frac{\chi}{\varepsilon_0} = 0, \quad \tilde{C} = 1$

### 3.1.1. Irreversible chemical reactions

The effect of the reaction rate in the case of an irreversible chemical reaction of an arbitrary order on the interphase mass transfer mechanism for gas-liquid system is discussed in [7] with the following chemical reaction



where the component  $A_1$  of the gaseous mixture reacts with the component  $A_2$  of the liquid absorbent and the yield is the substance  $A_3$ .

The reaction rate is determined by

$$r_i = -k_i c_1^m c_2^n,$$

$$\frac{k}{a_i} = k_0 > 0, \quad i = 1, 2, \quad (3.24)$$

where  $k_i$  are the rate constants and  $c_i$  are the concentrations of the substances  $A_i$  ( $i = 1, 2$ ) in the liquid.

In fact the substances  $A_2$  and  $A_3$  are non-volatile and for the determination of their concentrations equations for the liquid phase are only required. Thus, the mathematical description of the absorption process may be obtained from (3.1), where  $\tilde{c}$  is the concentration of  $A_1$  in the gas, while the desired equation for  $c$  must be replaced with two equations for  $c_1$  and  $c_2$  in the liquid:

$$u \frac{\partial c_i}{\partial x} + v \frac{\partial c_i}{\partial y} = D_i \frac{\partial^2 c_i}{\partial y^2} - k_i c_i^m c_2^n, \quad i = 1, 2. \quad (3.25)$$

The boundary conditions follow from (3.2) taking into account the non-volatility of the substance  $A_2$ :

$$\begin{aligned} x = 0, \quad \tilde{c} = \tilde{c}_0, \quad c_2 = c_{02}; \\ y = 0, \quad \tilde{c} = \chi c_1, \quad D \frac{\partial \tilde{c}}{\partial y} = D_i \frac{\partial c_1}{\partial y}, \quad \frac{\partial c_2}{\partial y} = 0; \\ y \rightarrow \infty, \quad \tilde{c} = \tilde{c}_0; \quad y \rightarrow -\infty \quad c_1 = 0, \quad c_2 = c_{02}. \end{aligned} \quad (3.26)$$

The theoretical analysis of the effect of the irreversible reaction on the interphase mass transfer mechanism needs the dimensionless variables defined by (3.3) taking into consideration that there are two diffusing substances in the liquid phase:

$$\begin{aligned} Y_i = \frac{y}{\delta_i}, \quad V_i = \frac{v}{\varepsilon_i u_0}, \quad \varepsilon_i = \frac{\delta_i}{L}, \\ C_i = \frac{c_i}{c_{0i}}, \quad i = 1, 2, \end{aligned} \quad (3.27)$$

where

$$c_{01} = \frac{\tilde{c}_0}{\chi}. \quad (3.28)$$

Hence, the equations (3.4) take the form:

$$\tilde{U} \frac{\partial \tilde{C}}{\partial X} + \tilde{V} \frac{\partial \tilde{C}}{\partial \tilde{Y}} = \tilde{F} o \frac{\partial^2 \tilde{C}}{\partial \tilde{Y}^2},$$

$$\begin{aligned}
 U \frac{\partial C_i}{\partial X} + V_i \frac{\partial C_i}{\partial Y_i} &= F_{O_i} \frac{\partial^2 C_i}{\partial Y_i^2} - K_i C_i^m C_2^n, \quad i = 1, 2 \\
 X = 0, \quad \tilde{C} &= 1, \quad C_1 = 0, \quad C_2 = 1; \\
 \tilde{Y} = Y_1 = Y_2 = 0, \quad \tilde{C} &= C_1, \quad \frac{\partial C_2}{\partial Y_2} = 0, \quad \frac{\chi}{\varepsilon_{01}} \frac{\partial \tilde{C}}{\partial \tilde{Y}} = \frac{\partial C_1}{\partial Y_1}; \\
 \tilde{Y} \rightarrow \infty, \quad \tilde{C} &= 1; \quad Y_1 \rightarrow -\infty, \quad C_1 = 0; \quad Y_2 \rightarrow -\infty, \quad C_2 = 1,
 \end{aligned} \tag{3.29}$$

where

$$\begin{aligned}
 F_{O_i} &= \frac{D_i L}{u_0 \delta_i^2}, \quad K_i = \frac{k_i L}{u_0} \frac{\tilde{c}_0^{m-2+i} c_{02}^{n+1-i}}{\chi^{m-2+i}}, \\
 \varepsilon_{01} &= \frac{D_j \tilde{\delta}}{\tilde{D} \delta_i}, \quad i = 1, 2
 \end{aligned} \tag{3.30}$$

and the value of  $\tilde{\delta}$  may be obtained from (3.7).

The dimensionless rate constants of the chemical reaction are always interrelated:

$$\frac{K_1}{K_2} = \frac{c_{02}/a_2}{\tilde{c}_0/\chi a_1}, \tag{3.31}$$

where the ratios  $\frac{c_{02}}{a_2}$  and  $\frac{\tilde{c}_0}{\chi a_1}$  may be considered as the maximum values of the concentrations of the substances  $A_1$  and  $A_2$  in the liquid. It is clear that  $\frac{K_1}{K_2}$  may vary in an unlimited range.

Equations (3.29) show that in the case of slow chemical reactions  $K_1 < 10^{-2}$  and the term  $K_i C_i^m C_2^n$  in left hand part of the equation may be neglected. In this way it is possible to substitute  $K_1 = 0$  in (3.29). The result is that the equation for  $C_2$  becomes superfluous because the interphase mass transfer of  $A_1$  between the gas and the liquid no longer depends on the mass transfer of  $A_2$  in the liquid phase. It follows that at

$$\frac{k_i L}{u_0} \frac{\tilde{c}_0^{m-1} c_{02}^n}{\chi^{m-1}} < 10^{-2} \tag{3.32}$$

the change of the chemical reaction rate as well as the initial concentrations of the reagents and the physical solubility of the absorbing gas do not affect the mass transfer process in the liquid phase.

From (3.32) it follows that it is possible to substitute  $K_1 = 0$  in (3.29), i.e.

$$F_{O_i} \sim 1. \tag{3.33}$$

That allows to establish the order of diffusion boundary layer thickness:

$$\delta_1 = \sqrt{\frac{D_1 L}{u_0}}. \quad (3.34)$$

It is evident that the chemical reaction rate and the initial concentrations of the reagents as well the physical solubility of the absorbing substance affect the mass transfer rate in the liquid phase if  $K_1 > 10^{-2}$ . In the range of

$$10^{-2} < K_1 < 1 \quad (3.35)$$

the effect of the chemical reaction in the liquid is always lower with respect of that of the convective transport. Taking unto account that the convective and the diffusion transport must be of equal orders the value of  $\delta_1$  should be evaluated from (3.34) when

$$K_1 < 1. \quad (3.36)$$

It is clear from (3.37) that in the range defined by (3.35) the order of  $K_2$  may vary in an unlimited range. If  $K_2 < 10^{-2}$  then  $K_2 = 0$  is assumed in (3.29). Thus, for  $C_2$  the result is:

$$C_2 \equiv 1. \quad (3.37)$$

If substitute (3.37) in (3.29) the result is a mathematical description of an absorption process in the case of chemical reaction of a pseudo-order  $m$ . For  $m=1$  the resulting equation has a pseudo-first order [6].

When  $10^{-2} < K_2 < 1$  it is possible in a similar way to obtain

$$Fo_2 \sim 1, \quad \delta_2 = \sqrt{\frac{D_2 L}{u_0}}. \quad (3.38)$$

The effects of the parameters  $K_1$  and  $K_2$  on the interphase mass transfer mechanism is considerable when  $K_1 > 1$  and  $K_2 > 1$ . For the purposes of the theoretical analysis of the absorption process under these conditions the equation for  $C_i$  ( $i = 1, 2$ ) should be presented in the form:

$$\frac{1}{K_i} \left( U \frac{\partial C_i}{\partial X} + V_i \frac{\partial C_i}{\partial Y_i} \right) = \frac{Fo_i}{K_i} \frac{\partial^2 C_i}{\partial Y_i^2} - C_i^m C_2^n, \quad i = 1, 2. \quad (3.39)$$

It follows from (3.39) that in the range defined by (3.35) the increase of  $K_2 > 1$  leads to a decrease in the convective transport of the substance  $A_2$ , while at the same time the effects of both the diffusion transport and the chemical reaction must be of equal order:

$$\frac{Fo_2}{K_2} \sim 1. \quad (3.40)$$

Thus, when  $K_2 > 1$  the thickness of the diffusion boundary layer for  $A_2$  has an order defined by

$$\delta_2 = \sqrt{\frac{D_2}{K_2}} \frac{\chi^{m/2}}{\tilde{c}_o^{m/2} c_{02}^{(n-l)/2}}. \quad (3.41)$$

When  $K_2 > 10^2$  the hydrodynamics does not affect the interphase mass transfer of  $A_2$ , and one may substitute  $K_2^{-1} = 0$  in (3.29).

The increase of the parameter  $K_1 > 1$  leads to significant changes of the mass transfer mechanism for the substance  $A_1$  in the liquid as well as the overall gas-liquid interphase mass transfer mechanism. It is evident from (3.39) that this is accompanied by a decreasing effect of the convective transport. In this case it is possible to establish the thickness of the diffusion boundary layer with respect the substance  $A_1$  in the liquid phase

$$\delta_1 = \sqrt{\frac{D_1}{K_1}} \frac{\chi^{(m-l)/2}}{c_o^{(m-l)/2} c_{01}^{n/2}}, \quad (3.42)$$

i.e.

$$Fo_1 \sim K_1. \quad (3.43)$$

There are no hydrodynamic effects on the mass transfer if  $K_1 > 10^2$ . This allows to substitute  $K_1^{-1} = 0$  in (3.29). In all the situations where  $K_1 > 1$  the parameter  $K_2$  may assume values in an unrestricted range. Despite this, all the conclusions about the effect of  $K_2$  on the transport of the substance  $A_2$  in the liquid already done for  $K_1 < 1$  are valid also in the case when  $K_1 > 1$ .

The distribution of the diffusion resistances in both phases is determined like in the case of first order chemical reactions. It is clear from (3.29) that the transport processes in the liquid (in the gas) limit the mass transfer if  $\frac{\chi}{\varepsilon_{01}} > 10^2$  ( $\frac{\chi}{\varepsilon_{01}} < 10^{-2}$ ). The diffusion resistances are commensurable if  $10^{-2} < \frac{\chi}{\varepsilon_{01}} < 10^2$ .

If  $K_1 > 1$  the parameter  $\frac{\chi}{\varepsilon_{01}}$  depends on the chemical reaction rate and the initial concentrations of the reagents. Thus, it is possible to derive conditions under which the process is limited by the mass transport in the gas phase only:

**Table 3.2.**  
The values of the parameters in the model (3.29)

$K_1 < 10^{-2}$	$K_1 = 0$	$K_2 < 10^{-2}$	$K_2 = 0$	$C_2 \equiv 0$
	$Fo_1 = 0$	$K_2 < 1$		$C_2 \equiv 0$
		$K_2 > 1$		$C_2 \equiv 0$
		$K_2 > 10^2$	$K_2^{-1} = 0$	$C_2 \equiv 0$
$K_1 < 1$	$Fo_1 = 1$	$K_2 < 10^{-2}$	$K_2 = 0$	$C_2 \equiv 1$
		$K_2 < 1$	$Fo_2 = 1$	
		$K_2 > 1$	$\frac{Fo_2}{K_2} = 1$	
		$K_2 > 10^2$	$\frac{Fo_2}{K_2}$	
			$K_2^{-1} = 0$	$\frac{Fo_2}{K_2} = 1$
$K_1 > 1$	$\frac{Fo_1}{K_1} = 1$	$K_2 < 10^{-2}$	$K_2 = 0$	$C_2 \equiv 1$
		$K_2 < 1$	$Fo_2 = 1$	
		$K_2 > 1$	$\frac{Fo_2}{K_2} = 1$	
		$K_2 > 10^2$	$\frac{Fo_2}{K_2}$	
			$K_2^{-1} = 0$	$\frac{Fo_2}{K_2} = 1$
$K_1 > 10^2$	$K_1^{-1} = 0$	$K_2 < 10^{-2}$	$K_2 = 0$	$C_2 \equiv 1$
	$\frac{Fo_1}{K_1} = 1$	$K_2 < 1$	$Fo_2 = 1$	
		$K_2 > 1$	$\frac{Fo_2}{K_2} = 1$	
		$K_2 > 10^2$	$\frac{Fo_2}{K_2}$	
			$K_2^{-1} = 0$	$\frac{Fo_2}{K_2} = 1$
$10^{-2} < K_1 < 10^2$	$\frac{\chi}{\varepsilon_{01}} < 10^{-2}$	$\frac{\chi}{\varepsilon_{01}} = 0$	$C_1 \equiv 1$	
		$\frac{\chi}{\varepsilon_{01}}$	$\tilde{C}_1 \equiv 1$	
	$\frac{\chi}{\varepsilon_{01}} > 10^2$	$\frac{\varepsilon_{01}}{\chi} = 0$		

$$\chi \sqrt{\frac{\tilde{D}\tilde{u}_0}{D_I u_0 K_1}} = \frac{\chi^{(m+I)/2}}{c_0^{(m-I)/2} c_{02}^{n/2}} \sqrt{\frac{\tilde{D}\tilde{u}_0}{D_I K_1 L}} < 10^{-2} \quad (3.44)$$

and the mass transfer rate is independent of the reaction rate.

The effect of the chemical reaction rate of an arbitrary order on the interphase mass transfer mechanism discussed here depends on the physical solubility of the gas. The

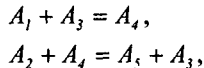
relationship may be obtained (see Fig.3.1) by replacing  $\varepsilon_0$  and  $K$  with  $\varepsilon_{0l}$  and  $K_l$ , i.e. the zones on the figure remain the same.

The existence of a mass transport of the substance  $A_2$  in the liquid phase is the reason for various possible interphase mass transfer mechanisms and the respective mathematical models in comparison with the pseudo-first order chemical reaction. All of these mathematical descriptions of the process may be obtained from (3.29) if suitable parameters and functions are used (see Table 3.2). In the table it is noted by a convention  $C_2 \equiv 0$  because when  $K_l < 10^{-2}$  the equation for  $C_2$  in (3.29) is unnecessary.

The effect of the chemical reactions on the interphase mass transfer mechanism becomes more complicated with the increase of the number of the reactions considered.

### 3.1.2. Homogenous catalytic reactions

The homogenous catalytic processes in gas-liquid systems are widely used for the synthesis of new substance [2], as well as for enhancement of the separation of gas mixtures by absorption [3]. In these cases there are at least two chemical reactions in the liquid phase. Consider a simple example of a homogenous catalytic process.



where  $A_3$  is the catalyst for the interaction between  $A_1$  and  $A_2$  in the liquid phase. The reaction rates (3.45) may be expressed as:

$$\begin{aligned} r_1 &= -\frac{\partial c_1}{\partial t} = k_1 c_1 c_3, \\ r_2 &= -\frac{\partial c_2}{\partial t} = k_2 c_2 c_4, \\ r_3 &= -\frac{\partial c_3}{\partial t} = r_1 - r_2, \\ r_4 &= -\frac{\partial c_4}{\partial t} = -r_1 + r_2, \end{aligned} \tag{3.46}$$

where  $c_i$  are the concentrations of the substances  $A_i$  ( $i = 1, \dots, 4$ ).

The equations describing the process are:

$$\begin{aligned} \tilde{u} \frac{\partial \tilde{c}_i}{\partial x} + \tilde{v} \frac{\partial \tilde{c}_i}{\partial y} &= \tilde{D}_i \frac{\partial^2 c_i}{\partial y^2}; \\ u \frac{\partial c_i}{\partial x} + v \frac{\partial c_i}{\partial y} &= D_i \frac{\partial^2 c_i}{\partial y^2} - r_i; \end{aligned}$$

$$\begin{aligned}
& u \frac{\partial c_j}{\partial x} + v \frac{\partial c_j}{\partial y} = D_j \frac{\partial^2 c_j}{\partial y^2} - r_j ; \\
& x = 0, \quad \tilde{c}_i = \tilde{c}_{0i}, \quad c_i = 0, \quad c_j = c_{0j} \quad (c_{04} = 0) , \\
& y = 0, \quad \tilde{c}_i = \chi_i c_i, \quad \tilde{D}_i \frac{\partial \tilde{c}_i}{\partial y} = D_i \frac{\partial c_i}{\partial y}, \quad \frac{\partial c_j}{\partial y} = 0; \\
& y \rightarrow \infty, \quad \tilde{c}_i = \tilde{c}_{0i}; \\
& y = -\infty, \quad c_i = 0, \quad c_j = c_{0j}, \quad (c_{04} = 0); \\
& i = 1, 2; \quad j = 3, 4,
\end{aligned} \tag{3.47}$$

where the symbols are same as those used in (3.1) and (3.2).

The analysis of (3.47) requires of dimensionless variables like those in (3.3):

$$\begin{aligned}
& X = \frac{x}{L}, \quad \tilde{Y}_i = \frac{y}{\delta_i}, \quad Y_i = \frac{y}{\delta_i}, \\
& \tilde{U} = \frac{\tilde{u}}{\tilde{u}_0}, \quad V_i = \frac{\tilde{v}}{\tilde{\epsilon}_i \tilde{u}_0}, \quad \tilde{C}_i \frac{\tilde{c}_i}{\tilde{c}_{0i}}, \\
& U = \frac{u}{u_0}, \quad V_i = \frac{v}{\epsilon_i u_0}, \quad V_j = \frac{v}{\epsilon_j u_0}, \\
& C_i = \frac{c_i}{c_{0i}}, \quad C_j = \frac{c_j}{c_{0j}}, \quad c_{0i} = \frac{\tilde{c}_{0i}}{\chi_i}, \\
& \tilde{\epsilon}_i = \frac{\delta_i}{L}, \quad \epsilon_i = \frac{\delta_i}{L}, \quad \epsilon_j = \frac{\delta_j}{L}, \\
& i = 1, 2, \quad j = 3, 4.
\end{aligned} \tag{3.48}$$

In this way as results 6 coupled boundary problems are obtained:

$$\begin{aligned}
& \tilde{U} \frac{\partial \tilde{C}_i}{\partial X} + V_i \frac{\partial \tilde{C}_i}{\partial \tilde{Y}_i} = \tilde{F} o_i \frac{\partial^2 C_i}{\partial \tilde{Y}_i^2}; \\
& X = 0, \quad \tilde{C}_i = 1; \\
& \tilde{Y}_i = 0, \quad \tilde{C}_i = C_i; \\
& \tilde{Y}_i \rightarrow \infty, \quad \tilde{C}_i = 1; \quad i = 1, 2.
\end{aligned} \tag{3.49}$$

$$U \frac{\partial C_i}{\partial X} + V_i \frac{\partial C_i}{\partial Y_i} = F o_i \frac{\partial^2 C_i}{\partial Y_i^2} - R_i;$$

$$X = 0, \quad C_i = 0;$$

$$Y_i = 0, \quad \frac{dC_i}{dY_i} = \frac{\chi_i}{\epsilon_{0i}} \left( \frac{\partial \tilde{C}_i}{\partial \tilde{Y}_i} \right)_{\tilde{Y}_i=0};$$

$$Y_i \rightarrow -\infty, C_i = 0, \quad i = 1, 2. \quad (3.50)$$

$$\begin{aligned} U \frac{\partial C_j}{\partial X} + V_j \frac{\partial C_j}{\partial Y_j} &= Fo_j \frac{\partial^2 C_j}{\partial Y_j^2} - R_j; \\ X = 0, \quad C_3 &= 1, \quad C_4 = 0; \\ Y_j = 0, \quad \frac{\partial C_j}{\partial Y_j} &= 0; \\ Y_j \rightarrow -\infty, \quad C_3 &= 1, \quad C_4 = 0, \quad j = 3, 4. \end{aligned} \quad (3.51)$$

$$\begin{aligned} \tilde{F}o_i &= \frac{\tilde{D}_i L}{\tilde{u} \delta_i^2}, \quad Fo_i = \frac{D_i L}{u \delta_i^2}, \quad Fo_j = \frac{D_j L}{u \delta_j^2}, \\ K_i &= \frac{k_i L}{u_0}, \quad \varepsilon_{oi} = \frac{D_i \tilde{\delta}_i}{\tilde{D}_i \delta_i}, \quad i = 1, 2, \quad j = 3, 4, \\ R_1 &= K_1 c_{03} C_1 C_3, \quad R_2 = K_2 c_{03} C_2 C_4, \\ R_3 &= K_1 \frac{c_{01}}{\chi_1} C_1 C_3 - K_2 \frac{\tilde{c}_{02}}{\chi_2} C_2 C_4, \\ R_4 &= -K_1 \frac{\tilde{c}_{01}}{\chi_1} C_1 C_3 + K_2 \frac{\tilde{c}_{02}}{\chi_2} C_2 C_4. \end{aligned} \quad (3.52)$$

The boundary problems (3.49)-(3.51) allow to determine the effect of the chemical reaction rate (and the physical solubilities of the substances  $A_1$  and  $A_2$  in the liquid too) on the interphase mass transfer mechanism by the method described in 3.1.1. and 3.1.2.

In fact, the chemical reaction rates (3.45) are greater. In situations where the following conditions are satisfied

$$K_1 c_{03} > 10^2, \quad K_2 c_{03} > 10^2, \quad K_1 \frac{\tilde{c}_{01}}{\chi_1} \sim K_2 \frac{\tilde{c}_{02}}{\chi_2} > 10^2, \quad (3.53)$$

the equations (3.50) and (3.51) take the form:

$$\begin{aligned} \frac{\partial^2 C_i}{\partial Y_i^2} &= C_i C_{i+2}; \\ Y_i = 0, \quad \frac{\partial C_i}{\partial Y_i} &= \frac{\chi_i}{\varepsilon_{oi}} \left( \frac{\partial C_i}{\partial \tilde{Y}_i} \right)_{\tilde{Y}_i=0}; \\ Y_i \rightarrow -\infty, \quad C_i &= 0, \quad i = 1, 2. \end{aligned} \quad (3.54)$$

$$\frac{\partial^2 C_3}{\partial Y_3^2} = C_1 C_3 - a C_2 C_4;$$

$$\begin{aligned} \frac{\partial^2 C_4}{\partial Y_j^2} &= -C_1 C_3 + \alpha C_2 C_4; \\ Y_j &= 0, \quad \frac{\partial C_j}{\partial Y_j} = 0; \\ Y_j &\rightarrow -\infty, \quad C_3 = 1, \quad C_4 = 0, \end{aligned} \tag{3.55}$$

where

$$\begin{aligned} \alpha &= \frac{K_2 \tilde{c}_{02} \chi_1}{K_1 \tilde{c}_{01} \chi_2}, \quad \delta_i \sqrt{\frac{D_i L}{u_0 K_i c_{03}}}, \quad i = 1, 2; \\ \delta_j &= \sqrt{\frac{D_j L \chi_1}{u_0 K_j \tilde{c}_{01}}}, \quad j = 3, 4. \end{aligned} \tag{3.56}$$

From (3.55) it follows that if  $D_3 \approx D_4$  one may write that  $C_4 \approx 1 - C_3$ .

When the reactions (3.45) are fast,  $\delta_i = 0, \varepsilon_{0i} \rightarrow \infty$  ( $i = 1, 2$ ), i.e. the homogenous reaction becomes heterogeneous. In these cases the reactions (3.45) may occur on the liquid surface and the mass transfer in the gaseous phase limits the whole process.

### 3.1.3. Reversible chemical reactions

The reversible gas absorption is applied in the cases when the regeneration of the absorbent is needed. In the practical situations the absorption is reversible due to the reversibility of the chemical reaction. The rates of both the forward and backward reactions affect the interphase mass transfer mechanism as in the case of irreversible processes. These effects become more complicate due to a simultaneous reversibility of both the physical and the chemical parts of the absorption process.

An example of a reversible absorption has been described in [8] with a simple reversible chemical reaction.



where the assumption that the absorbed substance  $A_1$  from the gas reacts with the substance  $A_2$  in the liquid. Far from the equilibrium the rate of interaction between  $A_1$  and  $A_2$  is:

$$r_i = -\frac{\partial c_i}{\partial t} = k_i c_i^m c_2^n - k_{3i} c_3^p, \tag{3.58}$$

$$\frac{k_1}{a_1} = \frac{k_2}{a_2} = -\frac{k_3}{a_3} = k_0 > 0. \tag{3.59}$$

Here  $c_i$  are the concentrations of  $A_i$  ( $i = 1, 2, 3$ ).

### The introduction of the constant of chemical equilibrium

$$R = \frac{k_{3i}}{k_i}, \quad i = 1, 2, 3, \quad (3.60)$$

from (3.58) leads to

$$r_i = k_i(c_i^m c_2^n - R c_3^p), \quad i = 1, 2, 3, \quad (3.61)$$

i.e., the equilibrium constants and the forward reaction rate constant may express the process rate.

The mathematical description of absorption complicated with a reversible chemical reaction in the liquid is:

$$\begin{aligned} \tilde{u} \frac{\partial \tilde{c}}{\partial x} + \tilde{v} \frac{\partial \tilde{c}}{\partial y} &= \tilde{D} \frac{\partial^2 \tilde{c}}{\partial y^2}; \\ u \frac{\partial c_i}{\partial x} + v \frac{\partial c_i}{\partial y} &= D_i \frac{\partial^2 c_i}{\partial y^2} - k_i(c_i^m c_2^n - R c_3^p), \quad i = 1, 2, 3; \\ x = 0, \quad \tilde{c} &= \tilde{c}_0, \quad c_1 = 0, \quad c_2 = c_{02}, \quad c_3 = 0; \\ y = 0, \quad \tilde{c} &= \chi c_1, \quad \tilde{D} \frac{\partial \tilde{c}}{\partial y} = D_i \frac{\partial c_i}{\partial y}, \quad \frac{\partial c_2}{\partial y} = 0, \quad \frac{\partial c_3}{\partial y} = 0; \\ y \rightarrow \infty, \quad \tilde{c} &= \tilde{c}_0; \\ y \rightarrow -\infty, \quad c_1 &= 0, \quad c_2 = c_{02}, \quad c_3 = 0. \end{aligned} \quad (3.62)$$

The analysis of the reversible reaction effect on the interphase mass transfer mechanism needs the following dimensionless variables:

$$\begin{aligned} X &= \frac{x}{L}, \quad \tilde{Y} = \frac{y}{\tilde{\delta}}, \quad \tilde{C} = \frac{\tilde{c}}{\tilde{c}_0}, \\ Y_i &= \frac{y}{\delta_i}, \quad C_i = \frac{c_i}{c_{0i}}, \quad (c_{0i} = \tilde{c}_0 / \chi), \\ \tilde{U} &= \frac{\tilde{u}}{\tilde{u}_0}, \quad \tilde{V} = \frac{\tilde{v}}{\tilde{\epsilon} \tilde{u}_0}, \quad U = \frac{u}{u_0}, \quad V_i = \frac{v}{\epsilon_i u_0}, \\ \tilde{\epsilon} &= \frac{\tilde{\delta}}{L}, \quad \epsilon_i = \frac{\delta_i}{L}, \quad r_0 = \frac{k_0 \tilde{c}_0^m c_{02}^n}{\chi^m}, \\ \tilde{F}o &= \frac{\tilde{D} L}{\tilde{u}_0 \tilde{\delta}}, \quad Fo_i = \frac{D_i L}{u_0 \delta_i^2}, \quad \alpha = \frac{r_0 L}{u_0}, \\ \alpha_1 &= \frac{a_1 \alpha}{c_{01}}, \quad \alpha_2 = \frac{a_2 \alpha}{c_{02}}, \quad \alpha_3 = -\frac{a_3 \alpha}{c_{03}}, \end{aligned}$$

$$c_{03} = \frac{c_{01}^{m/p} c_{02}^{n/p}}{\chi^{m/p}}, \quad \varepsilon_{0l} = \frac{D_l \tilde{\delta}}{\tilde{D} \delta_l}, \quad i = 1, 2, 3. \quad (3.63)$$

In this way equations (3.62) take the form

$$\begin{aligned} \tilde{U} \frac{\partial \tilde{C}}{\partial X} + \tilde{V} \frac{\partial \tilde{C}}{\partial \tilde{Y}} &= \tilde{F}_o \frac{\partial^2 \tilde{C}}{\partial \tilde{Y}^2}; \\ U \frac{\partial C_i}{\partial X} + V_i \frac{\partial C_i}{\partial Y_i} &= F_{O_i} \frac{\partial^2 C_i}{\partial Y_i^2} - \alpha_i (C_i^m C_2^n - R C_3^p); \\ X = 0, \quad \tilde{C} &= 1, \quad C_1 = 0, \quad C_2 = 1, \quad C_3 = 0; \\ \tilde{Y} = Y_i = 0, \quad \tilde{C} &= C_i, \quad \frac{\partial C_i}{\partial Y_i} = \frac{\chi}{\varepsilon_{0l}} \frac{\partial \tilde{C}}{\partial \tilde{Y}}, \quad \frac{\partial C_2}{\partial Y_2} = \frac{\partial C_3}{\partial Y_3} = 0; \\ \tilde{Y} \rightarrow \infty, \quad \tilde{C} &= 1; \\ Y_i \rightarrow -\infty, \quad C_1 &= 0, \quad C_2 = 1, \quad C_3 = 0. \end{aligned} \quad (3.64)$$

It follows from (3.64) that the process depends on the parameters  $K, \alpha_i, F_o$ , and  $\frac{\chi}{\varepsilon_{0l}}$ .

Their values determine the interphase mass transfer mechanism.

If  $R > 10^2$  the chemical reactions are practically irreversible. If it is substituted  $R = 0$  in (3.64), the problem of determination of  $C_i$  becomes drops not. Thus, then  $R > 10^2$  the equations for  $C_i$  ( $i = 1, 2, 3$ ) become:

$$U \frac{\partial C_i}{\partial X} + V_i \frac{\partial C_i}{\partial Y_i} = F_{O_i} - R \alpha_i \left( \frac{1}{R} C_i^m C_2^n - C_3^p \right), \quad i = 1, 2, 3, \quad (3.65)$$

Here it is possible to substitute  $R^{-1} = 0$ . From the boundary problem for  $C_3$  it follows that  $C_3 \equiv 0$  and consequently  $C_2 \equiv 1$ . For  $C_1$  the resulting equations describe the case of a physical absorption of the substance  $A_1$ .

A reversible absorption occurs if  $10^{-2} < R < 10^2$  and the mass transfer mechanism depends strongly on the rate of the forward reaction, i.e. on the parameters  $\alpha_i$  ( $i = 1, 2, 3$ ).

If  $\alpha_i < 10^{-2}$  it is possible to substitute  $\alpha_i = 0$  in (3.64) which corresponds to the case of a physical absorption (at various values of  $\alpha_2$  and  $\alpha_3$ ).

If  $\alpha_2 < 10^{-2}$  it follows from (3.64) that at  $\alpha_2 = 0$  and  $C_2 \equiv 1$ , i.e. this is the case of a forward reaction of pseudo- $m$  order.

When  $\alpha_3 < 10^{-2}$  it follows that  $C_3 \equiv 0$  and the case corresponds to the situation of an irreversible reaction.

The correlation between the effects of both the diffusion and the convective transport as well as the diffusion boundary layer thickness depends on the values of the parameters  $\alpha_i$  and  $R$ .

At  $\alpha_i > 10^2$  and  $10^{-2} < R < 1$  ( $i=1,2,3$ ) it is possible to substitute  $\alpha_i^{-1} = 0$  ( $i = 1,2,3$ ) in (3.64). This means that the convective transport may be neglected and the thickness of the diffusion boundary layer may be evaluated from the condition:

$$Fo_i \sim \alpha_i, \quad i=1,2,3, \quad (3.66)$$

i.e.

$$\delta_i = \sqrt{\frac{D_i L}{u_0 \alpha_i}}, \quad i = 1,2,3. \quad (3.67)$$

At  $\alpha_i R > 10^2$  and  $1 < R < 10^2$  one may substitute  $(\alpha_i R)^{-1} = 0$  ( $i = 1,2,3$ ) in (3.64) and neglect the left-hand sides of the equations for  $C_i$  ( $i = 1,2,3$ ). In this case the result for the boundary layer thickness is:

$$Fo_i \sim \alpha_i R, \quad i = 1,2,3, \quad (3.68)$$

i.e.

$$\delta_i = \sqrt{\frac{D_i L}{u_0 \alpha_i R}}, \quad i = 1,2,3. \quad (3.69)$$

In the case of slow reactions  $\alpha_i < 1$ ,  $\alpha_i R < 1$ ,  $i = 1,2,3$  the thickness of the diffusion boundary layer may be obtained from a relationship similar to (3.10):

$$\delta_i = \sqrt{\frac{D_i L}{u_0}}, \quad i = 1,2,3. \quad (3.70)$$

The distribution of the diffusion resistances is determined by the conditions (3.18)-(3.20), where  $\varepsilon$  must be replaced by  $\varepsilon_{0i}$  from (3.63). The determination of  $\tilde{\delta}$  and  $\delta_i$  must be performed from (3.7), (3.67), (3.69) and (3.70).

The analysis of the boundary problem (3.64) does not consider processes in which

$$C_i'' C_2^n - R C_3^p \approx 0, \quad \alpha_i (C_i'' C_2^n - R C_3^p) \neq 0. \quad (3.71)$$

It corresponds to a situation when in the bulk of the liquid there is a chemical equilibrium and the rates of both the forward and the backward reactions are significant, but the difference between them significantly affect the mass transfer. In this situation the solution must take into account both the physical and the chemical equilibrium.

### 3.1.4. Relationships between the chemical and physical equilibriums during absorption

The absorption process in various systems like  $\text{NH}_3 - \text{H}_2\text{O}$ ,  $\text{SO}_2 - \text{H}_2\text{O}$  etc., is characterized by a fast establishment of the chemical equilibrium in the liquid phase. The chemical reaction significantly increases the gas-liquid mass transfer rate. The mathematical description uses a model of physical absorption where Henry's constant may be assumed as a conditional value relating the physical solubility of the gas and the chemical equilibrium in the liquid. Under these assumptions the liquid absorbs the substance  $A_1$  from the gas. After that  $A_1$  reacts with the liquid component  $A_2$  and the reaction is followed by a dissociation of the reaction product. Generally, the reversible reaction may be expressed as



where  $A_1$  represents the gas molecule ( $\text{NH}_3$ ,  $\text{SO}_2$ ,  $\text{HCl}$ , etc) and  $A_2$  are the molecules of the reagent in the liquid ( $\text{H}_2\text{O}$ ).  $A_3$  is the ionic form of the molecule  $A_1$  while  $A_4$  are the hydroxyl or hydrogen ions.

The kinetic equations are:

$$r_i = -\frac{\partial c_i}{\partial t} = k_i (c_i^m c_2^n - R c_3^p c_4^q), \quad i = 1, \dots, 4, \quad (3.73)$$

where

$$k_1 = \frac{k_2}{a_2} = -k_3 = -\frac{k_4}{a_4} = k_0 > 0, \quad (3.74)$$

and  $R$  is the chemical equilibrium constant.

Substituting  $r_i$  ( $i = 1, \dots, 4$ ) from (3.73) in (3.62) the yield is the mathematical description of an absorption process with a reversible chemical reaction (3.72). It should be taken into account, that the boundary conditions for  $c_3$  and  $c_4$  are equal.

In the situations where the rate of establishment of the chemical equilibrium is high and the corresponding rates of both reactions (forward and backward) are also significant the equations (3.73) indicate that:

$$\begin{aligned} c_1^m c_2^n - R c_3^p c_4^q &\approx 0, \\ k_i (c_i^m c_2^n - R c_3^p c_4^q) &\neq 0, \quad i = 1, \dots, 4. \end{aligned} \quad (3.75)$$

The concentration of  $A_1$  in the liquid ( $c$ ) may be expressed by the concentrations of its molecular and ionic forms:

$$c = c_1 + c_3, \quad (3.76)$$

while their coefficients of diffusion may be assumed practically equal:

$$D_1 = D_3 = D. \quad (3.77)$$

This allows a summation of the equations for  $c_1$  and  $c_3$ :

$$u \frac{\partial c}{\partial x} + v \frac{\partial c}{\partial y} = D \frac{\partial^2 c}{\partial y^2} \quad (3.78)$$

with boundary conditions

$$\begin{aligned} x = 0, \quad c &= 0; \\ y = 0, \quad c &= \frac{\tilde{c}}{\chi} \left( 1 + \frac{\tilde{c}^{m/p-1} c_2^{n/p}}{\chi^{m/p-1} R^{1/p} c_4^{q/p}} \right), \quad D \frac{\partial c}{\partial y} = \tilde{D} \frac{\partial \tilde{c}}{\partial y}; \\ y \rightarrow \infty, \quad c &= 0. \end{aligned} \quad (3.79)$$

The boundary conditions follow from the conditions imposed by the physical and chemical equilibriums:

$$c_1 = \tilde{c}/\chi, \quad c_1^m c_2^n - R c_3^p c_4^q = 0. \quad (3.80)$$

The boundary conditions (3.79) permit to obtain an apparent Henry's constant:

$$H = \chi \left( 1 + \frac{\tilde{c}^{m/p-1} c_2^{n/p}}{\chi^{m/p-1} R^{1/p} c_4^{q/p}} \right)^{-1}, \quad (3.81)$$

which takes into account both the physical and the chemical equilibriums.

In most of the cases of practical interest the substance  $A_2$  is water, so  $c_2$  is a large value that does not change during the process. This means that the reaction is of a pseudo-first order:

$$c_2 \equiv c_{02} = const, \quad m = n = p = q = 1. \quad (3.82)$$

Moreover, it follows from (3.72) and (3.76) that

$$c_1 = c - c_3, \quad c_3 = c_4/a_4. \quad (3.83)$$

Hence, the mathematical description of the process may be expressed in the following form:

$$\begin{aligned} \tilde{u} \frac{\partial \tilde{c}}{\partial x} + \tilde{v} \frac{\partial \tilde{c}}{\partial y} &= D \frac{\partial^2 \tilde{c}}{\partial y^2}, \\ u \frac{\partial c}{\partial x} + v \frac{\partial c}{\partial y} &= D \frac{\partial^2 c}{\partial y^2}, \end{aligned}$$

$$\begin{aligned}
 u \frac{\partial c_4}{\partial x} + v \frac{\partial c_4}{\partial y} &= D_4 \frac{\partial^2 c_4}{\partial y^2} - k_4 \left( c_{02} c - \frac{1}{a_4} c_{02} c_4 - R \frac{1}{a_4} c_4^2 \right); \\
 x = 0, \quad \tilde{c} &= \tilde{c}_0, \quad c = 0, \quad c_4 = 0; \\
 y = 0, \quad \tilde{c} &= HC, \quad \tilde{D} \frac{\partial \tilde{c}}{\partial y} = D \frac{\partial c}{\partial y}, \quad \frac{\partial c_4}{\partial y} = 0; \\
 y \rightarrow \infty, \quad \tilde{c} &= \tilde{c}_0; \\
 y \rightarrow -\infty, \quad c &= 0, \quad c_4 = 0,
 \end{aligned} \tag{3.84}$$

where:

$$H = \chi \left( 1 + \frac{c_{02}}{R c_4} \right)^{-1}. \tag{3.85}$$

In the cases when there is no chemical reaction in the liquid phase ( $R \rightarrow \infty$ ) it follows from (3.85) that  $H = \chi$ . When the chemical reaction is irreversible ( $R = 0$ ) and the rate constant is high the relationship (3.85) gives  $H = 0$ , i.e. the mass transfer is limited by the mass transfer in the gas.

In the situations when  $c_4 = c_{04} = \text{const}$  (there is absorption of  $\text{SO}_2$  or  $\text{NH}_3$  by means of buffer solutions and  $c_4$  is the concentration of the hydrogen or hydroxyl ions) there is no need the equation for  $c_4$  in (3.84). A model of a physical absorption may describe the process with a Henry's constant given by (3.85).

The evaluations of the boundary layer thickness as well as the distribution of the diffusion resistances in both phases are similar to those discussed in 3.1.4.

## CHAPTER 3.2. MACROKINETICS OF THE CHEMICAL TRANSFORMATIONS

The macrokinetics of the chemical transformations in gas-liquid systems is determined by the interphase mass transfer rate between both phases taking into consideration the reaction rate in the liquid. Taking into account that the initial concentration of the absorbed substances in the liquid is always zero, the driving force of the mass transfer depends on the initial concentration gradient in the gas phase. In this way the mass transfer rate may be expressed by the interphase mass transfer rate in the gas or liquid depending on the limiting stage of the process:

$$J = \tilde{\beta} \tilde{c}_0 = \beta \frac{\tilde{c}_0}{\chi}, \tag{3.86}$$

where  $\tilde{\beta}$  and  $\beta$  are the mass transfer coefficients in the gas and the liquid respectively. The left part of (3.86) is the average rate  $J$  of interphase mass transfer through the face interphase with a length  $L$ . The value of  $J$  may be determined by means of the average value of the mass flux across that interphase surface:

$$J = \frac{I}{L} \int_0^L \tilde{D} \left( \frac{\partial \tilde{c}}{\partial y} \right)_{y=0} dx = \frac{I}{L} \int_0^L D \left( \frac{\partial c}{\partial y} \right)_{y=0} dx . \quad (3.87)$$

The equations (3.86) and (3.87) permit to establish relationships for the Sherwood number:

$$\begin{aligned} \tilde{Sh} &= \frac{\tilde{\beta}L}{\tilde{D}} = \frac{I}{\tilde{c}_0} \int_0^L \left( \frac{\partial c}{\partial y} \right)_{y=0} dx , \\ Sh &= \frac{\beta L}{D} = \frac{\chi}{\tilde{c}_0} \int_0^L \left( \frac{\partial c}{\partial y} \right)_{y=0} dx . \end{aligned} \quad (3.88)$$

In the case of an irreversible chemical reaction of a first order and with the help of the dimensionless variables (3.3) the Sherwood number becomes:

$$\begin{aligned} \tilde{Sh} &= \tilde{\varepsilon}^{-1} \int_0^I \left( \frac{\partial \tilde{C}}{\partial \tilde{Y}} \right)_{Y=0} dX , \\ Sh &= \varepsilon^{-1} \int_0^I \left( \frac{\partial C}{\partial Y} \right)_{Y=0} dX , \end{aligned} \quad (3.89)$$

where  $\varepsilon$  and  $\tilde{\varepsilon}$  depend on the thickness of the diffusion boundary layer, i.e. their values depend on the interphase mass transfer mechanism.

Equations (3.89) relate the macrokinetics rate constants ( $\tilde{\beta}$  and  $\beta$ ) of the mass transfer process and the chemical rate constant ( $K$  in (3.5)) of the chemical reactions (microkinetics) through the solution of the boundary problem (3.4)).

When an irreversible reaction occurs (of arbitrary order) the substitution  $Sh = Sh_i$  should be made in (3.89):

$$Sh_i = \frac{\beta_i L}{D_i} = \varepsilon_i^{-1} \int_0^I \left( \frac{\partial C_i}{\partial Y_i} \right)_{Y_i=0} dX , \quad (3.90)$$

where in the general situation  $\beta_i$  is a function of  $K_1$  and  $K_2$  obtained from (3.29).

In the case of homogeneous catalytic reactions the equations (3.89) take the form:

$$\begin{aligned} \tilde{Sh}_i &= \frac{\tilde{\beta}_i L}{\tilde{D}_i} = \tilde{\varepsilon}_i^{-1} \int_0^I \left( \frac{\partial \tilde{C}_i}{\partial \tilde{Y}_i} \right)_{\tilde{Y}_i=0} dX , \\ Sh_i &= \frac{\beta_i L}{D_i} = \varepsilon_i^{-1} \int_0^I \left( \frac{\partial C_i}{\partial Y_i} \right)_{Y_i=0} dX , \quad i = 1, 2 , \end{aligned} \quad (3.91)$$

where  $\tilde{\beta}$  and  $\beta$  are functions of  $K_i$  ( $i = 1, 2$ ) obtained from the solution of (3.29).

Applying the conditions valid for a reversible reaction (3.57) the relationships for Sherwood number take the same form like those obtained for irreversible reactions. However,  $\tilde{\beta}$  and  $\beta$  are functions of  $k_i$  ( $i = 1, 2, 3$ ) and  $R$ , and may be obtained as solutions of (3.64).

Equations (3.86)-(3.89) permit to calculate the mass transfer rate in reacting gas-liquid systems through the solution of the basic equation of the convective diffusion in both phases. This will be done in several particular cases.

### 3.2.1. Chemosorption in a falling liquid film

The analysis of the kinetics of irreversible absorption in the case of a laminar liquid film flow is interesting from two points of view. The first is from the position of the general mass transfer theory upon the conditions of a concurrent kinetics, while the second - to obtain theoretically the mass transfer coefficients in various practically important cases. For example, such processes are the absorption processes performed in film flow devices: packed bed columns, falling liquid film, etc.

Let the practically important case be considered when the gas movement does not affect the liquid film flow and the velocity profile in it may be determined by of Nusselt equation [4]:

$$u = u_0 \left( \frac{2y}{h_0} - \frac{y^2}{h_0^2} \right), \quad v = 0, \quad (3.92)$$

where  $u_0$  and  $h_0$  are the surface film velocity and its thickness. Moreover, the mass transfer is intensified mainly due to the irreversible chemical reaction of a first or a pseudo-first order. If the mass transfer limits the reaction rate in the liquid phase [9,10] the concentration at the film surface becomes equal the equilibrium one.

$$c^* = \frac{\tilde{c}_0}{\chi}. \quad (3.93)$$

The mathematical description of this process may be obtained from (3.1) and (3.2) taking into consideration (3.92) and (3.93):

$$\begin{aligned} u \frac{\partial c}{\partial x} &= D \frac{\partial^2 c}{\partial y^2} - kc; \\ x = 0, \quad c &= 0; \\ y = 0, \quad c &= 0; \\ y = h_0, \quad c &= c^*. \end{aligned} \quad (3.94)$$

The mass transfer rate for a film of a length  $L$  may be determined from the equations (3.87). It may be calculated by averaging the local diffusion fluxes.

$$J = \beta c^* = \frac{1}{L} \int_0^L D \left( \frac{\partial c}{\partial y} \right)_{y=h_0} dx. \quad (3.95)$$

Thus the Sherwood number is

$$Sh = \frac{\beta L}{D} = \frac{1}{c^*} \int_0^\infty \left( \frac{\partial c}{\partial y} \right)_{y=h_0} dx, \quad (3.96)$$

i.e. (3.94) must be solved.

The solution of (3.94) may be obtained [10] by means of the dimensionless variables of the diffusion boundary layer :

$$X = \frac{x}{L}, \quad Y = \frac{y - h_0}{\delta}, \quad \delta = \sqrt{\frac{DL}{u_0}}, \quad C = \frac{c}{c^*}.$$

Hence,

$$\begin{aligned} (1 - \theta Y^2) \frac{\partial C}{\partial X} &= \frac{\partial^2 C}{\partial Y^2} - KC; \\ X = 0, \quad C &= 0; \\ Y = 0, \quad C &= 1; \\ Y \rightarrow -\infty, \quad C &= 0, \end{aligned} \quad (3.97)$$

where

$$K = \frac{kL}{u_0}, \quad \theta = \frac{\delta^2}{h_0^2} \ll 1.$$

The new variables allow to express (3.96) in the form:

$$Sh = \sqrt{Pe} \int_0^\infty \left( \frac{dC}{dY} \right)_{Y=0} dx. \quad (3.98)$$

In equations (3.97) the small parameter  $\theta$  permits to obtain the solution in the form

$$C = C_0 + \theta C_1 + \theta C_2 + \dots . \quad (3.99)$$

The boundary problems [9,10] for  $C_i$  ( $i = 0, 1, 2$ ) may be solved by means of integral transformations

$$\bar{C}_i(p, Y) = p \int_0^\infty C_i(X, Y) \exp(-pX) dX, \quad i = 0, 1, 2. \quad (3.100)$$

The same result may be obtained if one substitutes

$$C_i(X, Y) = F_i(X, Y) \exp(-KX), \quad i = 0, 1, 2, \quad (3.101)$$

because for  $F_i(X, Y)$  ( $i = 0, 1, 2$ ) the boundary problems may be solved by Green functions. The result in this case is:

$$\begin{aligned} C_0 &= \frac{1}{2} \left[ \exp(-Y\sqrt{K}) \operatorname{erfc} \left( \frac{Y}{2\sqrt{X}} - \sqrt{KX} \right) + \exp(Y\sqrt{K}) \operatorname{erfc} \left( \frac{Y}{2\sqrt{X}} + \sqrt{KX} \right) \right], \\ C_1 &= \frac{1}{2\sqrt{\pi}} \left( \frac{Y^3}{3\sqrt{X}} + Y\sqrt{X} \right) \exp \left( -KX - \frac{Y^2}{4X} \right), \\ C_2 &= \frac{1}{12\sqrt{\pi}} \left( \frac{19}{2} Y X^{3/2} + \frac{19}{4} Y^3 X^{1/2} - \frac{4}{5} Y^5 X^{-1/2} + \right. \\ &\quad + \frac{1}{12} Y^7 X^{-3/2} - \frac{19}{5} K Y X^{5/2} - \frac{38}{15} K Y^3 X^{3/2} - \\ &\quad \left. - \frac{1}{3} K Y^5 X^{1/2} \right) \exp \left( -KX - \frac{Y^2}{4X} \right). \end{aligned} \quad (3.102)$$

The basic equation of the chemosorption kinetics in a falling liquid film follows from (3.98) and (3.102):

$$\begin{aligned} Sh &= \sqrt{Pe} \left\{ \frac{1}{\sqrt{\pi}} \exp(-K) + \left( \frac{3}{2} \frac{1}{\sqrt{K}} - \sqrt{K} \right) \operatorname{erf} \sqrt{K} - \right. \\ &\quad \left. - \theta \left[ -\frac{1}{2K\sqrt{\pi}} \exp(-K) + \frac{1}{4K^{3/2}} \operatorname{erf} \sqrt{K} \right] - \theta^2 \frac{19}{60\sqrt{\pi}} \exp(-K) \right\}. \end{aligned} \quad (3.103)$$

In the absence of a chemical reaction ( $K = 0$ ) the kinetic equation of the physical absorption [11,12] follows from (3.103):

$$Sh = \sqrt{\frac{Pe}{\pi}} \left( 1 - \frac{\theta}{3} - \frac{19\theta^2}{60} \right). \quad (3.104)$$

When fast chemical reactions take place ( $K \gg 1, \theta \ll 1$ ) it follows that

$$Sh = \sqrt{KPe}, \quad (3.105)$$

i.e. the well-known [3] equation:

$$\beta = \sqrt{kD}. \quad (3.106)$$

The relationship (3.103) demonstrates the increase of mass transfer rate as a function of the chemical reaction rate in a range bounded by  $K = 0$  and by an upper limit defined by (3.19), i.e. the case of an interphase mass transfer limited by the process in the gas.

### 3.2.2. Sulphuric acid alkylation process in a film flow reactor

The film flow reactors are usually designed as a bundle of tubes with liquid flowing down on their inner surfaces. The flow is oriented upward and the absorption occurs in a countercurrent mode. A cooling agent cools the tubes bundle enclosed in a cylindrical shell.

The film flow reactors are employed for gas-liquid reactions in two principle cases:

- When the gas absorbed by the liquid reacts with the reagents of the absorbent;
- When the liquid absorbs two components of a gas mixture, which react there after in the bulk of the absorbent.

In the second case the reaction is usually homogenous catalytic, where the liquid plays the role of the catalyst.

In the film flow reactors the conditions allow an intensive heat exchange (cooling). In this way these reactors are suitable for carrying out gas-liquid reactions accompanied with high thermal effects. A propre example for such type of reaction is the alkylation of iso-butane with butene with concentrated sulphur acid as a catalyst [13].

The process is performed in the following manner. The gas mixture of iso-butane ( $A_1$ ) and butene ( $A_2$ ) flows downward in a co-current mode with the liquid film inside a cylindrical tube. Both gases are absorbed in the liquid where homogeneous catalytic reactions of alkylation and oligomerization take place.

$$\begin{aligned} A_1 + A_2 &= A_3, \\ A_2 + A_2 &= A_4. \end{aligned} \quad (3.107)$$

The reaction products are iso-oktane ( $A_3$ ) and oktene ( $A_4$ ). The first reaction in (3.107) gives desired products, while in the second reaction a by-product is generated.

The reactions (3.107) are exothermic with large thermal effects. The cooling is effected by water flowing on the outer surface of the tube. In this way a constant temperature along the tube length is maintained.

The mathematical description of the mass transfer process [13,16] may be obtained by means of (3.1) and (3.94):

$$\begin{aligned} \tilde{u} \frac{\partial \tilde{c}_i}{\partial x} + \tilde{v} \frac{\partial \tilde{c}_i}{\partial y} &= \tilde{D}_i \frac{\partial^2 \tilde{c}_i}{\partial y^2}, \\ u \frac{\partial c_i}{\partial x} &= D_i \frac{\partial^2 c_i}{\partial y^2} - r_i; \\ y = 0, \quad c_i &= 0; \\ y = h_0, \quad \tilde{c}_i &= \chi_i c_i, \quad \tilde{D}_i \frac{\partial \tilde{c}_i}{\partial y} = D_i \frac{\partial c_i}{\partial y}; \\ y \rightarrow \infty, \quad \tilde{c}_i &= \tilde{c}_{0i}, \quad i = 1, 2, \end{aligned} \quad (3.108)$$

where

$$\begin{aligned} r_1 &= -\frac{\partial c_1}{\partial t} = k_1 c_1 c_2, \\ r_2 &= -\frac{\partial c_2}{\partial t} = k_1 c_1 c_2 + k_2 c_2^2. \end{aligned} \quad (3.109)$$

The solution of the boundary problem requires dimensionless variables and parameters as follows:

$$\begin{aligned} X &= \frac{x}{L}, & \tilde{Y}_i &= \frac{y - h_0}{\tilde{\delta}}, & Y_i &= \frac{h_0 - y}{\delta_i}, \\ \tilde{U} &= \frac{\tilde{u}}{\tilde{u}_0}, & \tilde{V}_i &= \frac{\tilde{v}}{\tilde{\varepsilon}_i \tilde{u}_0}, & U &= \frac{u}{u_0}, & \tilde{\varepsilon}_i &= \frac{\tilde{\delta}_i}{L}, & \varepsilon_i &= \frac{\delta_i}{L}, \\ \tilde{C}_i &= \frac{\tilde{c}_i}{\tilde{c}_{0i}}, & C_i &= \frac{c_i}{c_{0i}}, & c_{0i} &= \frac{\tilde{c}_{0i}}{\chi_i}, & \varepsilon_{0i} &= \frac{D_i \tilde{\delta}_i}{\tilde{D}_i \delta_i}, \\ \tilde{F}o_i &= \frac{\tilde{D}_i L}{\tilde{u}_0 \tilde{\delta}_i^2}, & F_o_i &= \frac{D_i L}{u_0 \delta_i^2}, & K_i &= \frac{k_i L}{u_0}, \\ R_i &= \frac{r_i L}{u_0 c_{0i}}, & i &= 1, 2, \end{aligned} \quad (3.110)$$

where  $\tilde{\delta}_i, \delta_i$  ( $i = 1, 2$ ) are the diffusion boundary layer thicknesses in the gas and the liquid. In this way (3.108) takes the form:

$$\begin{aligned} \tilde{U} \frac{\partial \tilde{C}_i}{\partial X} + \tilde{V}_i \frac{\partial \tilde{C}_i}{\partial \tilde{Y}_i} &= \tilde{F}o_i \frac{\partial^2 \tilde{C}_i}{\partial \tilde{Y}_i^2}; \\ U \frac{\partial C_i}{\partial X} &= F_o_i \frac{\partial^2 C_i}{\partial Y_i^2} - R_i; \\ X = 0, & \quad \tilde{C}_i = 1, & C_i &= 0; \\ \tilde{Y}_i = Y_i = 0, & \quad \tilde{C}_i = C_i, & \frac{\partial \tilde{C}_i}{\partial \tilde{Y}_i} &= \frac{\varepsilon_{0i}}{\chi_i} \frac{\partial C_i}{\partial Y_i}; \\ \tilde{Y}_i \rightarrow \infty, & \quad \tilde{C}_i = 1; & Y_i \rightarrow \infty, & C_i = 1, \quad i = 1, 2, \end{aligned} \quad (3.111)$$

where

$$\begin{aligned} R_1 &= K_1 c_{02} C_1 C_2, \\ R_2 &= K_2 c_{01} C_1 C_2 + K_2 c_{02} C_2^2. \end{aligned} \quad (3.112)$$

Using (3.86) it is possible to express the mass transfer rate as

$$J_i = \tilde{\beta}_i \tilde{c}_{0i} = \beta_i c_{0i}, \quad i = 1, 2. \quad (3.113)$$

The rate is determined by means of the average value of the diffusion flux. For a liquid film of a length  $L$  the results is:

$$J_i = \frac{1}{L} \int_0^L \tilde{D}_i \left( \frac{\partial \tilde{c}_i}{\partial y} \right)_{y=h} dx = \frac{1}{L} \int_0^L D_i \left( \frac{\partial c_i}{\partial y} \right)_{y=h} dx, \quad i = 1, 2 \quad (3.114)$$

or for the Sherwood number

$$\begin{aligned} \tilde{Sh}_i &= \frac{\tilde{\beta}_i L}{\tilde{D}_i} = \tilde{\varepsilon}_i^{-1} \int_0^1 \left( \frac{\partial \tilde{C}_i}{\partial \tilde{Y}_i} \right)_{\tilde{Y}=0} dX, \\ Sh_i &= \frac{\beta_i L}{D_i} = \varepsilon_i^{-1} \int_0^1 \left( \frac{\partial C_i}{\partial Y_i} \right)_{Y=0} dX, \quad i = 1, 2. \end{aligned} \quad (3.115)$$

The relationships (3.115) permit to determine the kinetics of the sulphuric acid alkylation process on the basis of the solution of (3.111).

The second reaction in (3.107) is undesirable. Because of that in the practical situations the condition  $c_{02} \ll c_{01}$  is satisfied. From experimental data [14] for the microkinetics of the reaction (3.107) and based on the experiments performed in [13,16] ( $u_0 = 0.224 m/s$ ,  $L = 2m$ ) one is obtained that

$$K_1 = 0.4 \cdot 10^7, \quad K_2 = 1.6 \cdot 10^7. \quad (3.116)$$

It is evident from (3.111) and (3.112) that the liquid hydrodynamics does not affect the mass transfer.

In the practical situations the condition  $K_1 c_{01} > K_2 c_{02}$  is satisfied. It was shown in 3.1.2 that it is possible to determine the thicknesses of the diffusion boundary layers

$$\begin{aligned} \tilde{Fo}_i &\approx 1, \quad Fo_i = K_i \frac{c_{01} c_{02}}{c_{0i}}, \\ \tilde{\delta}_i &= \sqrt{\frac{\tilde{D}_i L}{\tilde{u}_0}}, \quad \delta_i = \sqrt{\frac{D_i L c_{0i}}{u_0 K_i c_{01} c_{02}}}, \quad i = 1, 2. \end{aligned} \quad (3.117)$$

The experimental conditions reported in [13,16] ( $\tilde{u}_0 = 0.23 m/s$ ) and the data published in [14] permit to establish that

$$\frac{\varepsilon_{01}}{\chi_1} = 0.53, \quad \frac{\varepsilon_{02}}{\chi_2} = 0.36, \quad (3.118)$$

i.e. the diffusion resistances are located in both phases.

The results obtained (3.116)-(3.118) allow to solve the problem (3.111) consequently for the gas and the liquid:

$$\begin{aligned} \tilde{U} \frac{\partial \tilde{C}_i}{\partial X} + \tilde{V}_i \frac{\partial \tilde{C}_i}{\partial \tilde{Y}_i} &= \tilde{F}_o i \frac{\partial^2 \tilde{C}_i}{\partial \tilde{Y}_i^2}; \\ X = 0, \quad \tilde{C}_i &= 1; \\ \tilde{Y}_i = 0, \quad \tilde{C}_i &= \tilde{C}_i^*; \\ \tilde{Y}_i \rightarrow 0, \quad \tilde{C}_i &= 1, \quad i = 1, 2. \end{aligned} \quad (3.119)$$

$$\begin{aligned} \frac{\partial^2 C_1}{\partial Y_2^2} &= \frac{\delta_2}{\delta_1} C_1 C_2; \\ \frac{\partial^2 C_2}{\partial Y_2^2} &= C_1 C_2 + \frac{k_2 c_{20}}{k_1 c_{10}} C_2^2; \\ Y_2 = 0, \quad C_i &= \tilde{C}_i^*; \\ Y_2 \rightarrow \infty, \quad C_i &= 0, \quad i = 1, 2, \end{aligned} \quad (3.120)$$

where  $Y_i$  is replaced by  $Y_2$ . The unknown constants  $\tilde{C}_i^*$  ( $i = 1, 2$ ) must be determined in a way allowing the satisfaction by  $\tilde{C}_i$  and  $C_i$  ( $i = 1, 2$ ) of the following boundary condition:

$$\left( \frac{\partial \tilde{C}_i}{\partial \tilde{Y}_i} \right)_{\tilde{Y}_i=0} = \frac{\varepsilon_{oi}}{\chi_i} \left( \frac{\partial C_i}{\partial Y_i} \right)_{Y_i=0}, \quad i = 1, 2. \quad (3.121)$$

The problem (3.119) has been solved in [16]. In this case (3.121) takes the form:

$$\left( \frac{\partial C_i}{\partial Y_2} \right)_{Y_2=0} = -A_i (1 - \tilde{C}_i^*) \chi_i \left( \frac{I}{\varphi_{oi}} + \frac{\theta_i}{\alpha \varphi_{oi}^2} \right), \quad i = 1, 2, \quad (3.122)$$

where

$$\begin{aligned} A_i &= \sqrt{\frac{\tilde{D}_i \tilde{u}_0 \chi_i D_2}{D_i^2 u_0 K_i \tilde{c}_{oi}}}, \quad i = 1, 2, \\ \theta_i &= \frac{u_0}{\tilde{u}_0}, \quad \alpha = 0.332. \end{aligned} \quad (3.123)$$

Here  $\varphi_{oi}$  is a function of the Schmidt number of the gas phase [4].

The problem (3.120) has been solved numerically [13,16] by an iterative procedure. The values of  $\tilde{C}_i^*$  ( $i = 1, 2$ ) have been varied in order to satisfy the condition (3.122). After the

determination of  $\tilde{C}_i^*$  ( $i = 1, 2$ ) the Sherwood number has been established by means of (3.115) and (3.116):

$$Sh_i = \tilde{Sh}_{0i} (1 - \tilde{C}_i^*), \quad i = 1, 2, \quad (3.124)$$

where

$$\tilde{Sh}_{0i} = \frac{\chi_i}{D_i} \sqrt{\tilde{D}_i L \tilde{u}_0} \left( \varphi_{0i}^{-1} + \frac{\theta}{\alpha} \varphi_{0i}^{-2} \right), \quad i = 1, 2 \quad (3.125)$$

is the Sherwood number in the case of a mass transfer limited by the transport in the gas. The term  $(1 - \tilde{C}_i^*)$ , where  $i = 1, 2$  indicates that the diffusion resistance in the liquid plays an important role.

The process discussed here depends strongly on the effective utilization of the butene. This indicates that the values of  $Sh_2$  and  $\beta_2$  are enough to establish the macrokinetics. Because of the fact that butene reacts vigorously during its dissolution in the sulphuric acid the evaluation of Henry's constant is practically impossible. This may be done through a comparison of  $Sh_2$  with experimental data.

The analysis of the experimental data for the Sherwood number ( $Sh_{exp}$ ) published in [13] shows that the turbulence in the gas phase must be taken into account (a linear relationship between the coefficient of a turbulent diffusion and the gas velocity). Thus,  $\tilde{D}_2$  in (3.125) may be replaced by  $\tilde{D}'_2$ :

$$\tilde{D}'_2 = d \tilde{D}_2 u_0, \quad (3.126)$$

where  $d$  is a constant.

The above mentioned demonstrates the possibility to obtain a theoretical relationship for the Sherwood number by means of (3.125):

$$Sh_T = \frac{\chi_2 \sqrt{d} \tilde{u}_0 \sqrt{\tilde{D}_2 L}}{D_2} \left( \varphi_{02}^{-1} + \frac{\theta}{\alpha} \varphi_{02}^{-2} \right) (1 - \tilde{C}_2^*). \quad (3.127)$$

The comparison of the experimental data and  $Sh_T$  permits to establish that

$$\chi_2 \sqrt{d} = 14.5 \quad (3.128)$$

and to substitute it in (3.127).

The parity plot of both the theoretical and experimental values of Sherwood number is shown on Fig.3.2.

### 3.2.3. Non-linear mass transfer in a falling liquid film

The mathematical description of the non-linear mass transfer in a falling liquid film with an irreversible chemical reaction has been made in [17] excluding the contribution of the gas phase hydrodynamics. However, in the real situations of practical interest from a practical point of view the following condition is valid

$$\frac{h_0}{L} \ll 1. \quad (3.129)$$

Using this approximation the mathematical description of the non-linear mass transfer in a falling liquid film at high concentration gradients caused by the irreversibility of the chemical reaction may be expressed in the following form

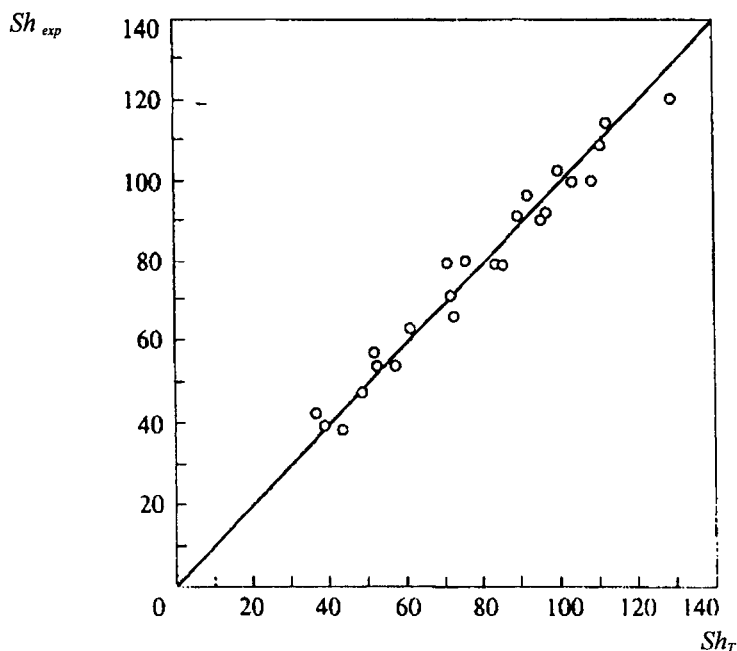


Fig. 3.2 A parity plot of the experimental ( $Sh_{exp}$ ) and the theoretical ( $Sh_T$ ) Sherwood numbers.

$$\nu \frac{\partial^2 u}{\partial y^2} + g = 0, \quad \frac{\partial u}{\partial x} + \frac{\partial v}{\partial y} = 0; \\ y = 0, \quad u = v = 0; \quad y = h(x), \quad \frac{\partial u}{\partial y} = 0. \quad (3.130)$$

$$u \frac{\partial c}{\partial x} + v \frac{\partial c}{\partial y} = D \frac{\partial^2 c}{\partial y^2} - kc; \\ x = 0, \quad c = 0; \quad y = 0, \quad \frac{\partial c}{\partial y} = 0; \quad y = h, \quad c = c^*. \quad (3.131)$$

$$(h' u - v)_{y=h} = \frac{MD}{\rho_0^*} \left( \frac{\partial c}{\partial y} \right)_{y=h}; \\ x = 0, \quad h = h_0. \quad (3.132)$$

Here  $\rho_0^*$  is the density of the liquid at the gas-liquid interphase, while  $M$  is its molecular mass.

The boundary problems (3.130)-(3.132) shows that the high concentration gradients affect both the hydrodynamics and the mass transfer due the change of the film thickness (see 3.132).

Applying the approximations of the linear mass transfer theory the right-hand side of the differential equation (3.132) becomes zero (the condition for a “non-leakage” at the film surface, i.e. the normal velocity component at the liquid film is zero).

Under conditions of intensive mass transfer [21,22] the normal velocity component at the film surface is equal to the velocity induced due to the high concentration gradients (the conditions for a “leakage” as a result of the intensive mass transfer).

In this case the mass transfer rate [17] may be determined from (3.86) and (3.87):

$$J = \beta M c^* = \frac{MD\rho_0^*}{L\rho_0^* c^*} \int_0^L \left( \frac{\partial c}{\partial y} \right)_{y=h} dx, \quad (3.133)$$

i.e.

$$\beta = \frac{D\rho_0^*}{L\rho_0^* c^*} \int_0^L \left( \frac{\partial c}{\partial y} \right)_{y=h} dx. \quad (3.134)$$

The solution of the equation (3.130) is:

$$u = \frac{g}{2\nu} (2hy - y^2), \quad v = -\frac{g}{2\nu} h' y, \quad (3.135)$$

where  $h(x)$  is an arbitrary function and may be determined by (3.131) and (3.132).

The intensive mass transfer occurs at high reaction rates, i.e. the boundary layer thickness may be determined from (3.16). Setting these conditions the equation (3.131) may be solved by means of the following dimensionless variables:

$$\begin{aligned} x = LX, \quad y = h - \delta Y, \quad c = c^* C, \quad h = h_0 H, \\ \theta = \frac{\delta}{h_0} = \frac{1}{h_0} \sqrt{\frac{D}{k}}, \quad \theta_0 = \frac{u_0 h_0}{L \sqrt{k D}}, \quad u_0 = \frac{g h_0^2}{2 \nu}. \end{aligned} \quad (3.136)$$

Thus, (3.131) assumes the following form:

$$\begin{aligned} \theta \theta_0 (H^2 - \theta^2 Y^2) \frac{\partial C}{\partial X} + \theta_0 (2H^2 H' - 2\theta H H' Y) \frac{\partial C}{\partial Y} = \frac{\partial^2 C}{\partial Y^2} - C; \\ X = 0, C = 0; \quad Y = 0, C = 1; \quad Y \rightarrow \infty, C = 0, \end{aligned} \quad (3.137)$$

where  $H$  may be determined from

$$\begin{aligned} -\varepsilon_0 \left( \frac{\partial C}{\partial Y} \right)_{Y=0} = 2H^2 H'; \\ X = 0, \quad H = 1, \end{aligned} \quad (3.138)$$

and  $\varepsilon_0$  from

$$\varepsilon_0 = \frac{\rho^* - \rho_0^*}{\rho_0^*} \frac{L \sqrt{k D}}{u_0 h_0}, \quad \rho^* = \rho_0^* + M c^*. \quad (3.139)$$

The intensive mass transfer affects the hydrodynamics when  $\varepsilon_0 > 10^{-2}$ .

In the case of a chemical reaction when  $\theta < 10^{-2}$  the problem (3.137) may be solved by means of a first-order approximation with respect to the small parameter  $\theta$ :

$$\begin{aligned} 2\theta_0 H^2 H' \frac{\partial C}{\partial Y} = \frac{\partial^2 C}{\partial Y^2} - C; \\ Y = 0, \quad C = 1; \quad Y \rightarrow \infty, \quad C = 0. \end{aligned} \quad (3.140)$$

The solution of (3.140) may be expressed as

$$C = \exp \left\{ - \left[ \sqrt{\frac{u_0^2 H^4 H'^2 h_0^2}{D^2 L^2} + \frac{k}{D}} - \frac{u_0 H^2 H' h_0}{DL} \right] (h_0 H - h_0 Y) \right\}, \quad (3.141)$$

This allows to determine  $H$  from (3.138):

$$H = \sqrt[3]{1 + \frac{3}{2} \varepsilon_0 X \sqrt{\frac{\rho^*}{\rho_0^*}}} . \quad (3.142)$$

By means of the relationships (3.141) and (3.142) the mass transfer coefficient may be expressed as

$$\beta = \sqrt{kD \frac{\rho^*}{\rho_0^*}} . \quad (3.143)$$

It is evident from (3.106) and (3.143) that the non-linear effect depends on the following term

$$\sqrt{\frac{\rho^*}{\rho_0^*}} . \quad (3.144)$$

In the case of a very fast chemical reaction ( $\theta < 10^{-2}$ ), it follows from (3.137) that

$$\begin{aligned} \frac{\partial^2 C}{\partial Y^2} - C = 0 ; \\ Y = 0, C = 1 ; Y \rightarrow \infty, C = 0 , \end{aligned} \quad (3.145)$$

i.e.

$$C = \exp \left[ h_0 (Y - H) \sqrt{\frac{k}{D}} \right] , \quad (3.146)$$

Thus,  $H$  may be obtained from (3.138) as

$$H = \sqrt[3]{1 + \frac{3}{2} \frac{h_0}{L} X} , \quad (3.147)$$

while the mass transfer coefficient may be expressed as

$$\beta = \frac{\rho^*}{\rho_0^*} \sqrt{kD} . \quad (3.148)$$

It is clear from (3.148) and (3.106) that the non-linear effect contributes with the ratio

$$\frac{\rho^*}{\rho_0^*} . \quad (3.149)$$

In gas-liquid systems the ratio (3.149) is practically equal to unity except in the systems under high pressures.

The theoretical results obtained for the mass transfer kinetics under high concentration gradients caused by the chemical reactions indicate that under normal pressure the non-linear effects may be neglected as shown in Part 1 of this book. Moreover, in the absence of a chemical reaction the velocities of the induced flows are insignificant and have no effect on the mass transfer kinetics. The increase of the chemical reaction rate leads to the increase of the concentration gradients and the velocities of the secondary induced flows, but upon these conditions the hydrodynamics has no effect on the mass transfer rate (see 3.17).

### CHAPTER 3.3. EFFECTS OF THE PHYSICAL PARAMETERS

The results obtained show that the chemical reactions in the liquid phase increase the overall mass transfer rate. The increase depends on the chemical reaction rate. At very slow reactions the mass transfer in the liquid limits the interphase mass transfer rate. However, if the reaction is very fast the mass transfer in the gas limits the whole process.

The mechanism of that intensification of the interphase mass transfer is related with the decrease of the concentration and temperature boundary layer thicknesses, i.e. with increased concentration and temperature gradients in the liquid. Under these conditions the concentration and the temperature effect on the physical parameters and thus on the mass transfer kinetics and must be taken into consideration.

#### 3.3.1. Concentration effects

The effect of the high concentration gradients on the physical parameters of the hydrodynamics, the heat and the mass transfer will be discussed on the bases of falling liquid film, taken as an example. For this purpose the mathematical description (3.130)- (3.132) of the process will be used in the following form:

$$\begin{aligned} \frac{\partial}{\partial y} \left( \mu \frac{\partial u}{\partial y} \right) + \rho g &= 0, \\ \frac{\partial}{\partial x} (\rho u) + \frac{\partial}{\partial y} (\rho v) &= 0; \\ y = 0, \quad u = v &= 0; \\ y = h, \quad \frac{\partial u}{\partial y} &= 0. \end{aligned} \tag{3.150}$$

$$\begin{aligned} u \frac{\partial c}{\partial x} + v \frac{\partial c}{\partial y} &= \frac{\partial}{\partial y} \left( D \frac{\partial c}{\partial y} \right) - kc + c \left( \frac{\partial u}{\partial x} + \frac{\partial v}{\partial y} \right); \\ x = 0, \quad c &= 0; \\ y = h, \quad c &= c^*; \\ y = 0, \quad \frac{\partial c}{\partial y} &= 0. \end{aligned} \tag{3.151}$$

$$(h'u - v)_{y=h} = \frac{MD}{\rho_0^*} \left( \frac{\partial c}{\partial y} \right)_{y=h}; \\ x=0, \quad h=h_0. \quad (3.152)$$

The solution of (3.150)-(3.152) needs the following dimensionless variables

$$\begin{aligned} X &= \frac{x}{L}, & Y &= \frac{y}{h_0}, & U &= \frac{u}{u_0}, & V &= \frac{v}{\epsilon u_0}, \\ C &= \frac{c}{c^*}, & H &= \frac{h}{h_0}, & \epsilon &= \frac{h_0}{L}, & u_0 &= \frac{gh_0^2 \rho_0}{2\mu_0}, \\ Fo &= \frac{D_0 L}{u_0 h_0^2}, & Da &= \frac{kL}{u_0}, & A &= \frac{Mc^*}{\rho_0^*} Fo. \end{aligned} \quad (3.153)$$

Hereafter the relationships between the parameters and the concentration will be assumed linear:

$$\begin{aligned} \rho &= \rho_0(I + \bar{\rho}C), \\ \mu &= \mu_0(I + \bar{\mu}C), \\ D &= D_0(I + \bar{D}C). \end{aligned} \quad (3.154)$$

In this way (3.150)-(3.152) take the form [18]:

$$\begin{aligned} 2(I + \bar{\rho}C) + \frac{\partial}{\partial Y} \left[ (I + \bar{\mu}C) \frac{\partial U}{\partial Y} \right] &= 0; \\ \frac{\partial}{\partial X} [(I + \bar{\rho}C)U] + \frac{\partial}{\partial Y} [(I + \bar{\rho}C)V] &= 0; \\ Y = 0, \quad U = V = 0; \\ Y = H, \quad \frac{\partial U}{\partial Y} &= 0. \end{aligned} \quad (3.155)$$

$$\begin{aligned} U \frac{\partial C}{\partial X} + V \frac{\partial C}{\partial Y} &= Fo \frac{\partial}{\partial Y} \left[ (I + \bar{D}C) \frac{\partial C}{\partial Y} \right] - DaC + C \left( \frac{\partial U}{\partial X} + \frac{\partial V}{\partial Y} \right); \\ X = 0, \quad C = 0, \quad Y = 0, \quad \frac{\partial C}{\partial Y} &= 0, \quad Y = H, \quad C = 1. \end{aligned} \quad (3.156)$$

$$(H'U - V)_{Y=H} = A(I + \bar{D}C) \left( \frac{\partial C}{\partial Y} \right)_{Y=H}; \quad X = 0, \quad H = 1, \quad (3.157)$$

where  $\bar{\rho}$ ,  $\bar{\mu}$  and  $\bar{D}$  could in many cases be considered as small parameters. This permits to find the solutions of (3.155)-(3.157) in the form:

$$\begin{aligned}
U &= U_0 + \bar{\rho}U_1 + \bar{\mu}U_2 + \bar{D}U_3 + \dots, \\
V &= V_0 + \bar{\rho}V_1 + \bar{\mu}V_2 + \bar{D}V_3 + \dots, \\
C &= C_0 + \bar{\rho}C_1 + \bar{\mu}C_2 + \bar{D}C_3 + \dots, \\
H &= H_0 + \bar{\rho}H_1 + \bar{\mu}H_2 + \bar{D}H_3 + \dots .
\end{aligned} \tag{3.158}$$

The zero-order approximation has been obtained in [18]:

$$\begin{aligned}
U_0 &= 2H_0Y - Y^2, & V_0 &= -H'_0Y^2, \\
C_0 &= \exp a_0\eta, & H_0 &= \left(1 - \frac{3\varepsilon_0 a_0 X}{2}\right)^{1/3},
\end{aligned} \tag{3.159}$$

where

$$\begin{aligned}
\varepsilon_0 &= \frac{Mc^* \sqrt{kD_0}}{\rho_0^* u_0 \varepsilon}, & a_0 &= a - \sqrt{a^2 + 1} = \sqrt{\rho_0^*/\rho^*}, \\
a &= \theta_0 H_0^2 H'_0 = \frac{\rho^* - \rho_0^*}{2\sqrt{\rho_0^* \rho^*}}, & \theta_0 &= \frac{\varepsilon u_0}{\sqrt{kD_0}}, \\
\eta &= \frac{H_0 - Y}{\theta}, & \theta &= \frac{\delta}{h_0}, & \delta &= \sqrt{\frac{D_0}{k}}.
\end{aligned} \tag{3.160}$$

Taking into account that  $\theta < 10^{-2}$ , it was demonstrated in [18] that the zero-order approximation with respect to the small parameters  $\theta$  allows to obtain

$$\begin{aligned}
U_1 &\equiv 0, & V_1 &\equiv 0, & C_1 &\equiv 0, & H_1 &\equiv 0, \\
U_2 &\equiv 0, & V_2 &\equiv 0, & C_2 &\equiv 0, & H_2 &\equiv 0, \\
U_3 &\equiv 0, & V_3 &\equiv 0, \\
C_3 &= \frac{2a_0^2}{4aa_0 + 3} (\exp a_0\eta - \exp 2a_0\eta), \\
H_3 &= \frac{2\rho^*}{\rho^* + 2\rho_0^*} (H_0 - 1).
\end{aligned} \tag{3.161}$$

The mass transfer rate and the respective mass transfer coefficient are available from (3.133) and (3.134) taking into account the concentration effect on  $D$ :

$$\beta = -\sqrt{kD_0} \frac{\rho^*}{\rho_0^*} \left[ \int_0^1 (1 + \bar{D}C) \frac{\partial C}{\partial \eta} dX \right]_{\eta=0} \tag{3.162}$$

The introduction of (3.158)-(3.161) in (3.162) gives

$$\beta = \sqrt{kD_0} \sqrt{\frac{\rho^*}{\rho_o^*} \left( I + \bar{D} \frac{\rho^*}{\rho^* + 2\rho_o^*} \right)}. \quad (3.163)$$

The comparison of (3.143) and (3.163) indicates that the concentration effect on the diffusion coefficient may be expressed as

$$\bar{D} \frac{\rho^*}{\rho^* + 2\rho_o^*}. \quad (3.164)$$

In the cases of very fast chemical reactions ( $\theta < 10^{-2}$ ) the relationships (3.159) and (3.161) take the forms:

$$\begin{aligned} C_o &= \exp(-\eta), & H_o &= \left( I + \frac{3\varepsilon_o X}{2} \right)^{1/3}, \\ C_3 &= \frac{2}{3} [\exp(-\eta) - \exp(-2\eta)], & H_3 &= \frac{2}{3} (H_o - I), \end{aligned} \quad (3.165)$$

i.e.

$$\beta = \sqrt{kD} \frac{\rho^*}{\rho_o^*} \left( I + \frac{\bar{D}}{3} \right). \quad (3.166)$$

The comparative analysis of (3.148) and (3.166) shows that the concentration effect must be taken into account by including the following addition term:

$$\bar{D}/3. \quad (3.167)$$

### 3.3.2. Temperature effects

The chemical reactions in a gas-liquid system are often accompanied by significant thermal effects which lead to high temperature gradients in the liquid phase. However, all the physical parameters depend on the temperature. This poses the problem of assessing the contribution of the temperature effect in the mathematical description of the process.

In gas-liquid systems the temperature changes induce the surface tension gradients. This thermocapillary effect is important when the liquid flows downward as a thin liquid film. The considered process becomes more complicated if the liquid contains surfactants. It becomes a problem of the capillary hydrodynamics [23-27]. From a practical point of view it is interesting to make a theoretical analysis of the effect of the chemical reaction on the surface tension gradient taking into account all other temperature effects on the physical parameters of the liquid.

Let an example of the thermocapillary effects in a falling liquid film [19, 20] be considered accompanied with a chemical reaction of a first order and significant temperature effects. The mathematical description of the process (taking into account the approximations (3.129)) is :

$$\begin{aligned}
& \frac{\partial}{\partial y} \left[ \mu(t) \frac{\partial u}{\partial y} \right] + \rho g = 0 ; \\
& \frac{\partial u}{\partial x} + \frac{\partial v}{\partial y} = 0 ; \\
& h' = \left( \frac{v}{u} \right)_{y=h} ; \\
& u \frac{\partial c}{\partial x} + v \frac{\partial c}{\partial y} = \frac{\partial}{\partial y} \left[ D(t) \frac{\partial c}{\partial y} \right] - k(t)c ; \\
& \rho c_p \left( u \frac{\partial t}{\partial x} + v \frac{\partial t}{\partial y} \right) = \frac{\partial}{\partial y} \left[ \lambda(t) \frac{\partial t}{\partial y} \right] \pm qk(t)c ; \\
& x = 0, \quad h = h_0, \quad c = 0, \quad t = t_0 ; \\
& y = 0, \quad u = 0, \quad v = 0, \quad c = 0, \quad t = t_0 ; \\
& y = h, \quad \mu(t) \frac{\partial u}{\partial y} = \frac{\partial \sigma(t)}{\partial x} + h' \frac{\partial \sigma(t)}{\partial y}, \\
& c = c^*, \quad \lambda(t) \frac{\partial t}{\partial y} = \pm \alpha q D(t) \frac{\partial c}{\partial y}, \tag{3.168}
\end{aligned}$$

where  $q$  is the thermal effect of the chemical reaction. If  $\alpha = 1$  the chemical reaction occurs at the gas-liquid interface, while when  $\alpha = 0$  the reaction takes place in the bulk of the liquid. The equations (3.168) take into consideration the fact that for many liquids the temperature effect on the density ( $\rho$ ) and the heat capacity ( $c_p$ ) is negligible.

$$\begin{aligned}
I_c &= \beta_c c^* = \frac{1}{L} \int_0^L D(t) \left( \frac{\partial c}{\partial y} \right)_{y=h} dx, \\
I_t &= \beta_t t_0 = \frac{1}{L} \int_0^L \lambda(t) \left( \frac{\partial t}{\partial y} \right)_{y=h} dx, \tag{3.169}
\end{aligned}$$

where  $\beta_c$  and  $\beta_t$  are the mass and heat transfer coefficients.

The temperature effects on the physical parameter of the liquid may be expressed by the following linear approximations:

$$\begin{aligned}
\mu(t) &= \mu_0 (1 - \bar{\mu} T), \\
\sigma(t) &= \sigma_0 (1 - \bar{\sigma} T), \\
D(t) &= D_0 (1 + \bar{D} T), \\
\lambda(t) &= \lambda_0 (1 + \bar{\lambda} T), \\
T &= t/t_0, \tag{3.170}
\end{aligned}$$

where  $\bar{\mu}$ ,  $\bar{\sigma}$ ,  $\bar{D}$  and  $\bar{\lambda}$  are small parameters.

The temperature effect on the chemical reaction constant is

$$k(t) = k_0 \exp\left[-\frac{E}{R[273 + t_0 T]}\right]. \quad (3.171)$$

In most of the practical situations the relationship may be linearized:

$$\begin{aligned} k(t) &\approx k_0 (1 + \bar{t}T) \exp(-A), \\ A &= \frac{E}{273R}, \quad \bar{t} = \frac{At_0}{273}, \end{aligned} \quad (3.172)$$

where  $\bar{t}$  is a small parameter.

The theoretical analysis of the thermocapillary effects in a falling liquid film will be carried out by means of the following dimensionless parameters:

$$\begin{aligned} x &= LX, & y &= h_0 Y = h - \delta_c \eta = h - \delta_t \xi, \\ u(x, y) &= u_0 U(X, Y), & h(x) &= h_0 H(X), \\ v(x, y) &= \varepsilon_0 u_0 V(X, Y) = -\varepsilon_c u_0 V_c(X, \eta) = -\varepsilon_t u_0 V_t(X, \xi), \\ h_0 &= \left( \frac{3\mu_0^2 Re}{g\rho^2} \right)^{1/3}, & \varepsilon &= \frac{h_0}{L}, & \varepsilon_c &= \frac{\delta_c}{L}, & \varepsilon_t &= \frac{\delta_t}{L}, \\ Re &= \frac{Q\rho}{\mu_0}, & u_0 &= \frac{gh_0^2 \rho}{3\mu_0}, & Da &= \frac{k^* L}{u_0}, \\ k^* &= k_0 \exp(-A), & Fo_D &= \frac{D_0 L}{u_0 \delta_c^2}, & Fo_a &= \frac{aL}{u_0 \delta_t^2}, \\ a &= \frac{\lambda_0}{\rho c_p}, & \theta &= \frac{\varepsilon_0 Re \bar{\sigma}}{We}, & We &= \frac{\rho u_0^2 h_0}{\delta_0}, & \bar{q} &= \frac{qc^*}{t_0 \rho c_p}, \end{aligned} \quad (3.173)$$

where  $\delta_c$  and  $\delta_t$  are the orders of the concentration and the temperature boundary layer thickness respectively,  $Q$  is the liquid flow per unit width of the film,  $a$ - the thermal diffusivity.

The new variables (3.173) allow to reduce (3.168) into four coupled boundary problems:

$$\frac{\partial}{\partial Y} \left\{ \left[ 1 - \bar{\mu} T \left( X, \frac{H - Y}{\delta_t/h_0} \right) \right] \frac{\partial U}{\partial Y} \right\} = -3;$$

$$\frac{\partial U}{\partial X} + \frac{\partial V}{\partial Y} = 0;$$

$$Y = 0, \quad U = V = 0;$$

$$Y = H, \quad (I - \bar{\mu}T)_{\xi=0} \left( \frac{\partial U}{\partial Y} \right)_{Y=H} = -\theta \left( \frac{\partial T}{\partial X} + \frac{h_0}{\delta_t} H' \frac{\partial T}{\partial \xi} \right)_{\xi=0}. \quad (3.174)$$

$$H' = \left( \frac{V}{U} \right)_{Y=H}; \\ X = I, \quad H = I. \quad (3.175)$$

$$U \left( X, H - \frac{\delta_c}{\delta_t} \eta \right) \frac{\partial C}{\partial X} + V_c(X, \eta) \frac{\partial C}{\partial \eta} = Fo_D \frac{\partial}{\partial \eta} \left\{ \left[ I + \bar{D}T \left( X, \frac{\delta_c}{\delta_t} \eta \right) \right] \frac{\partial C}{\partial \eta} \right\} - \\ - Da \left[ I + \bar{t}T \left( X, \frac{\delta_c}{\delta_t} \right) \right] C; \\ X = 0, \quad C = 0; \\ \eta = 0, \quad C = 1; \\ \eta \rightarrow \infty, \quad C = 0. \quad (3.176)$$

$$U \left( X, H - \frac{\delta_t}{h_0} \xi \right) \frac{\partial T}{\partial X} + V_t(x, \xi) \frac{\partial T}{\partial \xi} = Fo_a \frac{\partial}{\partial \xi} \left[ \left( I + \bar{\lambda}T \right) \frac{\partial T}{\partial \xi} \right] \pm \\ \pm \bar{q}Da(I + \bar{t}T)C \left( X, \frac{\delta_t}{\delta_c} \xi \right); \\ X = 0, \quad T = I; \\ \xi = 0, \quad \left( I + \bar{\lambda}T \right) \left( \frac{\partial T}{\partial \xi} \right)_{\xi=0} = \pm \alpha \bar{q} \frac{D_0 \delta_t}{a \delta_c} \left( I + \bar{D}T \right) \left( \frac{\partial C}{\partial \eta} \right)_{\eta=0}; \\ \xi \rightarrow \infty, \quad T = I. \quad (3.177)$$

The new variables lead to the following relationships for the Sherwood and the Nusselt numbers:

$$Sh = \frac{\beta_c L}{D_0} = - \frac{L}{\delta_c} \int_0^I \left( I + \bar{D}T \right)_{\xi=0} \left( \frac{\partial C}{\partial \eta} \right)_{\eta=0} dX, \\ Nu = \frac{\beta_t L}{\lambda_0} = - \frac{L}{\delta_t} \int_0^I \left[ \left( I + \bar{\lambda}T \right) \frac{\partial T}{\partial \xi} \right]_{\xi=h/\delta_t} dX. \quad (3.178)$$

In the equations (3.174)-(3.177) one has to introduce  $\delta_c$  and  $\delta_t$ , which are dependent on the values of  $Da$  and  $\bar{q}Da$ . By the help of a theoretical analysis (similar to that carried out in 3.1) one is obtained:

$$Da < 1, \quad Fo_D \sim 1, \quad \delta_c = \sqrt{D_0 L / u_0};$$

$$\begin{aligned} Da > 1, \quad & Fo_D \sim Da, \quad \delta_c = \sqrt{D_0/k^*}; \\ \bar{q}Da < 1, \quad & Fo_a \sim 1, \quad \delta_c = \sqrt{aL/u_0}; \\ \bar{q}Da > 1, \quad & Fo_a \sim \bar{q}Da \quad \delta_t = \sqrt{a/\bar{q}k^*}. \end{aligned} \quad (3.179)$$

It was demonstrated that when very fast chemical reactions occur

$$Da > 10^2 \quad (3.180)$$

and the hydrodynamics does not affect the mass transfer. This has been confirmed experimentally. In a similar way it could be assumed that at

$$\bar{q}Da > 10^2 \quad (3.181)$$

the hydrodynamics does not affect the mass transfer, too. Unfortunately, there are no experimental data confirming that. However, this fact has a theoretical explanation.

From (3.179) it follows and (3.178) that

$$\delta_c = \sqrt{\frac{D_0}{k^*}}, \quad \frac{\delta_c}{h_0} < 10^{-2}, \quad (3.182)$$

i.e. the chemical reaction occurs at the film surface and in (3.177) there is no volumetric heat source, so in the boundary condition one must assume  $\alpha = 1$ .

The absence of a volumetric heat source in (3.176) allows to express the thickness of the temperature boundary layer as

$$\delta_t = \sqrt{\frac{aL}{u_0}} \sim h_0, \quad (3.183)$$

i.e. the equation shows that the temperature boundary layer does not practically exist. From (3.181) it follows and (3.182) that

$$\frac{\delta_t}{\delta_c} > 10^2, \quad C\left(X, \frac{\delta_t}{\delta_c} \xi\right) \approx C(X, \infty) = 0. \quad (3.184)$$

This result confirms the absence of a volumetric heat source in (3.177). Thus, the heat transfer is affected by the hydrodynamics. Here the possibility for occurrence of a natural convection is not taken into account despite that fact that the high temperature gradients lead to density differences.

The theoretical analysis of the possibility to create a powerful heat source due to a chemical reaction leading to elimination of the convective transport mechanism (like in the mass transfer situations at  $Da > 10^2$ ) shows that it is possible in the case of medium reaction rates:

$$10 < Da < 10^2. \quad (3.185)$$

However, in the practical situations

$$\bar{q} < 10, \quad (3.186)$$

i.e.

$$\bar{q}Da < 10^2. \quad (3.187)$$

This inequality shows that the hydrodynamics always effects the heat transfer.

The quantitative description of the mass transfer kinetics with the contribution of the thermocapillary effects has been done in [20] for the cases of very fast chemical reactions. This permits to use the following approximations:

$$\begin{aligned} Da^{-1} &= 0, \quad \delta_c = \sqrt{\frac{D_0}{k^*}}, \quad \delta_t = h_0, \\ \frac{\delta_c}{\delta_t} &= \frac{\delta_c}{h_0} = 0, \quad \alpha = 1. \end{aligned} \quad (3.188)$$

Applying these approximations the equations (3.174)-(3.177) take the form:

$$\begin{aligned} \frac{\partial}{\partial Y} \left\{ [I - \bar{\mu}T(X, H - Y)] \frac{\partial U}{\partial Y} \right\} &= -3; \\ \frac{\partial U}{\partial X} + \frac{\partial V}{\partial Y} &= 0; \\ Y = 0, \quad U = V &= 0; \\ Y = H, \quad (I - \bar{\mu}T)_{\xi=0} \left( \frac{\partial U}{\partial Y} \right)_{Y=H} &= -\theta \left( \frac{\partial T}{\partial X} - H' \frac{\partial T}{\partial \xi} \right)_{\xi=0}. \end{aligned} \quad (3.189)$$

$$\begin{aligned} H' &= \left( \frac{V}{U} \right)_{Y=H}; \\ X = 0, \quad H &= 1. \end{aligned} \quad (3.190)$$

$$\begin{aligned} 0 &= \frac{\partial}{\partial \eta} \left\{ [I + \bar{D}T(X, 0)] \frac{\partial C}{\partial \eta} \right\} - [I + \bar{T}T(X, 0)]C; \\ \eta = 0, \quad C &= 1; \\ \eta \rightarrow \infty, \quad C &= 0. \end{aligned} \quad (3.191)$$

$$U(X, H - \xi) \frac{\partial T}{\partial X} - V(X, H - \xi) \frac{\partial T}{\partial \xi} = Fo_a \frac{\partial}{\partial \xi} \left[ (I - \bar{\lambda}T) \frac{\partial T}{\partial \xi} \right] \pm$$

$$\pm \bar{q} D a (I + \bar{t} T) C(X, \infty); \\ X = 0, \quad T = I;$$

$$\xi = 0, \quad (I + \bar{\lambda} T) \frac{\partial T}{\partial \xi} = b(I + \bar{D} T) \left( \frac{\partial C}{\partial \eta} \right)_{\eta=0}; \\ \xi = H, \quad T = I, \quad (3.192)$$

where

$$b = \pm \frac{qc^* h_0}{t_0 \lambda_0} \sqrt{D_0 k^*} = \pm \bar{q} \frac{h_0}{a} \sqrt{D_0 k^*}, \\ C(X, \infty) = 0. \quad (3.193)$$

The change of the last boundary conditions in (3.192) is a result of the absence of a thermal boundary layer at the film surface (this follows from (3.183)).

The solutions of the boundary problems (3.189)-(3.192) depend on five small parameters ( $\bar{\mu}, \bar{D}, \bar{\lambda}, \theta, \bar{t}$ ). Because of that they may be obtained by the perturbation method in the following form

$$F = F_0 + \bar{\mu} F_1 + \bar{D} F_2 + \bar{\lambda} F_3 + \theta F_4 + \bar{t} F_5 + \dots, \quad (3.194)$$

where  $F$  is a vector-function

$$F = (U, V, H, C, T). \quad (3.195)$$

The substitution of (3.194) and (3.195) in (3.189)-(3.192) yields a number of boundary problems for the functions  $U_j, V_j, H_j, C_j, T_j$  ( $j = 0, 1, \dots, 5$ ).

The zero-order approximations follow from (3.189)-(3.192) if one is substituted  $\bar{\mu} = \bar{D} = \bar{\lambda} = \theta = \bar{t} = 0$ .

The velocity profile problem is:

$$\frac{\partial^2 U_0}{\partial Y^2} = -3, \quad \frac{\partial U_0}{\partial X} + \frac{\partial V_0}{\partial Y} = 0; \\ Y = 0, \quad U_0 = V_0 = 0; \quad \left( \frac{\partial U_0}{\partial Y} \right)_{Y=H_0} = 0, \quad (3.196)$$

It may be solved in the following way:

$$U_0 = 3H_0 Y - \frac{3}{2} Y^2, \quad V_0 \equiv 0, \quad (3.197)$$

where  $H_\theta$  is determined by

$$H'_\theta = \left( \frac{V_\theta}{U_\theta} \right)_{Y=H_\theta}; \\ X = 0, \quad H_\theta = I, \quad (3.198)$$

i.e.

$$H_\theta \equiv I. \quad (3.199)$$

The problem for the concentration distributions is

$$\frac{\partial^2 C_\theta}{\partial \eta^2} - C_\theta = 0; \\ \eta = 0, \quad C_\theta = I; \quad \eta \rightarrow \infty, \quad C_\theta = 0. \quad (3.200)$$

The solution of (3.200) is:

$$C_\theta = \exp(-\eta). \quad (3.201)$$

The zero-order approximation of the temperature distribution problem is:

$$\frac{3}{2}(1-\xi^2)\frac{\partial T_\theta}{\partial X} = Fo_a \frac{\partial^2 T_\theta}{\partial \xi^2}; \\ X = 0, \quad T_\theta = I; \\ \xi = 0, \quad \frac{\partial T_\theta}{\partial \xi} = -b; \\ \xi = 1, \quad \frac{\partial T_\theta}{\partial \xi} = I. \quad (3.202)$$

The solution may be found [20] in a form of series of orthogonal eigenfunctions [28,29]:

$$T_\theta(X, \xi) = I - (I+b) \left[ \xi - I - \sum_{i=1}^{\infty} \tilde{\Psi}_i(\psi_i, \xi) - \frac{\exp\left(-\psi_i^2 \frac{2Fo_a X}{3}\right)}{\psi_i^2} \right] \tilde{\Psi}_i(\psi_i, 0), \quad (3.203)$$

where

$$\tilde{\Psi}_i(\psi_i, \xi) = \frac{\Psi_i(\psi_i, \xi)}{\sqrt{N_i}}, \quad i = 1, \dots, \infty. \quad (3.204)$$

$\Psi_i$ ,  $\psi_i$ , and  $N_i$  ( $i = 1, \dots, \infty$ ) are eigenfunctions, eigenvalues and  $L_2$ -norms of the problem:

$$\begin{aligned} \Psi_i'' + \psi_i^2(1 - \xi^2)\Psi_i &= 0; \\ \xi = 0, \quad \Psi_i' &= 0; \\ \xi = 1, \quad \Psi_i' &= 0; \quad i = 1, \dots, \infty. \end{aligned} \quad (3.205)$$

The problem (3.205) has a solution by the method given in [29,30]. The values of  $\psi_i$ ,  $\Psi_i(0)$ ,  $\Psi_i(1)$  and  $\sqrt{N_i}$  for  $i=1, \dots, 10$  are listed in Table 3.3.

The temperature effects on the hydrodynamics take place only thorough the temperature effects on the viscosity and the surface tension. The first-order approximations lead to boundary problems for other temperature effects:

$$\begin{aligned} \frac{\partial^2 U_j}{\partial Y^2} &= 0, \quad \frac{\partial U_j}{\partial X} + \frac{\partial V_j}{\partial Y} = 0; \\ Y = 0, \quad U_j = V_j &= 0; \quad Y = 1, \quad \frac{\partial U_j}{\partial Y} = 0, \quad j = 2, 3, 5, \end{aligned} \quad (3.206)$$

with trivial solutions:

$$U_j \equiv 0, \quad V_j \equiv 0, \quad j = 2, 3, 5. \quad (3.207)$$

Table 3.3.  
Eigenfunctions and eigenvalues of the problem (3.205)

$i$	$\psi_i$	$\sqrt{N_i}$	$\Psi_i(0)$	$\Psi_i'(1)$
1	1.68159	0.64875	1.5414	-2.2029
2	5.66879	0.62921	1.5893	6.0505
3	9.66821	0.62754	1.5935	-9.4340
4	13.66765	0.62710	1.5946	12.5854
5	17.66737	0.62692	1.5961	-15.5856
6	21.66720	0.62683	1.5953	18.4732
7	25.66704	0.62678	1.5955	-21.2736
8	29.66704	0.62675	1.5955	24.0015
9	33.66692	0.62672	1.5956	-26.6690
10	37.66691	0.62672	1.5956	29.2833

The effect of the viscosity on the hydrodynamics may be expressed as:

$$\frac{\partial^2 U_I}{\partial Y^2} = -3(I-Y) \left( \frac{\partial T_0}{\partial \xi} \right)_{\xi=I-Y} - 3(T_0)_{\xi=I-Y};$$

$$Y = 0, \quad U_I = V_I = 0; \quad Y = I, \quad \frac{\partial U_I}{\partial Y} = 0. \quad (3.208)$$

The solution is:

$$U_I = 3Y + \frac{3}{2}bY^2 - (I+b)Y^3 +$$

$$+ 3(I+b) \sum_{i=1}^{\infty} I_i(\psi_i, Y) \frac{\exp\left(-\psi_i^2 \frac{2Fo_a X}{3}\right)}{\psi_i^2} \tilde{\Psi}_i(\psi_i, 0), \quad (3.209)$$

where

$$I_i(\psi_i, Y) = - \int_{I-Y}^I \xi \tilde{\Psi}_i(\psi_i, \xi) d\xi, \quad i = 1, \dots, \infty. \quad (3.210)$$

The result obtained (3.209) permits to determine  $V_I$ :

$$V_I = - \int_0^Y \frac{\partial U_I}{\partial X} dY. \quad (3.211)$$

The determination of  $U_4$  and  $V_4$  follows from the solution of the following boundary problem:

$$\frac{\partial^2 U_4}{\partial Y^2} = 0, \quad \frac{\partial U_4}{\partial X} + \frac{\partial V_4}{\partial Y} = 0;$$

$$Y = 0, \quad U_4 = V_4 = 0; \quad Y = I, \quad \left( \frac{\partial U_4}{\partial Y} \right)_{Y=I} = - \left( \frac{\partial T_0}{\partial X} \right)_{\xi=0}. \quad (3.212)$$

The solution of (3.212) allows the determination of the influence of the thermocapillary effects on the hydrodynamics:

$$U_4 = (I+b) \frac{2Fo_a}{3} Y \sum_{i=1}^{\infty} \tilde{\Psi}_i^2(\psi_i, 0) \exp\left(-\psi_i^2 \frac{2Fo_a X}{3}\right),$$

$$V_4 = - \int_0^Y \frac{\partial U_4}{\partial X} dY. \quad (3.213)$$

The temperature effect on the film thickness may be evaluated by means of the velocity distribution:

$$\begin{aligned} H'_j U_{\theta}(X, H_{\theta}) &= V_j(X, H_{\theta}); \\ X = 0, \quad H_j = 0 \quad j &= 1, \dots, 5. \end{aligned} \quad (3.214)$$

The result is

$$H_j = \frac{2}{3} \int_0^1 [U_j(0, Y) - U_j(X, Y)] dY, \quad (3.215)$$

where

$$H_2 = H_3 = H_5 \equiv 0. \quad (3.216)$$

The temperature effect on the mass transfer exists only through the temperature effects on the diffusivity and the chemical reaction rate constant. Because of that in the first-order approximation the new boundary problems for other temperature effects are:

$$\begin{aligned} \frac{\partial^2 C_j}{\partial \eta^2} - C_j &= 0; \\ \eta = 0, \quad C_j &= 0; \quad \eta \rightarrow \infty, \quad C_j = 0; \quad j = 1, 3, 4 \end{aligned} \quad (3.217)$$

with a trivial solution:

$$C_j \equiv 0, \quad j = 1, 3, 4. \quad (3.218)$$

The solution of the problem

$$\begin{aligned} \frac{\partial^2 C_j}{\partial \eta^2} - C_j &= -T_{\theta}(X, 0) \exp(-\eta); \\ \eta = 0, \quad C_j &= 0; \quad \eta \rightarrow \infty, \quad C_j = 0; \quad j = 2, 5 \end{aligned} \quad (3.219)$$

gives the temperature effect on the mass transfer.

$$C_j = \frac{1}{2} T_{\theta}(X, 0) \eta \exp(-\eta), \quad j = 2, 5. \quad (3.220)$$

The results allow the calculation of the Sherwood number by (3.177):

$$Sh = L \sqrt{\frac{k^*}{D_0}} \left\{ 1 + \frac{1}{2} (\bar{D} - \bar{t}) \left[ 2 + b - \frac{3(I+b)}{2Fo_a} \sum_{i=1}^{\infty} \frac{\tilde{\Psi}_i^2(\psi_i, \theta)}{\psi_i^4} \left[ \exp\left(-\psi_i^2 \frac{2Fo_a}{3}\right) - 1 \right] \right] \right\}. \quad (3.221)$$

In this example the rate of the heat transfer may be evaluated by means of the mass transfer rate. The relationship for Nusselt number follows from (3.178) taking into account (3.188):

$$Nu = \frac{\beta_t L}{\lambda_0} = - \frac{L}{h_0} \int_0^L \left[ (I + \bar{\lambda}T) \frac{\partial T}{\partial \xi} \right]_{\xi=1} dX. \quad (3.222)$$

The determination of  $T(X, \xi)$  does not require a solution of the equations for  $T_j$  ( $j = 1, \dots, 5$ ), because the heat transfer rate may be determined from the thermal balance within the film of a length  $L$ :

$$\begin{aligned} \int_0^L \left[ \lambda(T) \frac{\partial t}{\partial y} \right]_{y=0} dx &= \int_0^L \left[ \lambda(T) \frac{\partial t}{\partial y} \right]_{y=h} dx - \\ &- \rho c_p \int_0^h u \left[ t(L, y) - t_0 \right] dy. \end{aligned} \quad (3.223)$$

The dimensionless form of (3.223) is (see also (3.173)):

$$\begin{aligned} \int_0^L \left[ (I + \bar{\lambda}T) \frac{\partial T}{\partial \xi} \right]_{\xi=1} dX &= \int_0^L \left[ (I + \bar{\lambda}T) \frac{\partial T}{\partial \xi} \right]_{\xi=0} dX + \\ &+ B \int_0^h U [T(1, 1 - Y) - I] dY, \end{aligned} \quad (3.224)$$

where

$$B = \frac{\rho c_p u_0 h_0^2}{\lambda_0 L}. \quad (3.225)$$

The second boundary condition in (3.192) may be averaged with respect the variable  $X$ :

$$\int_0^L \left[ (I + \bar{\lambda}T) \frac{\partial T}{\partial \xi} \right]_{\xi=0} dX = b \int_0^L \left[ (I + \bar{D}T)_{\xi=0} \left( \frac{\partial C}{\partial \eta} \right)_{\eta=0} \right] dX. \quad (3.226)$$

The parameter  $B$  in (3.224) is a small parameter, i.e. for the latter integral it is possible to use the zero-order approximations for  $U$ ,  $T$  and  $H$ . Thus, using (3.224) and (3.226) it is possible to obtain the following result:

$$\begin{aligned} \int_0^l \left[ (I + \bar{\lambda} T) \frac{\partial T}{\partial \xi} \right]_{\xi=1} dX &= b \int_0^l (I + \bar{D} T)_{\xi=0} \left( \frac{\partial C}{\partial \eta} \right)_{\eta=0} dX + \\ &+ B \int_0^l U_0 \left[ T_0(l, l - Y) - 1 \right] dY . \end{aligned} \quad (3.227)$$

The substitution of (3.222) and the Sherwood number (3.178) in (3.227) permits to establish a relationship between the Nusselt and the Sherwood numbers:

$$Nu = \frac{bSh}{h_0} \sqrt{\frac{D_0}{k}} - \frac{LB}{h_0} \int_0^l U_0 \left[ T_0(l, l - Y) - 1 \right] dY , \quad (3.228)$$

The integral can be solved numerically solved and the result is a function of  $Fo_a$ .

The theoretical results developed here indicate that the thermocapillary effects occur when low-rate chemical reactions and high temperature effects exist. The cases of fast chemical reactions show that the temperature gradient along the film length affects the mass transfer through its effects on the diffusion coefficient and the rate constant of the reaction, while the hydrodynamics has no effect.

♦

In Part 3 it was demonstrated that both the mechanism and the kinetics of the interphase mass transfer depends on the chemical reaction kinetics and the mass transfer in the liquid phase. By slow chemical reactions the interphase mass transfer rate depends on the mass transfer in the liquid phase under conditions of a physical absorption. The increase of the chemical reaction rate leads to the consequent increase of the mass transfer rate and a reduction of the effect of the convective transport. By fast chemical reactions this effect is practically absent (the mass transfer rate is independent of the velocity in the liquid phase). The very fast chemical reactions occur at the face interphase and the interphase mass transfer rate depends on the mass transfer in the gas phase.

When the chemical reaction is reversible the thermodynamic gas-liquid equilibrium depends of the apparent Henry's constant. It includes implicitly both the Henry's constant at a physical equilibrium and the chemical equilibrium constant. Probably the Henry's constants for different gases have equal orders of magnitude and the experimentally determined ones are different due to the contribution of the chemical equilibrium constant.

The mass transfer processes complicated with a chemical reaction become more complex under non-stationary conditions. These problems will be discussed the next part this book.

## References

1. Chr.Boyadjiev, Chem. Eng. Sci, 38 (1983) 641.
2. F. R. E. Danckwerts, Gas-Liquid Reactions, McGraw-Hill, New York, 1970.
3. V. M. Ramm, Gas Absorption, Khimia, Moscow, 1966 (in Russian).
4. Chr.Boyadjiev and V. Beschkov, Mass Transfer in Liquid Film Flows, Mir, Moscow, 1988 (in Russian).
5. G. Astarita, Mass Transfer with Chemical Reactions, Elsevier, New York, 1967.
6. Chr. Boyadjiev, Chem. Technology (Russia), 5 (1990) 48.
7. Chr. Boyadjiev, Chem. Technology (Russia), 6 (1990) 53.
8. Chr. Boyadjiev, Hung. J. Ind. Chem., 13(1985) 163.
9. Chr. Boyadjiev, Int.Chem. Eng., 14 (1974) 514.
10. Chr. Boyadjiev, Comptes Rendue Bulg. Acad. Sci., 25 (2) (1974) 205.
11. V. S. Krylov, Chr. Boyadjiev and V. Levich, Dokl.AN SSSR, 175 (1967) 156.
12. Chr. Boyadjiev, V. Levich and V.S.Krylov, Int.Chem. Eng., 8 (1968) 393.
13. I. M. Parvez, Ph.D. Thesis, Higher Inst. Chem. Technol, Sofia, 1988 (in Bulgarian).
14. L. Lee and P. Harriott , Ind. Eng. Chem. Process Des. Dev., 16 (1977) 282.
15. J. S. Naworski and P. Harriott, , Ind. Eng. Chem. Fund., 8 (1969) 397.
16. I. M. Parvez, Chr.Karagiozov and Chr.Boyadjiev, Chem. Eng. Sci, 46 (1991) 1589.
17. Chr. Boyadjiev, Int. J. Heat Mass Transfer, 25 (1982) 535.
18. Chr. Boyadjiev, Int. J. Heat Mass Transfer, 27 (1984) 1277.
19. Chr. Boyadjiev, Hung. J. Ind. Chem., 16 (1988) 195.
20. Chr. Boyadjiev, Hung. J. Ind. Chem., 16 (1988) 203.
21. V. S. Krylov, Advances in Chemistry (Russia), 49 (1980) 118.
22. A. Tamir, J. C. Merchuk and P. D. Virkar, Chem. Eng. Sci, 35 (1980) 1393.
23. L. E. Scriven and Sterling, C. V., Nature (London), 187 (1960) 186.
24. M. Hennenberg, P. M. Bisch, M. Vignes-Adler and A. Sanfeld, Lecture Note in Physics, Springer-Verlag, Berlin, 105 (1979) 229.
25. A. Sanfeld, A. Steichen, M. Hennenberg, P.M.Bisch, D.van Lamswerde-Gallez and W. Dalle-Vedore, Lecture Note in Physics, Springer-Verlag, Berlin 105 (1979) 168.
26. H. Linde, P. Schwartz and H. Wilke, Lecture Note in Physics, Springer-Verlag, Berlin 105 (1979) 75.
27. Yu. V. Axel'rod and V. V.Dil'man, Theor. Fund. Chem. Technol. (Russia), 14 (1980) 837.
28. G. M. Brown, AIChEJ., 6 (1960) 179.
29. M. M. Mikhailov and M. N.Ozisik, Unified Analysis of Heat and Mass Diffusion, J. Wiley Int., New York, 1984.
30. M. M. Mikhailov and N. L. Vulchanov, J. Comput. Phys., 50 (1983) 323.

This Page Intentionally Left Blank

## PART 4

### Non-Stationary Interphase Mass Transfer with Chemical Reactions

The steady-state mass transfer in two-phase systems complicated with a chemical reaction was developed in Part 3. It was demonstrated that the chemical reaction affects the mass transfer kinetics in two different ways. On the one hand there are non-linear effects when the chemical reaction order differs from unity and the mass transfer coefficient depends on the initial concentration of the transferred substance. On the other hand the mass transfer mechanisms depend on the chemical reaction rate.

The mass transfer with a chemical reaction becomes significantly complicated when the contact time between the phases is a parameter depending on the interphase mass transfer mechanism. This effect may be illustrated with an example considering a mass transfer with an irreversible chemical reaction of a first order.

Let the liquid flows in the area  $0 \leq x \leq L, 0 \leq y \leq \delta$  along the axis  $x$ . The mathematical model is a mass conservation balance

$$\frac{\partial c}{\partial t} + u \frac{\partial c}{\partial x} + v \frac{\partial c}{\partial y} = D \left( \frac{\partial^2 c}{\partial x^2} + \frac{\partial^2 c}{\partial y^2} \right) \pm kc.$$

In any elementary (finite) volume of the area (without the boundaries) the change of the concentration with time  $\left( \frac{\partial c}{\partial t} \right)$  is a result of the disbalance of the substance leaving the volume through its surface due to convection  $\left( u \frac{\partial c}{\partial x} + v \frac{\partial c}{\partial y} \right)$  and diffusion  $D \left( \frac{\partial^2 c}{\partial x^2} + \frac{\partial^2 c}{\partial y^2} \right)$ . The mass conservation balance equation takes into account the “creation” (“disappearing”) of a substance due to the chemical reaction of a first order ( $\pm kc$ ).

The boundary conditions of the equation are:

$$\tau = 0, \quad c = 0; \quad x = 0, \quad c = 0; \quad y = 0, \quad c = 0;$$

$$x = L, \quad c = c^*; \quad y = \delta, \quad c = c^*.$$

The above equation assumes that the diffusion in the considered area is a result of the concentration differences at the boundaries.

Moreover, the velocity components  $u$  and  $v$  satisfy the continuity equation:

$$\frac{\partial u}{\partial x} + \frac{\partial v}{\partial y} = 0.$$

If  $u_0(v_0)$  is the average velocity of the flow along the axis  $x(y)$  the above equation may be rewritten in a dimensionless form

$$\frac{\partial U}{\partial X} + \frac{v_0 L}{u_0 \delta} \frac{\partial V}{\partial Y} = 0$$

by means of the following dimensionless variables:

$$x = LX, \quad y = \delta Y, \quad u = u_0 U, \quad v = v_0 V.$$

If the flow is stratified:

$$\frac{v_0 L}{u_0 \delta} \ll 1, \text{ i.e. } \frac{\partial U}{\partial x} = 0, \quad V \equiv 0$$

and the characteristic velocity  $v_0$  does not exist.

In the situation

$$\frac{v_0 L}{u_0 \delta} \sim 1, \text{ i.e. } v_0 = u_0 \frac{\delta}{L}, \quad \frac{\partial U}{\partial X} + \frac{\partial V}{\partial Y} = 0.$$

The introduction of the dimensionless concentration  $C = \frac{c}{c^*}$  and time  $T = \frac{\tau}{t_0}$  leads to:

$$St \frac{\partial C}{\partial T} + U \frac{\partial C}{\partial X} + V \frac{\partial C}{\partial Y} = Fo \left( L_0 \frac{\partial^2 C}{\partial X^2} + \frac{\partial^2 C}{\partial Y^2} \right) \pm Da C;$$

$$T = 0, \quad C = 0; \quad X = 0, \quad C = 0; \quad Y = 0, \quad C = 0;$$

$$X = 1, \quad C = 1; \quad Y = 1, \quad C = 1,$$

where  $St = \frac{L}{u_0 t_0}$ ,  $Fo = \frac{DL}{u_0 \delta^2}$ ,  $Da = \frac{kL}{u_0}$  are the Struchal, the Fourier and the Damkohler numbers respectively.

The boundary problem developed shows that the model of the non-stationary mass transfer is affected by three parameters and depending on their orders. This allows various mass transfer mechanisms between two phases with a chemical reaction in one of them. In contrast to the problems discussed in Part 3 of this book, here the time for contact between the phases  $t_0$  appears. Obviously, it affects the interphase mass transfer mechanism.

The non-stationary interphase mass transfer complicated with a chemical reaction is the basis of many batch chemical processes in two-phase systems. Their models usually employ steady state methods. These methods assume that the both phases (gas and liquid for example) are in a closed volume for a fixed period of time and the process rate depends on the changes of the partial pressure in the gaseous phase at the corresponding concentrations in the liquid [1]. The intensification of the process is usually due to a mixing by a stirrer [2]. The simulation of these processes requires the solution of the above mentioned equations together with the Navier-Stokes equations with corresponding boundary and initial conditions.

The great number of parameters and various mathematical difficulties are the reasons for the relatively low number of published works considering the problem solution in its general formulation. Usually, the cases limited by the mass transfer in one of the phases are considered [3,4]. In such cases the contact time is small and the diffusion boundary layers on the phase interface are not developed [5 - 8]. In some cases the solution of the problem exist for particular values of the physicochemical and hydrodynamic properties and a given reactor geometry.

A great number of chemical reactions are characterized with large chemical reaction rates or small times for a contact between the phases. In this situations

$$St_h \gg 1, \quad Da \gg 1.$$

Under such conditions the mass transfer rate does not depend on the convective transport. This allows the use of the models developed for the interphase mass transfer between two stagnant fluids complicated with a chemical reaction in one of them. Depending on the order of the parameters of the model there are various mass transferring mechanisms. They will be developed in this part of the book.

## CHAPTER 4.1. NON-STATIONARY PHYSICAL ABSORPTION

Non-stationary mass transfer between two phases in the case of a physical solubility of component  $A$  is shown schematically on Fig. 4.1. There are two layers of fluids - a liquid layer of depth  $h$  and a gas layer of height  $b$ . The gas layer is an admixture of an inner component  $B$  and the diffusing component  $A$ . The interface is flat and the area of contact is  $S$ . In an one-dimensional co-ordinate system shown in Fig.4.1 the problem of the non-stationary two-phase diffusion may be formulated as follows:

$$\begin{aligned} \frac{\partial c'_1}{\partial \tau} &= D_1 \frac{\partial^2 c'_1}{\partial y^2}, \quad \frac{\partial c'_2}{\partial \tau} = D_2 \frac{\partial^2 c'_2}{\partial y^2}, \\ c'_{2s} &= kc'_{s1} + p, \quad D_1 \left( \frac{\partial c'_1}{\partial y} \right)_s = D_2 \left( \frac{\partial c'_2}{\partial y} \right)_s, \\ t = 0, \quad c'_1 &= c_{01}, \quad c'_2 = c_{02}, \end{aligned} \tag{4.1}$$

where  $y$  is the vertical co-ordinate, m;  $y = 0$  at the bottom of the vessel;  $\tau$  - time, s;  $c_i$  - the concentration of  $A$ , moles per liter,  $D_i$  - the coefficient of binary molecular diffusion (of  $A$

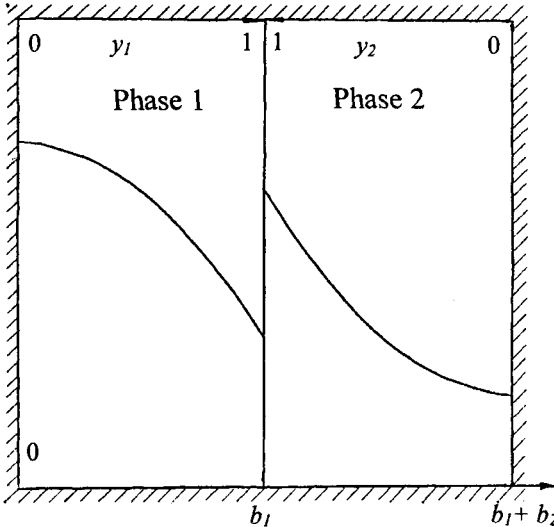


Fig.4.1. Schematic presentation of non-stationary mass transfer in the case of a physically soluble component  $A$ .

through  $B$ ),  $\text{m}^2/\text{s}$ ;  $i=1,2$ - indicates the phase; subscripts denote:  $s$  -the interface and  $0$  – the time  $\tau = 0$ .

Two conditions for equality are satisfied at the interface: a) the diffusion fluxes are equal; b) the linear Henry's law with respect the concentrations  $c'_{is}$  ( $k$  and  $p$  are constants depending on the temperature,  $T$ ) is valid.

During a time  $\tau$  the quantity of  $I'$  moles of the substance  $A$  passes through the interface. It may be expressed by the concentrations in both phases:

$$I' = -S \int_0^\tau D_i \left( \frac{\partial c'_i}{\partial y} \right) d\tau = -S \left[ c_{0i} b_i - \int_{b_i}^{b_i+b_2} c'_i dy \right] = -S \int_0^\tau D_2 \left( \frac{\partial c'_2}{\partial y} \right) d\tau = -S \left[ \int_0^{b_2} c'_2 dy - b_2 c_{02} \right]. \quad (4.2)$$

In order to simplify the further problem discussion the equations will be rewritten in a dimensionless form. The dimensionless concentrations  $c_i$  are:

$$\begin{aligned} c'_1 &= (c_{01} - c_{01}^*) c_1 + c_{01}^*, \\ c'_2 &= (c_{02}^* - c_{02}) c_2 + c_{02}, \end{aligned} \quad (4.3)$$

where the asterisk denotes the corresponding equilibrium concentrations in both phases at  $\tau = 0$ :

$$c_{02} = kc_{01}^* + p, \quad c_{02}^* = kc_{01} + p.$$

Taking into account that

$$(c_{02}^* - c_{02}) = k(c_{01} - c_{01}^*), \quad (4.4)$$

it is easy to demonstrate the continuity of the concentrations  $c_i$  ( $i = 1, 2$ ) at the interface:

$$c_{S1} = c_{S2} = c_S.$$

The dimensionless coordinates  $y_i$  and the time  $\tau_i$  ( $i = 1, 2$ ) may be introduced on the basis of the following physical assumptions (Fig. 4.1):

$$y = (b_1 + b_2) - b_1 y_1 = b_2 y_2, \quad t = \frac{b_i^2}{D_i} \tau_i, \quad i = 1, 2. \quad (4.5)$$

Hence, the general dimensionless formulation of the problem is:

$$\begin{aligned} \frac{\partial c_i}{\partial \tau_i} &= \frac{\partial^2 c_i}{\partial y_i^2}; \\ y_i &= I, \quad c_{S1} = c_{S2} = c_S, \quad \left( -\frac{\partial c_i}{\partial y_i} \right)_S \left( \frac{1}{\varepsilon \beta^2} \right) = \left( \frac{\partial c_i}{\partial y_i} \right)_S; \\ \tau_i &= 0, \quad c_{01} = 1, \quad c_{02} = 0; \quad i = 1, 2. \end{aligned} \quad (4.6)$$

Here two dimensionless parameters  $\beta^2 = \left( \frac{b_1}{b_2} \right)^2 \frac{D_2}{D_1}$  and  $\varepsilon = k(b_2 / b_1)$  are introduced. The physical sense of the first parameter is the ratio of the characteristic time scales of both phases. The second parameter follows from the mass balance equation (4.2) rewritten in a dimensionless form:

$$I' = -Sb_1 \left( c_{01} - c_{01}^* \right) \left( 1 - \int_0^I c_1 dy_1 \right) = -Sb_2 \left( c_{02}^* - c_{02} \right) \int_0^I c_2 dy_2 \quad (4.7)$$

or

$$I_2 = \int_0^I c_2 dy_1 = \varepsilon \left( 1 - \int_0^I c_1 dy_1 \right) = \varepsilon \int_0^I c_2 dy_2 = \varepsilon I_2. \quad (4.8)$$

Here  $\varepsilon = Sb_2 (c_{02}^* - c_{02}) / Sb_1 (c_{01} - c_{01}^*) = k(b_2 / b_1)$  is the ratio of the maximum amounts of mols absorbed by the second phase and those that may be released by the first one. Thus  $\varepsilon$  may be considered as a relative capacity of the second phase.

#### 4.1.1. Problem solution

The problem (4.6) may be solved by variable separation method [9]:

$$C = \sum_{\lambda} c_{\lambda} Y_{\lambda}(y) \exp(\lambda t), \quad (4.9)$$

where  $\lambda < 0$  are the eigenvalues,  $c_{\lambda}$  and  $Y_{\lambda}(y)$  are the respective coefficients and characteristic functions. The vector-functions  $Y_{\lambda}$  and  $C$  are expressed as:

$$C = \begin{bmatrix} c_1(\tau_1, y_1) \\ c_2(\tau_2, y_2) \end{bmatrix}, \quad Y_{\lambda} = \begin{bmatrix} Y_{\lambda}^1(y_1) \\ Y_{\lambda}^2(y_2) \end{bmatrix}.$$

The upper rows correspond to the first phase, while the lower rows represent the second phase. The characteristic functions  $Y_{\lambda}^i(y_i)$  satisfy the linear differential equations

$$-z^2 Y_{\lambda}^{(2)} = \frac{d^2 Y_{\lambda}^{(2)}}{dy_2^2}, \quad -r^2 Y_{\lambda}^{(1)} = \frac{d^2 Y_{\lambda}^{(1)}}{dy_1^2} \quad (4.10)$$

with boundary conditions

$$\begin{aligned} Y_{\lambda}^{(1)}(1) &= Y_{\lambda}^{(2)}(1) = 1; \quad \left( \frac{dY_{\lambda}^{(1)}}{dy_1} \right)_{y_1=0} = \left( \frac{dY_{\lambda}^{(2)}}{dy_2} \right)_{y_2=0} = 0; \\ \left( \frac{dY_{\lambda}^{(2)}}{dy_2} \right)_s &= - \left( \frac{dY_{\lambda}^{(1)}}{dy_1} \right)_s = \left( \frac{1}{\epsilon \beta^2} \right)_s, \end{aligned} \quad (4.11)$$

where  $z$  and  $r$  are the characteristic roots related to  $\lambda$  as follows:

$$\lambda \tau = -r^2 \tau_1 = -z^2 \tau_2. \quad (4.12)$$

The initial conditions (4.6) may be rewritten as:

$$\begin{bmatrix} 0 \\ 1 \end{bmatrix} = \sum_{\lambda} c_{\lambda} \begin{bmatrix} Y_{\lambda}^1 \\ Y_{\lambda}^2 \end{bmatrix}. \quad (4.13)$$

The solution of the set of equations (4.10 - 4.11) could be expressed as:

$$Y_{\lambda}^{(1)} = \frac{\cos(ry_1)}{\cos(r)}, \quad Y_{\lambda}^{(2)} = \frac{\cos(zy_2)}{\cos(z)}. \quad (4.14)$$

The characteristic roots  $z$  (or  $r$ ) follow from the characteristic equation (4.11):

$$-\operatorname{ctg}(z) = (\varepsilon\beta)\operatorname{ctg}(r), \quad r = \beta z. \quad (4.15)$$

The determination of the coefficients  $c_\lambda$  requires the introduction of a scalar product in the space of the functions  $Y_\lambda$  transforming these functions in an orthogonal system.

Taking into consideration (4.11) it is easy to demonstrate that for two arbitrary functions  $Y_\lambda$  and  $Y_{\lambda'}$  the following relationship is satisfied [10]:

$$\int_0^l Y_\lambda^{(1)} Y_{\lambda'}^{(1)} dy_1 + \varepsilon \int_0^l Y_\lambda^{(2)} Y_{\lambda'}^{(2)} dy_2 = 0, \quad \lambda \neq \lambda'. \quad (4.16)$$

The left-hand part of (4.16) has the properties of a scalar product [10]. Thus, the relationship for  $c_\lambda$  (through (4.13)) is:

$$c_\lambda = \frac{\int_0^l Y_\lambda^l dy_1}{\int_0^l Y_\lambda^{(1)} Y_\lambda^{(1)} dy_1 + \varepsilon \int_0^l Y_\lambda^{(2)} Y_\lambda^{(2)} dy_2}. \quad (4.17)$$

In the particular case of  $\lambda = 0$

$$Y_0 = \begin{bmatrix} l \\ 1 \end{bmatrix}, \quad c_0 = \frac{l}{l + \varepsilon}. \quad (4.18)$$

At  $\lambda \neq 0$  the explicit relationships for  $Y_\lambda$  [11] give:

$$c_\lambda = \frac{2(tgr/r)}{(1 + tg^2 r) + \varepsilon(1 + tg^2 z)}. \quad (4.19)$$

The final relationships for the average concentrations  $\bar{c}_i$  in the bulks of the phases and at the interface  $c_s$  are:

$$\begin{aligned} \bar{c}_1 &= \frac{1}{1 + \varepsilon} + \left( \frac{\varepsilon}{1 + \varepsilon} \right) b(\tau), \quad \bar{c}_2 = \left( \frac{1}{1 + \varepsilon} \right) (1 - b(\tau)), \\ c_s &= \frac{1}{1 + \varepsilon} + \sum_{z \neq 0} \frac{2\varepsilon(rctgr)e^{-z^2 t_1}}{[r^2(1 + ctg^2 r)\varepsilon + z^2(1 + ctg^2 z)]}, \end{aligned} \quad (4.20)$$

where

$$b(\tau) = \sum_{z=0}^{\infty} \frac{2(1+\varepsilon)e^{-\tau^2 t_z}}{[r^2(1+ctg^2 r)\varepsilon + z^2(1+ctg^2 z)]}. \quad (4.21)$$

It follows from (4.20 - 4.21) that at sufficiently large values of  $\tau$  the system reaches equilibrium through out its volume:

$$c_1 = c_2 = c_s = \frac{I}{I + \varepsilon}. \quad (4.22)$$

In this case the dimensionless fluxes  $I_i$  aspire to their equilibrium values:

$$I_1 \Rightarrow \frac{\varepsilon}{I + \varepsilon}, \quad I_2 \Rightarrow \frac{I}{I + \varepsilon}. \quad (4.23)$$

The time for the establishment of the equilibrium ( $\tau^*$ ) will be calculated from the condition assuring only 5% accuracy of the equality (4.23) that is enough for most of the practical cases. The value  $\tau^*$  depends on the parameters  $\varepsilon$  and  $\beta$ . In the next chapter a number of particular analytical solutions of (4.6) will be discussed.

#### 4.1.2. Solutions at short contact times

When in both the gas and the liquid phase there are diffusion boundary layers [9] and the contact times are small ( $\tau \rightarrow 0$ ) the solution has the form:

$$\begin{aligned} 1 - c_1(\eta_1) &= (1 - c_s)erfc(\eta_1 / 2), \\ c_2(\eta_2) &= c_s erfc(\eta_2 / 2), \end{aligned} \quad (4.24)$$

where  $\eta_i$  are the similarity variables for the  $i^{\text{th}}$  phase

$$\eta_i = \frac{(1 - y_i)}{\sqrt{\tau_i}}. \quad (4.25)$$

At small times  $\tau$  the concentration  $c_s$  is constant and may be determined by the condition defining the equality of the diffusion fluxes (4.6):

$$(1 - c_s) \frac{2}{\sqrt{\pi}} \left( \frac{1}{2\sqrt{\tau_1}} \right) \left( \frac{1}{\varepsilon\beta^2} \right) = c_s \left( \frac{2}{\sqrt{\pi}} \right) \left( \frac{1}{2\sqrt{\tau_2}} \right).$$

Thus

$$c_s \approx 1/(1 + \varepsilon\beta). \quad (4.26)$$

The dimensionless mass fluxes  $I_i$  are:

$$I_1 = \frac{2}{\sqrt{\pi}} \left( \frac{\varepsilon\beta}{1+\varepsilon\beta} \right) \sqrt{\tau_1}, \quad I_2 = \frac{2}{\sqrt{\pi}} \frac{\sqrt{\tau_2}}{1+\varepsilon\beta}. \quad (4.27)$$

#### 4.1.3. Interphase mass transfer resistance located in one of the phases

If it is supposed that the change of  $c_s$  with time is monotonic (this will be demonstrated further by numerical calculations) the limiting relationships (4.22) and (4.26) and the simultaneous satisfaction of the inequalities

$$\varepsilon \gg 1, \quad \varepsilon\beta \gg 1. \quad (4.28)$$

lead to the fact that the for the surface concentration  $c_s(\tau) \ll 1$  is valid. Thus, the problem (4.6) may be solved for the first phase only under the unique condition at the interface  $c_s = 0$ . In this case the solution is well known [9]:

$$\bar{c}_1 = \sum_{n=0}^{\infty} \frac{2}{\pi^2 (n+1/2)^2} \exp[-\pi^2 (n+1/2)^2 \tau_1]. \quad (4.29)$$

In the other case

$$\varepsilon \ll 1, \quad \varepsilon\beta \ll 1 \quad (4.30)$$

and the concentration  $c_s(\tau) \approx 1$ , so the problem may be solved for the second phase only at  $c_s(\tau) = 1$ . The corresponding solution is [9]:

$$\bar{c}_2 = 1 - \sum_{n=0}^{\infty} \frac{2}{\pi^2 (n+1/2)^2} \exp[-\pi^2 (n+1/2)^2 \tau_2]. \quad (4.31)$$

It should be noted that the formal treatment of the equations describing a given physical problem with the view to express it in a dimensionless form provides a possibility to reduce the number of the decisive parameters by grouping them in dimensionless complexes. Various systems of independent combinations of these complexes in accordance with the theory of the dimensions are equivalent, but an unique condition imposed is that the dimensions of all these systems must be invariant [12].

The choice of the particular system of decisive parameters should be made on the basis of the physical assumptions. In the case of two-phase physical absorption discussed here it is suitable to choose  $(\varepsilon, \varepsilon\beta)$  or  $(X, Y)$ :

$$X = \lg \varepsilon, \quad Y = \lg(\varepsilon\beta). \quad (4.32)$$

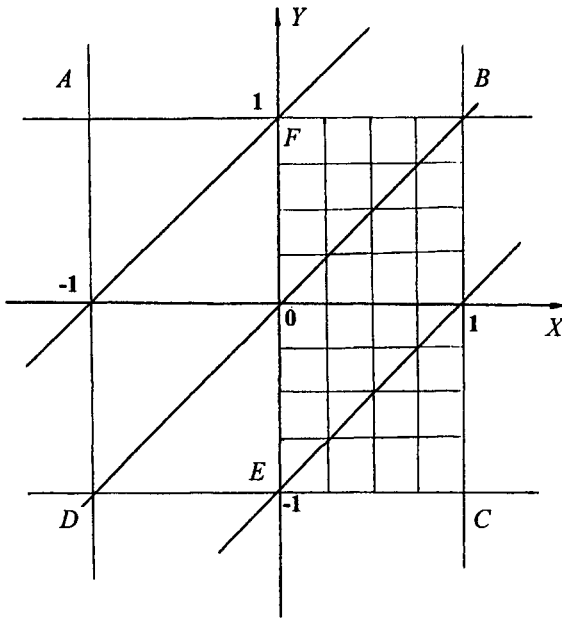


Fig.4.2. The Cartesian co-ordinate system  $X - Y$ .

The Cartesian co-ordinate system  $X - Y$  is shown in Fig.4.2. The solution of (4.6) is considered in that absorption plane.

It is evident from

$$Y = X + \lg \beta,$$

that along the straight lines parallel to the bisectrix of the second quadrant the parameter  $\beta$  has constant values (Fig. 4.2).

#### 4.1.4. Solution on the line $\beta = I$

In this case the solution of the characteristic equation of (4.6) is trivial:

$$ctgr = ctgZ = 0, \quad r = \pi(n + 1/2) \quad n = 0, 1, \dots$$

and the distribution in both phases has the form :

$$\bar{c}_l = \frac{1}{1+\varepsilon} + \frac{\varepsilon}{1+\varepsilon} \left[ \sum_{n=0}^{\infty} \frac{2}{\pi^2 (n + 1/2)^2} \exp(-\pi^2 (n + 1/2)^2 \tau_l) \right],$$

$$\bar{c}_2 = \left( \frac{1}{1+\varepsilon} \right) \left[ I - \sum_{n=0}^{\infty} \frac{2}{\pi^2 (n+1/2)^2} \exp(-\pi^2 (n+1/2)^2 \tau_2) \right],$$

$$c_s = \frac{I}{1+\varepsilon}, \quad \tau_1 = \tau_2. \quad (4.33)$$

Taking into account that the characteristic times of both phases are equal  $\left( \frac{b_2^2}{D_2} = \frac{b_1^2}{D_1} \right)$ ,

the absorption will be carried out under a constant surface concentration  $c_s$ . At  $\varepsilon \gg 1$  (the upper right corner of the plane  $X-Y$ ) the inequalities  $\bar{c}_2 \ll I$ ,  $c_s \ll I$  are satisfied and the relationships (4.29) and (4.33) developed for  $\bar{c}_i$  are identical. In this case the mass transfer in the first phase limits the overall absorption rate (see 4.1.3).

#### 4.1.5. Solution in the upper part of $X-Y$ plane

It is clear from Fig. 4.2 that in this part of the  $X-Y$  the condition  $\beta \gg 1$  is always satisfied. The characteristic equation (4.15) and the relationships (4.20 - 4.21) become simpler as follows:

$$ctgr \approx \left( -\frac{1}{\varepsilon r} \right), \quad b \approx \sum_r \frac{2(1+\varepsilon)\varepsilon}{(\varepsilon r)^2 + \varepsilon + 1} \exp(-r^2 \tau_1), \quad \bar{c}_1 = \frac{I}{1+\varepsilon} + \frac{\varepsilon}{1+\varepsilon} b(\tau_1),$$

$$\bar{c}_2 \approx c_s \approx \frac{I}{1+\varepsilon} - \sum_r \frac{2\varepsilon}{[(\varepsilon r)^2 + \varepsilon + 1]} \exp(-r^2 \tau_1). \quad (4.34)$$

Hence, the lateral variations of the concentration in the second phase may be neglected. The integration along the co-ordinate  $y_2$  of the second transport equation in (4.6) yields:

$$\frac{\partial c_s}{\partial \tau_2} = \left( \frac{\partial c_2}{\partial y_2} \right)_s. \quad (4.35)$$

In this case the two-phase problem (4.6) becomes one-phase problem:

$$\frac{\partial c_1}{\partial \tau_1} = \frac{\partial^2 c_1}{\partial y_1^2} \quad \frac{\partial c_s}{\partial \tau_1} = \frac{1}{\varepsilon} \left( -\frac{\partial c_1}{\partial y_1} \right)_s, \quad c_s(0) = 0, \quad c_1(0, y_1) = 1. \quad (4.36)$$

The solution of the one-phase problem  $c_i(\tau_1, y_1)$  depends on  $\varepsilon$  and obviously coincides with (4.34). The dimensionless diffusion flux is  $I_i^B(X, \tau_1)$ . For small and large values of  $\varepsilon$  there are analytical solutions for  $\bar{c}_i$ ,  $i = 1, 2$  (by means of (4.34)).

In the case  $\varepsilon \ll 1$  the roots of the characteristic equation are equal to  $r = \pi k$  ( $k = 1, 2, \dots$ ). By replacing in (4.34) the summation with respect to the discrete variable  $r$  by an integration with respect the continuous variable  $x = (\varepsilon r)$  yields:

$$\begin{aligned} b(\tau_1) &\approx \sum_r \frac{2\varepsilon}{(\varepsilon r)^2 + 1} \exp[-(\varepsilon r)^2 \tau_1 \varepsilon^2] \approx \frac{2}{\pi} \int_0^\infty \frac{\exp[-x^2 (\tau_1 \varepsilon^2)]}{1+x^2} dx = \\ &= \exp(p) \operatorname{erfc}(\sqrt{p}), \end{aligned} \quad (4.37)$$

where  $dx = \pi \varepsilon \ll 1$ ,  $p = \tau_1 \varepsilon^2$ . Thus the relationship about the concentration is:

$$\bar{c}_2 \approx c_s \approx 1 - \exp(p) \operatorname{erfc}(\sqrt{p}), \quad \bar{c}_1 \approx 1. \quad (4.38)$$

In the case of  $\varepsilon \gg 1$  it is easy to demonstrated by the help of (4.34) that:

$$b(\tau_1) \Rightarrow \sum_r \frac{2}{r^2} \exp(-r^2 \tau_1), \quad \bar{c}_2 \approx c_s \approx 0,$$

where  $r = \pi(k+1/2)$ ,  $p = 0, 1, \dots$ . The concentration distribution in the first phase coincides with (4.29). From a physical point of view it is easy to understand the result. In this case the problem is located in a part of  $X-Y$  where the interphase mass transfer is limited by the mass transfer in the first phase.

#### 4.1.6. Solution in the lower part of the $X-Y$ plane

In this part of the plane the interesting situation occurs when  $\beta \ll 1$  (Fig. 4.1). The corresponding characteristic equation (4.15) and the relationships (4.20 - 4.21) become simpler:

$$\begin{aligned} \operatorname{ctgz} &= -\frac{\varepsilon}{z}, \\ b(\tau_2) &\approx \sum_z \frac{2(1+\varepsilon)}{\varepsilon + \varepsilon^2 + z^2} \exp(-z^2 \tau_2), \\ \bar{c}_1 \approx c_s &\approx \frac{1}{1+\varepsilon} + \sum_z \frac{2\varepsilon}{\varepsilon + \varepsilon^2 + z^2} \exp(-z^2 \tau_1). \end{aligned} \quad (4.39)$$

The relationships show that the lateral variations of the concentrations in the first phase may be neglected. By integration with respect to the variable  $y_1$  from zero to unity the transport equation (4.6) for the first phase gives:

$$\frac{\partial c_s}{\partial \tau_1} = \left( \frac{\partial c_1}{\partial y_1} \right)_s. \quad (4.40)$$

Hence, in the lower part of the  $X-Y$  plane the two-phase problem (4.6) may be reduced to an one-phase problem

$$\frac{\partial c_2}{\partial \tau_2} = \frac{\partial^2 c_2}{\partial y_2^2},$$

$$\left( -\frac{\partial c_s}{\partial \tau_2} \right) \left( \frac{1}{\varepsilon} \right) = \left( \frac{\partial c_2}{\partial y_2} \right)_s, \quad c_s(0) = 1, \quad c_2(0, y_2) = 0. \quad (4.41)$$

The solution of (4.41) is  $c_2(\tau_2, y_2)$ . It depends on  $\varepsilon$  (like (4.36)) and coincides with (4.39).

In the cases of small and large values of  $\varepsilon$  the set (4.39) allows to obtain analytical relationships for  $\bar{c}_i$ .

In the case when  $\varepsilon \ll 1$  it is clear that

$$b(\tau_2) \approx \sum_z \frac{2}{z^2} \exp(-z^2 \tau_2), \quad \bar{c}_i \approx c_s \approx 1,$$

where  $z = \pi(k + 1/2)$ ,  $k = 0, 1, \dots$ . The average concentration in the second phase coincides with (4.31). The last result indicates that the process in the second phase limits the interphase mass transfer (the problem corresponds to the left corner of the  $X - Y$  plane (see Fig. 4.2)).

At  $\varepsilon \gg 1$  the roots of the characteristic equation (4.15) are  $z = \pi k$ ,  $k = 1, 2, \dots$ . The replacement of the summation with respect to  $z$  in (4.39) by an integration with respect to the variable  $x = \pi k / \varepsilon$  [11], leads to:

$$\begin{aligned} b(\tau_2) &\approx \sum_k^{\infty} \frac{2(\pi/\varepsilon)}{1 + \left(\frac{\pi k}{\varepsilon}\right)^2} \exp\left[-\left(\frac{\pi k}{\varepsilon}\right)^2 \varepsilon^2 \tau_2\right] \approx \frac{2}{\pi} \int_0^{\infty} \frac{\exp(-\varepsilon^2 \tau_2 x^2)}{1+x^2} dx = \\ &= \exp(p) \operatorname{erfc}(\sqrt{p}), \end{aligned} \quad (4.42)$$

where  $dx = \pi/\varepsilon \ll 1$ ,  $p = \varepsilon^2 \tau_2$ . In this case the corresponding relationship for the average concentration is:

$$\bar{c}_i \approx c_s \approx \exp(p) \operatorname{erfc}(\sqrt{p}), \quad \bar{c}_2 \approx 0. \quad (4.43)$$

#### 4.1.7. Solution in the left part of $X - Y$ plane

It is clear from Fig. 4.2 that in this part of the plane  $\beta \gg 1$  and the characteristic time of the first phase ( $b_1^2 / D_1$ ) is significantly greater than the characteristic time of the second phase ( $b_2^2 / D_2$ ). This means that the time  $\tau^*$  required for the establishment of the equilibrium is smaller than the time required for the complete development of the boundary layers throughout the depth of the first phase. The introduction of a new variable  $y_{IS}$ :

$$l - y_1 = \frac{y_{IS}}{\beta} \quad (4.44)$$

and replacement of the conditions at  $y_1 = 0$  by  $y_{IS} = \infty$ , leads to the following form of the two-phase problem (4.6):

$$\begin{aligned}
\frac{\partial c_1}{\partial \tau_2} &= \frac{\partial^2 c_1}{\partial y_{IS}^2}, \quad \frac{\partial c_2}{\partial \tau_2} = \frac{\partial^2 c_2}{\partial y_2^2}, \\
\left( \frac{\partial c_1}{\partial y_{IS}} \right)_S \left( \frac{1}{\varepsilon} \right) &= \left( \frac{\partial c_2}{\partial y_2} \right)_S, \quad c_{2S} = c_{IS}, \\
\left( \frac{\partial c_1}{\partial y_{2S}} \right)_\infty &= 0; \quad c_1(0, y_{IS}) = 1, \quad c_2(0, y_2) = 0.
\end{aligned} \tag{4.45}$$

The subscripts “ $\infty$ ” and “ $0$ ” correspond to the co-ordinates  $y_{IS}$  and  $y_2$ . The problem (4.45) is one-parametric. Thus the concentrations  $c_2(\tau_2, y_2)$  and  $c_1(\tau_2, y_{IS})$  and the dimensionless fluxes  $I_2$  and  $I_{IS} \equiv \int_0^\infty (1 - c_1) dy_{IS}$  depend on  $\varepsilon\beta$  only. It is easy to demonstrate, that the following equalities are satisfied:

$$I_I = \int_0^1 (1 - c_1) dy_I \approx \frac{1}{\beta} \int_0^\beta (1 - c_1) dy_{IS} \approx \frac{1}{\beta} \int_0^\infty (1 - c_1) dy_{IS}.$$

Hence,

$$I_{IS}(\tau_2) = (\varepsilon\beta) I_2(\tau_2). \tag{4.46}$$

The function  $I_2(\tau_2)$  depends on  $Y$  in the considered area of the plane, so its graphical presentation is simpler.

The small and larger values of  $(\varepsilon\beta)$  do permit analytical solutions. The first case ( $\varepsilon\beta \gg 1$ ) corresponds to the upper left corner of the  $X - Y$  plane. Here, the lateral variations of the concentration  $c_2(\tau_2, y_2)$  may be neglected (see 4.2.4). The integration of the second transport equation (4.45) with respect to  $y_2$  from zero to unity gives the relationship (4.35). The substitution of the co-ordinates  $\tau_1, y_{IS}$  with  $\tau_1, y_1$  transforms the two-phase problem (4.45) into the one-phase problem (4.36). The solution of (4.36) in the left half-plane ( $\varepsilon \ll 1$ ) has been obtained in the form (4.38):

$$I_2 = 1 - \exp(p) \operatorname{erfc}(\sqrt{p}), \tag{4.47}$$

where

$$p = \frac{\tau_2}{\varepsilon^2} = \frac{\tau_2}{(\varepsilon\beta)^2}.$$

In the second case ( $\varepsilon\beta \ll 1$ ) the equality of the fluxes (4.45) leads to  $c_1(\tau) \approx 1$ . Thus the problem (4.45) may be solved in the second phase with a boundary condition at the

interface  $c_{2S} \approx 1$ . In the whole lower left part of the plane  $X - Y$  (see 4.2.2) it is possible to obtain solutions for  $\bar{c}_2(\tau_2)$  in the form of (4.31), i.e. the mass transfer resistance is located in the second phase.

#### 4.1.8. Solution in the right part of $X - Y$ plane

Let the case  $\beta \ll 1$  when the characteristic time of the second phase is significantly greater than the characteristic time of the first phase be considered. This means that during the time  $\tau^*$  the boundary layer of the lower phase cannot grow through out the whole its depth. The introduction of the lateral co-ordinate  $y_{2S}$  by:

$$1 - y_2 = \beta y_{2S} \quad (4.48)$$

and the change of the condition at  $y_2 = 0$  by  $y_{2S} = \infty$  transform the two-phase problem (4.6) to the following form :

$$\begin{aligned} \frac{\partial c_1}{\partial \tau_1} &= \frac{\partial^2 c_1}{\partial y_1^2}, \quad \frac{\partial c_2}{\partial \tau_1} = \frac{\partial^2 c_2}{\partial y_{2S}^2}, \\ \left( \frac{\partial c_1}{\partial y_1} \right)_S \left( \frac{1}{\varepsilon \beta} \right) &= \left( \frac{\partial c_2}{\partial y_{2S}} \right)_S, \quad c_{1S} = c_{2S}, \\ \left( \frac{\partial c_1}{\partial y_1} \right)_0 &= \left( \frac{\partial c_2}{\partial y_{2S}} \right)_\infty = 0, \quad c_1(0, y_1) = 1, \quad c_2(0, y_{2S}) = 0. \end{aligned} \quad (4.49)$$

This is an one-parametric problem like (4.45). The dimensionless fluxes  $I_1(\tau_1)$  and  $I_{2S}(\tau)$  depend on  $\varepsilon \beta$ .

$$I_1(\tau_1) = (\varepsilon \beta) I_{2S}(\tau_1), \quad I_{2S}(\tau_1) \equiv \int_0^\infty c_2 dy_{2S}. \quad (4.50)$$

The dimensionless flux  $I_1$  will be expressed as  $I_{1Y}(\tau_1)$ . Obviously, the function depends on  $Y$  only.

At small and large values of  $(\varepsilon \beta)$  the solution of (4.49) could be obtained analytically. The first case corresponds to  $\varepsilon \beta \ll 1$  (the lower right corner of the  $X - Y$  plane). The lateral changes of the concentration  $c_1(\tau_1, y_1)$  may be neglected (see 4.2.5.). Thus, it is easy to obtain the relationship (4.40). The latter allows the transformation of the two-phase problem (4.49) (by the change of the co-ordinates to  $\tau_2, y_2$ ) to the one-phase problem (4.41). The solution of (4.42) at  $\varepsilon \gg 1$  is :

$$I_1(p) = 1 - \exp(p) \operatorname{erfc}(\sqrt{p}) \approx I_{1C}(p), \quad (4.51)$$

where  $p \equiv \varepsilon^2 \tau_2 = (\varepsilon\beta)^2 \tau_1$ .

In the second case  $\varepsilon\beta \gg 1$  (and from the equality of the fluxes (4.49)) it follows that  $c_2(\tau_2) \approx 0$ . Thus, the problem (4.6) could be solved in the first phase only under the condition  $c_{1S} \approx 0$ . The final result for  $\bar{c}_1(\tau_1)$  is valid for the whole upper right corner of  $X - Y$  and has the form of (4.29). Thus, the mass transfer resistance is located in the first phase.

#### 4.1.9. Numerical solutions

The theoretical analysis performed above shows that at high and small values of the parameters  $\varepsilon$  or  $\varepsilon\beta$  the problem (4.6) becomes simpler and one-parametric. This means that the numerical calculations may be carried out inside a limited area of the  $X - Y$  plane. Let this area be defined. In order to increase the accuracy of the calculations of the two functions in all the points of  $I_1$  of  $X - Y$  the desired area must be defined as large as possible. The mass balance (4.8) indicates that in the right half of the plane ( $X > 0$ ) the dimensionless flux is  $I_1$ , while in the left part ( $X \leq 0$ ) the corresponding flux is  $I_2$ . Thus, it is sufficient to solve the problem in one of these half-planes. The latter follows from the symmetry of the problem (4.6).

Let two arbitrary points  $(X_0, Y_0)$  and  $(-X_0, -Y_0)$  located symmetrically with respect the co-ordinate system origin (Fig. 4.2) be considered.

Further, introduce the functions  $s_1$  and  $s_2$  by means of

$$s_1 = I - c_1, \quad s_2 = I - c_2.$$

These functions satisfy the following two-phase problem:

$$\begin{aligned} \frac{\partial s_1}{\partial \tau_1} &= \frac{\partial^2 s_1}{\partial y_1^2}, \quad \frac{\partial s_2}{\partial \tau_2} = \frac{\partial^2 s_2}{\partial y_2^2}, \\ s_{2S} &= s_{1S} = s_S, \quad -\left(\frac{\partial s_2}{\partial y_2}\right)_S \varepsilon\beta^2 = \left(\frac{\partial s_1}{\partial y_1}\right)_S; \\ \tau_1 &= 0, \quad s_1 = 0, \quad s_2 = 1. \end{aligned} \tag{4.52}$$

The comparison between (4.6) and (4.52) leads to the following relationship between the equations  $s_i$  and  $c_i$  at the symmetrical points:

$$\begin{aligned} s_1(-X_0, -Y_0, y_1, \tau_1) &= c_2(X_0, Y_0, y_2, \tau_2), \\ s_2(-X_0, -Y_0, y_2, \tau_2) &= c_1(X_0, Y_0, y_1, \tau_1) \end{aligned} \tag{4.53}$$

satisfying the conditions that  $y_1 = y_2$ ,  $\tau_1 = \tau_2$ .

The integration of (4.53) with respect the lateral co-ordinates yields:

$$I_1(X_0, Y_0, \tau_1) = I_2(-X_0, -Y_0, \tau_2), \quad (4.54)$$

where  $\tau_1 = \tau_2$ .

Further the dimensionless flux  $I_1(\tau_1)$  will be calculated in the right half-plane  $X - Y$  ( $X > 0$ ) only. The corresponding solution for  $(I_2)$  in the left half-plane follows automatically from the symmetry condition (4.54).

After a certain period of time the dimensionless diffusion fluxes  $I_i$  will approach the limiting values (4.23). The time required to reach 90 % of the maximum value will be denoted as  $\tau_i^*$ . This time is termed a time required for the establishment of the equilibrium in the two-phase system. The order of the  $\tau_i^*$  could be determined by means of the simplified non-stationary diffusion model. It is assumed that a diffusion boundary layer exists in one of the phases at least till the establishment of the equilibrium conditions at  $\tau_i^*$ . The fluxes  $I_1$  and  $I_2$  (at all the points of the right and left half-plane  $X - Y$ ) are:

$$I_1 \leq \frac{\varepsilon}{1+\varepsilon}, \quad I_2 \leq \frac{1}{1+\varepsilon},$$

and the value of  $\tau_i^*$  may be established from (4.27) :

$$\begin{aligned} \sqrt{\tau_i^*} &= \left( 1 + \frac{1}{\varepsilon\beta} \right) \quad \text{at} \quad X \geq 0; \\ \sqrt{\tau_i^*} &= (1 + \varepsilon\beta) \quad \text{at} \quad X < 0. \end{aligned} \quad (4.55)$$

The dimensionless co-ordinate  $Z$  for both the left and the right half-planes  $X - Y$  may be determined by the relationships:

$$Z = \begin{cases} \frac{\tau_1}{(1 + \frac{1}{\varepsilon\beta})^2} & , \quad X \geq 0; \\ \frac{\tau_2}{(1 + \varepsilon\beta)^2} & , \quad X < 0. \end{cases} \quad (4.56)$$

The variable  $Z$  has an advantage with respect to the other time co-ordinates ( $\tau_1$  or  $\tau_2$  for example) because the equilibrium occurs at  $Z \approx 1$  for every  $X, Y$ .

Hence, the calculation of the function  $I_i(Z)$  may be carried out in a limited interval with respect to the variable  $Z$ . Taking into account that at the symmetrical points  $(X_0, Y_0)$  and  $(-X_0, -Y_0)$  at  $\tau_1 = \tau_2$  the variables  $Z$  are equal the symmetry conditions (4.54) take the form

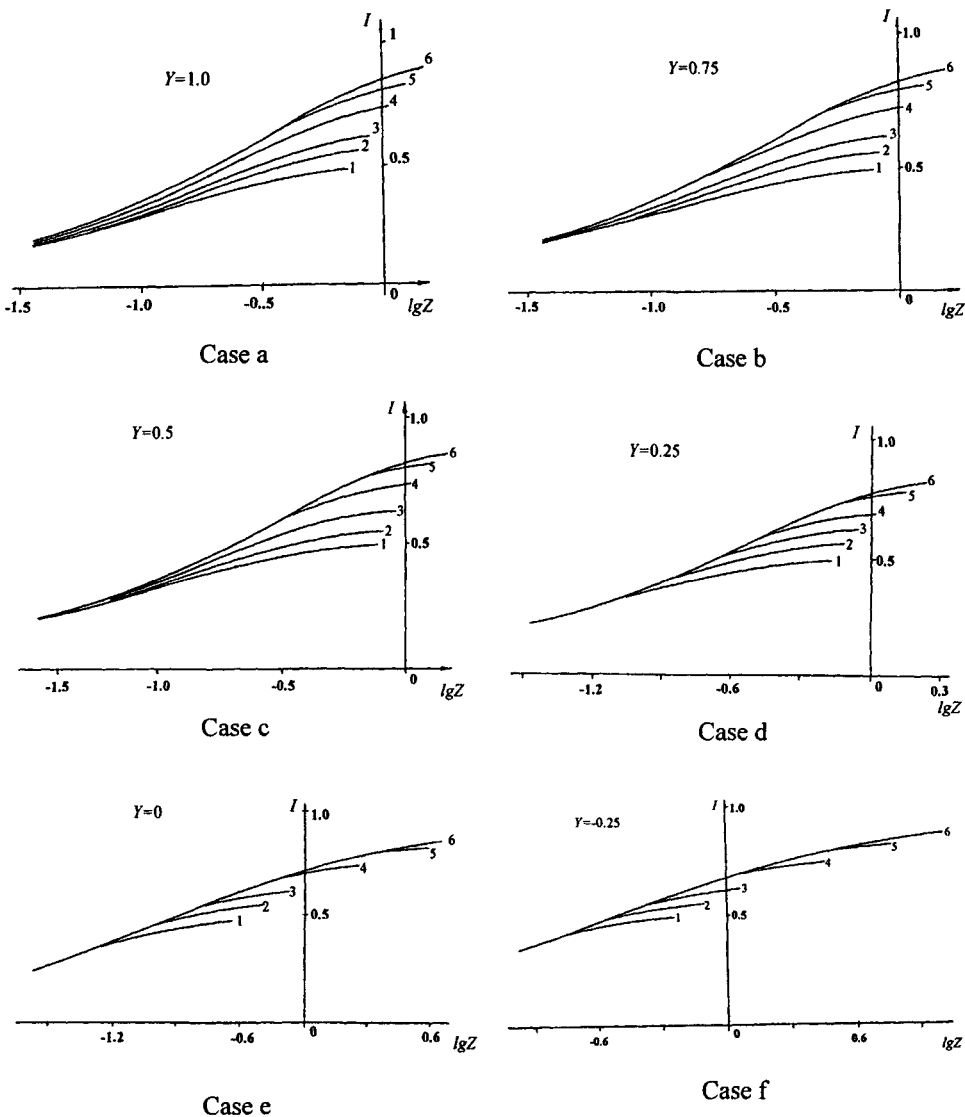


Fig. 4.3. Calculation results for  $I_l(Z)$  in the right half-plane  $X-Y$ , according to (4.20) in cases of: a)  $Y \geq 1.0$ ; b)  $Y=0.75$ ; c)  $Y=0.5$ ; d)  $Y \geq 0.25$ ; e)  $Y=0.0$ ; f)  $Y=-0.25$ ; (1)  $X=0$ ; (2)  $X=0.125$ ; (3)  $X=0.25$ ; (4)  $X=0.5$ ; (5)  $X=0.75$ ; (6)  $X \geq 1$ .

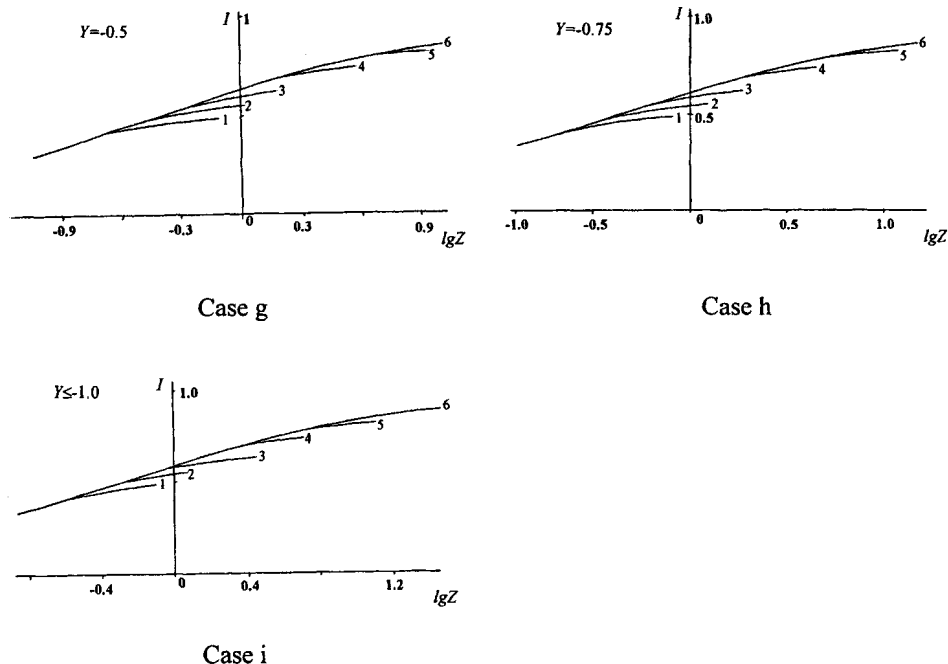


Fig. 4.3. Calculation results for  $I_l(Z)$  in the right half-plane  $X-Y$ , according to (4.20) in cases of: g)  $Y=-0.5$ ; h)  $Y=-0.75$ ; i)  $Y \leq -1.0$ ; (1)  $X=0$ ; (2)  $X=0.125$ ; (3)  $X=0.25$ ; (4)  $X=0.5$ ; (5)  $X=0.75$ ; (6)  $X \geq 1$ .

$$I_2(-X_0, -Y_0, Z) = I_l(X_0, Y_0, Z), \quad (4.57)$$

Here for  $I_2$  the value of  $Z$  is calculated in the point  $(-X_0, -Y_0)$  while in the case of  $I_l$  the corresponding point is  $(X_0, Y_0)$ .

The other advantage of  $Z$  is that at  $Z \rightarrow 0$  the asymptotic behaviour of the function  $I_l(Z)$  is invariant in  $X-Y$  (see (4.27) and (4.56)):

$$\begin{aligned} I_l &\rightarrow \frac{2}{\sqrt{\pi}} \sqrt{Z} \quad \text{at} \quad X \geq 0, \\ I_2 &\rightarrow \frac{2}{\sqrt{\pi}} \sqrt{Z} \quad \text{at} \quad X < 0. \end{aligned} \quad (4.58)$$

The function  $I_1(Z)$  has been calculated in the right half-plane  $X - Y$  through (4.20), (4.21) in points of a set shown on Fig. 4.2. The results are shown on Fig. 4.3 (Cases: a-i).

Some problems occurring during these calculations will be discussed. Let an accuracy of 10% is assumed for the calculation of the fluxes  $I_1(T)$  and define an area of the plane  $X - Y$ , where the approximations made in 4.1.2 are valid.

It is easy to prove that in the upper right corner with the apex  $B$  ( $X \geq I$ ,  $Y \geq I$ ) the dimensionless flux  $I_1(Z)$  can be analytically determined:

$$I_1(Z) = I_{IB}(Z) \equiv 1 - \sum_{n=0}^{\infty} \frac{2}{\pi^2(n+1/2)^2} \exp[-\pi^2(n+1/2)^2 Z]. \quad (4.59)$$

Taking into account that in this area the inequalities  $\varepsilon \geq 10$  and  $\varepsilon\beta \geq 10$  are satisfied, so  $Z \approx \tau_1$  ( see (4.56)) and the solution obtained coincides with (4.29). Thus, the mass transfer resistance is located in the first phase.

In the symmetrical area located in the lower left corner of  $X - Y$  with an apex  $D$  ( $X \leq -I$ ,  $Y \leq -I$ ) the following equality is satisfied:

$$I_2(Z) = I_{ID}(Z). \quad (4.60)$$

Taking into consideration that  $Z \approx \tau_2$  the flux  $I_2(Z)$  coincides with the relationship (4.31), i.e. the mass transfer resistance is located in the second phase.

The results are shown graphically on Fig. 4.3. Each figures presents a family of functions  $I_1(Z)$  (with a parameter  $X$ ) at a fixed value of  $Y$ . It is clear that the functions grow monotonously with  $X > 0$ . Moreover, the locus of each family coincides with the solution  $I_{II}$  of the one-phase limiting problem (4.49) (curves 5 on Fig. 4.3 (Cases: a - i))

The dimensionless fluxes  $I_{II}(Z)$  are shown on Fig. 4.4. Obviously, the solution of the problem (4.45) (see 4.1.7) is:

$$I_{2Y}(Y, Z) = I_{II}(-Y, Z). \quad (4.61)$$

In the area located above the horizontal line  $AB$  ( $Y \geq I$ ) these families are independent of the parameter  $Y$  and practically coincide with the limiting solution  $I_{IX}^B(Z)$  (4.36) developed in 4.1.5. It is shown on Fig.4.3 (Case a). On the other hand in the area below the line  $CD$  ( $Y \leq -I$ ) the dimensionless fluxes  $I_1(Z)$  coincide with the limiting solutions  $I_{IX}^*(Z)$  developed in 4.1.6 (see Fig. 4.3 (Case i)).

It is easy to prove that in the upper right corner with an apex  $B$  (Fig. 4.2) the equality is satisfied:

$$I_{IX}^B(Z) = I_{II}(Z) = I_{IB}(Z). \quad (4.62)$$

while in the lower right corner ( with the apex  $C$  ) the corresponding relation is

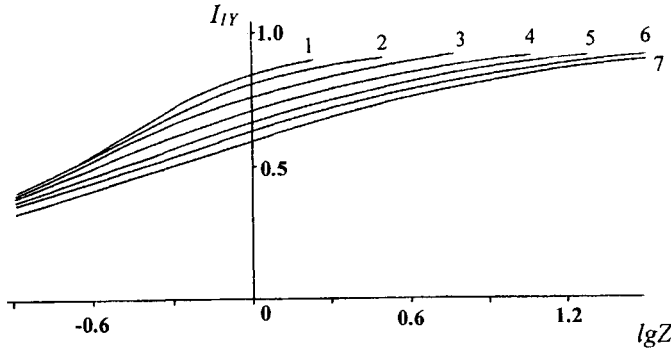


Fig. 4.4. Dimensionless fluxes  $I_{IY}(Z)$  in case of large volume of the second phase: 1)  $Y \geq 0.75$ ; 2)  $Y = 0.5$ ; 3)  $Y = 0.25$ ; 4)  $Y = 0$ ; 5)  $Y = -0.25$ ; 6)  $Y = -0.5$ ; 7)  $Y \leq -0.75$ .

$$I_{IX}^u(Z) = I_{IY}(Z) = I_{IC}(Z), \quad (4.63)$$

Here  $I_{IC}(Z)$  is the analytical relationship (4.51).

The solution in the left half-plane  $X - Y$  (where the points are located above the line  $AB$  and below the line  $CD$ ) may be obtained by means of the symmetry condition (4.57).

In the first case ( $Y \geq 1$ ):

$$I_2(X, Y, Z) = I_{2X}^B(X, Z) = I_{IX}^u(-X, Z). \quad (4.64)$$

In the second case ( $Y \leq -1$ ):

$$I_2(X, Y, T) = I_{2X}^u(X, T) = I_{IX}^B(-X, Z). \quad (4.65)$$

In the area of the upper left corner with an apex  $A$

$$I_2(Z) = I_{IC}(Z) \quad (4.66)$$

and in the lower left corner with the apex  $D$

$$I_2(Z) = I_{IB}(Z). \quad (4.67)$$

The above discussion shows that the numerical solution of the two-phase problem (4.6) may be carried out in a limited area of the  $(X - Y)$  plane. The internal points inside the square  $ABCD$  define this area (Fig. 4.2). The more precise solution corresponds to the

rectangular area  $EBCF$ . Outside that area (if the accuracy of 10% is enough for the calculations of the diffusion mass fluxes) the solution becomes simpler because the problem becomes one-parametric one:

- $I_{ix}^B(X, Z)$  -above the line  $AB$ ;
- $I_{ix}^n(X, Z)$  -below  $CD$ ;
- $I_{iy}(Y, Z)$  - to the right of  $BC$ ;
- $I_{2y}(Y, Z)$  - to the left of  $AC$ ,

if analytical solutions are available (in the areas  $B$  and  $D$  or  $C$  and  $A$ ).

The plots on Fig. 4.3 (Cases: a - i) allow (with an accuracy of 10%) the determination of the dimensionless fluxes  $I_i(X, Y, Z)$  in every point of the square  $ABCD$ . Moreover, if the considered point  $(X - Y)$  is not a node (Fig. 4.2), a linear approximation of the values calculated at the neighboring nodes (two or four) could be applied.

#### 4.1.10. Approximations of the numerical solutions

The analysis of the numerical solutions done in the previous sub-section indicates that it is possible to obtain reliable approximations of the integral fluxes  $I_i(X, Y, Z)$  required for fast calculus of approximations and estimations. It should be noted that inside the angle  $BOF$  and at  $\tau \leq \tau^*$   $I_i \leq 0.9(\varepsilon/(1+\varepsilon))$  the fluxes  $I_i(Z)$  do not practically decline from the locus's of the families corresponding to given  $Y$  values (Fig. 4.3 (Cases: a-i)). This is satisfied in Fig. 4.3 (Cases: a-d) at  $X \geq Y$  and for every  $X \geq 0$  in Fig. 4.3 (Cases: e - i) (curves 1 - 5).

Taking into consideration that the locus coincides with  $I_{iy}(Y, Z)$  inside  $BOF$ :

$$I_1 = I_{iy}(Y, Z), \text{ where } I_1 \leq 0.9(\varepsilon/(1+\varepsilon)). \quad (4.68)$$

It is clear that in the symmetrical area (inside the angle  $DOF$ ):

$$I_2(X, Y, Z) = I_{iy}(-Y, Z), \text{ where } I_2 \leq 0.9/(1+\varepsilon). \quad (4.69)$$

The physical sense of the above results may be understood if iso-lines of the function  $\sqrt{\tau_i^*}$  are drawn on the plane  $X - Y$ . These lines at  $\sqrt{\tau_i^*} < 1$  practically coincide with maximum boundary layer thickness' at ( $T_o = 273K$ ). The lines may be obtained from the simplified mass transfer model assuming that the relationship (4.27) is applicable up to the saturation point.

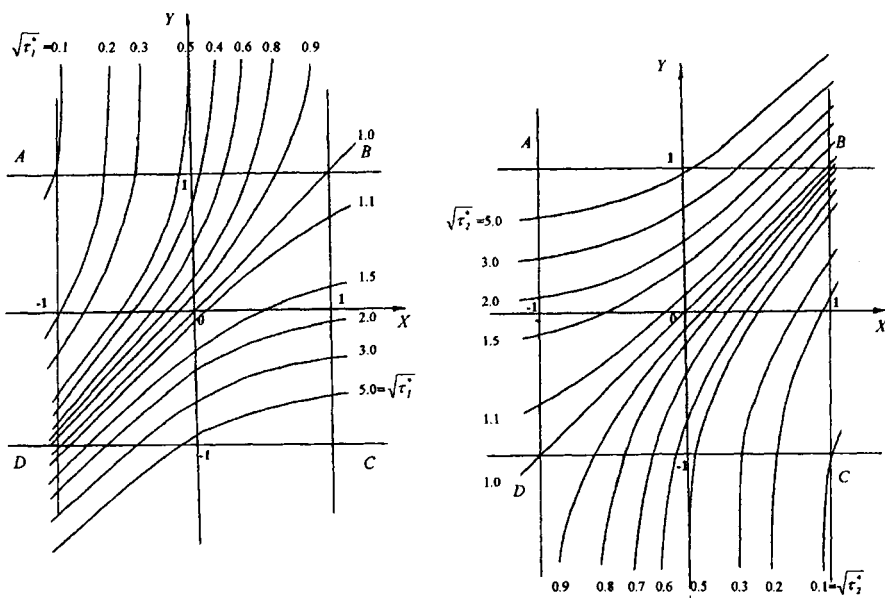
$$\sqrt{\tau_i^*} = \frac{1+1/\varepsilon\beta}{1+1/\varepsilon} \quad \text{at } X \leq 0; \quad \sqrt{\tau_2^*} = \frac{1+\varepsilon\beta}{1+\varepsilon} \quad \text{at } X > 0. \quad (4.70)$$

The lines are shown in Fig. 4.5. It is clear that in the left half-plane of the beam  $OB$  the equality  $\sqrt{\tau_2^*} = 1$  is satisfied, while inside the angle  $FOB$  the inequality  $\sqrt{\tau_2^*} < 1$  is valid. This means that in the area considered diffusion boundary layers exist in the second phase down to point where the absorbed substance in the first phase is completely depleted. Moreover, the assumptions done during the development of the simple diffusional model

(4.49) are valid in that area. In the left half-plane (inside the angle  $EOD$ ) diffusion boundary layers exist in the first phase up to the complete saturation of the second phase. Thus, the assumptions made during the development the one-parametric problem (4.45) are satisfied.

In this way the solutions inside the adjacent angles formed by the lines  $EF$  and  $DB$  (Fig. 4.2) may be obtained on the basis on the functions  $I_{IY}(Y, Z)$  only (Fig. 4.4). Taking into account that they are bounded by the analytical curves  $I_{IB}(Z)$  and  $I_{IC}(Z)$  the effect of the parameter  $Y$  is practically linear in the rage  $-1 \leq Y \leq 1$ . Thus by means of  $I_{IB}$  and  $I_{IC}$  it is possible to develop a numerical approximation of  $I_{IY}(Z)$ :

$$I_{IY}^{\text{app}} = \begin{cases} I_{IC}(Z) & \text{at } Y \leq -1, \\ I_{IC}(Z) + [I_{IB}(Z) - I_{IC}(Z)] \frac{(Y+1)}{2} & \text{at } -1 \leq Y \leq 1, \\ I_{IB}(Z) & \text{at } Y \geq 1. \end{cases} \quad (4.71)$$



Case (a)

Case (b)

Figs. 4.5. Iso-lines:  $\sqrt{t_i^*} = \text{const.}$  Cases: a) -  $i = 1$ ; b) -  $i = 2$ .

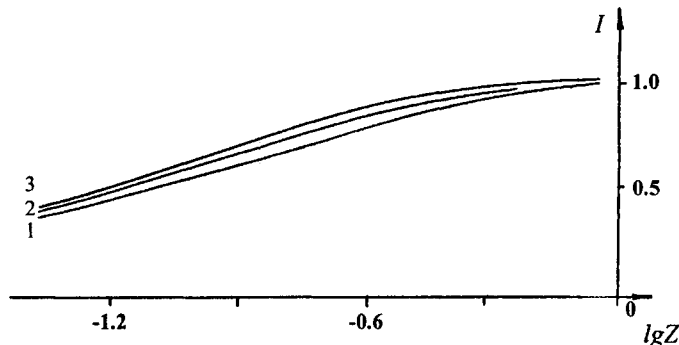


Fig. 4.6. Dimensionless flax on the axis  $X \geq 0$ . (1) -  $Y \geq 1$ ; (2) -  $Y = 0.5$ ; (3) -  $Y = 0$ .

The test performed shows that the maximum error does not exceed 5%.

Let a suitable approximation of the numerical solution inside the adjacent angles formed by the lines  $EF$  and  $DB$  be developed. The analysis of the plots  $I_i(X,Y,Z)$  in that area (see for example Figs. 4.3 (Cases: a – e)) indicates that at a given  $Y$  ( $0 \leq Y \leq 1$ ) the effect of the parameter  $X$  in the range  $0 \leq X \leq Y$  is practically linear, so:

$$I_i(X,Y,Z) = I_i(0,Y,Z) + [I_i(Y,Y,Z) - I_i(0,Y,Z)]X/Y \quad 0 \leq (X/Y) \leq 1. \quad (4.72)$$

Here  $I_i(Y,Y,Z)$  is the analytical solution along the line  $DB(\beta^2 = 1)$  at a given  $Y$  (4.33):

$$I_i(Y,Y,Z) = \left( \frac{\varepsilon\beta}{1 + \varepsilon\beta} \right) \left\{ 1 - \sum_{n=0}^{\infty} \frac{2}{\pi^2(n+1/2)^2} \exp[-\pi^2(n+1/2)^2 Z] \right\}. \quad (4.73)$$

The functions  $I_i(0,Y,Z)$  in (4.72) are the numerical solutions on the axis  $Y$  (Fig. 4.6). It is evident that the effect of  $Y$  on  $I_i(0,Y,Z)$  is weak and the function  $I_i(0,Y,Z)$  in (4.72) may be replaced by the analytical relationship  $I_i(0,0,Z)$  at the co-ordinate origin (Fig. 4.2):

$$I_i(0,0,Z) = \frac{1}{2} \left\{ 1 - \sum_{n=0}^{\infty} \frac{2}{\pi^2(n+1/2)^2} \exp[-\pi^2(n+1/2)^2 Z] \right\}. \quad (4.74)$$

The final expression of the approximating formula for the area defined by the adjacent angles formed by the lines  $EF$  and  $DB$  under the condition  $X > 0$  is :

$$I_1^{\text{app}}(X, Y, Z) = \left[ \frac{1}{2} + \left( \frac{\varepsilon\beta}{1+\varepsilon\beta} - \frac{1}{2} \right) \left( \frac{X}{Y} \right) \right] \left\{ 1 - \sum_{n=0}^{\infty} \frac{2}{\pi^2 (n+1/2)^2} \exp \left[ -\pi^2 \left( n + \frac{1}{2} \right)^2 Z \right] \right\}. \quad (4.75)$$

In the opposite case of  $X \leq 0$  the relationship (4.57) gives:

$$I_2^{\text{app}}(X, Y, Z) = I_1^{\text{app}}(-X, -Y, Z), \quad Y \leq 0, \quad Y \leq X \leq 0. \quad (4.76)$$

The approximation error of (4.75) does not exceed 5%. The approximations (4.75) and (4.76) allow fast development of an approximated solution of the general problem (4.6) at arbitrary values of the dimensionless decisive parameters  $X, Y, Z$ , thus avoiding numerical calculations.

#### 4.1.11. Physical absorption

The problem considered in the previous point shows that the absorption of physically soluble gases is defined by the position of the point  $(X, Y)$  on the characteristic plane (Fig. 4.2), i.e. by the values of the parameters

$$\varepsilon = k \frac{b_2}{b_1}, \quad \varepsilon\beta = k \sqrt{\frac{D_2}{D_1}}. \quad (4.77)$$

Let the relationships describing the effect of the temperature  $T$  and the pressure  $P$  on the transport coefficients be accepted. This effect on the coefficients of a binary diffusion (a component  $A$  diffuses through an inner gas  $B$  under pressure  $P$  and temperature  $T$ ) is [13]:

$$D_{AB} = D_{AB}^0 \left( \frac{T}{T_0} \right)^{1.75} \frac{1}{P}, \quad (4.78)$$

where  $P$  is in  $\text{atm}$  and the subscript “0” denotes the value at the standard temperature ( $T_0 = 273K$ ).

The diffusivities in the liquid phase depend on the temperature and the solution viscosity  $\mu$  only [13]:

$$D_A = D_A^0 \left( \frac{T}{T_0} \right) \left( \frac{\mu_0}{\mu} \right). \quad (4.79)$$

On the other hand the viscosity depends on the temperature in accordance with the Andrade's correlation [14]:

$$\mu = A 10^{B/T} \quad \text{or} \quad \left( \frac{\mu}{\mu_0} \right) = 10^{B \left( \frac{1}{T} - \frac{1}{T_0} \right)}, \quad (4.80)$$

where  $A, B$  are experimentally defined constants (for example in this case  $B = 650K$  ).

The Henry's constant generally depends on the temperature and in a narrow temperature range  $(T - T_0) \leq 50K$  it can be approximated by power functions:

$$k = k_0 10^{-\alpha(T-T_0)}. \quad (4.81)$$

Experimentally determined values of  $D_{AB}^0$ ,  $D_A^0$ ,  $k_0$  for gases of different solubility at  $T_0 = 273K$  are summarized in Table 4.1 [13]. The values of  $\alpha$  were calculated by means of experimentally verified relationships between the distribution coefficient  $m_{px}$  and the temperature of aqueous solutions [1]:

$$m_{px} = P/x, \quad k = \left( \frac{\rho}{M} \right) \frac{RT}{m_{px}},$$

where  $P$  is the pressure of the pure gas above the solution;  $x$  is the molar part of the soluble gas in the liquid (water);  $\rho$  and  $M$  are the density and the molecular weight of water respectively. Air was used as an inner gas ( $B$ ).

Table 4.1. Experimentally determined diffusivity and Henry's constants for gases.

gas	$D_{AB}^0$ , cm <sup>2</sup> /s	$D_A^0$ , cm <sup>2</sup> /s	$k_0$	$\alpha$ , 1/g	$X_0$	$Y_0$
N <sub>2</sub>	0.13	$1.05 \times 10^{-5}$	0.026	$1.1 \times 10^{-2}$	-1.6	-3.6
O <sub>2</sub>	0.18	$1.15 \times 10^{-5}$	0.046	$0.7 \times 10^{-2}$	-1.34	-3.45
CO <sub>2</sub>	0.14	$1.13 \times 10^{-5}$	1.41	$2.1 \times 10^{-2}$	0.15	-1.9
H <sub>2</sub> S	0.13	$0.9 \times 10^{-5}$	4.26	$0.9 \times 10^{-2}$	0.63	-1.47
Cl <sub>2</sub>	0.12	$0.78 \times 10^{-5}$	4.15	$1.0 \times 10^{-2}$	0.63	-1.48
SO <sub>2</sub>	0.12	$0.94 \times 10^{-5}$	40	$1.3 \times 10^{-2}$	1.6	-0.75
NH <sub>3</sub>	0.20	$1.13 \times 10^{-5}$	566	$1.66 \times 10^{-2}$	2.75	0.65

Using (4.78 - 4.80) one could be written:

$$\sqrt{\frac{D_2}{D_1}} = \sqrt{\frac{D_2^0}{D_1^0}} \left( \frac{T_0}{T} \right)^{0.38} P^{1/2} I 10^{\left[ \frac{13}{2} \left( \frac{1}{T_0} - \frac{1}{T} \right) \right]}.$$

Thus, the co-ordinates  $X, Y$  (Fig. 4.2) may be expressed as:

$$X = \lg \varepsilon = \lg k + \lg \frac{b_2}{b_1} = X_0 + \lg \frac{b_2}{b_1} - (\alpha T_0) \left( \frac{\Delta T}{T_0} \right), \quad (4.82)$$

$$Y = \lg(\varepsilon\beta) = \lg k + \frac{I}{2} \lg \left( \frac{D_2}{D_I} \right) = Y_0 + \left[ \frac{B}{2} \left( \frac{1}{T_0} - \frac{1}{T} \right) + 0.38 \lg \left( \frac{T_0}{T} \right) - \alpha(T - T_0) \right] + \\ + \frac{I}{2} \lg P = Y_0 + \frac{I}{2} \lg P + \left( \frac{\Delta T}{T_0} \right) \left[ \left( \frac{B}{2T_0} \right) + 0.16 + (\alpha T_0) \right]. \quad (4.83)$$

where the terms are proportional to  $(T - T_0)$  in (4.82 - 4.83) obtained under the condition  $(T - T_0) \ll T_0$ . The parameters  $X_0$ ,  $Y_0$  are:

$$X_0 = \lg k_0, \quad Y_0 = \lg k_0 + \frac{I}{2} \lg \left( \frac{D_2^0}{D_I^0} \right). \quad (4.84)$$

The physical sense of  $X_0, Y_0$  is the that they are the absorption co-ordinates under standard conditions:  $T = T_0$ ,  $P = 1 \text{ atm}$ ,  $b_2 = b_I$ .

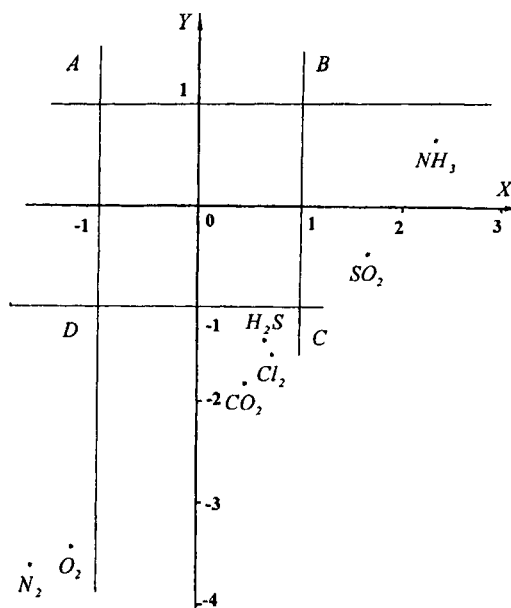


Fig. 4.7. Position of the co-ordinates  $X_0$ ,  $Y_0$  for gases of different solubilities.

The relationships (4.82 - 4.83) permit investigations of the pressure and the temperature effects as well as the effect of the liquid layer geometry  $\frac{b_2}{b_1}$  on the two-phase absorption process. The change of any of these quantities moves the point  $X, Y$  inside the characteristic plane, i.e. the absorption mechanism is changed.

The right-hand parts of (4.82) and (4.83) contain terms allowing for the effects of the water layer depth, the pressure and the temperature as well. By means of the symbols used in Table 4.1 it is easy to demonstrate that the temperature effects may be neglected in the range  $(T - T_0) \leq 50^{\circ}\text{C}$  because the terms  $(T - T_0)/T_0$  are close to unity. Thus:

$$X = X_0 + \lg\left(\frac{b_2}{b_1}\right), \quad Y = Y_0 + \frac{1}{2} \lg P, \quad (4.85)$$

i.e. the relative bed depth affects the variable  $X$ , while the pressure controls  $Y$ .

Figure 4.7 shows the position of the co-ordinates  $X_0, Y_0$  for gases with different solubilities (Table. 4.1).

It is evident, that for gases of low-solubility such as  $\text{N}_2$  and  $\text{O}_2$  ( $k_0 \approx 10^{-2}$ ) the diffusion resistances under ambient conditions are located in the liquid phases because the standard co-ordinates belong to the lower left part of the plane  $X - Y$  (the area  $D$ ). Thus, for the purposes of the calculations it is easy to use the relationship (4.31). When other gases from Table 1 are absorbed the points  $X_0, Y_0$  belong to the inside area of the angle  $FOB$  and the approximations of the diffusion boundary layer in the liquid phase are applicable (see the formulation of (4.49) in 4.1.8). In this case the equality  $I_1 = I_{1Y}(Y, Z)$  (see Fig. 4.7 and the approximation (4.71)) is valid till the complete depletion of the absorbing gas from the gaseous admixture. ( $I_1 \leq 0.9\varepsilon/(1+\varepsilon)$ ). The data in Table 4.1 indicate that the increase of the pressure ( $P > 5$  atm) may transfer the absorption of a highly soluble gas  $\text{NH}_3$  ( $k_0 = 566$ ) into the area  $B$ , where the diffusion resistance is located in the gas phase.

On the other hand, the pressure decrease ( $P \leq 0.3$  atm) could move the absorption of  $\text{SO}_2$  ( $k_0 = 40$ ) into the area  $C$  (the lower right corner of the plane  $X - Y$ ). It is easy to shift the absorption of  $\text{H}_2\text{S}$  and  $\text{Cl}_2$  from the standard position to this area. The solution is simple: the relative bed height must be increased two times.

#### 4.1.12. Non-stationary interphase heat transfer

Let the heat transfer between two media with temperatures  $t'_1 = t_{10}$  and  $t'_2 = t_{20}$  be considered at  $\tau' = 0$ . If the contacting fluids are liquids or gases a thin shell will be placed between them. The shell will prevent the mixing of the fluids and its thermal resistance could be assumed zero. The corresponding heat transfer problem is (it is equivalent to (4.1)):

$$\frac{\partial t'_i}{\partial \tau'} = a_i \frac{\partial t'_i}{\partial y^2}, \quad i = 1, 2;$$

$$\begin{aligned} t'_{2S} &= t'_{IS}, \quad \lambda_1 \left( \frac{\partial t'_1}{\partial y} \right)_S = \lambda_2 \left( \frac{\partial t'_2}{\partial y} \right)_S, \\ \tau' &= 0, \quad t'_1 = t_{10}, \quad t'_2 = t_{20}, \end{aligned} \quad (4.86)$$

where  $t'_i$  - phase temperature,  $^{\circ}\text{C}$ ;  $\lambda_i$  - phase thermal conductivity,  $\text{cal}/\text{m}\cdot\text{s}^{\circ}\text{C}$ ,

$a_i = \frac{\lambda_i}{\rho_i c_{pi}}$  - phase thermal diffusivity,  $\text{m}^2/\text{s}$ ;  $\rho_i$  - density,  $\text{kg}/\text{m}^3$ ;  $c_{pi}$  - thermal capacity at constant pressure,  $\text{cal}/\text{kg}^{\circ}\text{C}$ .

The problem solution requires the definition of a dimensionless temperature  $t_i$  in accordance with the relationship:

$$t'_i = (t_{10} - t_{20})t_i + t_{20} \quad (4.87)$$

which leads to the dimensionless form (4.6) as well as the change of variables  $c_i \rightarrow t_i$ . The co-ordinates  $\tau_i$  and the parameters  $\varepsilon$  and  $\beta$  are defined as follows:

$$t'_i = \frac{b_i^2}{a_i} \tau_i, \quad \varepsilon = \frac{(\rho_2 c_{p2} b_2)}{(\rho_1 c_{p1} b_1)}, \quad \rho = \left( \frac{b_1}{b_2} \right) \sqrt{\frac{a_2}{a_1}}, \quad (4.88)$$

$$X = \lg \varepsilon = \lg \left( \frac{b_2 \rho_2 c_{p2}}{b_1 \rho_1 c_{p1}} \right), \quad Y = \lg(\varepsilon \beta) = \frac{1}{2} \lg \left( \frac{\lambda_2 \rho_2 c_{p2}}{\lambda_1 \rho_1 c_{p1}} \right).$$

The heat flux  $I'$  through the interface (during a time interval  $\tau'$ ) is:

$$\begin{aligned} I' &= -S \int_0^{\tau'} \lambda_1 \left( \frac{\partial t'_1}{\partial y} \right) d\tau' = -Sc_{p1} \rho_1 \left[ t_{01} b_1 - \int_{b_1}^{(b_1+b_2)} t'_1 dy \right] = -Sb_2 c_{p2} \rho_2 (t_{10} - t_{20}) I_1 = \\ &= -S \int_0^{\tau'} \lambda_2 \left( \frac{\partial t'_2}{\partial y} \right) d\tau' = - \left[ \int_0^{b_2} t'_2 dy - b_2 t_{02} \right] (S \rho_2 c_{p2}) = -Sb_2 \rho_2 c_{p2} (t_{10} - t_{20}) I_2. \end{aligned} \quad (4.89)$$

The dimensionless integral fluxes  $I_1$  and  $I_2$  are defined as follows:

$$I_1(X, Y, Z) = \left( 1 - \int_0^l t_1 dy_1 \right), \quad I_2(X, Y, Z) = \int_0^l t_2 dy_2. \quad (4.90)$$

The time co-ordinate  $Z$  (see (4.56)) the mass balance (4.8) and the symmetry condition (4.57) remain unchanged.

The two-phase heat transfer may occur between liquid, solid or gaseous phases. The characteristic values of the transport coefficients for several cases are summarized below in the temperature range of  $(0^{\circ} - 100^{\circ}\text{C})$  what is interesting from a practical point of view.

Table 4.2 summarizes experimentally determined values of  $\rho^T$ ,  $c_p^T$ ,  $\lambda^T$  for solids and some combinations of them[15].

Table 4.2. Experimentally defined constants for solids in the 0-100°C.

No.	Substance	$\rho^T$ , g/cm <sup>3</sup>	$c_p^T$ , cal/gr·°C	$\lambda^T$ , cal/cm·s·°C	$a^T$ , cm <sup>2</sup> /s	$\rho^T c_p^T$ , cal/cm <sup>3</sup> ·°C	$\rho^T c_p^T \lambda^T$ , cal <sup>2</sup> /cm <sup>4</sup> ·°C <sup>2</sup> ·s
1	Al	2.7	0.21	0.56	0.98	0.57	0.32
2	Fe	7.8	0.11	0.17	0.21	0.82	0.14
3	Au	11.3	0.03	0.74	2.18	0.34	0.25
4	Ag	10.5	0.56	1.00	1.70	0.59	0.59
5	Cu	8.8	0.10	0.91	1.20	0.79	0.73

Most of the gases used in the industry have high critical temperatures  $T_c$  and under ambient conditions the following inequality is satisfied  $T < T_c$  (where  $T$  is temperature in K). In the practical cases where  $T \leq (0.7)T_c$  all these gases may be assumed as ideal and:

$$\rho_g = \frac{P}{RT} \approx (44.06) \left( \frac{T_0}{T} \right) P, \quad (4.91)$$

where  $\rho_g$  - gas density, mol/m<sup>3</sup>;  $P$  - pressure, atm;  $R = 8.3 \times 10^{-5}$  gas constant, (atm·m<sup>3</sup>)/(mol·°C),  $T_0 = 273K$  is the standard temperature.

The thermal capacity of an ideal gas  $c_p^{(0)}$  may be calculated by empirical relationships:

$$c_p^{(0)} = A + BT + CT^2 \quad [\text{cal/mol} \cdot ^\circ\text{C}], \quad (4.92)$$

where the coefficients  $A, B, C$  are tabulated for many cases [13].

The heat conductivity  $\lambda^g$  is usually calculated by the relationship [2, 13]:

$$\lambda^g = \frac{c_p^{(0)} \mu_g^0}{M Pr_g}, \quad (4.93)$$

where  $\lambda^g$  and  $\mu^g$  for an ideal gas are [2, 16]:

$$\lambda^g = \frac{c_p^{(0)}}{1.3c_p^{(0)} + 0.9}, \quad \mu_g^0 = (2.67)10^{-6} \sqrt{M} \frac{\sqrt{T}}{\sigma^2 \Omega_v} \quad [\text{kg/m's}]. \quad (4.94)$$

In the above equations  $\sigma$  is a parameter of collisions,  $A^0$ ,  $\Omega_v(T^*)$  - a Scteckmayer interval,  $T^* = \frac{T}{\left(\frac{\varepsilon}{k}\right)}$  - a dimensionless temperature,  $\left(\frac{\varepsilon}{k}\right)$  - a parameter,  $K$  [13].

Table 4.3 summarizes the values of some physico-chemical constants and their combinations for widely used gases. The relationships (4.91 - 4.94) were used to calculate the values at two temperature points  $T = 273K$  (the first values in the columns) and  $T = 373K$  (the second values in the columns).

Table 4.3. Values of experimental constants for some gases (0-100°C)

No.	gas	$c_p^{(0)}$ , cal/mol·°C	$\lambda^*$ , cal/cm·s·°C	$a^*$ , cm <sup>2</sup> /s	$(\rho c_p)^*$ , cal/cm <sup>3</sup> ·°C	$(\rho c_p \lambda)^*$ , cal <sup>2</sup> /cm <sup>4</sup> ·s·°C <sup>2</sup>
1	H <sub>2</sub>	7.1 - 7.3	(4.0 - 5.2)x10 <sup>-4</sup>	(1.3-2.2).P <sup>-1</sup>	(3.1-2.35)x10 <sup>-4</sup> .P	(12.5-12.2)x10 <sup>-8</sup> P
2	O <sub>2</sub>	7.0 - 7.15	(0.6 - 0.8)x10 <sup>-4</sup>	(0.2-0.34).P <sup>-1</sup>	(3.0-2.3)x10 <sup>-4</sup> .P	(1.7-1.8)x10 <sup>-8</sup> P
3	SO <sub>2</sub>	10.1 - 11.7	(0.2 - 0.4)x10 <sup>-4</sup>	(1.1-1.54).P <sup>-1</sup>	(4.4-3.8)x10 <sup>-4</sup> .P	(1.1-1.54)x10 <sup>-8</sup> P
4	CO <sub>2</sub>	8.6 - 9.6	(0.35 - 0.5)x10 <sup>-4</sup>	(0.1-0.17).P <sup>-1</sup>	(3.8-3.1)x10 <sup>-4</sup> .P	(1.3-1.6)x10 <sup>-8</sup> P
5	CH <sub>4</sub>	8.0 - 9.3	(0.7 - 1.0)x10 <sup>-4</sup>	(0.2-0.34).P <sup>-1</sup>	(3.5-3.0)x10 <sup>-4</sup> .P	(2.5-3.0)x10 <sup>-8</sup> P
6	air	6.95 - 7	(0.6 - 0.75)x10 <sup>-4</sup>	(0.2-0.34).P <sup>-1</sup>	(3.0-2.3)x10 <sup>-4</sup> .P	(1.8-1.7)x10 <sup>-8</sup> P

The dimension of the pressure  $P$  is atmospheres (atm). Table 4.3 indicates that the change of temperature up to 100°C affects significantly most of the values.

Under standard conditions ( $P = 1$  atm,  $T = 273^0K$ ) the densities (g/cm<sup>3</sup>) of the pure liquids are the orders of unity. For example, in the case of ethyl alcohol, water, nitric acid and sulphuric acid they are [15]:

$$\rho_{C_2H_5OH} = 0.785, \quad \rho_{H_2O} = 1, \quad \rho_{HNO_3} = 1.5, \quad \rho_{H_2SO_4} = 1.8.$$

For most of the liquids the density is independent of the pressure. The temperature effects (at  $T < T_c$ ) may be calculated by Yeu-Woofs [17] relationship:

$$\rho = \rho_c \left[ 1 + K_1 \left( I - \frac{T}{T_c} \right)^{\frac{1}{3}} + K_2 \left( I - \frac{T}{T_c} \right)^{\frac{2}{3}} \right], \quad (4.95)$$

Here  $\rho_c$  is the density at the critical point, g/cm<sup>3</sup>;  $K_i$  are coefficients of the order of unity.

Of the most important (from a practical point of view) liquids the value of  $T_c$  is in the range ( $T_c \approx 500 - 700K$ ). Because of that the temperature effects on the density will be neglected in the range of  $t \approx 0 - 100^{\circ}C$ .

The thermal capacity of the liquid may be calculated with a sufficient accuracy by an empirical relationship [18]:

$$\frac{C_p - C_p^{(0)}}{R} = (0.5 + 2.2\omega) \left[ 3.67 + 11.64 \left( 1 - \frac{T}{T_c} \right)^4 + \frac{0.634}{1 - \frac{T}{T_c}} \right], \quad (4.96)$$

where  $C_p^{(0)}$  is the thermal capacity of an ideal gas ( see 4.92), cal/mol·°C,  $\omega$  is eccentricity factor of the substance [13].

The following approximation exists for the heat transfer coefficient [20]:

$$\lambda_b = \frac{(2.64) \cdot 10^{-3}}{\sqrt{M}} \left[ \frac{1 + (20/3)(1 - T/T_c)^{2/3}}{1 + (20/3)(1 - T_b/T_c)^{2/3}} \right] [\text{cal/cm}\cdot\text{s}\cdot^\circ\text{C}], \quad (4.97)$$

where  $T_b$  is the boiling point at normal conditions, K.

Equation (4.97) gives adequate results for organic liquids, but it is inapplicable for water and aqueous solutions. In the latter situations the experimental data are more reliable.

Table 4.4 summarizes the values of most of the physico-chemical coefficients of some liquids. In the cases when the equations (4.95 - 4.97) gave significant errors experimental data were used.

Table 4.4.Physico-chemical constants of some liquids (the first values are for 0°C, the second for 100°C).

No.	Liquid	$\rho_L$ , g/cm <sup>3</sup>	$(\rho C_p)_L$ , cal/cm <sup>3</sup> ·°C	$(\rho C_p \lambda)_L$ , cal <sup>2</sup> /cm <sup>4</sup> ·s·°C <sup>2</sup>	$a_L$ , cm <sup>2</sup> /s	$\lambda_L$ , cal/cm·s·°C
1.	H <sub>2</sub> O	1 - 0.96	1 - 0.96	(1.4-1.65).10 <sup>-3</sup>	(1.4-1.7).10 <sup>-3</sup>	(1.43-1.64).10 <sup>-3</sup>
2.	C <sub>2</sub> H <sub>4</sub> O <sub>2</sub> (acetic acid)	1.05	0.65 - 0.85	(0.33-0.31).10 <sup>-3</sup>	(0.78-0.44).10 <sup>-3</sup>	(0.51-0.37).10 <sup>-3</sup>
3.	C <sub>3</sub> H <sub>6</sub> O (acetone)	0.79	0.46 - 0.58	(0.2-0.19).10 <sup>-3</sup>	(0.9-0.55).10 <sup>-3</sup>	(0.41-0.32).10 <sup>-3</sup>
4.	C <sub>6</sub> H <sub>5</sub> Br (brombenzol)	1.5	0.47 - 0.63	(0.13-0.15).10 <sup>-3</sup>	(0.58-0.37).10 <sup>-3</sup>	(0.27-0.23).10 <sup>-3</sup>
5.	C <sub>7</sub> H <sub>16</sub> (n-heptane)	0.68	0.44 - 0.6	(0.14-0.16).10 <sup>-3</sup>	(0.72-0.44).10 <sup>-3</sup>	(0.32-0.26).10 <sup>-3</sup>

#### 4.1.13. Interphase heat transfer regimes

As already mentioned each of the contacting phase may be in a solid, liquid or gaseous state. Thus, the following combinations are possible:

- Two solid phases (S-S);
- Two liquid phases( L-L);
- Two gaseous phases (G-G);
- The first (second) phase is solid body, while the second (first) is a liquid (S - L) or (L - S);
- One of the phases is liquid and the second one is a gas - (L - G) or (G - L) ;

- One of the phases is solid and the second one is a gas: (S - G) or (G - S).

Let a case be considered that a heat transfer occurs, but the initial temperature difference ( $t_{01} - t_{02}$ ) does not exceed 20 - 30°C. In this case one may assume (see Tables 4.2 - 4.4) that the coefficients for each of the phases are constant. Thus, one may introduce a characteristic density as a characteristic of the regime. Moreover, the characteristics plane  $X - Y$  may be used. The values of  $X$  and  $Y$  are calculated at an average temperature  $(t_{01} + t_{02})/2$ . The pressure ( $P_i$ ) and the dimensions ( $b_i$ ) for each phase may be different. The standard heat transfer conditions are assumed as valid, i.e.  $b_1 = b_2 = 1$ ,  $P_1 = P_2 = 1$  atm. The plane  $X - Y$  will be used to define the areas of the various heat transfer regimes existing at the various combinations of the phases in contact.

Interphase heat transfer between phases with same physical conditions. In the case of a S-S heat transfer (see Table 4.2) the minimum and the maximum values of  $Y$  are achieved if a contact between Cu and Al (second phase) exists:

$$(\varepsilon\beta)_{min} = \sqrt{\frac{(\rho C_p \lambda)_{Al}}{(\rho C_p \lambda)_{Cu}}}, \quad Y_{min} = -0.2,$$

$$(\varepsilon\beta)_{max} = \sqrt{\frac{(\rho C_p \lambda)_{Cu}}{(\rho C_p \lambda)_{Al}}}, \quad Y_{max} = 0.2.$$

The corresponding values for  $X$  are :

$$\varepsilon_{min} = \frac{b_2(\rho C_p)_{Au}}{b_1(\rho C_p)_{Fe}}, \quad X_{min} = -0.2 + \lg(b_2/b_1),$$

$$\varepsilon_{max} = \frac{b_2(\rho C_p)_{Fe}}{b_1(\rho C_p)_{Au}}, \quad X_{max} = 0.2 + \lg(b_2/b_1).$$

The range of variations for  $X, Y$  in the cases (S- S), (L - L) and (G - G) are presented in Table 4.5.

Table 4.5. Ranges of possible variations of  $X$  and  $Y$ .

Combination	$Y_{min}$	$Y_{max}$	$X_{min}$	$X_{max}$
S - S	-0.2	+0.2	$-0.38 + \lg\left(\frac{b_2}{b_1}\right)$	$+0.38 + \lg\left(\frac{b_2}{b_1}\right)$
L - L	-0.5	+0.5	$-0.36 + \lg\left(\frac{b_2}{b_1}\right)$	$+0.36 + \lg\left(\frac{b_2}{b_1}\right)$
G - G	$-0.53 + 1/2 \lg\left(\frac{P_2}{P_1}\right)$	$+0.53 + 1/2 \lg\left(\frac{P_2}{P_1}\right)$	$-0.2 + \lg\left(\frac{P_2 b_2}{P_1 b_1}\right)$	$+0.2 + \lg\left(\frac{P_2 b_2}{P_1 b_1}\right)$

The limits of the areas of the heat transfer regimes under normal conditions ( $b_1 = b_2$ ,  $P_1 = P_2 = 1$  atm) are shown in Fig.4.8 (the rectangular areas  $S_1, \dots, S_4$ ,  $L_1, \dots, L_4$  and  $G_1, \dots, G_4$ ). The variations of the ratio  $b_2 / b_1$  do not affect the shape of the areas, but move them along the axis  $X$  (from left to right or vice versa). Thus, if such contacts (S-S and L-L) are possible the change of the cell size  $b_i$  may occur indifferent heat transfer regimes in the area bounded by the parallel lines  $Y = -0.2$ ,  $Y = +0.2$  and  $Y = -0.5$ ,  $Y = +0.5$  respectively.

Under the G-G heat transfer conditions an additional possibility to move the area  $G_1 \dots G_4$  along the axis  $Y$  exists due to the change of the phase pressure, so various heat transfer regimes are available in the  $X - Y$  plane.

Liquid-solid interphase heat transfer. In the case of a liquid cooling (L – S) the data in Tables 4.2 and 4.3 show, that the ranges of variations of the parameters are:

$$(\varepsilon\beta)_{min} = \sqrt{\frac{(\lambda C_p \rho)_{Fe}}{(\lambda C_p \rho)_{H_2O}}}, \quad (\varepsilon\beta)_{max} = \sqrt{\frac{(\lambda C_p \rho)_{Cu}}{(\lambda C_p \rho)_{C_6H_5Br}}},$$

$$\varepsilon_{min} = \frac{b_2(\rho C_p)_{Au}}{b_1(\rho C_p)_{H_2O}}, \quad \varepsilon_{max} = \frac{b_2(\rho C_p)_{Fe}}{b_1(\rho C_p)_{n-heptane}}.$$

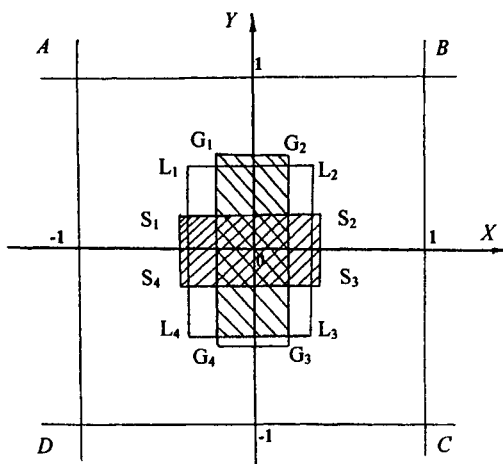


Fig. 4.8. The limits of the areas of heat transfer regimes under standard conditions.

In the case of heating of a liquid (S - L)

$$(\varepsilon\beta)_{min} = \sqrt{\frac{(\lambda C_p \rho)_{C_6H_5Br}}{(\lambda C_p \rho)_{Cu}}}, \quad (\varepsilon\beta)_{max} = \sqrt{\frac{(\lambda C_p \rho)_{H_2O}}{(\lambda C_p \rho)_{Fe}}},$$

$$\varepsilon_{min} = \frac{b_2(\rho C_p)_{n-hptane}}{b_1(\rho C_p)_{Fe}}, \quad \varepsilon_{max} = \frac{b_2(\rho C_p)_{H_2O}}{b_1(\rho C_p)_{Au}}.$$

The limits of  $X$  and  $Y$  for both cases are listed in Table 4.6.

Table 4.6. Limits of the variations of  $X$  and  $Y$  during cooling (L-S) or heating (S-L) of the liquid phase

Combinations	$Y_{min}$	$Y_{max}$	$X_{min}$	$X_{max}$
Liquid-Solid	+1	+1.9	$-0.47 + \lg\left(\frac{b_2}{b_1}\right)$	$+0.27 + \lg\left(\frac{b_2}{b_1}\right)$
Solid-Liquid	-1.9	-1	$-0.27 + \lg\left(\frac{b_2}{b_1}\right)$	$+0.47 + \lg\left(\frac{b_2}{b_1}\right)$

Under standard conditions ( $b_1 = b_2$ ) the limits are shown in Fig.4.9. It is clear that during the cooling of the liquid (L - S) the change of the cell size may create various heat transfer regimes in the range  $1 < Y < 1.9$  above the line  $AB$ . In that area (see 4.1.5) the lateral variations of the second phase temperature may be neglected ( $t_s \approx t_2$ ).

During liquid heating the phases allow heat transfer regimes inside the band  $-1.9 \leq Y \leq -1$  located above the line  $CD$ . In this case (see (4.1.6) the temperature variations of the first phase may be neglected ( $t_s \approx t_1$ ). In the two cases discussed the phase with negligible temperature variations is a metal. This may be attributed to the higher thermal conductivity of the metal compared to the liquids.

Interphase heat transfer when one of the phases is a gas. In the case of heating of the gas phase (L-G, S-G) the limits of the possible regimes are listed in Table 4.7. Figure 4.10 shows the areas defined by the standard conditions ( $b_1 = b_2$ ,  $P_2 = 1 \text{ atm}$ ). Both areas are located in the lower left corner  $D$  of the characteristic plane  $X - Y$ . This indicates that the heat transfer resistance is located in the second phase only. The temperature at the interface is  $t_s \approx t_1 \approx 1$  (see 4.1.3).

Cooling of the gas phase (G - L and G - S). In this case the possible regimes under standard conditions ( $b_1 = b_2$ ,  $P_2 = 1 \text{ atm}$ ) exist in the upper right corner  $B$  of the characteristics plane  $X - Y$  (see Table. 4.7 and Fig. 4.10). Moreover, the interphase heat transfer resistance is located in the first phase only. The temperature at the interface is  $t_s \approx t_2 \approx 0$  (see 4.1.3).

The examples discussed above show that when heating (cooling) a gas under normal conditions the gas phase limits the interphase heat transfer. That fact may be attributed to the low gas thermal conductivity and density. However, Table 4.7 indicates that at different cell sizes and the gas pressures various heat transfer regimes are possible for all system commented above.

Table 4.7. Limits of the heat transfer regimes

Combination	$Y_{min}$	$Y_{max}$	$X_{min}$	$X_{max}$
L - Gr	$-2.5 + \frac{1}{2} \lg P_2$	$-1.5 + \frac{1}{2} \lg P_2$	$-3.6 + \lg \left( \frac{b_2 P_2}{b_1} \right)$	$-3 + \lg \left( \frac{P_2 b_2}{b_1} \right)$
S - L	$-4 + \frac{1}{2} \lg P_2$	$-3 + \frac{1}{2} \lg P_2$	$-3.5 + \lg \left( \frac{b_2 P_2}{b_1} \right)$	$-3 + \lg \left( \frac{b_2 P_2}{b_1} \right)$
G - L	$1.5 - \frac{1}{2} \lg P_1$	$2.5 - \frac{1}{2} \lg P_1$	$3 + \lg \left( \frac{b_2}{b_1 P_1} \right)$	$3.6 + \lg \left( \frac{b_2}{b_1 P_1} \right)$
G - S	$3 - \frac{1}{2} \lg P_1$	$4 - \frac{1}{2} \lg P_1$	$3 + \lg \left( \frac{b_2}{b_1 P_1} \right)$	$3.5 + \lg \left( \frac{b_2}{b_1 P_1} \right)$

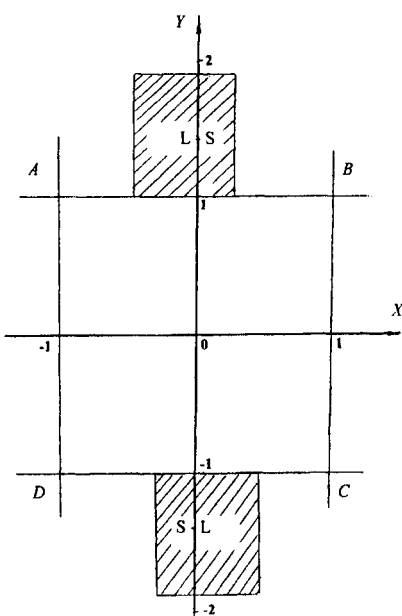


Fig. 4.9. The limits of the areas of the heat transfer regimes under normal conditions for L-S.

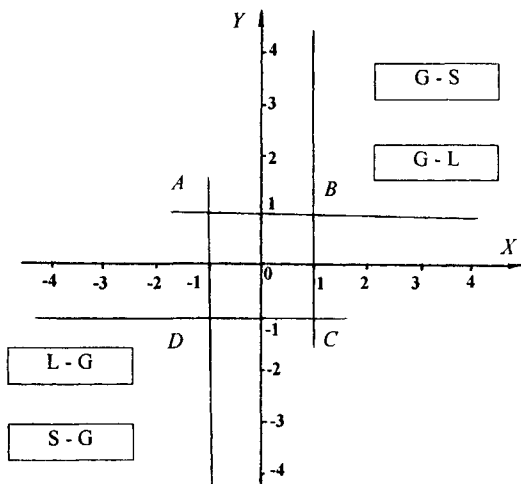


Fig. 4.10 The limits of the areas of the heat transfer regimes under normal conditions for (L - G), (S - G) heating and (G - L), (G - S) cooling.

## CHAPTER 4.2. NON-STATIONARY TWO-PHASE ABSORPTION COMPLICATED WITH FIRST ORDER CHEMICAL REACTION

The enhancement of gas admixture cleaning in laboratory scale usually is due to the use of chemical sorbent instead of pure water [1,19,20]. The commonly used vessels are vertical (see Fig.4.1). In this case the absorbed component *A* reacts with the absorbent. The common approach for creation of the model of such absorption process is to apply the idea of two additive diffusion resistances located in both phases [20]. The model usually calculates the augmentation coefficients in the liquid [20]. The common approach in theoretical studies on chemosorption [3,4] is to assume that the whole mass transfer resistance is located in the liquid phase.

Here a contemporary approach based on two-phase chemosorption processes is developed. The model includes differential equations for the gaseous (first) and the liquid (second) phase accounting the real chemical reactions in the liquid. The conditions describing the conjunction of the fluxes and the concentrations at the interface close the model [21, 22]. Moreover, in the case of a fast chemical reaction and short contact times the mass transfer in the liquid phase is independent of the convective transport.

Let the simpler case of an irreversible chemical reaction of first order in the liquid phase be considered:

$$A \rightarrow C, \quad (4.98)$$

where  $C$  is the reaction yield. The chemical reactions of this type occur very often in the chemical technology. For example the  $\text{CO}_2$  interaction with carbonate-bicarbonate buffer solutions (where the concentrations of the  $\text{CO}_3^{2-}$  and the  $\text{HCO}_3^-$  ions remain constant) may be considered as first order chemical reaction [23]. Similar situations exist in alcohol solutions with high alcohol concentrations as well as in primary amines solutions at small contact times [24]. Similar examples may be discussed for other liquids [25-28]. The problem development requires new algorithms for the mass transfer models considering first order chemical reactions in the liquid phase [29].

The following equations describing the mass transfer of  $A$  in both phase and the reaction yield  $C$  in the liquid build up the model (see also Fig. 4.1):

$$\frac{\partial c'_1}{\partial \tau'} = D_1 \frac{\partial^2 c'_1}{\partial y^2}, \quad \frac{\partial c'_2}{\partial \tau'} = D_2 \frac{\partial^2 c'_2}{\partial y^2} - \bar{k}_1 c'_2, \quad \frac{\partial c'}{\partial \tau'} = D_2 \frac{\partial^2 c'}{\partial y^2} + \bar{k}_1 c'_2,$$

where  $c'_i$  are the concentration of  $A$  in the gas ( $i = 1$ ) and the liquid ( $i = 2$ ), (mol/l);  $c'$  - the concentration in the liquid, (mol/l);  $D$  - diffusivity, ( $\text{m}^2/\text{s}$ )  $y$  - the vertical co-ordinate, (m);  $\tau'$  - time, (s);  $\bar{k}_1$  - the constant of the forward reaction, ( $\text{s}^{-1}$ ).

For simplicity of explanation equal diffusivities of both reagents in the liquid are assumed. Assuming that  $C$  is a non-volatile component, new conditions should be added to the model:

$$D_2 \left( \frac{\partial c'_2}{\partial y} \right)_s = D_1 \left( \frac{\partial c'_1}{\partial y} \right)_s, \quad \left( \frac{\partial c'}{\partial y} \right)_s = 0, \quad c'_{2s} = k c'_{1s} \quad \text{at } y = b_1; \\ \left( \frac{\partial c'}{\partial y} \right) = \left( \frac{\partial c'_2}{\partial y} \right) = 0 \quad \text{at } y = 0; \quad \frac{\partial c'_1}{\partial y} = 0 \quad \text{at } y = b_1 + b_2; \\ c'_1 = c_0, \quad c'_2 = c' = 0 \quad \text{at } \tau' = 0.$$

The dimensionless longitudinal ( $y_i$ ) and time ( $\tau_i$ ) co-ordinates are (Fig. 4.1):

$$y = (b_1 + b_2) - b_1 y_1 = b_2 y_2, \quad \tau' = \frac{b_i^2}{D_i} \tau_i, \quad i = 1, 2, \quad (4.99)$$

while the dimensionless concentrations  $c_1$ ,  $c_2$ , and  $c$  have the following:

$$c'_1 = c_0 c_1(\tau_1, y_1), \quad c'_2 = k c_0 c_2(\tau_2, y_2), \quad c' = k c_0 c(\tau_2, y_2). \quad (4.100)$$

The dimensionless form of the two-phase chemosorption problem is:

$$\frac{\partial c_1}{\partial \tau_1} = \frac{\partial^2 c_1}{\partial y_1^2}, \quad \frac{\partial c_2}{\partial \tau_2} = \frac{\partial^2 c_2}{\partial y_2^2} - a^2 c_2, \quad \frac{\partial c}{\partial \tau_2} = \frac{\partial^2 c}{\partial y_2^2} + a^2 c_2. \quad (4.101)$$

$$\begin{aligned} \left( \frac{\partial c_2}{\partial y_2} \right)_s &= - \left( \frac{1}{\varepsilon \beta^2} \right) \left( \frac{\partial c_1}{\partial y_1} \right)_s, \quad c_{1s} = c_{2s}, \quad \left( \frac{\partial c}{\partial y_2} \right)_s = 0, \quad \text{at } y_2 = y_1 = 1; \\ \left( \frac{\partial c_1}{\partial y_1} \right) &= 0 \quad \text{at } y_1 = 0; \quad \left( \frac{\partial c_2}{\partial y_2} \right) = \left( \frac{\partial c}{\partial y_2} \right) = 0 \quad \text{at } y_2 = 0; \\ c_1 &= 1, \quad c = c_2 = 0 \quad \text{at } \tau_1 = 0, \end{aligned} \quad (4.102)$$

where the parameters  $\varepsilon = k \frac{b_2}{b_1}$  and  $\beta^2 = \frac{b_1^2}{D_1} \frac{D_2}{b_2^2}$  are the liquid capacity and the dimensionless ratio of the phase dimensions, respectively. They were introduced earlier for the cases of the two-phase physical absorption (equations (4.7) in 4.1); the parameter  $a^2 = \vec{k}_1 \frac{b_2^2}{D_2}$  is the Damkohler number [1] for a stagnant liquid.

The two-phase chemosorption problem formulated above has been solved in [30] by the separation variables method. At a chemical reaction rate constant turned to  $K \equiv \frac{\vec{k}_1}{\vec{k}_2}$  infinity ( $\vec{k}_2$  - the rate constant of the backward reaction (4.98),  $s^{-1}$ ) it is easy to obtain the solution of (4.101-4.102):

$$I \equiv (1 - \bar{c}_1) = 1 - \varepsilon \sum_{z < a} \frac{2 \exp(\lambda \tau')}{S_1(z)} - \varepsilon \sum_{z > a} \frac{2 \exp(\lambda \tau')}{S_2(z)}, \quad (4.103)$$

$$\bar{c}_2 = \sum_{z < a} \frac{2 \left( \frac{z^2}{a^2 - z^2} \right)}{S_1(z)} \exp(\lambda \tau') - \sum_{z > a} \frac{2 \left( \frac{z^2}{z^2 - a^2} \right)}{S_2(z)} \exp(\lambda \tau'), \quad (4.104)$$

$$c_{1s} = \varepsilon \sum_{z < a} \frac{2r \operatorname{ctg}(r)}{S_1(z)} \exp(\lambda \tau') + \varepsilon \sum_{z > a} \frac{2r \operatorname{ctg}(r)}{S_2(z)} \exp(\lambda \tau'), \quad (4.105)$$

where the dash over the symbols means average values and  $\lambda \tau'$ ,  $r$ ,  $S_1(z)$  and  $S_2(z)$  have the forms :

$$\lambda \tau' = -z^2 \tau_2 - r^2 \tau_1, \quad r = \beta z,$$

$$S_1(z) = \varepsilon r^2 + \varepsilon(r \operatorname{ctg}(r))^2 + \varepsilon r \operatorname{ctg}(r) + \left[ \operatorname{cth}^2(\sqrt{a^2 - z^2}) - 1 + \frac{\operatorname{cth}(\sqrt{a^2 - z^2})}{\sqrt{a^2 - z^2}} \right] \frac{z^4}{a^2 - z^2},$$

$$S_2(z) = \varepsilon r^2 + \varepsilon(r \operatorname{ctg}(r))^2 + \varepsilon r \operatorname{ctg}(r) + \left[ \operatorname{ctg}^2(\sqrt{z^2 - a^2}) + 1 + \frac{\operatorname{ctg}(\sqrt{z^2 - a^2})}{\sqrt{z^2 - a^2}} \right] \frac{z^4}{z^2 - a^2}.$$

The eigenvalues  $z$  (or  $r$ ) are calculated from the characteristic equations:

$$\begin{aligned}\varepsilon\beta ctg(r) &= \frac{z}{\sqrt{a^2 - z^2}} \operatorname{cth}(\sqrt{a^2 - z^2}), \quad z < a; \\ \varepsilon\beta ctg(r) &= -\frac{z}{\sqrt{z^2 - a^2}} \operatorname{ctg}(\sqrt{z^2 - a^2}), \quad z > a.\end{aligned}\quad (4.106)$$

Three special solutions are known. The first is the well-known Danckwerts equation [31] concerning the case of interphase mass transfer with a diffusion resistance located in the liquid phase ( $c_{ls} \approx 1$ ) and short contact times ( $b_2 \rightarrow \infty$ ):

$$I_{Dan} = \left( \frac{\varepsilon}{a} \right) \left\{ \operatorname{erf}(\sqrt{a^2 \tau_2}) (a^2 \tau_2 + 1/2) + \frac{\sqrt{a^2 \tau_2}}{\sqrt{\pi}} \exp(-a^2 \tau_2) \right\}. \quad (4.107)$$

For small and large values of the independent variable argument in (4.107) it is possible to obtain well-known asymptotic solutions for physical absorption and fast chemical reaction, respectively [3, 4]:

$$I_{Dan} = \begin{cases} 2\varepsilon \sqrt{\frac{\tau_2}{\pi}} & (\tau_2 \ll 1/a^2); \\ (\varepsilon a) \tau_2 & (\tau_2 \gg 1/a^2). \end{cases} \quad (4.108)$$

The second solution concerns a slow chemical reaction with a constant rate over the whole liquid layer depth:

$$I^{seon} = I^{abs} + [1 - \exp(-\varepsilon a^2 \tau_2)], \quad (4.109)$$

Here  $I^{abs}$  is the dimensionless flux of the two-phase physical absorption.

The third solution corresponds to regime of maximum absorption where the surface concentration  $c_{ls} \approx 0$ , so the mass transfer resistance is totally located in the gas phase [32]:

$$I^{max} = 1 - \sum \frac{2}{\pi^2 (n+1/2)^2} \exp[-\pi^2 (n+1/2)^2 \tau_1]. \quad (4.110)$$

The conditions allowing the applications of these equations may be obtained through a theoretical analysis of the general problem (4.101-4.102) only. From a formal point of view it should be accepted that the solution is dependent on three dimensionless parameters:  $\varepsilon$ ,  $\varepsilon\beta$  and  $a^2$ . The first two parameters are related to the absorption process (already introduced in 4.1). The third parameter  $a^2$  will be termed here a chemosorption parameter, because it contains the rate constant  $\bar{k}_1$ .

At  $a = 0$  the problem (4.101-4.102) becomes a two-phase absorption problem. The further graphical treatment will be carried out in the absorption plane  $X - Y$  (Fig. 4.2):

$$X \equiv \lg(\varepsilon), \quad Y = \lg(\varepsilon\beta). \quad (4.111)$$

At every point in that plane the value  $a^2$  vary from zero to infinity.

In the next section the general solution (4.102) will be used to obtain relationships for further study of the chemical reaction rate effect on the absorption process. This will allow the build up of a generalized methodology for two-phase chemosorption design.

#### 4.2.1. Solution in $X-Y$ plane at $\varepsilon \ll 1, \varepsilon\beta \ll 1$

In the considered case the interphase mass transfer is concentrated in the liquid phase. For clarity of explanation the case of  $\beta^2 = 1$  will be developed. At small Damkohler numbers ( $a \ll 1$ ) the expansion of  $\text{ctg}(z)$  and  $\text{ctg}(\sqrt{a^2 - z^2})$  (at  $z < a$ ) in the characteristic equation (4.106) leads to the approximation  $z_1^2 = a^2\varepsilon$  of the first root. Thus:

$$S_1(z) \approx \varepsilon z + (z \text{ctg}(z))^2 + \varepsilon z \text{ctg}(z) + 2 \left( \frac{z^2}{a^2 - z^2} \right) \approx 2\varepsilon.$$

The roots  $z > a$  are located close to the sequences  $z_k = \pi(k + 1/2)$  and  $z_n = \pi n$  ( $n = 1, 2, \dots$ ,  $k = 0, 1, 2, \dots$ ). They may be obtained through an expansion of  $\text{ctg}(z)$  and  $\text{ctg}(\sqrt{z^2 - a^2})$  close to these points:

$$\Delta z_k \equiv z_k - \pi(k + 1/2) = a^2 / 2\pi(k + 1/2),$$

$$\Delta z_n \equiv z_n - \pi n = a^2\varepsilon / 2\pi n.$$

The functions  $S_2(z)$  may be simplified as :

$$S_2^k = \varepsilon z^2 + \varepsilon(1 + \varepsilon)(z \text{ctg}z)^2 + z^2 = (1 + \varepsilon)z_k^2 [1 + \varepsilon(\Delta z_k)^2] = z_k^2$$

$$S_2^n = (1 + \varepsilon)z^2 (1 + \varepsilon \text{ctg}^2 z) = (1 + \varepsilon)\varepsilon(z_n \text{ctg}z_n)^2 = \varepsilon z_n^2 / \Delta z_n^2.$$

The substitution of these approximations in (4.105) shows that in  $I(\tau)$  the terms proportional to  $z_n$  are small (with an equally distributed accuracy), while in the relationship for  $c_s$  (4.105) the major contribution belongs to the first root  $z_1$ . In this case

$$I(\tau) = [1 - \exp(-\varepsilon a^2 \tau_1)] + \varepsilon \left\{ 1 - \sum_{k=0}^{\infty} \frac{2}{\pi^2 (k + 1/2)^2} \exp[-\pi^2 (k + 1/2)^2 \tau_2] \right\} =$$

$$= [1 - \exp(-P \tau_1)] + I^{abs}(\tau_2),$$

$$c_{1s} = \exp(-P \tau_1), \quad (4.112)$$

where  $I^{abs}$  is the solution of the absorption problem in the defined area and  $P = \varepsilon a^2$  is a parameter.

At large Damkohler numbers ( $a \gg 1$ ) the solution depends on the product  $\varepsilon a$  and can be obtained for small and large values of this parameter. When  $\varepsilon a \ll 1$  among all the roots satisfying the condition  $z < a$  the principle role plays the first root  $z_1^2 = \varepsilon a$ , so :

$$S_1(z_1) = 2\varepsilon.$$

At  $z > a$  the difference between the roots of the characteristic equation (4.106) is  $\Delta z = 1/a \ll 1$ . By introduction of new variable  $y$ , where  $z = \sqrt{a^2 + y^2}$ ,  $y = \pi k$ ,  $k = 1, 2, \dots$  and the expression the  $S_2(z)$  through  $y$  one is obtained:

$$S_2(z) = \varepsilon z^2 \left[ ctg^2(z) + \frac{\frac{1}{\varepsilon} z^2}{z^2 - a^2} \right] = \frac{z^4}{z^2 - a^2} = \frac{(a^2 + y^2)^2}{y^2}.$$

Equations (4.103- 4.105) will be rewritten in the form:

$$I(\tau) = I - \exp(-z_1^2 \tau_2) - \sum_y \frac{2\varepsilon y^2}{(y^2 + a^2)^2} \exp(-y^2 \tau_2) \exp(-a^2 \tau_2),$$

$$c_{1s} = \exp(-z_1^2 \tau_2).$$

The substitution of the summation with respect to the discrete  $y$  by an integration with respect  $t = \frac{y}{a} = \frac{\pi k}{a}$  ( $dt = \frac{\pi}{a} \ll 1$ ) allows the  $I(\tau)$  to be expressed as :

$$I(\tau) = [I - \exp(\varepsilon a \tau_1)] + \left( \frac{1}{2} \frac{\varepsilon}{a} \right) \left\{ I - \frac{4}{\pi} \left[ \sum_y \frac{\left( \frac{y}{a} \right)^2 \frac{\pi}{a}}{\left( 1 + \frac{y^2}{a^2} \right)^2} \exp[-(a^2 \tau_2)(y/a)^2] \right] \exp(-a^2 \tau_2) \right\} =$$

$$= [I - \exp(-\varepsilon a \tau_1)] + \left( \frac{1}{2} \frac{\varepsilon}{a} \right) \left\{ I - \left[ \frac{4}{\pi} \int_0^\infty \frac{t^2 \exp(-a^2 \tau_2 t^2)}{(1+t^2)^2} dt \right] \exp(-a^2 \tau_2) \right\}.$$

The integral in the brackets can be expressed by means of the well-known functions [35]:

$$\frac{1}{2} \left( \frac{\varepsilon}{a} \right) \left\{ I - \left[ \frac{4}{\pi} \int_0^\infty \frac{t^2 \exp(-a^2 \tau_2) t^2}{(1+t^2)^2} dt \right] \exp(-a^2 \tau_2) \right\} =$$

$$= \left( \frac{\varepsilon}{a} \right) \left\{ \operatorname{erf} \left( \sqrt{a^2 \tau_2} \left( a^2 \tau_2 + \frac{1}{2} \right) \right) + \frac{\sqrt{a^2 \tau_2}}{\sqrt{\pi}} \exp(-a^2 \tau_2) - a^2 \tau_2 \right\}. \quad (4.113)$$

The comparison of (4.113) and (4.107) allows the solution at  $a\varepsilon \ll I$  to be developed as :

$$I(\tau) = [I - \exp(-P\tau_1)] + \left[ \frac{I_{\text{Dan}}}{a^2 \tau_2} - (\varepsilon a) \tau_2 \right],$$

$$c_{1s} = \exp(-P\tau_1), \quad (4.114)$$

where  $I_{\text{Dan}}$  is the classical Danckwerts solution and  $P = \varepsilon a \ll I$  is a parameter.

The solution at  $\varepsilon a \gg I$  and  $z < a$  cannot be confined to one root only, i.e.

$$z = \pi(k + 1/2), \quad k = 0, 1, \dots; \quad S_i(z) = \varepsilon z^2 \frac{1+z^2}{\varepsilon^2(a^2-z^2)}.$$

The roots available at  $z > a$  remain without changes. The summation of the derivatives  $(-\frac{dc_i}{d\tau_2})$  gives:

$$\begin{aligned} \left( -\frac{dc_i}{d\tau_2} \right) &= \sum_{z < a} \frac{2 \exp(-z^2 \tau_2)}{1 + \left( \frac{z}{\varepsilon a} \right)^2} + \sum_{z > a} \frac{2\varepsilon y^2}{(y^2 + a^2)} \exp[-(a^2 + y^2)\tau_2] = \\ &= (\varepsilon a) \left\{ \frac{2}{\pi} \int_0^\infty \frac{\exp[-(\varepsilon a)^2 \tau_2 t^2]}{1+t^2} dt \right\} + \\ &+ (\varepsilon a) \left\{ \frac{2}{\pi} \int_0^\infty \frac{t^2 \exp[-(a^2 \tau_2)t^2]}{1+t^2} dt \right\} \exp(-a^2 \tau_2). \end{aligned}$$

Here at  $z < a$  the variable is  $t = \frac{\pi(k + 1/2)}{\varepsilon a}$ , while at  $z > a$ ,  $t = \frac{\pi k}{a}$ .

The dimensionless flux  $I(\tau)$  can be obtained by an integration of  $\frac{dc_i}{d\tau_2}$  with respect to the time  $\tau_2$  under the condition  $\bar{c}_i(0) = 1$ :

$$I(\tau) = (\varepsilon a) \left\{ \frac{2}{\pi} \int_0^\infty \frac{1 - \exp[-(\varepsilon a)^2 \tau_2 t^2]}{(\varepsilon a)^2 t^2 (1+t^2)} dt \right\} +$$

$$+ \left( \frac{I}{2} \frac{\varepsilon}{a} \right) \left\{ I - \left[ \frac{4}{\pi} \int_0^\infty \frac{t^2 \exp[-(a^2 \tau_2)t^2]}{(1+t^2)^2} dt \right] \exp(-a^2 \tau_2) \right\}.$$

Both integrals in brackets can be expressed by the error function [11]. The first integral for example is expressed as:

$$P \left\{ \frac{2}{\pi} \int_0^\infty \frac{1 - \exp[-(P^2 \tau)t^2]}{P^2 t^2 (1+t^2)} dt \right\} = \frac{I}{P} \left\{ \frac{2}{\sqrt{\pi}} \sqrt{P^2 \tau} - [I - \exp(P^2 \tau)] \operatorname{erfc}(\sqrt{P^2 \tau}) \right\}. \quad (4.115)$$

The second integral was derived earlier (see (4.113)).

In this way the solution at  $\varepsilon a \gg I$  can be expressed in the form:

$$\begin{aligned} I(\tau) &= \frac{I}{P} \left[ \frac{2}{\sqrt{\pi}} \sqrt{P^2 \tau_1} - [I - \exp(-P^2 \tau_1)] \operatorname{erfc}(\sqrt{P^2 \tau_1}) \right] + [I_{D_{an}}(a^2 \tau_2) - \varepsilon a], \\ c_{ls} &= \frac{2}{\sqrt{\pi}} \int_0^\infty \frac{\exp[-(P^2 \tau_1)^2 t^2]}{1+t^2} dt, \end{aligned} \quad (4.116)$$

where  $P = a\varepsilon \gg I$ . The result for  $c_{ls}$  needs a summation in (4.105) like in the case of  $\left( \frac{dc_1}{d\tau_2} \right)$ .

It should be noted that the dimensionless flux  $I(\tau)$  is a sum of two groups of terms in all the cases discussed above: terms corresponding to  $z < a$  and  $z > a$  (4.101, 4.102). It is easy to show that at  $\tau_2 \gg 1/a^2$  the first terms are slightly greater than the second ones. Further, the process description for various areas of  $X - Y$  will be developed using the final results without making the intermediate calculations.

#### 4.2.2. Solution in the area with $\varepsilon \gg I$ , $\varepsilon \beta \ll 1$

In the area where the inequality

$$\frac{I}{\varepsilon^2} \ll \frac{I}{a^2} \quad (4.117)$$

is satisfied with equal accuracy with respect the time  $\tau$  (the lower right corner in Fig.4.2) the following relationships are valid

$$\begin{aligned} I(\tau) &= I - \exp(-\varepsilon^2 \tau_2) \operatorname{erfc}(\sqrt{\varepsilon^2 \tau_2}) = I^{abs}(\tau), \\ c_{ls} &= \exp(-\varepsilon^2 \tau_2) \operatorname{erfc}(\sqrt{\varepsilon^2 \tau_2}) = c_{ls}^{abs}(\tau). \end{aligned} \quad (4.118)$$

The relationship (4.118) is the solution of the absorption problem in the area  $D$  (see equation (4.51)). Obviously, with such weak reactions the depletion of the gas phase occurs due to the physical absorption because at  $\tau_2 \gg \frac{I}{\varepsilon^2}$  the flux  $I^{abs} \rightarrow I$ .

At sufficiently large values of  $a^2$ , and preferably when the inequality

$$\frac{I}{a^2} \ll \frac{I}{\varepsilon^2} \quad (4.119)$$

takes place the yields are the relationships (4.114) and (4.116) with a parameter

$$P = \varepsilon a \beta^2. \quad (4.120)$$

In this case the parameter  $P$  in (4.114) is  $P \ll 1$ , while in (4.116) -  $P \gg 1$ .

#### 4.2.3. Solution at $\varepsilon \gg 1$ and $\varepsilon \beta \gg 1$

It was demonstrated in chapter 4.1 that in the area considered (the upper right corner of Fig. 4.2) under the conditions of a physical absorption  $c_{ls} \ll 1$ . The solution may be obtained for the gas phase only with a boundary condition at the interface  $c_{ls} = 0$ . This is the regime of the maximal absorption and the corresponding flux is  $I = I^{max}(\tau_i)$  (4.110). When a chemisorption is carried out ( $a > 0$ ) this regime remains too. From a physical point of view the irreversible chemical reaction can make the inequality  $c_{ls} \ll 1$  stronger. Consequently, one may assume that for every  $a > 0$  the interphase mass transfer resistance is located in the gas phase only.

#### 4.2.4. Solution in the area with $\varepsilon \ll 1$ , $\varepsilon \beta \gg 1$

In this case (the upper left corner of Fig. 4.2) for various Damkohler numbers (or  $\frac{I}{a^2}$ ) it is possible to derive analytical solutions. For example, if the inequality

$$(\varepsilon \beta)^2 \ll \frac{I}{a^2} \quad (4.121)$$

takes place, the corresponding solution is:

$$I(\tau) = [I - \exp(-P\tau_i)] + \varepsilon \left\{ 1 - \exp\left(\frac{-\tau_i}{\varepsilon^2}\right) \operatorname{erfc}\left(\frac{\sqrt{\tau_i}}{\varepsilon}\right) \right\} = [I - \exp(-P\tau_i)] + I^{abs}(\tau),$$

$$c_{ls} = \exp(-P\tau_i) - \exp\left(\frac{-\tau_i}{\varepsilon^2}\right) \operatorname{erfc}\left(\frac{\sqrt{\tau_i}}{\varepsilon}\right), \quad (4.122)$$

with a parameter  $P$ :

$$P = \varepsilon \beta^2 a^2 \ll 1. \quad (4.123)$$

is valid.

If under the conditions (4.121) the parameter  $P \gg I$  the corresponding relationships are valid:

$$\begin{aligned} I(\tau) &= P \int_0^\infty \frac{1 - \exp[-(P^2 \tau_I)t^2]}{P^2 t^2 (1 + t^2)} dt + \varepsilon \left\{ 1 - \exp\left(-\frac{\tau_I}{\varepsilon^2}\right) \operatorname{erfc}\left(\frac{\sqrt{\tau_I}}{\varepsilon}\right) \right\} = \\ &= \frac{I}{P} \left\{ \frac{2}{\sqrt{\pi}} \sqrt{P^2 \tau_I} - [1 - \exp(-P^2 \tau_I)] \operatorname{erfc}\left(\sqrt{P^2 \tau_I}\right) \right\} + I^{abs}(\tau), \\ c_{ls}(\tau) &= \frac{2}{\pi} \int_0^\infty \frac{\exp[-(P^2 \tau_I)t^2]}{1 + t^2} dt - \exp\left(-\frac{\tau_I}{\varepsilon^2}\right) \operatorname{erfc}\left(\frac{\sqrt{\tau_I}}{\varepsilon}\right). \end{aligned} \quad (4.124)$$

It is evident, that the curve  $c_{ls}(\tau)$  has maxima equal to unity in both cases. In the range where  $\tau = \varepsilon^2$  the concentration rises from zero to unity and after that decreases to zero again.

In the first case (4.122) the maximum occurs at  $\tau_I \approx \frac{I}{P} \gg I$ , while in the second case (4.123) at  $\tau_I \approx \frac{I}{P^2} \ll I$ .

When the inequality

$$\frac{I}{a^2} \ll (\varepsilon \beta)^2 \quad (4.125)$$

is valid, the regime of the maximum absorption exists. The corresponding maximum flux is:

$$I = I^{max}(\tau_I), \quad c_{ls} \ll 1.$$

It is interesting to mention that in the case (4.125) the shape of the curve  $c_{ls}(\tau)$  depends on  $a^2$ . For example, at  $a^2 \ll I$ :

$$c_{ls}(\tau) = \frac{1}{(\varepsilon \beta) a} \left[ \frac{2}{\pi} \int_0^1 \frac{\exp[(a^2 \tau_2)t^2]}{1 - t^2} dt - \frac{2}{\pi} \int_1^\infty \frac{\exp[-(a^2 \tau_2)t^2]}{t^2 - 1} dt \right]. \quad (4.126)$$

The above function has a maximum  $c_{ls}^{max} \approx \frac{1}{\varepsilon \beta a} \ll 1$  at  $\tau_2 \approx \frac{I}{a^2}$ . Further,  $\tau_2 \gg \frac{I}{a^2}$

approaches zero.

Finally, at  $a^2 \gg I$  the following analytical relationship is the result:

$$c_{ls}(\tau) = \left( \frac{I}{\varepsilon \beta} \right) \left[ \frac{2}{\pi} \int_0^\infty \frac{\exp[-(a^2 \tau_2)t^2]}{\sqrt{1-t^2}} dt \right]. \quad (4.127)$$

The function is monotonous and varies from  $\frac{I}{\varepsilon \beta} \ll I$  at  $\tau_2 = 0$  down to zero at  $\tau_2 \gg \frac{I}{a^2}$ .

#### 4.2.5. Solution at $\beta^2 = 1$

The solution on the line DB corresponding to the condition  $\beta^2 = 1$  is available in an analytical form if the values of  $a^2$  are sufficiently small, i.e.

$$I \ll \frac{1}{a^2}. \quad (4.128)$$

and the solution can be expressed as :

$$\begin{aligned} I(\tau) &= \left( \frac{I}{1+\varepsilon} \right) \left[ 1 - \exp\left(-\frac{\varepsilon a^2}{1+\varepsilon} \tau_1\right) \right] + \left( \frac{\varepsilon}{1+\varepsilon} \right) \left\{ I - \sum_{k=0}^{\infty} \frac{2}{\pi^2 \left( k + \frac{I}{2} \right)^2} e^{-\pi^2 \left( k + \frac{I}{2} \right)^2 \tau_2} \right\} = \\ &= \left( \frac{I}{1+\varepsilon} \right) \left[ 1 - \exp\left(-\frac{\varepsilon a^2}{1+\varepsilon} \tau_1\right) \right] + I^{abs}(\tau), \\ c_{ls} &= \exp \frac{-\frac{\varepsilon a^2}{1+\varepsilon} \tau_1}{1+\varepsilon}. \end{aligned} \quad (4.129)$$

#### 4.2.6. Common properties of the solutions

The analysis of the solutions developed (see Chapters 4.1 and 4.2) in various particular cases allows several generalizing conclusions:

Characteristic time intervals. The term *characteristic time*  $\tau^{abs}$  was introduced in the case of a two-phase absorption discussed earlier. In co-ordinates  $\tau_1$  and  $\tau_2$  -  $\tau_1^{abs}$  and  $\tau_2^{abs}$  the characteristic time  $\tau^{abs}$  corresponds to the moment when the dimensionless flux  $I^{abs}(\tau)$  reaches (within the accuracy set for calculations) its limit value equal to  $\frac{\varepsilon}{1+\varepsilon}$ . The order of  $\tau_i^{abs}$  ( $i=1,2$ ) can be determined by using (4.70) (see chapter 4.1 and Fig. 4.5) or simpler relationships:

$$\begin{aligned}\tau_1^{abs} &= \left(1 + \frac{1}{\varepsilon \beta}\right)^2 && \text{at } X > 0; \\ \tau_2^{abs} &= (1 + \varepsilon \cdot \beta)^2 && \text{at } X < 0.\end{aligned}\quad (4.130)$$

Together with  $\tau^{abs}$  for the purposes of the analysis of chemical reacting systems [21, 22] a characteristic time  $\tau^{chem}$  ( $\tau_1^{chem}$ ,  $\tau_2^{chem}$ ) is employed. It corresponds to the time enough to detect the effect of the chemical reaction, i.e. the moment when  $I(\tau)$  becomes greater than  $I^{abs}(\tau)$ . It is easy to detect that (see the equations in 4.2.1-4.2.4) in cases discussed above (despite of the  $X, Y, a^2$ ) the orders of these characteristic times are:

$$\tau_1^{chem} = \frac{1}{A^2}, \quad \tau_2^{chem} = \frac{1}{a^2}, \quad A^2 = \beta^2 \alpha^2. \quad (4.131)$$

The latter relationships follow from the mass balance that may be expressed as:

$$I(\tau) = \varepsilon \left( c_2 + a^2 \int_0^{\tau} c_2 d\tau_2 \right). \quad (4.132)$$

In the case of irreversible chemical reactions additional characteristic time is usually introduced. The time  $\tau^{max}$  ( $\tau_1^{max}$ ,  $\tau_2^{max}$ ) corresponds to the time when  $\tau \geq \tau^{max}$  and the concentration  $c_{ls}(\tau)$  is practically zero (see (4.105)) so the regime of maximum absorption is established in the system (4.110).

Obviously, in the general case:

$$\tau^{max} \geq \tau^{chem}. \quad (4.133)$$

Shape of the curve  $c_{ls}(\tau)$  during a chemosorption. The shape depends on the function  $c_{ls}^{abs}(\tau)$ . At the initial time interval ( $\tau \ll \tau^{chem}$ ) both curves coincide. At  $\tau \approx \tau^{chem}$  the concentration  $c_{ls}$  starts to decrease from the value of  $c_{ls}^{abs}$  and at  $\tau \geq \tau^{max}$  it is practically zero. If at a certain point  $X, Y$  the function  $c_{ls}^{abs}(\tau)$  is decreasing with respect to the time  $\tau$ , it is clear that  $c_{ls}(\tau)$  will have the same behaviour. Such situation exists all the range along the line  $BD$  (Fig. 4.2) where  $\beta^2 \leq 1$  (see also equations 4.22, 4.26 as well as (4.118, 4.116, 4.114)).

The situation becomes more simpler if the point moves further along the line  $BD$  where  $\beta^2 > 1$  and  $c_{ls}^{abs}(\tau)$  is an increasing function. In that area  $\tau_2^{abs} > 1$  (Fig. 4.5). The latter indicates that at  $\tau_2^{chem} > 1$  the curve  $c_{ls}(\tau)$  must reach a maximum (see 4.122, 4.124). The increase of  $a^2$  in the range  $1 < \tau_2^{chem} < \tau_2^{abs}$  means that this maximum varies from  $\frac{1}{1+\varepsilon}$  down

to  $\frac{I}{1+\varepsilon\beta}$  (4.126). Further, when  $a > I$  this maximum disappears and the function of  $c_{ls}$  decreases monotonously. It varies from  $\frac{I}{1+\varepsilon\beta}$  at  $\tau=0$  down to zero at  $\tau_2 >> \frac{I}{a^2}$  (4.127).

Concentration profile in the liquid at  $\tau >> \tau^{chem}$ . The time interval corresponding to  $\tau \approx \tau^{chem}$  will be termed *initial time interval* hereafter. From the common properties of the parabolic differential equations with sources it follows that at  $\tau > \tau^{chem}$  the non-stationary terms in the left part of the transport equation for the liquid phase (4) become negligible and may be omitted [11]. Thus at  $\tau >> \tau^{chem}$  a steady state concentration profile exists in the liquid phase:

$$c_2 \Rightarrow c_{ls}(\tau) \frac{ch(ay_2)}{ch(a)}. \quad (4.134)$$

For example, it follows from (4.134) that if  $a^2 \ll I$  the chemical reaction has equal rate at  $\tau >> \tau^{chem}$  across the whole layer depth  $b_2$ . The latter indicates that at  $(c_{ls} \approx c_2)$  a kinetically controlled regime starts [3, 4]. On the other hand, at higher values of  $a^2$  and  $\tau >> \tau^{chem}$  a thin boundary layer occurs near the interface. Its thickness  $\frac{I}{a} \ll I$  remains constant, so

$$c_2 \approx c_{ls}(\tau) \exp(-ay_2).$$

Singularities of the solution when the mass transfer resistance is located in the liquid phase ( $\varepsilon \ll I$ ,  $\varepsilon\beta \ll I$ ). In that area of the  $X-Y$  plane the equality  $c_{ls}^{obs}(\tau^{chem}) = I$  takes place despite the chemical reaction rate. This means that at the initial time interval ( $\tau \leq \tau^{chem}$ ) the mass transfer resistance is located in the liquid phase and the solution may be derived from the one-parametric problem:

$$\begin{aligned} \frac{\partial c_2}{\partial \tau_2} &= \frac{\partial^2 c_2}{\partial y_2^2} - a^2 c_2; \\ c_{2s} &= I, \quad \left( \frac{\partial c_2}{\partial y_2} \right)_s = 0 \quad \text{at } y_2 = 0; \quad c_{2s} = 0, \quad \tau_2 = 0. \end{aligned} \quad (4.135)$$

The corresponding dimensionless flux is

$$I^L \equiv \varepsilon \int_0^{y_2} \left( \frac{\partial c_2}{\partial y_2} \right)_s dy_2. \quad (4.136)$$

The solution of the problem (4.135) at large and small  $a^2$  is well-known [4, 31]:

$$I^L = \begin{cases} I^{abs} + \varepsilon a^2 \tau_2, & a \ll I; \\ I_{Dan} & a \gg I. \end{cases} \quad (4.137)$$

It is clear that at  $\tau \ll \tau^{max}$  the flux is  $I = I^L$ . Taking into account that both characteristic times  $\tau^{max}$  and  $\tau^{chem}$  satisfy the inequality (it follows from the condition  $c_{ls}^{abs} = I$ )

$$\tau^{chem} \ll \tau^{max}, \quad (4.138)$$

the solution of the problem (4.101, 4.102) becomes simpler at  $\tau \gg \tau^{chem}$ . In this case (see (4.128)):

$$\left( \frac{\partial c_2}{\partial y_2} \right)_s = c_{ls} \frac{th(a)}{a}. \quad (4.139)$$

Taking into consideration that condition of coupled fluxes at the interface exists, the following problem for the gas phase only may be formulated:

$$\begin{aligned} \frac{\partial c_1}{\partial \tau_1} &= \frac{\partial^2 c_1}{\partial y_1^2}; \\ \left( \frac{\partial c_1}{\partial y_1} \right) &= 0 \quad \text{at } y_1 = 0; \\ \left( \frac{\partial c_1}{\partial y_1} \right)_s &= P c_{ls}(\tau_1) \quad \text{at } y_1 = I; \\ c_1 &= c_{ls} = I \quad \text{at } \tau_1 = 0. \end{aligned} \quad (4.140)$$

The problem depends on the parameter  $P$ :

$$P = \varepsilon \beta^2 a \ th(a). \quad (4.141)$$

It is easy to check that all the parameters  $P$  in the problems discussed (4.2.1-4.2.4) are particular cases of (4.141) in the respective areas of the  $X - Y$  plane. The integral flux corresponding to (4.140) will be noted as  $I^G(P, \tau_1)$  hereafter.

At arbitrary values of  $P$  the relationship for  $I^G(\tau_1)$  can be obtained numerically only. However, at small and high  $P$  analytical approximations could be derived:

$$I^G = \begin{cases} 1 - \exp(-P\tau_1), & P \ll I; \\ \frac{1}{P} \left\{ \sqrt{\frac{P^2 \tau_1}{\pi}} - [1 - \exp(-P^2 \tau_1)] \operatorname{erfc}(\sqrt{P^2 \tau_1}) \right\}, & P \gg I. \end{cases} \quad (4.142)$$

The latter follows directly from the comparison of the relationships (4.141, 4.112, 4.114, 4.116).

The relationships (4.142) allow the evaluation of the order of the characteristic time  $\tau^{\max}$  for  $I^G$  at an arbitrary value of  $P$ . Obviously,

$$\tau^{\max} = \begin{cases} \frac{I}{P}, & P \leq 1; \\ \frac{I}{P^2}, & P > 1. \end{cases} \quad (4.143)$$

In time range  $\tau^{\text{chem}} \ll \tau \ll \tau^{\max}$  the dimensionless fluxes  $I^L$  and  $I^G$  coincide :

$$I^L = \varepsilon a^2 \bar{c}_2 \tau_2 = P \tau_1 = I^G. \quad (4.144)$$

The solution may be expressed in the form (with an equally distributed accuracy with respect to  $\tau$ ) (see (4.116)):

$$I = I^G(P, \tau_1) - P \tau_1 + I^L. \quad (4.145)$$

The equivalent form of (4.145) is:

$$I = \begin{cases} I^L(\tau_2) & \text{at } \tau \ll \tau^{\max} \\ I^G(\tau_1) & \text{at } \tau \gg \tau^{\text{chem}}. \end{cases} \quad (4.146)$$

In this way in the lower left corner of the absorption plane the general chemosorption problem (4, 5) is divided into two monophasic problems. Each problem depends on one chemosorption parameter. In the range  $\tau \ll \tau^{\max}$  it is the Damkohler number ( $a^2$ ), while at  $\tau \gg \tau^{\text{chem}}$  the controlling parameter is  $P$  (4.141).

Singularities in the lower part of the absorption plane X-Y at  $\varepsilon\beta \ll 1$ . (Applicability of the Danckwerts' equation). In this area at  $\tau \ll \tau^{\text{abs}}$  the surface concentration in the case of the absorption is  $c_{ls}^{\text{abs}} = 1$ . This means that (in contrast to the situation in the lower left corner) the condition  $c_{ls}(\tau^{\text{chem}}) = 1$  is not valid for arbitrary values of  $\tau^{\text{chem}}$ , but only for those corresponding to fast interactions.

$$\tau_2^{\text{chem}} = \frac{I}{a^2} \ll \tau_2^{\text{abs}} = \frac{I}{1 + \varepsilon}. \quad (4.147)$$

It is clear that in this case  $a \gg 1$  and the flux  $I$  may be obtained by means of (4.145, 4.146) where  $I^L = I_{\text{Dan}}$ ,  $P = \varepsilon \beta^2 a$  (see (4.137), (4.141)). Moreover, the inequality (4.119), governing the analytical solutions (4.114, 4.116) in 4.2.2 is a particular case of the condition (4.147).

The results developed give the answer for the applicability of the Danckwerts' equation (4.107). Obviously, this equation can be employed in the lower part of  $X-Y$  ( $\varepsilon\beta \ll 1$ ) plane where the condition (4.147) is satisfied.

Singularities in the left part of the plane  $X-Y$  at  $\varepsilon \ll 1$ . In this area the relation  $c_{ls}^{abs} = 1$  is satisfied at  $\tau \gg \tau^{abs}$ . Thus, for slow chemical reactions :

$$\tau_2^{abs} = (I + \varepsilon\beta)^2 \ll \tau^{chem} = \frac{I}{A^2}, \quad (4.148)$$

the concentration is  $c_{ls}^{abs}(\tau^{chem}) = 1$ . The flux  $I$  (with an equally distributed accuracy with respect to the time  $\tau$ ) may be expressed as:

$$I(\tau) = I^{abs} + I^G(P, \tau_1), \quad (4.149)$$

where  $P = \varepsilon\beta^2 A^2$ , because  $A \ll 1$  (see (4.148)). Obviously, the condition (4.121) allowing the analytical solutions (4.122, 4.124) in chapter 4.2.4, is a particular case of (4.148).

Singularities in the upper part of the plane  $X-Y$  at  $\varepsilon\beta \gg 1$ . (The condition allowing the maximum absorption regime (4.110)). In this area of the plane (at  $\tau \leq \tau^{abs}$ ) the dimensionless flux becomes  $I^{abs} = I^{max}(\tau_1)$  and the surface concentration is  $c_{ls}^{abs} = 0$ . Thus, at sufficiently high values of the chemosorption parameter  $A^2$ , i.e. under the conditions allowing the inequality:

$$\tau_1^{chem} = \frac{I}{A^2} \leq \tau_1^{abs} = \left( \frac{\varepsilon}{I + \varepsilon} \right)^2, \quad (4.150)$$

Hence, a maximum absorption regime (4.110) exists for every arbitrary values of  $\tau$  because at the interface  $c_{ls} = 0$  (see also the solutions (4.126, 4.127) in 4.2.4 obtained under the condition (4.124) that is a particular case of (4.150)).

Thus, the maximum absorption regime (4.110) may occur:

- in the upper right corner of the absorption plane inspite of the chemical reaction rate (chapter 4.2.3);
- in the upper part of the plane if the condition (4.150) is satisfied;
- at arbitrary point  $X, Y$  when  $\tau \geq \tau^{max}$  (see (4.105)).

Singularities in the right half part of the plane  $X-Y$  at  $\varepsilon \gg 1$  (Conditions at which the chemical reaction does not affect the rate of absorption). In this case ( $\varepsilon \gg 1$ ) and if  $\tau \geq \tau^{abs}$  the dimensionless flux is  $I^{abs} \Rightarrow 1$ . The gas phase is totally depleted due the physical absorption. The latter means that under slight interactions allowing the inequality

$$\left( I + \frac{1}{\varepsilon\beta} \right)^2 = \tau^{abs} \leq \tau^{chem} = \frac{I}{A^2}, \quad (4.151)$$

the chemical reaction does not affect the mass transfer:

$$I = I^{\text{abs}}(\tau). \quad (4.152)$$

The condition (4.117) allowing the solution (4.118) in 4.2.2 is a particular case of (4.151).

Thus the chemical reaction effects may be omitted if:

- a) in the upper part of the plane  $X - Y$  ( $\varepsilon >> 1$ ) the condition (4.151) is satisfied;
- b) at every point of the absorption plane the contact time  $\tau$  is sufficiently small:

$$\tau \ll \tau^{\text{chem}}. \quad (4.153)$$

#### 4.2.7. Numerical investigation of the two-phase chemosorption in the initial time interval

The theoretical investigations performed in the previous chapters allow to make the suggestion that under chemosorption the deviations of the dimensionless diffusion flux  $I$  from the function  $I^{\text{abs}}$  corresponding to the initial time interval  $\tau \approx \tau^{\text{chem}}$  can be neglected. Usually the deviations may be expressed as a factor of augmentation of the chemical reaction  $\Phi$ . In the case of a mass transfer resistance totally located in the liquid phase the augmentation factor  $\Phi$  [3, 4] is:

$$\Phi = \frac{I(X, Y, a^2, z_a)}{I^{\text{abs}}(X, Y, \tau)}, \quad (4.154)$$

where the dimensionless time co-ordinate  $z$  is :

$$z_a = \tau / \tau^{\text{chem}} = a^2 \tau_2 = A^2 \tau_1. \quad (4.155)$$

Finally, the presentation of the results by functions  $I(\tau)$  or  $\Phi(z_a)$  are equivalent because both of them are one-parametric dependent (by the chemosorption parameter) functions. However, the expression through  $\Phi$  in the initial time interval has advantages. This expression allows the determination of (4.152) in a restricted time interval  $z_a \approx 1$ .

The formalistic treatment of the dimensionless problem (4.101, 4.102) shows that the Damkohler number ( $a^2$ ) or  $A^2$  may be used as a chemosorption parameter for  $\Phi(z_a)$ . However, in the course of building up a methodology of the chemosorption design under various conditions this approach does not lead to the desired success. The problem will be discussed in detail below.

First of all, let the solution of the problem (4.101, 4.102) be considered in the initial time interval and in two limiting cases – slow and fast reactions with respect to the absorption time. In the first case the condition  $\tau^{\text{chem}} >> \tau^{\text{abs}}$  must be satisfied, while in the second the situation is just the opposite  $\tau^{\text{chem}} \ll \tau^{\text{abs}}$  [3, 4].

In the case of slow chemical reaction ( $\tau^{\text{abs}} \ll \tau^{\text{chem}}$ ) the reaction rate affects the mass transfer at times  $\tau >> \tau^{\text{abs}}$ . This time interval is enough for the establishment of the equilibrium in entire the volumes of both phases (4.22, 4.23):

$$I^{abs} \Rightarrow \frac{\varepsilon}{1+\varepsilon}, \quad c_1^{abs} = c_2^{abs} = \frac{I}{1+\varepsilon}. \quad (4.156)$$

If suggest that at ( $\tau \gg \tau^{abs}$ ) the equality  $c_1 = c_2$  remains, the integration of the transport equation in the gas phase (4.101) (with respect to  $c_1$ ) along the transversal coordinate  $y_1$  allows to derive an ordinary differential equation for  $c_1$ :

$$\frac{dc_1}{d\tau} = -\left(\frac{\varepsilon}{1+\varepsilon}\right)c_1.$$

The junction of its solution in the range  $\tau^{abs} \ll \tau \ll \tau^{chem}$  with (4.156) gives an analytical relationship for the dimensionless flux:

$$I = I - \bar{c} = \frac{\varepsilon}{1+\varepsilon} + \frac{1 - \exp[-\varepsilon z_a / (1+\varepsilon)]}{1+\varepsilon}. \quad (4.157)$$

The corresponding augmentation factor  $\Phi_0(\varepsilon, z_a)$  is:

$$\Phi_0 = 1 + \frac{1}{\varepsilon} \left[ 1 - \exp \frac{-\varepsilon z_a}{1+\varepsilon} \right]. \quad (4.158)$$

The one-parametric function  $\Phi_0(X, z_a)$  ( $X$  is the parameter) is shown on Fig. 4.11. At  $\varepsilon \gg 1$  the factor  $\Phi_0 \Rightarrow 1$ . In this case the depletion of the gas phase is due to the physical absorption only and  $\tau \approx \tau^{abs}$ . The chemical reaction effect becomes detectable at  $\tau \approx \tau^{chem}$ , but it has no effect on the process. The decrease of  $\varepsilon$  increases the factor  $\Phi_0(z_a)$  and at  $\varepsilon \Rightarrow 0$  and a restricted time rage ( $z_a \approx 1$ ) it tends toward:

$$\Phi_0 \rightarrow 1 + z_a, \quad \varepsilon \rightarrow 0. \quad (4.159)$$

In the case of a fast chemical reaction  $\tau^{chem} \ll \tau^{abs}$  at  $\tau \leq \tau^{chem}$  there are boundary layers in both phases along the interface. The introduction of dimensionless lateral co-ordinates  $y_{10} = A(1 - y_1)$ ,  $y_{20} = a(1 - y_2)$ , transforms the problem (4.101, 4.102) to the form:

$$\begin{aligned} \frac{\partial c_1}{\partial z_a} &= \frac{\partial^2 c_1}{\partial y_{10}^2}, \quad \frac{\partial c_2}{\partial z_a} = \frac{\partial^2 c_2}{\partial y_{20}^2} - c_2; \\ \left( \frac{\partial c_1}{\partial y_{10}} \right)_s &= -(\varepsilon \beta) \left( \frac{\partial c_2}{\partial y_{20}} \right)_s \quad \text{at} \quad y_{10} = y_{20} = 0; \\ c_1 &= 1, \quad y_{10} \rightarrow \infty; \quad c_2 = 0, \quad y_{20} \rightarrow \infty; \\ c_1 &= 1, \quad c_2 = 0 \text{ at } z_a = 0. \end{aligned} \quad (4.160)$$

The solution of (4.160) and the corresponding augmentation factor  $\Phi_\infty(z_a)$  depend on the absorption parameter  $Y$ :

$$\Phi_\infty(Y, z_a) = \frac{\int_0^\infty (1 - c_{l0}) dy_{l0}}{\frac{2}{\sqrt{\pi}} \left( \frac{\varepsilon \beta}{1 + \varepsilon \beta} \right) \sqrt{z_a}} \quad (4.161)$$

The analytical relationship for  $I^{abs}$  (4.27) corresponding to  $\tau \ll \tau^{abs}$  is employed here. The numerical calculations of  $\Phi_\infty(z_a)$  for various discrete values of  $Y$  are presented in Fig. 4.12. It is clear that the effect of  $Y$  on the solution exists in a restricted range  $-1 \leq Y \leq 1$  only. Outside that range the augmentation factor  $\Phi_\infty(z_a)$  is practically independent of  $Y$ .

It is well known that at  $Y \geq 1$  and  $\tau \ll \tau^{abs}$  the mass transfer resistance of the physical absorption is controlled by the gas phase because  $c_{ls} \ll 1$  (see chapter 4.2.6). The occurrence of a chemical reaction may lead to a decrease of  $c_{ls}$ , without affecting on the diffusion flux  $I^{max}(\tau_l)$  and  $\Phi_\infty \Rightarrow 1$  ( $Y \leq -1$  in Fig. 4.12). In the other limiting case ( $Y \leq -1$ ) and at  $\tau \ll \tau^{abs}$  the chemosorption resistance is located in the liquid phase ( $c_{ls} = 1$ ) and the dimensionless flux may be evaluated by the Danckwerts' equation (4.107). Taking into consideration that  $I^{abs} = 2\sqrt{\tau_2/\pi} \varepsilon$  the factor  $\Phi_\infty$  may be expressed in the form:

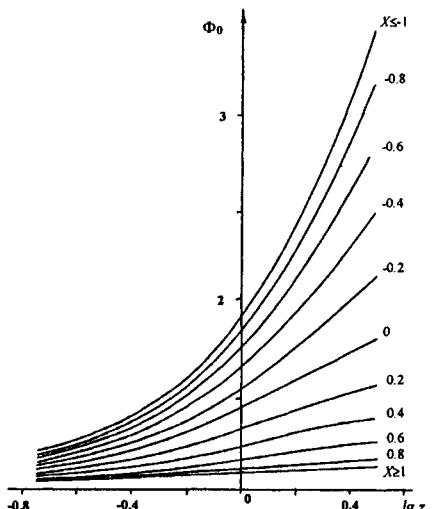


Fig. 4.11. Calculation of  $\Phi_0$  for different  $X$  in the case of a slow chemical reaction.

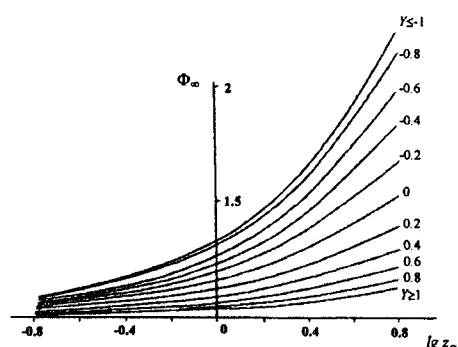


Fig. 4.12. Calculation of  $\Phi_0$  for different  $Y$  in the case of a fast chemical reaction.

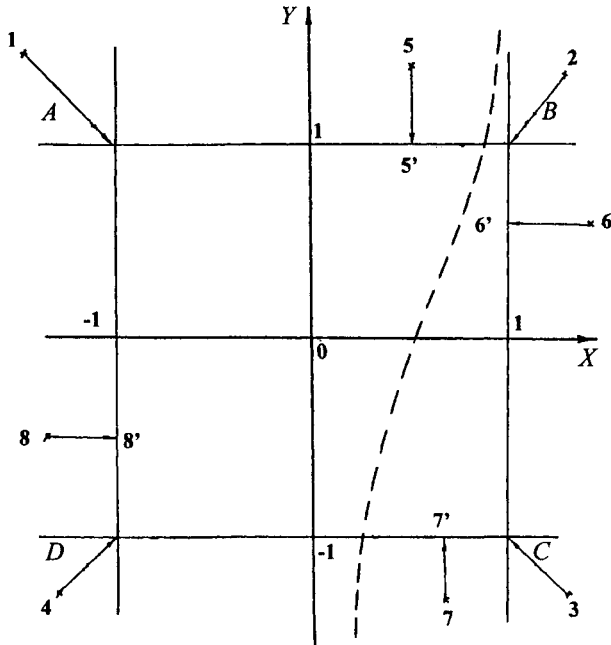


Fig. 4.13. The “absorption square” ABCD. The dashed line presents the case when  $\Phi_0 = \Phi_\infty(z)$ .

$$\Phi_\infty \Rightarrow \frac{\operatorname{erf}(\sqrt{z_a})(z_a + 1/2) + \sqrt{\frac{z_a}{\pi}} \exp(-z_a)}{2\sqrt{\frac{z_a}{\pi}}} \equiv \Phi_{Dan}(z_a) \quad (4.162)$$

It is easy to check that at  $Y \geq 1$  (Fig. 4.12) it practically coincides with the analytical line. Thus, supposing that at every point  $X, Y$  and in the time interval  $z_a \approx 1$  the factor  $\Phi(z_a)$  is monotonously dependent on the chemical reaction rate the following evaluations should be performed:

$$\Phi_{min}(z_a) \leq \Phi \leq \Phi_{max}(z_a),$$

where

$$\Phi_{min} = \min[\Phi_0(X, z_a), \Phi_\infty(Y, z_a)],$$

$$\Phi_{\max} = \max[\Phi_0(X, z_a), \Phi_\infty(Y, z_a)]. \quad (4.163)$$

The formulae (4.163) allow evaluations of the chemical reaction effect during the initial time interval without using the complete solution of (4.101, 4.102).

It was demonstrated earlier (see physical absorption in chapter 4.1) that it is enough to tabulate the values of  $I^{abs}$  inside the so-called "absorption square" ABCD ( $-1 \leq X \leq 1$ ,  $-1 \leq Y \leq 1$ ), shown in Fig. 4.13. Outside the square the solutions are the solutions at points belonging to the square border. For example, at point with a number 1 the corresponding point is A, 2 → B, 3 - C, 4 - D as well as 5 → 5', 6 → 6', 7 - 7', 8 - 8' (Fig. 4.13). It is clear that the interphase mass transfer augmentation due the chemical reaction effect depends on the concentration distribution under the condition of a physical absorption. Thus, the tabulation of  $\Phi(z_a)$  may be done inside the square ABCD only.

Figures 4.14 and 4.15 illustrate a typical example for the augmentation factor  $\Phi(z_a)$  calculation at the points A and C, respectively. The chemosorption parameter in the first case is  $\lg \alpha^2$ , while in the second it is  $-\lg A^2$ . At fixed values of the parameters the augmentation factor  $\Phi(z_a)$  is an increasing function of  $z_a$ . At  $z_a \rightarrow 0$  the factor  $\Phi \rightarrow 1$ . The plots demonstrate that the chemical reaction effect is important in a restricted range of variation of the absorption parameters. This is exactly the range [-1, 1]. Outside this range, the factor  $\Phi(z_a)$  is independent of  $\alpha^2(A^2)$  and practically coincides with  $\Phi_0(z_a)$  and  $\Phi_\infty(z_a)$ .

It should be noted that at point A the mass transfer resistance (in case of absorption) is located mainly in the liquid phase. There  $\tau_2^{abs} = 1$ , while at point B the situation is just the opposite – the gas phase exerts the limiting mass transfer resistance ( $\tau_1^{abs} = 1$ ). It has been already demonstrated that at arbitrary  $X, Y$  the value of  $\tau^{abs}$  is a characteristic time of  $\tau^{chim}$  (see the conditions for slow and fast reactions solutions), so their ratio ( $\kappa^2$ ) may be chosen as the absorption parameter [21]:

$$\kappa^2 = \frac{\tau_2^{abs}}{\tau_1^{chem}} = \tau_1^{abs} A^2 = \tau_2^{abs} \alpha^2. \quad (4.164)$$

In the particular case corresponding to the lower left corner of the absorption plane ( $X \leq -1$ ,  $Y \leq -1$ ,  $\tau_2^{abs} = 1$ ) the parameter is practically equal to  $\alpha^2$  (Fig. 4.14). In the upper right corner ( $X \geq 1$ ,  $Y \geq 1$ ,  $\tau_1^{abs} = 1$ ) it coincides with  $A^2$  (Fig. 4.15).

It is clear that at  $\kappa^2 \rightarrow 0$ ,  $\Phi \rightarrow \Phi_0$ , while at  $\kappa^2 \rightarrow \infty$   $\Phi \rightarrow \Phi_\infty$ .

The chemosorption parameter  $\kappa^2$  was derived on the basis of the physical assumption, that the range [ $\kappa_{min}^2$ ,  $\kappa_{max}^2$ ] defines the area where the chemical reaction effect on  $\Phi(z_a)$  is significant. Thus, the boundaries of that range should be conservative with respect to the position of the point on the absorption plane.

The calculation of the augmentation factor at  $z_a \leq 0.5$  for a number of discrete values inside the square ABCD (Fig. 4.13) is demonstrated on Figs. 4.16-4.20. The plots demonstrate

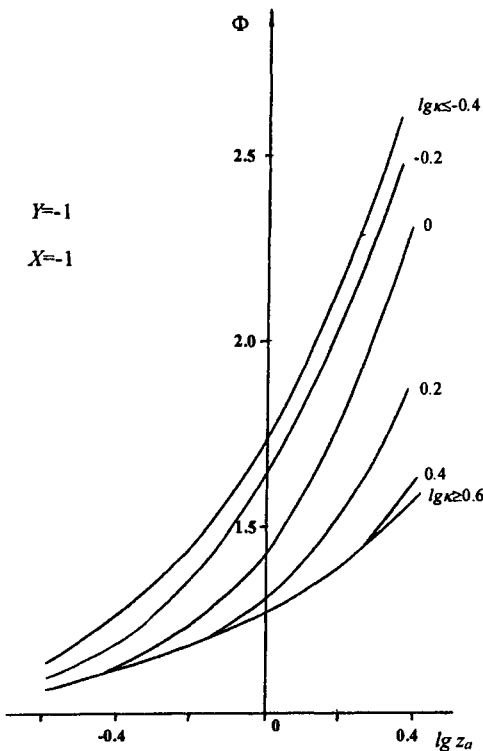


Fig. 4.14. Calculation of the factor  $\Phi$  in the point D (absorption resistance is concentrated in the liquid phase) for different  $\kappa$ .

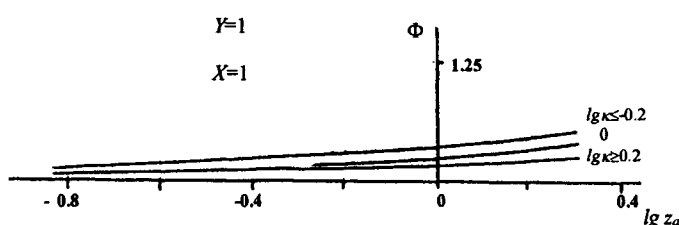


Fig. 4.15. Calculation of the factor  $\Phi$  in the point B (absorption resistance is concentrated in the gas phase) for different  $\kappa$ .

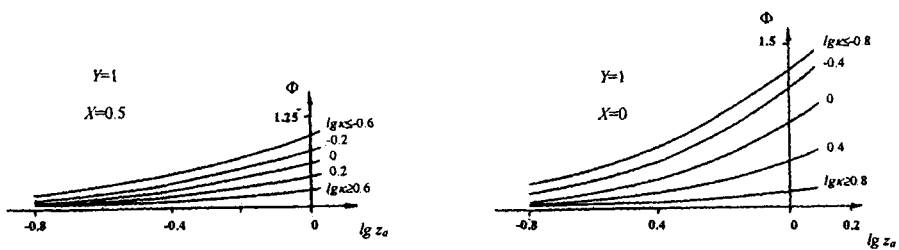
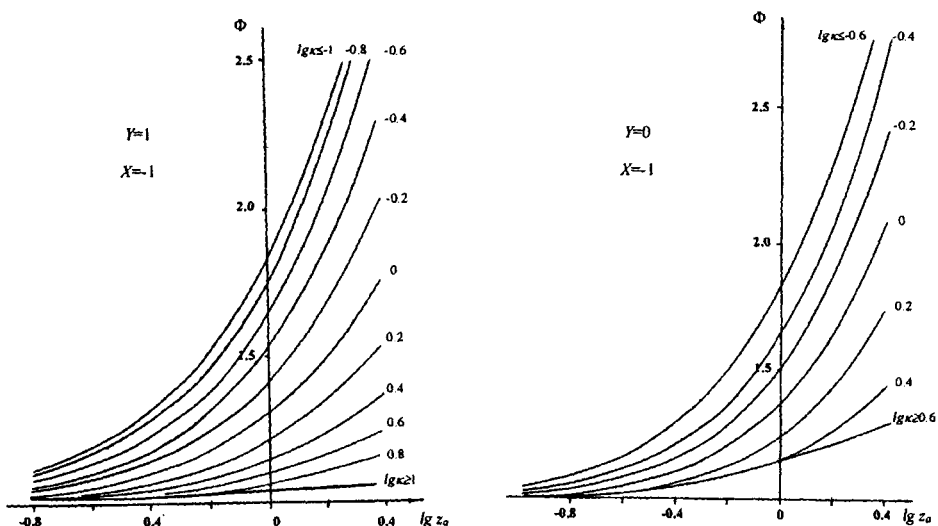
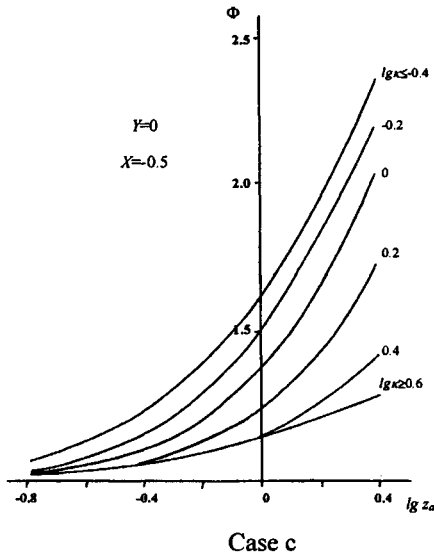


Fig. 4.16. Calculation of the factor  $\Phi$  in the points: a)  $Y = 1, X = 0.5$ ; b)  $Y = 1, X = 0$ .



Figs. 4.17 a, b. Calculation of the factor  $\Phi$  in the points: a)  $Y = 1, X = -1$ ; b)  $Y = 0, X = -1$



Case c

Fig. 4.17 c. Calculation of the factor  $\Phi$  in the points:  $Y = 0$ ,  $X = -0.5$ .

that the parameter  $\lg(\kappa^2)$  should be assumed as a constant:  $\lg(\kappa_{min}^2) = -1$ ,  $\lg(\kappa_{max}^2) = +1$ , so:

$$-1 \leq \lg \kappa^2 \leq 1. \quad (4.165)$$

Outside the range ( $\lg \kappa^2 > 1$ ,  $\lg \kappa^2 \leq -1$ ) the differences between  $\Phi(z_a)$  and the corresponding boundary values of  $\Phi_0(z_a)$  and  $\Phi_\infty(z_a)$  do not usually exceed 5 %. The function  $\Phi(z_a)$  generally depends on  $\lg(\kappa^2)$  monotonously within the range [-1, 1]. The areas, where  $\Phi$  increases or decreases, may be defined by means of the figures 4.11 and 4.12. The figures show that if the parameter  $Y$  is assumed as constant it is always possible to find a point where  $X = X_0(Y)$ , inside the square ABCD. In this case the limiting curves coincide:

$$\Phi_\infty(Y, z_a) = \Phi_0(X_0, z_a),$$

i.e.  $\Phi(z_a)$  is independent of  $\kappa^2$ .

The last relationship is obviously not a strong equality. It would be satisfied with a given accuracy when is a function of the value of  $z_a$ . The calculations made indicate that at  $\lg z_a \leq 0.5$  the relative error does not exceed 5%. (The limiting curve  $X_0(Y)$  is shown on

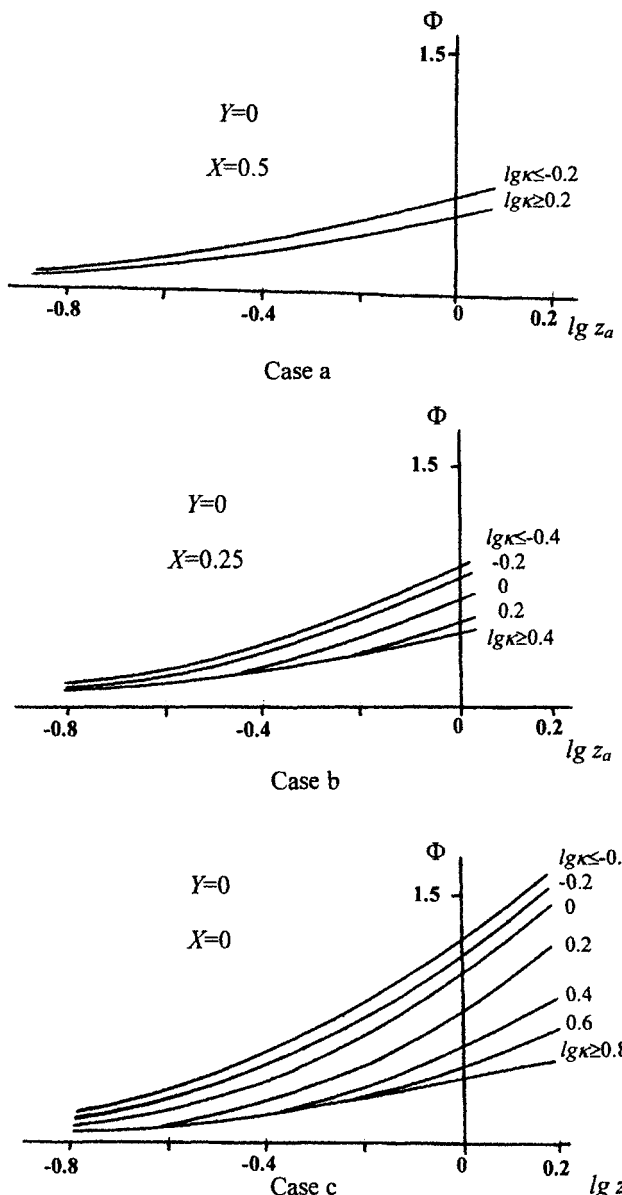


Fig. 4.18. Calculation of the factor  $\Phi$  in the points: a)  $Y = 0$ ,  $X = 0.5$ ; b)  $Y = 0$ ,  $X = 0.25$ ; c)  $Y = 0$ ,  $X = 0$ .

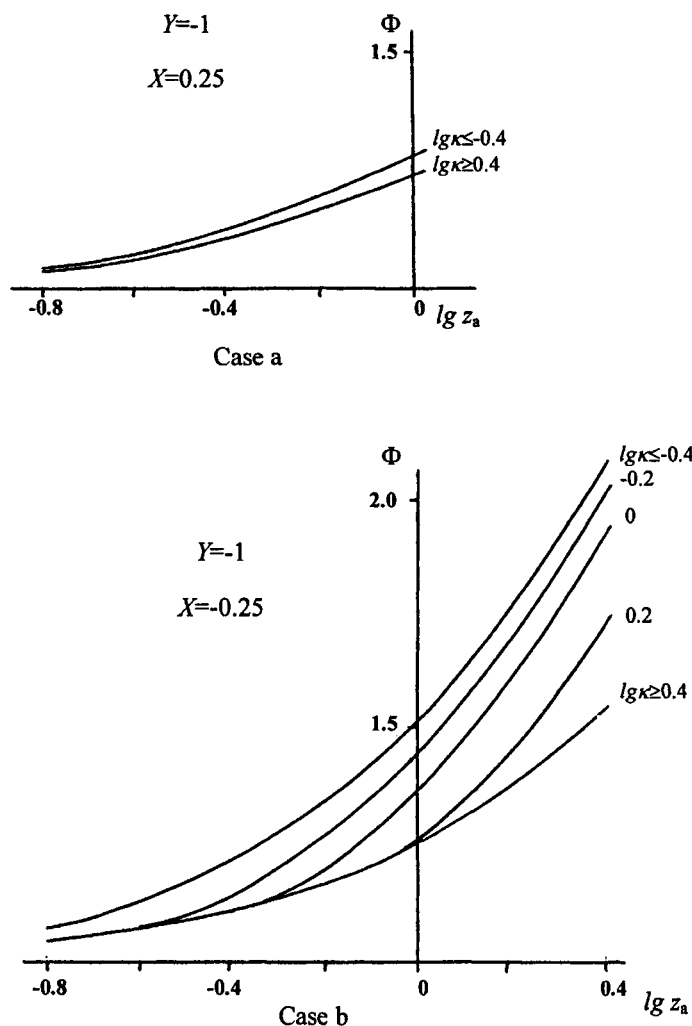


Fig. 4.19. Calculation of the factor  $\Phi$  in the points: a)  $Y = -1, X = -0.25$ ; b)  $Y = -1, X = 0.25$ .

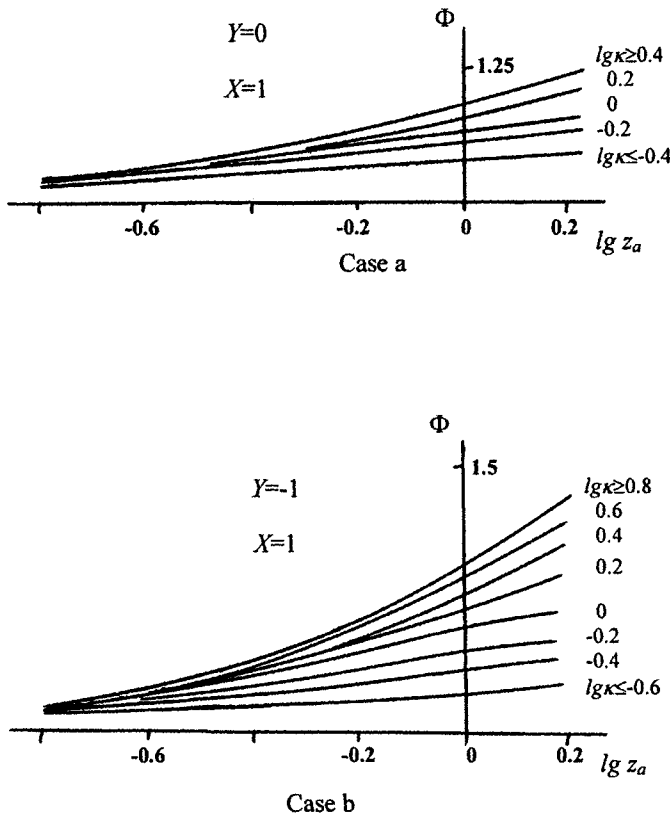


Fig. 4.20. Calculation of the factor  $\Phi$  in the points: a)  $Y = 0$ ,  $X = 1$ ; b)  $Y = -1$ ,  $X = 1$ .

Fig. 4.13 by a dashed line). At  $X \geq X_0(Y)$ , where  $\Phi_0(z_a) = \Phi_{\min}$  the factor  $\Phi(z_a)$  increases monotonously with  $\lg(\kappa^2)$ , while at  $X \leq X_0(Y)$  where  $\Phi_0(z_a) = \Phi_{\max}$  the behaviour is just the opposite. The analysis of the numerical solution proves that a significant mass transfer augmentation due to accompanying first order chemical reaction may be reached outside the boundaries of the initial time interval at higher values of  $z_a$ . At the initial interval the upper assessment of  $\Phi(z_a)$  is:

$$\Phi(z_a) \leq 1 + z_a. \quad (4.166)$$

The right hand side of (4.166) corresponds to the value of  $\Phi_{\max}(z_a)$  obtained for the left half-plane ( $X \leq -1$ ) at  $\lg(\kappa^2) \leq -1$  (4.159). For example, at  $\lg z_a \leq 0.5$  the factor  $\Phi \leq 4$ .

The intensification of the absorption due to a chemical reaction depends on the ratio of the two dimensionless fluxes  $I^{abs}(\tau)$  and  $I^{max}(\tau)$ . The ratio strongly depends on the position of the point on the absorption plane  $X - Y$ . For example, in the first quadrant of the plane where the surface concentration is lower than unity (or exactly  $c_{ls}^{abs} \leq 0.5$ ) the difference between these functions is small irrespective of  $\tau$ . Thus,  $c_{ls}^{abs}(\tau^{chem}) \leq 0.5$  and  $\tau^{max} \approx \tau^{chem}$ . Outside the limits of the initial time interval the following applies:

$$I \Rightarrow I^{max}(\tau), \quad \tau \geq \tau^{chem}. \quad (4.167)$$

An important intensification of the absorption occurs in the third quadrant of  $X - Y$ , where  $\varepsilon\beta \leq 1$ ,  $\varepsilon \leq 1$ ,  $c_{ls}^{abs} \geq 0.5$  and the difference between  $I^{abs}$  and  $I^{max}$  is significant. In this case the interphase mass transfer resistance is located in the liquid phase (lower left corner of Fig. 4.13). In this case  $c_{ls}^{abs}(\tau^{chem}) = 1$  and  $\tau^{max} \gg \tau^{chem}$ . Outside the initial time interval there is a transition:

$$I \Rightarrow I^G(P, \tau) \quad (\tau \geq \tau^{chem}). \quad (4.168)$$

In the second and the fourth quadrants the augmentations is possible upon satisfactions of some conditions. For example, in the second quadrant such augmentation is possible in the left half plane only ( $\varepsilon \ll 1$ ) and slow reactions ( $\tau^{abs} \ll \tau^{chem}$ ). In this case  $c_{ls}^{abs}(\tau^{chem}) = 1$ ,  $\tau^{max} \gg \tau^{chem}$  and the transition (4.168) occurs (see also 4.2.5).

A similar situation exists in the fourth quadrant of the lower half plane of  $X - Y$  ( $\varepsilon\beta \ll 1$ ) and fast chemical interactions ( $\tau^{chem} \ll \tau^{abs}$ ) (see also 4.2.5).

It is clear that in all the case when the mass transfer augmentation is not enough the dimensionless flux is  $I^G(P, \tau_i) \Rightarrow I^{max}(\tau_i)$  at  $\tau < \tau^{chem}$  (see. (4.143)). Thus, in a general situation at  $\tau \gg \tau^{chem}$  the transition (4.168) should occur everywhere on  $X - Y$  plane and for every  $\kappa^2$ . The numerical calculations indicate that everywhere inside  $ABCD$  (Fig. 4.13) at  $\lg z_a \geq 0.5$  such situation exists. The solution of the problem (4.140) and the graphical presentation of  $I^G(P, \tau_i)$  are not difficult because the problem is one-parametric.

#### 4.2.8. Numerical investigation of the chemosorption outside the initial interval

The analysis of the analytical solutions (4.142) at large and small values of the parameter  $P$  requires a dimensionless longitudinal co-ordinate:

$$z \equiv \begin{cases} P\tau_i & \text{if } P \leq 1; \\ P^2\tau_i & \text{if } P > 1. \end{cases} \quad (4.169)$$

The dimensionless objective function  $\varphi_i(z)$  allows the determination of the time  $\tau$  through the dimensionless flux  $I^G$  and the other way around. It could be determined as a function of the parameter  $P$ :

$$\varphi_I \equiv \begin{cases} I^G(z) & \text{if } P \leq 1; \\ PI^G(z) & \text{if } P > 1. \end{cases} \quad (4.170)$$

The numerical solution of (4.140) for small ( $\lg P \leq 0$ ) and large ( $\lg P > 0$ ) values of  $P$  is shown on Figs. 4.21 and 4.22 by means of the variables  $\varphi_I - z$ . At  $\lg P \leq 0$  the effect of the chemosorption parameter  $P$  on  $I^G(z)$  is insignificant. The maximum difference between  $I^G$  and the analytical prediction of  $I_o^G$  (4.142) at  $P \ll 1$  (curve 1 in Fig. 4.21) does not exceed 20%.

In the area where  $\lg P > 0$  the effect of  $P$  on  $\varphi_I(z)$  is detectable. It is clear that the analytical relationship  $PI_\infty^G$  (the function (4.142) at  $P \gg 1$ ) (curve 2 on Fig. 4.22) is a locus of the one-parametric curves  $\varphi_I(P, z)$ . At every  $P$  the range of variations of  $\lg z$ , defining the numerical calculations is restricted. At "small"  $z$  the objective function is  $\varphi_I = PI_\infty^G$ , while at high values of  $z$  it becomes  $\varphi_I \Rightarrow PI_{\max}^G(\tau_1)$ . The further transition (with an error of 5%) occurs at the line 3 on Fig. 4.22. Obviously, the magnitude of the  $\lg z$  defining the area of calculations decreases. Its maximum value is 0.6 (at  $\lg P = 0$ ), while the minimal is zero ( $\lg P = 0.8$ ). At  $\lg P \geq 0.8$  the objective functions  $\varphi_I(z)$  tend to deviate from the locus  $PI_\infty^G$  (curve 2 in Fig. 4.22) in the area defined by the condition  $\lg z \geq 1.5$ .

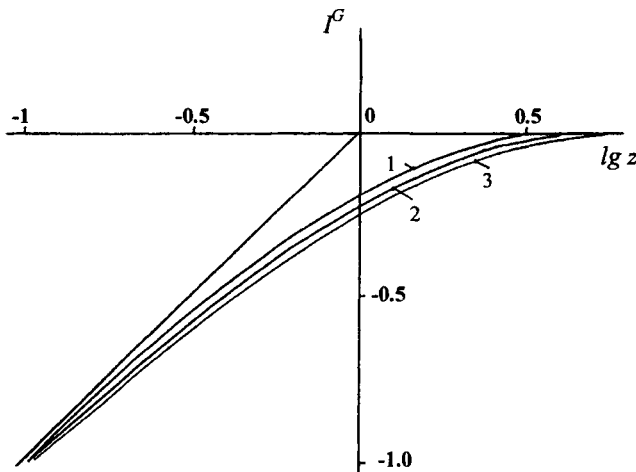


Fig. 4.21. Numerical solution of (4.140) for small  $P$  values ( $\lg P \leq 0$ ): 1)  $\lg P \leq -1$ ; 2)  $\lg P = -0.5$ ; 3)  $\lg P = 0$ .

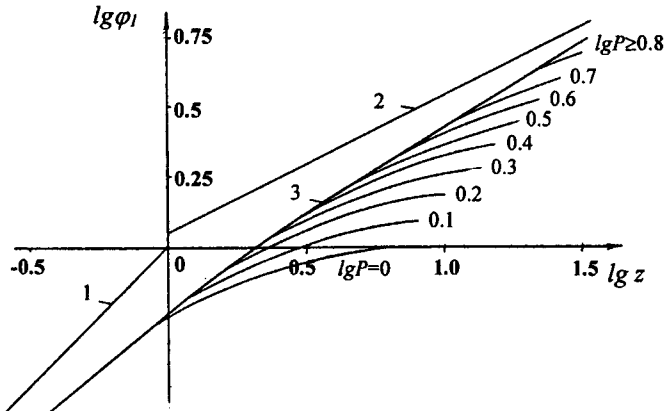


Fig. 4.22. Numerical solution of (4.140) for high  $P$  values ( $\lg P > 0$ ): 1)  $\varphi_I = z$ ;

$$2) \varphi_I = \frac{2}{\sqrt{\pi}} \sqrt{z}.$$

Thus, there is no need of numerical calculation for high  $P$  because the assumed accuracy of (5%) allows the detection of the transition  $\varphi_I \rightarrow PI^{max}(\tau_1)$  at  $\lg z = 1.5$ . The straight line 2 in Fig. 4.22 is asymptotic of  $I^{max}$  at small  $\tau_I$ :

$$PI^{max} = P \frac{2}{\sqrt{\pi}} \sqrt{\tau_I} = \frac{2}{\sqrt{\pi}} \sqrt{z}. \quad (4.171)$$

The plots on Fig. 4.22 and the analytical relationships (4.110) permit a solution of (4.101, 4.102) to be found at every value of the chemosorption parameter when  $\tau \gg \tau^{chem}$ , in the case of a fast chemical reaction ( $\lg z \geq 0.5$ ).

#### 4.2.9. Methodology of the chemosorption design

The methodology of the two-phase chemosorption with an irreversible chemical reaction of first order under an arbitrary contact time corresponding to every point of the plane  $X$ - $Y$  requires the following steps:

1. Calculation of the dimensionless time co-ordinate  $z_a$  (4.155) should be made.
2. If  $\lg z_a \leq 0.5$  the dimensionless flux  $I(z_a)$  should be calculated by means of the augmentation factor  $\Phi$ . Initially the dimensionless parameter  $\kappa^2$  should be calculated. If  $\lg \kappa^2$  does not belong to the range  $[-1, 1]$  the corresponding relationships for  $\Phi_o(z_a)$  and  $\Phi_a(z_a)$  should be determined through the plots on Fig. 4.11 and Fig. 4.12 or the formula

(4.158). In the opposite case ( $-1 \leq \lg(\kappa^2) \leq 1$ ) the numerical solution  $\Phi(z_a)$  (Figs. 4.14 - 4.20) should be employed..

The numerical calculations  $\Phi(z_a)$  at discrete points inside the absorption square  $ABCD$  were carried out with steps  $\Delta X = \Delta Y = 0.25$   $\lg \kappa^2 = 0.2$  ( $-1 \leq \lg(\kappa^2) \leq 1$ ).

The dimensionless integral diffusion flux is calculated as  $I = \Phi I^{abs}$ .

3. If the points  $X, Y$  do not belong to the square  $ABCD$  the function  $\Phi(z)$  practically coincides with the solutions corresponding to the points laying on the boundary of  $ABCD$  (see the points 1-8 in Fig. 4.13).

The numerical calculations made indicate that in the range of  $-1 \leq \lg(\kappa^2) \leq 1$  the effect of  $\lg(\kappa^2)$  on  $\Phi(z_a)$  is practically linear. Thus, the preliminary evaluations and the fast calculations of the augmentation factor may be carried out by means of the following approximation (at  $\lg z_a \leq 0.5$ ):

$$\Phi(z_a) = \Phi_0 + (\Phi_\infty - \Phi_0) [\lg(\kappa^2) + 1] / 2, \quad (4.172)$$

The function  $\Phi_\infty(z_a)$  is defined by :

$$\Phi_\infty = \Phi_{Dan} + (1 - \Phi_{Dan}) [Y + 1] / 2. \quad (4.173)$$

where  $\Phi_{Dan}$  is the analytical solution of Danckwerts (4.162).

If the point considered ( $X, Y$ ) is not a node of the calculation set (see Fig.4.13), a linear approximation should be used.

Finally, it should be mentioned that a significant augmentation of the mass transfer due to the accompanying first order chemical reaction is possible at sufficiently high values of  $z_a$ . The practical use of chemical sorbents at small ( $\lg z_a < 0.5$ ) steady water meets with certain difficulties. The difficulties are associated with the sorbent preparations and the corrosion of the preparation solution vessels. Consequently, at such values of  $z_a$  the problem is theoretical rather than a practical.

#### CHAPTER 4.3. NON-STATIONARY ABSORPTION WITH SECOND ORDER CHEMICAL REACTION

In the real chemosorption processes with reactive absorbing components of the gas phase there are usually several stages of elementary reactions. These elementary stages form a second order chemical reaction. The wide use of bimolecular processes is probably attributed to the fact that the double collisions occur more frequently than those occurring between three, four or more particles of the solution do [33].

In the present chapter the simple case of a non-stationary two-phase absorption is discussed. The process is accompanied by a chemical reaction between the component  $A$  soluble in the liquid and the chemical sorbent  $B$ . The reaction is irreversible. The problem is interesting and from a theoretical point of view. The need to elaborate a calculation procedure for the chemosorption process design is related to the problem set up here. It is enough to

mention as an example the processes of cleaning of synthese gases by solutions of primary amines (monoethanol amine, diethanol amine, triethanol amine) in the industrial ammonia synthesis [34], as well as the  $\text{CO}_2$  recovery from such gases by base solutions [35] etc.

The absorption complicated with a chemical reaction and an interphase mass transfer located in the liquid phase are well discussed in details in [3, 4]. In these studies there are many examples that enable the application of the results developed here.

Let an irreversible chemical reaction be assumed which is occurred in the liquid phase:



where one mole of the soluble component  $A$  consumes  $q$  moles of the absorbents  $B$ .

Usually the calculations of absorption devices are restricted within the frame of the diffusion boundary layer in the liquid phase under the assumption that the concentration of  $A$  remains constant at the interface [3, 4]. This procedure supposes that the mass transfer resistance is located in the liquid phase only. However, such assumptions need a strong theoretical support.

Like in the cases discussed earlier the problem is discussed from the positions of the two-phase mass transfer assuming a continuity of the fluxes and the concentrations across the interface. In the situation discussed here there are two transport equations in the liquid phase considering the particles  $A$  and  $B$ :

$$\begin{aligned} \frac{\partial c'_1}{\partial \tau'} &= D_2 \frac{\partial^2 c'_1}{\partial y^2}, \quad \frac{\partial c'_2}{\partial \tau'} = D_2 \frac{\partial^2 c'_2}{\partial y^2} - \vec{k}_2 c'_2 B', \\ \frac{\partial B'}{\partial \tau'} &= D_2 \frac{\partial^2 c'_2}{\partial y^2} - q \vec{k}_2 c'_2 B'. \end{aligned} \quad (4.175)$$

Here  $B'$  is the concentration of  $B$  in the liquid, mol/l;  $\vec{k}_2$  is the rate constant of the forward second order reaction between  $A$  and  $B$ , l/(mol·s). The co-ordinate system is shown on Fig. 4.1. The basic assumption is that the diffusion coefficients  $D_2$  of all the particles in the liquid are equal.

The boundary conditions at the interface considering the concentration are:

$$D_2 \left( \frac{\partial c'_2}{\partial y} \right)_s = D_l \left( \frac{\partial c'_1}{\partial y} \right)_s, \quad \left( \frac{\partial B'}{\partial y} \right)_s = 0, \quad c'_{2s} = k c'_{1s} \quad \text{at } y = b_2. \quad (4.176)$$

The above equations are expressed upon the assumption that  $B$  is the non-volatile component and the surface concentration of  $A$  satisfies the Henry's law.

The conditions at  $y = 0$  and  $y = (b_1 + b_2)$  are:

$$\left( \frac{\partial c'_1}{\partial y} \right) = 0 \quad \text{at } y = (b_1 + b_2); \quad \left( \frac{\partial B'}{\partial y} \right) = \left( \frac{\partial c'_2}{\partial y} \right) = 0 \quad \text{at } y = 0. \quad (4.177)$$

The initial conditions for the concentrations remain constant:

$$c'_1 = c_0, \quad c'_2 = 0, \quad B' = N_0 \quad \text{at} \quad \tau' = 0. \quad (4.178)$$

Let dimensionless functions  $c_1$  and  $c_2$  for  $A$  be introduced by

$$c'_1 = c_0 c_1(\tau_1, y_1), \quad c'_2 = k c_0 c_2(\tau_2, y_2). \quad (4.179)$$

The component  $A$  in the liquid phase exists not only as physically soluble substance ( $c'_2$ ), but also it exists in the form of chemical compounds. Taking into account that 1 mole of  $A$  consumes  $q$  moles of  $B$  the introduction of an effective concentration of  $A$  for its amount in the compounds ( $c'$ ) is required [3, 4]:

$$c' \equiv \frac{(N_0 - B')}{q} = \left( \frac{N_0}{q} \right) (1 - B). \quad (4.180)$$

The corresponding dimensionless concentrations for  $c'$  and  $B'$  are:

$$B' = N_0 B, \quad c' = \left( \frac{N_0}{q} \right) c. \quad (4.181)$$

If the concentration  $c$  is known, the equations (4.180, 4.181) permit to obtain the concentration of the absorbent  $B'$  in the liquid phase, because  $B$  is related to the effective concentration  $c$  linearly:

$$B = 1 - c. \quad (4.182)$$

The dimensionless two-phase problem about  $c_1$ ,  $c_2$  and  $c$  may be formulated as follows:

$$\begin{aligned} \frac{\partial c_1}{\partial \tau_1} &= \frac{\partial^2 c_1}{\partial y_1^2}, \quad \frac{\partial c_2}{\partial \tau_2} = \frac{\partial^2 c_2}{\partial y_2^2} - a^2 c_2 (1 - c), \\ \frac{\partial c}{\partial \tau_2} &= \frac{\partial^2 c}{\partial y_2^2} + \left( \frac{1}{N} \right) a^2 c_2 (1 - c) \end{aligned} \quad (4.183)$$

$$\begin{aligned} \left( \frac{\partial c_2}{\partial y_2} \right)_s &= - \left( \frac{1}{\varepsilon \beta^2} \right) \left( \frac{\partial c_1}{\partial y_1} \right)_s, \quad c_{1s} = c_{2s}, \\ \left( \frac{\partial c}{\partial y_2} \right)_s &= 0 \quad \text{at} \quad y_2 = y_1 = 1. \end{aligned} \quad (4.184)$$

$$\begin{aligned} \left( \frac{\partial c_1}{\partial y_1} \right) &= 0 \quad \text{at } y_1 = 0; \quad \left( \frac{\partial c_2}{\partial y_2} \right) = \left( \frac{\partial c}{\partial y_2} \right) = 0 \quad \text{at } y_2 = 0; \\ c_1 &= 1, \quad c = c_2 = 0 \quad \text{at } \tau_2 = 0. \end{aligned} \quad (4.185)$$

Here  $\tau_1, \tau_2, y_1, y_2$  are dimensionless co-ordinates (see Fig.4.1);  $a^2 \equiv \frac{\bar{k}_2 N_0 b_2^2}{D_2}$  is the Damkohler number, i.e. the chemosorption parameter;  $N = \frac{N_0}{q k c_0}$  is the concentration ratio.

The mass balance equation with an irreversible reaction (4.174) is :

$$\left( b_1 c_0 - \int_{b_2}^{(b_1+b_2)} c'_1 dy \right) = \left[ \int_0^{b_2} \left( c'_2 + \frac{N_0 - B'}{q} \right) dy \right]$$

or in a dimensionless form :

$$\begin{aligned} \left( 1 - \int_0^1 c_1 dy_1 \right) &= \left( \frac{b_2}{b_1} k \right) \left[ \int_0^1 \left( c_2 + \frac{N_0}{q k c_0} c \right) dy_2 \right], \\ (1 - \bar{c}_1) &= \epsilon [\bar{c}_2 + N \bar{c}] \end{aligned} \quad (4.186)$$

where  $N = N_0 / q k c_0$ .

Let the most important (from a practical point of view) case be considered where the concentration  $N_0$  is greater than the maximal equilibrium concentration in the liquid phase  $k c_0$ :

$$N \gg 1. \quad (4.187)$$

Further, it will be demonstrated that if (4.187) is satisfied the change of the concentration  $B'$  becomes significant. This means that the kinetics of the second order reaction affects the mass transfer at  $\tau_2 \gg 1/a^2$ . At moderate values of  $\tau_2$  ( $\tau_2 \sim 1/a^2$ ) the interaction between  $A$  and  $B$  may be assumed as a reaction of a pseudo-first order. In the latter case the equations (4.183) may be expressed in formalistic way with  $c \equiv 0$ . A such problem has been discussed in chapter 4.2.

The further investigations of the problem (4.183-4.185) the important case of a short contact times between the phases will be considered. The basic assumption here is that the whole interphase mass transfer resistance is located in the liquid phase.

#### 4.3.1. Mass transfer in the liquid at short contact times

Let an absorption with inevitable second order chemical reaction in liquid phase be considered at short contact times [36]. The selection of the problem is not casual, because it is

widely encountered in the practice. The transport equations (4.183) are considered for the liquid phase only:

$$\begin{aligned}\frac{\partial c_2}{\partial z_a} - \frac{\partial^2 c_2}{\partial y_a^2} &= -c_2(1-c), \\ \frac{\partial c}{\partial z_a} - \frac{\partial^2 c}{\partial y_a^2} &= \left(\frac{q k c_0}{N_0}\right)c_2(1-c).\end{aligned}\quad (4.188)$$

The boundary condition at the interface become simpler:

$$c_{2s} = 1, \quad \left(\frac{\partial c}{\partial y_a}\right)_s = 0.$$

The condition at the solid surface, i.e. at  $y=0$  is replaced with a condition at the infinity:

$$\left(\frac{\partial c_2}{\partial y_a}\right) = c = 0 \quad \text{at} \quad y_a = \infty. \quad (4.189)$$

The initial conditions remain unchanged:

$$c_2 = c = 0 \quad \text{at} \quad z_a = 0. \quad (4.190)$$

The dimensionless co-ordinates along the axis  $y$  and the time axis  $y_a$  and  $z_a$  are:

$$1 - y_2 = \frac{I}{a} y_a, \quad \tau_2 = \frac{I}{a^2} z_a. \quad (4.191)$$

The assumption  $a^2 \gg I$  is based on the fact that at  $\tau_2 \gg 1/a^2$  there is a thin diffusion layer of the substance  $A$  close to the gas-liquid interface.

Taking into account that at  $z_a = 0$  the concentration  $c = 0$  it is clear that at an arbitrary section  $z_a$  of the right parts of the set of equations (4.188) the term with  $c$  may be omitted. Thus, one may assume that  $B = 1$ . In this case the chemical reaction kinetics corresponds to that of a pseudo-first order reaction. In this case the substitution

$$c = c^{(0)} / N \quad \text{or} \quad c' = (k c_0) c^{(0)}, \quad (4.192)$$

allows the expression of the equations (4.188-4.190) in a simpler way:

$$\frac{\partial c_2}{\partial z_a} - \frac{\partial^2 c_2}{\partial y_a^2} = -c_2, \quad \frac{\partial c^{(0)}}{\partial z_a} - \frac{\partial^2 c^{(0)}}{\partial y_a^2} = c_2,$$

$$\begin{aligned} c_2 &= 1, \quad \frac{\partial c^{(0)}}{\partial y_a} = 0 \quad \text{at} \quad y_a = 0; \\ c_2 &= c^{(0)} = 0 \quad \text{at} \quad y_a = \infty; \quad c_2 = c^{(0)} = 0 \quad \text{at} \quad z_a = 0. \end{aligned} \quad (4.193)$$

The relationship for the diffusion flux of  $A$  is:

$$Q \equiv -D_2 \int_0^z \left( \frac{\partial c'_2}{\partial y'} \right)_s d\tau' = (k c_0) \sqrt{\frac{D_2}{\bar{k}_2 N_0}} \int_0^z \left( \frac{\partial c_2}{\partial y_a} \right)_s dz_a = k c_0 \sqrt{\frac{D_2}{\bar{k}_2 N_0}} (\bar{c}_2 + \bar{k}^{(0)}), \quad (4.194)$$

where the average concentrations are:

$$\bar{c}_2 = \int_0^\infty c_2 dy_a, \quad \bar{c}^{(0)} = \int_0^\infty c^{(0)} dy_a. \quad (4.195)$$

The analytical solution of the problem (4.193) has been developed in [31]. The result obtained for the augmentation coefficient  $\Phi$  (see (4.162) in 4.2) is:

$$\Phi = \frac{\sqrt{\pi}}{2\sqrt{z_a}} \left[ (z_a + 1/2) \operatorname{erf}(\sqrt{z_a}) + \sqrt{\frac{z_a}{\pi}} \exp(-z_a) \right]. \quad (4.196)$$

The solution indicates that if  $z_a \ll 1$  the factor  $\Phi \rightarrow 1$  and the concentration of the reaction product  $c$  may be neglected. In the opposite case at  $z_a \gg 1$  practically all the absorbed amount of  $A$  is in the form of a chemical compound ( $c^{(0)} \gg c_2$ ). In this case the derivative  $\left( \frac{\partial c_2}{\partial z_a} \right)$  in the equations (4.193) may be omitted.

For small and large values of  $z_a$  the corresponding analytical solutions with respect to  $c_2$  are:

$$c_2 = \begin{cases} \operatorname{erfc}(\eta), & \text{if } z_a \ll 1; \\ \exp(-y_a), & \text{if } z_a \gg 1, \end{cases} \quad (4.197)$$

where  $\eta = y_a / \sqrt{z_a}$  is a similarity variable.

Let the corresponding relationships for  $c$  be obtained. It is well known that the diffusion equation with an arbitrary right part  $f(x, y)$ :

$$\frac{\partial c}{\partial z_a} - \frac{\partial^2 c}{\partial y_a^2} = f(z_a, y_a)$$

with boundary conditions

$$\frac{\partial c}{\partial y_a} \text{ at } y=0, \quad c=0 \text{ at } y_a=\infty$$

and with initial condition

$$c=0 \text{ at } z_a=0$$

has a solution in the form of the Green's function [9]:

$$c(z_a, y_a) = \frac{1}{2\sqrt{\pi}} \int_0^{z_a} \left\{ \int_0^{\infty} f(\xi, t) \left[ \exp\left(-\frac{(y_a + \xi)^2}{4(z_a - t)}\right) + \exp\left(-\frac{(y_a - \xi)^2}{4(z_a - t)}\right) \right] d\xi \right\} \frac{dt}{\sqrt{z_a - t}}. \quad (4.198)$$

Obviously,  $c^{(0)}$  may be calculated by means of the substitution  $f = c_2(z_a, y_a)$  in (4.198). Let the surface concentration  $c_s^{(0)}(z_a)$  be defined by a substitution  $y_a = 0$  in (4.198).

At  $z_a \ll 1$  the result is:

$$\begin{aligned} c_s^{(0)}(z_a) &= \frac{1}{\sqrt{\pi}} \int_0^{z_a} \left\{ \int_0^{\infty} \operatorname{erfc}\left(\frac{\xi}{2\sqrt{t}}\right) \exp\left(-\frac{\xi^2}{4(z_a - t)}\right) d\xi \right\} \frac{dt}{\sqrt{z_a - t}} = \\ &= \frac{2}{\pi} \int_0^{z_a} \operatorname{arctg}\left(\frac{\sqrt{t}}{\sqrt{z_a - t}}\right) dt = \frac{2z_a}{\pi} \int_0^{\infty} \frac{dt}{(1+t^2)^2} = \frac{z_a}{2}. \end{aligned} \quad (4.199)$$

During the derivation of (4.199) the integrals

$$\int_0^{\infty} \operatorname{erfc}\left(\frac{\xi}{2\sqrt{t}}\right) \exp\left(-\frac{\xi^2}{4(z_a - t)}\right) d\xi = \frac{2}{\sqrt{\pi}} \operatorname{arctg}\left(\sqrt{\frac{t}{z_a - t}}\right) \left(\sqrt{z_a - t}\right)$$

and

$$\frac{2}{\pi} \int_0^{\infty} \frac{dt}{(1+t^2)^2} = \frac{1}{2},$$

were used in the forms developed in [11].

In the other limiting case ( $z_a \gg 1$ ) (see (4.197)) the result is:

$$c_s^{(0)} = \frac{1}{\sqrt{\pi}} \int_0^{z_a} \left\{ \int_0^{\infty} \exp(-\xi) \exp\left(-\frac{\xi^2}{4(z_a - t)}\right) d\xi \right\} \frac{dt}{\sqrt{z_a - t}} =$$

$$= \int_0^{z_a} \exp(-t) \operatorname{erfc}(\sqrt{t}) dt = \frac{2}{\sqrt{\pi}} \sqrt{z_a}. \quad (4.200)$$

The formulae 4.199 and 4.200 permit to define the applicability of the approximation (4.193), i.e. of the analytical equations of Danckwerts (4.196). In the general case  $c \leq c_s(z_a)$  and at  $z_a \gg 1$  the surface concentration is  $c_s = \frac{1}{N} \left( \frac{2\sqrt{z_a}}{\sqrt{\pi}} \right)$ . Thus, it is easy to prove that the assumption of the pseudo-first order of the chemical reaction is valid at  $z_a \ll N^2$ . It should be noted that in the case just considered  $N^2 \gg 1$  (4.187).

The further investigations of the solution of (4.188-4.190) in the area of the non-linear kinetics require new dimensionless co-ordinates  $x, y$ :

$$z_a = N^2 x, \quad y_a = Ny. \quad (4.201)$$

The new variables transform the set of equations (4.188-4.190) at high  $z_a$  to a simpler form:

$$\begin{aligned} \frac{\partial^2 c_2}{\partial y^2} &= (1-c)c_2 N^2, \\ \frac{\partial c}{\partial x} - \frac{\partial^2 c}{\partial y^2} &= (1-c)c_2 N. \end{aligned} \quad (4.202)$$

The solution of (4.202) at small  $x$  ( $x \ll 1$ ) is the approximation

$$c_2 = \exp(-yN). \quad (4.203)$$

The concentration  $c(x, y)$  is defined by the integral (4.198), where  $f = \exp(-\xi N)N$ . The integration with respect to the variable  $t$  gives:

$$c = \frac{\sqrt{x}}{\sqrt{\pi}} \int_0^\infty \exp(-\xi_0) \{ [\exp(-\eta_+^2) - \sqrt{\pi}\eta_+ \operatorname{erfc}(\eta_+)] + [\exp(-\eta_-^2) - \sqrt{\pi}\eta_- \operatorname{erfc}(\eta_-)] \} d\xi_0, \quad (4.204)$$

where

$$\eta_\pm = \left| \frac{y \pm \xi}{2\sqrt{x}} \right| = \varepsilon_0 |y_a \pm \xi_0|, \quad y = \frac{y_a}{N}, \quad \eta = \frac{y_a}{2\sqrt{z_a}}, \quad \varepsilon_0 = \frac{1}{2\sqrt{z_a}}.$$

If  $\eta \ll 1$  ( $y_a \ll 2\sqrt{z_a}$ ) the terms of (4.204) in the brackets may be expressed by Taylor's expansions. The next integration procedure gives the following approximations:

$$c(x, y) = \frac{2\sqrt{x}}{\sqrt{\pi}} \left\{ I - \varepsilon \sqrt{\pi} [y_a + \exp(-y_a)] \right\} = \frac{2\sqrt{x}}{\sqrt{\pi}} = c_s(x),$$

$$\frac{\partial c}{\partial \eta} = -c_s(x)\sqrt{\pi}[I - \exp(-y_a)], \quad y_a \ll 2\sqrt{z_a}. \quad (4.205)$$

It is clear from (4.204, 4.205) that the main variations of the concentration  $c_2$  occur near the gas-liquid interface at a distance  $y_a \approx 1$ . At  $y_a \gg 1$  one may substitute  $\eta_+ = \eta_- = \eta$  in the integral of (4.204). Thus, the result is:

$$c(x, y) = c_s(x) \left[ \exp(-\eta^2) - \sqrt{\pi}(\eta) \operatorname{erfc}(\eta) \right]. \quad (4.206)$$

It is easy to demonstrate, that at  $y_a \ll 2\sqrt{z_a}$  the relationships (4.206) and (4.205) are identical. Thus, the relationship (4.206) is valid everywhere (with an equally distributed accuracy) at  $\eta \gg 0$ . Note that the derivative of (4.206) is not zero at the interface in contrast to the derivative of the exact solution (4.205). The asymptotic behaviour of the function (4.206) is:

$$c(x, y) \Rightarrow c_s(x) \frac{\exp(-\eta^2)}{2\eta^2} \ll c_s(x), \quad \eta \gg 1.$$

The inequality means that at  $z_a \gg 1$  the thickness of the diffusion boundary layer is  $\delta y_a = 2\sqrt{z_a}$  and it is significantly greater than the dimension of the reaction zone. This allows to assume  $c = c_s$  during the solution of (4.202)

$$\frac{\partial^2 c_2}{\partial y^2} = (1 - c_s) c_2 N^2, \quad \frac{\partial c}{\partial x} - \frac{\partial^2 c}{\partial y^2} = (1 - c_s) c_2 N. \quad (4.207)$$

It is evident, that the above law-determined features should be valid at moderate values of  $x$ .

The solution of (4.207) with the associated boundary conditions (4.189-4.190) is:

$$c_2 = \exp\left(-\sqrt{1 - c_s} y N\right),$$

$$c = \frac{1}{\sqrt{\pi}} \int_0^x \frac{\sqrt{1 - c_s} \exp\left[-y^2/4(x-t)\right]}{\sqrt{x-t}} dt. \quad (4.208)$$

The substitution of  $y = 0$  in (4.208) gives the following non-linear integral equation with respect to the surface concentration  $c_s(x)$ :

$$c_s(x) = \frac{1}{\sqrt{\pi}} \int_0^x \frac{\sqrt{1-c_s}}{\sqrt{x-t}} dt. \quad (4.209)$$

It should be noted that at  $x \ll 1$  the result is the relationship (4.200).

The solution of (4.209) will be found in the form of a power series:

$$\sqrt{1-c_s} = a_0 + a_1 x^{1/2} + \dots + a_k x^{k/2} + \dots . \quad (4.210)$$

The substitution of the series in (4.209) and the equalizing of the terms of both sides (having equal powers) with respect the  $x$  gives recurrent relationships for the coefficients  $a_n$ :

$$A_1 = 2, \quad A_2 = \pi/2, \quad A_n = (n-1)/n \quad \text{at } n \geq 3;$$

$$a_0 = 1, \quad a_1 = -2/\sqrt{\pi}, \quad a_2 = 1 - 2/\pi,$$

$$a_n = \begin{cases} \frac{1}{2} \left[ (a_1 a_{n-1}) A_n - 2 \sum_{i=1}^{\frac{n-1}{2}} (a_i a_{n-i}) \right], & n \geq 3, \text{ odd numbers,} \\ \frac{1}{2} \left[ (a_1 a_{n-1}) A_n - a_{n/2}^2 - 2 \sum_{i=1}^{\frac{n-1}{2}} (a_i a_{n-i}) \right], & n \geq 4, \text{ even numbers.} \end{cases} \quad (4.211)$$

The first five coefficients are:

$$a_0 = 1, \quad a_1 = -1.13, \quad a_2 = 0.36, \quad a_3 = 0.136, \quad a_4 = 2.64 \times 10^{-3}, \quad a_5 = -5.1 \times 10^{-2}.$$

It is sufficient restrict the series (4.210) up to five terms only. The calculations of  $c_s(x)$  at  $k$ , equal to 5 and 100 are practically equal. The solution of the integral equation (4.209) exists as a series (4.210) if  $x < 1$  only. The asymptotic values of the function  $\sqrt{1-c_s}$  at  $x \gg 1$  is:

$$\sqrt{1-c_s} \rightarrow \frac{1}{2\sqrt{\pi x}} \quad \text{or} \quad c_s \rightarrow 1 - \frac{1}{4\pi x}. \quad (4.212)$$

The latter is easy to check directly by a substitution in (4.209).

The distribution of the concentrations  $c_2$  and  $c$  at high values of  $x$  may be evaluated by mean of the formulae (4.208) and (4.212). The result is [11]:

$$c_2 = \exp(-\eta_a), \quad (4.213)$$

$$c(x, y) = \frac{1}{\pi} \int_0^{\infty} \frac{\exp[-(\eta \operatorname{cth}(t))^2]}{\operatorname{cth}(t)} dt = \frac{1}{2} \operatorname{erfc}(\eta), \quad (4.214)$$

where

$$\eta = \sqrt{\pi} \frac{\eta_a}{N}, \quad \eta_a = \frac{y_a}{2\sqrt{z_a}} = \frac{y}{2\sqrt{x}}.$$

The concentration  $c_s$  is different from zero (see (4.197) and (4.206)) in a rather narrow zone in comparison with the diffusion boundary layer thickness (with respect to  $c$ )  $\delta \approx 2\sqrt{x}$ . On the other hand, the function (4.214) is valid everywhere if  $\eta \geq 0$  despite the fact that its derivative does not satisfy the zero condition at the gas-liquid interface. It is easy to demonstrate that close to the interface the following approximations of  $\left(\frac{\partial c}{\partial \eta}\right)_s$  valid:

$$\frac{\partial c}{\partial \eta} = \begin{cases} -\frac{1}{\sqrt{\pi}} [1 - \exp(-\eta_a)], & \eta \ll 1; \\ -\frac{1}{\sqrt{\pi}} \exp(-\eta^2), & \eta_a \gg 1. \end{cases} \quad (4.215)$$

The calculated dimensionless concentration  $c_s(x)$  is shown on Fig. 4.23.

The average dimensionless concentration  $\bar{c}(x)$  may be obtained by an integration of (4.208) with respect to  $y$  in the range  $(0, \infty)$ :

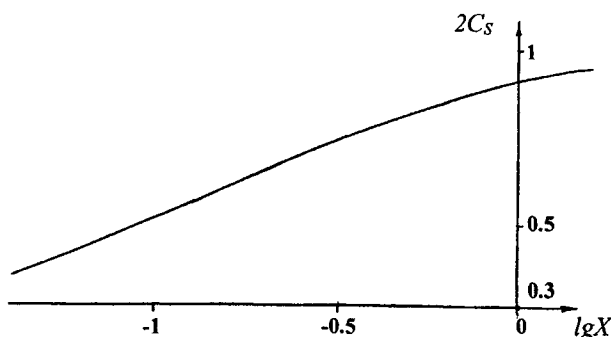


Fig. 4.23. Relationship between the product concentration and the time at short time contact and resistance in the liquid phase.

$$\bar{c}(x) = \frac{1}{\sqrt{\pi}} \left[ \int_0^x \int_0^\infty \frac{\exp \frac{-y^2}{4(x-t)}}{\sqrt{x-t}} dy \right] \sqrt{I - c_s} dt = \int_0^x \sqrt{I - c_s} dt. \quad (4.216)$$

The corresponding augmentation factor  $\Phi$  is :

$$\Phi = \frac{\bar{c}(x)}{2\sqrt{x/\pi}} N.$$

There are many approximations of  $\Phi$  available in the literature.

The equality of the diffusion coefficients in the liquid phase leads to the following semi-empirical relationship [37]:

$$\Phi = \left( \frac{\sqrt{\pi x}}{\sqrt{\pi x} + \exp(-0.35\sqrt{\pi x})} \right) N. \quad (4.217)$$

Figure 4.24 illustrates the approximation (4.217) and the analytical solution (4.210) obtained earlier. The error does not exceed 15%.

The absorption process at  $x \gg 1$  is well known as a *very fast chemical reaction*[3, 4]. In this case the set of exact equations (4.188-4.190) may be replaced by a model problem [3, 4]:

$$c = I, \quad \frac{\partial c_2}{\partial x} = \frac{\partial^2 c_2}{\partial y^2} \quad \text{at } y \leq y_s; \quad c_2 = 0, \quad \frac{\partial c}{\partial x} = \frac{\partial^2 c}{\partial y^2} \quad \text{at } y \geq y_s;$$

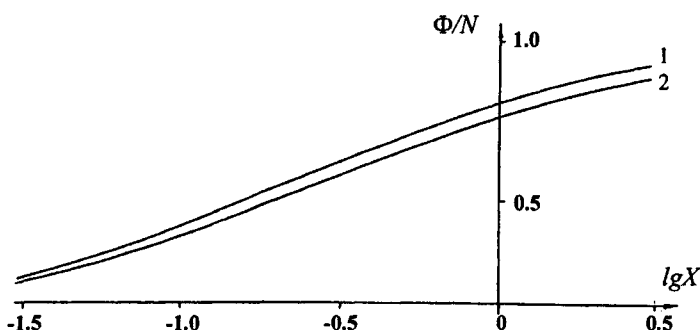


Fig. 4.24. Relationship between the factor  $\Phi$  and the time: 1) analytical solution according to (4.210); 2) approximation according (4.217).

$$\left( \frac{\partial c}{\partial y} \right)_s = \left( \frac{1}{N} \right) \left( \frac{\partial c_2}{\partial y} \right)_s, \quad c_2 = 0, \quad c_s = 1 \quad \text{at } y_s = 2\sqrt{\beta x}; \\ c = 0 \quad \text{at } y = \infty; \quad c_2 = 1 \quad \text{at } y = 0, \quad (4.218)$$

where the constant  $\beta = (1/N^2)$  is a solution of (4.218).

The main assumption of the model that the reaction between  $A$  and  $B$  occurs at the reaction plane  $y = y_s = 2\sqrt{x}/N$ , ( $\eta_a = 1$ ) only. It is easy to demonstrate, that the solution of (4.218) exists in the form

$$c_2 = 1 - \frac{\operatorname{erfc}(\eta)}{\operatorname{erfc}(\beta)} = 1 - \eta_a, \quad c = 1 \quad \text{at } \eta_a \leq 1, \\ c = \operatorname{erfc}(\eta), \quad c_2 = 0 \quad \text{at } \eta_a > 1. \quad (4.219)$$

The concentration  $c(\eta)$  defined by the model (4.218) practically coincides with the exact solution (4.214). However, there are differences between the concentration distribution ( $c_2$ ) (see also (4.213) and (4.219)). The exact solution demonstrates that at  $a \gg 1$ ,  $z_a \gg 1$  there is a thin diffusion boundary layer of the soluble component  $A$ . The thickness of this layer is significantly lower than the corresponding layer of the absorbent  $B$  (or  $C$ ). The term *reaction front* ( $y = y_s$ ) defined as the surface where the chemical interaction between  $A$  and  $B$  takes place (the basic assumption of the model) has no physical meaning. It is a mathematical idealization of the real processes. However, the values of the augmentation factor ( $\Phi = N$ ) derived by both models are equal.

#### 4.3.2 Transformation of the problem of two-phase chemisorption to a two-phase absorption problem with non-linear boundary conditions

The results obtained in the previous chapter may be applied to the general case of non-linear chemical kinetics at  $\tau_2 \gg 1/a^2$ . The satisfaction of the condition (4.187) in the transport equations for  $A$  in the liquid phase allows the non-stationary term  $\frac{\partial c_2}{\partial \tau_2}$  to be omitted. In a similar way the equation with respect to  $B$  may lose his volumetric source term. Moreover, in this time interval one may assume  $c = c_s(\tau)$ . The latter assumption allows the determination of the distribution of  $A$  in the liquid:

$$c_2(\tau_2, y_2) = c_{ls}(\tau) \frac{ch[a y_2 \sqrt{1 - c_s(\tau)}]}{ch[a \sqrt{1 - c_s(\tau)}]}, \quad \tau_2 \gg 1/a^2. \quad (4.220)$$

Thus, there is no need to solve the transport equation for the soluble component  $A$  in the liquid phase:

Thus, the dimensionless form of the problem (4.183-4.185) becomes simpler:

$$\frac{\partial c_1}{\partial \tau_1} = \frac{\partial^2 c_1}{\partial y_1^2}, \quad \frac{\partial c}{\partial \tau_2} = \frac{\partial^2 c}{\partial y_2^2}; \quad (4.221)$$

$$\left( \frac{\partial c}{\partial y_2} \right)_s = P_2 \sqrt{1 - c_s} \frac{\operatorname{th}(a\sqrt{1 - c_s})}{\operatorname{th}(a)} c_{ls},$$

$$\left( \frac{\partial c_1}{\partial y_1} \right)_s = -P_1 \sqrt{1 - c_s} \frac{\operatorname{th}(a\sqrt{1 - c_s})}{\operatorname{th}(a)} c_{ls}, \text{ at } y_1 = y_2 = 1; \quad (4.222)$$

$$\left( \frac{\partial c_1}{\partial y_1} \right) = 0 \quad \text{at } y_1 = 0;$$

$$\left( \frac{\partial c}{\partial y_2} \right) = 0 \quad \text{at } y_2 = 0;$$

$$c_1 = 1, \quad c = 0 \quad \text{at } \tau_1 = 0, \quad (4.223)$$

where  $P_2 = \frac{a}{N} \operatorname{th}(a)$ ,  $P_1 = \varepsilon \beta^2 N P_2 = \varepsilon \beta^2 a \operatorname{th}(a)$ .

The new dimensionless variables transform the integral mass balance equation (in the case of chemisorption when  $\tau_2 \gg 1/a^2$ ) to:

$$I \equiv (1 - \bar{c}_1) = (\varepsilon N) \bar{c}. \quad (4.224)$$

The result coincides with that obtained in the case of a physical absorption (4.8). The absorption parameter  $\varepsilon$  is replaced here by  $\varepsilon N$ . Moreover, the concentration of  $A$  in the chemical compounds  $\bar{c}$  replace the concentration  $\bar{c}_2$ . This is attributed to the fact that all the time the component  $A$  exists in the chemical compound only.

Despite that the diffusion flux of the reaction product  $C$  is zero at the gas-liquid interface in accordance with the model (4.221-4.223) and the concentration distributions with respect to  $c_1$ ,  $c_2$ ,  $c$ , derived by both models at  $\tau_2 \gg 1/a^2$  are practically equivalent. The analysis done shows that the main changes of the concentration  $c_2$  (in the liquid) occur near the interface at a distance where the concentration  $c$  is practically equal  $c_s$ . When  $a \gg 1$  (see 4.3.1) the concentration  $c_2$  varies from  $c_{ls}$  down to zero within a thin diffusion layer with respect to the component  $A$  (4.203, 4.213). The characteristic dimensions of the area of variation of  $c$  are greater than the layer dimensions because faraway  $c_2 = 0$ . This permits to omit the source term in the transport equation, so the concentration of the product across the whole layer  $b_2$  varies in accordance with the molecular diffusion law (4.221).

At moderate values of  $a^2$  ( $a^2 \sim 1$ , taking into account the case  $a \ll 1$ , too) and times  $\tau_2 \gg 1/a^2$ , the non-stationary term in the transport equations with respect to  $c_2$  may be neglected. In this case the product concentration  $c$  grows across entire the layer depth  $b_2$ , so it may be assumed that  $c = c_s$  and the equation (4.220) is valid.

From a formalistic point of view the transformation of a set containing three differential equations (4.183) into the set of equations (4.221) may be carried out by means of an expression of the solution of (4.183) assuming  $1/N \ll 1$  as a small parameter.

The unknown concentration at the interface  $c_s(\tau)$  follows from the conditions governing the equality of the fluxes  $\left(\frac{\partial c_1}{\partial y_1}\right)_s$  and  $\left(\frac{\partial c_2}{\partial y_2}\right)_s$ , taking into account that:

$$\begin{aligned} \left(\frac{\partial c_2}{\partial y_2}\right)_s &= c_{1s} a \sqrt{1 - c_s} \operatorname{th}(a \sqrt{1 - c_s}) = a^2 \bar{c}_2(1 - \bar{c}), \\ \frac{\partial \bar{c}}{\partial \tau_2} &= \left(\frac{\partial c}{\partial y_2}\right)_s = \frac{a^2 \bar{c}_2(1 - \bar{c})}{N}. \end{aligned} \quad (4.225)$$

The model ignores the condition  $\left(\frac{\partial c}{\partial y_2}\right)_s = 0$  at the interface.

In this way the two-phase chemisorption problem governed by a non-liner kinetics at  $\tau_2 \gg 1/a^2$  is transformed into an equivalent two-phase problem (4.221-4.223). The equivalent problem resembles the non-stationary two-phase absorption problem, but here  $\varepsilon \Rightarrow \varepsilon N$ ,  $c_2 \Rightarrow c$ . Moreover, the concentration  $c_s$  is governed by the non-linear conditions (4.222).

The solution of (4.221-4.223) depends on four dimensionless parameters:  $\varepsilon$ ,  $\beta^2$ ,  $a^2$ ,  $N$ . Further one should take into consideration the analogy between (4.221-4.223) and the corresponding two-phase absorption problem (see 4.1). The independent parameters are:

$$\varepsilon N, \varepsilon \beta N, \frac{a}{N}, a. \quad (4.226)$$

For clarity of explanation a Cartesian co-ordinate system  $X_N - Y_N$  is introduced:

$$X_N \equiv \lg(\varepsilon N), \quad Y_N \equiv \lg(\varepsilon \beta N). \quad (4.227)$$

Obviously, these co-ordinates are related with  $X = \lg \varepsilon$ ,  $Y = \lg \varepsilon \beta$  (employed in the case of two-phase absorption see Fig. 4.3) by linear relationships:

$$X_N = X + \lg N, \quad Y_N = Y + \lg N. \quad (4.228)$$

The latter means that the planes  $(X - Y)$  and  $(X_N - Y_N)$  are shifted at a distance  $\lg N$  as shown on Fig. 4.25.

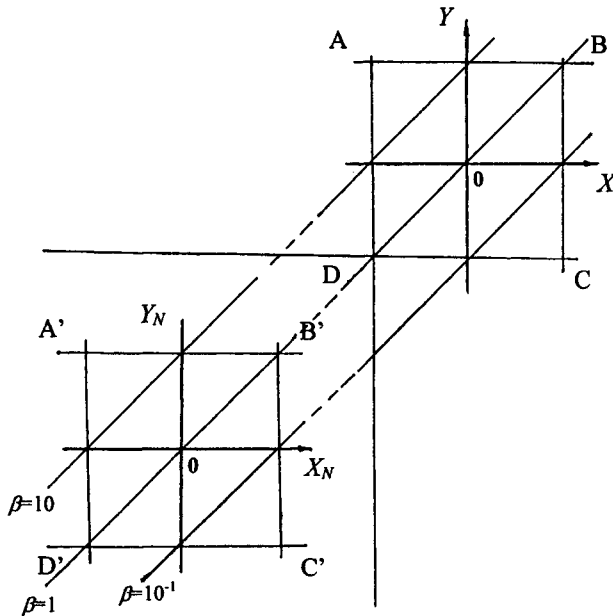


Fig. 4.25. Comparative positions of the planes  $X - Y$  and  $X_N - Y_N$ .

Like in the case of two-phase absorption the solution (4.221-4.223) is investigated at all the points of the chemosorption plane ( $X_N - Y_N$ ). The parameters  $\frac{a}{N}$  and  $a$  may take any values from zero to infinity. It will be proved further that it is enough to tabulate the solution in a restricted area of the plane  $X_N - Y_N$  only:

$$-1 \leq X_N \leq 1, \quad -1 \leq Y_N \leq 1, \quad (4.229)$$

i. e. in the so-called "chemosorption square" (Fig. 4.25). That entire square is located in the lower left corner of the absorption plane  $X - Y$  if  $N \gg 1$  and the following inequalities (see Fig. 4.2 or Fig. 4.25) are satisfied:

$$\varepsilon \ll 1, \quad \varepsilon \beta \ll 1. \quad (4.230)$$

The latter condition means that in the entire chemosorption square the diffusion resistance of the physical absorption is located in the liquid phase and  $c_{ls}^{abs}(\tau) = 1$ . Because at  $\tau \rightarrow 0$  the chemical reaction may be ignored the chemosorption of  $A$  at the interface must satisfy the condition:

$$c_{ls}(\tau) \rightarrow 1 \quad \text{at } \tau \rightarrow 0. \quad (4.231)$$

The time interval, where  $c_{ls} = 1$  (with an accuracy of 5% for example) is termed *initial chemosorption interval*.

The aim of the investigation is to find solutions of (4.221-4.223) in the form of dimensionless fluxes  $\Sigma(\tau)$  and  $I(\tau)$  at arbitrary values of  $\tau$  in the entire chemosorption plane  $X_N - Y_N$ . If the fluxes  $\Sigma(\tau)$  or  $I(\tau)$  are known the chemosorption design (the calculation of  $\tau$  by known  $I$  or *vice versa*) is a trivial problem. However, it will be demonstrated further that the solution strongly depends on the position of the point  $X_N, Y_N$  in the different quadrants of the chemosorption plane. Because of that the two-phase chemosorption problem will be discussed at each quadrant separately. In a way similar to that used in the case of the two-phase absorption the left half plane  $X_N - Y_N$  ( $X_N \leq 0$ ) will be used for the determination of  $\Sigma(\tau)$ , while the right one ( $X_N > 0$ ) for the flux  $I(\tau)$ .

#### 4.3.3. Solution with parameters $\varepsilon N \leq 1$ , $\varepsilon \beta N \leq 1$

From a physical point of view the dimensionless complexes  $\varepsilon N$  and  $\varepsilon \beta N$  are the liquid capacities (or the chemosorption factors) at "short" and "long" contact times. The definition for long times (high  $\tau$ ) follows directly from the mass balance equation (4.224), while the short time contact definition of the liquid capacity follows from equation (4.245) at small  $\tau$ .

A special feature of the two-phase transport problems discussed here is the existence of characteristic time intervals  $\left(\frac{b_2^2}{D_L}\right)$  and  $\left(\frac{b_1^2}{D_g}\right)$ , i.e. two dimensionless variables  $\tau_1$  and  $\tau_2$ . The partial differential equations (4.221) are parabolic. In accordance with the theory [9] inspite the boundary conditions at the interface at small  $\tau_2$  (in the liquid) and  $\tau_1$  (in the gas) there are diffusion boundary layers with thicknesses  $\delta_2 = \sqrt{\tau_2}$  ( $\delta_1 = \sqrt{\tau_1}$ ). They grow throughout the entire phase (liquid or gas)  $\tau_2 \cong I(\tau_1 \cong 1)$ . At long times  $\tau_2 \gg I(\tau_1 \gg 1)$  and the change of the concentration in the lateral direction (along  $y$ ) may be neglected:

$$c(\tau_2, y_2) = c_s(\tau_2), \quad c_i(\tau_1, y_1) = c_{ls}(\tau_1). \quad (4.232)$$

The ratios  $\left(\frac{b_2^2}{D_2}\right)$  and  $\left(\frac{b_1^2}{D_1}\right)$  determine where the boundary layer grows faster.

Obviously, in the general case the following relation is valid:

$$\delta_2 = \beta \delta_1. \quad (4.233)$$

By the help of the chemosorption plane  $X_N - Y_N$  (Fig. 4.25) it is easy to detect that on the bisectrix  $AC$  (first quadrant), the parameter  $\beta^2$  remains constant. For all point located

below  $AC$  the inequality  $\beta^2 \leq 1$  is satisfied, while for all of them located above that line the condition  $\beta^2 \geq 1$  takes place.

For better understanding of the problem (4.221-4.223) two important limiting cases will be studied. The first case corresponds to the situation where both boundary layers grow throughout the entire phases. The second case considers existing boundary layers in both phases.

Solution when boundary layers in both phases grow throughout the entire phases. The solution in the first case exists at sufficiently long contact times ( $\tau \Rightarrow \infty$ ). The mass balance equation (4.232) gives:

$$c_s = \sum, \quad c_{ls} = 1 - (\varepsilon N) \sum. \quad (4.234)$$

The integration along  $y_2$  from zero to  $I$  permits to obtain (taking into account the conditions at the interface for  $\Sigma(\tau)$ ) an ordinary differential equation :

$$\frac{d \Sigma_o}{dz_o} = \sqrt{I - \sum} \left[ \frac{th(a\sqrt{I - \Sigma_o})}{th(a)} \right] [I - (\varepsilon N) \sum_o], \quad \Sigma_o(0) = 0, \quad (4.235)$$

where the dimensionless time  $z_o$  and the chemosorption parameter  $P_2$  are:

$$z_o = P_2 \tau_2, \quad P_2 = a \frac{h(a)}{N}.$$

Let  $\Sigma_o(X_N, a, z_o)$  is a solution of (4.235). The function  $\Sigma_o(z_o)$  is two-parametrical and depends on  $a$  and  $\varepsilon N$ . Taking into account that the main variations of  $\Sigma_o$  occur in the area  $z_o \sim 1$  one may suppose that the solution of the general problem (4.183-4.185) could be confined to (4.235) at sufficiently small parameters  $P_2$  ( $P_2 \leq P_2^{min}$ ). At moderate values of  $P_2$  the investigation of the general two-phase problem may be restricted for  $a \gg 1$ . The latter follows from the definition of  $P_2$  and the inequality  $N \gg 1$  (4.187). The substitution  $th(\sqrt{a(1 - c_s)}) \Rightarrow 1$  in (4.235) leads to [38]:

$$[I - \Sigma_o(\infty, X_N, z)]^{1/2} = \frac{I - \left( \frac{1 - \varepsilon N}{\varepsilon N} \right)^{1/2} tg[(\varepsilon N)^{1/2} (I - \varepsilon N)^{1/2} z/2]}{I + \left( \frac{1 - \varepsilon N}{\varepsilon N} \right)^{1/2} tg[(\varepsilon N)^{1/2} (I - \varepsilon N)^{1/2} z/2]}, \quad (4.236)$$

where  $z \equiv \frac{a}{N} \tau_2$  because  $a \gg 1$ . The same substitution in the boundary condition (4.222) yields the dimensionless problem (4.221-4.223) at  $a \gg 1$ :

$$\frac{\partial c_1}{\partial \tau_1} = \frac{\partial^2 c_1}{\partial y_1^2}, \quad \frac{\partial c}{\partial \tau_1} = \frac{\partial^2 c}{\partial y_2^2}; \quad (4.237)$$

$$\begin{aligned} \left( \frac{\partial c}{\partial y_2} \right)_s &= P_2 \sqrt{1 - c_s(\tau)} c_{ls}(\tau); \\ \left( \frac{\partial c_1}{\partial y_1} \right)_s &= -P_1 \sqrt{1 - c_s(\tau)} c_{ls}. \end{aligned} \quad (4.238)$$

The conditions (4.223) remain the unchanged. The problem (4.237-4.238, 4.223) is three-parametric and depends on the parameters

$$X_N, Y_N, P_2 \equiv a/N \quad (4.239)$$

in the third quadrant. The corresponding dimensionless flux is  $\Sigma_\infty(X_N, Y_N, P_2, \tau_2)$ .

In this way the four-parametric problem (4.221-4.223) has been split into two problems. The first one (4.235) is two-parametric, while the second (4.238, 4.223) is three-parametric. A criterion for applicability of each of them is the value of the parameter  $P_2$ . It is evident that

$$\Sigma = \begin{cases} \Sigma_\infty(P_2, X_N, Y_N, z), & \text{if } P_2 \geq P_2^{\min}(X_N, Y_N); \\ \Sigma_0(a, X_N, z_0), & \text{if } P_2 < P_2^{\min}(X_N, Y_N). \end{cases} \quad (4.240)$$

From the discussion above it is clear that  $P_2^{\min} \ll 1$ . Its value depends on the location of the point in the plane  $X_N - Y_N$  as well as on the accuracy of satisfaction of the equality (4.240) and may be obtained by numerical calculations only. Usually its value should be chosen from the condition that in the entire quadrant it would remain constant.

The case where the boundary layers exist in both phases. At these conditions very small contact times occur. The introduction of the dimensionless variables

$$1 - y_1 = \left( \frac{1}{P_2 \beta} \right) y_{ls}, \quad 1 - y_2 = \frac{1}{P_2} y_{2s}, \quad z = P_2^2 \tau_2 = (P_2 \beta) \tau_1, \quad (4.241)$$

along the axes  $y_1$ ,  $y_2$  and  $\tau_2$  transform the problem (4.221-4.223) in:

$$\frac{\partial c_1}{\partial z} = \frac{\partial^2 c_1}{\partial y_{ls}^2}, \quad \frac{\partial c}{\partial z} = \frac{\partial^2 c}{\partial y_{2s}^2}, \quad (4.242)$$

$$\left( \frac{\partial c}{\partial y_{2s}} \right)_s = -\sqrt{1 - c_s(z)} c_{ls},$$

$$\left( \frac{\partial c_1}{\partial y_{ls}} \right)_s = (\varepsilon \beta N) \sqrt{1 - c_s(z)} c_{ls}; \quad (4.243)$$

$$\begin{aligned} \left( \frac{\partial c}{\partial y_{2s}} \right)_\infty &= \left( \frac{\partial c_1}{\partial y_{ls}} \right)_\infty = 0 \quad \text{at} \quad y_{2s} \rightarrow \infty, y_{ls} \rightarrow \infty; \\ c = 0, \quad c_1 = 1 &\quad \text{at} \quad z = 0. \end{aligned} \quad (4.244)$$

It is clear that the solution of this problem is:

$$\begin{aligned} \Sigma_p(z) &\equiv \int_0^\infty c dy_{2s}, \\ I_p(z) &\equiv \int_0^\infty (1 - c_1) dy_s, \end{aligned}$$

and depends on the dimensionless parameter  $Y_N$  only. From a formal point of view the latter problem follows from (4.221-4.223) at  $P_2 \rightarrow \infty$ . The corresponding mass balance equation is:

$$I_p = (\varepsilon \beta N) \Sigma_p. \quad (4.245)$$

Obviously

$$\Sigma_p \equiv \lim_{P_2 \rightarrow \infty} [P_2 \Sigma(P_2, Y_N, z)]. \quad (4.246)$$

Further, it will be demonstrated that at any points of the third quadrant at sufficiently high value of  $P_2$  and in the range  $z \sim 1$  the equality  $P_i \Sigma \approx \Sigma_p$  is satisfied.

Figure 4.26 presents the numerical calculation of the function  $\Sigma_p(z)$  in the range  $-1.2 \leq \lg z \leq 1.2$  for various discrete values of the parameter  $Y_N \geq 0$ . It is clear that its effect on the solution is not significant. Moreover, at  $Y_N \geq 1$  (curve 3) this effect disappears. The asymptotic relationships  $\Sigma_p$  at low and high values of  $z$  are independent of  $Y_N$  (curves I and II), too:

$$\Sigma_p \rightarrow \begin{cases} z & (z \rightarrow 0), \\ 2\sqrt{\frac{z}{\pi}} & (z \rightarrow \infty). \end{cases} \quad (4.247)$$

It is easy to demonstrate that the first relationship (4.247) follows directly from (4.242-4.244) at  $c_s(z) \ll 1$ , while the second is the result at  $c_s \rightarrow 1$ . Several analytical solutions of the general problem (4.221-4.223) in various parts of the third quadrant of  $X_N - Y_N$  plane will be developed in the next pages.

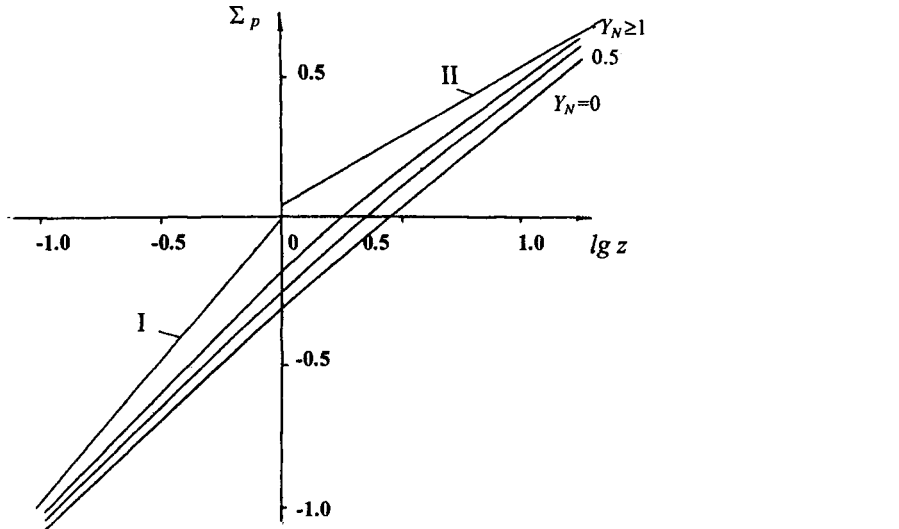


Fig.4.26. Numerical calculation of  $\Sigma_p(z)$  at  $Y_N \leq 0$ .

Solution at  $\beta^2 \leq 1$ . This solution corresponds to the points located below the line BD ( $\beta^2 = 1$ ), i.e. the boundary layers in the gas and in the liquid have thicknesses covering the entire phases at  $\tau_1 \approx \tau_2 \approx 1$ . It is clear that if  $P_2 \ll 1$  the conditions allowing the development of the equation (4.235) are satisfied. Thus, the solution should be determined by the formulae (4.234, 4.236). At high values of  $P_2 \gg 1$  one may suppose that both boundary layers exist ( $\delta_1 = \delta_2$ ). In this case in the initial interval, i.e. at  $c_s \ll 1$ ,  $c_{ls} \approx 1$ , the concentrations in both phases are:

$$I - c_1 = (\tau_1)^{1/2} f_{1/2}(\eta_1) \frac{-\varepsilon N \beta^2 P_2}{df_{1/2}/d\eta} + \dots,$$

$$c = (\tau_2)^{1/2} f_{1/2}(\eta_2) \frac{-P_2}{df_{1/2}/d\eta} + \dots . \quad (4.248)$$

Two similarity variables has been introduced in (4.248):

$$\eta_1 = \frac{I - y_1}{\sqrt{\tau_1}}, \quad \eta_2 = \frac{I - y_2}{\sqrt{\tau_2}}. \quad (4.249)$$

The function  $f_{1/2}(\eta)$  satisfies the ordinary differential equation obtained from (4.242) by a substitution of (4.248):

$$\frac{d^2 f_r}{d\eta^2} + \frac{\eta}{2} \frac{df_r}{d\eta} - \gamma f_r = 0; \quad f_r(0) = 1, \quad f_r(\infty) = 0. \quad (4.250)$$

The solution of this equation at  $\gamma = 1/2$  is [38]:

$$f_{1/2}(\eta) = \exp\left(-\frac{\eta^2}{4}\right) - \left(\frac{\eta}{4}\right)_\eta^\infty \exp\left(-\frac{t^2}{4}\right) dt.$$

Hence, in the initial time interval the surface concentration variations at  $P_2 \gg I$  are:

$$c_s = -\frac{P_2}{f'_{1/2}(0)} \sqrt{\tau_2} = 2\sqrt{\frac{z}{\pi}},$$

$$c_{ls} = 1 - (\epsilon \beta N) 2\sqrt{\frac{z}{\pi}}, \quad z \ll I. \quad (4.251)$$

Here the dimensionless co-ordinate along the  $\tau$  axis is  $z = P_2^2 \tau_2$ . It is clear that the initial chemosorption area corresponds to  $z \ll I$ .

The concentration  $c_s$  cannot be greater than unity (see (4.243)), so using the first equality (4.251) one may suppose that at  $z \geq I$  it approaches  $c_s \Rightarrow I$ . Therefore, the dimensionless flux  $\Sigma$  "approaches" the limiting regime well known as instantaneous chemical reaction regime ( $B_s \rightarrow 0$ ) [3, 4]:

$$\Sigma \Rightarrow \Sigma_s \equiv I - \sum_{n=0}^{\infty} \frac{2}{\pi^2 \left(n + \frac{1}{2}\right)^2} \exp\left[-\pi^2 \left(n + \frac{1}{2}\right)^2 \tau_2\right] \quad \text{at} \quad \tau_2 \gg \frac{I}{P_2^2}. \quad (4.252)$$

The concentration distributions in both the liquid and the gas are:

$$c(\tau_2, y_2) = erfc(\eta_2),$$

$$c_i = I - (1 - c_{ls}) erfc(\eta_1), \quad \tau_2 = \tau_1 \ll I. \quad (4.253)$$

The substitution of these distributions in (4.253) leads to the fact that at  $\tau_i \ll I$ , the surface concentration  $c_{ls}$  tends to a constant value:

$$c_{ls} \Rightarrow I - \varepsilon \beta N. \quad (4.254)$$

At high  $\tau_1 = \tau_2 \gg 1$  it follows from (4.252), (4.234)-(4.236) that:

$$c \Rightarrow I, \quad c_1 \Rightarrow I - \varepsilon N. \quad (4.255)$$

In this case the boundary layers cover the entire phases.

When  $\beta^2 \ll 1$  the transversal variations of the concentration in the gas phase may be neglected because  $\frac{b_1^2}{D_1} \rightarrow 0$ . At small  $P_2$  the formulae (4.234 and 4.236) are valid. In this case the flux  $\Sigma = c_s(z)$ . At  $z = P_2 \tau_2 > 1$  it approaches unity ( $\Sigma \Rightarrow I$ ).

At high values of  $P_2$  and ( $z \ll 1$ ) the concentration  $c_s(z)$  is determined by (4.251), while the relationship between  $c_{ls}$  and  $\Sigma$  at arbitrary  $\tau$  is:

$$c_{ls} = I - (\varepsilon N) \Sigma(\tau). \quad (4.256)$$

The relationship (4.256) follows from the mass balance equation (4.224). At  $z = P_2^2 \tau_2 \gg 1$  the approximation (4.252) is valid. Taking into account that  $c_{ls} = I$  at  $\tau_2 \ll 1$  the concentration of  $A$  at the interface (with equally distributed accuracy with respect to  $\tau_2$ ) is:

$$c_{ls} = I - (\varepsilon N) \left\{ I - \sum_{n=0}^{\infty} \frac{2}{\pi^2 (n+1/2)^2} \exp[-\pi^2 (n+1/2)^2 \tau_2] \right\}. \quad (4.257)$$

The function monotonically decreases with the increase of  $\tau_2$ . At  $\tau_2 \geq 1$  it approaches to its asymptotic value ( $I - \varepsilon N$ ).

The analysis performed at various values of the parameter  $\beta^2$  allows the conclusion that everywhere in the plane, but below the line  $BD$  ( $\beta^2 \leq 1$ ) the concentrations  $c_s$  and  $c_{ls}$  are monotonic functions of  $\tau$ . The former varies from zero to unity, while the second from unity to ( $I - \varepsilon N$ ).

Solution at  $\beta^2 \geq 1$ . This solution for the points located above the line  $BD$  ( $\beta^2 \geq 1$ ) will be investigated upon the condition  $\beta^2 \gg 1$  (the case  $\beta^2 = 1$  was developed above). The solution is investigated under the assumption that the concentration variations in the liquid phase are negligible ( $\frac{b_2^2}{D_2} \rightarrow 0$ ). Under these conditions one may assume that at every value of  $\tau$

$$c_s = \Sigma. \quad (4.258)$$

At sufficiently small  $P_2$  the boundary layers cover the entire areas of both phases and in the initial interval ( $c_s \ll I$ ,  $c_{ls} = I$ ) the following approximations are valid:

$$c_s = \sum = P_2 \tau_2 = z, \quad c_l = c_{ls} = I - \varepsilon N z, \quad z \ll I, \quad P_2 \ll 1/\beta^2. \quad (4.259)$$

At  $z \gg I$  the concentrations in both phases approach their equilibrium values (see (4.255)).

The further increase of the parameter  $P_2$  ( $1/\beta^2 \ll P_2 \ll I$ ) and  $z \ll I$  leads to:

$$c_s = \sum = z, \quad c_{ls} = I - (\varepsilon \beta N) \sqrt{\frac{z P_2}{\pi}}, \quad z = P_2 \tau_2. \quad (4.260)$$

The formula (4.260) may be obtained by means of (4.251) if (under the condition  $P_2 \ll I$ ) the dimensionless time co-ordinate is  $z = P_2 \tau_2$ . At  $z \gg I$  the concentration  $c$  in the volume of the liquid phase tends to the equilibrium ( $c_s = \sum \rightarrow I$ ). Hence, the mass balance equation (4.224) gives:  $I \rightarrow \varepsilon N < I$ . These reaction times permit to use the following one-phase formulation of the problem:

$$\begin{aligned} \frac{\partial c_l}{\partial \tau_l} &= \frac{\partial^2 c_l}{\partial y_l^2}; \\ c_l &= I \quad \text{at } y_l = 0; \quad I - \int_0^l c_l dy_l = \varepsilon N. \end{aligned} \quad (4.261)$$

The solution at  $\tau_l \ll I$  is:

$$I - c_l = \frac{(\varepsilon N) f_{-1/2}(\eta_l)}{\left( \int_0^\infty f_{-1/2}(\eta) d\eta \right) \sqrt{\tau_l}},$$

where the function  $f_{-1/2}$  satisfies the equation (4.250) at  $\gamma = -1/2$  [38].

$$f_{-1/2}(\eta) = \exp(-\eta^2/4).$$

Therefore, at  $z \gg 1$  the concentration  $c_{ls}$  is a monotonously increasing function:

$$c_{ls} = I - \frac{1}{\left( \int_0^\infty f_{-1/2} d\eta \right) \sqrt{\tau_l}} \frac{\varepsilon N}{\sqrt{\tau_l}} = I - \frac{(\varepsilon \beta N)}{\sqrt{\pi}} \frac{\sqrt{P}}{\sqrt{z}},$$

$$\tau_l \ll I, \quad 1/\beta^2 \ll P_2 \ll I, \quad z = P_2 \tau_2. \quad (4.262)$$

The comparison between (4.260) and (4.262) (obtained at small and large values of  $z$ ) indicates that the curve  $c_{ls}(z)$  has a minimum at  $z \approx 1$ . The order of this minimum is  $1 - (\varepsilon\beta N)\sqrt{P_2}$ . Obviously, the further increase of  $\tau_1$  ( $\tau_1 \geq 1$ ) leads to the situation where the boundary layers cover the entire phases and the approximations (4.255) are valid. The solution at  $P_2 \gg 1$  corresponds to  $z = P_2^2$ ,  $\tau_2 \ll 1$  in the initial interval, so the formulae (4.251) are applicable.

The further investigations at  $z \gg 1$  show that the concentrations  $c_s \rightarrow 1$ ,  $c_{ls} \rightarrow 1 - \varepsilon\beta N$  (see 4.253, 4.254). The latter relationships are valid for values of  $\tau_2 \leq 1$  ( $z \leq P_2^2$ ) only. At  $\tau_2 > 1$  the approximations (4.262, 4.255) should be applied. Hence, everywhere above the line  $BD$  (Fig. 4.25) the surface concentration  $c_{ls}(\tau)$  is a composite function of  $\tau$ . Its minimum value in that area is equal to  $1 - \varepsilon\beta N$ .

The results obtained at various  $\beta^2$  permit the conclusion that the minimum of the surface concentration  $c_{ls}$  in the third quadrant of  $X_N - Y_N$  plane at ( $\varepsilon N \leq 1$ ,  $\varepsilon\beta N \leq 1$ ) is:

$$c_{ls}^{min} = \min(1 - \varepsilon\beta N, 1 - \varepsilon N). \quad (4.263)$$

Usually the assumption [3, 4], that the chemosorption resistance is located in the liquid phase only, is valid ( $c_{ls} = 1$ ), irrespective of the chemical reaction rate and the time. The relationship (4.263) developed here allows the conclusion that a sufficient condition of the existence of such regime is the simultaneous satisfaction of the following conditions:

$$\varepsilon N \ll 1, \quad \varepsilon\beta N \ll 1. \quad (4.264)$$

The area where the conditions (4.264) are satisfied is located in the lower left corner of the plane  $X_N - Y_N$  (Fig. 4.25). The exact boundaries of that area may be determined after the calculation of the values of the flux  $\Sigma(\tau)$  and the comparison of the value obtained with the relationships developed for the simplified chemosorption problem with a condition  $c_{ls} = 1$ .

A characteristic feature of the solutions of the problem (4.221-4.223) obtained in the third quadrant is that the concentration  $c_s$  is a monotonous function of the time. It varies from zero to unity in a time interval  $\tau_2$  that may be termed *two-phase chemosorption interval*  $\tau_2^*$ . The analysis done indicates that the length of the *two-phase chemosorption interval* depends on  $P_2$ :

$$\tau_2^* = \begin{cases} 1/P_2 & \text{if } P_2 \ll 1; \\ 1/P_2^2 & \text{if } P_2 \gg 1. \end{cases} \quad (4.265)$$

Hence, it is enough to carry out the numerical calculations of  $\Sigma(\tau)$  at  $\tau_2 \leq \tau_2^*$  because at  $\tau_2 \geq \tau_2^*$  the concentration  $c_s \Rightarrow 1$  and the system reaches the regime of an instantaneous chemical reaction (the analytical relationship (4.252) is valid). The latter conclusion means that at  $\tau \geq \tau_2^*$  the chemosorption process is limited by the diffusion of the reaction product

through the second phase. The reaction product concentration at the interface  $c'_s = \frac{N_\varrho}{q}$  (see 4.181) is  $N$  times greater than the corresponding concentration  $c'_{ls} = kc_0$  of the soluble component  $A$  under the conditions of physical absorption. Therefore, the augmentation factor is  $\Phi \Rightarrow N \gg 1$ . This is the maximum value of the augmentation factor available in the entire system.

The results developed indicate the condition requires the transformation of the two-phase chemosorption problem into the problem formulated by equations (4.188-4.190) in 4.3.2. The latter is valid if  $\varepsilon N \ll 1$ ,  $\varepsilon\beta N \ll 1$  (the lower left corner of the plane  $X_N - Y_N$ , Fig. 4.25). Moreover, the case considered occurs at  $P_2 \gg 1$  and  $\tau_2 \ll 1$ . It is easy to see that the co-ordinate  $X$  (4.201) introduced in (4.207) coincides with the time co-ordinate:

$$z = P_2^2 \tau_2 = \left( \frac{a}{N} \right)^2 \tau_2.$$

Graphical presentation of the numerical solution of the three-parametric problem (4.237-4.238) in the two-phase chemosorption interval. For convenience of the further presentation of the solutions at arbitrary values of the parameters, the dimensionless contact time  $z$  is defined as (see (4.265)):

$$z = \begin{cases} \tau_2 P_2, & P_2 \leq 1; \\ \tau_2 P_2^2, & P_2 > 1. \end{cases} \quad (4.266)$$

The corresponding objective function  $\varphi_3(P_2, X_N, Y_N, z)$  (see (4.235) and (4.246)) is:

$$\varphi_3 = \begin{cases} \sum(P_2, X_N, Y_N, z), & P_2 \leq 1; \\ P_2 \sum(P_2, X_N, Y_N, z), & P_2 > 1. \end{cases} \quad (4.267)$$

The integration of the transport equation with respect to  $c(\tau, y_2)$  along the transverse co-ordinate  $y_2$  indicates that inspite of the values of  $P_2$ :

$$\varphi_3(z, P_2) = z \quad \text{if } z \ll 1. \quad (4.268)$$

The calculation of the functions  $\varphi_3(z)$  at a fixed point of the plane ( $X_N - Y_N$ ) will be presented as parametric curves  $\varphi_3 - z$  (with a parameter  $\lg P_2$ ).

It is clear that at  $z \ll 1$  all the curves coincide (see (4.268)) which is an advantage of the co-ordinate  $z$ . The next advantage in contrast to the other co-ordinates  $(\tau_1, \tau_2)$  is that the limiting values (4.252) at arbitrary  $P_2$  appear at  $z \gg 1$ . This allows the calculation of the objective functions in a restricted interval of  $z$  ( $-1 \leq \lg z \leq 1$ ). The problem (4.221-4.223) was solved numerically by the Gauss successive method with respect to  $\tau$  [9, 39]. The forward

step starts from the depth of the corresponding phase ( $y_2 = y_1 = 0$ ). The unknown functions were determined by the conjunction conditions (4.238). After that the backward pass of the method started for the estimation of the concentration profiles in the phases. Figure 4.27 presents results of such calculations at  $X_N = Y_N = 0$ . It was detected that at sufficiently small  $P_2$  (practically at  $\lg P_2 \leq -0.8$ ) the function  $\Sigma(\tau)$  coincides with the solution of (4.235) at  $a \gg 1$  (see 4.236). Hence, in accordance with the general theory there is a transition of the three-parametric problem (4.237, 4.238, 4.223) into the two-parametric (4.235) at  $P = P_2^*$  ( $\lg P_2^* = -0.8$ ), so:

$$\Sigma(P_2, X_N, Y_N, z) \Rightarrow \Sigma_0(X_N, \infty, z) \Rightarrow \Sigma_0(X_N, a, z_0).$$

The first step of the transition occurs at  $P_2 = P_2^*$ , while the second one corresponds to  $a \approx 1$  (see the definition of  $P_2$  (4.236)).

The transport equations (4.237) are parabolic partial differential equations so the objective functions  $\varphi_3(z)$  ( $\Sigma(\tau)$  and  $P_2 \Sigma(\tau)$ ) are monotonous functions of  $z$ . The asymptotic values at small  $z$  are (4.268) (the lines I on Fig. 4.27). At high values of  $z$  it is clear that  $\Sigma \Rightarrow 1$  ( $P_2 < 1$ ) and  $P_2 \Sigma \Rightarrow P_2$  ( $P_2 > 1$ ). Figure 4.27 shows that in the case

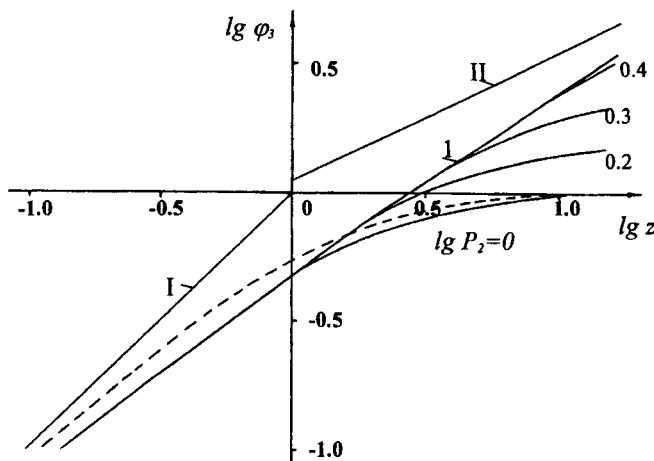


Fig. 4.27. Calculation of the objective function  $\varphi_3(z)$  in the points  $X_N = Y_N = 0$ . Curve 1 – the relation  $\Sigma_p(0, z)$ ; lines I and II – the asymptotic solutions of the problem (4.247); dashed line – the solution of the problem (4.236) at  $X_N = 0$ .

$\lg P_2 \geq 0$  all the curves  $P_2 \Sigma(\tau)$  at  $z$  lower than a certain value  $z^*$  coincide with the limiting function  $\Sigma_p(Y_N, z)$ . In this case all the conditions allowing the employment of the problem formulation (4.242-4.244) are satisfied, i.e. boundary layers exist in both phases. The quantity  $\lg z^*$  increases monotonously with the parameter  $\lg P_2$ . At sufficiently high values of  $P_2$  ( $\lg P_2 \geq 0.8$ ) it reaches the condition  $\lg z^* > 1$ . Hence,  $P_2 \Sigma(z)$  coincides with  $\Sigma_p(z)$  in the entire interval  $-1 \leq \lg z \leq 1$  (curve 1 on Fig. 4.27).

It was estimated, that at  $\lg z > 1$  and arbitrary  $P_2$  the analytical relationship (4.252) is valid for  $\Sigma(\tau)$ . In this case  $c_s \Rightarrow 1$ . Therefore, there is no need to calculate the objective function at  $\lg P_2 \geq 0.8$ , because it is easy to use the limiting solution  $\Sigma_p(Y_N, z)$  (Fig. 4.26) and the equation (4.252). The numerical calculations indicate, that similar behaviour of the objective functions occur in the entire third quadrant. This is an effect of the method for presentation of problem solutions in the form  $\varphi_3(z) - z$ . The plane  $X_N - Y_N$  contains areas where the solution of the general problem (4.221-4.223) is simpler which may be attributed to the behaviour of the concentrations  $c_{ls}$  and  $c_s$  in the phases. The number of the controlling parameters in these areas is reduced. These areas will be considered further.

Numerical solution at small phase capacities. The problem considers the area of the plane  $X_N - Y_N$ , where the chemosorption resistance is located in the liquid phase only. The situation corresponds to  $\varepsilon N \rightarrow 0$ ,  $\varepsilon \beta N \rightarrow 0$ ,  $c_{ls} \rightarrow 1$  (see 4.263 and 4.264). The solution is available through the simplified one-phase problem formulation:

$$\begin{aligned} \frac{\partial c}{\partial \tau_2} &= \frac{\partial^2 c}{\partial y_2^2}; \\ \left( \frac{\partial c}{\partial y_2} \right)_s &= P_2 \sqrt{1 - c_s} \quad \text{at } y_2 = l; \\ \left( \frac{\partial c}{\partial y_2} \right) &= 0 \quad \text{at } y_2 = 0; \quad c = 0 \quad \text{at } \tau_2 = 0. \end{aligned} \quad (4.269)$$

The problem (4.269) depends on the single parameter  $P_2$ . The numerical results concerning the objective functions (denoted as  $\varphi_D$ ) are shown on Fig. 4.28. The main features of the solution remain (see Fig. 4.27), because at  $\lg P_2 \leq -0.8$  the analytical relationship (4.236) is valid (assuming  $\varepsilon N = 0$  (the dashed curve)). The solution  $\Sigma_p$  is reached at  $\lg P_2 \geq 0.8$  (see Fig. 4.26).

Obviously, the exact boundaries of the areas, where the solution (4.269) is valid, depend on the accuracy required. A comparison of the numerical solutions of the general formulation (4.221-4.223) and the simpler one (4.269) at equal values of  $P_2$  may determine them. Assuming an accuracy of about 5% in the calculations of  $\Sigma(z)$  it can be demonstrated that the chemosorption resistance is in the liquid phase only if the following conditions are satisfied:

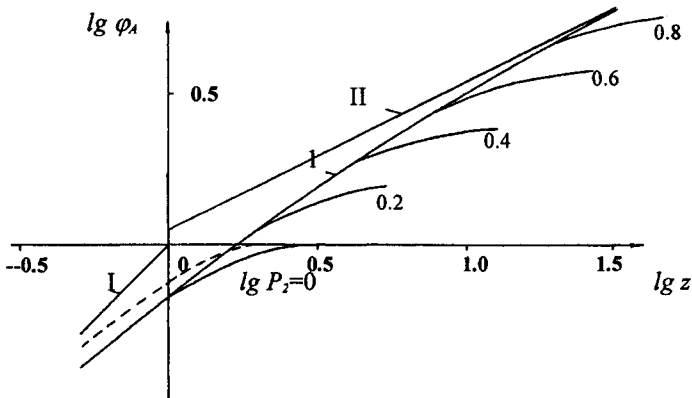


Fig. 4.28. Solution ( $\varphi_A$ ) of problem (4.269) in case of chemosorption resistance in the liquid phase. Curve 1 -  $\sum_p(z)$  at  $Y_N = -\infty$ ; lines I and II - the asymptotic solution (4.247); dashed line the solution according (4.236) at  $X_N = -\infty$ .

$$X_N \leq -1, \quad Y_N \leq -1. \quad (4.270)$$

This area is located in the lower left corner of Fig. 4.25 (the internal points of the right angle with a vertex  $D$ ).

Let the problem (4.221-4.223) be considered at  $\varepsilon N \rightarrow 0$ . The situation corresponds to  $\beta^2 \gg 1$  (Fig. 4.25). One may assume that in the gas phase there is a boundary layer, so the general problem could be simplified:

$$\begin{aligned} \frac{\partial c_1}{\partial \tau_2} &= \frac{\partial^2 c_1}{\partial y_{ls}^2}; \quad \frac{\partial c}{\partial \tau_2} = \frac{\partial^2 c}{\partial y_2^2}; \\ \left( \frac{\partial c}{\partial y_2} \right)_s &= P_2 \sqrt{1 - c_s} c_{ls}(\tau_2), \quad \left( \frac{\partial c_1}{\partial y_{ls}} \right)_s = -(\varepsilon \beta N) \left( \frac{\partial c}{\partial y_2} \right)_s; \\ \left( \frac{\partial c_1}{\partial y_{ls}} \right) &= 0 \quad \text{at } y_{ls} = \infty; \quad c_1 = 1, \quad c = 0 \quad \text{at } \tau_2 = 0. \end{aligned} \quad (4.271)$$

For the purposes of the further analysis a dimensionless co-ordinate  $y_{ls} = \beta(1 - y_1)$  will be introduced. The problem (4.271) is two-parametric. The objective function  $\varphi_3(\tau)$  in the area considered will be denoted as  $\varphi_{3Y}(P_2, Y_N, z)$ . The numerical calculations of the family of functions  $\varphi_{3Y}(z)$  (with a parameter  $P_2$ ) at  $Y_N = (0, -1)$  are illustrated on Fig. 4.29. The

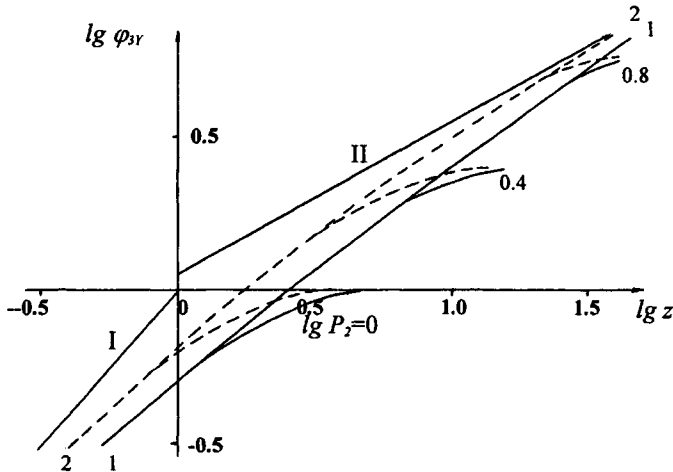


Fig. 4.29. Solution ( $\varphi_{3Y}$ ) of problem (4.271) at  $\varepsilon N \rightarrow 0$ . Solid curves -  $Y_N = 0$ ; dashed curves -  $Y_N = -\infty$ ; Curves 1 and 2 -  $\Sigma_p(0, z)$  and  $\Sigma_p(-\infty, z)$ .

effect of  $Y_N$  on the solution is weak, because the maximum difference between the curves (obtained at different  $Y_N$  and  $\lg P_2 \geq 0$ ) does not exceed 30%. The effect becomes more insignificant within the decrease of the parameter  $\lg P_2$ . At  $\lg P_2 \leq -0.8$  it practically disappears, so  $\varphi_{3Y} \Rightarrow \Sigma_0(-\infty, +\infty, z)$  (4.236). The solution (4.271) (with an equally distributed accuracy with respect to  $P_2$ ) is valid in the area located on the left of the vertical line  $AB$  (Fig. 4.25).

The next interesting situation is the case  $\varepsilon \beta N \rightarrow 0$ . The mass balance equation gives the relationship (4.256), so the problem (4.237-4.238, 4.223) becomes simpler (one phase problem):

$$\begin{aligned} \frac{\partial c}{\partial \tau_2} &= \frac{\partial^2 c}{\partial y_2^2}; \\ \left( \frac{\partial c}{\partial y_2} \right)_s &= P_2 \sqrt{1 - c_s(\tau_2)} [I - (\varepsilon N) \Sigma(\tau_2)] \\ \left( \frac{\partial c}{\partial y_2} \right) &= 0 \quad \text{at } y_2 = 0; \quad c = 0 \quad \text{at } \tau_2 = 0. \end{aligned} \tag{4.272}$$

The objective function  $\varphi_3 = \varphi_{3X}(P_2, X_N, z)$  depends on two parameters:  $X_N$  and  $P_2$ . The numerical calculations of  $\varphi_{3X}(P_2, X_N, z)$  are shown on Fig. 4.30. The increase of the value

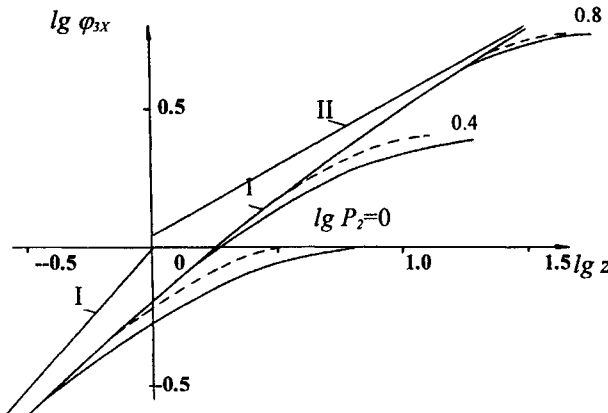


Fig. 4.30. Solution ( $\varphi_{3X}$ ) of problem (4.272) at  $\varepsilon\beta N \rightarrow 0$ , for high  $P_2$ .  
Solid curves -  $X_N = 0$ ; dashed curves -  $X = X_{NY}$ .

of  $P_2$  reduces the effect of  $X_N$  on the solution and at  $\lg P_2 \geq 0.8$  it practically disappears. In this limiting situation  $\varphi_{3X} \rightarrow \Sigma_p(-\infty, z)$  (curve 1). The effect of  $X_N$  is stronger at  $\lg P_2 \leq -0.8$  and  $\Sigma_X$  coincides with the analytical relationship  $\Sigma_0(X_N, +\infty, z)$  (4.236). The comparison of the solutions of (4.272) and (4.221-4.223) indicates that the approximation is valid in the area defined by ( $Y_N \leq -1$ ). The points are located below the horizontal line  $CD$  (see Fig. 4.25). It is clear that at any internal point of the angle  $A$  all the limiting solutions of (4.269, 4.271, and 4.272) coincide at values of  $P_2$ , i.e.  $\varphi_{3X} = \varphi_{3Y} = \varphi_D$ .

Numerical solution of the two-parametric problem. The objective function  $\Sigma_0(X_N, a, z_0)$  is a solution of the problem (4.235) and depends on the two parameters  $a$  and  $X_N$ , and the dimensionless time  $z_0 = a \frac{th(a)}{N} \tau_2$ . At large and small values of the parameter  $a$  analytical solutions for  $\Sigma_0(z_0)$  are available. In the former case ( $a \rightarrow \infty$ ) the solution has been developed already in 4.3.4.1 (see (4.236) under the assumption  $z \rightarrow z_0$ ). The latter case ( $a \rightarrow 0$ ) has a solution in the form [38]:

$$\Sigma_0(X_N, 0, z_0) = \frac{\exp[(1 - \varepsilon N)z_0] - 1}{\exp[(1 - \varepsilon N)z_0] - \varepsilon N}. \quad (4.273)$$

Equation (4.235) was solved by the Runge-Kutta method. Examples of the objective functions  $\Sigma_0(z_0)$  at  $X_N = -0.3$  and various discrete values of  $\lg a$  are illustrated on Fig. 4.31. It is enough to perform the calculations in a restricted interval  $-1 \leq X_N \leq 0$  because at

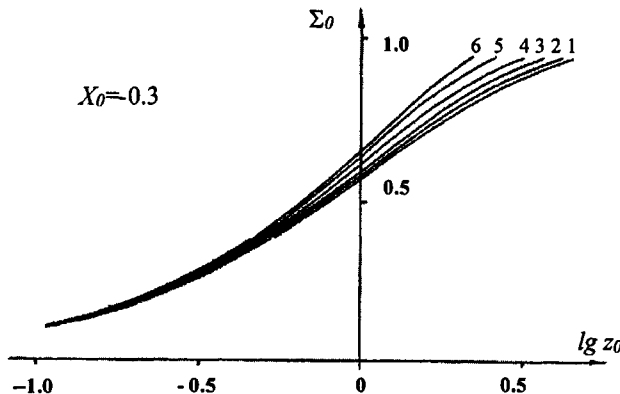


Fig. 4.31. Solution ( $\Sigma_0$ ) of two parameters problem (4.235) at  $X_N = -0.3$ ,  
 1) -  $\lg a \leq -0.1$ ; 2) -  $\lg a = -0.2$ ; 3) - 0; 4) - 0.2; 5) - 0.4; 6) -  $\lg a \geq 0.6$ .

$X_N \leq -1$  the solution (4.235) becomes independent of  $X_N$ . With an accuracy of 5% the following equality is valid:

$$\Sigma_0(X_N, a, z_0) = \Sigma_0(-\infty, a, z_0) \quad (4.274)$$

at any value of  $a$ . Here  $\Sigma_0(a, -\infty, z_0)$  is the solution of (4.235) for  $\varepsilon N = 0$ . An advantage of the dimensionless time  $z_0$  with respect  $\tau_1$  or  $\tau_2$  is the fact that despite the values of  $a$  and  $X_N$  the main variations of  $\Sigma_0(z_0)$  occur at  $z_0 \sim 1$ . Moreover, the asymptotic behaviour of these functions at  $z_0 \rightarrow 0$  and  $z_0 \rightarrow \infty$  does not depend on any parameter:

$$\Sigma_0(z_0) \Rightarrow z_0 \quad \text{at } z_0 \Rightarrow 0; \quad \Sigma_0(z_0) \Rightarrow 1 \quad \text{at } z_0 \gg 1. \quad (4.275)$$

The latter feature follows directly from (4.235). It was proved that at every  $X_N = \text{const.}$  and sufficiently "small" of  $a$  ( $\lg a \leq \lg a_0$ ) the function  $\Sigma_0(z_0)$  practically coincides with the limiting relationship (4.273). At  $\lg a \geq \lg a_\infty$  the limiting relationship is (4.236). If an accuracy of 5% is assumed, it is easy to demonstrate that during the calculations of  $\Sigma_0(z_0)$   $\lg a_0 = -0.4$ ,  $\lg a_\infty = 0.6$  despite the value of  $X_N$ . Moreover, the relationship between the solution and  $\lg a$  is practically linear in the range  $-0.4 \leq \lg a \leq 0.6$ . This allows a presentation of the numerical results as approximating relationships:

$$\Sigma_0(X_N, a, z_0) \approx \Sigma_0(X_N, 0, z_0) + (\lg a + 0.4) [\Sigma_0(X_N, \infty, z_0) - \Sigma_0(X_N, 0, z_0)]$$

$$-0.4 \leq \lg a \leq 0.6. \quad (4.276)$$

The relative error does not exceed 5%.

Numerical solution of the three-parametric problem in the third quadrant of  $(X_N - Y_N)$ . The numerical calculations of the objective functions  $\varphi_3(z)$  were performed at discrete points of the third quadrant  $-1.25 \leq X_N \leq 0$ ,  $-1.25 \leq Y_N \leq 0$  with steps  $\Delta X_N = \Delta Y_N = 0.125$ . The chemosorption parameter  $\kappa_3$  (see the previous sub-chapters) was defined as:

$$\lg \kappa_3 = \lg P_2 = \lg \frac{a}{N}. \quad (4.277)$$

Obviously, at  $a \gg 1$  the parameter  $P_2$  becomes  $P_2 = \frac{a}{N}$ . The calculations have been carried out in the range  $-1.2 \leq \lg \kappa_3 \leq 1.2$  and with a step of  $\Delta \lg \kappa_3 = 0.2$ . The graphical presentations have been separated in two groups: "strong" ( $\lg \kappa_3 \geq 0$ ) and "weak" ( $\lg \kappa_3 < 0$ ) chemical interactions.

At "strong" chemical interactions ( $\lg \kappa_3 > 0$ ) it is easy to present the data by logarithmic co-ordinates  $\lg[\kappa_3 \Sigma_\infty(\kappa_3, z)] - \lg z$  and a parameter  $\lg \kappa_3$ . The dimensionless co-ordinate  $z$  is defined by (4.266). In the situation considered a three-parametric function  $\Sigma_\infty(\kappa_3, X_N, Y_N, z)$  is assumed. The subscript " $\infty$ " is omitted. Typical calculation results are shown on Figs. 4.32-4.34. The numerical experiments indicate that in a given area of the  $X_N - Y_N$  plane (at a fixed value of  $\kappa_3$ ) the differences between the objective functions  $\varphi_3(z)$  are insignificant both qualitatively and quantitatively. This is a consequence of the method chosen for the solution presentation by logarithmic co-ordinates  $\lg \varphi_3 - \lg z$ . Moreover, at fixed values of  $\kappa_3$  and  $Y_N$  the effect of  $X_N$  on  $\varphi_3$  is monotonous. This allows presentations of the numerical results on horizontal lines  $Y_N = \text{const.}$  by a number of plots. The investigations performed indicate that it is enough to restrict the calculations to the cases  $Y_N = 0, -0.5, -1$  only. For the other  $Y_N$  in the range ( $-1 \leq Y_N \leq 0$ ) the accuracy of (5%) could be obtained by means of linear approximations.

It is clear that the functions  $\lg(\kappa_3 \Sigma)$  are monotonous regarding the variable  $\lg z$ . Their asymptotic behaviour at  $z \leq z^*$  coincides with the limiting case of  $\Sigma_p$  (curves 1 on Figs. 4.32 - 4.34). At sufficiently high values of  $z$  there is a transition  $\Sigma \Rightarrow \Sigma_s(\tau_2)$  (4.252). This is the so-called "instantaneous chemical reaction regime" with a maximum available value of the augmentation factor  $\Phi \Rightarrow N$  [3, 4]. The latter follows directly from the fact that the chemosorption square ( $-1 \leq X_N \leq 1$ ,  $-1 \leq Y_N \leq 1$ ) considered here is located in the part of the  $X - Y$  plane where the adsorption resistance located in the liquid phase dominaes. In this situation the relationship (4.31) is valid.

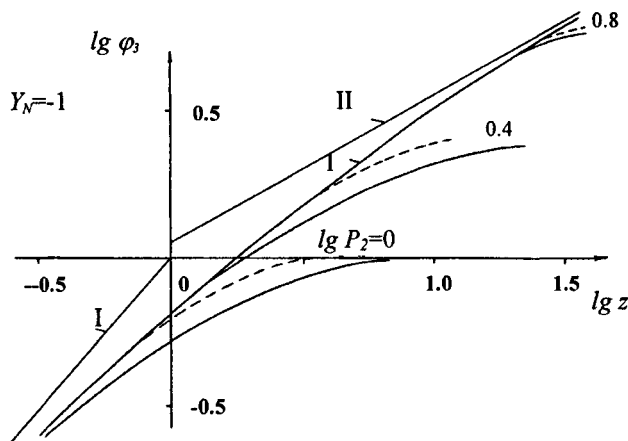


Fig. 4.32. Solution  $\varphi_3(X_N, Y_N, z)$  on the horizontal line  $Y_N = -1$ . Solid curves -  $\varphi_3(0, -1, z)$ ; dashed curves -  $\varphi_{3y}$ ; curve 1) -  $\Sigma_p(-1, z)$ , lines I and II - asymptotic solution of (4.247).

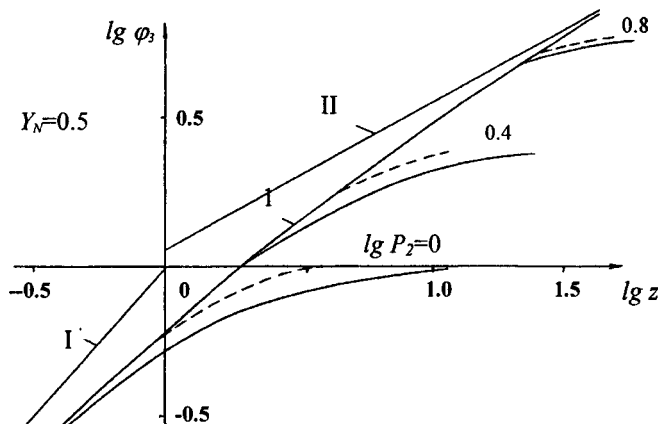


Fig. 4.33. Solution  $\varphi_3(X_N, Y_N, z)$  on the horizontal line  $Y_N = -0.5$ . Solid curves -  $\varphi_3(0, -0.5, z)$ ; dashed curves -  $\varphi_{3y}$ ; curve 1) -  $\Sigma_p(-1, z)$ , lines I and II - asymptotic solution of (4.247).

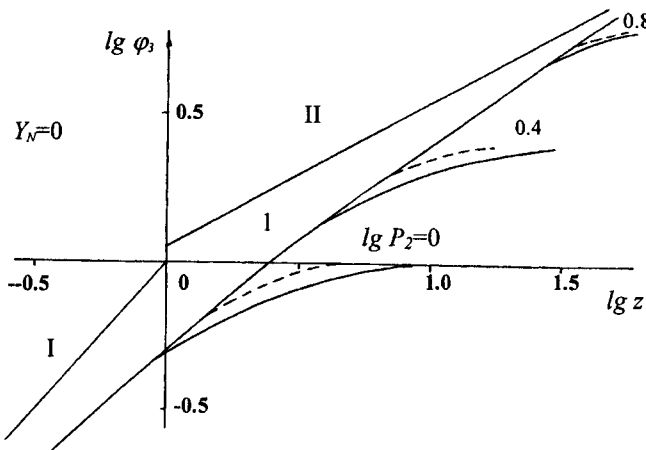


Fig. 4.34. Solution  $\varphi_3(X_N, Y_N, z)$  on the horizontal line  $Y_N = 0$ . Solid curves -  $\varphi_3(0, -l, z)$ ; dashed curves -  $\varphi_{3Y}$ ; curve 1) -  $\Sigma_p(-l, z)$ , lines I and II - asymptotic solution of (4.247).

Note that at sufficiently high values of  $\kappa_3$  the transition into the limiting curve  $\Sigma_s(\tau_2)$  occurs for shorter contact times ( $\tau_2 \approx \frac{l}{\kappa_3^2} \ll 1$ ) and a boundary layer in the liquid phase  $\delta_2 \ll l$ . It is well known that the asymptotic expression  $\Sigma_s(\tau_2)$  at  $\tau_2 \rightarrow 0$  approaches  $2\sqrt{\frac{\tau_2}{\pi}}$  [40]. Hence, in co-ordinates  $lg z$  the function  $lg \varphi_3$  should approach the following linear relationship (the inclined lines II on Figs. 4.32 - 4.34):

$$\lg[\kappa, \Sigma(\kappa_3, z)] \Rightarrow \frac{l}{2} \lg z + \lg\left(\frac{2}{\sqrt{\pi}}\right), \quad z \gg l. \quad (4.278)$$

The calculation was stopped when the equality  $\Sigma = \Sigma_s$  was satisfied with 5% accuracy.

The weak chemical interaction ( $lg \kappa_3 < 0$ ) is easy to present by parametric curves  $lg \Sigma - lg z$  (a parameter  $\kappa_3$ ). The investigations performed show that in the range  $-1 \leq lg \kappa_3 \leq 0$  the effect of  $lg \kappa_3$  on the solution is practically linear. Moreover, at small values of  $\kappa_3$  ( $lg \kappa_3 \leq -1$ ) the function  $\Sigma(\tau_2)$  coincides with the analytical relationship (4.236). This permits the approximation of the objective functions  $\Sigma(\kappa_3, X_N, Y_N, z)$  by relationships valid at  $lg \kappa_3 < 0$ :

$$\begin{aligned} \lg \Sigma(\kappa_3, X_N, Y_N, z) &= \lg \Sigma(I, X_N, Y_N, z) - \lg \kappa_3 [\lg \Sigma_0(\infty, X_N, z) - \lg \Sigma(I, X_N, Y_N, z)] \\ -1 \leq \lg \kappa_3 &\leq 0, \end{aligned} \quad (4.279)$$

Here,  $\Sigma(I, X_N, Y_N, z)$  is the objective function at  $\lg \kappa_3 = 0$  (Figs. 4.32 - 4.34). The relationship (4.279) is valid in the entire third quadrant and the relative error with respect to  $\Sigma$  does not exceed 5%. The accuracy required for better calculation of the function  $\Sigma(I, X_N, Y_N, z)$  may be determined by means of the plots presented on Figs. 4.32 - 4.34. When  $\lg \kappa_3 \leq 0$  the effect of the parameters  $X_N, Y_N, \kappa_3$  on  $\Sigma(\tau)$  is insignificant which is consequence of the dimensionless co-ordinate  $z$  expressed in the form (4.236).

As a conclusion it should be mentioned that the area defined by the limiting solutions  $\Sigma_X, \Sigma_Y$  and  $\Sigma_D$  is wider (from a general point of view) than that defined in 4.4.6. This may be attributed to the fact that the boundaries depend on the parameter  $\kappa_3$ . For example, at strong chemical interactions ( $\lg \kappa_3 \geq 0.8$ ) the equality  $\kappa_3 \Sigma_D = \kappa_3 \Sigma_X = \Sigma_p(-\infty, z)$  is satisfied and the corresponding area defining  $\Sigma_A(z)$  becomes larger (all the points are below the line  $CD$  (Fig. 4.25)). It was mentioned earlier that the boundaries of the area defining the objective function  $\Sigma_X$  coincide with the lower boundary of the chemosorption square (the line  $CD, Y_N \leq -1$ ) irrespective of the value of  $\kappa_3$ .

However, this is not valid for the other objective function  $\Sigma_Y(P_2, Y_N, z)$ . Its area of definition depends on  $\lg \kappa_3$ . For example, at small  $\kappa_3$  ( $\lg \kappa_3 \leq -1$ ) the function  $\Sigma$  coincides with  $\Sigma_0(\infty, X_N, z)$  (4.236) inspite of the value of  $Y_N$ . This solution is shown on Fig. 4.35. It is clear, that outside the boundaries of the chemosorption square ( $X_N \leq -1$ ) the effect of  $X_N$  (with an equally distributed accuracy with respect  $z$ ) disappears. Hence  $\Sigma \Rightarrow \Sigma_Y(Y_N, z) = \Sigma_0(+\infty, -\infty, z)$  (curve 6 on Fig. 4.35). Thus, at sufficiently small values of  $\kappa_3$  the boundaries of the area defining  $\Sigma_Y$  coincide with the boundaries of the chemosorption square ( $X_N = -1$ ). On the other hand at sufficiently high  $\kappa_3$  ( $\lg \kappa_3 \geq 1$ ) the objective function  $\kappa_3 \Sigma$  is independent of  $X_N$  (curves 7 on Figs. 4.32 - 4.34) and consequently  $\Sigma = \Sigma_Y$ . The area defining  $\Sigma_Y$  is  $X_N \leq 0$ .

In the general situation for every  $\kappa_3$  belonging to the range  $-1 \leq \lg \kappa_3 \leq 1$  the boundaries of the area defining  $\Sigma_Y$  may be estimated by calculations of the objective functions at discrete values of the parameter  $X_N$  and fixed values of  $Y_N$ . Evidently, to any fixed values of  $\kappa_3$  and  $Y_N$  there is a corresponding value of  $X_{NY}$  ( $X_N \leq X_{NY}$ ) allowing the function  $\Sigma(\kappa_3, X_N, Y_N, z)$  to be independent of  $X_N$  and consequently  $\Sigma \Rightarrow \Sigma_Y(\kappa_3, Y_N, z)$ . The numerical investigations indicate that the limiting values of  $X_{NY}$  depend on  $\kappa_3$  and monotonously increase from -1 to 0 (Fig. 4.36) when the parameter varies in the range  $-1 \leq \lg \kappa_3 \leq 1$ . In the range  $X_{NY} \leq X_N \leq 0$  the effect of  $X_N$  on the objective function is practically linear:

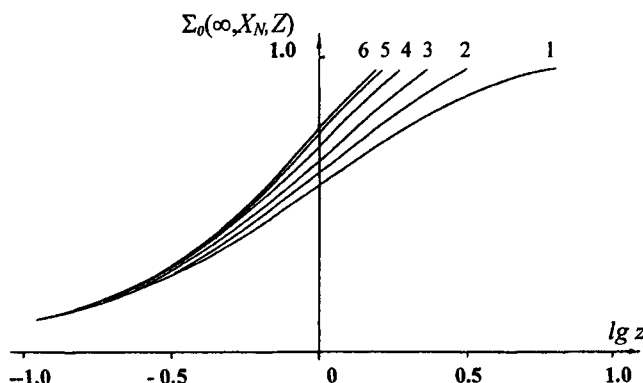


Fig. 4.35. Function  $\Sigma_0(\infty, X_N, z)$  (4.236) at different  $X_N$ . Curves: 1) -  $X_N = 0$ ;  
2)  $X_N = -0.125$ ; 3)  $X_N = -0.25$ ; 4)  $X_N = -0.5$ ; 5)  $X_N = -0.75$ ; 6)  $X_N = -1$ .

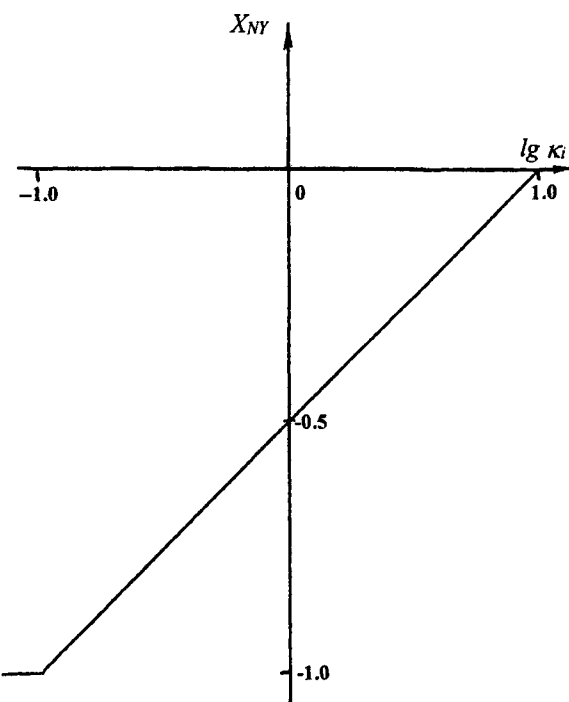


Fig. 4.36. Dependence of the limit values  $X_{NY}$  of the defining range function  $\Sigma_Y$ , from  $P_2$ .

$$\Sigma = \Sigma(\kappa_3, 0, Y_N, z) + \frac{X_N}{X_{NY}} [\Sigma(\kappa_3, X_{NY}, Y_N, z) - \Sigma(\kappa_3, 0, Y_N, z)] \quad (4.280)$$

In the particular case corresponding to  $\lg \kappa_3 = 0$  the objective function is  $\Sigma(I, X_N, Y_N, z)$  already used in the approximating relationship (4.279) at  $\lg \kappa_3 \leq 0$ . The analysis made in the respective part of the book has shown that it is possible to simplify the two-phase problem. The plots on Figs. 4.32-4.34 together with the limiting relationships of  $\Sigma_X$ ,  $\Sigma_Y$  (Figs. 4.30, 4.29),  $\Sigma_A$  (Fig. 4.28) and  $\Sigma_p$  (Fig. 4.26) allow to solve the problem without performing numerical calculations in any particular case. The use of the dimensionless controlling parameters  $X_N, Y_N, a, \kappa_3$  permits various simplifications of the general two-phase problem (4.221-4.223) and solutions at various points within the area of the chemosorption plane defined by the third quadrant.

#### 4.3.4. Solution with parameters $\varepsilon N \geq I$ and $\varepsilon \beta N \geq 1$

In the first quadrant  $X_N \geq 0$ , so the dimensionless flux  $I(\tau)$  will be calculated for the gas phase only. The solution will be developed for large and small contact times.

At large contact times ( $\tau_i \rightarrow \infty$ ) the boundary layers cover the entire phases and the concentrations corresponding to the flux  $I$  ( $0 \leq I \leq 1$ ) are (see (4.235)):

$$c = c_s = \frac{I}{\varepsilon N}, \quad c_i = c_{is} = I - I. \quad (4.281)$$

The integration of the above equation in the gas phase (with respect to  $y_i$ ) gives the following problem for  $I(\tau)$ :

$$\frac{dI_0}{dz_0} = \sqrt{1 - \frac{I_0}{\varepsilon N}} \frac{\operatorname{th}\left[a\sqrt{1 - \frac{I_0}{\varepsilon N}}\right]}{\operatorname{th}(a)} (I - I_0), \quad I_0(0) = 0, \quad (4.282)$$

where

$$z_0 = P_i \tau_i = \varepsilon N P_2 \tau_2, \quad P_i = \varepsilon \beta^2 a \operatorname{th}(a).$$

The function  $I_0(z_0)$  is two-parametric and depends on  $a^2$  and  $X_N$ . For small and large values of  $a^2$  the solutions are [38]:

$$\left(1 - \frac{I_0}{\varepsilon N}\right)^{1/2} = \left(1 - \frac{I}{\varepsilon N}\right)^{1/2} \begin{cases} \frac{\left[1 + \varepsilon N \left[I - \left(1 - \frac{I}{\varepsilon N}\right)^{1/2}\right]^2\right] \exp\left[-\left(1 - \frac{I}{\varepsilon N}\right)^{1/2} z_0\right]}{\left[1 - \varepsilon N \left[I - \left(1 - \frac{I}{\varepsilon N}\right)^{1/2}\right]^2\right] \exp\left[-\left(1 - \frac{I}{\varepsilon N}\right)^{1/2} z_0\right]}, & a^2 \ll 1; \\ \text{other form for } a^2 \gg 1. \end{cases}$$

$$I_0 = \frac{1 - \exp\left[-\left(\frac{\varepsilon N - 1}{\varepsilon N}\right)z_0\right]}{1 - \exp\left[-\left(\frac{\varepsilon N - 1}{\varepsilon N}\right)z_0\right]/\varepsilon N}, \quad a^2 \gg 1. \quad (4.283)$$

The equation (4.282) has been solved numerically for arbitrary values of  $a^2$ . The results obtained by Runge-Kutta method for  $I_0(z_0)$  at  $X_N = 0, \geq 0.5$  are shown on Fig. 4.37. It is clear that the effect of  $a^2$  is weak and monotonous. At "small" ( $\lg a \leq -0.4$ ) and "large"  $a^2$  ( $\lg a \geq 0.6$ ) the functions  $I(z_0)$  practically coincides with these expressed by (4.283). The maximum differences between the limiting curves plotted on Fig. 4.37 decrease with the increase of  $X_N$ . For example, at  $X_N = 0$  the difference does not exceed 10%, at  $X_N = 0.25$  it decreases at 5%, while at  $X_N \geq 0.5$  it becomes smaller than 1%. These facts allow to restrict the calculations by an accuracy of 5% for the points of the entire plane  $X_N - Y_N$ . The diffusion fluxes  $I(z_0)$  may be obtained as arithmetic mean values of the analytical function (4.283). Moreover, it is possible to use an approximation relationship (like (4.276), but with the substitution  $\Sigma \rightarrow I$ ):

$$I_0(X_N, a^2, z_0) = I_0(X_N, -\infty, z_0) + (\lg a + 0.4)[I(X_N, +\infty, z_0) - I(X_N, -\infty, z_0)] \\ (-0.4 \leq \lg a \leq 0.6). \quad (4.284)$$

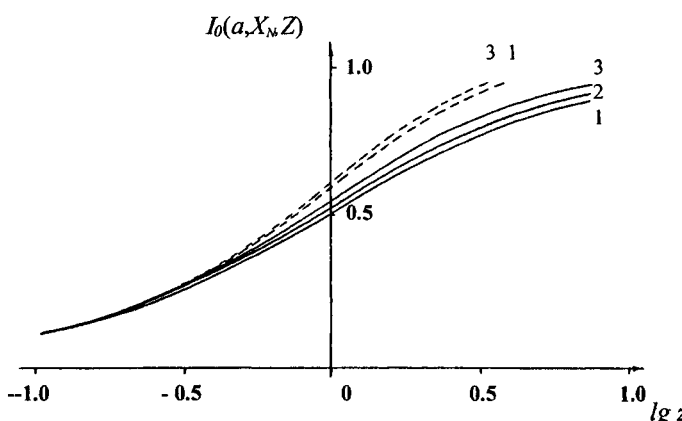


Fig. 4.37. Solution ( $I_0$ ) of the two parameter problem (4.282) at different  $X_N$ . Solid curves -  $X_N = 0$ ; dashed curves -  $X_N \geq 0.5$ ; 1) -  $\lg a \leq -0.4$ ; 2) -  $\lg a = 0$ ; 3) -  $\lg a \geq 0.6$ .

In the particular case of  $z_0 \gg I, I_0 \Rightarrow I$  the equations (4.281) give:

$$c_s \Rightarrow \frac{I}{\varepsilon N}, \quad c_{ls} \Rightarrow 0, \quad z_0 \gg I. \quad (4.285)$$

Taking into account that the main variations of  $I_0(z_0)$  occur at  $z_0 \sim I$  the relationship (4.283) indicates that the solution of the problem (4.221-4.223) may be reduced to the solution of (4.282) at sufficiently small parameters  $P_l$  ( $P_l \ll 1$ ). Hence, at moderate  $P_l$  ( $P_l \geq 10^{-1}$  for example) the investigation of the two-phase problem may be restricted to values  $a \gg I$  only (see the definition of  $P_l$  by (4.282)).

The substitution of the boundary conditions (4.222)  $th(a\sqrt{1-c_s}) \Rightarrow I$  leads to the dimensionless three-parametric problem (4.237-4.238, 4.223). The parameters controlling the solution are:

$$X_N, \quad Y_N, \quad P_l = \varepsilon \beta^2 a th(a) \approx \varepsilon \beta^2 a. \quad (4.286)$$

The solution will be the dimensionless flux in the gas phase  $I_\infty(X_N, Y_N, P_l, \tau_l)$ . Hence, in the first quadrant the problem (4.221-4.223) may be split into two independent problems. The first problem is two-parametric (4.282), while the second one is three-parametric (4.237-4.238). The criterion for applicability of both solutions ( $I_0$  or  $I_\infty$ ) is the value of  $P_l$ :

$$I \approx \begin{cases} I_\infty(X_N, Y_N, P_l, \tau_l) & \text{if } P_l \geq P_l^*; \\ I_0(X_N, a, z_0) & \text{if } P_l \leq P_l^*. \end{cases} \quad (4.287)$$

The subscript " $\infty$ " will be omitted during the development of the three-parametric problem.

It follows from the comments above that  $P_l^* \ll 1$  and its value depends on the location of the point in the plane  $X_N - Y_N$ . The further discussion will demonstrate that the value of  $P_l^*$  may be assumed as a constant in the entire first quadrant if a certain accuracy of the calculations of  $I$  is accepted.

Short contact times ( $\tau_l \rightarrow 0$ ). In this time interval the changes of  $c_{ls}$  occur in both phases but in the frames of the existing boundary layers. By the introduction of new variables  $y_{lp}$ ,  $y_p$  and  $z$ :

$$1 - y_1 = \frac{I}{P_l} y_{lp}, \quad 1 - y_2 = \frac{\beta}{P_l} y_p, \quad z = P_l^2 \tau_l, \quad (4.288)$$

the problem (4.237-4.238) may be formulated as :

$$\frac{\partial c_1}{\partial z} = \frac{\partial^2 c_1}{\partial y_{lp}^2}, \quad \frac{\partial c}{\partial z} = \frac{\partial^2 c}{\partial y_p^2};$$

$$\begin{aligned} \left( \frac{\partial c_l}{\partial y_{lp}} \right)_s &= \sqrt{1 - c_s} c_{ls}, \quad \left( \frac{\partial c}{\partial y_p} \right)_s = \left( \frac{1}{\varepsilon \beta N} \right) \sqrt{1 - c_s} c_{ls}, \\ \left( \frac{\partial c}{\partial y_p} \right)_\infty &= \left( \frac{\partial c_l}{\partial y_{lp}} \right)_\infty = 0, \quad (y_p \rightarrow \infty, y_{lp} \rightarrow \infty); \\ c_l &= 1, \quad c = 0 \quad \text{at} \quad z = 0. \end{aligned} \quad (4.289)$$

The problem (4.289) may be derived from (4.237-4.238) at  $P_i \rightarrow \infty$ . The corresponding dimensionless flux  $I_p(z)$  is related with  $I(z)$  by:

$$I_p \equiv \int_0^\infty (1 - c_l) dy_{lp} = P_i \int_0^l (1 - c_l) dy_l = P_i I(z).$$

The flux  $I_p(z)$  depends on the parameter  $Y_N$  only. The numerical calculations of the function are shown on Fig. 4.38. The plots indicate the weak effect of  $Y_N$ . At  $Y_N \geq 0.5$  (curve II on Fig. 4.38) the effect disappears.

The analytical solution of (4.289) (in the initial time interval ( $c_s \ll l$ ,  $c_{ls} = 1$ )) in the form (4.248) will be developed below. It is easy to demonstrate that the surface concentrations are:

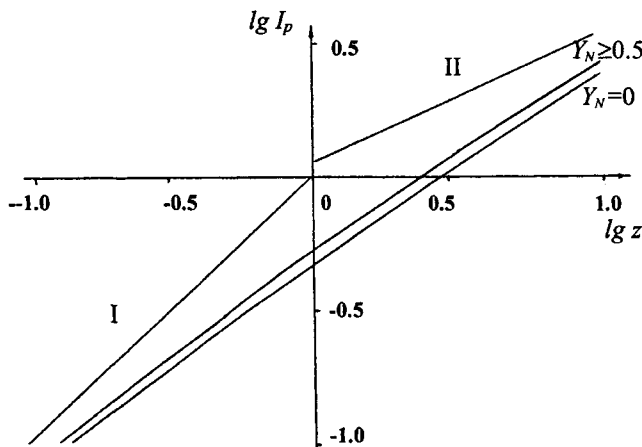


Fig. 4.38. Numerical calculation of the function  $I_0(Y_N, z)$  at  $Y_N \geq 0$ . Lines I and II – asymptotic relationships (4.293).

$$c_{ls} = I - \frac{2\sqrt{z}}{\sqrt{\pi}}, \quad c_s = \left( \frac{I}{\epsilon\beta N} \right) \frac{2\sqrt{z}}{\sqrt{\pi}}, \quad z = P_l^2 \tau_l. \quad (4.290)$$

Thus, the relationships (4.290) and the corresponding approximation (4.248) are valid at  $z \ll 1$ . Obviously, at high values of  $z$  ( $z \gg 1$ ) the concentration

$$c_{ls} \rightarrow 0. \quad (4.291)$$

is valid.

This means that at such values of  $z$  the chemosorption resistance is located in the gas phase. The concentration distributions in both phases are:

$$c_l \rightarrow \text{erf}(\eta_l), \quad c \rightarrow \left( \frac{1}{\epsilon\beta N} \right) \text{erfc}(\eta_2), \quad c_s \rightarrow \frac{I}{\epsilon\beta N} \leq 1, \quad z \gg 1. \quad (4.292)$$

It is possible to obtain the asymptotic relationships for  $I_p(z)$  by means of (4.290) and (4.292):

$$I_p \rightarrow \begin{cases} z & z \ll 1, \\ 2\sqrt{\frac{z}{\pi}} & z \gg 1. \end{cases} \quad (4.293)$$

The numerical solutions  $I_p(z)$  (Fig. 4.38) approach the asymptotic relationship (4.293) at high and low  $z$ . The conditions allowing the application of the simplified problem formulations (4.282) and (4.289) will be obtained further as results of the general solution of the two-phase chemosorption problem (4.237-4.238). It should be noted that the solutions developed in 4.5.1 and 4.5.2 are not unique in the first quadrant. Several simplifications will be developed below.

Solutions at  $\beta^2 \leq 1$ . They will be derived in the area located below the line  $DB$  on Fig. 4.25 and in several time intervals.

At  $\tau_2 > 1$  the boundary layers of both phases cover their entire areas, while at  $\tau_1 > 1, \tau_2 < 1$  a boundary layer exist in the liquid phase only. The situation  $\tau_1 < 1$  corresponds to the existence of boundary layers in both phases. If the two-phase chemosorption interval belongs to the range  $\tau_2 > 1$  the fluxes  $I_o(z_0)$  and the concentrations are defined by the relationships developed in 4.5.1 (see. (4.281), (4.282)). These relationships are monotonous and at  $z_0 \gg 1$ :

$$c_s \rightarrow \frac{I}{\epsilon N}, \quad I \rightarrow I, \quad c_{ls} \rightarrow 0. \quad (4.294)$$

Obviously, the case corresponds to a very small  $\beta^2$  ( $P_l < \beta^2 < 1$ ).

When the two-phase chemosorption process is characterized by  $I < \tau_1$ ,  $\tau_2 < I$ , the solution corresponding to the initial time interval ( $c_{ls} = I$ ,  $c_s \ll I$ ) is:

$$I = P_l \tau_1 = z, \quad c_{ls} = I - I = I - z,$$

$$c_s = \frac{P_2}{(-f'_{l/2}(0))} \tau_2^{l/2} = \frac{\sqrt{P_l}}{\varepsilon \beta N} 2 \sqrt{\frac{z}{\pi}}, \quad z \ll I. \quad (4.295)$$

Taking into account that  $I < I$  it may be assumed that at  $z \gg I$  the function  $I \rightarrow I$ ,  $c_{ls} \rightarrow 0$  and therefore  $\bar{c} \rightarrow \frac{I}{\varepsilon N} < I$ . The latter means that at  $z \gg I$  the distribution of  $c_s$  in the gas is determined by (4.292), while the concentration  $c$  is a solution of the following one-phase problem:

$$\frac{\partial c}{\partial \tau_2} = \frac{\partial^2 c}{\partial y_2^2}, \quad c = 0 \quad \text{at} \quad \tau_2 = 0; \quad \int_0^I c dy_2 = \frac{I}{\varepsilon N}.$$

The solution of the problem at  $\tau_2 < I$  exists in the form:

$$c = \frac{1}{\varepsilon N} \frac{1}{\int_0^\infty f_{-l/2}(\eta_2) d\eta_2} \frac{f_{-l/2}(\eta_2)}{\sqrt{\tau_2}}, \quad (4.296)$$

where the function  $f_{-l/2}(\eta_2)$  satisfies the equation (4.250) at  $\gamma = -I/2$  [38]:

$$f_{-l/2}(\eta_2) = \exp(-\eta_2^2/4).$$

At  $z \geq I$  the concentration  $c_s(z)$  at the interface decreases:

$$c_s = \frac{\sqrt{P_l}}{\varepsilon \beta N} \frac{1}{\sqrt{\pi z}} = \frac{I}{\varepsilon N \sqrt{\tau_2}}, \quad I \ll z, \quad \tau_2 < I, \quad (4.297)$$

where  $z = P_l \tau_1$ .

The comparison between (4.295) and (4.297) indicates that at  $z \approx I$  the concentration  $c_s$  has a maximum  $\sim \frac{\sqrt{P_l}}{\varepsilon \beta N} > \frac{I}{\varepsilon N}$ . It is clear that at  $\tau_2 > I$  the boundary layers will cover the entire phases and the relationship (4.294) will be valid. The case discussed above (4.295-4.297) is available at  $\beta^2 \ll P_l \ll 1$ .

Finally, if the two-phase chemosorption interval belongs to the range  $\tau_1 \ll I$  the concentration distributions are defined by the relationships developed in 4.5.2 (see 4.290-

4.293) and  $z = P_l^2 \tau_l$ . At  $z \gg 1$  the concentrations  $c_{ls} \rightarrow 0$ ,  $c_s \rightarrow \frac{I}{\varepsilon \beta N}$ . Further, at  $1 \ll \tau_l$ ,  $\tau_2 \ll 1$  the solution in the liquid is defined by (4.296-4.297), while at  $\tau_2 \gg 1$  the approximations (4.294) take place. This case is available at  $P_l \gg 1$ .

Solutions at  $\beta^2 > 1$  (the area above the line DB). There are three time intervals that corresponds to the chemosorption process: ( $\tau_l > 1$ ) with boundary layers covering the entire phases; ( $1 \ll \tau_2$ ,  $\tau_l \ll 1$ ) with a boundary layer in the gas phase only; ( $\tau_2 \ll 1$ ) with boundary layers in both phases.

In the first case the flux  $I$  and the concentrations may be determined by the relationships developed in 4.5.1. Taking into account that  $z = P_l \tau_l$ , it becomes clear that the regime may be occurred at sufficiently small values of  $P_l \ll 1$ .

In the second case ( $\tau_l < 1$ ,  $\tau_2 > 1$ ) the results corresponding to the initial time interval (see. (4.290)) are:

$$\begin{aligned} I &= P_l \tau_l = \frac{z}{P_l}, \quad I_p = z, \\ c_{ls} &= 1 - 2\sqrt{\frac{z}{\pi}}, \quad c_s = \frac{z}{P_l \varepsilon N}, \quad z = P_l^2 \tau_l \ll 1. \end{aligned} \quad (4.298)$$

Further, at  $z \gg 1$  the concentration  $c_{ls} \Rightarrow 0$ , and therefore (see. (4.292, 4.293)):

$$\begin{aligned} I &= \frac{2}{\sqrt{\pi}} \sqrt{\tau_l} = \frac{2}{P_l} \sqrt{\frac{z}{\pi}}, \quad I_p = \frac{2}{\sqrt{\pi}} \sqrt{z}, \\ c_s &= \frac{1}{P_l \varepsilon N} 2\sqrt{\frac{z}{\pi}}, \quad \tau_l \ll 1. \end{aligned} \quad (4.299)$$

The area corresponding to the condition  $1 \ll \tau_l$  has two boundary layers covering the entire phases and the results developed in 4.5.1 are valid (see (4.294)). The case is available at

$$I \ll P_l \ll \beta.$$

The third case ( $\tau_2 \ll 1$ ) has concentration distributions at  $z = P_l^2 \tau_l \ll 1$  (defined by (4.248)) and the surface concentrations can be obtained by (4.290). Outside the initial time ( $1 \ll z$ ,  $\tau_2 < 1$ ) the approximations (4.292) are applicable. Moreover,  $c_{ls} \Rightarrow 0$ . Further at  $1 \ll \tau_2$ ,  $\tau_l \ll 1$  the relationship (4.299) is valid, while at  $1 < \tau_l$  those developed in 4.5.1 ( $c_s \Rightarrow 1/\varepsilon N$ ,  $c_{ls} = 0$ ) are applicable. The third case is available at sufficiently high  $P_l$  ( $P_l \gg \beta$ ).

The generalization of the results obtained shows that a characteristic feature of the chemosorption solution in the first quadrant is the monotonous variation of the concentration

$c_{ls}$  with the time. The function ( $c_{ls}$ ) varies from one to zero (the two-phase chemosorption range) in a time interval of the order of  $\tau_i^*$ :

$$\tau_i^* \approx \begin{cases} \frac{1}{P_i} & \text{at } P_i \ll I; \\ \frac{1}{P_i^2} & \text{at } P_i \gg I. \end{cases} \quad (4.300)$$

Outside this range the general two-phase (4.237-4.238) problem may be simplified because  $c_{ls} \Rightarrow 0$  and the dimensionless flux  $I$  is available from the solution of the transport equation of the gas phase with a boundary condition  $c_{ls} = 0$  [40]:

$$I \Rightarrow I_i \equiv I - \sum_{n=0}^{\infty} \frac{2}{\pi^2 (n+1/2)^2} \exp[-\pi^2 (n+1/2)^2 \tau_i], \quad \tau_i \gg \tau_i^*. \quad (4.301)$$

Obviously, this is the maximum absorption regime.

For convenience of presentation of the solution in the first quadrant a dimensionless time should be introduced:

$$z = \begin{cases} \tau_i P_i & \text{at } P_i < I; \\ \tau_i P_i^2 & \text{at } P_i \geq I. \end{cases} \quad (4.302)$$

The corresponding objective function  $\varphi_i$  is:

$$\varphi_i = \begin{cases} I(z) & \text{at } P_i < I; \\ P_i I(z) & \text{at } P_i \geq I. \end{cases} \quad (4.303)$$

At small  $z$  the function approaches the  $\varphi_i = z$  irrespective of the value of  $P_i$  (compare with (4.268)). The calculations of  $\varphi_i(z)$  may be performed in a restricted interval  $z \sim 1$  only, because at  $z \gg 1$  the problem transforms to the one-phase problem ( $I \Rightarrow I_i(z)$ ):

$$\varphi_i \Rightarrow \begin{cases} 1 & \text{if } P_i < I; \\ P_i I_i \frac{z}{P_i^2} & \text{if } P_i \geq I. \end{cases} \quad (4.304)$$

The concentration  $c_s(\tau)$  is presented by a curve depending mainly on a relationship between

$\frac{b_1}{D_1^2}$  and  $\frac{b_2^2}{D_2}$ . At  $\beta^2 > 1$  (above the line  $DB$  on Fig. 4.25) the function  $c_s(\tau)$  is monotonous at every  $P_i$ . It varies from zero to its maximum  $\frac{I}{\varepsilon N} < 1$  (see 4.5.4).

At  $\beta^2 < 1$  (below the line  $DB$ ) the monotonous behaviour of  $c_s(\tau)$  exists only at sufficiently small values of  $P_i$  ( $P_i \leq \beta^2$ ). Under strong interactions ( $\beta^2 \leq P_i \leq 1$ ) the curve  $c_s(\tau)$  has a maximum  $\sim \frac{\sqrt{P_i}}{\varepsilon \beta N}$  (4.295, 4.297) at  $\tau \approx \tau^*$ . The magnitude of that maximum is always restricted by  $\frac{1}{N} < c_s^{\max} < \frac{1}{\varepsilon \beta N}$ . When intensive reactions take place ( $P_i > 1$ )  $c_s^{\max} = \frac{1}{\varepsilon \beta N}$  (see for example (4.292)).

The results obtained at various  $\beta^2$  yield the conclusion that in the general case (inspite of  $P_i$ ) the value of  $c_s^{\max}$  in the first quadrant is restricted with the range :

$$\min\left(\frac{1}{\varepsilon N}, \frac{1}{\beta N}\right) \leq c_s^{\max} \leq \max\left(\frac{1}{\varepsilon \beta N}, \frac{1}{N}\right). \quad (4.305)$$

Therefore, the surface concentration  $c_s$  satisfies the condition  $c_s < 1$  or  $B_s > 0$  in the entire area. Hence, inside the first quadrant the instantaneous chemical reaction regime ( $c_s = 1$  or  $B_s = 0$  [3, 4]) cannot occur at any  $\tau$ . However, the regime always exists in the third quadrant at  $\tau \gg \tau^*$ , but the maximum absorption regime is impossible in the same area (because  $c_{Is} > 0$  is always valid).

The results developed allow the estimation of the conditions required to consider a second order chemical reaction as a pseudo-first order reaction (see 4.2). It follows from (4.305) that at sufficiently high phase capacities ( $\varepsilon N \gg 1$ ,  $\varepsilon \beta N \gg 1$ ) the product concentration at the interface  $c_s$  (in the liquid volume too) satisfies the condition  $c_s(\tau) \ll 1$  ( $B_s = B_0$ ). In this case one may substitute  $c_s = 0$  in (4.237-4.238) and transform the problem into a simplified formulation (4.140) in 4.2.6 (the case of  $z_a \gg 1$ ). The area of the pseudo-first order chemical reaction is located in the upper right corner of the chemosorption plane  $X_N - Y_N$  (Fig. 4.25). The exact boundaries may be estimated by a comparing the numerical results (problem 4.237-4.238) with the corresponding curves on Fig. 4.22. Such comparison for  $X_N = Y_N = 0.5$  is shown on Fig. 4.39). The curves are similar to those on Fig. 4.22 (with 5% accuracy). The latter means that if the assumption of 5% accuracy for the dimensionless flux calculations is applicable the area corresponding to the pseudo-first order chemical reaction is the internal area of the right angle with a vertex at  $X_N = Y_N = 0.5$ . It will be demonstrated further, that this area is larger and its boundaries depend on the parameter  $P_i$ , because in the two-phase chemosorption interval ( $z \sim 1$ ) the maximum value of  $c_s$  is lower then that one following from the general condition (4.305). Thus, in the upper right corner

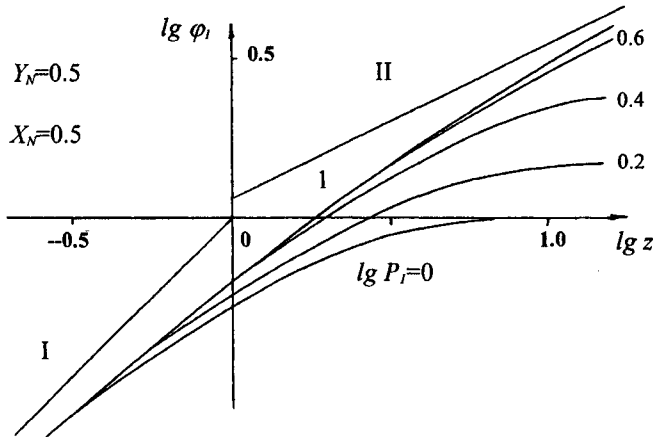


Fig. 4.39. Calculation of the objective functions  $\varphi_i(z)$  in the point  $X_N = Y_N = 0.5$ . Lines I and II – asymptotic relationships (4.293); curve 1) – relationship  $I_p(\infty, z)$ .

of Fig. 4.25 the graphical presentation becomes simpler because the problem solution depends on  $P_i$  only (Fig. 4.22).

In the first quadrant there are two areas, where the number of the controlling parameters may be reduced.

Solution of the problem (4.221-4.223) at  $\varepsilon N \rightarrow \infty$ . In this case one may assume that  $\beta \rightarrow 0$  (Fig. 4.25) and there is a diffusion boundary in the liquid phase. Under these assumptions the general problem may be expressed in a simpler form:

$$\frac{\partial c_I}{\partial \tau_I} = \frac{\partial^2 c_I}{\partial y_I^2}, \quad \frac{\partial c}{\partial \tau_I} = \frac{\partial^2 c}{\partial y_{2p}}, \quad y_{2p} = \frac{1-y_2}{\beta}; \quad (4.306)$$

$$\left( \frac{\partial c}{\partial y_{2p}} \right)_s = - \left( \frac{P_I}{\varepsilon \beta N} \right) \sqrt{I - c_s(\tau_I)} c_{Is}, \quad \left( \frac{\partial c_I}{\partial y_I} \right)_s = - P_I \sqrt{I - c_s(\tau_I)} c_{Is},$$

$$\text{at } y_I = I, \quad y_{2p} = 0; \quad (4.307)$$

$$\left( \frac{\partial c_I}{\partial y_I} \right) = 0 \quad \text{at} \quad y_I = I; \quad \left( \frac{\partial c}{\partial y_{2p}} \right) = 0 \quad \text{at} \quad y_{2p} \rightarrow \infty;$$

$$c_I = I, \quad c = 0 \quad \text{at} \quad \tau_I = 0. \quad (4.308)$$

The problem (4.306-4.308) depends on two parameters. The objective function  $\varphi_i(z)$  is  $\varphi_{iY}(P_i, Y_N, z)$  and it depends on  $P_i$  and  $Y_N$  as parameters.

The numerical solutions of the one-parametric curves  $\varphi_{iY}(P_i, Y_N, z)$  (with a parameter  $P_i$ ) at fixed  $Y_N$  ( $Y_N = 0, Y_N \geq 0.5$ ) are illustrated on Fig. 4.40. It is clear that the effect of  $Y_N$  is insignificant and that the solution strongly depends on  $P_i$ . At  $\lg P_i \leq -0.8$  this effect disappears and  $\varphi_{iY} = 1 - \exp(-z)$  (see. (4.283) at  $a \gg 1$  and  $\varepsilon N \rightarrow \infty$ ), while at  $\lg P_i \geq 0.8$  the solution has a maximum (see Fig. 4.40) that coincides with the relationships  $I_p(Y_N, z)$  on Fig. 4.38). The problem (4.306-4.308) indicates that at  $\varepsilon \beta N \gg 1$  the transport equation for  $c$  is not required because at  $c \rightarrow 0$  the problem considers a first order chemical reaction between  $A$  and  $B$ . The numerical results indicate that the solution  $\varphi_{iY}$  is valid in the area defined by  $X_N \geq 0.5$  (on the right of the vertical line  $X_N = 0.5$ ).

Solution at  $\varepsilon \beta N \rightarrow \infty$  ( $\beta \rightarrow \infty$ ). In this case the transversal variations of the concentration in the liquid phase may be neglected ( $\frac{b_2^2}{D_2} \rightarrow 0$ ). The mass balance equation gives:

$$c_s = \sum = \frac{I}{\varepsilon N}. \quad (4.309)$$

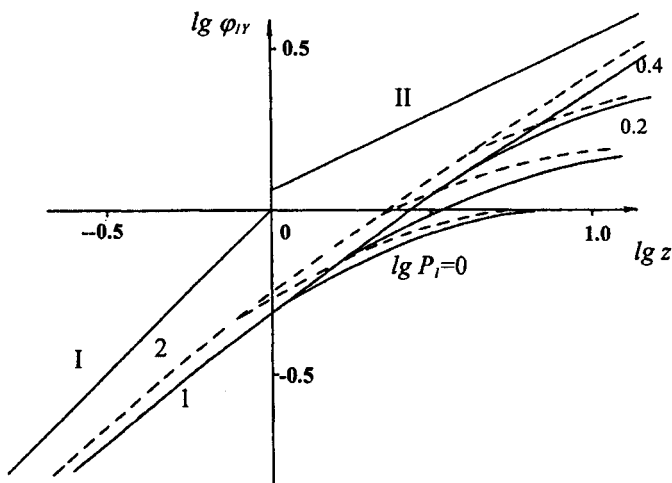


Fig. 4.40. Calculation of  $(\varphi_{iY})$  at  $\varepsilon N \rightarrow \infty$ , problem (4.306-4.308). Solid curves -  $Y_N = 0$ ; dashed curves -  $Y_N = \infty$ ; curves 1) -  $I_p(0, z)$ ; 2) -  $I_p(\infty, z)$ .

The substitution of (4.309) in (4.221-4.223) yields the one-phase problem:

$$\begin{aligned}\frac{\partial c_i}{\partial \tau_i} &= \frac{\partial^2 c_i}{\partial y_i^2}; \\ \left( \frac{\partial c_i}{\partial y_i} \right)_s &= -P_i \sqrt{1 - \frac{1}{\varepsilon N}}, \\ \left( \frac{\partial c_i}{\partial y_i} \right) &= 0 \text{ at } y_i = 0, \quad c_i = 1 \text{ at } \tau_i = 0.\end{aligned}\tag{4.310}$$

The objective function  $\varphi_{IX}(P_i, X_N, z)$  depends on  $P_i$  and  $X_N$  as parameters. The calculations are shown on Fig. 4.41. The effect of  $X_N$  has maximum at  $P_i \rightarrow 0$ . In this case  $\varphi_{IX}$  coincides with the analytical relationship  $I_0(X_N, \infty, z)$  (4.283). With the increase of  $P_i$  the effect of  $X_N$  on  $\varphi_{IX}$  decreases and at  $\lg P_i \geq 0.8$  it disappears, because  $\varphi_{IX}$  coincides with  $I_p(Y_N, z)$  at  $\lg z \leq 1$  ( $Y_N \rightarrow \infty$  and curve 4 on Fig. 4.41). The calculations indicate that, the approximations (4.309-4.310) are applicable (with an equally distributed error with respect  $P_i$ ) at  $Y_N \geq 0.5$  (above the horizontal line  $Y_N = 0.5$  on Fig. 4.25). The results obtained show that in the area of the pseudo-first order chemical reaction ( $X_N \geq 0.5$ ,  $Y_N \geq 0.5$ ) the objective functions  $\varphi_{IY}$  and  $\varphi_{IX}$  coincide.

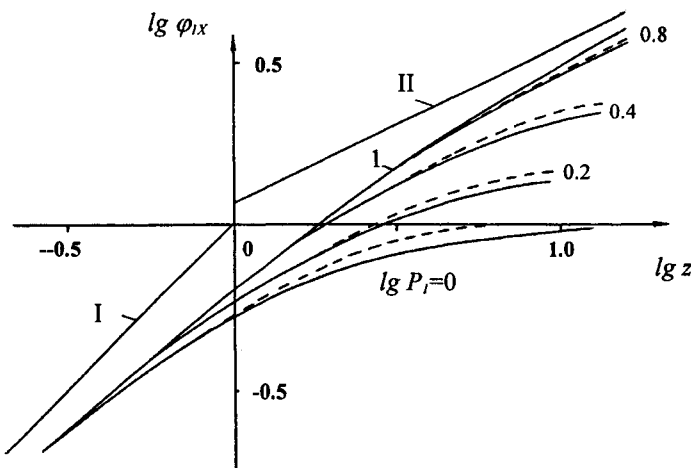


Fig. 4.41. Solution  $\varphi_{IX}$  of the problem (4.310) at  $\varepsilon\beta N \rightarrow \infty$ . Solid curves -  $X_N = 0$ ; dashed curves -  $X_N > 0$ ; curve 1) -  $I_p(\infty, z)$ ; lines I and II - asymptotic relationships (4.293).

The tabulation of the objective functions  $\varphi(P_i, X_N, Y_N, z)$  as well as  $\varphi_{II}$ ,  $\varphi_{IX}$  and  $I_i(\tau_i)$  in a restricted area of the first quadrant defined by  $0 \leq X_N \leq 0.5$ ,  $0 \leq Y_N \leq 0.5$  allows the solution of the general chemosorption problem in its entire area at any moment of the process  $\tau$ .

Numerical solution in the square  $X_N \leq 0.5$ ,  $Y_N \leq 0.5$ . The area of the plane  $X_N - Y_N$  defined in first quadrant is four times smaller than the corresponding square of the third quadrant. All the calculations have been carried out at  $a \gg 1$  and the  $P_i \ll 1$  (where the effect of  $a$  may be neglected (see Fig. 4.37)). The value of  $P_i$  ( $\kappa_i \equiv P_i$ ) has been chosen as a chemosorption parameter.

At strong chemical interactions ( $\lg \kappa_i > 0$ ) the corresponding calculations in logarithmic co-ordinates (4.302, 4.303) are shown on Figs. 4.42-4.44 for three values of  $Y_N$  (0, 0.25, 0.5) and two values of  $X_N$  (0,  $X_{NY}$ ). At a fixed  $Y_N$  and at  $X_N \geq X_{NY} (\kappa_i)$  the equality  $\varphi_i = \varphi_{II}$  is satisfied with an accuracy of 5%. The relationship  $X_{NY} (\kappa_i)$  is shown on Fig. 4.45. The values of  $X_{NY}$  increase monotonously with the increase of  $\lg P_i$  when  $-1 \leq \lg \kappa_i \leq 1$ . At  $\lg \kappa_i \leq -1$  the value of  $X_{NY}$  is  $X_{NY} = 0.5$ , while at  $\lg \kappa_i \geq 1$  it is zero ( $X_{NY} = 0$ ). The function  $X_{NY}$  is practically independent of  $Y_N$ .

In the general case and sufficiently high  $z (\lg z \geq 1)$  there is a transition  $I \Rightarrow I_i(\tau_i)$ . For small  $z$  ( $z \leq z^*$ ) the objective function  $\varphi_i(z)$  coincides with  $I_p(z)$  (Fig. 4.38 in 4.5.2).

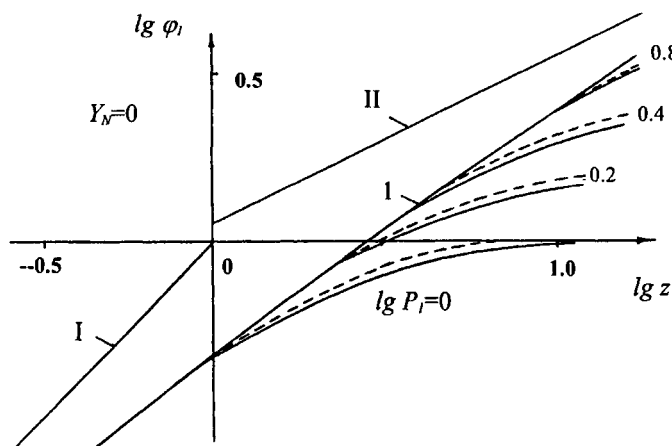


Fig. 4.42. Solution  $\varphi_i(X_N, Y_N, z)$  on the horizontal line  $Y_N = 0$ . Solid curves -  $\varphi_i(0,0,z)$ ; dashed curves -  $\varphi_{II}$ ; 1 -  $I_p(0,z)$ ; lines I and II - asymptotic relationships (4.293).

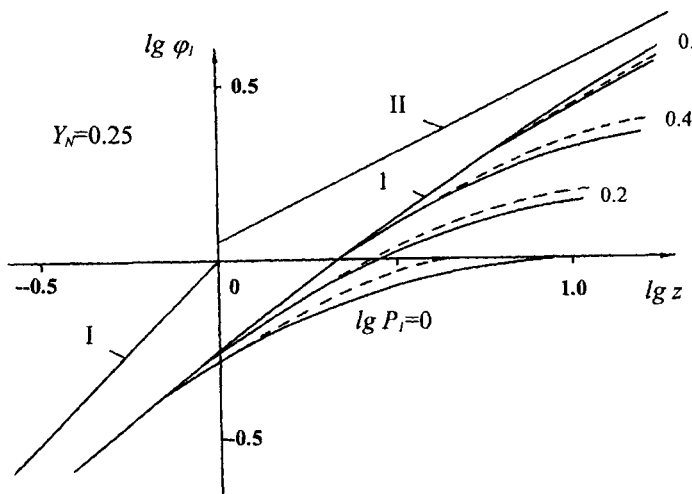


Fig. 4.43. Solution  $\varphi_I(X_N, Y_N, z)$  on the horizontal line  $Y_N = 0.25$ . Solid curves -  $\varphi_I(0,0,z)$ ; dashed curves -  $\varphi_{IY}$ ; 1) -  $I_p(0,z)$ ; lines I and II - asymptotic relationships (4.293).

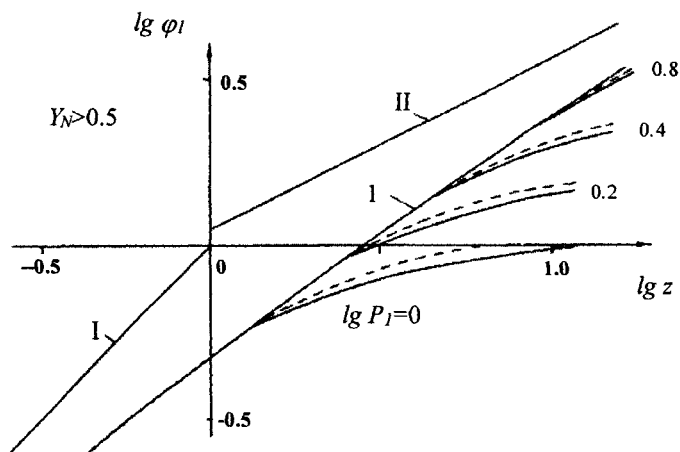


Fig. 4.44. Solution  $\varphi_I(X_N, Y_N, z)$  on the horizontal line  $Y_N = 1$ . Solid curves -  $\varphi_I(0,0,z)$ ; dashed curves -  $\varphi_{IY}$ ; 1) -  $I_p(0,z)$ ; lines I and II - asymptotic relationships (4.293).

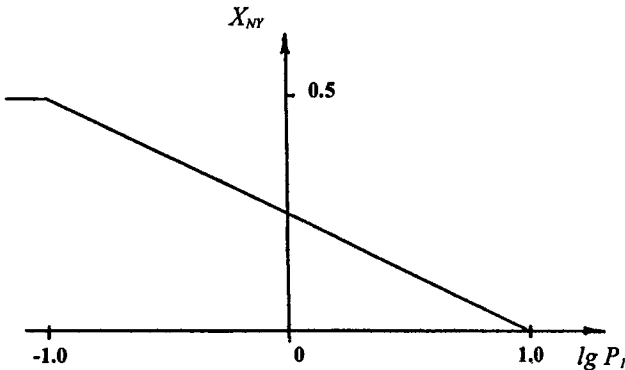


Fig. 4.45. Dependence of the limits  $X_{NY}$  of the range determination function  $I_Y$  from  $P_I$ .

All the calculations should be carried out in a restricted range  $0 \leq \lg \kappa_I \leq 1$  because for  $\lg \kappa_I \geq 1$  and  $\lg z \leq 1$  the function  $\varphi_I(z)$  practically coincides with  $I_p(z)$ .

At a fixed value of  $Y_N$  of the range  $[0, X_{NY}]$  the relationship between  $\varphi_I(z)$  and  $X_N$  is practically linear:

$$\varphi_I(P_I, X_N, Y_N, z) = \varphi_I(P_I, 0, Y_N, z) + \left( \frac{X_N}{X_{NY}} \right) [\varphi_I(P_I, X_{NY}, Y_N, z) - \varphi_I(P_I, 0, Y_N, z)]. \quad (4.311)$$

The relationships  $\varphi_I(z)$  at  $X_N = 0$  and  $X_{NY}$  required for calculations may be found by the help of the plots on Figs. 4.42-4.44.

Weak chemical interactions  $\lg \kappa_I \leq 0$ . Under these conditions it is more suitable to present the numerical results in the form  $\lg I - \lg z$ . It was proved that inspite of the position of the point  $X_N, Y_N$  at  $\lg \kappa_I \leq -1$  the solution practically coincided with the analytical relationship (4.283) at  $a \gg 1$ . In the range  $-1 \leq \lg \kappa_I \leq 0$  the effect of  $\lg \kappa_I$  is practically linear:

$$\lg I(\kappa_I, X_N, Y_N, z) = \lg I(I, X_N, Y_N, z) - (\lg \kappa_I) [\lg I_0(X_N, z) - \lg I(I, X_N, Y_N, z)]. \quad (4.312)$$

The functions  $I(I, X_N, Y_N, z)$  required for the calculations may be found through (4.311) with the substitution  $\lg \kappa_I = 0$ .

Finally, it is possible to make conclusions about the area of application of the limiting solutions  $I_Y$ ,  $I_X$  and  $I_p$ . The calculations indicate that the difference between the objective

functions at  $Y_N = 0.5$  and the corresponding relationships  $I_X(\kappa_1, X_N, z)$  does not exceed 5% (with equally distributed accuracy with respect to  $X_N$  and  $\kappa_1$ ). Therefore, the boundary of the area defining  $I_X(z)$  coincides with the horizontal line  $Y_N = 0.5$  (Fig. 4.25).

However, the area of determination of  $I_Y$  depends on the value of  $\kappa_1$ . At  $\lg \kappa_1 \leq -1$  the flux is  $I = I_0(+\infty, X_N, z)$ . The function  $I_0$  becomes independent of  $X_N$  at  $X_N \geq 0.5$ . Hence, at sufficiently small  $\kappa_1$  the area determining the limiting solution  $I_Y$  contains the points located on the left of the vertical line  $X_N = 0.5$ . At sufficiently high  $\kappa_1$  ( $\lg \kappa_1 \geq 1$ ) the objective function  $\varphi_1 \Rightarrow I_p$ , i.e. it is independent of  $X_N$  (Fig. 4.38). Therefore, the area of determination of  $\kappa_1 I = \kappa_1 I_Y = I_p$  contains every points of the entire first quadrant ( $X_N \geq 0$ ). In the general case the area of determination of  $I_Y(z)$  is located in the first quadrant on the right of the line  $X_{NY}(\kappa_1)$  (Fig. 4.45).

#### 4.3.5. Investigations in the fourth quadrant of the plane $X_N - Y_N$

The presentation of the solutions needs dimensionless complexes. The formalistic expression of the general two-phase chemosorption problem (see for example (4.221-4.223)) shows that the problem solutions dependence from the time (the dimensionless fluxes  $\Sigma(\tau_i)$  and  $I(\tau_i)$ ) is controlled by four dimensionless parameters. Obviously, the choice of these parameters is arbitrary. Using the analogy between the two-phase absorption (chapter 4.1) and the two-phase chemosorption discussed here the dimensionless phase capacities  $X_N$  and  $Y_N$  ( $\varepsilon N$  and  $\varepsilon \beta N$ ) may be chosen as two of them. Moreover, the solutions are presented in the plane  $X_N - Y_N$  (Fig. 4.25). The other two parameters usually characterize the chemosorption process (i.e. the chemical rate constant  $\bar{k}$  should be included, too). They should vary at any point  $(X_N, Y_N)$  from zero to infinity. Such parameter is the dimensionless thickness of the liquid layer  $a$  (or the well known Damkohler number  $\sqrt{M}$  (4.183)).

The investigations performed in the first and the third quadrants indicate that the main advantage of  $a$  is its weak effect on the solution. The existence of some two-phase systems or regimes (kinetics-controlled regime, instantaneous chemical reaction or the regime of a maximum absorption) depend on other controlling chemosorption parameter ( $\kappa_i$ ). This parameter in contrast to  $\varepsilon N$ ,  $\varepsilon \beta N$  and  $a$  should depend on the position of the point  $(X_N, Y_N)$  considered, i.e. on the choice of the quadrant. For example, in the situations discussed in the third quadrant  $\kappa_3 \equiv P_2$  (chapter 4.4), while in the first quadrant  $\kappa_1 \equiv P_1$  (chapter 4.5). Hence, in these areas the controlling parameters coincide with dimensionless complexes obtained through the problem expression in the form of (4.221-4.223).

The investigations show that the solution of the two-phase chemosorption problem in the form (4.221-4.223) may be obtained in a restricted time interval. Its length depends on the value of the controlling parameter  $P_i$  (or  $\kappa_i$ ). Outside this interval (it was termed *two-phase chemosorption interval*) the problem (4.221-4.223) is reduced to the well-known two one-phase problem formulations. In the former (first quadrant) the mass transfer

resistance is located in the gas phase only ( $c_{ls} = 0$ ), while in the second (third quadrant) the mass transfer resistance is in the liquid phase only ( $c_s = 1$ ).

In order to obtain solutions at various parameter values similarity, time co-ordinates  $z$  have been introduced. They are related to the co-ordinates  $\tau_i$  by the relationship (4.266) (in the third quadrant) and (4.302) (in the first quadrant) respectively. The advantage of  $z$  with respect to  $\tau_i$  is the fact that the dimensionless fluxes ( $\Sigma(z)$  or  $I(z)$ ) may be considered in a time interval of the order of unity ( $z \sim I$ ) irrespective of the value of  $P_i$ .

For the purposes of the numerical solutions under the condition of the "strong" chemical interactions (i.e. for  $P_i \geq 1$ ) the dimensionless fluxes  $\Sigma(z)$  (third quadrant) and  $I(z)$  (first quadrant) were replaced by the products  $P_2 \Sigma$  and  $P_1 I$  respectively. The objective functions  $\varphi_i(X_N, Y_N, P_i, a, z)$ , defined by (4.267) and (4.303) were introduced due to the same reasons.

It was demonstrated that the values of the objective functions corresponding to the two-phase chemosorption interval ( $z \sim I$ ) are always greater than unity inspite the values of  $P_i$ . Moreover, at every point  $X_N, Y_N$  and sufficiently high  $P_i$  (in fact at  $\lg P_i \geq 1$ ) the objective functions depend on the parameter  $Y_N$  (i.e.  $\varphi_i \cong \varphi_i(Y_N, z)$ ) only. In the other limiting case of sufficiently low values of  $P_i$  (practically at  $\lg P_i \leq -1$ ) these functions depend on  $X_N$  and  $a$  only. Thus, the presentation of the solution of (4.221-4.223) in the form of  $\varphi_i = \varphi_i(X_N, Y_N, P_i, a, z)$  permits to obtain a solution at every point  $X_N, Y_N$  and every chemical interactions (i.e. various  $k$ ) and arbitrary time intervals  $\tau$ .

Hereafter, the theoretical investigations of the solutions at various points of fourth quadrant will determine the corresponding values of the controlling parameter  $\kappa_i$ , the objective function  $\varphi_i$  and the dimensionless time co-ordinate  $z$ . These investigations allow the evaluation of the solution in that  $X_N - Y_N$  semi-plane.

The solution on the axis  $Y_N \leq 0$ . This solution should take into account that the axis belongs simultaneously to the fourth and third quadrants and may be obtained as a particular case of the solutions already obtained in the third quadrant at  $\varepsilon N = 1$  (chapter 4.4).

In the third quadrant the controlling parameter is  $P_2$  and the corresponding time co-ordinate may be determined by the relationship (4.266). A characteristic feature of the solution of the problem (4.221-4.223) in that part of the plane (i.e. on the vertical line  $X_N = 0$  too) there is a monotonous increase of the product concentration  $c_s(z)$ . The range of variations is from zero to unity at the time interval  $z \sim I$  (two-phase chemosorption interval). Outside that range ( $z \gg I$ ) it is possible to obtain analytically the dimensionless flux  $I(z)$  because the concentration at the interface is almost equal to the equilibrium ( $c_s = 1$ ):

$$I \Rightarrow (\varepsilon N) \left\{ 1 - \sum_{n=0}^{\infty} \frac{2}{\pi^2 (n + 1/2)^2} \exp[-\pi^2 (n + 1/2)^2 \tau_2] \right\} = (\varepsilon N) \Sigma_s(\tau_2). \quad (4.313)$$

This means that an instantaneous reaction regime with  $B_s \rightarrow 0$  occurs in the system [3, 4]. Further the regime remains unchanged at every  $\tau$ .

The objective functions  $P_2 I(z)$  (if  $P_2 > 1$ ) and  $I(z)$  (if  $P_2 \leq 1$ ) may be obtained by the plots on Figs. 4.32-4.34 or by the approximating relationship (4.279) ( $X_N = 0, a \gg 1$ ).

In accordance with the features of the "splitting" (4.267) the effect of the Damkohler number on the objective function exists at low values of  $P_2$  (practically at  $\lg P_2 \leq -1$ ). In this case the dimensionless flux  $I(z)$  may be calculated by the approximating relationship (4.276) with a substitution  $X_N = 0$  ( $I = \Sigma_0(0, a, z)$ ). On the axis  $Y_N \leq 0$  the flux depends on the parameter  $a$  only. At low and high values of that parameter analytical solutions are available (see (4.283)):

$$I_0(0, a, z) = \begin{cases} z/(1+z) & \text{at } a \rightarrow 0; \\ 1 - 1/(1+z/2)^2 & \text{at } a \rightarrow \infty. \end{cases} \quad (4.314)$$

The difference between the limiting curves does not exceed 10%, so one may decide that the effect of the parameter  $a$  on that axis is weak.

Solution on the axis  $X_N \geq 0$ . This axis belongs simultaneously to the first and the fourth quadrant, so the solution on it may be obtained as a particular case of the solution in the first quadrant at  $Y_N = 0$  ( $\epsilon\beta N = 1$ ). In this case the controlling parameter is  $P_1$ , while (4.302) and (4.303) define the time co-ordinate  $z$  and the objective functions respectively.

A characteristic feature of the general problem (4.221-4.223) solution on the horizontal line axis  $Y_N = 0$  ( $X_N > 0$ ) is the monotonous decrease of the surface concentration  $c_{ls}(z)$  from unity to zero in the time range  $z \sim 1$ . At  $z \gg 1$  and  $c_{ls} = 0$  the problem becomes one-phase problem and the flux  $I(\tau)$  may be defined analytically by (4.301). In this case the mass transfer resistance is totally located in the gas phase. The conditions correspond to the maximum absorption regime existing further at every  $\tau$ .

The objective functions  $P_1 I(z)$  (if  $P_1 > 1$ ) and  $I(z)$  (if  $P_1 \leq 1$ ), corresponding to the two-phase chemosorption interval, may be obtained by the plots on Fig. 4.42 and the approximation (4.312) ( $Y_N = 0, a \gg 1$ ).

The effect of the Damkohler number on  $I(z)$  exists at low values of the controlling parameter ( $\lg P_1 \leq -1$ ). In this case the flux coincides with the solution of the two-parametric  $I_0(X_N, a, z)$  (4.282) and the approximation (4.284) may be employed. The effect considered decreases monotonously with the increase of  $X_N$ . The effect is maximal (about 10%) at  $X_N = 0$  (see 4.3.5) and practically disappears at  $X_N \geq 0.5$ . In the latter situation the analytical relationship  $I_0 = 1 - \exp(-z)$  (4.283) is valid.

The solution of the general problem (4.221-4.223) has interesting feature in the close proximity of the central point  $X_N = Y_N = 0$  of the plane. There the characteristic dimensions of the gas phase  $\frac{b_1^2}{D_1}$  and the liquid  $\frac{b_2^2}{D_2}$  coincide, and the parameter  $\beta^2 = 1$ . Therefore, the dimensionless time intervals  $z$  defined in the third (4.266) and the first (4.302) quadrants coincide too. Outside that range and  $z \gg 1$  the conditions  $c_s \rightarrow 1$  and  $c_{ls} \rightarrow 0$  are satisfied. Thus, the chemosorption regime established in the system may be assumed as a regime of an

instantaneous chemical reaction and as a maximum absorption regime too. Obviously, the equality  $I_a(\tau_1) = \varepsilon N \sum_s(\tau_2)$  remains with the further increase of the time.

The solution of (4.221-4.223) in the internal points of the square of the fourth quadrant is investigated below under the strong conditions  $\varepsilon N > 1$ ,  $\varepsilon \beta N < 1$ .

The solution at  $\beta^2 \ll 1$ . This solution should take into account that the ratio  $\beta^2 = \left( \frac{b_1^2}{D_1} \right) / \left( \frac{b_2^2}{D_2} \right)$  remains constant along the lines parallel to  $AC$  (Fig. 4.25). Several analytical solutions corresponding to various time intervals will be developed below on the lines  $\beta^2 = \text{const} \ll 1$  for the possible time intervals: 1)  $\tau_1 \ll 1$ ; 2)  $\tau_1 \gg 1$ ,  $\tau_2 \ll 1$ ; 3)  $1 \ll \tau_2$ .

It is clear, that at  $\tau_1 \ll 1$  (and  $\tau_2 \ll 1$  too) the diffusion boundary layers exist in both phases. The solution of (4.221-4.223) corresponding to the initial time intervals ( $c_{ls} = 1$ ,  $c_s \ll 1$ ) exists in the form (4.248, 4.249).

At the surface ( $z \ll 1$ ):

$$c_{ls} = 1 - P_1 \frac{2}{\sqrt{\pi}} \sqrt{\tau_1} = 1 - (\varepsilon \beta N) \frac{2}{\sqrt{\pi}} \sqrt{z}, \quad (4.315)$$

$$c_s = P_2 \frac{2}{\sqrt{\pi}} \sqrt{\tau_2} = \frac{2}{\sqrt{\pi}} \sqrt{z}, \quad (4.316)$$

where  $z = P_2^2 \tau_2$ . Taking into account that  $c_s \leq 1$  the result (4.316) allows the suggestion that at  $z \gg 1$  the concentration  $c_s \rightarrow 1$ . In this case the solution of (4.221-4.223) is available in the forms (4.253, 4.254) and the concentrations on the interface are equal (4.254). The relationships (4.253, 4.254) are not asymptotic, but they are valid in the restricted time interval  $\tau_1 \ll 1$ .

At  $\tau_1 \gg 1$ ,  $\tau_2 \ll 1$  the diffusion boundary layer in the gas tends to cover the entire phase that corresponds to the condition  $c_s = c_{ls}(\tau)$ . Under such conditions the equations (4.253, 4.254) are not correct. The concentration distribution in the gas phase may be obtained by the mass balance equation (4.224). Hence:

$$c_{ls} = 1 - \varepsilon N \frac{2}{\sqrt{\pi}} \sqrt{\tau_2}, \quad c_s = 1. \quad (4.317)$$

It follows from (4.254) and (4.317) that the concentration in the gas phase corresponding to  $1 \leq \tau_1$ ,  $\tau_2 \leq \frac{1}{(\varepsilon N)^2} < 1$  decreases from a moderate value of  $(1 - \varepsilon \beta N)$  down to zero. Further, at  $(\frac{1}{(\varepsilon N)^2} < \tau_2)$  the gas phase depletion is complete ( $c_{ls} = 0$ ,  $I = 1$ ),

so the distribution  $c(\tau, y)$  in the liquid is available by the simplified problem formulation (one-phase problem):

$$\frac{\partial c}{\partial \tau_2} = \frac{\partial^2 c}{\partial y_2^2}, \quad \int_0^l c dy_2 = \frac{I}{\varepsilon N}. \quad (4.318)$$

It is easy to check that the solution of the latter problem corresponding to  $\tau_2 \ll I$  is:

$$c = \left( \frac{I}{\varepsilon N} \right) \frac{1}{\sqrt{\pi}} \frac{\exp\left(-\frac{\eta_2^2}{4}\right)}{\sqrt{\tau_2}}, \quad c_s = \frac{I}{\varepsilon N} \frac{1}{\sqrt{\pi}} \frac{1}{\sqrt{\tau_2}}. \quad (4.319)$$

At  $\tau_2 \gg I$  the boundary layer in the liquid covers the entire phase and the solution of (4.318) is trivial:

$$c_s = \frac{I}{\varepsilon N}. \quad (4.320)$$

The above approximations (4.315-4.320) need better definitions of the conditions under which they may be applied. The transition into the instantaneous chemical reaction regime (4.317) occurs in the range  $z \sim I$  or  $\tau_2 \sim \frac{I}{P_2^2}$  (solutions 4.315 and 4.316). The same regime occurs at  $\tau_2 \sim \frac{I}{(\varepsilon N)^2}$  and in this case the solutions (4.319) and (4.320) are valid.

Therefore, it may be decided that the required condition of the existence of that regime is the satisfaction of the following condition:

$$\frac{I}{P_2^2} \ll \frac{I}{(\varepsilon N)^2} \quad \text{or} \quad \kappa_s \gg I, \quad (4.321)$$

where the parameter  $\kappa_s$  is defined by :

$$\kappa_s \equiv \frac{P_2}{N} = \frac{P_1}{(\varepsilon \beta N)^2}. \quad (4.322)$$

At sufficiently high values of the parameter  $\kappa_s$  one may suppose that in the two-phase chemosorption interval there are boundary layers in both phases. This requires the introduction of dimensionless time and space co-ordinates by the definition (4.241). The next step is the simplified problem formulation (4.242-4.244). Its solution is the dimensionless flux  $\Sigma_p(z)$  (see (4.246)):

$$\Sigma_p(Y_N, z) \equiv \int_0^\infty c dy_{2p} = P_2 \Sigma(z). \quad (4.323)$$

Hence, at sufficiently high  $\kappa_s$ , the dimensionless flux  $I(z)$  may be expressed as:

$$I(z) = \left( \frac{\varepsilon N}{P_2} \right) \Sigma_p(Y_N, z) = \frac{\Sigma_p(Y_N, z)}{\kappa_s}, \quad (4.324)$$

or

$$\kappa_s I(z) = \Sigma_p(Y_N, z) \quad (\kappa_s \gg 1). \quad (4.325)$$

Thus, at high  $\kappa_s$ , the functions  $\kappa_s I(z)$  depend on the parameter  $Y_N$  only. Moreover, they coincide with the limiting relationships shown on Fig. 4.26.

The solution of the general problem (4.221-4.223) when the opposite condition ( $\kappa_s \ll 1$ ) is satisfied is of a special interest. In this case during the initial chemosorption interval ( $c_{ls} \approx 1$ ,  $c_s \ll 1$ ) the condition  $\tau_2 \gg \frac{1}{(\varepsilon N)^2}$  or  $\tau_1 \gg \frac{1}{(\varepsilon \beta N)^2} > 1$  is valid. This

means that the boundary layer in the gas covers the entire phase and therefore  $c_l = c_{ls}(\tau)$ . The concentration distribution corresponding to the initial time interval is defined by the relationship (4.316). Assuming that  $\tau_2 < 1$ , the yield of the mass balance equation (4.224) is:

$$c_{ls} = 1 - z, \quad c_s = \sqrt{\kappa_s} \frac{2}{\sqrt{\pi}} \sqrt{z} \quad (z \ll 1), \quad (4.326)$$

where  $z = P_1 \tau_1$  is the dimensionless time.

If accept that at  $z \sim 1$  the gas phase depletion is complete ( $c_{ls} \rightarrow 0$ ,  $I \rightarrow 1$ ) and the corresponding concentration distribution in the liquid at  $z \gg 1$  is available by the simplified problem formulation (4.318). In this particular case at the interface there are (4.319, 4.320):

$$c_s = \begin{cases} \sqrt{\kappa_s} \frac{1}{\sqrt{\pi}} \frac{1}{z}, & z \gg 1, \quad \tau_2 < 1; \\ \frac{1}{\varepsilon N}, & \tau_2 > 1. \end{cases} \quad (4.327)$$

The formulae (4.326, 4.327) indicate that the curve  $c_s(z)$  has a maximum of the order  $c_s^{\max} \approx \sqrt{\kappa_s}$  at  $z \sim 1$ . Moreover, the inequality:

$$\frac{1}{\varepsilon N} < \sqrt{\kappa_s} < 1. \quad (4.328)$$

is satisfied.

The latter indicates that at small  $\kappa_4$ , the regime of an instantaneous chemical reaction  $c_s \approx 1$  does not exist for any  $\tau$ . However, the value  $(\frac{I}{\varepsilon N})$  is asymptotic for  $c_s(\tau)$  (see (4.327)), so at  $\kappa_4 > 1$  the condition  $c_s^{\max} = 1$  (4.317) takes place. It may be suggested that the condition  $\sqrt{\kappa_4} > \frac{I}{\varepsilon N}$  is enough to assure the maximum of  $c_s(\tau)$ . If the opposite condition  $\sqrt{\kappa_4} < \frac{I}{\varepsilon N}$  is satisfied the maximum disappears and the surface concentration  $c_s(\tau)$  increases monotonously with the time  $\tau$ . In the latter case during the two-phase chemosorption interval ( $z = P_1\tau_1 \sim I$ ) the boundary layers cover the entire phases because  $\tau_2 > 1$ . Hence, the flux  $I(z)$  satisfies the equation (4.282) and the following equality:

$$c_s = \frac{I_0(X_N, a, z)}{\varepsilon N}, \quad c_I = 1 - I_0, \quad I = I_0(X_N, a, z), \quad (4.329)$$

is valid.

In this situation the chemical reaction has a constant rate across the entire film thickness (kinetics-controlled regime). It should be mentioned that at  $\kappa_4 \ll 1$  the equality  $I = I_0(X_N, a, z)$  is always valid inspite of the behaviour of the curve  $c_s(z)$  (i.e. the occurrence of a maximum or not).

The solution in the fourth quadrant at various values of the chemosorption parameters require the introduction of dimensionless time co-ordinates  $z$  and objective functions  $\varphi_4$  that should be of the orders of unity in the two-phase chemosorption interval.

It follows from the discussion above that the requirement may be satisfied by the following quantities:

$$\varphi_4(z) = \begin{cases} \kappa_4 I(z) & \text{at } \kappa_4 \geq 1; \\ I(z) & \text{at } \kappa_4 < 1; \end{cases} \quad (4.330)$$

$$z = \begin{cases} P_2^2 \tau_2 & \text{at } \kappa_4 \geq 1 \\ P_1 \tau_1 & \text{at } \kappa_4 < 1 \end{cases} = \begin{cases} \kappa_4^2 \tau^* & \text{at } \kappa_4 \geq 1 \\ \kappa_4 \tau^* & \text{at } \kappa_4 < 1 \end{cases}. \quad (4.331)$$

Here, the dimensionless time co-ordinate  $\tau^*$  is related with the co-ordinates  $\tau_i$  by:

$$\tau^* \equiv (\varepsilon N)^2 \tau_2 = (\varepsilon \beta N)^2 \tau_1. \quad (4.332)$$

The second brackets of (4.331) show that in the fourth quadrant the parameters  $\kappa_4$  and  $\tau^*$  have the same sense like  $P_2$ ,  $\tau_2$  in the third and  $P_1$ ,  $\tau_1$  in the first quadrants, respectively.

It should be mentioned that on the axis  $X_N \geq 0$ , where  $\varepsilon\beta N = 1$ , the conditions  $\kappa_4 = P_1$ ,  $\tau^* = \tau_1$ , and  $\varphi_4 = \varphi_1(z)$  are valid, while on the vertical axis  $Y_N \leq 0$ , where  $\varepsilon N = 1$ , the conditions are  $\kappa_4 = P_2$ ,  $\tau^* = \tau_2$ ,  $\varphi_4(z) = \varphi_2(z)$ . Moreover, on these axes the dimensionless time co-ordinates  $z$  in the fourth quadrant defined by (4.331) coincide with  $z$  defined in the first (4.302) and third (4.266) quadrants. Therefore, during the transitions from the fourth quadrant into the first (or the second) quadrant there are discontinuities of the dimensionless parameters and functions.

The comments made above give possibility to decide that the two-phase chemosorption problem (4.221-4.223) may be defined in the fourth quadrant as:

$$\begin{aligned} (\varepsilon\beta N)^2 \frac{\partial c_1}{\partial \tau^*} &= \frac{\partial^2 c_1}{\partial y_1^2}, \quad \frac{\partial c}{\partial \tau^*} = \frac{\partial^2 c}{\partial y_2^2}; \\ \left( \frac{\partial c}{\partial y_2^*} \right)_s &= \kappa_4 \sqrt{1-c_s} c_{ls}, \quad \left( \frac{\partial c_1}{\partial y_1} \right)_s = (\varepsilon\beta N)^2 \kappa_4 \sqrt{1-c_s} c_{ls}; \\ \left( \frac{\partial c}{\partial y_2^*} \right) &= 0 \quad \text{at } y_2^* = \varepsilon N; \\ \left( \frac{\partial c_1}{\partial y_1} \right) &= 0 \quad \text{at } y_1 = 0; \\ c &= 0, \quad c_1 = 1 \quad \text{at } \tau^* = 0. \end{aligned} \tag{4.333}$$

The corresponding dimensionless flux  $I$  is:

$$I = I - \int_0^1 c_1 dy_1 = \int_0^{\alpha} c dy_2^*. \tag{4.334}$$

A transversal co-ordinate in the liquid phase  $y_2^* = (1-y_2)(\varepsilon N)$  has been introduced above. Moreover, the assumption that the Damkohler number  $\alpha \gg 1$  was applied.

It is easy to find that the dimensionless co-ordinates  $\tau^*$  and  $z$  (the second definitions in (4.331)) are interrelated by relationships similar to those defined by (4.266) and (4.302) in the third and the first quadrants respectively. The problem (4.333) is an analogue of the dimensionless three-parametric problem (4.237-4.238). Moreover, the time dependence of the dimensionless flux  $\varphi_4(z)$  during the two-phase chemosorption interval ( $z \sim I$ ) is controlled by the parameters  $X_N, Y_N$  and  $\kappa_4$ .

At sufficiently high values of the controlling parameter  $\kappa_4$ , the objective functions  $\varphi_4(z)$  become one-parametric because  $\varphi_4(z) \Rightarrow \Sigma_p(Y_N, z)$ . The latter is easy to prove, if dimensionless co-ordinates  $y_{2p}$  and  $y_{1p}$  are applied (see for example (4.241)):

$$y_{2p} = y_2^* \kappa_4 \equiv (1-y_2)P_2, \quad y_{1p} = (\varepsilon\beta N)\kappa_4(1-y_1) \equiv \beta P_2(1-y_1).$$

The result is the two-phase problem formulation (4.242-4.244) with one controlling parameter. Therefore, the objective function  $\varphi_4$  may be determined by (4.325) (see Fig. 4.26). One should remember that  $z = \kappa_4^2 \tau^* = P_2^2 \tau_2$  (4.331). Obviously, in this case the diffusion boundary layers exist in both phases.

In the next limiting case corresponding to low values of  $\kappa_4$  one could assume that the diffusion boundary layers cover the entire phases and therefore the relationships (4.281) are applicable.

The integration of any transport equation (4.333) along the transversal co-ordinate with the appropriate condition at the interface yields an ordinary differential equation (4.282) corresponding to  $a \gg 1$ . Hence, (see also (4.283)):

$$\varphi_4 = I_0(X_N, +\infty, z), \quad z = \kappa_4 \tau^* \equiv P_1 \tau_1. \quad (4.335)$$

Here  $P_1 \equiv \varepsilon \beta^2 a$ , so at  $\kappa_4 \ll 1$  the objective function depends on two parameters ( $X_N$  and  $a$ ), and the approximation (4.284) is applicable.

The approach results in the fact that the solution of the two-phase chemosorption problem (4.221-4.223) in the fourth quadrant splits in two solutions. The first one at  $\kappa_4 \geq \kappa_4^*$  coincides with that of the three-parametric problem  $\varphi_4 = \varphi_4(X_N, Y_N, \kappa_4, z)$  (4.333), while the second at  $\kappa_4 \leq \kappa_4^*$  is equal to the solution of the two-parametric function  $\varphi_4 = I_0(X_N, a, z_0)$  (4.282). The limiting value of  $\kappa_4^*$  slightly depends on the position of the point  $X_N, Y_N$  in the plane  $X_N - Y_N$ . In the general case the condition  $\kappa_4^* \ll 1$  is satisfied. It will be demonstrated further (see the numerical calculation of the objective functions) that in the entire fourth quadrant the values of  $\kappa_4^*$  may be assumed constant.

It should be mentioned that the above feature of the solution splitting follows directly from the definition of  $\kappa_4$  (4.322) presented in the form:

$$ath(a) \equiv \kappa_4(\varepsilon N)N, \quad (4.336)$$

taking into account that in the quadrant considered  $\varepsilon N \geq 1$ .

In the fourth quadrant there are two areas where the solution ( $\varphi_4(X_N, Y_N, \kappa_4, z)$ ) of the three-parametric problem (4.333) allows further simplifications because the effect of the one of the parameters ( $X_N$  or  $Y_N$ ) disappears. These areas correspond to higher values of the liquid phase capacity ( $\varepsilon N$  or  $\varepsilon \beta N$ ).

The solution at high  $\varepsilon N$  (in the right half plane  $X_N - Y_N$ , where  $\varepsilon N \gg 1$ ) corresponds to the condition  $\beta^2 \ll 1$ . Therefore, one may assume that in the liquid phase there is always a diffusion boundary layer, because  $\frac{b_2^2}{D_2} \rightarrow \infty$ . The substitution of the

boundary condition  $\frac{\partial c}{\partial y_2^*} = 0$  at  $y_2^* = \varepsilon N$  by  $\frac{\partial c}{\partial y_2^*} = 0$  at  $y_2^* = \infty$  transforms the dimensionless problem formulation (4.333) to expressions corresponding to the case

$\varepsilon N \rightarrow \infty$ . The dimensionless flux  $I_Y(z)$  of the new problem may be obtained by (see also (4.334)):

$$I_Y = I - \int_0^1 c_I dy_I = \int_0^\infty c dy_2^*. \quad (4.337)$$

The objective function  $\varphi_4(z)$  depends on two parameters ( $Y_N$  and  $\kappa_4$ ) only. Moreover, at high and low  $\kappa_4$ , simplifications are possible. In the former case  $\varphi_{4Y} \Rightarrow \sum_p(Y_N, z)$  (4.325), while in the latter  $\varphi_{4Y} \Rightarrow 1 - \exp(-z)$  (4.283). The area, where the function  $\varphi_{4Y}(z)$  may be determined, is possible to define by numerical calculation only. It will be demonstrated below that the boundaries of that area depend on the chemosorption parameter  $\kappa_4$ .

The solution at low values of  $\varepsilon\beta N$  may be obtained by the transport equation in the gas phase (see 4.333)) at  $\varepsilon\beta N \rightarrow 0$ , i.e.  $\frac{\partial^2 c_I}{\partial y^2} = 0$ . Therefore, the variations of the concentration  $c_I$  in a transversal direction may be neglected ( $c_I = c_{Is}(\tau)$ ). Thus, there is no need to solve the equation. The problem (4.333) may be transformed in the following one-phase problem:

$$\begin{aligned} \frac{\partial c}{\partial \tau^*} &= \frac{\partial^2 c}{\partial y_2^{*2}}; \\ \left( \frac{\partial c}{\partial y_2^*} \right)_s &= \kappa_4 \sqrt{1 - c_s} (1 - I); \\ \left( \frac{\partial c}{\partial y_2^*} \right) &= 0 \quad \text{at } y_2^* = \varepsilon N; \quad c = 0 \quad \text{at } \tau^* = 0, \end{aligned} \quad (4.338)$$

where

$$I = I - c_{Is} = \int_0^{\varepsilon N} c dy_2^*.$$

Like in the case in the third quadrant, the dimensionless flux (the objective function)  $I_X(z)$  ( $\varphi_4(z)$ ) must be defined at ( $\varepsilon\beta N \rightarrow 0$ ). It follows from (4.338) that both functions depend on the parameters  $X_N$  and  $\kappa_4$  only, so they may be expressed as  $\varphi_{4X} = \varphi_{4X}(X_N, \kappa_4, z)$ . In the particular case of  $\kappa_4 \gg 1$  the objective function is  $\varphi_{4X} \Rightarrow \sum_p(-\infty, z)$  (Fig. 4.26), while in the other extreme situation ( $\kappa_4 \ll 1$ ) the function  $\varphi_{4X}$  is defined by (4.283) (the case of  $a \gg 1$ ).

The analysis performed above shows that the dimensionless complex  $\kappa_4$  (4.322) has all the features of a controlling parameter in the fourth quadrant. Its value determines the

regime of absorption in the two-phase system during both the initial chemosorption interval and the rest of the process.

The effect of the second chemosorption parameter (the Damkohler number) is not strong in the general case and it may be detected when weak chemical interactions between  $A$  and  $B$  occurs in kinetics-controlled regimes (low  $\kappa_4$ ). The investigations carried out indicate that outside the two-phase chemosorption interval ( $z \gg 1$ ) the numerical solution of the general problem (4.221-4.223) is not required, because the dimensionless flux  $I(\tau)$  may be obtained analytically.

When strong chemical interactions occur ( $\kappa_4 \gg 1$  at  $z \gg 1$ ) the system passes into the instantaneous chemical reaction regime. Taking into account that during the two-phase chemosorption the depletion of the gas is negligible (because  $I \ll 1$ ) it may be decided that the main absorption of the component  $A$  occurs outside that interval during the instantaneous reaction regime. Moreover,  $B_s = 0$  may be assumed at every  $\tau$ . In the opposite case of weak chemical interactions ( $\kappa_4 \ll 1$ ) the gas depletion occurs mainly during the two-phase chemosorption interval under kinetics control ( $c_s = c$ ).

In the general case at any values of  $\kappa_4$  one may assume that

$$I \Rightarrow \min\{(\varepsilon N) \sum_s(\tau_2), I_s(\tau_1)\} \text{ at } z \gg 1. \quad (4.339)$$

Particularly, at the boundary between the third and the fourth quadrants ( $X_N = 0$ ) the inequality  $(\varepsilon N) \sum_s \leq I_s$  takes place inspite of  $\kappa_4$  and  $I \Rightarrow (\varepsilon N) \sum_s(\tau_2)$ . In a similar way, at the boundary between the fourth and the first quadrants ( $Y_N = 0$ ) the opposite condition is satisfied  $I_s < (\varepsilon N) \sum_s$  and therefore  $I \Rightarrow I_s(\tau_1)$  if  $z \gg 1$ .

The solution in the fourth quadrant may be considered as marginal between those obtained in the first and the third quadrants. In the former the maximum absorption regime exists ( $I \Rightarrow I_s(\tau_1)$ ), while in the latter the instantaneous chemical reaction regime occurs ( $I \Rightarrow (\varepsilon N) \sum_s(\tau_2)$ ). In both cases the transition into these limiting regimes occurs inspite of the values of  $k_i$  ( $i = 1, 3$ ). However, in fourth quadrant all the processes depend on the value of  $\kappa_4$ . The calculations indicate that at  $\kappa_4 \geq 1$  the system usually passes into the instantaneous chemical reaction regime.

During the numerical studies on the two-parametric problem the integration of (4.282) was carried out in 4.3.5. (see the approximation (4.284)). Taking into account that the effect of the parameter  $a$  is weak, it may be assumed that the analytical approximation (4.283) may be applied with an error of about 10%:

$$I_0(X_N, a, z) = \frac{1 - \exp\left[-\left(\frac{\varepsilon N - 1}{\varepsilon N}\right)z\right]}{1 - \exp\left[-\left(\frac{\varepsilon N - 1}{\varepsilon N}\right)z\right] \quad \text{(at any } a\text{)}} \quad (4.340)$$

The numerical investigations of the three-parametric problem ( $a \rightarrow \infty$ ) in the fourth quadrant. The dimensionless flux  $I(X_N, Y_N, \kappa_4, z)$  will be presented as one-parametric curves  $\varphi_4(z)$  ( $\kappa_4$  as a parameter) and will be separated in two groups of strong ( $\lg \kappa_4 \geq 0$ ) and weak ( $\lg \kappa_4 < 0$ ) chemical interactions.

At a strong chemical interaction ( $\lg \kappa_4 \geq 0$ ) a logarithmic co-ordinate system  $\lg[\kappa_4 \cdot I] - \lg z$  is suitable for better presentation of the results. The numerical results indicate, that the effect of  $X_N$  and  $Y_N$  on  $\varphi_4$  is weak and monotonous. The plots of  $\lg[\varphi_4]$  at fixed values of  $Y_N$  are shown on Fig. 4.46. From the qualitative point of view, the behaviour is like that observed in the first and the third quadrants. During the initial chemosorption interval ( $c_s \ll l, c_{ls} = 1$ ) the objective functions  $\varphi_4(z)$  are linear with respect to the time co-ordinate  $z$ . In that area:

$$I = P_l \tau_l = \kappa_4 \tau^* \text{ or } \varphi_4 = z.$$

If  $\lg z \geq \lg \frac{P_l^2}{(\varepsilon N)^2} = 2 \lg \kappa_4$ , then  $\varphi_4 \Rightarrow \kappa_4$ , because at  $\tau_2 \geq \frac{l}{(\varepsilon N)^2}$  the flux  $I \rightarrow I$  (4.317).

The decrease of  $z$  leads to  $\varphi_4 \rightarrow \Sigma_p(Y_N, z)$ . Thus, in accordance with the general theory it approaches the approximation (4.325) corresponding to the case of boundary layers in both phases. The value  $z^*$ , at which the transition occurs, increases monotonically with the increase of  $\kappa_4$ . Hence, under sufficiently intensive chemical interactions ( $\lg \kappa_4 \geq 1$ ) the

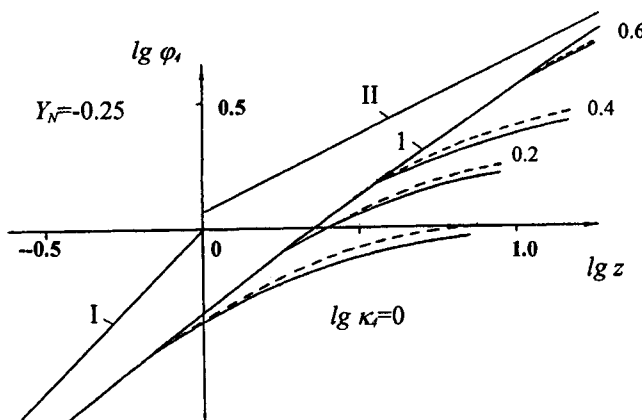


Fig. 4.46. Solution  $\varphi_4(X_N, Y_N, z)$  on the horizontal line  $Y_N = -0.25$ . Solid curves -  $\varphi_4(0, -0.25, z)$ ; dashed curves -  $\varphi_{4Y}; 1$  -  $I_p(-0.25, z)$ ; lines I and II - asymptotic relationships (4.247).

equality  $\varphi_4 = \sum_p$  is valid at  $\lg z \leq 1.5$ . Further, at  $\lg z > 1.5$  the flux is  $\sum_p = 2\sqrt{\frac{z}{\pi}}$ .

The numerical results show that the effect of  $Y_N$  on the solution exists at  $Y_N \geq -1$  only (Figs. 4.46-4.48). In the area  $Y_N \leq -1$  the objective function is independent of  $Y_N$ , so it is a two-parametric function ( $\kappa_4$  and  $X_N$  are the parameters)  $\varphi_4 = \varphi_{4X}(z)$  (4.338) (Fig. 4.48).

Figures 4.46-4.48 show that the effect of the parameter  $X_N$  on the solution at  $\lg \kappa_4 > 0$  is significant in the range  $0 < X_N \leq X_{NY}$  only and the approximation (4.311) is valid.

At any fixed  $Y_N$  and  $\kappa_4$  in the area defined by  $X_N \geq X_{NY}$  the objective function becomes independent of  $X_N$  and coincides with the limiting objective function  $\varphi_{4Y}(Y_N, \kappa_4, z)$  (see the problem formulation (4.333) when  $\varepsilon N \rightarrow \infty$ ). The boundaries of the area where  $\varphi_{4Y}$  may be determined (i.e.  $X_{NY}$ ) depend mainly on the chemosorption parameter  $\kappa_4$  (see Fig. 4.45).

In the general case the decrease of  $\kappa_4$  leads to a smaller area of determination of  $\varphi_{4Y}$ . The maximum difference between  $\varphi_4(\kappa_4, 0, Y_N, z)$  and  $\varphi_4(\kappa_4, X_{NY}, Y_N, z)$  at  $\lg \kappa_4 \geq 0$  does not exceed 10% (Fig. 4.46) because at  $\lg \kappa_4 \geq 0$  in the entire fourth quadrant one may assume that  $\varphi = \varphi_{4Y}$  (Figs. 4.46-4.48). Hence, the effect of  $X_N$  may be neglected ( $X_{NY} = 0$ ).

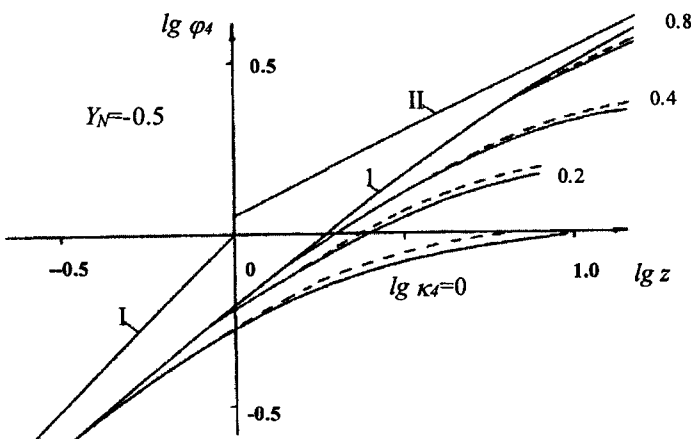


Fig. 4.47. Solution  $\varphi_4(X_N, Y_N, z)$  on the horizontal line  $Y_N = -0.5$ . Solid curves -  $\varphi_4(0, -0.25, z)$ ; dashed curves -  $\varphi_{4Y}(1, -0.25, z)$ ; lines I and II - asymptotic relationships (4.247).

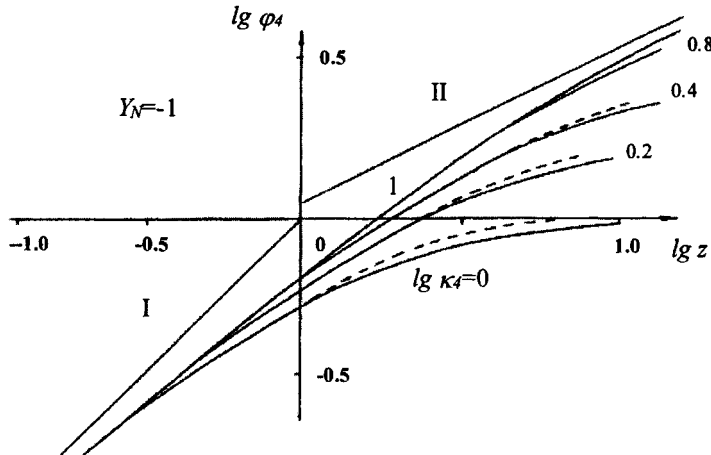


Fig. 4.48. Solution  $\varphi_4(X_N, Y_N, z)$  on the horizontal line  $Y_N = -1$ . Solid curves -  $\varphi_4(0, -0.25, z)$ ; dashed curves -  $\varphi_{4Y}; 1 - I_p(-0.25, z)$ ; lines I and II - asymptotic relationships (4.247).

Weak chemical interactions ( $\lg \kappa_4 < 0$ ). In this case there is no need to calculate the objective function  $I(z)$  because at any point of the fourth quadrant (like in the first) the approximation (4.312) is valid. That approximation is applicable if the substitution  $\lg P_i \rightarrow \lg \kappa_4$  is made. Taking into account the weak effect of  $X_N$  on  $\varphi(1, X_N, Y_N, z)$  one may assume that  $\varphi(1, X_N, Y_N, z) = \varphi_{4Y}(1, Y_N, z)$ . The effect of  $\lg \kappa_4$  on the solution is practically linear and at sufficiently small  $\lg \kappa_4 \leq -1$  the dimensionless flux coincides with the two-parametric function  $I_0(X_N, a, z)$ . In the latter case the area of determination of  $\varphi_{4Y}(z)$  contains the points located on the right side of the vertical line  $X_N = 0.5$  (Fig. 4.25).

In the area  $D$  (the points of the right angle with a vertex at  $D$  (Fig. 4.25)) the solution is independent of the parameters  $X_N$  and  $Y_N$ . It may be obtained by the simplified one-phase problem formulation (4.338) with the substitution  $\varepsilon N = \infty$ . The corresponding objective functions may be determined by the plots on Fig. 4.48 at  $X_N \geq X_{NY}$  ( $\lg \kappa_2 > 0$ ) or by the approximation (4.312) ( $\lg \kappa_2 \leq 0$ ).

The plots on Figs. 4.46-4.48, the limiting functions  $\Sigma_s(\tau_2), I_s(\tau_1)$  and the approximations for  $I_0(X_N, a, z_0)$  (4.284) and  $I(X_N, Y_N, \kappa_2, z)$  ( $\lg \kappa_2 < 0$ ) allow easy determination of the solution of the problem (4.221-4.223) in the fourth quadrant of the plane  $X_N - Y_N$ .

#### 4.3.6. Investigations in the second quadrant on the plane $X_N - Y_N$

In that part of the chemosorption plane the liquid phase capacity is  $\varepsilon N \leq 1$ , so the dimensionless flux  $\Sigma(\tau)$  will be used as a characteristic of the process. In order to determine the controlling parameter  $\kappa_2$ , the objective functions  $\varphi_2(z)$  and the dimensionless time co-ordinates  $z$  the solution of the general problem (4.221-4.223) will be investigated in different areas of the second quadrant.

The solution on the axis  $Y_N \geq 0$ . The positive axis  $Y_N$  belongs simultaneously to the first and the second quadrants (Fig. 4.25). Because of that the solution may be obtained as a particular case of the solution derived in the first quadrant (chapter 4.5) at  $\varepsilon N = 1$ . In the first quadrant the controlling parameter is  $P_1$ , while the dimensionless time co-ordinate is defined by (4.302).

A characteristic feature of the solution in the first quadrant (i.e. on the axis  $Y_N \geq 0$ ) is the monotonous decrease of the concentration  $c_{ls}(z)$  from unity to zero during the two-phase chemosorption interval  $z \sim 1$ . Hence, the maximum absorption regime is established in the system with a mass transfer resistance controlled totally by the gas phase. Outside that range the concentrations  $c_{ls} \rightarrow 0$  and the flux  $\Sigma(\tau)$  may be determined analytically (4.301):

$$\Sigma(\tau) \Rightarrow \frac{I(\tau_1)}{\varepsilon N}, \quad z \gg 1. \quad (4.341)$$

However, on the axis considered the dimensionless flux is  $I(z) = \Sigma(z)$ . Therefore the objective functions (corresponding to the two-phase chemosorption interval) are  $P_1 \Sigma$  (if  $P_1 > 1$ ) and  $\Sigma$  (if  $P_1 < 1$ ). The plots on Figs. 4.42-4.44 and the approximation (4.312) at  $X_N = 0$  ( $a \gg 1$ ) may be used to obtain them.

In accordance with the features of the “splitting” (4.287) the effect of the second chemosorption parameter (Dankohler number  $a$ ) on the objective function exists when the controlling parameter  $P_1$  is sufficiently small  $P_1$  ( $\lg P_1 \leq -1$ ) and  $\Sigma = \Sigma_0(0, a, z)$ . The effect on the axis  $Y_N \geq 0$  may be evaluated if the equation (4.282) is integrated at  $\varepsilon N = 1$  in two limiting cases:  $a \rightarrow 0$  and  $a \rightarrow \infty$ . The result is (see also (4.283)):

$$\Sigma_0(0, a, z) = \begin{cases} \frac{z}{1+z} & \text{at } a \rightarrow \infty; \\ 1 - \frac{1}{(1+z/2)^2} & \text{at } a \rightarrow 0. \end{cases} \quad (4.342)$$

At any  $z$  the difference between the objective functions does not exceed 10%. Therefore the effect of  $a$  on  $\Sigma(z)$  along the axis  $Y_N \geq 0$  is weak.

The solution on the axis  $X_N \leq 0$ . This is a particular case of the solution obtained in the third quadrant at  $Y_N = 0$  (see 4.3.3) because the axis belongs simultaneously to the third and the second quadrants (Fig. 4.25). In the third quadrant  $P_2$  is the controlling parameter, while the dimensionless time co-ordinate  $z$  is defined by (4.266).

A characteristic feature of the solution of (4.221-4.223) in the third quadrant is that the surface concentration  $c_s(z)$  increases monotonously from zero to unity at  $z \sim 1$ . The problem is transformed into one-phase problem at  $z \gg 1$  and when  $c_s = 1$ . The corresponding flux  $\Sigma(\tau)$  is available analytically:

$$\Sigma(z) \Rightarrow \Sigma_s(\tau_2) \equiv 1 - \sum_{n=0}^{\infty} \frac{2}{\pi^2(n+1/2)^2} \exp[-\pi^2(n+1/2)^2 \tau_2]. \quad (4.343)$$

In this case the mass transfer resistance is located in the liquid. The system passes into the instantaneous chemical reaction regime with an absorbent concentration at the interface  $B_s \rightarrow 0$ . Obviously, the feature is an attribute of the process carried out on the axis  $X_N \leq 0$ .

The objective functions  $P_2 \Sigma(z)$  (at  $P_2 > 1$ ) and  $\Sigma(z)$  (at  $P_2 < 1$ ) corresponding to  $z \sim 1$  may be determined by the approximation (4.279) ( $Y_N = 0$ ,  $a \gg 1$ ) and the plots on Fig.4.32.

According to the “splitting” features the Damkohler number effect on the solution occurs at sufficiently small values of the controlling parameter  $P_2$  ( $\lg P_2 \leq -1$ ), so  $\Sigma \Rightarrow \Sigma_0(X_N, a, z)$  (see (4.276)). The effect monotonously increases with the decrease of  $\varepsilon N$ . The substitution  $\varepsilon N = 0$  in (4.235) yields:

$$\Sigma_0(-\infty, a, z) = \begin{cases} 1 - \exp(-z) & \text{at } a \rightarrow 0; \\ 1 - (1-z/2)^2 & \text{at } a \rightarrow \infty. \end{cases} \quad (4.344)$$

The maximal difference between these limiting relationships does not exceed 15%, so it may be assumed the effect of  $a$  on the solution obtained on the axis  $X_N \leq 0$  as insignificant.

The solution of the problem (4.221-4.223) will be investigated in the internal part of the second quadrant under the strong inequalities  $\varepsilon N < 1$ ,  $\varepsilon \beta N > 1$ .

Solution at  $\beta^2 \gg 1$ . This solution corresponds to a solution on a line parallel to  $AC$  (Fig. 4.25). The solution should be considered in three time intervals: 1)  $\tau_2 \ll 1$ ; 2)  $1 \ll \tau_2$ ,  $\tau_1 \ll 1$ ; 3)  $1 \ll \tau_1$ .

In the first case  $\tau_1 \ll \tau_2 \ll 1$  boundary layers exist in both phases. During the initial time interval ( $c_{ls} = 1$ ,  $c_s \ll 1$ ) the concentration distribution is defined by (4.248, 4.249). In the particular case on the surface the concentrations are:

$$\begin{aligned} c_{ls} &= 1 - P_1 \frac{2}{\sqrt{\pi}} \sqrt{\tau_1} = 1 - \frac{2}{\sqrt{\pi}} \sqrt{z}, \\ c_s &= P_2 \frac{2}{\sqrt{\pi}} \sqrt{\tau_2} = \left( \frac{1}{\varepsilon \beta N} \right) \frac{2}{\sqrt{\pi}} \sqrt{z}, \end{aligned} \quad (4.345)$$

where  $z = P_i^2 \tau_i$ . Taking into account that in the general case  $c_{ls} \leq 1$  one may assume that at  $z \gg 1$  the surface concentration  $c_{ls} \rightarrow 0$ . Therefore the solution of (4.221-4.223) exists in the form (4.292). The concentrations on the interface are:

$$c_{ls} = 0, \quad c_s = \frac{I}{\varepsilon \beta N} \quad z \gg 1. \quad (4.346)$$

The relationships (4.292) and (4.346) are not asymptotic, because they are valid in the restricted time interval  $\tau_2 \leq I$  only.

In the second case ( $I \ll \tau_2$ ,  $\tau_1 \ll I$ ), the diffusion layer in the liquid covers the entire phase and  $c = c_s(\tau)$ . The relationships (4.292, 4.346) are not valid in this case for the liquid phase, while the corresponding relationships for the gas phase remain unchanged. The corresponding solution for the liquid phase is available by the mass balance equation (4.224):

$$c = \left( \frac{I}{\varepsilon N} \right) \frac{2}{\sqrt{\pi}} \sqrt{\tau_1}. \quad (4.347)$$

It follows from (4.346-4.347) that the concentration  $c$  corresponding to the time interval  $I \leq \tau_2$ ,  $\tau_1 \leq (\varepsilon N)^2 < I$  increases from an intermediate value of  $\frac{I}{\varepsilon \beta N} < 1$  up to unity (i.e. the saturation point). The time interval  $(\varepsilon N)^2 < \tau_1$  corresponds to a completely saturated liquid phase ( $\Sigma = I$ ). The concentration distribution is available by the one-phase simplified problem formulation

$$\frac{\partial c_1}{\partial \tau_1} = \frac{\partial^2 c_1}{\partial y_1^2}, \quad 1 - \int_0^1 c_1 dy_1 = \varepsilon N. \quad (4.348)$$

It is easy to demonstrate that the solution of (4.348) at  $\tau_1 \ll I$  may be expressed as:

$$1 - c_1 = (\varepsilon N) \frac{1}{\sqrt{\pi}} \frac{\exp(-\eta_1^2 / 4)}{\sqrt{\tau_1}}, \quad c_{ls} = 1 - \frac{\varepsilon N}{\sqrt{\tau_1}}. \quad (4.349)$$

In the third case the boundary layer in the gas phase covers the entire phase and the solution of the problem (4.348) is trivial:

$$c_1 = 1 - \varepsilon N. \quad (4.350)$$

The sufficient conditions needed to permit the application of the approximations (4.345-4.350) are of special interest. The transition into the maximum absorption regime ( $\Sigma \rightarrow \frac{I_1}{\varepsilon N}$ ) occurs at  $z \approx I$  ( $\tau_1 \approx I / P_i^2$ ), while the maximum saturation regime  $\Sigma \rightarrow I$  is

available at  $\tau_1 \approx (\varepsilon N)^2$  (4.348). Therefore, the condition that assures the transition into the maximum absorption regime is defined by the inequality

$$\frac{I}{P_1^2} \leq (\varepsilon N)^2 \quad \text{or} \quad \kappa_2 \equiv P_1(\varepsilon N) = P_2(\varepsilon \beta N)^2 \geq 1, \quad (4.351)$$

where the parameter  $\kappa_2$  is defined by:

$$\kappa_2 \equiv P_1(\varepsilon N) = P_2(\varepsilon \beta N)^2. \quad (4.352)$$

At sufficiently high  $\kappa_2$ , the system passes into the former regime ( $\tau_1 \ll \tau_2 \ll 1$ ) and the two-phase chemosorption problem (4.221-4.223) is transformed into the simplified problem formulation (4.288-4.289). The solution of the latter is the dimensionless flux  $I_p \equiv P_1 I(z)$  (i.e.  $\Sigma(z)$  at sufficiently high  $\kappa_2$ ):

$$\Sigma(z) = \frac{I}{\varepsilon N} = \frac{I_p}{(P_1 \varepsilon N)} = \frac{I_p}{\kappa_2}$$

or

$$\kappa_2 \Sigma(z) = I_p(Y_N, z) \quad \kappa_2 \gg 1. \quad (4.353)$$

Hence, at high  $\kappa_2$ , the functions  $\kappa_2 \Sigma(z)$  depend on  $Y_N$  and coincide with the relationships on Fig. 4.38.

The solution of (4.221-4.223) on the lines  $\beta^2 \gg 1$  where the opposite condition ( $\kappa_2 \ll 1$ ) is satisfied needs the consideration of the situations in the cases 2 and 3 only, because at  $z \sim 1$   $(\varepsilon N)^2 \ll \tau_1$  or  $1 < (\varepsilon \beta N)^2 \ll \tau_2$ . Thus, it may be assumed that when the two-phase chemosorption occurs the boundary layer in the liquid covers the entire phase and  $c = \Sigma(\tau)$ . The concentration at  $z \ll 1$  is defined by the relationships (4.248, 4.345). If one assume  $\tau_1 < 1$  (case 2), a dimensionless co-ordinate  $z = P_2 \tau_2$  should be introduced. The corresponding concentration distribution is:

$$\Sigma = c_s = z, \quad c_{ls} = 1 - \sqrt{\kappa_2} \sqrt{\frac{z}{\pi}}. \quad (4.354)$$

Obviously, at  $z > 1$  the liquid phase is saturated ( $\Sigma \rightarrow 1$ ). This allows the employment of the simplified one-phase formulation (4.348) for concentration distribution in the gas phase at  $z > 1$ . The particular case considering the points of the interface (4.349, 4.350) gives the following concentration distributions:

$$c_{ls} = \begin{cases} 1 - \frac{\sqrt{\kappa_2}}{\sqrt{\pi z}}, & I \ll z, \quad \tau_i \ll I; \\ 1 - \varepsilon N, & I \ll \tau_i. \end{cases} \quad (4.355)$$

The relationships (4.354) and (4.355) indicate that the curve  $c_{ls}(z)$  has a minimum  $c_{ls}^{\min} = 1 - \sqrt{\kappa_2} > 0$  at  $z \sim 1$ . The inequality means that under weak chemical interactions ( $\sqrt{\kappa_2} < 1$ ) the maximum absorption regime ( $c_{ls} = 0$ ) is impossible. Moreover,  $(1 - \varepsilon N)$  is asymptotic value of  $c_{ls}$ , while at  $\kappa_2 > 1$  the minimum value is  $c_{ls}^{\min} = 0$  (4.346). Hence, it may be assumed that the condition  $\sqrt{\kappa_2} > \varepsilon N$  is enough for the existence of a minimum on the curve  $c_{ls}(z)$ . If the opposite condition ( $\sqrt{\kappa_2} < \varepsilon N$ ) is satisfied the minimum is not available and the function  $c_{ls}(z)$  decreases monotonously with  $z$ . In the latter case the boundary layers at  $z \sim 1$  cover the entire phases (case 3,  $\tau_i > I$ ). Therefore the flux is  $\Sigma = \Sigma_0(X_N, a, z)$  (4.235) and the solution is:

$$c_i = 1 - (\varepsilon N) \Sigma_0(z), \quad c = \Sigma_0(z). \quad (4.356)$$

It should be mentioned that at  $\kappa_2 \ll I$  the equality  $\Sigma = \Sigma_0(z)$  is valid despite the behaviour of the curve  $c_{ls}(z)$  (the existence of a minimum or not).

Choice of the controlling parameter and the objective functions in the second quadrant. This problem calls for a special discussion. First of all, the dimensionless time co-ordinate  $z$  and the objective functions  $\varphi_2(z)$  should be defined at any values of the chemosorption parameters. The experience from the previous problem considered allows the following definitions:

$$\varphi_2(z) \equiv \begin{cases} \kappa_2 \Sigma(z) & \text{at } \kappa_2 \geq I; \\ \Sigma(z) & \text{at } \kappa_2 < I; \end{cases} \quad (4.357)$$

$$z \equiv \begin{cases} P_i^2 \tau_i & \text{at } \kappa_2 \geq I, \\ P_2 \tau_2 & \text{at } \kappa_2 < I \end{cases} = \begin{cases} \kappa_2^2 \tau^* & \text{at } \kappa_2 \geq I, \\ \kappa_2 \tau^* & \text{at } \kappa_2 < I \end{cases}. \quad (4.358)$$

The dimensionless time co-ordinates  $\tau^*$  and  $\tau_i$  are related by:

$$\tau^* = \frac{\tau_i}{(\varepsilon N)^2} = \frac{\tau_2}{(\varepsilon \beta N)^2}. \quad (4.359)$$

It is easy to prove that on the axis  $X_N \leq 0$ , where  $\varepsilon \beta N = I$ , the conditions  $\kappa_3 = \kappa_2 = P_2$ ,  $\tau^* = \tau_2$  and  $\varphi_2(z) = \varphi_3(z)$  are satisfied. The time co-ordinates  $z$  defined in the second quadrant by (4.358) coincide on the above axes with the corresponding definitions

for the first (4.302) and the third (4.266) quadrants. Thus, on the boundaries of the second quadrant all the dimensionless variables defined for all internal points coincide with the corresponding variables defined for the adjacent quadrants.

The parameter  $\kappa_2$  has all the attributes of a controlling parameter in the entire area considered. Therefore, taking into account all the specific conditions in the second quadrant the two-phase chemosorption problem (4.221-4.223) may be formulated as ( $a \gg 1$ ):

$$\frac{\partial \Delta_l}{\partial \tau^*} = \frac{\partial^2 \Delta_l}{\partial y_l^{*2}}, \quad \frac{1}{(\varepsilon \beta N)^2} \frac{\partial c}{\partial \tau^*} = \frac{\partial^2 c}{\partial y_l^2}; \quad (4.360)$$

$$\begin{aligned} \left( \frac{\partial c}{\partial y_2} \right)_s &= \frac{\kappa_2}{(\varepsilon \beta N)^2} \sqrt{1 - c_s} (1 - \Delta_{ls}), \\ \left( \frac{\partial \Delta_l}{\partial y_l^*} \right)_s &= \kappa_2 \sqrt{1 - c_s} (1 - \Delta_{ls}); \end{aligned} \quad (4.361)$$

$$\begin{aligned} \left( \frac{\partial \Delta_l}{\partial y_l^*} \right) &= 0 \quad \text{at} \quad y_l^* = \frac{1}{\varepsilon N}; \\ \left( \frac{\partial c}{\partial y_2} \right) &= 0 \quad \text{at} \quad y_2 = 0; \end{aligned} \quad (4.362)$$

$$c = \Delta_l = 0 \quad \text{at} \quad \tau^* = 0. \quad (4.363)$$

where  $y_l^* = \frac{(1 - y_l)}{\varepsilon N}$  is a transversal co-ordinate in the gas phase, while  $\Delta_l = 1 - c_l$  is a dimensionless function.

The dimensionless flux  $\Sigma(\tau^*)$  is:

$$\Sigma(z) = \frac{I}{\varepsilon N} = \int_0^{\frac{1}{\varepsilon N}} \Delta_l dy_l^*. \quad (4.364)$$

The problem (4.360-4.363) is an analogue of the dimensionless three-parametric formulation (4.237-4.238), and

$$\varphi_2(z) = \varphi_2(X_N, Y_N, \kappa_2, z). \quad (4.365)$$

At sufficiently high values of the controlling parameter  $\kappa_2$ , the objective functions  $\varphi_2(z)$  become one-parametric  $\varphi_2(z) \Rightarrow I_p(Y_N, z)$  (4.353). In this case in the chemosorption interval the boundary layers exist in both phases. With the help of the transversal co-ordinates  $y_{1p}$  and  $y_{2p}$  (see also. (4.288)):

$$y_{1,p} = \kappa_2 y_i^* = P_i(1 - y_i), \quad y_{2,p} = \left( \frac{\kappa_2}{\varepsilon \beta N} \right) (1 - y_2) = \frac{P_i}{\beta} (1 - y_2),$$

the problem is transformed into a two-phase one-parametric formulation (4.289) as well as in the formulation (4.353) because  $\kappa_2 \Sigma \equiv P_i I$ .

At sufficiently small  $\kappa_2$  the diffusion boundary layers cover the entire phases and the relationships (4.234) are valid. The integration of any of the transport equations (4.360) along a transversal co-ordinate (under the boundary condition at the interface (4.361)) yields in an ordinary differential equation (4.235) at  $a \gg 1$  (see also (4.236)).

Therefore,

$$\varphi_2 \Rightarrow \Sigma_0(X_N, a, z_0), \quad (4.366)$$

where  $z_0 = \kappa_2 \tau^* = P_2 \tau_2$ . The latter means that at  $\kappa_2 \ll 1$  the objective function depends on two parameters ( $X_N$  and  $a$ ) and the approximation (4.276) is valid.

In the second quadrant of  $X_N - Y_N$  plane the solution of the general problem (4.221-4.223) "splits" and when  $\kappa_2 \geq \kappa_2^*$  it coincides with the solution of the three-parametric problem (4.360-4.363), i.e. the formula (4.365) is valid. On the other hand, at  $\kappa_2 \leq \kappa_2^*$  the approximation (4.366) (i.e. the approximating relationship (4.276)) is applicable. The limiting value  $\kappa_2^*$  must satisfy the condition  $\kappa_2^* \ll 1$ , i.e. it must depend weakly on the location of the point  $X_N, Y_N$  on the plane  $X_N - Y_N$  (Fig. 4.25). The numerical calculations indicate that it must be accepted as a constant in the entire second quadrant.

There are two areas of the second quadrant where the solution of the three-parametric problem (4.360-4.363) becomes simpler and depends on one parameter ( $X_N$  or  $Y_N$ ) only. In these areas the capacity of the liquid phase holds two extreme values – low capacity  $\varepsilon N$  and high capacity  $\varepsilon \beta N$ .

Particular solutions considering points of the area outside the chemosorption square. The solutions at small  $\varepsilon N$  ( $\varepsilon N \ll 1$ ) belong to the area of Fig. 4.25 where the condition  $\beta^2 \gg 1$  is satisfied. Therefore, it may be suggested that in the gas phase there is a boundary layer of the soluble component and it may be assumed that  $\frac{b_i^2}{D_i} \rightarrow \infty$ . The substitution of the boundary condition  $\left( \frac{\partial \Delta_i}{\partial y_i^*} \right)_s = 0$  (at  $y_i^* = \frac{1}{N}$ ) by  $\left( \frac{\partial \Delta_i}{\partial y_i^*} \right)_s = 0$  (at  $y_i^* = \infty$ ) in the dimensionless equations (4.340-4.343) yields the dimensionless problem formulation of that particular case. The dimensionless flux  $\Sigma_y(z)$ , is (see also (4.364)):

$$\Sigma_y(z) = \int_0^\infty \Delta_i dy_i^*. \quad (4.367)$$

The objective function  $\varphi_{2Y}(z)$  depends on two parameters ( $Y_N$  and  $\kappa_2$ ). The small  $\kappa_2$  lead to the simpler case  $\varphi_{2Y} \Rightarrow 1 - (1 - z/2)^2$  (see (4.334)). On the other hand the large  $\kappa_2$  give  $\varphi_{2Y} \Rightarrow I_p(Y_N, z)$  (4.353). The area of determination of  $\varphi_{2Y}(z)$  may be found by numerical calculations only. Further, it will be demonstrated that the boundaries of that area depend on the parameter  $\kappa_2$ .

The higher values of  $\varepsilon\beta N$  lead to a simplification of the transport equation of the liquid phase (4.340) because at  $\varepsilon\beta N \Rightarrow \infty$  the yield is  $\frac{\partial^2 c}{\partial y_2^2} = 0$ . Therefore the variations of the concentration  $c$  along the transversal direction may be neglected ( $c = c_s(\tau)$ ). Hence, the problem (4.360-4.363) becomes simpler (one-phase problem):

$$\begin{aligned}\frac{\partial \Delta_l}{\partial \tau^*} &= \frac{\partial^2 \Delta_l}{\partial y_l^{*2}}; \\ \left( \frac{\partial \Delta_l}{\partial y_l^*} \right)_s &= \kappa_2 \sqrt{1 - \sum} (1 - \Delta_{ls}); \\ \left( \frac{\partial \Delta_l}{\partial y_l^*} \right) &= 0 \quad \text{at } y_l^* = \frac{l}{\varepsilon N}; \\ \Delta_l &= 0 \quad \text{at } \tau^* = 0,\end{aligned}\tag{4.368}$$

where the dimensionless flux  $\Sigma$  is defined by (4.364) because  $c_s(\tau) = \Sigma(\tau)$ .

Like in the situations discussed earlier (the solution in the first quadrant) the dimensionless flux  $\Sigma_x$  at ( $\varepsilon\beta N \rightarrow \infty$ ) will be expressed as  $\Sigma_x$  ( $\varphi_{2X}(z)$ ). The problem formulation (4.368) shows that these functions depend on  $X_N$  and  $\kappa_2$  only, i.e.  $\varphi_{2X} = \varphi_{2X}(X_N, \kappa_2, z)$ . In the particular case of  $\kappa_2 \gg 1$  the objective function is  $\varphi_{2X} \Rightarrow I_p(+\infty, z)$  (see Fig. 4.38). In the other limiting case of  $\kappa_2 \ll 1$  the function  $\varphi_{2X}$  is determined by (4.236).

The analysis performed above shows that the dimensionless complex  $\kappa_2$  (4.351) is a controlling parameter in the second quadrant. It controls the regimes of absorption available in the two-phase system. The effect of the Damkohler number is weak and it may be considered when the weak chemical interactions take place (small  $\kappa_2$ ). In this case the process is kinetics-controlled and its rate remains constant across the entire liquid layer. Outside the two-phase chemosorption interval ( $z \gg 1$ ) there is no need to solve the equations (4.221-4.223) numerically, because the dimensionless flux  $\Sigma(\tau)$  is available analytically.

Under strong chemical interactions ( $\kappa_2 \gg 1$ ) and at  $z \gg 1$  the system passes into the maximum absorption regime. Taking into account that during the two-phase chemosorption interval the liquid saturation is not reached ( $\Sigma \ll 1$ ) it may be suggested that the main part of the saturation occurs outside of that time interval. Moreover, it may be assumed that the

condition  $c_{ls} = 0$  is satisfied at any  $\tau$ . On the other hand, under weak chemical reactions ( $\kappa_2 \ll 1$ ) the liquid saturation occurs during the two-phase chemosorption interval.

In the general case one may assume that at any  $\kappa_2$ ,

$$\Sigma \Rightarrow \min \left\{ \frac{I_l(\tau_1)}{\varepsilon N}, \Sigma_s(\tau_2) \right\} \quad \text{at } z \gg 1. \quad (4.369)$$

In the particular case existing on the boundary between the second and the first quadrants ( $X_N = 0$ ) the inequality  $\Sigma_s(\tau_2) \geq \frac{I_l(\tau_1)}{\varepsilon N}$  is satisfied inspite of  $\kappa_2$ . Hence, the condition (4.369) becomes simpler  $\Sigma \Rightarrow \frac{I_l}{\varepsilon N}$ . In the other case (on the boundary between the second and the third quadrants), where  $\Sigma_s \leq \frac{I_l}{\varepsilon N}$  the condition (4.369) is  $\Sigma \Rightarrow \Sigma_s(\tau_2)$ .

In the second quadrant (like in the fourth one) the transitions into the maximum absorption regime or into the instantaneous chemical reaction regime depend on the value of  $\kappa_2$ . The numerical calculations indicate that at  $\kappa_2 \geq 1$  the system passes into the maximum absorption regime.

The numerical investigation of the three-parametric problem in the second quadrant will be performed below in the several limiting cases.

Figures 4.49-4.50 show the numerical results of the family of objective functions  $\varphi_2(z)$  ( $\kappa_2$  is the family parameter) under weak chemical interactions ( $\lg \kappa_2 \geq 0$ ). The investigations were carried out for fixed  $Y_N$  and a variable parameter  $X_N$ . The solid lines correspond to  $X_N = 0$ , while the dashed ones to the case  $X_N \leq X_{NY}$ . The relationship  $X_{NY}(\kappa_2)$  is shown on Fig. 4.45. At fixed  $Y_N$ ,  $\kappa_2$  the effect of  $X_N$  on  $\varphi_2(z)$  is monotonous and occurs in a narrow range  $X_{NY} \leq X_N \leq 0$ . For  $X_N \leq X_{NY}$  the objective functions do not depend on the parameter  $X_N$ . Moreover, they coincide with  $\varphi_{2Y}(Y_N, \kappa_2, z)$  and as well as Figs. 4.49-4.50. In the initial chemosorption interval ( $c_s \ll 1$ ,  $c_{sl} = 1$ ) all the functions  $\varphi_2(z)$  approach asymptotically a linear relationship (the inclined lines on Figs. 4.49-4.50) (see also (4.268)):

$$\Sigma = P_2 \tau_2 = \kappa_2 \tau^* \quad \text{or} \quad \varphi_2 = z. \quad (4.370)$$

For high  $z$  the function  $\lg \varphi_2 \rightarrow \lg \kappa_2$ . The latter transition occurs at  $\lg z \geq 2 \lg \kappa_2$  because at  $\tau_1 \geq (\varepsilon N)^2$  the flux  $\Sigma \Rightarrow 1$ . At fixed  $X_N, Y_N, \kappa_2$  there is a value  $z^*$  ( $z \leq z^*$ ) assuring that the objective functions  $\varphi_2 \rightarrow I_p(Y_N, z)$  (see (4.353)). The value of  $z^*$  depends mainly on  $\kappa_2$  (increases monotonously with the increase of  $\kappa_2$ ).

Under conditions of intensive chemical interactions ( $\lg \kappa_2 \geq 0.8$ ) the approximation (4.353) is applicable at  $\lg z \leq 1.2$  because  $\lg z^* > 1.2$ . At higher  $z$  ( $\lg z > 1.2$ ) the limiting

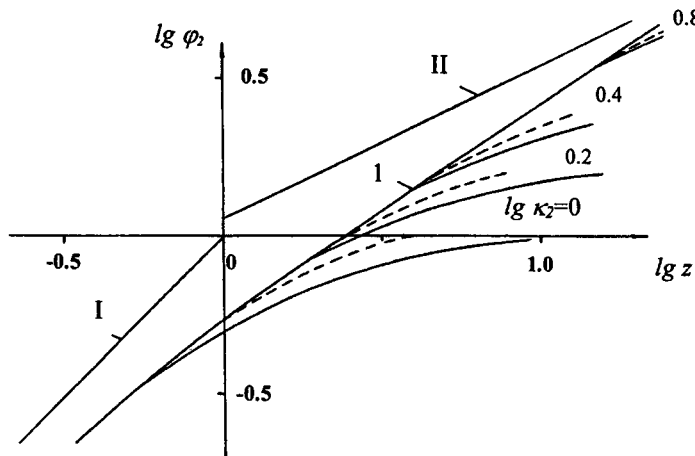


Fig. 4.49. Solution  $\varphi_2(X_N, Y_N, z)$  on the horizontal line  $Y_N = 0.25$ . Solid curves -  $\varphi_2(0, 0.25, z)$ ; dashed curves -  $\varphi_{2y}$ ; 1) -  $I_p(0.25, z)$ ; I and II - asymptotic relationships (4.293).

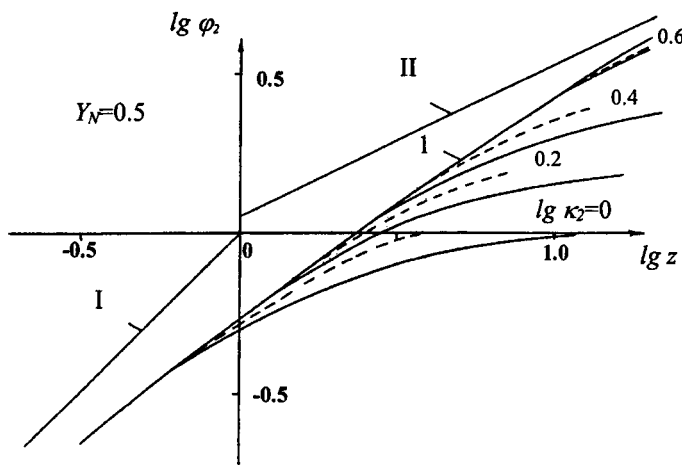


Fig. 4.50. Solution  $\varphi_2(X_N, Y_N, z)$  on the horizontal line  $Y_N = 0.5$ . Solid curves -  $\varphi_2(0, 0.25, z)$ ; dashed curves -  $\varphi_{2y}$ ; 1) -  $I_p(0.25, z)$ ; I and II - asymptotic relationships (4.293).

function is  $I_p \rightarrow 2\sqrt{\frac{z}{\pi}}$  (the inclined line I on Fig. 4.49-4.50).

In the second quadrant the effect of  $Y_N$  on  $\varphi_2(z)$  at  $\lg \kappa_2 \geq 0$  occurs only below the horizontal line  $Y_N = 0.5$  (Fig. 4.25). In the half-plane above ( $Y_N \geq 0.5$ ) the plots on Fig. 4.50 may be used because in that area  $\Sigma = \Sigma_{2X}$  (in accordance with the simplified one-phase formulation 4.368).

Weak chemical interactions ( $\lg \kappa_2 < 0$ ). The small  $\kappa_2$  allows the dimensionless flux  $\varphi_2(z)$  to be determined analytically by the approximation (4.279) (with a substitution  $\kappa_3 \Rightarrow \kappa_2$ ) that eliminates the numerical calculations. At  $\lg \kappa_2 \leq -1$  in the entire second quadrant the approximation:

$$\Sigma(X_N, Y_N, \kappa_2, z) \approx \Sigma_0(X_N, \infty, z), \quad a \gg 1 \quad (4.371)$$

is valid.

Further, the decrease of the Damkohler number permits the employment of the approximation (4.276) (where  $\Sigma_0(X_N, 0, z_0)$  is determined by (4.273)).

In the upper left corner of the plane  $X_N - Y_N$  the functions  $\Sigma_X$  and  $\lg \Sigma$  coincide at any  $\kappa_2$  because this is a common area of the sets ( $Y_N \geq 0.5, X_N \leq -1$ ). They may be obtained by the one-phase problem formulation (4.368) (one-parametric problem with a substitution  $\frac{1}{\varepsilon N} = \infty$ .

When  $\lg \kappa_2 > 0$  the curves plotted on Fig. 4.50 at  $X_N \leq X_{Ny}$  (weak chemical interactions ( $\lg \kappa_2 < 0$ )) represent the approximations (4.279).

The plots on Figs. 4.49-4.50 and the approximations for  $\Sigma_0(X_N, a, z_0)$  (4.276) (and  $\Sigma(X_N, Y_N, \kappa_2, z)$  at  $\lg \kappa_2 \leq 0$  respectively) as well as the limiting functions  $\Sigma_s(\tau_2), I_s(\tau_1)$  permit the solution of (4.221-4.223) to be obtained at any values of the parameters in the entire second quadrant of the plane  $X_N - Y_N$ .

#### 4.3.7. Analysis of the basis relations of the two-phase absorption

It was commented in chapter 4.2 that the effect of the chemical reaction on the two-phase absorption may be significant from a practical point of view in the third quadrant of the absorption plane  $X - Y$  (Fig. 4.2). The area  $D$  where the mass transfer resistance is located in the liquid phase only ( $X \leq -1, Y \leq -1$ ) is of a special interest. In that area the difference between  $I^{act}$  and  $I^{max}$  is significant at any  $\tau$  in contrast to the other parts of  $X - Y$  plane. The latter indicates that a significant augmentation of the mass transfer (see 4.2.6) is available when chemical sorbents are used for absorption of low-soluble gases as  $\text{CO}_2, \text{O}_2, \text{N}_2, \text{He}$  (see 4.1.11).

At high values of  $N$  the second order kinetics must be taken into account (i.e. the variations of the chemical sorbent concentration with time) at sufficiently high values of the

time co-ordinate ( $z_a \gg I$ ). However, during this time interval the transport equations in both phases become similar to those of the two-phase physical absorption. Despite the similarity of the equations it should be taken into account that in the liquid phase there is a component  $A$  which is not in a dissolved state ( $c_2$ ) but it is in the chemical compounded state ( $c$ ). In this case the liquid phase capacity (with respect to the component  $A$ ) increases significantly. The latter is attributed to the fact that in the mass balance equation (4.224) there is a parameter  $\varepsilon N$  instead the parameter  $\varepsilon$  in (4.372). The parameter  $\varepsilon N$  may be expressed as:

$$\varepsilon N = k \frac{b_2}{b_1} \frac{N'}{qkc_0} = \left( \frac{N'_0}{qc_0} \right) \frac{b_2}{b_1},$$

where  $q$  is a coefficient of the order of unity.

The comparison of the above expression with  $\varepsilon$  indicates that the distribution coefficient during a chemosorption  $\left( \frac{N'_0}{qc_0} \right)$  is significantly greater than the corresponding coefficient  $k$  ( $k \leq 1$ ) in the case of low-soluble gases. This is the reason for the significantly high mass transfer rates during a chemosorption.

The dimensionless fluxes in the gas phase ( $I = I - \bar{c}_1$ ) and in the liquid phase ( $\Sigma = \bar{c}$ ) (see (4.224)) is investigated by logarithmic co-ordinates in the plane  $X_N - Y_N$  (by the substitutions  $X_N = \lg(\varepsilon N)$ ,  $Y_N = \lg(\varepsilon \beta N)$ ) like in the case of physical absorption (4.183-4.185). The location of both the absorption ( $X - Y$ ) and the chemosorption ( $X_N - Y_N$ ) planes are shown on Fig. 4.25 for high values of  $N$ .

It is easy to defined that the chemosorption square  $ABCD$  is totally located in the lower left corner of the  $X - Y$  plane, i.e. where the mass transfer resistance is located in the liquid phase only ( $X \leq -I$ ,  $Y \leq -\Sigma$ ). All the investigations on the two-phase chemosorption were carried out in that area (see 4.2.4 - 4.2.7).

Like in the case of a physical absorption at any point  $X_N, Y_N$  the greater of both dimensionless fluxes was chosen for the solution. In the right half-plane ( $X_N > 0$ ) the dimensionless flux is  $I(\tau)$ , while in left half-plane ( $X_N < 0$ ) the flux is  $\Sigma(\tau)$  (see (4.224)).

At  $\tau \rightarrow \infty$  the greater flux approaches the unity. The time corresponding to the point where the difference between  $I$  (or  $\Sigma$ ) and its equilibrium value is negligible (5% accuracy is enough) is termed the saturation period (or the saturation time)  $\tau_\infty$ .

Under chemosorption there are three characteristic time intervals. The first interval is the so-called "initial interval". The second one is the "two-phase chemosorption interval", while the last one is the interval of the instantaneous chemical reaction (or of the maximum absorption regime). Each of them will be discussed separately.

During the initial chemosorption interval the concentrations of the component  $A$  in the gas  $c_0$  and that of the chemical sorbent in the liquid  $N'_0$  remain constant. The corresponding dimensionless fluxes ( $I$  or  $\Sigma$ ) are linear functions of the time:

$$I = P_1 \tau_1, \quad \Sigma = P_2 \tau_2, \quad z_a \geq 1.$$

In a dimensionless form all these conditions may be expressed as:

$$c_{ls} = 1, \quad c_s = 0, \quad \varphi(z) = z, \quad z_a \geq 1.$$

In this case the chemosorption resistance is in the liquid phase. The concentration of the product  $C$  at the interface and in the bulk of the liquid is far from the saturation point. The absorption of  $A$  occurs as a fast chemical reaction and all the amount of  $A$  is transformed in a chemical compound. From a mathematical point of view the latter means that the time-dependent term of the transport equation for  $A$  (4.175) may be omitted.

By the help of the universal time co-ordinate  $z$  the initial interval is represented always by a value  $z \ll 1$  irrespective of  $X_N, Y_N$  and  $\kappa$  (see the calculation of the objective functions  $\varphi(z)$ ). Moreover, the component  $A$  interacts with the chemical sorbent, but not with the solvent in the liquid phase. Because of that the first order chemical reaction (chapter 4.2) is considered as a particular case of the chemosorption with a second order chemical reaction. The latter assumption considers that during the whole process the concentration of the chemical sorbent is constant ( $N' = N'_0$ ). Hence, the rate constant  $\bar{k}_1$  (see the transport equations 4.101-4.102) is an apparent rate constant of a chemical reaction of pseudo-first order related to  $\bar{k}_2$  (4.175) by the relationship  $\bar{k}_1 = \bar{k}_2 N'_0$ . The sufficient conditions assuring this approximation ( $N' = N'_0$  or  $c_s = 0$ ) are of a significant interest. Moreover, in the initial time interval it is assumed that  $c_s = 0$ , so the interaction between  $A$  and  $B$  occurs as a pseudo-first order chemical reaction.

The second order chemical kinetics dominates at moderate values of  $z \sim 1$ . This corresponds to variations of the chemical sorbent concentration and the diffusion interactions between the phases (the concentration  $c_{ls}$  differs from unity). In fact, in that time interval (defined by  $1 \leq \lg z \leq 1$ ) the solution of (4.183-4.185) may be obtain only numerically.

The formalistic procedure expressing the two-phase chemosorption problem in a dimensionless form shows that the functions  $I(z)$  and  $\Sigma(z)$  depend on four dimensionless parameters.

However, the introduction of the plane  $X_N - Y_N$  (Fig. 4.25) does not facilitate the graphical solution of the problem. The difficulties come from the fact that at a fixed point  $X_N, Y_N$  the functions  $I(z)$  and  $\Sigma(z)$  depend on two chemosorption parameters. However, if one of these parameters is the Damkohler number (while the second is  $\kappa$ ) (see 4.235, 4.282, 4.322, and 4.352) the graphical presentation becomes simpler.

The controlling parameter  $\kappa$  was chosen to satisfy the condition  $\lg \kappa \leq -1$ . Thus, for small  $\kappa$  the two-phase chemosorption problem is transformed in ordinary differential equations ((4.235) or (4.282)):

$$\begin{aligned} \Sigma &= \Sigma_0(X_N, a, z_0) && \text{at } X_N \leq 0; \\ I &= I_0(X_N, a, z_0) && \text{at } X_N > 0. \end{aligned}$$

These relationships may be derived from the approximation (4.276) or (4.284). In this case the chemosorption occurs in a plug flow regime and the concentration distributions along

the co-ordinate  $y$  in both phases may be neglected at any time. Obviously, the latter is related to the intensive diffusion processes in the contracting phases and the low absorption rate.

The dimensionless Damkohler number in (4.376) may vary from zero to large values ( $a \gg 1$ ). When ( $a \gg 1$ ):

$$\begin{aligned}\Sigma_0(X_N, a, z_0) &\Rightarrow \Sigma_0(X_N, \infty, z), \quad X_N \leq 0, \\ I_0(X_N, a, z_0) &\Rightarrow I_0(X_N, \infty, z), \quad X_N > 0\end{aligned}\tag{4.372}$$

and the condition  $\lg \kappa \leq 1$  is always satisfied. Therefore, it may be assumed that the solutions  $\Sigma_0$  and  $I_0$  correspond to the case of weak chemical interceptions (see below).

If the controlling parameter  $\kappa$  satisfies the condition  $\lg \kappa > -1$  the Damkohler number is always greater than unity. Hence, under such  $\kappa$  the general set of equations (4.183-4.185) is enough to investigate the case at  $a \rightarrow \infty$ . In this case

$$\begin{aligned}\Sigma = \Sigma_\infty(X_N, Y_N, \kappa, z) &\equiv \Sigma(X_N, Y_N, \infty, \kappa, z), \quad X_N \leq 0; \\ I = I_\infty(X_N, Y_N, \kappa, z) &\equiv I(X_N, Y_N, \infty, \kappa, z), \quad X_N \geq 0.\end{aligned}\tag{4.373}$$

The functions  $\Sigma_\infty(z)$  and  $I_\infty(z)$  may be presented graphically without problems because at any point of the plane  $X_N - Y_N$  (Fig. 4.17 case c) there is a family of one-parametric curves (with  $\kappa$  as a parameter). The numerical calculations show that when  $\lg \kappa = -1$  the solution of the three-parametric problem (4.373) coincides with (4.372). Hence, the solution  $I_\infty$  (or  $\Sigma_\infty$ ) at  $\lg \kappa = -1$  passes into  $I_0$  (or  $\Sigma_0$ ) without discontinuities.

The “splitting” is a specific feature of the equations (4.221-4.223). Because of that the numerical solutions are enough to carry out at  $a \rightarrow \infty$ , i.e. in the case of the three-parametric problem.

The controlling parameter  $\kappa$  affects significantly the concentration distributions in the contacting phases. Its major effect is on the absorption regime. It is possible to divide the situations into weak chemical interactions for  $\kappa < 1$  ( $\lg \kappa \leq 0$ ) and strong chemical interactions for  $\kappa > 1$  ( $\lg \kappa > 0$ ).

Weak chemical interactions ( $-1 \leq \lg \kappa \leq 0$ ). Under the conditions of a weak chemical interactions ( $\lg \kappa \leq -1$ ) the surface concentrations  $c_{ls}$  and  $c_s$  vary monotonously with time. At  $X_N < 0$  the concentration  $c_s$  changes from zero to unity, while  $c_{ls}$  decreases from unity to its minimum ( $1 - \varepsilon N$ ). In the left half-plane of  $X_N - Y_N$  ( $X_N > 0$ )  $c_s$  increases from zero to

$\frac{1}{\varepsilon N}$ , while  $c_{ls}$  decreases from unity to zero (see (4.234) and (4.281)).

Moreover, in the left half-plane ( $X_N < 0$ ) the increase of  $\kappa$  disturbs the monotonous behaviour of the curve  $c_{ls}(\tau)$  in the area located above the line  $DB$  ( $\beta^2 > 1$ ) and moderate values of  $\varepsilon \beta N$ . However, the behavior of the surface concentration  $c_s(\tau)$  remains monotonous and at  $z \geq 1$ :  $c_s \Rightarrow 1$ ,  $\Sigma \Rightarrow 1$ . The latter indicates that the saturation occurs at  $z = z_\infty \approx 1$  in the two-phase system considered.

In the right half-plane ( $X_N > 0$ ) the increase of  $\kappa$  disturbs the monotonous behaviour of the curve  $c_s(\tau)$ , too. The latter is significant in the area below the line  $DB$  ( $\beta^2 < 1$ ) and moderate values of  $\varepsilon\beta N$ . On the other hand, the surface concentration  $c_{1s}$  decreases monotonously and at  $z > I$ :  $c_{1s} \Rightarrow 0$ ,  $I \Rightarrow 1$ . The complete depletion of the gas phase occurs at  $z = z_\infty \approx I$ .

The solution corresponding to the case of weak chemical interactions depends slightly on  $X_N, Y_N$  and  $\kappa$ . Because of that it may be derived by the approximations (4.279) and (4.312) (with 5% accuracy) at  $X_N < 0$  and  $X_N \geq 0$ , respectively.

Therefore, when weak chemical interactions ( $\lg \kappa < 0$ ) dominate the two-phase chemosorption, the process stops usually at  $z \approx z_\infty \approx I$  and the two-phase chemosorption interval practically coincides with the chemosorption interval  $\tau_\infty$ .

Strong chemical interactions ( $\lg \kappa > 0$ ). In this case the increase of  $\kappa$  leads to new features of the concentration distributions in both phases. They are related to the diffusion interactions between the phases in the two-phase chemosorption interval. The main problem is that the latter time interval  $z \leq I$  does not coincide with the chemosorption interval  $\tau_\infty$ . The effect strongly depends on the location the point  $X_N, Y_N$  (in the upper part  $X_N - Y_N$  or in the lower part ( $Y_N \geq 0$ )).

In the first and the second quadrants  $Y_N \geq 0$  and  $z \leq I$  and the concentration  $c_{1s}$  always decreases from unity to zero. At  $z > I$  the system enters into the maximum absorption regime  $I \Rightarrow I^{max}(\tau_1)$  (4.301). The regime remains in the left half-plane ( $X_N \leq 0$ ) up to the complete saturation by the reaction products  $C$   $\left( \Sigma = \frac{I^{max}}{\varepsilon N} \leq 1 \right)$ . The same regime exists in the right half-plane ( $X_N > 0$ ) down to the complete depletion of the component  $A$  from the gas phase ( $I = I^{max} \leq 1$ ).

In the fourth and the third quadrants ( $Y_N \leq 0$ ) and at ( $z \leq I$ ) (two-phase chemosorption interval) the concentration of the reaction product  $c_s$  always varies from zero to unity. Outside this interval the instantaneous chemical reaction regime occurs (4.252). The regime persists till the end of the process. In the left half-plane ( $X_N - Y_N$  ( $X_N < 0$ )) the yield is  $\Sigma = \Sigma_s(\tau_2) < 1$  while in the right counterpart ( $X_N > 0$ ) the flux is  $I = \varepsilon N \Sigma_s \leq 1$ .

Therefore, under strong chemical interactions the solution of the problem outside the two-phase chemosorption interval becomes simpler. Generally, this is the area defined as  $I \leq z \leq \kappa^2$ . A simpler problem is the one-phase problem formulation. Hence, there is no need to perform numerical calculations in that area.

All the numerical calculations described in 4.2.4 - 4.2.7 were carried out within a restricted time interval  $-I \leq \lg z \leq I$ . The objective function (a dimensionless flux) in the left half-plane ( $X_N \leq 0$ ) is  $\varphi \equiv \kappa \Sigma(z)$  and  $\varphi \equiv \kappa I(z)$  in the right half-plane ( $X_N > 0$ ) respectively. The family of functions  $\varphi(\kappa, z)$  depends slightly on the location of the point  $X_N, Y_N$  in the plane (Fig. 4.17 case c). For small and large values they are practically

independent of these parameters (see for example (4.247)), while at  $z \sim 1$  the value of  $\varphi$  is of the order of unity.

Sufficient conditions for limiting regimes (maximum absorption and the instantaneous chemical reaction). These conditions need a special consideration. It follows from the discussion above that under strong chemical interactions (practically at  $\lg \kappa \geq 1$ ) and  $z \sim 1$  the dimensionless fluxes  $\Sigma$  and  $I$  (i.e.  $\frac{\varphi}{\kappa}$ ) satisfy the condition  $\frac{\varphi}{\kappa} \ll 1$ .

The latter means that the mass transfer becomes significant outside the two-phase chemosorption interval (at  $z \gg 1$ ). However, in this time interval there is no need of numerical calculations because one of the two mentioned limiting regimes exists. Therefore, under strong chemical interactions ( $\kappa \gg 1$ ) in the upper half-plane on Fig. 4.17 case c ( $Y_N \geq 0$ ) it may be assumed that the chemosorption process is in the maximum absorption regime (4.301) at any  $\tau$ . In the opposite half-plane ( $Y_N < 0$ ) the system is in the instantaneous chemical reaction regime (4.252).

Mass transfer resistance located in the liquid phase. In the general case the concentration of the component  $A$  at the interface varies with the time  $c_{ls}(\tau)$ . In the left half-plane ( $X_N < 0$ ) at  $\beta^2 \geq 1$  and ( $z \geq 1$ ) that concentration decreases down to its minimum ( $c_{sl}^{min} < 1$ ). Further then it increases again to its equilibrium value ( $1 - \varepsilon N$ ) at  $\tau \rightarrow \infty$  (see the solution of (4.260-4.262, 4.354-4.355) in 4.2.4 and 4.2.7).

However, the concentration at the interface is usually assumed as a constant  $c_{ls} = 1$ , but this is true when low-soluble gases are absorbed [1, 3, 4, 20]. Because of that three cases may be considered.

1. The surface concentration  $c_{ls}$  one is assumed  $c_{ls} = 1$  in the initial chemosorption interval at  $z \ll 1$  inspite of the value of the chemosorption parameter  $\kappa$  and the position of the point on the plane  $X_N, Y_N$ .
2. There are areas of  $X_N - Y_N$  (Fig. 4.17, case c), where the condition  $c_{ls} = 1$  is valid for particular values of  $\kappa$ . Most of these points belong to the area located to the left of the vertical line  $AD(X_N \leq -1)$ , where  $\kappa \ll 1$ . In these areas the concentration  $c_{ls}$  satisfies the condition  $(1 - \varepsilon N) \leq c_{ls} \leq 1$ , so  $c_{ls} = 1$ . Moreover, in the area located above the horizontal line  $DC(Y_N \leq -1)$  at  $\kappa \gg 1$  and  $z \sim 1$  (more precisely at  $\tau \ll \tau_\infty$ ) it may be assumed that  $c_{ls} = 1$  (see the solutions of (4.317) and (4.257) in 4.2.4 and 4.2.6).
3. In the area  $D$  of the plane  $X_N - Y_N$  (the lower left corner on Fig. 4.17 case c) the condition  $c_{ls} = 1$  is always satisfied irrespective of the parameter  $\kappa$  and the time  $\tau$  (see for example the condition (4.263)). Particularly, in that area the analytical solution in 4.3.2 (at  $a \gg 1$ ,  $\kappa \gg 1$  and short contact time  $\tau_2 \ll 1$ ) was obtained.

Pseudo-first order chemical reactions. It is well known that a second order chemical reaction may be considered as a pseudo-first order reaction if  $c_s(\tau) \approx 0$  (or the concentration of the chemical sorbent is  $N'_0$ ). The surface concentration of the reaction product  $c_s(\tau)$  is a function of the time  $\tau$ . However, there are conditions under which  $c_s(\tau) \equiv 0$ . Three situations will be commented.

1. In the initial chemosorption interval ( $z \ll I$ ) the concentration  $c_s = 0$  inspite of the values of  $X_N, Y_N$  and  $\kappa$  (in accordance with its definition).
2. In some areas of the plane  $X_N - Y_N$  the condition  $c_s = 0$  is satisfied for particular values of  $\kappa$ . For example, in the upper part of  $X_N - Y_N$  ( $Y_N \geq 0.5$ ) and sufficiently high  $\kappa \gg I$  the condition  $c_s = 0$  is satisfied for  $\tau \ll \tau_\infty$ . On the other hand, at the points of the area  $X_N \geq 0.5$  the condition  $c_s = 0$  is satisfied for small  $\kappa \ll I$  (see the solutions (4.294), (4.295-4.297), as well as (4.326-4.327) and (4.329)).
3. In the upper right corner of Fig. 4.17, case a ( $X_N \geq 0.5, Y_N \geq 0.5$ ) is always valid  $c_s(\tau) = 0$  inspite of  $\kappa$  and  $\tau$  (see the condition (4.305)). The solution considering a first order chemical reaction (see 4.2) is applicable in that area of the plane  $X_N - Y_N$  (see the location of both the absorption and the chemosorption squares ABCD on Fig. 4.17, case c). More precisely, this is the area of the pseudo-first order chemical reaction.

Other simplifications of the concentration distributions. Often the solution of particular problems may be obtained under simplifying assumptions considering the concentration distributions in the phases. The simplifications lead to a decreased number of parameters. Moreover, in some specific cases the simplification is the only approach allowing a solution of the problem. However, these simplifications should be made carefully because the equations obtained on that basis should be adequate to the real systems described.

The theoretical analysis and the numerical calculations performed in 4.2.4 - 4.2.7 show that it is enough to consider the two-phase chemosorption in a restricted area of the plane ( $X_N - Y_N$ ) (Fig. 4.17 case c). Outside of that area the solution is simpler at any values of the controlling parameter  $\kappa$  and any type of the chemical interactions. The simpler solution does not depend on  $\kappa, X_N$  or  $Y_N$  and practically coincides with the solution on the boundary of this area (see Fig. 4.13 in chapter 4.2). It is easy to find that all these effects on the solutions are dues to the concentration distributions in the phases.

For example, in the area  $X_N \geq 0.5$  the diffusion boundary layer  $\delta_L$  of the reaction product  $C$  does not cover the entire liquid phase during the chemosorption interval  $\tau \leq \tau_\infty$  (see the problem formulations (4.306-4.308) and (4.333)) in I and IV quadrants - Fig.4.17, case c). The situation is different in the case of weak chemical interactions ( $\kappa \ll 1$ ) only (see the solutions (4.294), (4.295-4.297) and (4.326-4.327)). However, in the latter case the surface concentration  $c_s$  satisfies the condition  $c_s \ll I$  and the concentration distribution does not affect the chemosorption process.

In the area located on the left of the vertical line  $AD$  ( $X_N \leq -I$ ) on Fig. 4.17 (case c) there is a diffusion boundary layer of the component  $A$  in the gas phase during the whole chemosorption interval (see the formulations (4.360-4.363) and (4.271)). The situation differs only when  $\kappa \ll I$  and the surface concentration is  $c_{ls}(\tau) = I$ , i.e. the mass transfer resistance is totally located in the liquid phase. Therefore, the concentration distribution in the gas phase does not affect the mass transfer.

In the upper part of Fig.4.17, case c, (the area ( $Y_N \geq 0.5$ )) the concentration changes in the liquid phase along the transversal co-ordinate may be neglected ( $c_s = \Sigma$ ) (see formulations (4.368) and (4.310)). In a similar way, in the area located below the line

$DC, Y_N \leq -1$ ) it is possible to neglect the variations of the concentration in the gas phase along the same co-ordinate (see the formulations (4.272) and (4.338)).

Outside the chemosorption square in the upper left corner of Fig. 4.17 (case c) where the sets  $Y_N \geq 0.5$  and  $X_N \leq -1$  have a common area the conditions  $c_s = \Sigma$ ,  $\delta_L \ll 1$  are satisfied. The latter is valid under any type of chemical interaction (any  $\kappa$ ) during the whole chemosorption interval ( $\tau \leq \tau_\infty$ )  $c_s = \Sigma$  and  $\delta_L \ll 1$ . In a similar way in the symmetrical area ( $Y_N \leq -1, X_N \geq 0.5$ ) located in the lower right corner of Fig. 4.25  $\tau \leq \tau_\infty$  always applies and it may be assumed that  $c_{1s} = c_1$  and  $\delta_G \ll 1$ .

In the two latter areas the families of the objective functions  $\varphi(\kappa, z)$  are independent of the co-ordinates  $X_N, Y_N$  and coincide with the solutions at the points  $a$  and  $c$  (Fig. 4.25) (see the formulation (4.368) at  $\varepsilon N = 0$  and (4.338) at  $\varepsilon N = \infty$ ).

Finally, it should be mentioned that the choice of the chemosorption parameters  $\kappa$  was made in order to satisfy the condition that the numerical calculations of the objective functions  $\varphi(X_N, Y_N, \kappa, z)$  will correspond to a narrow range of the parameters ( $-1 \leq \lg \kappa \leq 1$ ). Outside that range and under weak chemical interactions ( $\lg \kappa \leq 1$ ) the transverse concentration variations in both phases may be neglected. Moreover, outside the chemosorption square the objective functions  $\varphi(z)$  are independent of the parameter  $Y_N$  and solutions of the ordinary differential equations (4.282) and (4.235) are available. The latter depends on the locations of the point  $X_N, Y_N$ . The corresponding objective functions are:

$$\varphi \Rightarrow \varphi_o = \begin{cases} I_o(X_N, a, z_o) & \text{if } X_N > 0; \\ \Sigma_o(X_N, a, z_o) & \text{if } X_N \leq 0. \end{cases}$$

In the other limiting case ( $\lg \kappa \geq 1$ ) there are two boundary layers in both phases during the whole chemosorption interval. The objective functions  $\varphi(z)$  are independent of the parameter  $X_N$ . The solutions are:

$$\varphi \Rightarrow \varphi_p = \begin{cases} I_p(Y_N, z) & \text{if } Y_N \geq 0; \\ \Sigma_p(Y_N, z) & \text{if } Y_N < 0. \end{cases}$$

It should finally be noted that the controlling chemosorption parameters  $\kappa$ , and the time co-ordinates  $z_i$  depends on the location of the point  $X_N, Y_N$  (in which quadrant it is located) on the plane. Moreover, the co-ordinates  $z_o$  depend on  $X_N$ :

$$z_o = \begin{cases} P_2 \tau_2 & \text{if } X_N \leq 0; \\ P_1 \tau_1 & \text{if } X_N > 0. \end{cases}$$

(see also (4.235) and (4.282)).

It may be decided that the co-ordinates  $X_N, Y_N, \kappa, a, z$  allow the solution of the two-phase chemosorption problem (4.183-4.185) in a wide range of variations of the physical,

chemical and geometrical quantities at any time  $\tau$ . The calculations of these parameters permit the solution of the problems considering various simplifications of concentration distributions.

#### 4.3.8. Applications

Some gases absorbed in a liquid interact chemically with the soluble chemical compounds. These reactions are usually bimolecular because the binary collisions are most probable with respect to the others from the chemical kinetics point of view [35]. In fact, most of the reactions are series of elementary steps. Each of these steps is a second order reversible chemical reaction.

Chemosorption of CO<sub>2</sub>. Consider the well-known process of CO<sub>2</sub> absorption by base solutions (NaOH for example) [35]. Nowadays, it is a well-established fact that the absorption of CO<sub>2</sub> by a liquid is a series of the following elementary reactions:

- a) CO<sub>2</sub> + H<sub>2</sub>O ⇌ H<sub>2</sub>CO<sub>3</sub>      ( $\bar{k}_a \cong 1.6 \times 10^{-2}$  L·mol<sup>-1</sup>·s<sup>-1</sup>,  $K_a \cong 1.5 \times 10^{-3}$  L·mol<sup>-1</sup>);
- b) CO<sub>2</sub> + OH<sup>-</sup> ⇌ HCO<sub>3</sub><sup>-</sup>      ( $\bar{k}_b = 6 \times 10^3$  L·mol<sup>-1</sup>·s<sup>-1</sup>,  $K_b = 6 \times 10^7$  L·mol<sup>-1</sup>);
- 1) H<sub>2</sub>CO<sub>3</sub> = H<sup>+</sup> + HCO<sub>3</sub><sup>-</sup>      ( $K_1 = 2 \times 10^{-4}$  mol·L<sup>-1</sup>);
- 2) HCO<sub>3</sub><sup>-</sup> = H<sup>+</sup> + CO<sub>3</sub><sup>2-</sup>      ( $K_2 = 4 \times 10^{-11}$  mol·L<sup>-1</sup>);
- 3) H<sub>2</sub>O = H<sup>+</sup> + OH<sup>-</sup>      ( $K_w = 0.6 \times 10^{-14}$  mol·L<sup>-1</sup>).      (4.372)

The values of the forward reaction rate constants  $\bar{k}$  and the equilibrium constants  $K$  are given at ambient temperature 20°C [3, 4]. The temperature relationships are valid in a wide interval [35].

Let the transport equation be expressed for the liquid phase with source terms representing the real chemical reactions:

$$\begin{aligned} \frac{\partial[\text{CO}_2]}{\partial\tau} - D_L \frac{\partial^2[\text{CO}_2]}{\partial y^2} &= -Q_a - Q_b, \\ \frac{\partial[\text{HCO}_3^-]}{\partial\tau} - D_L \frac{\partial^2[\text{HCO}_3^-]}{\partial y^2} &= Q_b + Q_l - Q_1, \\ \frac{\partial[\text{H}_2\text{CO}_3]}{\partial\tau} - D_L \frac{\partial^2[\text{H}_2\text{CO}_3]}{\partial y^2} &= Q_a - Q_l, \\ \frac{\partial[\text{CO}_3^{2-}]}{\partial\tau} - D_L \frac{\partial^2[\text{CO}_3^{2-}]}{\partial y^2} &= Q_2, \end{aligned} \quad (4.373)$$

where  $D_L$  is the diffusivity of the particles in the liquid phase. As a first approximation all the diffusion coefficients are assumed equal.  $Q$  is the rate of vanishing and nucleation of particles ( $\text{mol L}^{-1} \text{s}^{-1}$ ),  $[\text{CO}_2] = c_L$ .

For example one may express the reactions a) and b) as :

$$\begin{aligned} Q_a &= \vec{k}_a [\text{CO}_2] - \bar{k}_a [\text{H}_2\text{CO}_3] = \vec{k}_a [\text{CO}_2] \left\{ 1 - \frac{[\text{H}_2\text{CO}_3]}{K_a [\text{CO}_2]} \right\}, \\ Q_b &= \vec{k}_b [\text{CO}_2][\text{OH}^-] - \bar{k}_b [\text{HCO}_3^-] = \vec{k}_b [\text{CO}_2][\text{OH}^-] \left\{ 1 - \frac{[\text{HCO}_3^-]}{K_b [\text{CO}_2][\text{OH}^-]} \right\}. \end{aligned}$$

In contrast to the relatively slow reactions a) and b) the reactions 1)-3) are fast reaction of proton exchange with large rate constants of both the forward ( $\vec{k}$ ) and the backward ( $\bar{k}$ ) reactions [40]. Therefore the transport equations for  $\text{H}_2\text{CO}_3$ ,  $\text{CO}_3^{--}$  (as well as for  $\text{H}^+$ ) may be replaced by the following local equilibrium equations:

- 1)  $[\text{HCO}_3^-][\text{H}^+] = K_1 [\text{H}_2\text{CO}_3]$ ,
- 2)  $[\text{CO}_3^{--}][\text{H}^+] = K_2 [\text{HCO}_3^-]$ ,
- 3)  $[\text{H}^+][\text{OH}^-] = K_w$ , (4.374)

where  $K_w = 0.68 \times 10^{-14}$   $\text{mol L}^{-1}$  is the ionic product of the water ( $20^\circ\text{C}$ ). The summation of the last three equations of (4.376) yields the following transport equations:

$$\begin{aligned} \frac{\partial c'_G}{\partial \tau} - D_G \frac{\partial^2 c'_G}{\partial y^2} &= 0, \\ \frac{\partial [\text{CO}_2]}{\partial \tau} - D_L \frac{\partial^2 [\text{CO}_2]}{\partial y^2} &= -Q_a - Q_b, \\ \frac{\partial \Sigma'}{\partial \tau} - D_L \frac{\partial^2 \Sigma'}{\partial y^2} &= Q_a + Q_b, \end{aligned} \quad (4.375)$$

where  $\Sigma' = [\text{HCO}_3^-] + [\text{CO}_3^{--}] + [\text{H}_2\text{CO}_3]$  is the  $\text{CO}_2$  concentration in the liquid (in a chemical compound state).

The equations (4.375) must be solved with the following boundary and initial conditions (Fig. 4.1):

$$D_a \left( \frac{\partial c'_G}{\partial y} \right)_s = D_L \left( \frac{\partial c'_L}{\partial y} \right)_s; \quad \frac{\partial \Sigma'}{\partial y} = 0, \quad c'_{Ls} = K c'_{Gs} \quad \text{at } y = b_2. \quad (4.376)$$

The conditions at  $y = 0$  and  $y = b_1 + b_2$  are:

$$\frac{\partial c'_G}{\partial y} = 0 \text{ at } y = b_1 + b_2; \quad \left( \frac{\partial \Sigma'}{\partial y} \right) = \frac{\partial c_L}{\partial y} = 0 \text{ at } y = 0; \\ c'_G = c'_0, \quad c'_L = \Sigma' = 0 \text{ at } \tau = 0. \quad (4.377)$$

The closure of the equations (4.375-4.377) requires that the concentrations of all the particles of the process (and the sources  $Q_a$ ,  $Q_b$ , too) be expressed through the concentration of  $[\text{CO}_2]$  and  $\Sigma'$ . By means of (4.374) it is easy to write:

$$[\text{H}_2\text{CO}_3] = \left[ \frac{\frac{K_w / K_1}{[\text{OH}^-]}}{I + \frac{K_w / K_1}{[\text{OH}^-]} + (K_2 / K_w)[\text{OH}^-]} \right] \Sigma'; \\ [\text{HCO}_3^-] = \frac{\Sigma'}{I + \frac{K_w / K_1}{[\text{OH}^-]} + (K_2 / K_w)[\text{OH}^-]}; \\ [\text{CO}_3^{--}] = \left[ \frac{(K_2 / K_w)[\text{OH}^-]}{I + (K_2 / K_w)[\text{OH}^-] + \frac{K_w / K_1}{[\text{OH}^-]}} \right] \Sigma'; \\ [\text{H}^+] = \frac{K_w}{[\text{OH}^-]}. \quad (4.378)$$

The relationship between  $[\text{OH}^-]$  and  $\Sigma'$  may be obtained by means of the condition for the electroneutrality [41]:

$$[\text{Na}^+] + [\text{H}^+] = [\text{HCO}_3^-] + 2[\text{CO}_3^{--}] + [\text{OH}^-], \quad (4.379)$$

where  $[\text{Na}^+] = N'$  is the condition for the complete disassociation of the base solution.

The final result is an explicit relationship  $\Sigma' ([\text{OH}^-])$ :

$$\Sigma' = \frac{\left[ N' + \frac{K_w}{[\text{OH}^-]} - [\text{OH}^-] \right] \left[ I + (K_2 / K_w)[\text{OH}^-] + \frac{K_w / K_1}{[\text{OH}^-]} \right]}{I + 2(K_2 / K_w)[\text{OH}^-]}. \quad (4.380)$$

In these alkaline solutions at  $\Sigma' \leq N'$  the concentrations of  $[H^+]$  and  $[H_2CO_3]$  may be neglected. From a mathematical point of view the latter means that the terms  $\frac{K_w}{[OH^-]}$  and  $\frac{K_w / K_2}{[OH^-]}$  in (4.380) may be omitted. Finally, the following equation for  $[OH^-]$  and  $\Sigma'$  is available:

$$\left( \frac{K_2}{K_w} [OH^-] \right)^2 - \left[ \frac{K_2}{K_w} N' - 1 - 2 \left( \frac{K_2}{K_w} \right) \Sigma' \right] \left( \frac{K_2}{K_w} [OH^-] \right) - \frac{K_2}{K_w} (N' - \Sigma') = 0.$$

The solution of the equation is:

$$\frac{K_2}{K_w} [OH^-] = \frac{1}{2} \left[ \frac{K_2}{K_w} N' - 1 - 2 \frac{K_2}{K_w} \Sigma' + \sqrt{\left( \frac{K_2}{K_w} N' - 2 \frac{K_2}{K_w} \Sigma' - 1 \right)^2 + 4 \frac{K_2}{K_w} (N' - \Sigma')} \right]. \quad (4.381)$$

It is easy to check that at  $t = 20^\circ C$  the term  $(K_2 / K_w) Kc_0$  satisfies the condition:

$$\frac{K_2}{K_w} Kc_0 = \frac{K_2}{K_w} \frac{p_a y_a}{RT} \approx 2.10^2 y_a p_a > 1, \quad (4.382)$$

where  $y_a$  is the molar part of  $CO_2$  in the gas phase,  $p_a$  is the gas pressure in atm.

Further, the solution of (4.381) at  $N' \gg Kc_0$  will be considered. Table 4.8 shows the variations of  $\frac{K_2}{K_w} [OH^-]$  with  $\Sigma'$  obtained by the relationship (4.379).

Table 4.8 Variation of  $\frac{K_2}{K_w} [OH^-]$  with  $\Sigma'$  (4.379).

$\frac{K_2}{K_w} [OH^-]$	$\frac{K_2}{K_w} N'$	$\sqrt{\frac{K_2}{K_w} \frac{N'}{2}}$	1	0.1	0.01
$\Sigma'$	0	$\frac{1}{2} N'$	$\frac{2}{3} N'$	$0.9 N'$	$0.99 N'$

In the case considered the condition  $\frac{K_2}{K_w} N' \gg 1$  is satisfied.

The relationship for the source terms  $(Q_a + Q_b)$  in the transport equations (4.375) may be expressed as :

$$\begin{aligned}
 Q_a + Q_b &= \bar{k}_a [\text{CO}_2] \left\{ I - \frac{[\text{H}_2\text{CO}_3]}{K_a [\text{CO}_2]} \right\} + \bar{k}_b [\text{OH}^-] [\text{CO}_2] \left\{ I - \frac{[\text{HCO}_3^-]}{K_b [\text{OH}^-] [\text{CO}_2]} \right\} = \\
 &= (\bar{k}_a + \bar{k}_b [\text{OH}^-]) [\text{CO}_2] \left\{ I - \frac{[\text{HCO}_3^-]}{K_b [\text{CO}_2] [\text{OH}^-]} \right\} = \\
 &\quad \bar{k}_a \left[ I + \frac{\bar{k}_b}{\bar{k}_a} \frac{K_w}{K_2} \left( \frac{K_2 [\text{OH}^-]}{K_w} \right) \right] [\text{CO}_2] \left\{ I - \left( \frac{K_2}{K_a K_l} \right) \left( \frac{N'}{Kc_0} \right) \frac{\frac{\Sigma'}{N'}}{c_L \left( I + \frac{K_2 [\text{OH}^-]}{K_w} \right) \left( \frac{K_2 [\text{OH}^-]}{K_w} \right)} \right\} \quad (4.383)
 \end{aligned}$$

where  $c_L = \frac{[\text{CO}_2]}{Kc_0}$  is the dimensionless concentration of  $\text{CO}_2$  in the liquid (4.179). Usually  $c_L \sim 1$ . Here, the equations 1) and 3) of (4.374) were used. It is clear that the equality  $K_b K_w = K_a K_l$  is satisfied.

It follows from Table 4.8 that the increase of  $\Sigma'$  leads to a decrease of the concentration of  $[\text{OH}^-]$  in the solution and consequently the chemical reaction rate (b) decreases too. At  $t = 20^\circ\text{C}$  the constants  $\left( \frac{\bar{k}_b K_w}{\bar{k}_a K_2} \right)$  and  $\left( \frac{K_2}{K_a K_l} \right)$  of the equation (4.381) are:

$$\frac{\bar{k}_b K_w}{\bar{k}_a K_2} = 2.10^2, \quad \frac{K_2}{K_a K_l} = 10^{-4}.$$

It is obvious, that at  $\Sigma' \leq 0.99 N'$  the second term in the square brackets of (4.381) may be omitted. On the other hand the second term in the large brackets is significantly greater than the first term. This means that the both reactions ((a) and (b)) in the area defined by  $\Sigma' \leq \frac{N'}{2}$  are irreversible. Moreover, the depletion of the physically soluble  $\text{CO}_2$  is due to the reaction b) ( $\bar{k}_b [\text{OH}^-] \gg \bar{k}_a$ ).

The area of concentrations defined by  $\Sigma' \leq \frac{N'}{2}$  is of a main practical interest. The further increase of  $\Sigma'$  leads to the decrease of the concentration  $[\text{OH}^-]$  and the reaction rate of the elementary reaction b) (4.372) decreases too. The absorption of  $\text{CO}_2$  occurs in accordance with the mechanism of a slow chemical reaction a). In this case the use of alkaline solutions for  $\text{CO}_2$  absorption becomes a disadvantageous operation ( $\bar{k}_a = 1.610^{-2} \text{ s}^{-1}$ ). At sufficiently high alkaline concentrations  $\left( \frac{N' K_2}{K_w} \gg 1 \right)$  the solution of the equation (4.379) is:

$$[\text{OH}^-] = N' - 2\Sigma'. \quad (4.384)$$

The condition for the applicability of that approximation is:

$$\frac{I}{\sqrt{\frac{K_2}{K_w} N}} \leq I - 2 \frac{\Sigma'}{N'}$$

The latter means, that the relationship (4.384) may be used practically up to the equilibrium  $\Sigma' = \frac{N'}{2}$ . This is the so-called "metastable" equilibrium [33]. In that area practically all the  $[\text{H}_2\text{CO}_3] = [\text{CO}_3^-]$  because the inequalities  $[\text{H}_2\text{CO}_3] \ll \Sigma'$ ,  $[\text{HCO}_3^-] \ll \Sigma'$  are satisfied.

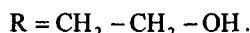
Therefore, the  $\text{CO}_2$  absorption by alkali solutions is irreversible chemical reaction of a second order (4.174) with a coefficient  $q = 2$ .

Absorption of  $\text{CO}_2$  by primary amines and  $\text{NH}_3$ . The technology of the ammonia synthesis is based on the natural gas (with approximately 20%  $\text{CO}_2$  contamination). The removal of  $\text{CO}_2$  is performed by concentrated ( $\sim 1 \text{ mol L}^{-1}$ ) solutions of ethanol amines (monoethanol amine (MEA), diethanol amine (DEA), triethanol amine (TEA) and  $\text{NH}_3$ ) under high pressures ( $\sim 1-20 \text{ atm}$ ) [33, 41]. Such process will be considered as an example below in the analysis of the real chemical reactions.

In the liquid phase two additional reactions exist in parallel with the reactions (4.372) [3, 4]:



where, for example in the case of MEA, the inner radical is :



The corresponding constants (at  $t = 20^\circ\text{C}$ ) are listed in Table 4.9.

Table 4.9. Values of the forward reaction rate constant ( $\bar{k}$ ) and equilibrium constant ( $K$ ).

Substance	$K_4, \text{L mol}^{-1}$	$\bar{k}_c, \text{L mol}^{-1} \text{s}^{-1}$	$K_c$
$\text{NH}_3$	$4.55 \times 10^9$	$0.44 \times 10^3$	$1.47 \times 10^{-6}$
MEA	$6.45 \times 10^9$	$7.6 \times 10^3$	$17.3 \times 10^{-6}$
DEA	$1.67 \times 10^9$	$1.5 \times 10^3$	$2.6 \times 10^{-6}$

The transport equations in the liquid phase are:

$$\hat{O}[\text{CO}_2] = -Q_a - Q_b - Q_c. \quad (4.386)$$

$$\begin{aligned}\hat{O}[\text{HCO}_3^-] &= Q_a + Q_b - Q_2, & \hat{O}[\text{RNH}_2] &= -Q_c - Q_4, \\ \hat{O}[\text{H}_2\text{CO}_3] &= Q_a - Q_1, & \hat{O}[\text{RNHCOO}^-] &= Q_c, \\ \hat{O}[\text{CO}_3^{--}] &= Q_2, & \hat{O}[\text{RNH}_3^+] &= Q_4,\end{aligned} \quad (4.387)$$

where  $\hat{O}$  is the operator

$$\hat{O} \equiv \frac{\partial}{\partial \tau} - D_L \frac{\partial^2}{\partial y^2}.$$

The rate of nucleation of the radicals  $[\text{RNHCOO}^-]$  may be expressed in the form:

$$\begin{aligned}Q_c &= \tilde{k}_c [\text{CO}_2][\text{RNH}_2] - \tilde{k}_c [\text{RNHCOO}^-][\text{H}^+] = \\ &= \tilde{k}_c [\text{RNH}_2][\text{CO}_2] \left\{ I - \left( \frac{K_w}{K_c} \right) \frac{[\text{RNHCOO}^-]}{[\text{RNH}_2][\text{OH}^-][\text{CO}_2]} \right\},\end{aligned} \quad (4.388)$$

In contrast to the slow chemical reaction c) the reaction 4) is a reaction of a proton exchange (see (4.385)). In this case the condition of the local equilibrium is:

$$[\text{RNH}_3^+] = K_4 [\text{RNH}_2][\text{H}^+]. \quad (4.389)$$

The summation of the transport equation (4.387) gives a set of transport equations describing the absorption process:

$$\begin{aligned}\frac{\partial c'_G}{\partial \tau} - D_G \frac{\partial^2 c'_G}{\partial y^2} &= 0, \\ \hat{O}[\text{CO}_2] &= -Q_a - Q_b - Q_c, \\ \hat{O}\Sigma' &= Q_a + Q_b, \\ \hat{O}[\text{RNHCOO}^-] &= Q_c, \\ \hat{O}[\text{R}'] &= 0,\end{aligned} \quad (4.390)$$

where  $\Sigma' = [\text{HCO}_3^-] + [\text{CO}_3^{--}] + [\text{H}_2\text{CO}_3]$  is the total  $\text{CO}_2$  concentration in the chemical compounds while  $[\text{R}'] = [\text{RNH}_2] + [\text{RNHCOO}^-] + [\text{RNH}^+]$  is the total concentration of the amine in the chemical compounds.

The problem (4.390) should be solved under the same boundary and initial conditions like in (4.376-4.377). Moreover, additional conditions about the concentrations of  $[\text{R}']$  and  $[\text{RNHCOO}^-]$  are needed:

$$\begin{aligned}\frac{\partial[\text{RNHCOO}^-]}{\partial y} &= \frac{\partial[\text{R}']}{\partial y} = 0 \quad \text{at } y = b_2; \\ \frac{\partial[\text{RNHCOO}^-]}{\partial y} &= \frac{\partial[\text{R}']}{\partial y} \quad \text{at } y = 0; \\ [\text{RNHCOO}^-] &= 0, \quad [\text{R}'] = N' \quad \text{at } \tau = 0.\end{aligned}\tag{4.391}$$

The solution of the last equation of (4.390) with respect to  $[\text{R}']$  (under the conditions (4.391) is:

$$N' \equiv [\text{RNH}_2] + [\text{RNHCOO}^-] + [\text{RNH}_3^+].\tag{4.392}$$

Hence, the total amine concentration during the process remains constant. The completion of the system of equations (4.390, 4.376-4.377, 4.391) by the local chemical equilibria (4.374, 4.389) and the equalities (4.392) should be expressed through all the actants in the process. This may be done by the help of the concentrations  $\Sigma'$  and  $[\text{RNHCOO}^-]$ . The results concerning the concentrations of  $[\text{H}_2\text{CO}_3]$ ,  $[\text{HCO}_3^-]$  and  $[\text{CO}_3^{--}]$  are the relationships (4.378)).

The corresponding relationships about  $[\text{RNH}_2]$  and  $[\text{RNH}_3^+]$  are:

$$\begin{aligned}[\text{RNH}_2] &= \frac{\frac{[\text{OH}^-]}{K_4 K_w}}{1 + \frac{[\text{OH}^-]}{K_4 K_w}} (N' - [\text{RNHCOO}^-]); \\ [\text{RNH}_3^+] &= \frac{N' - [\text{RNHCOO}^-]}{1 + \frac{[\text{OH}^-]}{K_4 K_w}}.\end{aligned}\tag{4.393}$$

With the help of the equations (4.378) and (4.393) as well as the condition of the solution electroneutrality

$$[\text{RNH}_3^+] + [\text{H}^+] = [\text{OH}^-] + [\text{HCO}_3^-] + 2[\text{CO}_3^{--}] + [\text{RNHCOO}^-],\tag{4.394}$$

one may express the implicit relationship between  $[\text{OH}^-]$  and the concentrations  $\Sigma'$  and  $[\text{RNHCOO}^-]$  as:

$$\frac{N' - [\text{RNHCOO}^-]}{1 + \frac{[\text{OH}^-]}{K_4 K_w}} + \frac{K_w}{[\text{OH}^-]} = [\text{OH}^-] + \frac{\left(1 + 2 \frac{K_2}{K_w} [\text{OH}^-]\right) \Sigma'}{1 + \frac{K_2}{K_w} [\text{OH}^-] + \frac{K_w}{K_l} [\text{OH}^-]} + [\text{RNHCOO}^-].\tag{4.395}$$

The further simplifications of the problem are related to the real values of the physical and the chemical constants. In the practically important situations  $N' \gg Kc_0 = 4 \cdot 10^{-2} y_a p_a$ .

Moreover, the values of the coefficients  $K_w$  and  $\left(\frac{K_w}{K_1}\right)$  are small ( $K_w \sim 10^{-14}$ ,  $\frac{K_w}{K_1} \sim 10^{-11}$ ).

Hence, it is easy to demonstrate that in the condition of the electroneutrality (4.395) the terms  $\frac{K_w}{[OH^-]}$  and  $\frac{K_w}{K_1}[OH^-]$  may be neglected if the condition  $[OH^-] \geq 10^{-11}$  is satisfied.

Moreover, if it is assumed that three parallel reactions a), b) and c), take place the main role belongs to the mechanism c, i.e. the conditions

$$\mathcal{Q}_c \gg \mathcal{Q}_a + \mathcal{Q}_b \quad \text{or} \quad \Sigma' \ll [RNHCOO^-], \quad (4.396)$$

are valid. Thus, it follows from (4.395) that the explicit relationship between  $[OH^-]$  and the concentration of  $[RNHCOO^-]$  is:

$$\frac{[OH^-]}{K_4 K_w} = \frac{1}{2} \left\{ \sqrt{\left( \frac{1 + [RNHCOO^-]}{K_4 K_w} \right)^2 + 4 \left( \frac{N'}{K_4 K_w} - \frac{2[RNHCOO^-]}{K_4 K_w} \right)} - \left( 1 + \frac{[RNHCOO^-]}{K_4 K_w} \right) \right\}. \quad (4.397)$$

For high  $N \equiv \frac{N'}{Kc_0}$  the ratio  $\frac{N'}{K_4 K_w} \gg 1$ . In this case by the help of (4.397) it is easy to derive the following approximations:

$$[RNH_3^+] = [OH^-] = \frac{N'}{\sqrt{\frac{N'}{K_w K_4}}}, \quad [RNH_2] = N',$$

$$(\text{if } [RNHCOO^-] \leq \frac{N'}{\sqrt{\frac{N'}{K_w K_4}}} \quad \text{or} \quad \frac{[RNHCOO^-]}{K_w K_4} \leq \sqrt{\frac{N'}{K_w K_4}});$$

$$[RNH_3^+] = [RNHCOO^-], \quad [OH^-] = \frac{N' - 2[RNHCOO^-]}{[RNHCOO^-]}, \quad [RNH_2] = N' - 2[RNHCOO^-]$$

$$(\text{if } [RNHCOO^-] \geq \frac{N'}{\sqrt{\frac{N'}{K_w K_4}}} \quad \text{or} \quad \frac{[RNHCOO^-]}{K_w K_4} \geq \sqrt{\frac{N'}{K_w K_4}}). \quad (4.398)$$

The relationships (4.398) shows that (with an equally distributed accuracy with respect  $[RNHCOO^-]$ ) in the entire area defined by  $0 \leq [RNHCOO^-] \leq \frac{N'}{2}$  (and practically up to the equilibrium) the following conditions are satisfied:

$$[RNH_2] \approx N' - 2[RNHCOO^-] \gg [OH^-]. \quad (4.399)$$

The evaluation of the source terms of the transport equations (4.390) is:

$$\begin{aligned} (Q_a + Q_b) &= (\bar{k}_a + \bar{k}_b [OH^-]) [CO_2] \left\{ I - \frac{[HCO_3^-]}{K_b [OH^-] [CO_2]} \right\} = \\ &= (\bar{k}_a + \bar{k}_b [OH^-]) [CO_2] \left\{ I - \frac{\Sigma' [RNHCOO^-]}{(K_b K_4 K_c K_{c_0}) [N' - 2[RNHCOO^-]] c_L} \right\}; \\ Q_c &= \bar{k}_c [N' - 2[RNHCOO^-]] [CO_2] \left\{ I - \frac{I}{(K_4 K_c K_{c_0})} \left( \frac{[RNHCOO^-]}{N' - 2[RNHCOO^-] c_L} \right) \right\}. \end{aligned} \quad (4.400)$$

The constants  $\frac{I}{K_b K_4 K_c K_{c_0}}$  and  $\frac{I}{K_4 K_c K_{c_0}}$  in (4.400) satisfy the following conditions (see Table 4.9):

$$\frac{I}{K_b K_4 K_c K_{c_0}} \leq \frac{I}{50 y_a p_a}, \quad \frac{I}{K_4 K_c K_{c_0}} \leq \frac{10^{-3}}{2 p_a y_a}. \quad (4.401)$$

The rate constants of the forward reactions b) and c) are practically equal ( $\bar{k}_c = \bar{k}_b = 6 \cdot 10^3$ ). Moreover, the concentration  $[RNH_2] \gg [OH^-]$  in the entire area defined by  $[RNHCOO^-] \leq \frac{N'}{2}$  (i.e. up to the metastable equilibrium). Thus, the above made suggestions for the mechanism c) (4.396) really take place. Furthermore,  $\Sigma' \ll 1$  and the second terms in the large brackets of (4.400) may be omitted up to the complete saturation  $[RNHCOO^-] \leq \frac{N'}{2}$ .

The above results indicate that all the three reactions a), b) and c) are irreversible. Moreover, the absorption of  $CO_2$  by solutions of amines occurs mainly following the mechanism c) (4.385). When the process approaches the metastable equilibrium  $([RNHCOO^-] \Rightarrow \frac{N'}{2})$  the reaction rate decreases due to the significant decrease of the concentration of the chemical sorbent ( $[RNH_2]$  - the free amine) in the solution. In this case the chemical reaction a) is slow (the same is valid for the absorption of  $CO_2$  by alkali), and

the case is not interesting from a practical point of view. It should note that the rate of the reaction b) is always lower than that of the reaction c) (4.398).

The ratio between the  $\text{CO}_2$  in the chemical compound and the concentration of the chemical sorbent (which is constant during the process,  $N' = \text{const}$ ) is termed a degree of carbonization of the solution ( $\alpha$ ). The physically soluble  $\text{CO}_2$  may be neglected at  $N' \gg Kc_0$ .

Therefore, it was established that when the degree of carbonization is  $\alpha \leq 0.5$ , the both processes discussed above may be considered as one irreversible chemical reaction of a second order between  $\text{CO}_2$  and the chemical sorbent. In the first case the sorbent is  $[\text{OH}^-]$ , while in the second case the free amine plays that role. In both cases the coefficient  $q = 2$  (see. (4.178)). Hence, all the results obtained in 4.2.3-4.2.7 are applicable to these processes.

The examples discussed above demonstrate how real chemical processes may be presented as simple irreversible chemical reactions of first or second orders. This indicates that the two-phase chemoabsorption problem investigated here is an important scientifically and practically oriented problem.

◆

The non-stationary diffusion in gas-liquid systems has been considered. The analysis has been carried out on the basis of the two-phase mass transfer phenomenon. The transport equations on both phases have been solved under boundary conditions coupling the concentrations and the diffusion fluxes at the interface.

The results obtained show that it is possible to construct a system of absorption parameters that enables easy presentations of the numerical results of the dimensionless flux evolution with the time. Particularly, the tabulation of the numerical solution in a narrow range allows an easy process design under conditions imposed by various controlling parameters. Several zones of the absorption plane have been defined. These zones define parts of the absorption plane where the mass transfer resistance is dominated by one of the phases (the gas or the liquid). The results developed have been applied for solving non-stationary heat transfer problems.

The analysis has been successfully applied for complex processes of two-phase non-stationary diffusion complicated with a irreversible chemical reaction (first or second order). Particularly, the conditions allowing a second order chemical reaction to be considered as pseudo-first order one, have been defined. Moreover, the conditions defining the system transition into a particular regime (kinetics-controlled, maximum absorption or instantaneous reaction regime) have been described.

The theory developed has been applied for the analysis of  $\text{CO}_2$  absorption by alkali and amine solutions when under certain conditions the process may be considered as a second order irreversible chemical reaction .

## References

1. V. M. Ramm, *Gas Absorption*, Khimia, Moscow, 1966 (in Russian).
2. T. K. Sherwood, R. L. Pigford, C. R. Wilke, *Mass Transfer*, McGraw-Hill, New York, 1975.
3. G. Astarita, *Mass Transfer with Chemical Reactions*, Elsevier, New York, 1967.
4. F. R. E. Danckwerts, *Gas-Liquid Reactions*, McGraw-Hill, New York, 1970.
5. M. H. Kishinevskii, *Theor. Fundam. Chem. Technol. (Russia)* 1 (1967) 759.
6. Chr.Boyadjiev and V. Beschkov, *Mass Transfer in Liquid Film Flows*, Publ. House Bulg. Acad.Sci., Sofia,1984.
7. Chr. Boyadjiev and V. Beshkov, *Mass Transfer in Following Liquid Films*, Mir, Moskow, 1988 (in Russian).
8. V. S. Krylov and Chr. Boyadjiev, *Non-Linear Mass Transfer*, Inst. Thermophysics, Novosibirsk, 1996 (in Russian).
9. L. N. Tikhonov and A. A. Samarskii, *The Equations of the Mathematical Physics*, Fizmatgiz, Moscow, 1966 (in Russian).
10. V. N. Babak, L. P., Kholpanov, V. A. Malussov and N. M. Zhavoronkov, *Theor. Fundam. Chem. Technol. (Russia)* 5 (1971) 13 .
11. I. S. Gradstein and I.M.Rizhik, *Tables of Integrals, Sums, Series and Products*, Fizmatgiz, Moscow, 1963 (in Russian).
12. V. G. Levich, *Physico-Chemical Hydrodynamics*, Prentice Hall, Englewood Cliffs, New York, 1962.
13. R. C. Reid and J. M. Prausnitz , *The properties of Gases and Liquids*, 3<sup>rd</sup> Ed., McGraw-Hill, New York, 1977
14. E. N. Andrade, *Nature*, 125 (1930) 309.
15. G. W. Kaye, T. H. Laby, *Tables of Physical and Chemical Constants*, Longmans, Green&Co., New York, 1956.
16. R. B. Bird, W.E. Steward and E. N. Lightfoot, *Transport Phenomena*, John Wiley, New York, 1965.
17. L. C. Yeu and S. S.Woofs, *AICHEJ*, 12 (1966) 95.
18. I. S. Rowlinson, *Liquids and Liquid Mixtures*, Butterworth, London, 1969.
19. I. L. Leites, T. A Semenova and Yu. V. Axelrod, *Cleaning of Technological Gases*, Khimia, Moscow, 1977 (in Russian).
20. Yu. V. Axelrod, *Gas-liquid Chemosorption Processes*, Khimia, Moscow, 1989 (in Russian).
21. V. N. Babak and Chr. Boyadjiev , In: Proc. 1<sup>st</sup> Workshop on Transport Phenomena in Two-phase Flows , Nessebar, Bulgaria, 1996.
22. Chr. Boyadjiev , T. B. Babak and V.N. Babak, In: Proc. of 1<sup>st</sup> Workshop on Transport Phenomena in Two-phase Flows , Nessebar, Bulgaria, 1996.
23. R. Nijsing, H. Kramers , In Proc.of 1st Europ. Symp. React. Eng., Amsterdam, 1957.
24. I. B. Stepanek and S. K. Achwal S.K, *Canad. J. Chem. Eng.*, 53 (1975) 35.
25. A. L. Shrier and P. V. Danckwerts, *Ind. Eng. Chem. Fund.*, 8 (1969) 415.
26. I. C. Gottifredi and O.D. Quiroga, *Int. J. Heat Mass Transfer*, 22 (1995) 839.
27. B. B. Benadda and M. Otterbein, *Chem. Eng. Process*, 35 (1996) 247.
28. R. Pohorecki and E. Kucharski, *Chem. Eng. J.*, 1 (1991) 1.
29. I. Romanainen I., *Chem. Eng. Process*, 36 (1997) 1.
30. V. N.Babak, Ph.D Thesis, IONH, Moscow, 1972 (in Russian).

31. P. V. Danckwerts, Trans. Faraday Soc., 46 (1950) 328.
32. V. V. Vyasovov, J. Techn. Physics (Russia), 18 (1940) 1519.
33. L. Pauling, General Chemistry, W. H. Freeman Co, San-Francisco, (Mir, Moscow, 1974 (in Russian)).
34. V. P. Semenov ( Ed), Ammonia Synthesis, Khimia, Moscow, 1985 (in Russian).
35. I. L. Leites (Ed), Cleaning of Technological Gases, Khimia, Moscow, 1977(in Russian).
36. V. N. Babak, T. B. Babak, L. P. Kholpanov, V. A. Malussov and N. M. Zhavoronkov, Theor. Fundam. Chem. Techol. (Russia), 15 (1981) 170.
37. M. H. Kishinevskii and A. S. Armash, J. Appl. Chemistry (Russia), 39 (1966) 1487.
38. E. Kamke, Diffrentialgleickungen, Leiptzig,1959.
39. A. A. Samarskii, Theory of Finite-Difference Schemes, Nauka, Moscow, 1975 (in Russian).
40. J. Coldin, Fast Chemical Reactions in Solutions, Mir, Moscow, 1979 (in Russian).
41. J. Newman, Electrochemical Systems, Prentice-Hall, Englewoods Cliffs, N.J., 1973.
42. R. R. Bottoms, US Patent1 783 901 (1927).
43. A. M. Kutepov, The future of KATEKA, Chemistry and Life (Russia), No. 4, 1987.

This Page Intentionally Left Blank

## PART 5

### Hydrodynamic Stability in Systems with Intensive Interphase Mass Transfer

In Part 1 of the book it was shown that the systems with intensive mass transfer are characterized by a number of non-linear effects. They change significantly both the kinetics and the mass transfer mechanism as a result of the mass transfer effects on the hydrodynamics of the system. The change may have significantly greater effect if the system loses its stability and reaches a new stable state (a self-organization of a dissipative system). The mathematical description of these systems may be done on the basis of the stability theory.

#### CHAPTER 5.1. STABILITY THEORY

Various problems are referred to the behaviour of the systems (mechanical, chemical, and physical, economical) when they are far from their equilibrium state. The behaviour depends on the system stability, i.e. it is related to the ability for a sharp change of its reaction to a smooth change of the external conditions.

The system stability is a feature also of its mathematical description. This needs a short description of the theory of the mathematical stability required for further development of the hydrodynamic stability theory. However, in all the situations the stability will be considered as a specific feature of a particular process.

##### 5.1.1. Evolution equations

Let consider that the features of the systems may be determined by the quantities  $x_i$  ( $i = 1, \dots, n$ ). This permits to consider the state of the system as a point in  $n$ -dimensional space with co-ordinates  $x_i$  ( $i = 1, \dots, n$ ) (a phase space) [5.1-5.3].

The rate of change of the system features in time is a vector in the  $n$ -dimensional space. The projections on the co-ordinate axis'  $\frac{dx_i}{dt}$  ( $i = 1, \dots, n$ ) satisfy the "evolution" law of the system:

$$\frac{dx_i}{dt} = X_i(x_1, \dots, x_n, t), \quad x_i(0) = x_{i0}, \quad i = 1, \dots, n. \quad (5.1)$$

The evolution equations (5.1) for systems with laws independent of the time are termed autonomous equations:

$$\frac{dx_i}{dt} = X_i(x_1, \dots, x_n), \quad x_i(0) = x_{i0}, \quad i = 1, \dots, n. \quad (5.2)$$

The components of the phase velocity  $X_i(i, \dots, n)$  are the co-ordinates of the vector field of the same phase velocity and determine the velocity of the system in the phase space. The points  $x_i(t)(i, \dots, n)$  represent a curve (a phase trajectory) in the scalar phase space (field).

For simplicity of explanation consider the autonomous equation

$$\frac{dx}{dt} = X(x), \quad x(0) = x_0. \quad (5.3)$$

Let assume that the solutions is

$$X(x) = 0, \quad (5.4)$$

i.e.

$$X(a) = 0. \quad (5.5)$$

It follows from (5.5) that the point  $x = a$  may be considered as a stationary point (the system velocity is zero). If  $a = x_0$  it clear that

$$x(t) \equiv a \quad (5.6)$$

is a solution of (5.3) for  $a = x_0$ , where  $a$  is a singular point.

For exactness consider the linear version of the equation (5.3) and its solution:

$$\frac{dx}{dt} = \lambda x, \quad x(0) = x_0, \quad x = x_0 \exp(\lambda t). \quad (5.7)$$

It is clear from (5.7) that  $x = 0$  is a singular point, i.e.  $x_0 = 0$  and the solution of (5.7) has the following features (see Fig. 5.1):

$$\lambda < 0, \quad \lim_{t \rightarrow \infty} x(t) = 0, \quad \forall x_0; \quad (5.8)$$

$$\lambda = 0, \quad x = x_0, \quad \forall x_0; \quad (5.9)$$

$$\lambda > 0, \quad x = x_0 \text{ at } x = 0;$$

$$\lambda > 0, \quad \lim_{t \rightarrow \infty} x(t) \rightarrow \infty, \quad \forall x_0 > 0;$$

$$\lambda > 0, \quad \lim_{t \rightarrow \infty} x(t) \rightarrow -\infty, \quad \forall x_0 < 0. \quad (5.10)$$

The multiformity of the solution at  $\lambda > 0$  is not a result of its non uniqueness, but is due to the solution instability with respect of the small perturbation of the initial condition ( $x_0$ ).

The inequality (5.8) leads to the following conclusions:

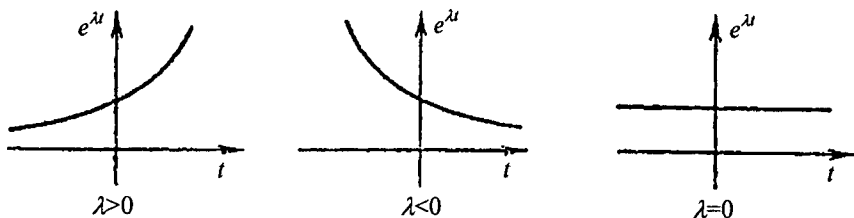


Fig.5.1. Solution of the equation (5.7)

1. The solution (the process) is unstable at  $\lambda > 0$  and the small deviations of the initial state  $x_0 \neq 0$  lead to deviations of the solution  $x = 0$ .
2. At  $\lambda \leq 0$  the solution is unstable for each  $x_0$ .
3. At  $\lambda \leq 0$  the solution is approaching to the singular point  $x = 0$ , i.e. the stationary point become a focus of attraction of the solution (an attractor).

The linear equation (5.7) together with the conditions for the solution stability are attractive because they give the basis of the kinetics models of many important processes (evolution of the organisms, nuclear processes, chemical reactions etc.) These features in the area of the real number ( $R$ ) become more interesting in the complex area ( $C$ ) where the equation (5.7) has the form:

$$\frac{dz}{dt} = \lambda z, \quad z \in C, \quad \lambda \in C, \quad t \in R, \\ z(0) = z_0, \quad z(t) = z_0 \exp(\lambda t). \quad (5.11)$$

It follows from (5.11) that if  $\lambda$  is a real number, the same is valid for  $z$ .

In the cases when  $\lambda$  is an imaginary number ( $\lambda = i\omega$ ,  $i^2 = -1$ ) the solution of (5.11) is a complex number because from the Euler formula gives:

$$z = z_0 \exp(\lambda t) = z_0 \exp(i\omega t) = z_0 (\cos \omega t + i \sin \omega t) = \zeta + i\eta. \quad (5.12)$$

Thus the solution (5.12) is circle in the plane of the complex numbers (Fig. 5.2) and the phase points moves along that circular trajectory clockwise ( $\omega < 0$ ) or in the opposite direction ( $\omega > 0$ ).

When  $\lambda$  is complex number

$$\lambda = \alpha + i\omega t \quad (5.13)$$

it follows directly from (5.11) that

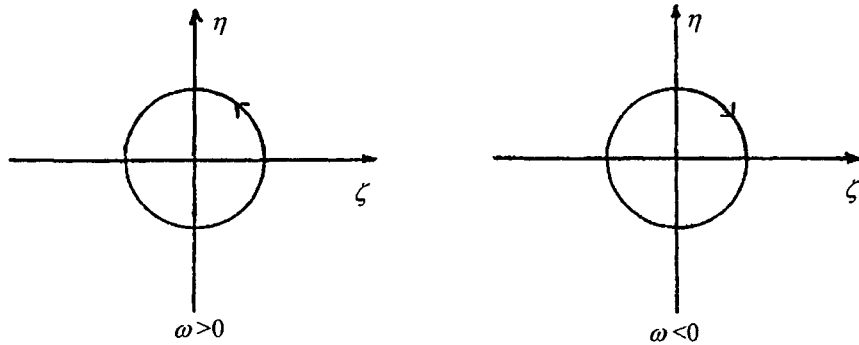


Fig.5.2. The solution of the equation (5.12) in the plane of the complex numbers.

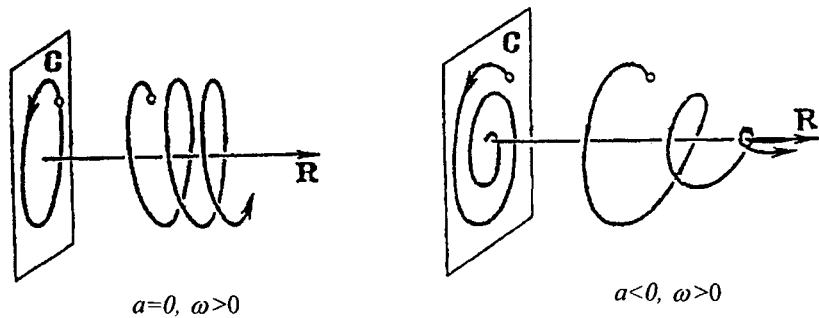


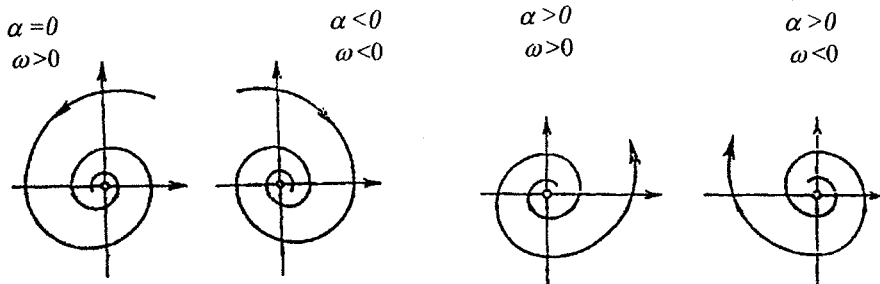
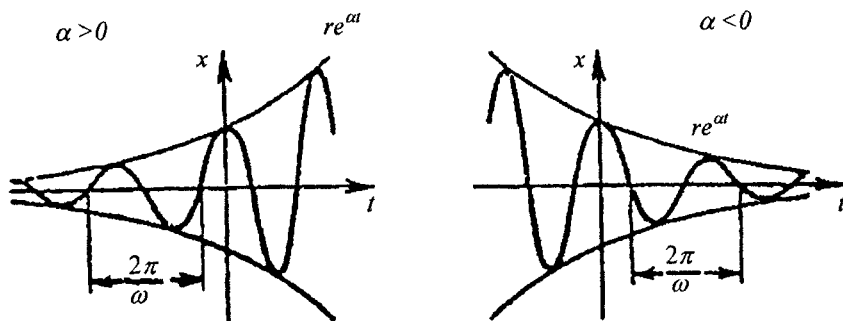
Fig. 5.3. Complex solution (5.14)

$$z = z_0 \exp(\lambda t) = z_0 \exp(\alpha t) \exp(i\omega t) = z_0 \exp(\alpha t) (\cos \omega t + i \sin \omega t) = x + iy, \quad (5.14)$$

i.e. the solution is a complex number. However, this periodic solution has variable amplitude  $z_0 \exp(\alpha t)$  depending on  $\alpha$ . At  $\alpha > 0$  the solution is unstable:

$$\lim_{t \rightarrow \infty} z(t) = \pm\infty .$$

At  $\alpha \leq 0$  the solution (5.14) is stable (see Fig. (5.3)). In Fig. 5.3, C denotes the complex plane  $(x, y)$ , R corresponds to the real axis  $t$ .

Fig. 5.4. Stable ( $\alpha < 0$ ) and unstable ( $\alpha > 0$ ) focuses.Fig. 5.5. Stable ( $\alpha < 0$ ) and unstable ( $\alpha > 0$ ) periodic solutions.

The solution (5.14) shows that at  $z = 0$  is the unique singular point, termed a *focus*. The focuses may be stable or unstable depending on the fact if they are attractors for the solution or not (see Fig. 5.4). At  $\alpha < 0$  the focuses are stable, while at  $\alpha > 0$  - unstable.

At  $\alpha \neq 0$  and  $\omega \neq 0$  the phase curves are circles (Fig. 5.2) and the singular point is their centre.

The use of complex variables gives a number of advantages of the mathematical analysis of the process stability. However, with the real processes the real parts make sense, i.e the physical solutions are identical to the real parts of the mathematical solutions. Thus for real processes it follows from (5.14) that:

$$z = r \exp(\alpha t) \cos \omega t, \quad r = z_0. \quad (5.15)$$

The solution obtained is a periodic solution and it may be stable ( $\alpha < 0$ ) or unstable ( $\alpha > 0$ ) as shown in Fig. 5.5.

The simulation of stable processes may be carried out with stable models. The unstable models are applicable for investigations on the transitions from one stable state into the next. During the last decades of the century they have been applied for the simulation of the transition from stable into unstable states (processes such as explosions) and lay in the basis of the theory of the catastrophes.

### 5.1.2. Bifurcation theory

The bifurcation theory [4] is widely applied for investigations of jump reactions of systems as responses of smooth changes of the external conditions. For the real systems it has been developed recently as a theory of the catastrophes. Here, the bifurcation theory will be considered in two-dimensional phase space only.

For clarity of explanation, consider that a real evolutionary process occurring in the phase plane  $(x, y)$  and the corresponding model is:

$$\begin{aligned} \frac{dx}{dt} &= X(x, y, \mu), & \frac{dy}{dt} &= Y(x, y, \mu), \\ x(0) &= x_0, & y(0) &= y_0. \end{aligned} \quad (5.16)$$

The system evolution in time is represented by the phase trajectory (the trajectory of the phase point) of the process

$$F(x, y, \mu) = 0, \quad (5.17)$$

where  $x(t)$  and  $y(t)$  in (5.16) are determined from the solution of (5.16). Depending on the form of the relationships for  $X$  and  $Y$  in (5.16), the parameter  $\mu$  and the initial conditions  $x_0$  and  $y_0$  various phase trajectories are possible.

The variations of the parameter  $\mu$  lead to several interesting cases of the solution of (5.16) shown in Fig. 5.6. The case shown in Fig. 5.6a corresponds to a periodic process that is attenuating with the time and approaching to a focus (a stationary state point). If other value of  $\mu$  is chosen the process might be unstable and periodic (Fig. 5.6b). The stable periodic processes (limit cycles) have closed trajectories in the phase space (Fig. 5.6c). The change of the initial state ( $y_0$ ) of the stable processes leads to attenuating processes approaching a stable periodic state. (Fig. 5.6d).

Figure 5.6 may be developed for more complicated cases (see Fig. 5.7). It is possible the existence of two limit cycles (periodic processes and solutions,), where one of them (the internal) is stable if the initial conditions are in the entire internal area of the large cycle. The internal cycle attracts all the solutions, while the external cycle is unstable (Fig. 5.7a).

The variations of the parameter  $\mu$  may lead to a junction of both cycles (Fig. 5.7b). The junction of an unstable and a stable cycle (as these in Fig. 5.7a) may lead to an abnormal limit cycle (Fig. 5.7b). In this case the solutions go from the initial conditions in internal area, approach the cycle and then due to small perturbations may go out of the cycle, so the process becomes unstable.

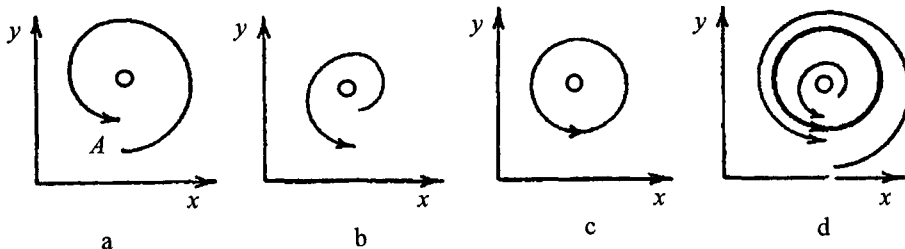


Fig. 5.6. Phase trajectories.

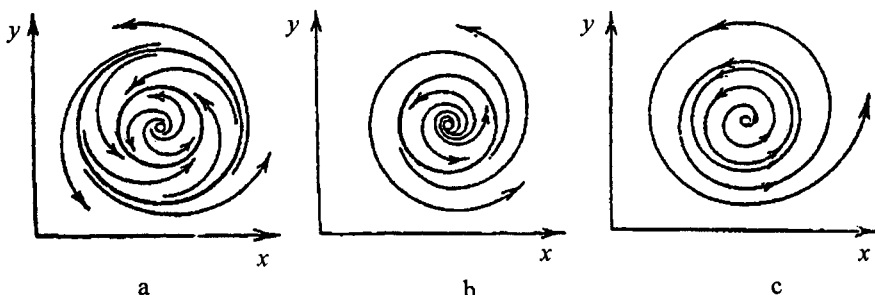


Fig. 5.7. Limit cycles.

The further changes of  $\mu$  may lead to a situation when the limit cycle disappear and the process becomes unstable (Fig. 5.7c).

The results obtained here show that the bifurcation theory considers qualitatively the changes of the movement of phase point as a result of a continuous variation of the model parameters. Parallel to the existence of stable points (foci) there are stable cycles. They describe stationary periodic oscillations of the systems (self-oscillations). They differ from the free oscillations (of a pendulum for example) where the system does not interact with the environment as well as from the forced oscillations provoked by external periodic impacts. The foci and the limit cycles attracting the solution (the phase point) are termed *attractors*.

The phase trajectory (5.17) depends on  $\mu$  because it follows from (5.16) that:

$$x = x(t, \mu), \quad y = y(t, \mu). \quad (5.18)$$

Let assume that  $\bar{x}$  and  $\bar{y}$  are the co-ordinates of a singular point moving with liquid having a dynamic viscosity  $\mu$ :

$$\bar{x} = x(\infty, \mu) < \infty, \quad \bar{y} = y(\infty, \mu) < \infty, \quad (5.19)$$

The different values of  $\mu$  determine different singular points (5.19) forming a continuos curve in the phase space:

$$F(\bar{x}, \bar{y}, \mu) = F[p(\mu)] = 0. \quad (5.20)$$

Here  $p(\mu)$  is a continuos function and is geometric locus of the singular points for various values of the parameter  $\mu$ .

Let assume that the point  $(\mu, p(\mu))$  attracts the solution for  $\mu > \mu_0$ . In this case the point  $(\mu_0, p(\mu_0))$  is pitchfork point (a bifurcation point) of the flux  $F(x, y, \mu)$  in the vector field determined by (5.16). This means that at  $t \rightarrow \infty$  the trajectory of the flux approaches  $p(\mu)$  for  $\mu < \mu_0$ . At  $\mu > \mu_0$  the singular point  $p(\mu)$  is unstable. Further, such bifurcations leading to stable regimes for  $\mu > \mu_0$  will be considered.

Let suppose that there are several curves  $p_i(\mu)$ ,  $i = 1, 2, \dots$ , where

$$F(p_i(\mu)) = 0, \quad i = 1, 2, \dots$$

At  $\mu = \mu_0$  it is possible to find a common point of the curves  $p_1(\mu_0) = p_2(\mu_0) = \dots$ . Moreover, it is possible some of these curves to stable at  $\mu > \mu_0$ , so they are a locus of singular points. Thus, different types of bifurcations are possible. The further discussion will consider a bifurcation leading to a development cycle from a focus that is important for the hydrodynamics and hydrodynamic stability.

Figure 5.8 shows bifurcations of cycle transitions from focuses. For that purpose the space map of  $F(x, y, \mu)$  is used. The case (a) correspond to a supercritical bifurcation (stable closed trajectories), while the case (b) presents a subcritical bifurcation (unstable and closed trajectories).

In the Fig. 5.8a the points  $(x, y, \mu)$  are singular at  $x = 0, y = 0, \mu \leq 0$  (i.e.  $F(0, 0, \mu) = 0$ ) and become stable at  $\mu \leq 0$ . The points  $(0, 0, \mu)$  at  $(\mu > 0)$  are unstable singular points. The trajectories  $F(x, y, \mu_0) = 0$  at  $\mu_0 > 0$  are closed and stable. Moreover, it is clear from Fig. 5.8a that due to the shape of the surface  $F(x, y, \mu) = 0$  there are closed unstable trajectories  $F(x, y, \mu_0) = 0$  at  $\mu_0 < 0$ .

Further, Fig. 5.8a shows the mechanism of a transition from a stable point (focus) toward a stable orbit (cycle). This type of bifurcation is shown in Fig. 5.9. The stages of that transition are: 1) a stable point; 2) the occurrence of a closed trajectory; 3) an increase of the closed trajectory amplitude. This order leads to the existence of stable three-dimensional torus.

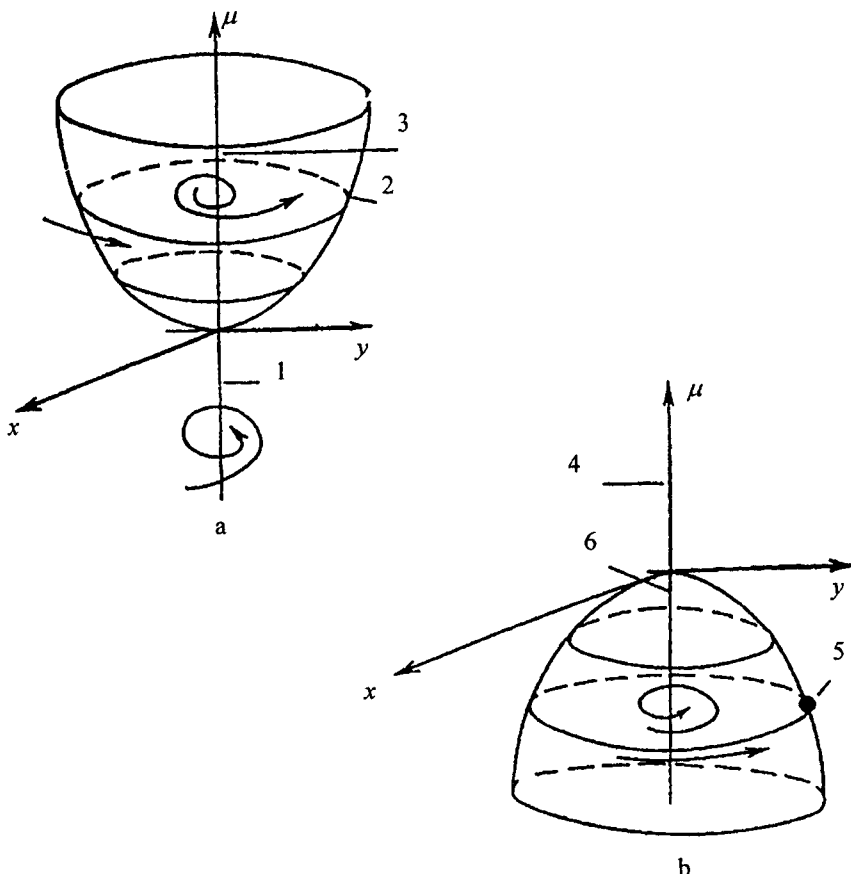


Fig.5.8. Bifurcation of cycle transitions from focuses.

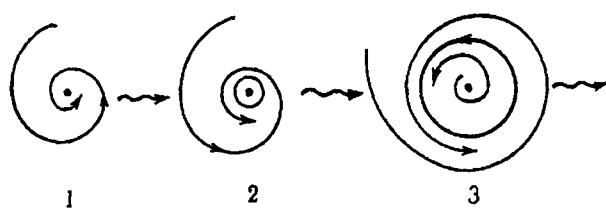


Fig. 5.9. Mechanism of a transition from a focus toward a cycle.

### 5.1.3. Eigenvalue problems

The analysis of the processes and the systems made in the previous section concerns the stability of the solutions as functions of the model parameters. This requires a solution of differential equations with parameters. When the boundary conditions contain function values in two different points this leads to eigenvalue problems. The solution of such problem will be demonstrated in an example of a homogeneous equation in the real numbers area:

$$y' + [f(x) + \lambda g(x)]y = 0, \quad (5.21)$$

with boundary conditions

$$y(b) = \alpha y(b), \quad \alpha \neq 0, \quad (5.22)$$

where  $\lambda$  is a parameter.

The solution of (5.21) is well known

$$y = C \exp \left[ - \int_a^x (f + \lambda g) dx \right]. \quad (5.23)$$

The substitution of (5.23) in (5.22) made in order to estimate the constant  $C$  shows that the condition (5.22) is satisfied only when  $\lambda = \lambda_0$ :

$$\lambda_0 = \frac{\ln \lambda + \int_a^b f dx}{\int_a^b g dx}, \quad (5.24)$$

well known as an eigenvalue. The substitution of (5.24) in (5.23) leads to an eigenfunction. Thus, for example at  $f \equiv 0$  and  $g \equiv 1$  it follows directly that

$$\lambda_0 = \frac{\ln \alpha}{b-a}, \quad y = C \exp \left[ - \frac{\ln \alpha (x-a)}{b-a} \right].$$

It is well demonstrated in the differential equation theory [5] that if  $\int_a^b g dx \neq 0$  there is an infinite set of eigenvalues:

$$\lambda_k = \lambda_0 + \frac{2k\pi i}{\int_a^b g dx}, \quad k = 0, \pm 1, \pm 2, \dots, \quad (5.26)$$

The results obtained allow the further development of the hydrodynamics stability problem.

## CHAPTER 5.2.HYDRODYNAMIC STABILITY

Most of the industrial scale processes depend on the fluid flow stability. The equations describing such fluid (gas or liquid) flows are typical evolutionary equations and relate the change of both the velocity and the pressure with the time. This permits to use the already developed approaches for stability analysis of evolutionary equations for these hydrodynamic equations [6].

### 5.2.1. Fundamental equations

Let consider a fluid (liquid or gas) flow with a kinematic viscosity  $\nu$  under the action of external forces  $F(x, t)$  or due the movement of the boundary  $S(t)$  of a closed volume  $V(t)$ . The velocity field  $U(x, t)$  is determined by the Navier-Stokes equations expressed for the velocity  $U$  and the pressure  $\pi$  in a volume  $V$ :

$$\frac{\partial U}{\partial t} + (\text{grad.} U)U - \nu \nabla^2 U + \text{grad}\pi - F(x, t) = 0, \\ \text{div} U = 0, \quad (5.27)$$

where  $x$  is the co-ordinate vector,  $\rho_0\pi$  - the pressure,  $\rho_0$  - the density and  $F$  the external forces.

The boundary conditions for (5.27) are

$$U(x, t) = U_s(x, t), \quad x \in S(t), \quad t \geq 0, \quad (5.28)$$

The corresponding initial conditions are

$$U(x, 0) = U_0(x), \quad x \in V(0). \quad (5.29)$$

The solution of (5.27)-(5.29) is the function

$$U = U(x, t; \nu, U_0). \quad (5.30)$$

In (5.30) there is no term for  $\pi$  because the pressure is determined directly from the velocity function solution  $U$  and it may be omitted [7] in (5.27).

The hydrodynamic stability will be considered as the flow stability (solution stability) under the variation of the parameters  $U_0$  and  $\nu$ . Two solutions at a given value of  $\nu$  and different initial conditions will be considered:

$$U = U(x, t; U_0), \quad U^a = U(x, t; U_0 + u_0), \quad (5.31)$$

where  $\mathbf{U}$  is the velocity of the main flow,  $\mathbf{U}^a$ - the velocity of the disturbed flow,  $\mathbf{u}_0 = \mathbf{u}_0(\mathbf{x})$ - a perturbation. The difference between the velocity of the main flow and the disturbed one is a function representing the perturbation evolution:

$$\mathbf{u}(\mathbf{x}, t) = \mathbf{U}^a - \mathbf{U}. \quad (5.32)$$

It may be determined directly from (5.27)-(5.32) that:

$$\begin{aligned} \frac{\partial \mathbf{u}}{\partial t} + (\mathbf{grad} \cdot \mathbf{U}) \mathbf{u} + (\mathbf{grad} \cdot \mathbf{u}) \mathbf{U} + (\mathbf{grad} \cdot \mathbf{u}) \mathbf{u} - \nu \nabla^2 \mathbf{u} + \mathbf{grad} P &= 0 \\ \operatorname{div} \mathbf{u} = 0, \quad \mathbf{u}|_{s=0} = 0, \quad \mathbf{u}|_{t=0} = \mathbf{u}_0(\mathbf{x}), \quad P = \pi^a - \pi. \end{aligned} \quad (5.33)$$

The equations (5.33) are the vector forms of the evolutionary hydrodynamics equations. If the flow is stable the solutions  $\mathbf{u}^a$  confluence with  $\mathbf{U}$  at  $t \rightarrow \infty$ , i.e.

$$\mathbf{u}(\mathbf{x}, t) \equiv 0 \quad \text{at} \quad t \rightarrow \infty. \quad (5.34)$$

The problem concerning the stability of  $\mathbf{U}$  at  $t \rightarrow \infty$  with respect to the perturbation of the initial conditions  $\mathbf{u}_0 \neq 0$  leads to the problem of the stability of the zero-order solution of the system (5.33). This problem may be solved in the case of arbitrary perturbations (non-linear stability) or small perturbation (linear stability). The linear theory does not predict the perturbation amplitudes. The problem may be solved by the non-linear theory that usually employs power conditions.

### 5.2.2. Power theory

The mean kinetic energy of the perturbation is

$$E(t) = \frac{1}{2} \langle |\mathbf{u}|^2 \rangle, \quad (5.35)$$

where the symbol  $\langle \rangle$  means a suitable (usually integrating) averaging procedure. In accordance with the power theory [6] the condition for the stability of the zero-order solution  $\mathbf{u}(\mathbf{x}, t)$  with respect to the perturbations of the initial conditions  $\mathbf{u}_0(\mathbf{x})$  is

$$\lim_{t \rightarrow \infty} \frac{E(t)}{E(0)} = 0, \quad (5.36)$$

Here  $E(0)$  is the initial energy of the perturbation, i.e.  $\mathbf{u} \rightarrow 0$  at  $t \rightarrow 0$ .

The condition (5.36) is a criterion for an asymptotic stability if

$$E(0) < \delta, \quad \delta > 0. \quad (5.37)$$

For every  $\delta > 0$  there is a set of initial perturbations  $\mathbf{u}_0$  that attract the solution  $\mathbf{u}_0 \equiv 0$ , i.e.  $\delta$  is the radius of attraction of the conditionally stable solution  $\mathbf{u}_0 \equiv 0$ . If  $\delta \rightarrow \infty$  the zero-order solution is absolutely (globally) stable. If the solution is asymptotically stable and  $\frac{dE}{dt} \leq 0$  (at  $t > 0$ ) the zero-order solution is a monotonous stable solution.

There is a second formulation of the stability conditions in accordance with the power theory, i.e.

$$\langle |\mathbf{U}(\mathbf{x}, t; \mathbf{U}_0) - \mathbf{U}(\mathbf{x}, t; \mathbf{U}_0 + \mathbf{u}_0)| \rangle \rightarrow 0$$

at  $t \rightarrow \infty$ , when  $\langle |\mathbf{u}|^2 \rangle < 2\delta$ . (5.38)

The solution  $\mathbf{U} = \mathbf{U}(\mathbf{x}, t; \nu, \mathbf{U}_0)$  of the system (5.27)-(5.29) at fixed external conditions ( $\mathbf{U}_0$ ) presents one-parametric family of solutions with a variable parameter  $\nu$  (the Reynolds number in the dimensionless form of the equations). The solution of the problem for the absolute stability pursues values of  $\nu$  and  $\delta$  that allow  $\mathbf{u}(\mathbf{x}, t; \nu, \mathbf{U}_0)$  to be a stable solution of (5.33), i.e.  $\mathbf{U} = \mathbf{U}(\mathbf{x}, t; \nu, \mathbf{U}_0)$  is the stable solution of (5.27)-(5.29).

For every value of  $\delta$  the condition (5.38) may be disturbed for various values of  $\nu = \nu_c$ , which depend on  $\delta$  and will be termed critical conditions. The stability limit may be obtained as the relationship  $F(\nu_c, \delta) = 0$ , i.e.  $\delta(\nu_c)$  and  $\nu_c(\delta)$ . This allows the expression of (5.37) in the form:

$$E(0) < \delta(\nu_c). (5.39)$$

In this way, the power theory formulates various critical values of the viscosity  $\nu_c$ . They are shown on Fig. 5.10. For clarity of the presentation a co-ordinate axis  $\nu^{-1}$ , which is in proportion to the Reynolds number at fixed external flow conditions, is introduced. Thus, the following four zones are defined in the figure:

1.  $\nu > \nu_E$  is the area of the monotonic and global stability.
2.  $\nu_G < \nu < \nu_E$  is the area of the global stability because it is possible to achieve  $\frac{dE}{dt} > 0$  at  $t > 0$  for given perturbations.
3.  $\nu_L < \nu < \nu_G$  is the area of the conditional stability with a radius of attraction  $\delta(\nu)$ .
4.  $\nu < \nu_L$  and  $\nu < \nu_c(\delta)$  determine the area of the instability.

There are also absolutely stable flows, i.e.  $\nu_c = 0$ . This is possible under special conditions such as:

- a flow in a tube when the perturbations does not vary along its longitudinal axis;
- some flows with infinite small perturbations;
- flows without velocity gradients under arbitrary perturbations.

In many cases the stable solutions of (5.27) –(5.29) are independent of the initial conditions i.e.

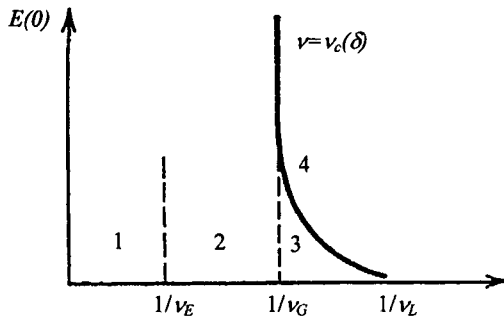


Fig. 5.10. Zones of stability.

$$U(x, t; \nu, U_0 + u_0) \rightarrow U(x, t; \nu) \text{ for } \langle |u|^2 \rangle < 2\delta. \quad (5.40)$$

The boundary flow  $U(x, t; \nu)$  depends mainly on the boundary conditions (5.28). When  $\nu > \nu_c$  the flow is called a basic flow.

The analysis of the flow stability by means of the power theory shows that the flow is stable if the perturbation energy is transmitted to the main flow. On the other hand, if the energy of the main flow is transmitted to the perturbation the flow becomes unstable. Thus, the first critical viscosity  $\nu_E$  shows the existence (or not) of perturbations which energy at the initial stage grows with the time. At  $\nu > \nu_E$  there is unique stable flow and all other flows are approaching to it.

In the situations where  $\nu < \nu_E$  there are perturbations with energy growing with the time, but at  $\nu > \nu_G$  that energy is approaching zero. Thus,  $\nu_G$  is the limit of the global stability.

If  $\nu \leq \nu_G$  there are more than one stable solutions. However, the questions about number of these solutions, their dependence on the parameters and the stability conditions could be set. These problems are solved particularly by the bifurcation theory. The latter is a non-linear theory of periodic motions with small but finite amplitudes. By its application one can follow the behaviour of the stable solutions, which are branched-out from the main flow in case of its stability loosing due to the perturbations with infinite small amplitudes. Under these conditions the perturbations grow, i.e. their amplitudes increase with the time, approaching to a finite value. The decrease of  $\nu$  leads to deficiency of the stability of these bifurcations and becomes the onset of new bifurcations. This demonstrates that the bifurcation theory starts with the linear stability analysis with respect to infinite small perturbations.

### 5.2.3. Linear theory

The linear theory [6] of the hydrodynamic stability considers the main flow  $U(x, v)$  and its non-stationary perturbation  $v(x, t; v)$  satisfying the set of equations (5.33). If one assume that the perturbations are small it is possible to write that:

$$v = \varepsilon v, \quad P = \varepsilon p, \quad \varepsilon \ll 1. \quad (5.41)$$

The substitution of (5.41) in (5.33) leads to

$$\begin{aligned} \frac{\partial v}{\partial t} + L[U, v] + \varepsilon \cdot (\text{grad.} v) v + \text{grad} p &= 0, \\ \text{div } v = 0, \quad v|_S &= 0, \quad v|_{t=0} = v_0, \end{aligned} \quad (5.42)$$

where  $L$  is a linear differential operator that represents all the differential operators (gradients, Laplacians, etc).

At  $\varepsilon = 0$  the equations (5.42) become an autonomous linear set of equations with solutions in an exponential form:

$$v(x, t) = \exp(-\sigma t) \xi(x) \quad (5.43)$$

upon setting the condition that there a numbers  $\sigma$  for which the spectral problem (an eigenvalue problem) with respect to  $\xi$  is :

$$\begin{aligned} \sigma \xi + L[U, v] \xi + \text{grad} p &= 0, \\ \text{div } \xi = 0, \quad \xi|_S &= 0. \end{aligned} \quad (5.44)$$

The problem has a non-trivial solution  $\xi \neq 0$ . The values of  $\sigma$  are the eigenvalues of the equation (5.44) and  $\xi$  are the corresponding eigenfunctions (for every  $\sigma$ ).

In the general situation  $\sigma$  may be a complex number and the eigenvalues may be expressed as:

$$\sigma = \sigma_n = \sigma_{nr} + i\sigma_{ni}, \quad n = 1, 2, \dots, \quad (5.45)$$

i.e.

$$v(x, t) = \prod_{n=1}^{\infty} \exp(-\sigma_{nr} t) \exp(-i\sigma_{ni} y) \xi(x). \quad (5.46)$$

The solution of (5.44) leads to the determination of  $\sigma_{nr}, \sigma_{ni}$  and  $\xi(x)$ ,  $n = 1, 2, \dots$ . It follows from (5.46) that:

1. The flow is stable if  $\sigma_{nr} > 0$ ,  $n = 1, 2, \dots$ ;

2. The flow is unstable if  $\sigma_{nr} < 0$ ,  $n = n_0$ ;
3. The flow is neutrally stable when  $\sigma_{n_0r} = 0$ ,  $\sigma_{nr} > 0$ ,  $n = 1, 2, \dots, n_0 - 1, n_0 + 1, \dots$ ;
4. The flow is stationary stable when  $\sigma_{nr} = 0$ ,  $\sigma_m \neq 0$ ,  $\sigma_{nr} > 0$ ,  $n = 1, 2, \dots$ ;
5. The flow is periodically stable when  $\sigma_{n_0r} = 0$ ,  $\sigma_{n_0l} \neq 0$ ,  $\sigma_{nr} > 0$ ,  $n = 1, 2, \dots, n_0 - 1, n_0 + 1, \dots, n_0 + 1$ .

The eigenvalues may be ordered as

$$\sigma_{1r} < \sigma_{2r} < \dots . \quad (5.47)$$

In this case  $\sigma_{1r}$  is the principal eigenvalue (the perturbation with greatest amplitude),  $\sigma_{2r}$  is the second eigenvalue etc.

The eigenvalues depend on the viscosity

$$\sigma_{nr} = \sigma_{nr}(\nu), \quad \sigma_m = \sigma_m(\nu), \quad n = 1, 2, \dots . \quad (5.48)$$

This allows the definition of the first critical viscosity  $\nu_L$ . The value of  $\nu_L$  is the greatest value of  $\nu$  (the minimum critical Reynolds number) that allows the satisfaction of  $\sigma_{1r}(\nu_L) = 0$ . Thus,  $\nu_L$  coincides with the critical viscosity of the non-linear (power) theory for a conditional stability at  $\delta \ll 1$ .

The hydrodynamic stability of a periodic main flow may be investigated in a similar way:

$$U(x, t, \nu) = U(x, t + T, \nu). \quad (5.49)$$

Then

$$\nu(x, t) = \exp(-\gamma t) \xi(x, t), \quad (5.50)$$

where  $\gamma = \gamma_r + i\gamma_i$  are Floke's powers. When  $\gamma_r > 0$  the periodic flow is stable, i.e. the stable periodic flow is superposed by a secondary stable periodic perturbation.

The comparison between the linear and the non-linear (power) theories shows that:

$$\nu_L \leq \nu_E \quad (5.52)$$

and several main conclusions follow:

1. If the flow is unstable in accordance with the linear theory ( $\nu < \nu_L$ ), it is unstable according to the non-linear theory too.
2. If the flow is stable in accordance with the linear theory ( $\nu > \nu_L$ ) it may be unstable according to the non-linear theory ( $E(0) > \delta$ ) or conditionally stable ( $E(0) < \delta$ ), where  $\delta$  is the radius of attraction.
3. The linear theory does not predict the value of  $\delta$  and the condition ( $\nu > \nu_L$ ) does not guarantee a global stability.

4. The linear theory guarantees only the instability at  $\sigma_{lr} < 0$  ( $\nu < \nu_L$ ), which explains the cases of disagreement between the prediction of the linear theory and the experimental results (where the perturbation amplitudes are not infinitely small).

#### 5.2.4. Stability, bifurcation and turbulence

The invariant form of the flow corresponds to its stable periodic solution (neutral stability) that occurs as a solution of (5.44) at  $\sigma_{lr} = 0$ . Then

$$\sigma_l = \sigma_l(\nu_L) = \pm i\omega_0. \quad (5.53)$$

If  $\omega_0 = 0$  at  $\varepsilon_0 = 0$  the problem (5.42) becomes a linearized problem with unique stationary solution with amplitude

$$\varepsilon^2 = E(t) = E(0). \quad (5.54)$$

This is a boundary solution (at  $\varepsilon = 0$ ) for the one-parameter family of stationary branched out solutions of the non-linear problem (5.42).

If  $\omega_0 \neq 0$ , the linearized (at  $\varepsilon = 0$ ) problem (5.42) has periodic (with a time  $t$ ) complex conjugate solutions:

$$v(x, t, \nu) = \exp(\pm i\omega_0 t) \xi(x, t). \quad (5.55)$$

In this case there is an unique family of one-parameter periodic solutions of (5.42) with a parameter  $\varepsilon$  that branches out from the solution for  $U$ . Different ways are available for the determination of  $\varepsilon$ , but the more convenient approach is to express it as the energy of the stationary branched out solution (the average energy of the cycle for one period):

$$\varepsilon^2 = \frac{1}{T} \int_0^T E(t) dt. \quad (5.56)$$

The set of equations (5.42) does not have solutions for every  $\varepsilon$ . Because of that the problem focussed on a family of solutions with a parameter  $\varepsilon$  assuring that for every small value of  $\varepsilon$  there is a corresponding value of  $\nu(\varepsilon)$ . Moreover, the values of  $\nu(\varepsilon)$  would allow a periodic solution of (5.42). Thus,  $\nu(\varepsilon)$  is a bifurcation curve.

If  $\nu(\varepsilon) > \nu_L$  it is possible to obtain a periodic flow with invariant form  $U(x, \nu) + u(x, t, \varepsilon)$  with amplitude  $\varepsilon$  (sufficiently small) which permit the perturbation energy to be constant with the time. The branched-out solutions at  $\nu(\varepsilon) > \nu_L$  (the linear theory guarantees a stability in that range) are subcritical, while at  $\nu(\varepsilon) < \nu_L$  the bifurcations are supercritical.

The stability of the secondary stable periodic flows has been investigated [5,6] too. Let the branched-out solution be considered:

$$U(x; \nu(\varepsilon)) + u(x, s; \varepsilon), \quad (5.57)$$

where  $\mathbf{u}$  is periodic with respect to  $s$  with a period of  $2\pi$ . A condition for the stability of  $\mathbf{U} + \mathbf{u}$  with respect to the small perturbations  $\mathbf{q} = \mathbf{q}(x, t)$  is required. The problem may be solved by an equation similar to (5.42). After the linearization treatment (5.42) takes the form

$$\frac{\partial \mathbf{q}}{\partial t} + \mathbf{L}\mathbf{q} + \mathbf{grad} p = 0, \\ \operatorname{div} \mathbf{q} = 0, \quad \mathbf{q}|_s = 0, \quad (5.58)$$

where  $L$  is a linear differential operator representing all the linear operators:

$$L = L[\mathbf{U} + \mathbf{u}; \nu], \quad (5.59)$$

Here  $\mathbf{U}(x; \nu(\varepsilon))$ ,  $\mathbf{u}(x, s; \varepsilon)$  and  $\nu(\varepsilon)$  are calculated at a fixed value of  $\varepsilon$ . It has been proved in [5,6] that small  $\varepsilon$  the subcritical solutions (bifurcations) are unstable, while the supercritical are stable. In these cases  $\nu = \nu(\varepsilon^2)$ .

The laminar flow of a fluid may turn into a turbulent flow if the flow parameter changes (the viscosity for example). However, in the real situations there is a continuous transition with the reduction of the viscosity. The continuous decrease of the fluid viscosity leads to a continuous transition from an organized (laminar regime) flow through self-organized flow (dissipative structures) toward a complex non-organized flow (turbulent regime). This continuous transition is a series of supercritical bifurcations. The following sequence of physical phenomena takes place:

1. At  $\nu > \nu_L$  the basic stationary flow exists.
2. At  $\nu = \nu_L$  the flow loses its stability and a secondary (more complex) periodic flow occurs. This secondary flow is stable at  $\nu < \nu_L$  and its amplitude approaches zero when  $(\nu_L - \nu) \rightarrow 0$ .
3. At  $\nu = \nu_2 < \nu_L$  (the second critical point) the secondary flow becomes unstable and a next solution pitchfork occurs. The next tertiary flow is more complex and stable until  $\nu < \nu_2$  (when the next bifurcation will start).

The transition from one stable flow regime into the next one through a series of supercritical bifurcations is a continuous process, because the amplitudes of the consequent flows approach zero when  $(\nu - \nu_L) \rightarrow 0$  and  $(\nu - \nu_2) \rightarrow 0$ . Thus, there are sharp changes of the flow regime.

A possibility of transition into a turbulent flow exists through a series of subcritical bifurcations. In this case  $\nu < \nu_L$  and the branched out solution is unstable and there is no area of attraction. An arbitrary initial perturbation “goes away” from the basic flow, branches out into a secondary unstable flow and approaches a flow (or a family of flows) with a large amplitude.

The transition from a laminar flow into a turbulent flow regime as continuous process of supercritical bifurcations is the basic idea of Landau-Hopf [4,6,11,12] for the onset of the turbulence.

### 5.2.5. Stability of parallel flows

The theory of hydrodynamic stability uses the stability analysis of various flow types. Here, several results of the non-linear theory will be discussed in order to investigate parallel fluid flows (Poiseuille and Couette flows).

The stability of flows in pipes far away from the inlet region depends on the Reynolds number:

$$Re = \frac{U_m(b-a)}{\nu}, \quad (5.60)$$

where  $U_m$  is the maximum velocity value ;  $a$  and  $b$  are the radii of the co-axial tubes forming the annulus when the fluid flows. At  $a = 0$  there is Hagen-Poiseuille flow in the pipe. In a parallel plate channel  $a = 0$  and  $b$  is the channel width (parallel Poiseuille flow). In all these cases there are several critical values of the Reynolds number:

1. The flow is globally and monotonously stable at  $Re < Re_E \approx 85 \div 100$ .
2. The flow is globally stable at  $Re_E < Re < Re_G$ , where  $Re_G \approx 2000 \div 2300$ .
3. The flow is conditionally stable at  $Re_G < Re < Re_L > 11\,000$  ( $40\,000$ ,  $10^6$ , etc.).
4. The flow is unstable at  $Re > Re_L$ .

When  $Re_E > Re_G$  there are various stable and periodic flows having equal coefficients of wall drag resistance. The state is termed *a stable turbulence*.

The next example of a parallel flow is the Couette flow between two rotating cylinders. At given Reynolds numbers a laminar flow exists. The increase of the Reynolds number is followed by the occurrence of Taylor vortexes (a stationary bifurcation) that is in fact a stable periodic flow. The further increase of  $Re$  leads to a next stable periodic flow – wavy Taylor vortexes (non-stationary bifurcations).

A large class of problems analyzed by the hydrodynamic stability theory is related to the Oberbeck-Boussinesq equations. They follow from the Navier-Stokes equations by means of an introduction of additional terms taking into consideration the natural convection as a result of the density differences. These differences may occur due to concentration or temperature gradients and require additional equations considering the diffusion and the heat transfer [6,8]. Among these problems the Benard cell convection is the one, which has been subject to extensive investigation [6,8]. In fact the phenomenon is a series of supercritical bifurcations (a consequent transitions into secondary, tertiary flows, etc.).

Under controllable conditions the thermoconvective instability may pass into a thermocapillary instability [9] and approach the Marangoni effect.

## CHAPTER 5.3. ORR-SOMMERFELD EQUATION

The linear analysis of the hydrodynamic stability may be applied in the cases of parallel fluid flows (Poiseuille or Couette flows) [6,7,10] as well as to almost-parallel flows such as flows in jets or in laminar boundary layers [6,10,11]. All these situations lead to the solution of the Orr-Sommerfeld equation. It may be derived from (5.42) with the substitutions:

$$\begin{aligned} \mathbf{v} &= (u, v), \quad \mathbf{x} = (x, y), \quad \varepsilon = 0, \quad U = U(y), \\ u &= \frac{\partial \Psi}{\partial y}, \quad v = -\frac{\partial \Psi}{\partial x}, \\ \Psi(x, y, t) &= \varphi(y) \exp[i(\alpha x - \beta t)], \end{aligned} \tag{5.61}$$

where  $\varphi$ ,  $\alpha$  and  $\beta/\alpha$  are the perturbation amplitude, the wave number and the phase velocity respectively. It is assumed in (5.62) that the amplitude and the frequency are complex, while  $\lambda$  is the wavelength of the perturbation.

$$\varphi = \varphi_r + i\varphi_i, \quad \alpha = \frac{2\pi}{\lambda}, \quad \beta = \beta_r + i\beta_i, . \tag{5.62}$$

where  $\beta_r$  is the critical frequency and  $\beta_i$  is the increment factor. Thus, the current function of the perturbation may be expressed as:

$$\Psi(x, y, t) = \varphi(y) \exp(\beta_r t) \exp[i(\alpha x - \beta_r t)], \tag{5.63}$$

where  $\varphi$  may be determined from the Orr-Sommerfeld equation:

$$(u - c)(\varphi'' - \alpha^2 \varphi) - U'' \varphi = \frac{i}{\alpha Re} \varphi''' - 2\alpha^2 \varphi'' + \alpha^4 \varphi. \tag{5.64}$$

The boundary conditions of (5.64) have various forms [14] for parallel flows and almost parallel flows. In the former cases  $\varphi(\pm 1) = \varphi'(\pm 1) = 0$ , while in the latter  $\varphi(0) = \varphi'(0) = \varphi(\infty) = \varphi'(\infty) = 0$ .

### 5.3.1. Parallel flows

In the case of parallel flow for the Orr-Sommerfeld equations are:

$$\begin{aligned} c &= \frac{\beta}{\alpha} = c_r + i c_i, \\ Re &= \frac{U_m \delta}{\nu}. \end{aligned} \tag{5.65}$$

Equation (5.64) is a typical eigenvalue problem with respect to  $\alpha$ ,  $Re$ ,  $c_r$  and  $c_i$ . At a given value of  $Re$  (or  $\alpha$ ) there is need of variations of  $\alpha$  (or  $Re$ ) in order to find  $c_r$  satisfying the condition  $c_i = 0$ . The plot obtained neutral curve  $\alpha(Re)$  (see Fig. 5.11) allows determinations of the critical Reynolds numbers.

The analysis of the hydrodynamic stability of parallel flow shows that the stability is a feature of the velocity profile shape  $U(y)$  changing with  $Re$ . At  $Re = Re_{cr}$  this profile becomes unstable.

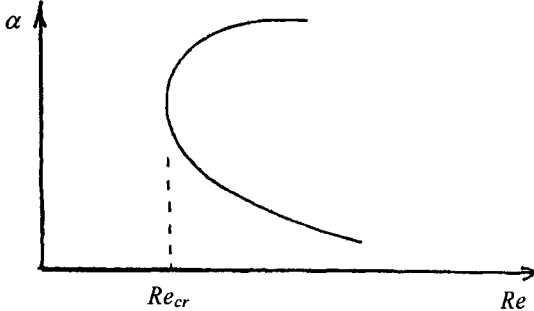


Fig. 5.11. The neutral curve.

### 5.3.2. Almost parallel flows

The almost parallel flows in jets and laminar boundary layers are characterized by the fact that the velocity profile  $U(y)$  changes along the boundary layer length. At a certain distance it becomes unstable, i.e. at a certain length the perturbation amplitude starts to grow. Finally this leads to turbulence developing further along the flow direction at lengths greater than that critical value. If the boundary layer is laminar the value of  $\delta$  in (5.65) is a function of the distance along the flow. Thus, there are coupled critical values of the length and the Reynolds number.

The relationship between the velocity of the main flow and the axial co-ordinate  $x$  is

$$\mathbf{U} = [u(x, y), v(x, y)]$$

leads to additional terms [16] in the Orr-Sommerfeld equation:

$$\left( u - \frac{\beta}{\alpha} \right) (\varphi'' - \alpha \varphi) - \frac{\partial^2 u}{\partial y^2} \varphi = - \frac{i\nu}{\alpha} (\varphi'' - 2\alpha^2 \varphi' + \alpha' \varphi) + \frac{i}{\alpha} \left[ v \varphi''' + \left( \frac{\partial^2 u}{\partial x \partial y} - \alpha^2 v \right) \varphi' \right]. \quad (5.66)$$

When a laminar boundary layer is investigated the values of  $u$  and  $v$  satisfy the Prandtl's equations

$$u \frac{\partial u}{\partial x} + v \frac{\partial u}{\partial y} = v \frac{\partial^2 u}{\partial y^2},$$

$$\frac{\partial u}{\partial x} + \frac{\partial v}{\partial y} = 0;$$

$$x = 0, u = U_\infty; \quad y = 0, u = v = 0; \quad y \rightarrow \infty, u = U_\infty.$$

(5.67)

The results obtained are the basis for the further theoretical development of the stability analysis in the case of systems with intensive mass transfer.

## CHAPTER 5.4. LINEAR STABILITY AND NON-LINEAR MASS TRANSFER

In Part 1, several problems have been discussed concerning the influence of the large concentration gradients on the velocity fields in the laminar boundary layer. The results obtained for the mass transfer rate coincide qualitatively with the experimental data which divert from the linear mass transfer theory predictions. However, some time the theory of non-linear mass transfer is missed the experimental results quantitatively. This could be explained with the lost flow stability which leads to the significant mass transfer rate arising. The induced secondary flow on the phases interface is the cause of the above phenomenon, which depending on the mass transfer direction produces suction (injection) from (to) the boundary layer and leads to increasing (decreasing) the hydrodynamic stability in the laminar boundary layer [7]. This effect will be discussed for the different systems with an intensive interphase mass transfer.

### 5.4.1. Gas (liquid)–solid system

Theoretical studies of the influence of the suction (injection) from (to) the boundary layer on the hydrodynamics and hydrodynamic stability have been carried out in cases where the normal component of the velocity on the phase boundary is constant along the boundary layer. In cases of non-linear mass transfer the rate of the suction (injection) effects on the local diffusion flux (see 1.2.1) and changes from  $\infty$  to 0 when  $x$  changes from 0 to  $\infty$ . The latter leads to a significant change in the flow stability.

The hydrodynamic stability in the gas (liquid)-solid systems will be demonstrated in the case of non-linear mass transfer in a stream flow along a semi-infinite plate [14,18]. In this case the mathematical model takes the following form:

$$\begin{aligned} u \frac{\partial u}{\partial x} + v \frac{\partial u}{\partial y} &= v \frac{\partial^2 u}{\partial y^2}, \\ \frac{\partial u}{\partial x} + \frac{\partial v}{\partial y} &= 0, \\ u \frac{\partial c}{\partial x} + v \frac{\partial c}{\partial y} &= D \frac{\partial^2 c}{\partial y^2}; \\ x = 0, \quad u = u_0, \quad c = c_0; \\ y = 0, \quad u = 0, \quad v = -\frac{MD}{\rho_0} \frac{\partial c}{\partial y}, \quad c = c^*; \\ y \rightarrow \infty, \quad u = u_0, \quad c = c_0, \end{aligned} \tag{5.68}$$

The solution of problem (5.68) can be obtained, if the following similarity variables are used:

$$\begin{aligned} u &= 0.5u_0\varepsilon\Phi', \quad v = 0.5\left(\frac{u_0v}{x}\right)^{0.5}(\eta\Phi' - \Phi), \\ c &= c_0 + (c^* - c_0)\Psi, \quad \Phi = \Phi(\eta), \quad \Psi = \Psi(\eta), \end{aligned}$$

$$\eta = y \left( \frac{u_0}{4Dx} \right)^{0.5}, \quad \varepsilon = Sc^{0.5}, \quad Sc = \frac{\nu}{D}, \quad (5.69)$$

where  $Sc$  is the Schmidt number.

The substitution of (5.69) in Eqn. system (5.68) leads to a system of ordinary differential equations:

$$\begin{aligned} \Phi'' + \varepsilon^{-1} \Phi \Phi'' &= 0, \quad \Psi'' + \varepsilon \Phi \Psi' = 0, \\ \Phi(0) &= \theta \Psi'(0), \quad \Phi'(0) = 0, \quad \Phi'(\infty) = 2\varepsilon^{-1}, \\ \Psi(0) &= 1, \quad \Psi'(\infty) = 0, \end{aligned} \quad (5.70)$$

where  $\theta$  is a small parameter, which characterises the non-linearity of the mass transfer and depends on the intensity of the interphase mass transfer.

The problem (5.70) has been solved [14, 18, 20] numerically and asymptotically as well. The results obtained by asymptotic theory [18] are confirmed through direct numerical experiments [18, 20] and show that the secondary flow with a rate  $\Phi(0) = \theta \Psi'(0)$  does not change the character of the flow in the boundary layer but only the shape of the velocity profile  $\Phi(\eta)$  [14]. This can also be proven by the following theoretical evaluations. The induction of secondary flows on the face boundary has an effect of injection to (suction from) the boundary layer, depending on the direction of the interphase mass transfer. This effect affects the potentiality of the flow at  $y \rightarrow \infty$  and is not in contradiction with the boundary layer approximations used [7]:

$$v_0 < u_0 Re_L^{-1/2}, \quad Re_L = \frac{u_0 L}{\nu}, \quad (5.71)$$

where  $v_0$  - is the mean rate of injection (suction) through a solid surface of a length  $L$ :

$$v_0 = \frac{1}{L} \int_0^L v dx, \quad v = \frac{MD}{\rho_0^*} \left( \frac{\partial c}{\partial y} \right)_{y=0}. \quad (5.72)$$

The introduction (5.69) into (5.72) leads to the following expression:

$$v_0 = -\theta u_0 Re_L^{-1/2} \Psi'(0). \quad (5.73)$$

The comparison of (5.72) with the equation (5.73) shows that (5.73) is valid if:

$$|\theta \Psi'(0)| < 1. \quad (5.74)$$

Taking into account that  $|\Psi'(0)| < 1$ , it is obvious that at  $|\theta| < 1$  the condition (5.74) is always valid.

Analytical and numerical solutions of the problem (5.70) for different values of  $\varepsilon$  and  $\theta$  allow the initial values of  $\Phi$  and its derivatives to be found:

$$\Phi(0) = a, \quad \Phi'(0) = 0, \quad \Phi''(0) = b \quad (5.75)$$

these values [18] are shown in Table 5.1.

Table 5.1.  
Initial values of  $\Phi$ , its derivatives and parameter  $k$  in eq.(5.93).

$\varepsilon$	$\theta$	$a$	$b$	$k$
1	-0.30	0.2546	1.710	1.232
	-0.20	0.1557	1.557	1.414
	-0.10	0.07162	1.432	1.576
	0.0	0.0	1.329	1.718
	0.10	-0.06196	1.239	1.849
	0.20	-0.1162	1.162	1.968
	0.30	-0.1643	1.095	2.076
10	-0.05	0.02295	0.01359	1.673
	0.0	0.0	0.01328	1.718
	0.05	-0.01237	0.01309	1.745
	0.10	-0.02074	0.01298	1.763
	0.20	-0.03196	0.01281	1.786
20	-0.05	0.02395	0.003389	1.668
	-0.03	0.01219	0.003375	1.697
	0.0	0.0	0.003321	1.718
	0.03	-0.00570	0.003321	1.734

The linear analysis has been made considerably easier considering (5.70) as a Cauchy problem.

It is seen from Table 5.1 that the initial conditions  $a$  and  $b$  include the effect of the mass transfer on the velocity profiles in the boundary layer. They depend considerably on the magnitude and the direction of the rate of the induced flow, i.e. on the direction and the rate of the intensive interphase mass transfer.

At high values of  $\theta$  in the case of liquids ( $\varepsilon \gg 1$ ), the numerical solution cannot converge due to an increasing singular perturbation (or stiffness) of the solution in the boundary layer.

It is seen from Table 5.1 that  $\theta > 0$  ( $\theta < 0$ ) corresponds to "injection" in ("suction" from) the boundary layer and according to the theory of the hydrodynamic stability [7] a decrease (increase) of the hydrodynamic stability of the flow in the boundary layer should be expected.

The influence of the intensive interphase mass transfer on the hydrodynamic stability of the flows in a laminar boundary layer is investigated applying the linear stability theory [7, 10]. This theory will be applied also for a almost parallel flow in a boundary layer, as it has been done in [6, 21] taking into account two linear scales:

$$x \text{ and } \delta = \sqrt{\frac{\nu x}{u_0}}. \quad (5.76)$$

The relation of these two scales for  $x = L$  is connected with the Reynolds number:

$$Re_L = \frac{u_0 L}{\nu} = \left( \frac{L}{\delta} \right)^2 \gg 1. \quad (5.77)$$

The approximations of the boundary layer (5.68) are zero-th order approximations regarding the small parameter  $(\delta/L)^2$ , i. e. the following relations are applicable:

$$\frac{\partial^2 v}{\partial x \partial y} \approx \frac{\partial^2 u}{\partial x^2} \ll \frac{\partial^2 u}{\partial y^2}, \quad \frac{\partial^2 v}{\partial x^2} \ll \frac{\partial^2 v}{\partial y^2}, \quad (5.78)$$

which will be used in the subsequent analysis.

The linear stability analysis considers a non-stationary flow  $(U, V, P, C)$ , obtained as a combination of a basic stationary flow  $(u, v, c)$  and two-dimensional periodic disturbances  $(u_i, v_i, p_i, c_i)$  with small amplitudes ( $\omega \ll 1$ ):

$$\begin{aligned} U(x, y, t) &= u(x, y) + \omega u_i(x, y, t), \\ V(x, y, t) &= v(x, y) + \omega v_i(x, y, t), \\ P(x, y, t) &= \omega p_i(x, y, t), \\ C(x, y, t) &= c(x, y) + \omega c_i(x, y, t). \end{aligned} \quad (5.79)$$

The non-stationary flow thus obtained satisfies the full system of Naier-Stokes equations:

$$\frac{\partial U}{\partial t} + U \frac{\partial U}{\partial x} + V \frac{\partial U}{\partial y} = -\frac{1}{\rho} \frac{\partial P}{\partial x} + \nu \left( \frac{\partial^2 U}{\partial x^2} + \frac{\partial^2 U}{\partial y^2} \right),$$

$$\frac{\partial V}{\partial t} + U \frac{\partial V}{\partial x} + V \frac{\partial V}{\partial y} = -\frac{1}{\rho} \frac{\partial P}{\partial y} + \nu \left( \frac{\partial^2 V}{\partial x^2} + \frac{\partial^2 V}{\partial y^2} \right),$$

$$\frac{\partial U}{\partial x} + \frac{\partial V}{\partial y} = 0,$$

$$\frac{\partial C}{\partial t} + U \frac{\partial C}{\partial x} + V \frac{\partial C}{\partial y} = D \left( \frac{\partial^2 C}{\partial x^2} + \frac{\partial^2 C}{\partial y^2} \right);$$

$$x = 0, \quad U = u_0, \quad V = 0, \quad P = p_0;$$

$$y=0, \quad U=0, \quad V=-\theta A_0 \frac{\partial C}{\partial y}; \\ y \rightarrow \infty, \quad U=u_0, \quad V=0, \quad P=p_0, \quad (5.80)$$

where  $A_0$ :

$$A_0 = \frac{\epsilon D}{c^* - c_0}. \quad (5.81)$$

After linearizing eqns. (5.80), i.e. in the zero approximation of the small parameters  $\omega^2$  and  $\theta\omega$ , the substitution of (5.78) and (5.79) in (5.80) leads to the following problem:

$$\begin{aligned} \frac{\partial u_I}{\partial t} + u \frac{\partial u_I}{\partial x} + v \frac{\partial u_I}{\partial y} + u_I \frac{\partial u}{\partial x} + v_I \frac{\partial u}{\partial y} &= -\frac{1}{\rho} \frac{\partial p_I}{\partial x} + v \left( \frac{\partial^2 u_I}{\partial x^2} + \frac{\partial^2 u_I}{\partial y^2} \right), \\ \frac{\partial v_I}{\partial t} + u \frac{\partial v_I}{\partial x} + v \frac{\partial v_I}{\partial y} + u_I \frac{\partial v}{\partial x} + v_I \frac{\partial v}{\partial y} &= -\frac{1}{\rho} \frac{\partial p_I}{\partial y} + v \left( \frac{\partial^2 v_I}{\partial x^2} + \frac{\partial^2 v_I}{\partial y^2} \right), \\ \frac{\partial u_I}{\partial x} + \frac{\partial v_I}{\partial y} &= 0; \\ x=0, \quad u_I=0, \quad v_I=0, \quad p_I=p_0; \\ y=0, \quad u_I=0, \quad v_I=0, \quad p_I=p_0; \\ y \rightarrow \infty, \quad u_I=0, \quad v_I=0. \end{aligned} \quad (5.82)$$

The equations (5.82) skip the equation for  $c_I$  since in the linear approximation ( $\theta\omega=0$ ) the disturbances in the velocity do not depend on the disturbances in the concentration.

The differentiation on  $y$  and  $x$  of the first two equations provides the opportunity to exclude the pressure  $p_I$ . The stability of the basic flow will be examined considering periodic disturbances of the form:

$$\begin{aligned} u_I &= F'(y) \exp i(\alpha x - \beta t), \\ v_I &= -i\alpha F(y) \exp i(\alpha x - \beta t), \end{aligned} \quad (5.83)$$

where  $F(y)$  is the amplitude of an one-dimensional disturbance (regarding  $y$ );  $\alpha$  and  $\beta/\alpha$  are its wave number and phase velocity respectively:

$$\alpha = \frac{2\pi}{\lambda}, \quad \beta = \beta_r + i\beta_i. \quad (5.84)$$

In the expression (5.84)  $\lambda$  is the wave length,  $\beta_r$ -the circle frequency,  $\beta_i$ -the increment factor. Obviously, the condition for stability of the flow is

$$\beta_i < 0. \quad (5.85)$$

In the case of  $\beta_i > 0$  the basic flow is unstable (the amplitude grows with time).

Introducing (5.83) into the equations. (5.82) leads to Orr-Sommerfeld type equations [11, 22, 23] for the amplitude of the disturbances:

$$\begin{aligned} \left( u - \frac{\beta}{\alpha} \right) (F'' - \alpha^2 F) - \frac{\partial^2 u}{\partial y^2} F = -\frac{i\nu}{\alpha} (F'^\vee - 2\alpha^2 F'' + \alpha^4 F) + \\ + \frac{i}{\alpha} \left[ v F''' + \left( \frac{\partial^2 u}{\partial x \partial y} - \alpha^2 v \right) F' \right], \\ y = 0, \quad F = 0, \quad F' = 0, \\ y \rightarrow \infty, \quad F = 0, \quad F' = 0. \end{aligned} \quad (5.86)$$

In equations. (5.86) the  $F = F(y)$  while  $u$  and  $v$  depend on  $y$ , and  $\nu x$ . Hence, the dependence on  $x$  is insignificant. This gives an opportunity to consider  $x$  as a parameter [11]. There are four constants in equations (5.86), where  $v$  and  $\alpha$  are known beforehand, while eigenvalues of  $\beta_r$  and  $\beta_i$  as well as eigenfunction  $F(y)$ , are sought. Obviously, eigenvalues of  $\beta_r$  and  $\beta_i$  thus determined depend on  $x$  and at some  $x_{cr}$

$$\beta_i(x_{cr}) = 0, \quad (5.87)$$

i.e. the velocity profile  $u(x, y)$  becomes unstable.

The assumption that the variable  $x$  is a parameter in the equations (5.86) allows a new variable to be introduced:

$$\xi = \frac{y}{\delta} = y \left( \frac{u_0}{\nu x} \right)^{0.5} = \frac{2}{\varepsilon} \eta. \quad (5.88)$$

Hence all functions in the equations (5.86) can be expressed by the new variable  $\xi$  (5.88):

$$\begin{aligned} u = u_0 f'(\xi), \quad v = 0.5 \left( \frac{u_0 \nu}{x} \right)^{0.5} (\xi f' - f), \\ F(y) = \varphi(\xi), \quad F^{(j)} = \delta^{-j} \varphi^{(j)}, \quad j = 1, \dots, 4. \end{aligned} \quad (5.89)$$

It is seen from (5.70), (5.71) and (5.89) that  $f$  can be determined from

$$\begin{aligned} 2f''' + ff'' = 0, \\ f(0) = a, \quad f'(0) = 0, \quad f''(0) = \frac{\varepsilon^2}{4} b. \end{aligned} \quad (5.90)$$

The introduction of (5.89) into equation (5.86) leads to the following Orr-Sommerfeld type of equation:

$$\begin{aligned}
 & (f' - C)(\varphi'' - A^2 \varphi) - f''' \varphi = \\
 & = -\frac{i}{A Re} \{(\varphi'' - 2A^2 \varphi'' + A^4 \varphi) - \frac{1}{2} (\xi f' - f) \varphi''' + \left[ \frac{1}{2} (\xi f''' + f'') \right. + \\
 & \left. + \frac{A^2}{2} (\xi f' - f) \right] \varphi' \}, \\
 & \varphi(0) = 0, \quad \varphi'(0) = 0, \quad \varphi(\infty) = 0, \quad \varphi'(\infty) = 0,
 \end{aligned} \tag{5.91}$$

where

$$A = \alpha \delta, \quad C = \frac{\beta}{\alpha u_0} = C_r + iC_i, \quad Re = 1.72 \frac{u_0 \delta}{\nu}. \tag{5.92}$$

The linear analysis of the hydrodynamic stability of a laminar boundary layer at the conditions of intensive interphase mass transfer are finally reduced to determining  $C$ , and  $\varphi(\xi)$  at  $C_i = 0$ , when  $Re$  and  $A$  are given. The minimum Reynolds number, i.e. the critical Reynolds number  $Re_{cr}$  at which the flow becomes unstabile, can be obtained from the dependence  $C_r(Re)$ .

The problem (5.91) is an eigenvalue problem about  $C$ , when  $Re, A$  are given. The imaginary part of the eigenvalue  $C$  determines whether or not the basic flow is stabile relative to the infinitesimal disturbances. Since this is a linear eigenvalue problem, in theory it could be solved for  $C = C(Re, A)$ . The solutions of this problem are usually presented in two ways: a) for specific values of the parameters  $A$  and  $Re$ , the corresponding values of  $C$  are tabulated or, b) the locus plane where  $C_i = 0$  (the "neutral stability curve") is plotted on the  $(Re, A)$ . The critical Reynolds number is the minimum Reynolds number at which having an infinitesimal disturbance will grow. The time growing disturbances are applied when  $Re$  and  $A$  are given real values whereas the parameter  $C$  is the searching complex eigenvalue.

In order to solve the problem (5.91) numerically in an infinite interval the boundary conditions ( $\varphi(\infty) = 0, \varphi'(\infty) = 0$ ) are assumed valid at finite distance  $\xi = \xi_\infty \gg 1$  far from the plate. The boundary conditions there will be replaced with two differential equations. In order to obtain these equations the solution [7] of (5.90) is used at high values of  $\xi$ :

$$f(\xi) = \xi - k + 0.231 \int_0^\xi d\xi \int_0^\xi \exp \left[ -\frac{1}{4} (\xi - k)^2 \right] d\xi. \tag{5.93}$$

The comparison of the numerical solution of (5.90) with (5.93) shows that an accuracy of  $10^{-4} - 10^{-6}$  is reached when  $\xi$  is greater than 6 and can assume:

$$f' = 1, \quad f'' = f''' = 0, \quad \xi f' - f = k, \quad \xi f''' = 0. \tag{5.94}$$

Thus, introducing (5.94) into (5.91) the following expression is obtained which is valid in case of  $\xi \geq 6$ :

$$(1-C)(\varphi'' - A^2\varphi) = -\frac{i}{A Re} \left[ (\varphi'^v - 2A^2\varphi'' + A^4\varphi) - \frac{1}{2}k\varphi''' + \frac{A^2}{2}k\varphi' \right]. \quad (5.95)$$

The solution of (5.95) depends on four constants [14, 20], two of them being equal to zero, because two of the solutions of the characteristic equation of (5.95) are positive, i. e. conditions  $\varphi(\infty) = \varphi'(\infty) = 0$  are satisfied:

$$\varphi = C_1 \exp(-A\xi) + C_2 \exp(-\gamma\xi), \quad (5.96)$$

where the constants  $C_1$  and  $C_2$  are determined using boundary conditions. The exclusion of these constants from (5.96) leads to the following relations for  $\xi \geq \xi_\infty = 6$ :

$$\begin{aligned} (\varphi'' - A^2\varphi)' - \gamma(\varphi'' - A^2\varphi) &= 0, \quad \xi = \xi_\infty, \\ (\varphi'' - \gamma^2\varphi)' + A(\varphi'' - \gamma^2\varphi) &= 0, \end{aligned} \quad (5.97)$$

and for  $\gamma$  the following is obtained:

$$\gamma = \frac{k}{4} - \frac{\sqrt{k^2 + 16A[A + iRe(1-C)]}}{4}. \quad (5.98)$$

The numerical solution of (5.90) for different values of  $\theta$  shows that  $k$  depends on  $\theta$  (Table 5.1.). In the case of  $\theta=0$  the comparison of the value  $Re_{cr} \approx 500$  obtained in [26, 27] in the approximations of parallel flows with the value  $Re_{cr} = 501$  obtained by us in the case of almost parallel flows shows that  $Re_{cr}$  depends slightly on  $k$ . Analogous results have been obtained at  $\theta \neq 0$ .

In a matrix form the equations. (5.91) receive the following form:

$$\begin{bmatrix} b_1 \\ b_2 \\ b_3 \\ b_4 \end{bmatrix}' + \begin{bmatrix} 0 & -1 & 0 & 0 \\ 0 & 0 & -1 & 0 \\ 0 & 0 & 0 & -1 \\ a_1 & a_2 & a_3 & a_4 \end{bmatrix} \begin{bmatrix} b_1 \\ b_2 \\ b_3 \\ b_4 \end{bmatrix} = 0, \quad (5.99)$$

and  $a_j$  ( $j = 1, \dots, 4$ ) are obtained directly from the equations (5.91):

$$\begin{aligned} a_1 &= [iA^3 Re(f' - B) - iA Re f''' + A^4], \\ a_2 &= \frac{1}{2}(\xi f''' - f'') + \frac{A^2}{2}(\xi f' - f), \quad a_3 = -[iA Re(f' - B) + 2A^2], \end{aligned}$$

$$a_4 = -\frac{1}{2}(\xi f' - f), \quad (5.100)$$

where  $b_j$  ( $j = 1, \dots, 4$ ) are

$$b_1 = \varphi, \quad b_2 = \varphi', \quad b_3 = \varphi'', \quad b_4 = \varphi'''.$$

The boundary conditions are transformed in

$$\begin{bmatrix} 1 & 0 & 0 & 0 \\ 0 & 1 & 0 & 0 \end{bmatrix} \begin{bmatrix} b_1 \\ b_2 \\ b_3 \\ b_4 \end{bmatrix} = 0, \quad \xi = 0; \quad (5.101)$$

and

$$\begin{bmatrix} -\gamma A^2 & -A^2 & \gamma & 1 \\ -A\gamma^2 & -\gamma^2 & A & 1 \end{bmatrix} \begin{bmatrix} b_1 \\ b_2 \\ b_3 \\ b_4 \end{bmatrix} = 0, \quad \xi = \xi_\infty = 6, \quad (5.102)$$

respectively.

Using the substitutions:

$$b_j = \varphi^{(j)}(\xi), \quad (j = 1, \dots, 4), \quad \mathbf{B} = (b_1, b_2, b_3, b_4)^T$$

the eigenvalue problem (5.101), (5.102) can be rewritten in the form:

$$\begin{aligned} \mathbf{B}'(\xi) + A(\xi; C)\mathbf{B}(\xi) &= 0, \quad \xi \in [0, \xi_\infty] \\ \Psi_\theta^T \mathbf{B} &= 0, \quad \xi = 0; \quad \Psi_\theta^T \mathbf{B} &= 0, \quad \xi = \xi_\infty, \end{aligned} \quad (5.103)$$

where  $A(\xi; C)$  is 4x4-matrix of the continuos components of  $\xi \in [0, \infty]$  and depends on  $C$ ;  $\Psi_\theta^T$  and  $\Psi_\theta^T$  are scalar matrices of order 4x2 ( $\Psi^T$  denotes the transposed matrix of  $\Psi$ ).

To solve the eigenvalue problem (5.103) the method proposed by Abramov [15] is used. Let  $\mathbf{B}(\xi; C)$  be an arbitrary solution of the system (5.103) satisfying the boundary condition at  $\xi = \xi_\infty$ . Then, as it has been shown in [15], the solution  $\Psi(\xi; C)$  of the initial value problem

$$\Psi' - (A^T + \Psi(\Psi^T \Psi)^{-1} \Psi^T A^T) \Psi = 0, \quad \xi \in [0, \infty]$$

$$\Psi = \Psi_1, \quad \xi = \xi_\infty, \quad (5.104)$$

satisfies

$$\Psi(\xi; C)B(\xi; C) = 0 \text{ for any } \xi \in [0, \infty], \quad (5.105)$$

i.e. can have the boundary conditions at  $\xi = \xi_\infty$  transferred to any  $\xi \in [0, \infty]$ .

Hence, integrating (5.104) up to  $\xi = 0$  the required eigenvalue relation is obtained in the form:

$$\det \begin{pmatrix} \Psi_o^T \\ \Psi_{1,0}^T(C) \end{pmatrix} = 0, \quad (5.106)$$

where  $\Psi_{1,0}(C)$  denotes the solution of (5.104) at  $\xi = 0$ .

The proposed method is reliable and  $\Psi\Psi^T = \text{const}$  along the integration path. The basic procedure is to iterate  $C$  until the solution  $C^*$  of the characteristic equation (5.106) is obtained with a given accuracy. The same procedure has to be repeated with greater  $\xi_\infty$  with a view to reach convergence of the successive approximations  $C^*$ . When a convergence is established with the prescribed accuracy the last computed  $C^*$  is taken as an eigenvalue of the original problem (5.91). The numerical experiments show that an accuracy of  $10^{-4} - 10^{-6}$  is reached when  $\xi_\infty$  is greater than 5–6.

The neutral curves presented on the  $(Re, A)$  as well as on the  $(Re, C)$  plane are shown on Figs. 5.12-5.17. They have been obtained for gases ( $\varepsilon = 1$ ) and for liquids ( $\varepsilon = 10, 20$ ).

The critical Reynolds numbers  $Re_{cr}$ , corresponding to the wave velocities  $C_r$ , and wave numbers  $A$  have been obtained.  $C_{r\min}$  and  $A_{\min}$  were obtained from these results too. Let  $C_{r\min}$  and  $A_{\min}$  denote the minimum values of the wave velocities and wave number at which the flow is stable at any value of the Reynolds number. They are shown in Table 5.2 in dependence on the magnitude and on the direction of the concentration gradient at the conditions of a intensive interphase mass transfer.

It could be seen from Figs. 5.12-5.17 and from Table 5.2, that the intensive interphase mass transfer directed toward the phase boundary ( $\theta < 0$ ) (the effect of "suction") stabilises the flow, i. e. the rise of the concentration difference  $|c_0 - c^*|$  leads to an increase of  $Re_{cr}$  and to a decrease of  $C_{r\min}$  and  $A_{\min}$ . In the case of intensive interphase mass transfer directed from the phase boundary toward the volume ( $\theta > 0$ ) (the effect of "injection") a destabilization of the flow is observed, i. e. the rise of the concentration difference  $|c_0 - c^*|$  leads to a decrease of  $Re_{cr}$  and to an increase of  $C_{r\min}$  and  $A_{\min}$ .

The high concentration gradients have a significantly stabilising effect at  $\theta < 0$ , then the destabilizing one in the case of a change in the direction of the mass transfer ( $\theta > 0$ ).

Table 5.2.

Values of the critical Reynolds number  $Re_{cr}$  corresponding to the wave velocities  $C_r$ , wave number  $A$  and  $C_{r\min}$ ,  $A_{\min}$  obtained.

$\varepsilon$	$\theta$	$Re_{cr}$	$A$	$C_r$	$A_{\min}$	$C_{r\min}$
1	-0.30	1619	0.259	0.3281	0.301	0.3310
	-0.20	1014	0.285	0.3587	0.322	0.3599
	-0.10	689	0.290	0.3816	0.340	0.3848
	0.0	501	0.305	0.4035	0.359	0.4067
	0.10	386	0.309	0.4196	0.373	0.4243
	0.20	310	0.320	0.4351	0.387	0.4396
	0.30	258	0.331	0.4488	0.398	0.4526
10	-0.05	555	0.300	0.3960	0.351	0.3990
	0.0	501	0.305	0.4035	0.359	0.4067
	0.05	476	0.305	0.4062	0.360	0.4097
	0.10	459	0.305	0.4085	0.361	0.4124
	0.20	437	0.310	0.4123	0.367	0.4155
20	-0.05	558	0.305	0.3959	0.351	0.3978
	-0.03	528	0.305	0.4010	0.354	0.4037
	0.0	501	0.305	0.4035	0.359	0.4067
	0.03	488	0.305	0.4064	0.362	0.4099

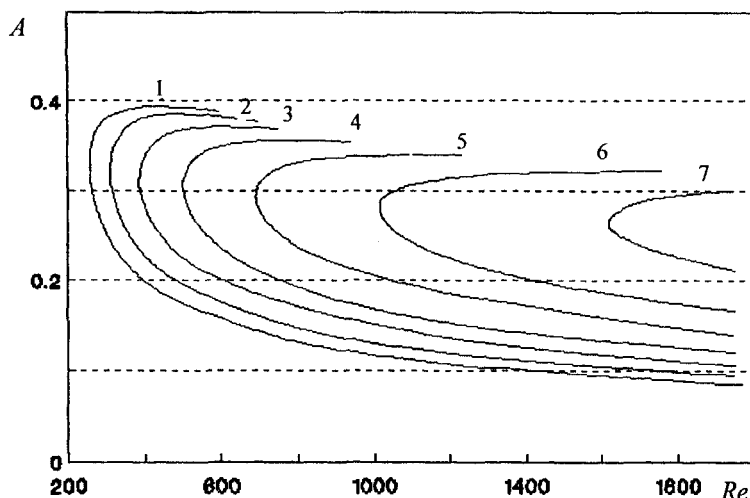


Fig. 5.12. The neutral curve for the wave number  $A$  as a function of the Reynolds number  $Re$  in the case of  $\varepsilon = 1$ : 1)  $\theta=0.3$ ; 2)  $\theta=0.2$ ; 3)  $\theta=0.1$ ; 4)  $\theta=0.0$ ; 5)  $\theta=-0.1$ ; 6)  $\theta=-0.2$ ; 7)  $\theta=-0.3$ .

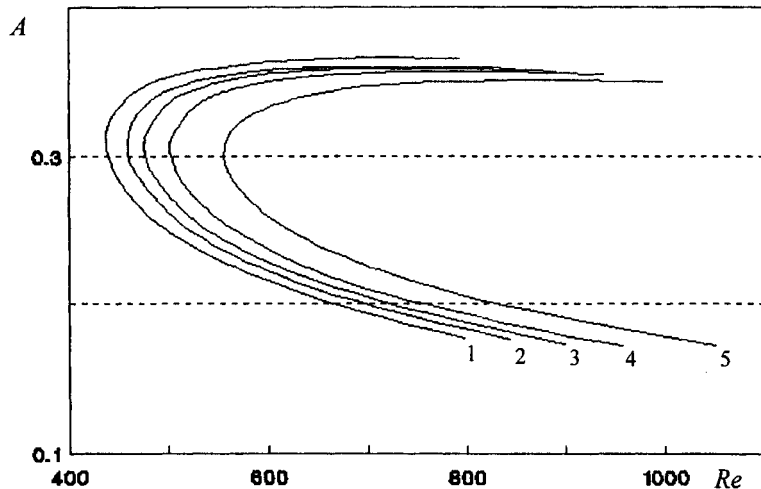


Fig. 5.13. The neutral curve for the wave number  $A$  as a function of the Reynolds number  $Re$  in the case of  $\varepsilon = 10$ : 1)  $\theta=0.2$ ; 2)  $\theta=0.1$ ; 3)  $\theta=0.05$ ; 4)  $\theta=0.0$ ; 5)  $\theta=0.05$ .

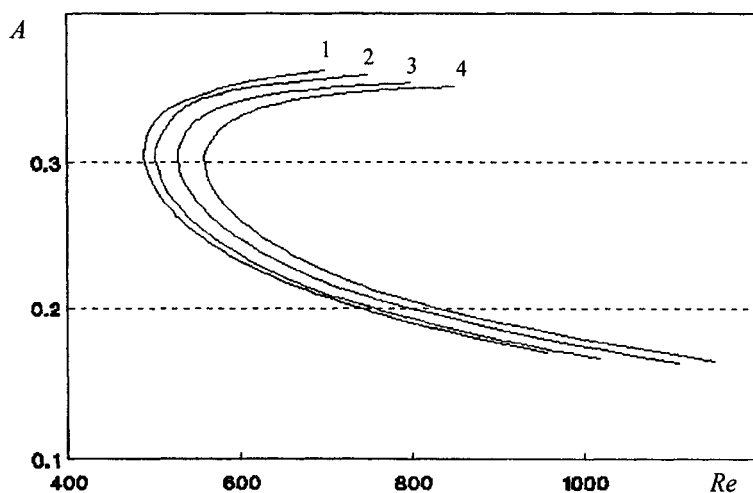


Fig. 5.14. The neutral curve for the wave number  $A$  as a function of the Reynolds number  $Re$  in the case of  $\varepsilon = 20$ : 1)  $\theta=0.03$ ; 2)  $\theta=0.0$ ; 3)  $\theta=-0.03$ ; 4)  $\theta=-0.05$ .

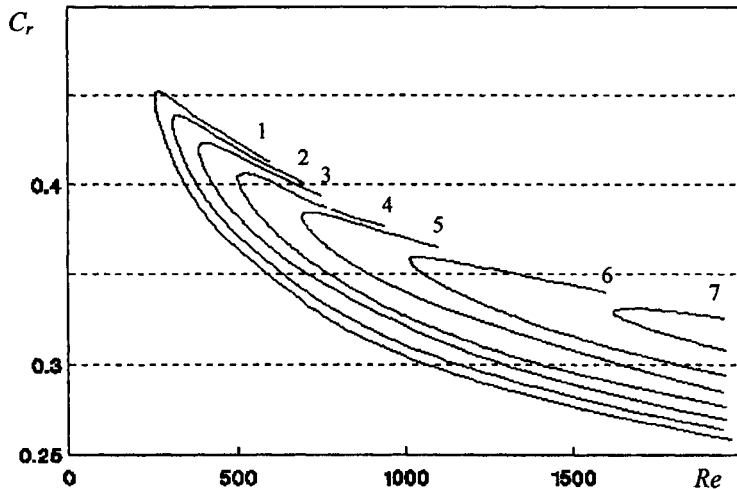


Fig. 5.15. The neutral curve for the wave velocities  $C_r$  as a function of the Reynolds number  $Re$  in the case of  $\varepsilon = 1$ : 1)  $\theta=0.3$ ; 2)  $\theta=0.2$ ; 3)  $\theta=0.1$ ; 4)  $\theta=0.0$ ; 5)  $\theta=-0.1$ ; 6)  $\theta=-0.2$ ; 7)  $\theta=-0.3$ .

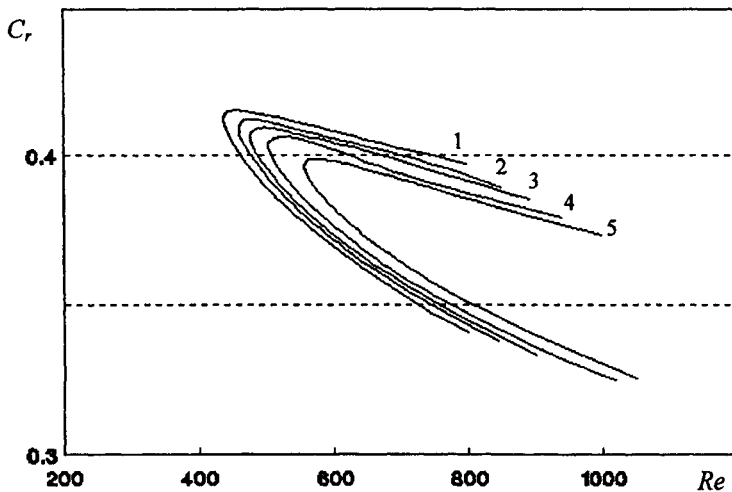


Fig. 5.16. The neutral curve for the wave velocities  $C_r$  as a function of the Reynolds number  $Re$  in the case of  $\varepsilon = 10$ : 1)  $\theta=0.2$ ; 2)  $\theta=0.1$ ; 3)  $\theta=0.05$ ; 4)  $\theta=0.0$ ; 5)  $\theta=0.05$ .

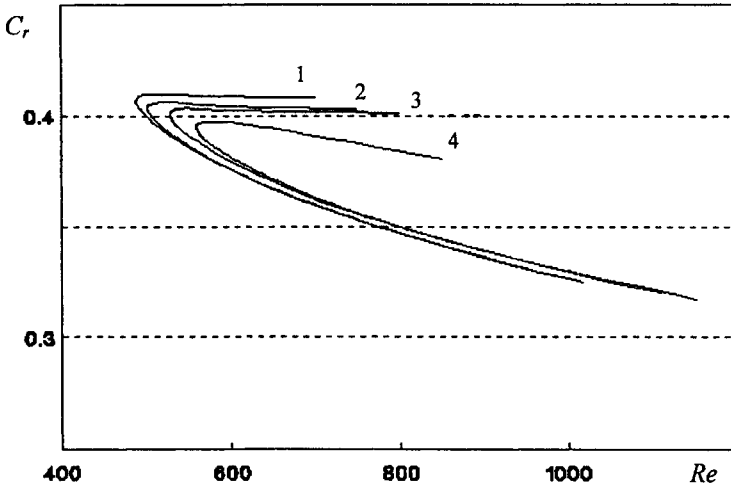


Fig. 5.17. The neutral curve for the wave velocities  $C_r$ , as a function of the Reynolds number  $Re$  in the case of  $\varepsilon = 20$  1)  $\theta=0.03$ ; 2)  $\theta=0.0$ ; 3)  $\theta=-0.03$ ; 4)  $\theta=-0.05$ .

In the above discussions the fact that the diffusive fluxes through the face boundary at ( $\theta < 0$ ) increase with the rise of the concentration difference  $|c_0 - c^*|$ , while at ( $\theta > 0$ ) they decrease with the rise of  $|c^* - c_0|$  has taking into account.

The results obtained could be of use in clarification of the mechanism and the kinetics of a number of practically interesting processes. For instance, in the liquid-solid systems the anode dissolution of metals in the electrolyte flow under conditions of intensive interphase mass transfer can rise substantially before of flow turbulence for comparatively small values of the Reynolds number, while the electrode position of metals out of concentrated solutions can be implemented at the laminar conditions at high values of Reynolds number. The intensive interphase mass transfer is of interest for the process of ablation (for example, launching a spacecraft in denser atmospheric layers). Intensive evaporation of a substance from a solid surface leads to an increase of the interphase heat transfer coefficients, i. e. to a decrease of the "undesired" heat flux toward the spacecraft (missile) rounded fuselage nose. It is evident from the results obtained that at these conditions the turbulization of the gas at considerably small Reynolds numbers is possible, which will affect also the rate of the interphase heat transfer.

The observed influence of the intensive interphase mass transfer on the hydrodynamic stability in the systems gas(liquid)-solid is much more interesting for systems with movable phase boundary (gas-liquid, liquid-liquid).

### 5.4.2. Gas – liquid system

Essential interaction between flows in gas and liquid will be observed if a movable liquid surface replaces the unmovable solid surface. There will be also the effect of induction of secondary flows as a result of intensive interphase mass transfer in the gas-liquid systems, but this effect is superposed with the hydrodynamic interaction between the above mentioned two phases. The stability at these conditions is not only of theoretical, but also of practical interest in view of the fact that it defines the rate of a number of industrial absorption and desorption processes.

The mathematical model of the non-linear mass transfer in gas-liquid systems (see 1.3.1) will be considered in the approximations of the boundary layer theory [29, 30, 42], taking into account, that the diffusive resistance is concentrated in the gas phase [31]. It was shown in [32] that the non-linear effects in the liquid can be neglected. Hence, the attention will be focused on the problem illustrated on Fig. 5.18. The mathematical description has the following form:

$$\begin{aligned} u_j \frac{\partial u_j}{\partial x} + v_j \frac{\partial u_j}{\partial y} &= v_j \frac{\partial^2 u_j}{\partial y^2}, \\ \frac{\partial u_j}{\partial x} + \frac{\partial v_j}{\partial y} &= 0, \quad j = 1, 2, \\ u_1 \frac{\partial c}{\partial x} + v_1 \frac{\partial c}{\partial y} &= D_l \frac{\partial^2 c}{\partial y^2}, \end{aligned} \tag{5.107}$$

where the indeces 1, 2 denote the gas and the liquid, respectively.

The boundary conditions of (5.107) are:

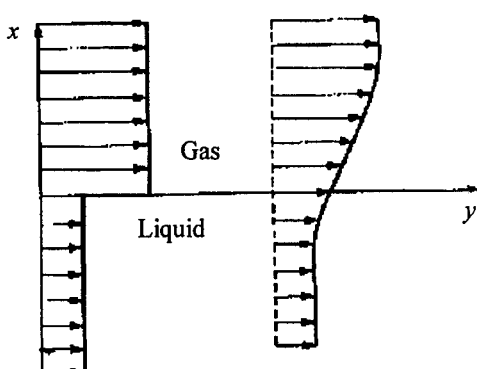


Fig. 5.18. Velocity profiles in gas and liquid flows in the boundary layer (gas - liquid system).

$$\begin{aligned}
x = 0, \quad u = u_{j0}, \quad c = c_0, \quad j = 1, 2; \\
y = 0, \quad u_1 = u_2, \quad c = c^*, \quad \mu_1 \frac{\partial u_1}{\partial y} = \mu_2 \frac{\partial u_2}{\partial y}, \\
v_1 = -\frac{MD_1}{\rho_0} \frac{\partial c}{\partial y}, \quad v_2 = 0; \\
y \rightarrow \infty, \quad u_1 = u_{10}, \quad c = c_0 \quad y \rightarrow -\infty, \quad u_2 = u_{20}. \tag{5.108}
\end{aligned}$$

The problem (5.107), (5.108) was solved numerically and asymptotically [13, 29, 33]. Further, similarity variables will be applied:

$$\begin{aligned}
u_j &= 0.5ju_{j0}\varepsilon_j\Phi'_j, \\
v_j &= (-1)^{j-1}0.5j\left(\frac{u_{j0}v_j}{x}\right)^{0.5}(\xi_j\Phi'_j - \Phi_j), \\
c &= c_0 - (c_0 - c^*)\Psi, \\
\Phi_j &= \Phi_j(\eta_j), \Psi_j = \Psi_j(\eta_j), \\
\eta_j &= (-1)^{j-1}y\left(\frac{u_{j0}}{4D_jx}\right)^{0.5}, \\
\varepsilon_j &= Sc_j^{0.5}, \quad Sc_j = \frac{V_j}{D_j}, \quad j = 1, 2. \tag{5.109}
\end{aligned}$$

The substitution of (5.109) in (5.107) and (5.108) leads to:

$$\begin{aligned}
\Phi''_1 + \varepsilon_1^{-1}\Phi'_1\Phi''_1 &= 0, \\
\Phi''_2 + 2\varepsilon_2^{-1}\Phi'_2\Phi''_2 &= 0, \\
\Psi'' + \varepsilon_1\Phi'_1\Psi' &= 0, \\
\Phi_1(0) &= -\theta_3\Psi'(0), \quad \Phi_2(0) = 0, \\
\Phi'_1(\infty) &= \frac{2}{\varepsilon_1}, \quad \Phi'_2(\infty) = \frac{1}{\varepsilon_2}, \\
\Phi'_1(0) &= 2\theta_1 \frac{\varepsilon_2}{\varepsilon_1} \Phi'_2(0), \\
\Phi''_2(0) &= -0.5\theta_2 \left(\frac{\varepsilon_1}{\varepsilon_2}\right)^2 \Phi''_1(0), \\
\Psi(0) &= 1, \quad \Psi(\infty) = 0. \tag{5.110}
\end{aligned}$$

The solution of the equations (5.110) is obtained [13, 33] by determining the initial values of  $f_j$ , which allows to define the velocity profiles in the gas and liquid, as solutions of a problem with initial conditions:

$$\begin{aligned} 2f_j''' + f_j f_j'' &= 0, \quad f_j = f_j(\xi_j), \quad \xi_j = \frac{2}{\varepsilon_j} \eta_j, \\ f_j(0) &= a_j, \quad f'_j(0) = b_j, \quad f''_j(0) = c_j, \quad (f'_j(\infty) = 1), \quad j = 1, 2, \end{aligned} \quad (5.111)$$

where

$$\begin{aligned} a_1 &= a_{10}, \quad b_1 = \frac{\varepsilon_1}{2} b_{10}, \quad c_1 = \frac{\varepsilon_1^2}{4} c_{10}, \\ a_2 &= 0, \quad b_2 = \varepsilon_2 b_{20}, \quad c_2 = -\frac{\varepsilon_2^2}{2} c_{20}, \end{aligned} \quad (5.112)$$

while the values of  $a_{10}$ ,  $b_{10}$ ,  $c_{10}$ ,  $b_{20}$  and  $c_{20}$  for  $\varepsilon_1 = 1$ ,  $\varepsilon_2 = 20$ ,  $\theta_1 = 0.1$ ,  $\theta_2 = 0.152$  are given in Tables 5.3 and 5.4.

Table 5.3.  
Initial values of  $f$ , its derivatives and the parameter  $k$  of the gas flow  
( $\varepsilon_1 = 1$ ,  $\theta_1 = 0.1$ ,  $\theta_2 = 0.152$ ,  $\theta_3 = \theta$ ).

$\theta$	$a_{10}$	$b_{10}$	$c_{10}$	$k$
-0.3	0.2797	0.2185	1.662	0.953
-0.2	0.1703	0.2166	1.520	1.133
-0.1	0.07852	0.2152	1.402	1.301
0.0	0.0	0.2138	1.304	1.428
0.1	-0.06822	0.2129	1.220	1.552
0.2	-0.1283	0.2118	1.084	1.665
0.3	-0.1816	0.2107	1.084	1.768

Table 5.4.  
Initial values of  $f$ , its derivatives and the parameter  $k$  of  
The liquid flow ( $\varepsilon_2 = 20$ ,  $\theta_1 = 0.1$ ,  $\theta_2 = 0.152$ ,  $\theta_3 = \theta$ ).

$\theta$	$b_{20}$	$c_{20}$	$k$
-0.3	0.0546	0.00033	-0.1
0.0	0.0536	0.00026	-0.086
0.3	0.0527	0.00022	-0.13

It was shown in [34] that the Orr-Sommerfeld equation in the approximations of almost parallel flows has the same form for the gas and the liquid, as follows:

$$\begin{aligned}
 & (f' - C)(\varphi'' - A^2 \varphi) - f''' \varphi = \\
 & = -\frac{i}{A Re} \{(\varphi'^{\vee} - 2A^2 \varphi'' + A^4 \varphi) - \frac{1}{2}(\xi f' - f)\varphi'' + \left[ \frac{1}{2}(\xi f''' + f'') \right. + \\
 & \left. + \frac{A^2}{2}(\xi f' - f) \right] \varphi'\}; \\
 & \xi = 0, \quad \varphi = 0, \quad \varphi' = 0; \\
 & \xi = \xi_{\infty} \geq 6, \quad (\varphi'' - A^2 \varphi)' - \gamma(\varphi'' - A^2 \varphi) = 0, \\
 & (\varphi'' - \gamma^2 \varphi)' + A(\varphi'' - \gamma^2 \varphi) = 0, \\
 & \gamma = \frac{k}{4} - \frac{\sqrt{k^2 + 16A[A + iRe(1-C)]}}{4}, \\
 & k = \lim_{\xi \rightarrow \infty} (\xi f' - f), \tag{5.113}
 \end{aligned}$$

where

$$f(\xi) = f_j(\xi_j), \quad \xi = \xi_j, \quad \varphi = \varphi_j, \quad \gamma = \gamma_j, \quad k = k_j, \quad j = 1, 2. \tag{5.114}$$

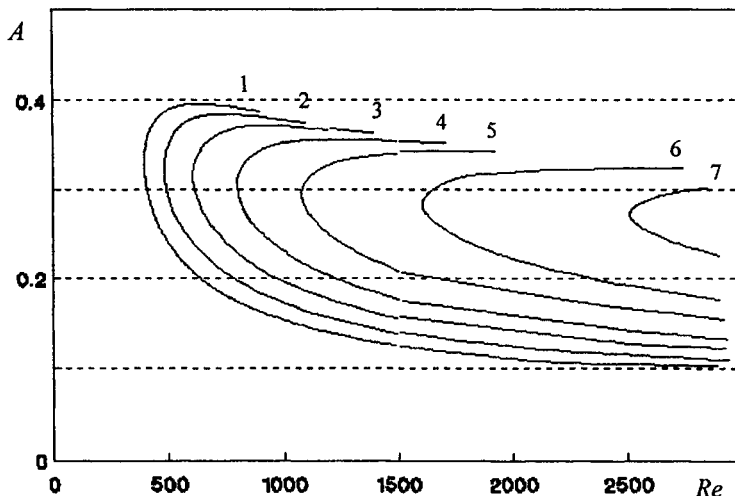


Fig. 5.19. The neutral curves for the wave number  $A$  as a function of the Reynolds number  $Re$  (in the gas phase) in the case of  $\varepsilon = 1:1$ : 1)  $\theta=0.3$ ; 2)  $\theta=0.2$ ; 3)  $\theta=0.1$ ; 4)  $\theta=0.0$ ; 5)  $\theta=-0.1$ ; 6)  $\theta=-0.2$ ; 7)  $\theta=-0.3$ .

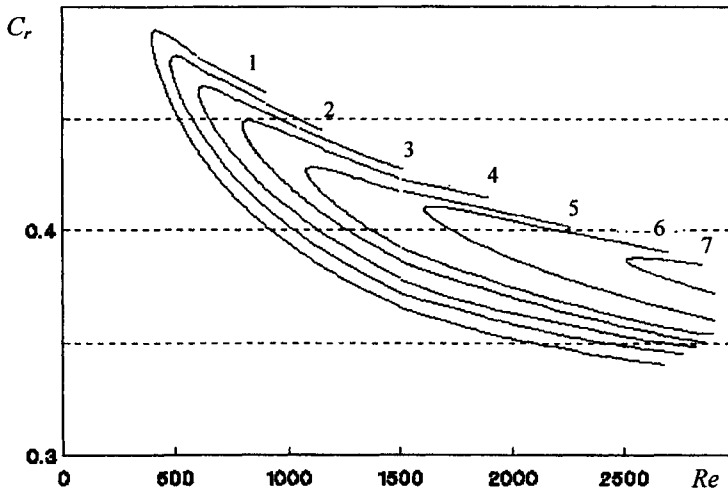


Fig. 5.20. The neutral curves for the phase velocity  $C_r$ , as a function of the Reynolds number  $Re$  (in the gas phase) in the case of  $\varepsilon = 1$ : 1)  $\theta=0.3$ ; 2)  $\theta=0.2$ ; 3)  $\theta=0.1$ ; 4)  $\theta=0.0$ ; 5)  $\theta=-0.1$ ; 6)  $\theta=-0.2$ ; 7)  $\theta=-0.3$ .

Table 5.5

Values of the critical Reynolds numbers  $Re_{cr}$ , wave velocities  $C_r$ , wave numbers  $A$  and  $C_{r min}, A_{min}$  obtained (in the gas phase).

$\theta$	$Re_{cr}$	$A$	$C_r$	$A_{min}$	$C_{r min}$
-0.3	2511	0.270	0.3863	0.304	0.3878
-0.2	1605	0.285	0.4095	0.325	0.4108
-0.1	1078	0.295	0.4264	0.341	0.4281
0.0	795	0.305	0.4469	0.356	0.4493
0.3	397	0.330	0.4866	0.398	0.4902
0.2	483	0.320	0.4749	0.386	0.4786
0.1	605	0.315	0.4620	0.373	0.4645

The values of  $k_j$  ( $j = 1, 2$ ) are calculated and shown in Tables 5.3 and 5.4.

The neutral curves  $(Re, A)$  and  $(Re, C_r)$  for the gas are shown on Fig. 5.19 and 5.20. The critical Reynolds numbers, corresponding wave numbers and phase velocities are presented in Table 5.5.

It is clearly seen, that the direction of the intensive interphase mass transfer influence the hydrodynamic stability of the flow in the gas phase boundary layer analogously to the case of the solid face boundary. Hence, in the case of absorption ( $\theta_s > 0$ ) the rise of stability is

observed. In the opposite case of desorption ( $\theta_3 < 0$ ) - the stability decreases. The motion of the interface ( $f'(0) > 0$ ) leads to decrease of the velocity gradients, which is the cause for flow stabilizing in all cases (increase of  $Re_{cr}$ ).

The solution of (5.113) for the liquid phase ( $f = f_2$ ) shows that the flow is stable at large Reynolds numbers ( $Re \approx 25\,000$ ), which can be explained by the fact that the velocity gradient in the liquid boundary layer is low (Fig. 5.21) and shaped as the profile of the Couette flow.

The effects of the intensive interphase mass transfer in the gas-liquid systems appear as a difference in the rates of absorption and desorption. In the cases, where the process is limited by the diffusion resistance in the gas phase this difference is explained by the Marangoni effect, which manifests itself in the liquid phase. The higher rate of absorption (compared with the rate of desorption) can be explained by the effect of non-linear mass transfer, i. e. the influence of the induced secondary flow on the kinetics of the mass transfer. Cases, where the desorption rate is higher than the absorption rate can be explained with loss of stability and transition to turbulence, since it is possible the flow in the gas phase to be turbulent for desorption and laminar for absorption at equal Reynolds numbers.

#### 5.4.3. Liquid-liquid system

In 5.4.1 and 5.4.2 it has been shown that the motion of the interface influences significantly the hydrodynamic stability of a flow in the gas boundary layer on the boundary with a flat liquid surface. In addition this motion and the effect of the intensive interphase mass transfer are superposed. This effect is expected to be considerably more pronounced at the conditions of intensive interphase mass

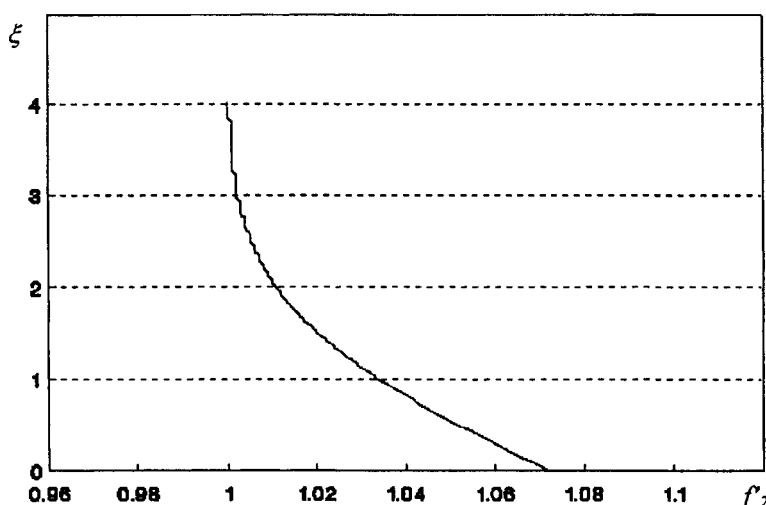


Fig. 5.21. Velocity profile in liquid flow ( $\theta=0$ ,  $\varepsilon=20$ ).

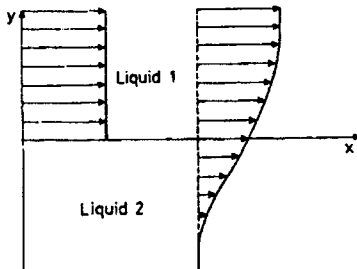


Fig. 5.22 Velocity profiles in liquid flows in the boundary layer (liquid - liquid system).

transfer between two liquids, where the hydrodynamic interaction between them is stronger and the surface velocity is higher.

Non-linear effects in the case of an intensive interphase mass transfer between two liquids can manifest themselves with the same intensity in both phases. In a number of extraction processes, where the motion of one of the phases (the dispersion medium) induces motion in the other (the dispersed phase), these effects are of great interest. Further, one could consider [35] the hydrodynamic stability at the conditions of an intensive interphase mass transfer between two liquid phases, where the velocity in the volume of one of them is zero (Fig. 5.22).

The mathematical model of the non-linear mass transfer in liquid - liquid systems, where the first liquid is in motion over the second one (which is at rest) can be obtained from the model "gas - liquid" (equations (1.59, 1.60)), when  $u_2=0$  and  $\chi=m$ , where  $m$  is the distribution coefficient, the indexes 1, 2 denote the liquid 1 and liquid 2 respectively.

The formulated problem has been solved numerically [29, 36] and the boundary values for the velocity and its derivatives obtained. This gives us opportunity to generate the velocity profiles of the following hydrodynamic problem:

$$\begin{aligned}
 u_j \frac{\partial u_j}{\partial x} + v_j \frac{\partial v_j}{\partial y} &= v_j \frac{\partial^2 u_j}{\partial y^2}, \\
 \frac{\partial u_j}{\partial x} + \frac{\partial v_j}{\partial y} &= 0; \\
 x = 0, \quad u_1 &= u_0, \quad u_2 = 0; \\
 y = 0, \quad u_j &= u_{j0}, \quad v_j = v_{j0}, \quad \frac{\partial u_j}{\partial y} = R_j, \quad j = 1, 2,
 \end{aligned} \tag{5.115}$$

where  $u_{j0}$ ,  $v_{j0}$  and  $R_j$  ( $j = 1, 2$ ) are determined in 1.3.3.

The introduction of the following similarity variables:

$$\begin{aligned}
 u_j &= u_0 f'_j(\xi_j), \quad v_j = \left( \frac{u_0 v_j}{4x} \right)^{0.5} (\xi_j f'_j - f_j) \\
 \xi_j &= (-1)^{j-1} y \left( \frac{u_0}{v_j x} \right)^{0.5}, \quad j = 1, 2,
 \end{aligned} \tag{5.116}$$

leads to a problem, which allows to determine the velocity profiles:

$$\begin{aligned}
 2f''_j + f_j f''_j &= 0, \\
 f_j(0) &= A_j, \quad f'_j(0) = B_j, \quad f''_j(0) = C_j, \quad j = 1, 2, \quad (f'_1(\infty) = I, \quad f'_2(\infty) = 0),
 \end{aligned} \tag{5.117}$$

where  $A_j$ ,  $B_j$  and  $C_j$  are results of the numerical solution [36] and they are displayed in Table 5.6.

The velocity profiles  $f'_j(\xi_j)$  ( $j = 1, 2$ ) depend substantially on the effect of the non-linear mass transfer ( $A_j$ ,  $j = 1, 2$ ), which is characterised by the parameters  $\theta_j$  ( $j = 1, 2$ ) [36]:

$$\theta_j = \frac{M(m c_{20} - c_{10})}{\rho_{j0}^* m^{j-1}}, \quad j = 1, 2. \tag{5.118}$$

Table 5.6

Computed values of  $A_j$ ,  $B_j$ ,  $C_j$  and  $k$ ; first part of the table - cases where the diffusion resistance is limited by the mass transfer in the phase 1 ( $m/b = 0$ ,  $\theta_1 = \theta$ ,  $\theta_2 = 0$ ); second part of the table - cases of diffusional resistances ( $b/m = 1$ ,  $\theta_1 = \theta_2 = \theta$ ).

$\varepsilon = 10$	$\theta$	$A_j$	$B_j$	$C_j$	$k$
$m/b = 0$	-0.5	0.66525	0.439	0.26565	0.673
	-0.3	0.032988	0.420	0.26565	0.747
	-0.1	0.0094	0.405	0.26565	0.805
	0.0	0.0	0.4	0.26565	0.823
	0.1	-0.008261	0.394	0.26565	0.846
	0.3	-0.022194	0.384	0.26565	0.883
	0.5	-0.033445	0.3755	0.26565	0.915
$b/m = 1$	-0.5	0.02117	0.4132	0.26565	0.773
	-0.3	0.012867	0.4075	0.26565	0.8
	-0.1	0.004316	0.402	0.26565	0.82
	0.0	0.0	0.4	0.26565	0.823
	0.1	-0.004316	0.3967	0.26565	0.836
	0.3	-0.012867	0.39	0.26565	0.862
	0.5	-0.02117	0.385	0.26565	0.88

This effect is superposed with the effect of the hydrodynamic interaction between the phases ( $C_j, j = 1, 2$ ). Hence, the interface velocity ( $B_j, j = 1, 2$ ) takes into account both the above mentioned effects.

The linear analysis of the hydrodynamic stability in the liquid - liquid systems is made similarly to that in the case of gas - liquid systems. The velocity profiles (5.117) are introduced into the Orr-Sommerfeld equation. The results obtained show, that the stability of the profiles depends considerably on the non-linear effects of the mass transfer  $\theta_j$  ( $j = 1, 2$ ), as well as on the interface velocity  $B_j$  ( $j = 1, 2$ ).

The effect of the non-linear mass transfer in the liquid 1 (Table 5.7,  $m/b = 0$ ) and the effects of the increase of the interface velocity are superposed and their total influence on the stability of the flow in phase 1 is shown on Figs. 5.23, 5.24.

Under the conditions of commensurable diffusive resistances in the two liquids (Table 5.7,  $m/b = 1$ ) the non-linear effects are lower (Figures 5.25, 5.26). The influence of the non-linear effects ( $\theta$ ) on the stability of the flow decreases.

The linear analysis of the hydrodynamic stability of the phase 2 [35] produces analogous results as those for the gas-liquid system. The flow is stable up to large Reynolds numbers ( $Re \approx 25\,000$ ), which can be explained with the velocity profile shape (approximately the same as the Couette one).

The studies on the hydrodynamic stability in the systems with intensive interphase mass transfer show, that the stability increases with the rise of the interface velocity and the rise of concentration gradients in the cases of interphase mass transfer directed from the volume to the phase boundary. The decrease of the interface velocity and the change of the direction of interphase mass transfer destabilize the flow in the boundary layer.

Table 5.7.

Values of the critical Reynolds numbers  $Re_{cr}$ , wave velocities  $C_r$ , wave numbers  $A$  and  $C_{rmin}, A_{min}$  obtained (in cases  $m/b = 0$ ,  $\theta_1 = \theta$ ,  $\theta_2 = 0$  and  $b/m = 1$ ,  $\theta_1 = \theta_2 = \theta$ ).

$\varepsilon = 10$	$\theta$	$Re_{cr}$	$A$	$C_r$	$A_{min}$	$C_{rmin}$
$m/b = 0$	-0.5	3145	0.315	0.6235	0.358	0.6246
	-0.3	2663	0.320	0.6155	0.364	0.6163
	-0.1	2343	0.325	0.6092	0.372	0.6101
	0.0	2243	0.330	0.6081	0.372	0.6085
	0.1	2145	0.320	0.6042	0.374	0.6053
	0.3	1983	0.320	0.5997	0.375	0.6009
	0.5	1859	0.330	0.5969	0.377	0.5974
$b/m = 1$	-0.5	2503	0.325	0.6130	0.367	0.6135
	-0.3	2398	0.325	0.6099	0.370	0.6111
	-0.1	2288	0.325	0.6079	0.371	0.6086
	0.0	2243	0.330	0.6081	0.372	0.6085
	0.1	2170	0.330	0.6064	0.374	0.6066
	0.3	2079	0.320	0.6020	0.375	0.6036
	0.5	1999	0.325	0.6008	0.375	0.6015

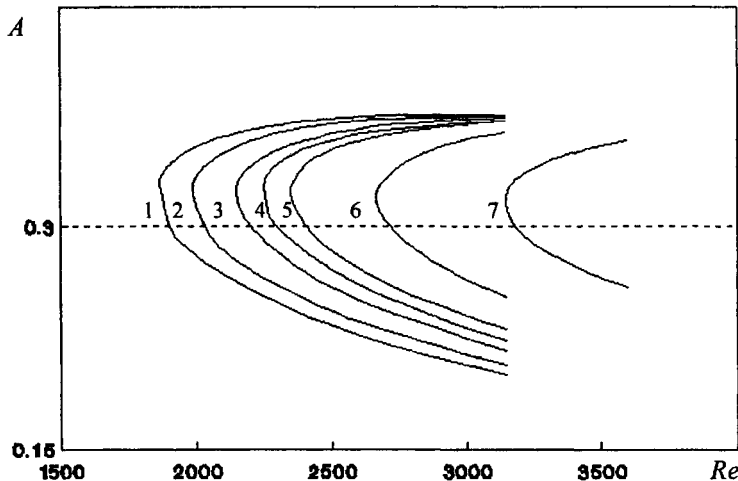


Fig. 5.23 The neutral curves for the wave number  $A$  as a function of the Reynolds number  $Re$  in the liquid 1 ( $\varepsilon = 10$ ,  $m/b = 0$ ,  $\theta_1 = \theta$ ,  $\theta_2 = 0$ ):  
1)  $\theta = 0.5$ ; 2)  $\theta = 0.3$ ; 3)  $\theta = 0.1$ ; 4)  $\theta = 0.0$ ; 5)  $\theta = -0.1$ ; 6)  $\theta = -0.3$ ; 7)  $\theta = -0.5$ .

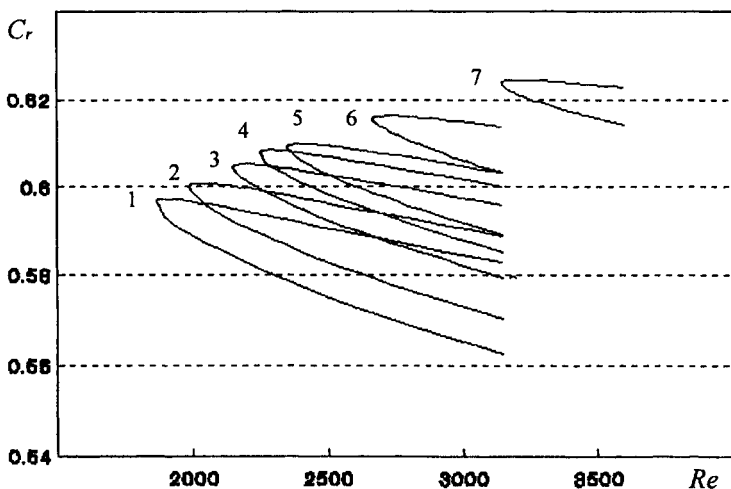


Fig. 5.24. The neutral curves for the phase velocity  $C_r$  as a function of the Reynolds number  $Re$  in the liquid 1 ( $\varepsilon = 10$ ,  $m/b = 0$ ,  $\theta_1 = \theta$ ,  $\theta_2 = 0$ ):  
1)  $\theta = 0.5$ ; 2)  $\theta = 0.3$ ; 3)  $\theta = 0.1$ ; 4)  $\theta = 0.0$ ; 5)  $\theta = -0.1$ ; 6)  $\theta = -0.3$ ; 7)  $\theta = -0.5$ .

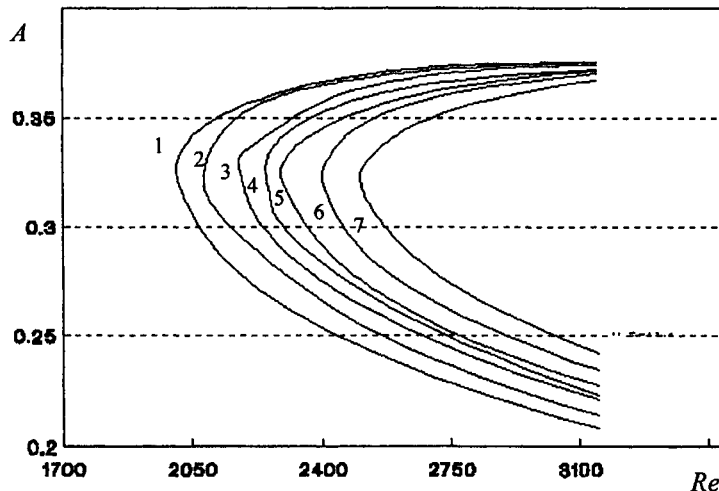


Fig. 5.25 The neutral curves for the wave number  $A$  as a function of the Reynolds number  $Re$  in the liquid I ( $\varepsilon = 10$ ,  $b/m = 1$ ,  $\theta_1 = \theta_2 = \theta$ ):  
 1)  $\theta = 0.5$ ; 2)  $\theta = 0.3$ ; 3)  $\theta = 0.1$ ; 4)  $\theta = 0.0$ ; 5)  $\theta = -0.1$ ; 6)  $\theta = -0.3$ ; 7)  $\theta = -0.5$ .

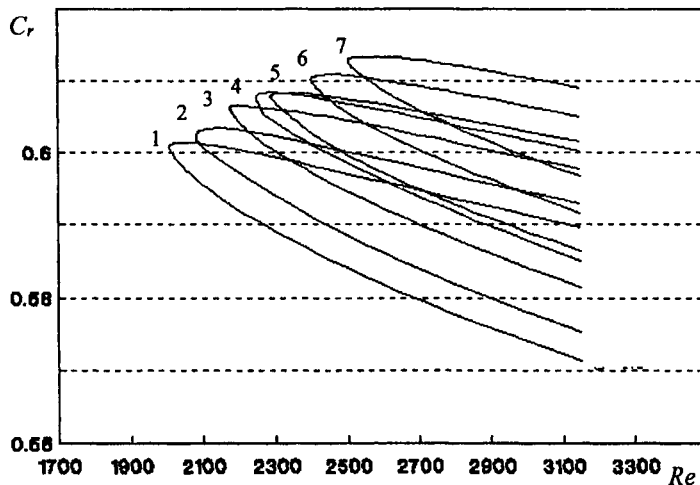


Fig. 5.26. The neutral curves for the phase velocity  $C_r$  as a function of the Reynolds number  $Re$  in the liquid I ( $\varepsilon = 10$ ,  $b/m = 1$ ,  $\theta_1 = \theta_2 = \theta$ ):  
 1)  $\theta = 0.5$ ; 2)  $\theta = 0.3$ ; 3)  $\theta = 0.1$ ; 4)  $\theta = 0.0$ ; 5)  $\theta = -0.1$ ; 6)  $\theta = -0.3$ ; 7)  $\theta = -0.5$ .

The experimental studies [37-39] of mass transfer in systems with intensive interphase mass transfer between two liquids show in number of cases a higher mass transfer rate compared with that predicted by the linear theory of mass transfer. So far this has been explained with the Marangoni effect, i. e. the creation of interfacial tension gradients as a result of temperature or concentration heterogeneity on the phase boundary. The interfacial tension gradient induces secondary flows directed tangentially to the phase boundary. They change the velocity profiles in the boundary layer. Thus, the mass transfer rate is directly effected. In the case of hydrodynamic instability of the new profiles, the flow spontaneously evolves from laminar into turbulent and the mass transfer rate drastically increases.

The results obtained show that at the conditions of intensive interphase mass transfer high mass fluxes induce secondary flows directed normally to the phase boundary. These secondary flows change the velocity profiles, consequentially they change the kinetics of mass transfer (non-linear mass transfer) and the hydrodynamic stability of the flow. This is a radically different mechanism of the intensive interphase mass transfer influence on the kinetics of the mass transfer and the hydrodynamic stability in liquid-liquid systems.

The theoretical results obtained allow the comparative analysis of the influence of the Marangoni effect and the effect of the non-linear mass transfer on the mass transfer rate and the hydrodynamic stability of systems with intensive interphase mass transfer.

#### 5.4.4. Gas-liquid film flow systems

The results obtained for gas-liquid and liquid-liquid systems show that the stability of the flow in the boundary layer depends considerably on the interface velocity. This velocity is a result of superposed influence of the flux of momentum (hydrodynamic interaction between the two phases) and the mass flux (inducing of parallel secondary flows) through the phase boundary. Based on the mentioned above, the study of the influence of the normal and the tangential components of the interface velocity on the hydrodynamic stability of the velocity profiles has been demonstrated [40]. For the practically interesting gas-liquid film flow systems this compound crossed effect can be observed in details.

The non-linear mass transfer at the conditions of intensive interphase mass transfer between gas and liquid film flow has been the subject of numerical and asymptotic analyses (1.4.1). The results show that the above mentioned crossed influence manifests itself, when the diffusion resistance is localized in the gas phase. In this case the velocity distribution in the gas can be expressed using the following similarity variables:

$$\tilde{u} = \tilde{u}_0 f(\xi), \quad \tilde{v} = 0.5 \left( \frac{\tilde{u}_0 \tilde{v}}{x} \right)^{0.5} (\xi f' - f), \quad \xi = y \left( \frac{\tilde{u}_0}{\tilde{v} x} \right)^{0.5}, \quad (5.119)$$

where  $f(\xi)$  is the solution of the problem

$$2f''' - ff'' = 0, \\ f(0) = a, \quad f'(0) = b, \quad f''(0) = c. \quad (5.120)$$

The associated set of initial conditions has been obtained in 1.4.1 and presented in Table 5.8, where the parameter  $k$  is determined by the expression:

$$k = \lim_{\xi \rightarrow \infty} (\xi f' - f). \quad (5.121)$$

Table 5.8.

Initial values of  $f$ , its derivates and parameter  $k$  (in the gas phase,  $\varepsilon = 1$ ,  $\theta_1 = 0.15$ ,  $\theta_3 = \theta$ )

$\theta$	$f(0)$	$f'(0)$	$f''(0)$	$k$
-0.3	0.30411	0.225	0.39250	0.702
-0.2	0.18788	0.225	0.36000	0.871
-0.1	0.08729	0.225	0.33240	1.023
0.0	0.0	0.225	0.30890	1.158
0.1	-0.07632	0.225	0.28900	1.278
0.2	-0.14399	0.225	0.27175	1.387
0.3	-0.20536	0.225	0.25650	1.486

The linear analysis of the stability of the velocity profiles  $f'(0)$  was carried out in the cases [41], where the hydrodynamic interaction between the gas and liquid film flows (see 1.4.1) is determined by the parameters

$$\varepsilon = (\tilde{v}/\tilde{D})^{1/2} = 1, \quad \theta_1 = \frac{u_0}{\tilde{u}_0} = 0.15, \quad \theta_3 = -\theta\varepsilon = \frac{M}{\tilde{\rho}_0^*} (\tilde{c}_0 - \chi c_0). \quad (5.122)$$

The initial conditions associated to (5.120) were obtained considering (5.122) for different values of  $\theta$  (Table 5.8) and they permit us to solve the problem (5.120) as a problem of Cauchy as well as the introduction of  $f(\xi)$  into the Orr-Sommerfeld equation. The Orr-Sommerfeld equation was solved analogously to that one in 5.4.1. The neutral curves and critical Reynolds numbers for different values of the dimensionless phase velocity ( $C_r$ ) and length number ( $A$ ) are obtained.

The neutral curves  $(Re, A)$  and  $(Re, C_r)$  are shown on Fig. 5.27 and Fig. 5.28. They allow us to obtain the critical Reynolds numbers  $(Re_{cr})$ , which are presented in Table 5.8. These results show the fact that the stability of the flow decreases with the rise of the parameter  $\theta$ .

The results presented in Table 5.9 and those shown in Tables 5.2, 5.5, 5.7 allow to study the influence of the tangential interface velocity component ( $f'(0)$ ) on the stability of the flow  $(Re_{cr})$ . These results are shown on Figure 5.29 at  $\theta = \text{const}$ . They clearly present a well-pronounced dependence, i. e. the rise of the interface velocity leads to stabilizing the flow.

The significant influence of the normal velocity at the interface  $f(0)$  upon the stability of the flow was shown in 5.4.1. – 5.4.3. Having this in mind it is of great interest to

find the dependence of  $Re_{cr}$  from  $f'(0)$  at  $f(0) = const$ . The results displayed on Fig. 5.30 demonstrate a dear-cut correlation.

Table 5.9.

Values of the critical Reynolds numbers  $Re_{cr}$ , wave velocities  $C_r$ , wave numbers  $A$  and  $C_{r\min}$ ,  $A_{r\min}$  obtained in the gas phase at the conditions  $\varepsilon = 1$ ,  $\theta_1 = 0.15$ ,  $\theta_3 = \theta$ .

$\theta$	$Re_{cr}$	$A$	$C_r$	$A_{r\min}$	$C_{r\min}$
-0.3	3760	0.280	0.4566	0.310	0.4576
-0.2	2484	0.290	0.4748	0.328	0.4760
-0.1	1714	0.305	0.4922	0.347	0.4928
0.0	1239	0.310	0.5064	0.361	0.5083
0.1	941	0.320	0.5200	0.376	0.5219
0.2	743	0.325	0.5311	0.390	0.5338
0.3	605	0.340	0.5429	0.402	0.5449

The results obtained so far allow to obtain the dependence of the critical Reynolds number  $Re_{cr}$  from the normal velocity component on the interface  $f(0)$  at the condition of constant value of tangential interface velocity component  $f'(0)$ . These results are shown on Fig. 5.31 and they express a continuous rise of the flow stability in the transition from injection to suction in the laminar boundary layer.

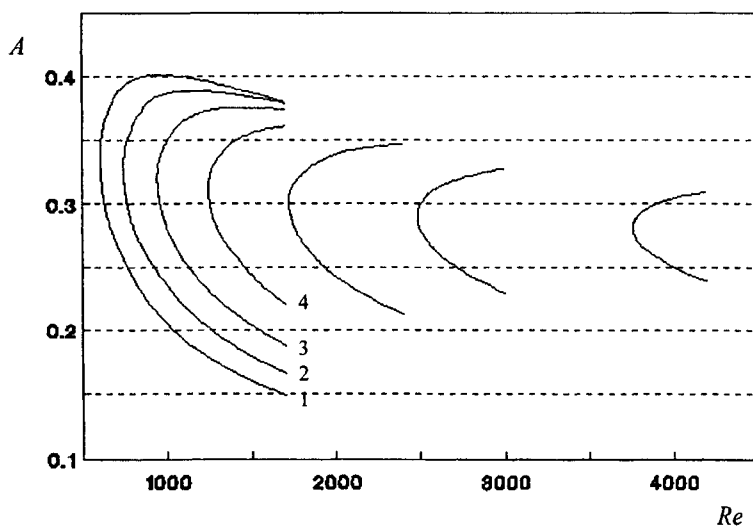


Fig. 5.27. The neutral curves for the wave number  $A$  as a function of the Reynolds number  $Re$  in the gas phase ( $\varepsilon = 1$ ). 1)  $\theta = 0.3$ ; 2)  $\theta = 0.2$ ; 3)  $\theta = 0.1$ ; 4)  $\theta = 0.0$ ; 5)  $\theta = -0.1$ ; 6)  $\theta = -0.2$ ; 7)  $\theta = -0.3$ .

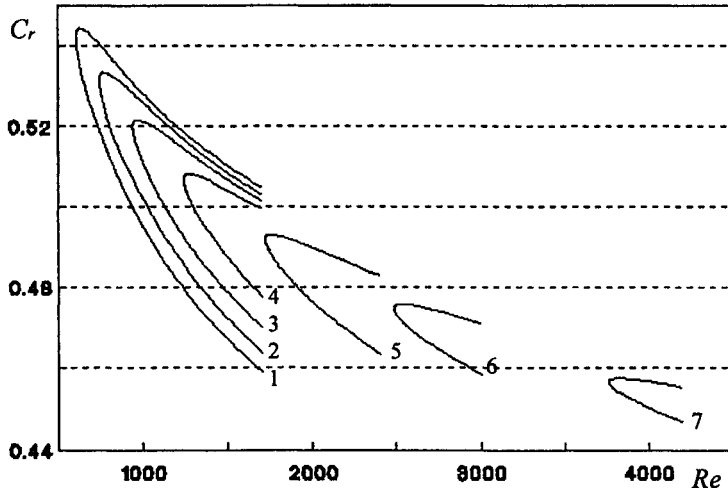


Fig. 5.28. The neutral cures for the phase velocity  $C_r$ , as a function of the Reynold number  $Re$  in gas phase ( $\varepsilon=1$ ): 1)  $\theta=0.3$ ; 2)  $\theta=0.2$ ; 3)  $\theta=0.1$ ; 4)  $\theta=0.0$ ; 5)  $\theta=-0.1$ ; 6)  $\theta=-0.2$ ; 7)  $\theta=-0.3$ .

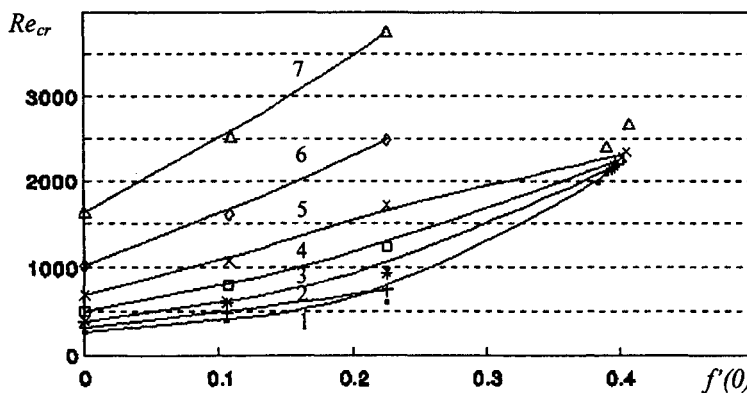


Fig. 5.29. The influence of the tangential interface velocity component ( $f'(0)$ ) on the stability of the flow ( $Re_{cr}$ ): 1)  $\theta=0.3$ ; 2)  $\theta=0.2$ ; 3)  $\theta=0.1$ ; 4)  $\theta=0.0$ ; 5)  $\theta=-0.1$ ; 6)  $\theta=-0.2$ ; 7)  $\theta=-0.3$ .

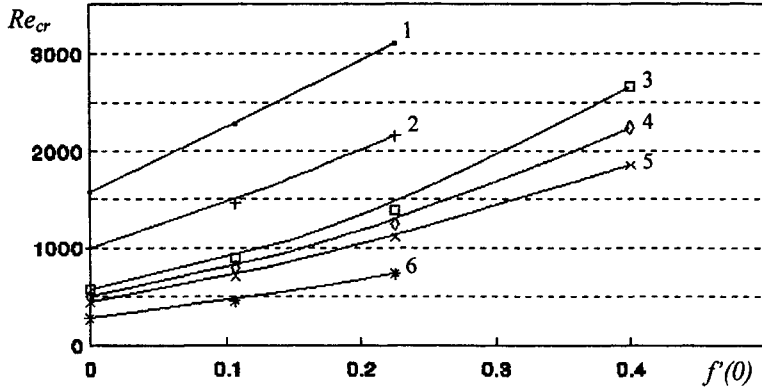


Fig. 5.30. The dependence of  $Re_{cr}$  on  $f'(0)$  at  $f(0) = \text{const}$ : 1)  $f(0)=0.25$ ; 2)  $f(0)=0.15$ ; 3)  $f(0)=0.03$ ; 4)  $f(0)=0.0$ ; 5)  $f(0)=-0.03$ ; 6)  $f(0)=-0.15$ .

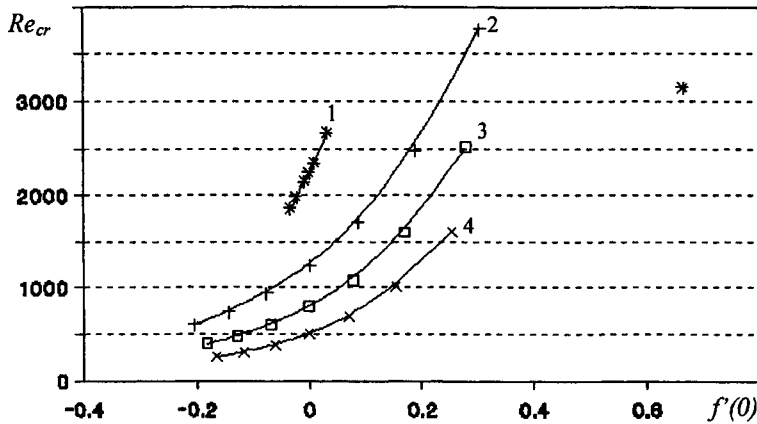


Fig. 5.31. The dependence of the critical Reynolds number  $Re_{cr}$  on the normal component of the velocity on the interface  $f(0)$  at the condition of constant value of the tangential interface velocity component  $f'(0)$ : 1)  $f'(0)=0.40$ ; 2)  $f'(0)=0.23$ ; 3)  $f'(0)=0.11$ ; 4)  $f'(0)=0.0$ .

The results obtained in 5.4.1–5.4.4 allow to draw some basic conclusions:

1. The flows in boundary layers with increasing velocity in the depth of the fluid ("Blasius flow") are characterized with hydrodynamic stability, which increases with the rise

of the tangential velocity component on the interface and the decrease of its normal component in the transition from "suction" ( $v < 0, f(0) > 0$ ) to "injection" ( $v > 0, f(0) < 0$ ) in the laminar boundary layer. The hydrodynamic stability of this type of flows in the boundary layer depends "independently" on the normal component of the velocity at the interface and on the tangential components of the interface velocity.

2. The flows in the boundary layers with decreasing velocity in the depth of the fluid ("Couette flow") are in practice globally stable, and they are not affected by changes in the normal and tangential component of the velocity on the interface.

3. The systems with intensive interphase mass transfer are characterized with the fact that the kinetics of mass transfer does not follow the linear theory of the mass transfer and the obvious changes in the hydrodynamic stability are observed. These effects have been explained quite often [37-39, 43] with the Marangoni effect, i. e. the induction of tangential secondary flow on the phase boundary. The investigations of the kinetics of mass transfer in the systems with intensive interphase mass transfer [33] and their hydrodynamic stability show that the same effects can be explained with the influence of the non-linear mass transfer, i. e. the induction of normal secondary flows on the phase boundary. Consequently, it is possible to compare the Marangoni effect with the effect of the non-linear mass transfer.

#### 5.4.5. Effect of concentration

It has been shown in 1.5.1. and 1.5.2. that the large concentration gradients in systems with intensive interphase mass transfer induce secondary flows on the phase boundary. The velocity of these flows depends on the concentration and its gradient:

$$v = \frac{MD\rho^*}{\rho_0^*} \left[ \frac{\partial}{\partial y} \left( \frac{c}{\rho} \right) \right]_{y=0}. \quad (5.123)$$

The influence of the concentration and its gradient on the velocity distribution in the laminar boundary layer has been assumed. This gives opportunity to study the hydrodynamic stability of the velocity profiles.

The flow in a laminar boundary layer will be examined as it was done in 1.5.1:

$$\rho \left( u \frac{\partial u}{\partial x} + v \frac{\partial u}{\partial y} \right) = \frac{\partial}{\partial y} \left( \mu \frac{\partial u}{\partial y} \right),$$

$$\frac{\partial}{\partial x} (\rho u) + \frac{\partial}{\partial y} (\rho v) = 0,$$

$$\rho \left( u \frac{\partial c}{\partial x} + v \frac{\partial c}{\partial y} \right) = \frac{\partial}{\partial y} \left( \rho D \frac{\partial c}{\partial y} \right);$$

$$x = 0, \quad u = u_0, \quad c = c_0;$$

$$y = 0, \quad u = 0, \quad v = - \frac{MD\rho^*}{\rho_0^*} \frac{\partial}{\partial y} \left( \frac{c}{\rho} \right), \quad c = c^*;$$

$$y \rightarrow \infty, \quad u = u_0, \quad c = c_0. \quad (5.124)$$

The linear stability analysis [44] considers a non-stationary flow  $(U, V, P)$ , obtained as a combination of a basic stationary flow  $(u, v)$  and two-dimensional periodic disturbances  $(u_l, v_l, p_l)$  with small amplitudes  $\omega$ :

$$\begin{aligned} U(x, y, t) &= u(x, y) + \omega u_l(x, y, t), \\ V(x, y, t) &= v(x, y) + \omega v_l(x, y, t), \\ P(x, y, t) &= \omega p_l(x, y, t), \\ C(x, y, t) &= c(x, y) + \omega c_l(x, y, t). \end{aligned} \quad (5.125)$$

The non-stationary flow  $(U, V, P)$ , thus obtained, satisfies the full system of Navier-Stokes equations:

$$\begin{aligned} \rho \frac{\partial U}{\partial t} + \rho U \frac{\partial U}{\partial x} + \rho V \frac{\partial U}{\partial y} &= -\frac{\partial P}{\partial x} + \frac{\partial}{\partial x} \left( \mu \frac{\partial U}{\partial x} \right) + \frac{\partial}{\partial y} \left( \mu \frac{\partial U}{\partial y} \right), \\ \rho \frac{\partial V}{\partial t} + \rho U \frac{\partial V}{\partial x} + \rho V \frac{\partial V}{\partial y} &= -\frac{\partial P}{\partial y} + \frac{\partial}{\partial x} \left( \mu \frac{\partial V}{\partial x} \right) + \frac{\partial}{\partial y} \left( \mu \frac{\partial V}{\partial y} \right), \\ \frac{\partial}{\partial x} (\rho U) + \frac{\partial}{\partial y} (\rho V) &= 0, \end{aligned} \quad (5.126)$$

with the following set of boundary conditions:

$$\begin{aligned} x = 0, \quad U &= u_0, \quad V = 0, \quad P = p_0; \\ y = 0, \quad U &= 0, \quad V = -\theta_0 \frac{\rho_0 D_0}{\Delta c_0} \frac{\partial}{\partial y} \left( \frac{c}{\rho} \right); \\ y \rightarrow \infty, \quad U &= u_0, \quad V = 0, \quad P = p_0, \end{aligned} \quad (5.127)$$

where

$$\theta_0 = \left( \frac{D \rho \Delta c_0}{\rho_0 \rho_0 D_0} \right)_{y=0}, \quad \Delta c_0 = c^* - c_0. \quad (5.128)$$

Linear approximations can be introduced into (5.126)-(5.128) for the dependencies of the density, viscosity and diffusivity on the concentration:

$$\rho = \rho_0(1 + \bar{\rho}\bar{c}), \quad \mu = \mu_0(1 + \bar{\mu}\bar{c}), \quad D = D_0(1 + \bar{D}\bar{c}), \quad \bar{c} = \frac{c - \theta_0 c_0 - c_0}{\Delta c_0}, \quad (5.129)$$

while the parameters  $\bar{\rho}$ ,  $\bar{\mu}$  and  $\bar{D}$  are small.

Upon consequential introduction of (5.124), (5.125) and (5.129) into (5.126) and (5.127) and after long transformations using the linear approximations for the small parameters  $\theta_0, \omega, \bar{\rho}, \bar{\mu}$  and  $\bar{D}$  a system of equations describing the evolution of the superposed periodic flow (disturbance) is obtained:

$$\begin{aligned} \frac{\partial u_I}{\partial t} + u \frac{\partial u_I}{\partial x} + v \frac{\partial u_I}{\partial y} + u_I \frac{\partial u}{\partial x} + v_I \frac{\partial u}{\partial y} &= -\frac{1}{\rho_0} \frac{\partial p_I}{\partial x} + v_0 \left( \frac{\partial^2 u_I}{\partial x^2} + \frac{\partial^2 u_I}{\partial y^2} \right), \\ \frac{\partial v_I}{\partial t} + u \frac{\partial v_I}{\partial x} + v \frac{\partial v_I}{\partial y} + u_I \frac{\partial v}{\partial x} + v_I \frac{\partial v}{\partial y} &= -\frac{1}{\rho_0} \frac{\partial p_I}{\partial y} + v_0 \left( \frac{\partial^2 v_I}{\partial x^2} + \frac{\partial^2 v_I}{\partial y^2} \right), \\ \frac{\partial u_I}{\partial x} + \frac{\partial v_I}{\partial y} &= 0; \\ x = 0, \quad u_I = 0, \quad v_I = 0, \quad p_I = p_0; \\ y = 0, \quad u_I = 0, \quad v_I = 0; \\ y \rightarrow \infty, \quad u_I = 0, \quad v_I = 0, \quad p_I = p_0. \end{aligned} \tag{5.130}$$

It includes no equations for the concentration ( $c_I$ ) in (5.130) because at the linear approximation for the small parameters  $\theta_0$  and  $\omega$  the disturbances do not influence the velocity ( $u_I, v_I$ ).

The periodic disturbances could be considered as a running wave with a variable amplitude:

$$\begin{aligned} u_I &= G'(y) \exp i(\alpha x - \beta t), \\ v_I &= -i\alpha G(y) \exp i(\alpha x - \beta t), \end{aligned} \tag{5.131}$$

where  $G(y)$  is the amplitude of the disturbance (regarding  $y$ );  $\alpha$  and  $\beta/\alpha$  are its wavenumber and phase velocity respectively (see (5.84)).

It is clearly seen that the amplitude of the disturbance decreases when  $\beta_I < 0$  ( $c_I < 0$ ), i.e. the basic flow is stable. At  $\beta_I > 0$  ( $c_I > 0$ ) the flow is unstable.

Hence, from (5.130) and (5.131) an equation of Orr-Sommerfeld type is directly obtained (for almost parallel flow):

$$\begin{aligned} \left( u - \frac{\beta}{\alpha} \right) (G'' - \alpha^2 G) - \frac{\partial^2 u}{\partial y^2} G &= -\frac{i v_0}{\alpha} (G'''' - 2\alpha^2 G'' + \alpha^4 G) + \\ + \frac{i}{\alpha} \left[ v G''' + \left( \frac{\partial^2 u}{\partial x \partial y} - \alpha^2 v \right) G' \right]; \\ y = 0, \quad G = 0, \quad G' = 0; \\ y \rightarrow \infty, \quad G = 0, \quad G' = 0. \end{aligned} \tag{5.132}$$

The analysis of stability requires the introduction of the basic flow velocity into (5.132). In the case of gases one is obtained:

$$\begin{aligned} u(x, y) &= u_0 \frac{\Phi'(\eta)}{\varphi}, \quad v = \frac{u_0 \delta}{2x} \frac{\eta \Phi'(\eta) - \Phi(\eta)}{\varphi}, \\ \eta &= \frac{y}{\delta}, \quad \delta = \sqrt{\frac{D_0 x}{u_0}}, \quad \varphi = 1 + \bar{\rho} F(\eta), \quad F(\eta) = \frac{c(x, y) - c_0}{c^* - c_0}, \\ G(y) &= \gamma(\eta), \quad \bar{\rho} \ll 1. \end{aligned} \quad (5.133)$$

The introduction of (5.133) into (5.132) leads to

$$\begin{aligned} &\left( \frac{\Phi'}{\varphi} - C \right) \left( \gamma'' - A_0^2 \gamma \right) - \left( \frac{\Phi''}{\varphi} - 2\bar{\rho} F' \frac{\Phi''}{\varphi^2} - \bar{\rho} F'' \frac{\Phi'}{\varphi^2} \right) \gamma = \\ &= -\frac{i}{A_0 Re_0} \left( \gamma'^v - 2A_0^2 \gamma'' + A_0^4 \gamma \right) + \frac{i}{2\varepsilon^2 A_0 Re_0} \frac{\eta \Phi' - \Phi}{\varphi} \gamma''' - \\ &- \frac{i}{2\varepsilon^2 A_0 Re_0} \left( \frac{\eta \Phi'' + \Phi''}{\varphi} - \frac{2\bar{\rho} \eta F' \Phi'' + \bar{\rho} \eta F'' \Phi' + \bar{\rho} F' \Phi'}{\varphi^2} + A_0^2 \frac{\eta \Phi' - \Phi}{\varphi} \right) \gamma', \end{aligned} \quad (5.134)$$

where

$$A = \alpha \delta, \quad C = \frac{\beta}{\alpha u_0} = C_r + iC_i, \quad Re_0 = \frac{u_0 \delta}{\nu_0}. \quad (5.135)$$

The solution of (5.133) has been accomplished as it was shown in [41], where the functions  $\Phi(\eta)$  and  $F(\eta)$  and their derivatives are taken from 1.5.2.

The neutral curves of stability are plotted on Figs. 5.32-5.34. The critical Reynolds numbers  $Re_{cr}$ , the corresponding wave velocities  $C_r$ , and the wave numbers  $A$  are obtained.  $C_{r\min}$  and  $A_{\min}$  have also been obtained from these results. Let  $C_{r\min}$  and  $A_{\min}$  denote the minimum values of the wave velocities and wave number at which the flow is stable at any Reynolds number  $Re$  respectively. They are shown in Table 5.10 in dependence on the concentration of the transferred substance ( $\bar{\rho}$  and  $\bar{\mu}$ ) and its gradient ( $\theta$ ), where  $Re = 1.72 Re_0$ .

The results obtained show that the effect of the concentration dependencies of the viscosity ( $\bar{\mu}$ ) is analogous to that of the large concentration gradient ( $\theta_0$ ), while the change in the density ( $\bar{\rho}$ ) has an insignificant effect and this dependence is not monotonous.

In the case of liquids the basic flow velocity is introduced into (5.132) as it has been defined in 1.5.2.:

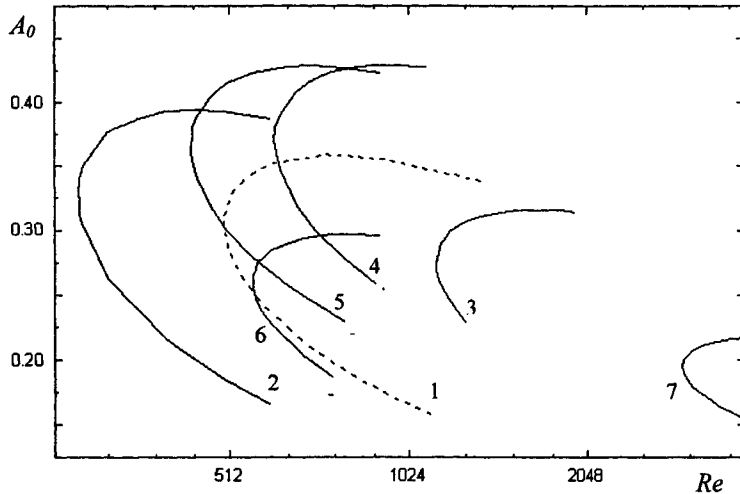


Fig. 5.32. The neutral curves of stability ( $Re$ ,  $A_0$ ) for flows of gases in the laminar boundary layer under the conditions of high concentrations:

- 1)  $\theta_0 = 0, \bar{\rho} = 0, \bar{\mu} = 0;$
- 2)  $\theta_0 = 0, \bar{\rho} = 0, \bar{\mu} = 0.2;$
- 3)  $\theta_0 = 0, \bar{\rho} = 0, \bar{\mu} = -0.2;$
- 4)  $\theta_0 = 0, \bar{\rho} = 0.15, \bar{\mu} = 0;$
- 5)  $\theta_0 = 0, \bar{\rho} = 0.15, \bar{\mu} = 0.2;$
- 6)  $\theta_0 = 0, \bar{\rho} = -0.15, \bar{\mu} = 0;$
- 7)  $\theta_0 = 0, \bar{\rho} = -0.15, \bar{\mu} = -0.2.$

$$\begin{aligned}
 u(x, y) &= u_0 \frac{\Phi'_l(\eta_l)}{\varphi}, \quad v = \frac{u_0 \delta_l}{2x} \frac{\eta_l \Phi'_l(\eta_l) - \Phi_l(\eta_l)}{\varphi}, \\
 \eta_l &= y \sqrt{\frac{u_0}{v_0 x}}, \quad \delta_l = \sqrt{\frac{v_0 x}{u_0}}, \quad \varphi = I + \bar{\rho} F_l(\eta_l), \\
 G(y) &= \gamma_l(\eta_l),
 \end{aligned} \tag{5.136}$$

where  $\Phi_l(\eta_l)$  and  $F_l(\eta_l)$  and their derivatives are obtained solving (5.124). The introduction of (5.136) into (5.132) leads to an equation of Orr-Sommerfeld type, which can be obtained directly from (5.134) using the substitutions:

$$\begin{aligned}
 \Phi(\eta) &= \Phi_l(\eta_l), \quad F(\eta) = F_l(\eta_l), \quad \gamma(\eta) = \gamma_l(\eta_l), \\
 \eta &= \eta_l, \quad A_0 = A_l = \alpha \delta_l, \quad Re_0 = Re_l = \frac{u_0 \delta_l}{v_0}, \quad \varepsilon = 1.
 \end{aligned} \tag{5.137}$$

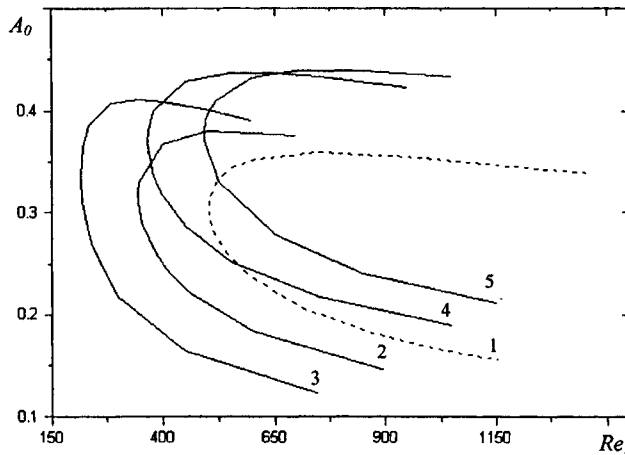


Fig. 5.33. The neutral curves of stability ( $Re$ ,  $A_0$ ) for flows of gases in the laminar boundary layer under the conditions of high concentrations and large concentration gradients: 1)  $\theta_0 = 0, \bar{\rho} = 0, \bar{\mu} = 0$ ; 2)  $\theta_0 = 0.3, \bar{\rho} = 0, \bar{\mu} = 0$ ; 3)  $\theta_0 = 0.3, \bar{\rho} = 0, \bar{\mu} = 0.2$ ; 4)  $\theta_0 = 0.3, \bar{\rho} = 0.15, \bar{\mu} = 0$ ; 5)  $\theta_0 = 0.3, \bar{\rho} = 0.15, \bar{\mu} = 0.2$ .

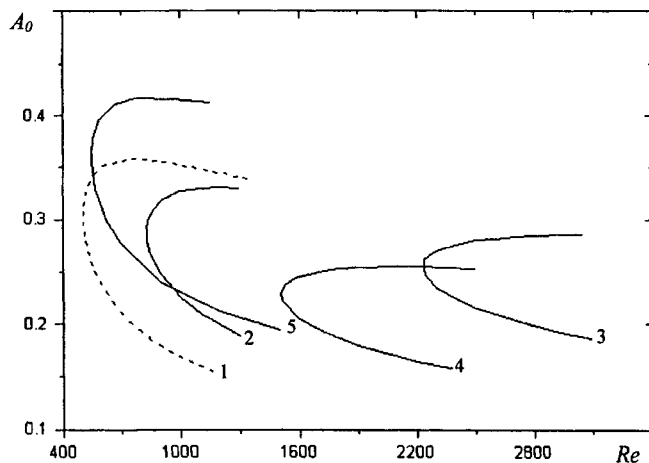


Fig. 5.34. The neutral curves of stability ( $Re$ ,  $A_0$ ) for flows of gases in the laminar boundary layer under the conditions of high concentrations and large concentration gradients: 1)  $\theta_0 = 0, \bar{\rho} = 0, \bar{\mu} = 0$ ; 2)  $\theta_0 = -0.3, \bar{\rho} = 0, \bar{\mu} = 0$ ; 3)  $\theta_0 = 0.3, \bar{\rho} = 0, \bar{\mu} = -0.2$ ; 4)  $\theta_0 = -0.3, \bar{\rho} = -0.15, \bar{\mu} = 0$ ; 5)  $\theta_0 = -0.3, \bar{\rho} = 0.15, \bar{\mu} = 0.2$ .

Table 5.10.

Values of the critical Reynolds numbers  $Re_{cr}$ , the corresponding wave velocities  $C_r$ , the wave numbers  $A$  and  $C_{r\min}, A_{\min}$  obtained at high concentrations (effects due to density ( $\bar{\rho} \neq 0$ ) and viscosity ( $\bar{\mu} \neq 0$ )) and large concentration gradients ( $\theta_0 \neq 0$ ) in gases.

No.	$\theta$	$\bar{\rho}$	$\bar{\mu}$	$Re_{cr}$	$A_{\max}$	$C_{\max}$
1		0.0	0.0	501	0.356	0.407
2		0.0	0.2	285	0.394	0.445
3		-0.2		1135	0.315	0.352
4	0.0	0.15	0.0	608	0.429	0.356
5			0.2	443	0.428	0.373
6		-0.15	0.0	559	0.296	0.403
7			-0.2	2972	0.217	0.289
8		0.0	0.0	1619	0.301	0.331
9	-0.3		-0.2	2238	0.286	0.312
10		-0.15	0.0	1508	0.255	0.332
11		0.15	0.2	547	0.418	0.361
12		0.0	0.0	345	0.380	0.431
13	0.3		0.2	215	0.411	0.467
14		0.15	0.0	491	0.439	0.369
15			0.2	367	0.437	0.384

Table 5.11.

Values of the critical Reynolds numbers  $Re_{cr}$ , the corresponding wave velocities  $C_r$ , the wave numbers  $A$  and  $C_{r\min}, A_{\min}$  obtained at the high concentrations (effects due to density ( $\bar{\rho} \neq 0$ ), viscosity ( $\bar{\mu} \neq 0$ ) and diffusivity ( $\bar{D} \neq 0$ )) and large concentration gradients ( $\theta_0 \neq 0$ ) in liquids.

No.	$\theta$	$\bar{\rho}$	$\bar{\mu}$	$\bar{D}$	$Re_{cr}$	$A_{\max}$	$C_{\max}$
1	0.0	0.0	0.0	0.0	501	0.356	0.407
2	0.3	0.0	0.0	0.0	422	0.367	0.418
3	-0.1	0.0	0.0	0.0	564	0.351	0.398
4	0.0	0.15	0.0	0.0	556	0.518	0.358
5	0.0	-0.15	0.0	0.0	1073	0.102	0.392
6	0.0	0.0	0.2	0.0	373	0.416	0.414
7	0.0	0.0	-0.2	0.0	742	0.300	0.395
8(□)	0.0	0.0	0.0	0.3	502	0.357	0.406
9(Δ)	0.0	0.0	0.0	-0.3	501	0.357	0.406

The solution of this equation is performed analogously to that of (5.134), while  $\Phi_i(\eta_i)$  and  $F_i(\eta_i)$  and their derivatives have been obtained in 1.5.2. The neutral curves of stability are shown on Fig. 5.35. The critical Reynolds numbers  $Re_{cr}$ , the corresponding wave velocities  $C_r$ , and the wave numbers  $A$  are obtained.  $C_{r\min}$  and  $A_{\min}$  are also obtained from

these results. They are shown in Table 5.11 in dependence on the concentration of transferred substance ( $\bar{\rho}$ ,  $\bar{\mu}$  and  $\bar{D}$ ) and its gradient ( $\theta_0$ ), where  $Re = 1.72 Re_1$ .

The neutral curves of stability for flows of gases and liquids in the laminar boundary layer under the conditions of high concentrations and large concentration gradients are shown on Figures 5.32-5.35. The scatter graphs on Fig. 5.35 having the same locus as the dotted line (1) are obtained in the case where the diffusivity depends on the concentration.

Data plotted on Figures 5.32-5.35 allow to determine the critical Reynolds numbers ( $Re_{cr}$ ),

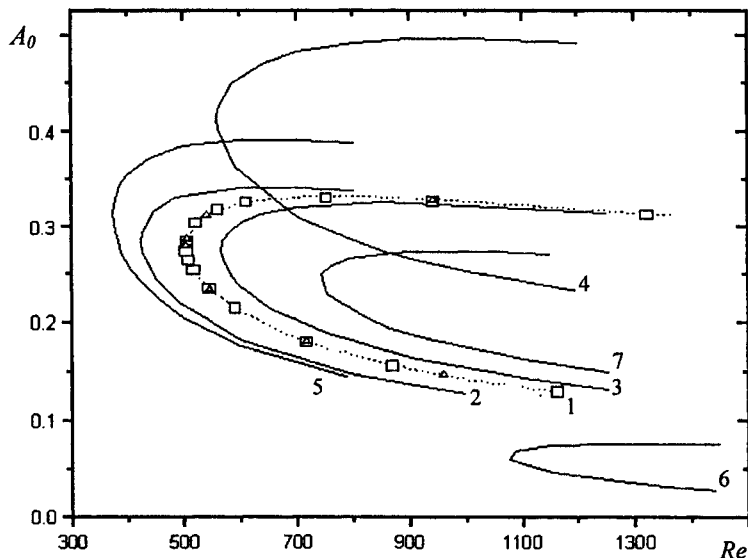


Fig. 5.35. The neutral curves of stability ( $Re_{cr}, A_0$ ) for flows of liquids in the laminar boundary layer under the conditions of high concentrations:

- 1)  $\theta_0 = 0, \bar{\rho} = 0, \bar{\mu} = 0, \bar{D} = 0;$
- 2)  $\theta_0 = 0.3, \bar{\rho} = 0, \bar{\mu} = 0, \bar{D} = 0;$
- 3)  $\theta_0 = -0.1, \bar{\rho} = 0, \bar{\mu} = 0, \bar{D} = 0;$
- 4)  $\theta_0 = 0, \bar{\rho} = 0.15, \bar{\mu} = 0, \bar{D} = 0;$
- 5)  $\theta_0 = 0, \bar{\rho} = 0, \bar{\mu} = 0.2, \bar{D} = 0;$
- 6)  $\theta_0 = 0, \bar{\rho} = -0.15, \bar{\mu} = 0, \bar{D} = 0;$
- 7)  $\theta_0 = 0, \bar{\rho} = 0, \bar{\mu} = -0.2, \bar{D} = 0;$
- $\square)$   $\theta_0 = 0, \bar{\rho} = 0, \bar{\mu} = 0, \bar{D} = 0.3;$
- $\Delta)$   $\theta_0 = 0, \bar{\rho} = 0, \bar{\mu} = 0, \bar{D} = -0.3.$

presented in Tables 5.10 and 5.11. They give the opportunity to define (Figures 5.36, 5.37) the dependence of  $Re_{cr}$  on the parameters characterizing the concentration dependencies on the density ( $\bar{\rho}$ ), viscosity ( $\bar{\mu}$ ), diffusivity ( $\bar{D}$ ) and large concentration gradients ( $\theta_0$ ).

The data presented in Tables 5.10, 5.11 and on Figs. 5.36 and 5.37 show that in gases and liquids:

- the stability of flows ( $Re_{cr}$ ) increases if the density depends on concentration ( $\bar{\rho} \neq 0$ );
- the decrease of the concentration gradient ( $\theta_0$ ) leads to a decrease of the stability ( $Re_{cr}$ );
- in the cases when the increase of the concentration leads to increase (decrease) of viscosity, i. e.  $\bar{\mu} > 0$  ( $\bar{\mu} < 0$ ), one can observe increase of stability, i.e. the high concentrations lead to high (low) mass transfer rates in gases;
- change in diffusivity ( $\bar{D}$ ) does not influence the stability (scattered plots on Fig. 5.35);
- additivity of the separated effects is observed.

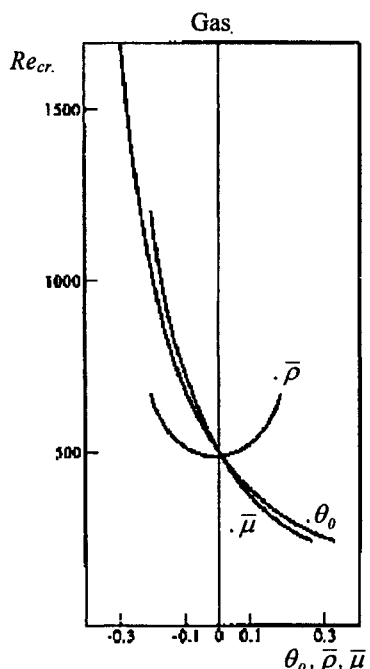


Fig. 5.36. Dependence of the critical Reynolds numbers ( $Re_{cr}$ ) on the high concentrations through the viscosity ( $\bar{\mu}$ ) and density ( $\bar{\rho}$ ), and the influence of the large concentration gradients ( $\theta_0$ ) in gases.

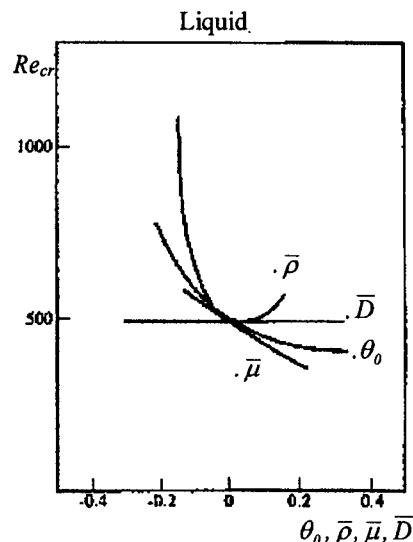


Fig. 5.37. Dependence of the critical Reynolds numbers ( $Re_{cr}$ ) on the high concentrations through the viscosity ( $\bar{\mu}$ ) and density ( $\bar{\rho}$ ) and diffusivity ( $\bar{D}$ ), and the influence of the large concentration gradients ( $\theta_0$ ) in liquids.

#### 5.4.6. Effect of temperature

In a great number of papers [9, 17, 19, 21, 25, 27, 37-39, 43, 46-49]) it has been shown that the tangential flows (as a result of interfacial tension gradients) affect considerably the hydrodynamic stability of the interface and the flow in the boundary layer.

The induction of normal flows (due to large concentration gradients) has an effect of "injection" or "suction" of fluid in the boundary layer, which also changes the hydrodynamic stability in the boundary layer [16, 23, 27, 34, 35, 40]. It has been shown [40] that changes in the normal component of the velocity on the interface influence the hydrodynamic stability stronger than changes in the tangential component.

The results obtained in 1.5.3. give the opportunity to define the influence of the non-linear mass transfer and the Marangoni effect on the hydrodynamic stability of the flow in the boundary layer.

The linear stability analysis uses the equation of Orr-Sommerfeld (5.132) where for  $u_j$  and  $v_j$  it can be written (see 1.5.3.):

$$\begin{aligned} u_j &= u_{j0} U_j(X, Y_j), \quad v_j = (-I)^{j+1} u_{j0} \frac{\delta_j}{L} V_j(X, Y_j), \\ x &= LX, \quad y = (-I)^{j+1} \delta_j Y_j, \quad \delta_j = \sqrt{\nu_j L / u_{j0}}, j=1, 2, \end{aligned} \quad (5.138)$$

Thus, it can be obtained directly:

$$\begin{aligned} (\bar{U}_j - C_j) \gamma_j'' - A_j^2 \gamma_j' &- \frac{\partial^2 U_j}{\partial Y_j^2} \gamma_j = \\ &= -\frac{i}{A_j Re_j} (\gamma_j''' - 2A_j^2 \gamma_j'' + A_j^4 \gamma_j) + \\ &+ \frac{i}{A_j Re_j} \left( \bar{V}_j \gamma_j'' - \frac{\partial^2 V_j}{\partial Y_j^2} \gamma_j' - A_j^2 \bar{V}_j \gamma_j' \right), \quad j=1, 2, \end{aligned} \quad (5.139)$$

where

$$\begin{aligned} C_j &= \frac{\beta_j}{\alpha_j u_{j0}}, \quad A_j = \alpha_j \delta_j, \quad Re_j = \frac{u_{j0} \delta_j}{\nu_j} = \sqrt{\frac{u_{j0} L}{\nu_j}}, \\ \bar{U}_j &= U_j(I, Y_j), \quad \bar{V}_j = V_j(I, Y_j), \quad \frac{\partial^2 U_j}{\partial Y_j^2} = \left( \frac{\partial^2 U_j}{\partial Y_j^2} \right)_{X=I}, \\ \frac{\partial^2 V_j}{\partial Y_j^2} &= \left( \frac{\partial^2 V_j}{\partial Y_j^2} \right)_{X=I}, \quad \gamma_j(Y_j) = G(y), \quad j = 1, 2. \end{aligned} \quad (5.140)$$

The solution of (5.139) could be found as it has been done in [45]. The results in the form of the neutral stability curves are presented on Fig. 5.38. The critical Reynolds numbers  $Re_{cr}$ , the corresponding wave velocities  $C_r$ , and the wave numbers  $A$  are obtained.  $C_{r\min}$  and  $A_{\min}$  are also obtained from these results. Let  $C_{r\min}$  and  $A_{\min}$  denote the minimum values for the wave velocities and the wave number at which the flow is stable at any Reynolds number  $Re$ , respectively. They are shown in Table 5.12 for different values of the parameters  $\theta_3, \theta_4$ , taking into account the intensity of the secondary flows induced by the concentration gradients and tangential temperature gradients.

**Table 5.12.**  
Values of the critical Reynolds numbers  $Re_{cr}$ , the corresponding wave velocities  $C_r$ , the wave numbers  $A$  and  $C_{r\min}, A_{\min}$  ( $Da=10, \theta_1=0.1, \theta_2=0.145, \theta_5=18.3, \theta_6=0.034$ ).

No.	$\theta_3$	$\theta_4$	$Re_{cr}$	$A_{\max}$	$C_{r\max}$
1.	0.0	0.0	800	0.357	0.4503
2.	0.2	0.0	1411	0.329	0.4187
3.	-0.2	0.0	512	0.382	0.4763
4.	0.0	$10^{-4}$	800	0.357	0.4503
5.	0.0	$10^{-3}$	800	0.357	0.4503
6.	0.0	$10^{-2}$	800	0.357	0.4503
7.	0.0	$10^{-1}$	799	0.356	0.4505
8.	0.0	1.0	799	0.356	0.4505

The numerical analysis of the influence of the effect of non-linear mass transfer and the Marangoni effect on the hydrodynamic stability in gas-liquid systems leads to some basic conclusions:

1. In the cases of absorption the increase in intensity of the mass transfer directed from the volume of the gas phase toward the phase boundary ( $\theta_3>0$ ) leads to an increase of the critical Reynolds numbers ( $Re_{cr}$ ), i. e. the flow is stabilized.
2. In the cases of desorption the increase in intensity of the mass transfer directed from the phase boundary toward the volume of the gas phase ( $\theta_3<0$ ) leads to a decrease of the critical Reynolds numbers ( $Re_{cr}$ ), i. e. the flow is destabilized.
3. The rise of the temperature gradient along the phase boundary length ( $\theta_4$ ) leads to a decrease of the critical Reynolds numbers ( $Re_{cr}$ ), i. e. destabilizes the flow. This Marangoni effect, however, is insignificant in gas-liquid systems with movable phase boundary.
4. The flow in the liquid phase is globally stable.

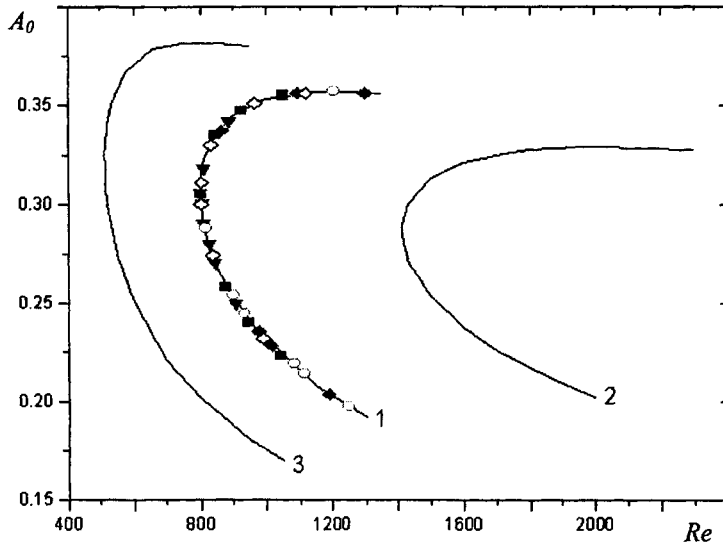


Fig. 5.38. The neutral curves of stability ( $Re$ ,  $A_0$ ) for flows of gases ( $Da=10$ ,  $\theta_1=0.1$ ,  $\theta_2=0.145$ ,  $\theta_5=18.3$ ,  $\theta_6=0.034$ ) in the laminar boundary layer:

- 1)  $\theta_4=0$ ,  $\theta_3=0$ ; 2)  $\theta_4=0$ ,  $\theta_3=0.2$ ; 3)  $\theta_4=0$ ,  $\theta_3=-0.2$ ;
- $\blacktriangleright$ )  $\theta_4=10^{-4}$ ,  $\theta_3=0$ ;  $\diamond$ )  $\theta_4=10^{-3}$ ,  $\theta_3=0.2$ ;  $\blacklozenge$ )  $\theta_4=-10^{-2}$ ,  $\theta_3=0.2$ ;
- $\circ$ )  $\theta_4=-10^{-1}$ ,  $\theta_3=0$ ;  $\blacksquare$ )  $\theta_4=-1$ ,  $\theta_3=0$ .

## CHAPTER 5.5. MECHANISM AND KINETICS OF THE TRANSPORT PROCESSES IN SYSTEMS WITH INTENSIVE INTERPHASE MASS TRANSFER

Experimental studies of systems with intensive mass transfer show in many cases serious deviations from the linear theory of mass transfer, which presumes independence of the velocity field from the fields of concentration and temperature. These effects are usually considered as Marangoni type effect [18, 20, 51] and are explained with the occurrence of tangential secondary flow on the phase boundary, caused by the surface tension gradient as a result of surface gradients of concentration or (and) temperature on the mass transfer surface.

Theoretical studies of systems with intensive interphase mass transfer (see Part 1) as a result of big concentration gradients showed [14, 23, 24, 31, 36] that these gradients induce normal secondary flows on the phase boundary. On this basis the non-linear theory of mass transfer [33] was built which provides a satisfactory explanations of the deviations of experimental results from the linear theory of mass transfer, too.

The above mentioned results illustrate the possibility for simultaneous or independent role of two mechanisms of heat mass transfer in systems with intensive mass transfer. This necessitates the definition of the conditions for occurrence of the effects of Marangoni and the non-linear mass transfer, which would allow the creation of adequate models of the chemical engineering processes under conditions of intensive interphase mass transfer between two phases.

The linear analysis of the hydrodynamic stability (see Chapter 4.4) in systems with intensive interphase mass transfer has shown [16, 34, 35, 40] that the normal and the tangential components of the velocity on the phase boundary influence the hydrodynamic stability of the flows in the boundary layer, and that the influence of the normally directed velocity component is significantly greater. This suggests that the occurrence of a marked considerable difference in the intensity of the effects of Marangoni and the non-linear mass transfer is possible.

The comparative analysis of these two effects has been made in the cases of mass transfer between two phases (gas – liquid and liquid – liquid) [45, 28], when substance from the first phase goes in to the second phase and reacts chemically with it. The big concentration gradients of the transferred substance create a normally directed secondary flow on the phase boundary. On the other hand, the thermal effect of the chemical reaction creates a gradient of the surface tension as a result of the temperature non-homogeneity at the phase interface.

The theoretical results obtained in 1.5.3. show [45, 28] that the Marangoni effect is negligible when compared with the effect of the non-linear mass transfer, i.e. the kinetics of mass transfer and the hydrodynamic stability do not depend on the surface tension gradient, caused by the temperature non-homogeneity at the phase interface as a result of the thermal effect of the chemical reaction. It should be noted, however, that the parameter, representing the Marangoni effect, increases with the decrease of the characteristic velocity in the second phase. The results obtained [28] when this phase is immovable show that under these conditions the Marangoni effect is also considerably smaller. Thus, the Marangoni effect may be expected in the limited case of interphase mass transfer between two immovable phases (for example in the absorption of pure gases in an immovable liquid). Under these conditions three processes are likely to take place: the natural convection, the non-linear mass transfer and the Marangoni effect.

Actually, these three effects may exhibit a dual influence on the mechanism and kinetics of the heat and mass transfer in systems with intensive interphase mass transfer. The first influence is relatively weak and is a result of the secondary flows, that change the velocity field. However, this may lead to changes in the hydrodynamic stability and therefore to the creation of self-organizing dissipative structures, having the form of stable periodic flows, that have a very strong influence on the mechanism and the kinetics of mass transfer. These two types of influences will be discussed consequently in the next presentation.

### 5.5.1. Mass and heat transfer kinetics

Let a vertical tube with a radius  $r_0$ , in which an immovable liquid ( $H_2O$ ) contacts an immovable gas ( $CO_2$ ,  $SO_2$ ,  $NH_3$ ) be considered. The gas is absorbed in the liquid, and the process is accompanied with a thermal effect. As a result several effects in the liquid may occur in the form of secondary flows due to the big concentration gradients on the phase

boundary (non-linear mass transfer), a density gradient in the volume (natural convection) and a surface tension gradient (Marangoni effect) [50, 61].

The mathematical description of the process will be made under the approximation of Oberbeck- Boussinesq equations [6, 8, 33], where the influence of the density gradient [52, 53], the concentration gradient [39] and the surface tension gradient will be considered [54-56]. In this way in cylindrical coordinates the problem assumes the form:

$$\begin{aligned}
 & \rho \left( \frac{\partial v_z}{\partial t} + v_z \frac{\partial v_z}{\partial z} + v_r \frac{\partial v_z}{\partial r} + \frac{v_\phi}{r} \frac{\partial v_z}{\partial \varphi} \right) = - \frac{\partial p}{\partial z} + \\
 & + \mu \left( \frac{\partial^2 v_z}{\partial z^2} + \frac{1}{r} \frac{\partial v_z}{\partial r} + \frac{\partial^2 v_z}{\partial r^2} + \frac{1}{r^2} \frac{\partial^2 v_z}{\partial \varphi^2} \right) + g(\rho - \rho_0), \\
 & \rho \left( \frac{\partial v_r}{\partial t} + v_z \frac{\partial v_r}{\partial z} + v_r \frac{\partial v_r}{\partial r} + \frac{v_\phi}{r} \frac{\partial v_r}{\partial \varphi} - \frac{v_\phi^2}{r} \right) = - \frac{\partial p}{\partial r} + \\
 & + \mu \left( \frac{\partial^2 v_r}{\partial z^2} + \frac{1}{r} \frac{\partial v_r}{\partial r} + \frac{\partial^2 v_r}{\partial r^2} - \frac{v_r}{r^2} + \frac{1}{r^2} \frac{\partial^2 v_r}{\partial \varphi^2} - \frac{2}{r^2} \frac{\partial v_\phi}{\partial \varphi} \right), \\
 & \rho \left( \frac{\partial v_\phi}{\partial t} + v_z \frac{\partial v_\phi}{\partial z} + v_r \frac{\partial v_\phi}{\partial r} + \frac{v_\phi}{r} \frac{\partial v_\phi}{\partial \varphi} + \frac{v_r v_\phi}{r} \right) = - \frac{1}{r} \frac{\partial p}{\partial \varphi} + \\
 & + \mu \left( \frac{\partial^2 v_\phi}{\partial z^2} + \frac{1}{r} \frac{\partial v_\phi}{\partial r} + \frac{\partial^2 v_\phi}{\partial r^2} - \frac{v_\phi}{r^2} + \frac{1}{r^2} \frac{\partial^2 v_\phi}{\partial \varphi^2} + \frac{2}{r^2} \frac{\partial v_r}{\partial \varphi} \right), \\
 & \frac{\partial \rho}{\partial t} + \frac{\partial(\rho v_z)}{\partial z} + \frac{\partial(\rho v_r)}{\partial r} + \frac{\rho v_r}{r} + \frac{1}{r} \frac{\partial(\rho v_\phi)}{\partial \varphi} = 0, \\
 & \frac{\partial c}{\partial t} + v_z \frac{\partial c}{\partial z} + v_r \frac{\partial c}{\partial r} + \frac{v_\phi}{r} \frac{\partial c}{\partial \varphi} = D \left( \frac{\partial^2 c}{\partial z^2} + \frac{1}{r} \frac{\partial c}{\partial r} + \frac{\partial^2 c}{\partial r^2} + \frac{1}{r^2} \frac{\partial^2 c}{\partial \varphi^2} \right), \\
 & \rho c_p \left( \frac{\partial \theta}{\partial t} + v_z \frac{\partial \theta}{\partial z} + v_r \frac{\partial \theta}{\partial r} + \frac{v_\phi}{r} \frac{\partial \theta}{\partial \varphi} \right) = \lambda \left( \frac{\partial^2 \theta}{\partial z^2} + \frac{1}{r} \frac{\partial \theta}{\partial r} + \frac{\partial^2 \theta}{\partial r^2} + \frac{1}{r^2} \frac{\partial^2 \theta}{\partial \varphi^2} \right), \\
 & \rho = \rho_0 \left[ 1 + \frac{c}{\rho_0} - \beta(\theta - \theta_0) \right]; \tag{5.141}
 \end{aligned}$$

with the corresponding initial and boundary conditions:

$$\begin{aligned}
 & t = 0, \quad v_z = v_r = v_\phi = c = 0, \quad \theta = \theta_0; \\
 & z = 0, \quad v_z = - \frac{D}{\rho_0} \frac{\partial c}{\partial z}, \quad \mu \left( \frac{\partial v_r}{\partial z} + \frac{\partial v_z}{\partial r} \right) = \frac{\partial \sigma}{\partial r} = \frac{\partial \sigma}{\partial \theta} \frac{\partial \theta}{\partial r}, \\
 & \mu \left( \frac{\partial v_\phi}{\partial z} + \frac{1}{r} \frac{\partial v_z}{\partial \varphi} \right) = \frac{1}{r} \frac{\partial \sigma}{\partial \varphi} = \frac{1}{r} \frac{\partial \sigma}{\partial \theta} \frac{\partial \theta}{\partial \varphi},
 \end{aligned}$$

$$\begin{aligned}
c &= c^*, \quad \lambda \frac{\partial \theta}{\partial z} = qD \frac{\partial c}{\partial z}; \\
z \rightarrow \infty, \quad v_z &= v_r = v_\varphi = c = 0, \quad \theta = \theta_0; \\
r = 0, \quad v_z, v_r, v_\varphi, c, \theta &- \text{finite}; \\
r = r_0, \quad v_z &= v_r = v_\varphi = 0, \quad \frac{\partial c}{\partial r} = \frac{\partial \theta}{\partial r} = 0. \tag{5.142}
\end{aligned}$$

Let assume that along the angle  $\varphi$  the processes are periodical with a period  $2\pi$ .

Equations (5.141) and (5.142) refer to the natural convection by means of the Archimedian force  $g(\rho - \rho_0)$ , the big concentration gradients through the connection between the velocity  $v_z$  and the concentration gradient  $\frac{\partial c}{\partial z}$  and the surface tension gradient ( $\sigma$ ) by means of its components on  $r$  and  $\varphi$  and their connection with the tangential components of the stress tensor at the surface  $z = 0$ .

The problem (5.141, 5.142) may be presented in a dimensionless form if the individual scales of the physical independent and dependent variables are used. These characteristic scales should be selected in such a way that the values of the dimensionless variables and parameters are not greater in order than unity.

The characteristic scales may be set in advance and for the example discussed they are of the following order for the time, radial coordinate, concentration and temperature:

$$t_0 \sim 10^2 \text{ s}, \quad r_0 \sim 10^{-2} \text{ m}, \quad c^* \sim (1-100) \text{ kg/m}^3 \text{ (for different gases)}, \quad \theta_0 \sim 10^0 \text{ C}. \tag{5.143}$$

The characteristic scales will be used in all cases when the character scales are not known in advance, and will be determined as a result of the qualitative analysis of the model (5.141, 5.142). If the characteristic scale of the velocity along the  $z$  axis is marked by  $u_0$ , then the scales of the other velocity components are determined in a way that the equation of continuity is satisfied in dimensionless variables, and for a characteristic scale of pressure the dynamic pressure  $\rho_0 u_0^2$  is used.

The difference in the orders of  $\mu$ ,  $D$  and  $\lambda$  shows that the basic change of the velocity, the concentration and the temperature will be reached at a different water depth in the tube. These characteristic depths for the velocity ( $l$ ), concentration ( $\delta$ ) and the temperature ( $h$ ) will be determined by the qualitative analysis of (5.141).

Using the above mentioned considerations, the following dimensionless variables are obtained:

$$\begin{aligned}
t &= t_0 T, \quad z = l Z_1 = \delta Z_2 = h Z_3, \quad r = r_0 R, \quad \varphi = 2\pi\Phi, \quad p = \rho_0 u_0^2 P, \\
v_z(t, z, r, \varphi) &= u_0 V_z(T, Z_1, R, \Phi) = u_0 \tilde{V}_z(T, Z_2, R, \Phi) = u_0 \tilde{V}_z(T, Z_3, R, \Phi), \\
v_r(t, z, r, \varphi) &= \frac{u_0 r_0}{l} V_r(T, Z_1, R, \Phi) = \frac{u_0 r_0}{l} \tilde{V}_r(T, Z_2, R, \Phi) = \frac{u_0 r_0}{l} \tilde{V}_r(T, Z_3, R, \Phi),
\end{aligned}$$

$$\begin{aligned}
v_\varphi(t, z, r, \varphi) &= 2\pi \frac{u_0 r_0}{l} V_\varphi(T, Z_1, R, \Phi) = 2\pi \frac{u_0 r_0}{l} \tilde{V}_\varphi(T, Z_2, R, \Phi) = \\
&= 2\pi \frac{u_0 r_0}{l} \tilde{\tilde{V}}_\varphi(T, Z_3, R, \Phi), \\
c(t, z, r, \varphi) &= c^* C(T, Z_1, R, \Phi) = c^* \tilde{C}(T, Z_2, R, \Phi) = c^* \tilde{\tilde{C}}(T, Z_3, R, \Phi), \\
\theta(t, z, r, \varphi) &= \theta_0 \Theta(T, Z_1, R, \Phi) = \theta_0 \tilde{\Theta}(T, Z_2, R, \Phi) = \theta_0 \tilde{\tilde{\Theta}}(T, Z_3, R, \Phi).
\end{aligned} \tag{5.144}$$

The introduction of (5.144) into (5.141, 5.142) converts the problem to a dimensionless form, where the dimensional characteristics parameters are grouped in such a way that the dimensionless parameters obtained be in order of unity, lower than unity ( $10^{-1}$ ) and many times lower than unity ( $\leq 10^{-2}$ ):

$$\begin{aligned}
&\left[ 1 + \frac{c^*}{\rho_0} C - \beta \theta_0 (\Theta - 1) \right] \left[ \frac{u_0 \rho_0}{gt_0 c^*} \frac{\partial V_z}{\partial T} + \frac{u_0^2 \rho_0}{glc^*} \left( V_z \frac{\partial V_z}{\partial Z_1} + V_r \frac{\partial V_z}{\partial R} + \frac{V_\varphi}{R} \frac{\partial V_z}{\partial \Phi} \right) \right] = \\
&= - \frac{u_0^2 \rho_0}{glc^*} \frac{\partial P}{\partial Z_1} + \frac{\mu u_0}{gl^2 c^*} \left[ \frac{\partial^2 V_z}{\partial Z_1^2} + \frac{l^2}{r_0^2} \left( \frac{1}{R} \frac{\partial V_z}{\partial R} + \frac{\partial^2 V_z}{\partial R^2} + \frac{1}{4\pi^2} \frac{1}{R^2} \frac{\partial^2 V_z}{\partial \Phi^2} \right) \right] + \\
&+ C - \frac{\rho_0 \beta \theta_0}{c^*} (\Theta - 1),
\end{aligned} \tag{5.145}$$

$$\begin{aligned}
&\left[ 1 + \frac{c^*}{\rho_0} C - \beta \theta_0 (\Theta - 1) \right] \left[ \frac{u_0 \rho_0}{gt_0 c^*} \frac{\partial V_r}{\partial T} + \right. \\
&\left. + \frac{u_0^2 \rho_0}{glc^*} \left( V_z \frac{\partial V_r}{\partial Z_1} + V_r \frac{\partial V_r}{\partial R} + \frac{V_\varphi}{R} \frac{\partial V_r}{\partial \Phi} - 4\pi^2 \frac{V_\varphi^2}{R} \right) \right] = - \frac{l^2}{r_0^2} \frac{u_0^2 \rho_0}{glc^*} \frac{\partial P}{\partial R} + \\
&+ \frac{\mu u_0}{gl^2 c^*} \left[ \frac{\partial^2 V_r}{\partial Z_1^2} + \frac{l^2}{r_0^2} \left( \frac{1}{R} \frac{\partial V_r}{\partial R} + \frac{\partial^2 V_r}{\partial R^2} - \frac{V_r}{R^2} + \frac{1}{4\pi^2} \frac{\partial^2 V_r}{\partial \Phi^2} - \frac{2}{R} \frac{\partial V_\varphi}{\partial \Phi} \right) \right],
\end{aligned} \tag{5.146}$$

$$\begin{aligned}
&\left[ 1 + \frac{c^*}{\rho_0} C - \beta \theta_0 (\Theta - 1) \right] \left[ \frac{u_0 \rho_0}{gt_0 c^*} \frac{\partial V_\varphi}{\partial T} + \right. \\
&\left. + \frac{u_0^2 \rho_0}{glc^*} \left( V_z \frac{\partial V_\varphi}{\partial Z_1} + V_r \frac{\partial V_\varphi}{\partial R} + \frac{V_\varphi}{R} \frac{\partial V_\varphi}{\partial \Phi} + \frac{V_r V_\varphi}{R} \right) \right] = - \frac{l^2}{r_0^2} \frac{u_0^2 \rho_0}{glc^*} \frac{1}{R} \frac{\partial P}{\partial \Phi} + \\
&+ \frac{\mu u_0}{gl^2 c^*} \left[ \frac{\partial^2 V_\varphi}{\partial Z_1^2} + \frac{l^2}{r_0^2} \left( \frac{1}{R} \frac{\partial V_\varphi}{\partial R} + \frac{\partial^2 V_\varphi}{\partial R^2} - \frac{V_\varphi}{R^2} + \frac{1}{4\pi^2} \frac{1}{R^2} \frac{\partial^2 V_\varphi}{\partial \Phi^2} + \frac{1}{2\pi^2} \frac{1}{R^2} \frac{\partial V_r}{\partial \Phi} \right) \right],
\end{aligned} \tag{5.147}$$

$$\begin{aligned} & \frac{lc^*}{\rho_0 u_0 t_0} \frac{\partial C}{\partial T} - \frac{\beta \theta_0 l}{t_0 u_0} \frac{\partial \Theta}{\partial T} + \left[ \frac{\partial V_z}{\partial Z_1} + \frac{V_r}{R} + \frac{\partial V_r}{\partial R} + \frac{l}{R} \frac{\partial V_\phi}{\partial \Phi} \right] \left[ 1 + \frac{c^*}{\rho_0} C - \beta \theta_0 (\Theta - 1) \right] + \\ & + V_z \left( \frac{c^*}{\rho_0} \frac{\partial C}{\partial Z_1} - \beta \theta_0 \frac{\partial \Theta}{\partial Z_1} \right) + V_r \left( \frac{c^*}{\rho_0} \frac{\partial C}{\partial R} - \beta \theta_0 \frac{\partial \Theta}{\partial R} \right) + \frac{V_\phi}{R} \left( \frac{c^*}{\rho_0} \frac{\partial C}{\partial \Phi} - \beta \theta_0 \frac{\partial \Theta}{\partial \Phi} \right) = 0, \quad (5.148) \end{aligned}$$

$$\begin{aligned} & \frac{\partial \tilde{C}}{\partial T} + \frac{u_0 t_0}{\delta} \left( \tilde{V}_z \frac{\partial \tilde{C}}{\partial Z_2} + \tilde{V}_r \frac{\partial \tilde{C}}{\partial R} + \frac{\tilde{V}_r}{R} \frac{\partial \tilde{C}}{\partial \Phi} \right) = \\ & = \frac{Dt_0}{\delta^2} \left[ \frac{\partial^2 \tilde{C}}{\partial Z_2^2} + \frac{\delta^2}{r_0^2} \left( \frac{1}{R} \frac{\partial \tilde{C}}{\partial R} + \frac{\partial^2 \tilde{C}}{\partial R^2} + \frac{1}{4\pi^2} \frac{1}{R^2} \frac{\partial^2 \tilde{C}}{\partial \Phi^2} \right) \right], \quad (5.149) \end{aligned}$$

$$\begin{aligned} & \left[ 1 + \frac{c^*}{\rho_0} \tilde{\tilde{C}} - \beta \theta_0 (\tilde{\tilde{\Theta}} - I) \right] \left[ \frac{\partial \tilde{\tilde{\Theta}}}{\partial T} + \frac{u_0 t_0}{h} \left( \tilde{\tilde{V}}_z \frac{\partial \tilde{\tilde{\Theta}}}{\partial Z_3} + \tilde{\tilde{V}}_r \frac{\partial \tilde{\tilde{\Theta}}}{\partial R} + \frac{\tilde{\tilde{V}}_\phi}{R} \frac{\partial \tilde{\tilde{\Theta}}}{\partial \Phi} \right) \right] = \\ & = \frac{at_0}{h^2} \left[ \frac{\partial^2 \tilde{\tilde{\Theta}}}{\partial Z_3^2} + \frac{h^2}{r_0^2} \left( \frac{1}{R} \frac{\partial \tilde{\tilde{\Theta}}}{\partial R} + \frac{\partial^2 \tilde{\tilde{\Theta}}}{\partial R^2} + \frac{1}{4\pi^2} \frac{1}{R^2} \frac{\partial^2 \tilde{\tilde{\Theta}}}{\partial \Phi^2} \right) \right]; \quad (5.150) \end{aligned}$$

$$T = 0, \quad V_z = V_r = V_\phi = \tilde{C} = 0, \quad \tilde{\tilde{\Theta}} = 1; \quad (5.151)$$

$$\begin{aligned} & Z_1 = Z_2 = Z_3 = 0, \quad V_z = -\frac{Dc^*}{u_0 \rho_0 \delta} \frac{\partial \tilde{C}}{\partial Z_2}, \\ & \frac{\partial V_r}{\partial Z_1} + \frac{l^2}{r_0^2} \frac{\partial V_z}{\partial R} = \frac{\partial \sigma}{\partial \theta} \frac{\theta_0}{\mu u_0} \frac{l^2}{r_0^2} \frac{\partial \tilde{\tilde{\Theta}}}{\partial R}, \\ & \frac{\partial V_\phi}{\partial Z_1} + \frac{l^2}{4\pi^2 r_0^2} \frac{1}{R} \frac{\partial V_z}{\partial \Phi} = \frac{\partial \sigma}{\partial \theta} \frac{\theta_0}{\mu u_0} \frac{l^2}{4\pi^2 r_0^2} \frac{1}{R} \frac{\partial \tilde{\tilde{\Theta}}}{\partial \Phi}, \\ & \tilde{C} = 1, \quad \frac{\partial \tilde{\tilde{\Theta}}}{\partial Z_3} = \frac{q D h c^*}{\delta \lambda \theta_0} \left( 1 + \frac{c^*}{\rho_0} \right) \frac{\partial \tilde{C}}{\partial Z_2}; \quad (5.152) \end{aligned}$$

$$Z_1 = Z_2 = Z_3 \rightarrow \infty, \quad V_z = V_r = V_\phi = \tilde{C} = 0, \quad \tilde{\tilde{\Theta}} = 1; \quad (5.153)$$

$$R = 0, \quad V_z, V_r, V_\phi, \tilde{P}, \tilde{C}, \tilde{\Theta} - \text{finite}; \quad (5.154)$$

$$R = 1, \quad V_z = V_r = V_\phi = 0, \quad \frac{\partial \tilde{C}}{\partial R} = \frac{\partial \tilde{\tilde{\Theta}}}{\partial R} = 0. \quad (5.155)$$

The qualitative analysis of the model (5.145 – 5.155) begins with the determination of the characteristic scales. The process under consideration is a result of the absorption of the gas and its thermal effect, i.e. the fields of concentration and temperature are determined by the diffusion and the heat transfer. From here it directly follows that the parameters in front of the Laplacians in (5.149) and (5.150) should be of the order of unity:

$$\frac{Dt_0}{\delta^2} = 1, \quad \frac{at_0}{h^2} = 1, \quad (5.156)$$

which makes the determination of the characteristic linear scales of  $\delta$  and  $h$  possible:

$$\delta = \sqrt{Dt_0} \sim 10^{-4} \text{ m}, \quad h = \sqrt{at_0} \sim 10^{-3} \text{ m}. \quad (5.157)$$

As a result of the diffusion and the heat transfer, conditions for a natural convection arise, which influence on the velocity field appears when the parameter in front of the Laplacian in (5.145 – 5.147) is of the order of unity (viscose flow):

$$\frac{\mu u_0}{gl^2 c^*} = 1. \quad (5.158)$$

From (5.158) it is obvious that it is not necessary to determine the characteristic velocity of the flow, which depends on the limitation process. Natural convection can not limit the velocity, because at diffusion and heat transfer in a stagnant liquid [6, 8, 32] there is a mechanical equilibrium ( $v_z = v_r = v_l \equiv 0$ ) and the natural convection is a result of the loss of stability only.

The big concentration gradients induce a secondary flow, which characteristic velocity may be determined, if the parameter of the non-linear mass transfer in (5.152) is of the order of unity:

$$\frac{Dc^*}{u_0 \rho_0 \delta} = 1. \quad (5.159)$$

In this way the characteristic scales  $l$  and  $u_0$  are obtained directly from (5.158) and (5.159):

$$u_0 = \frac{c^*}{\rho_0} \sqrt{\frac{D}{t_0}} \sim 10^{-7} \text{ m/s}, \quad l = \sqrt{\frac{\mu}{\rho_0 g}} \sqrt{\frac{D}{t_0}} \sim 10^{-7} \text{ m}. \quad (5.160)$$

The attempt to define the characteristic velocity from the Marangoni effect, i.e. from the condition

$$\frac{\partial \sigma}{\partial \theta} \frac{\theta_0}{\mu u_0} \frac{l^2}{r_0^2} = 1 \quad (5.161)$$

is not successful, because there is no value of  $u_0$  that can satisfy both (5.158) and (5.161). The natural convection and the Marangoni effect could arise simultaneously in the cases where the characteristic radius is very small:

$$r_0 = \sqrt{\frac{\partial \sigma}{\partial \theta} \frac{\theta_0}{\rho_0 \epsilon g}} \sim 10^{-3} \text{ m.} \quad (5.162)$$

The characteristic scales determined in this way in (5.157) and (5.160) do allow the determination of the order of the parameters in (5.145-5.153):

$$\begin{aligned} \epsilon &= \frac{c^*}{\rho_0} \sim 10^{-1}, \quad \frac{u_0 \rho_0}{g t_0 c^*} \sim 10^{-9}, \quad \frac{u_0^2 \rho_0}{g l c^*} \sim 10^{-7}, \quad \frac{l^2}{r_0^2} \sim 10^{-10}, \\ \frac{l c^*}{\rho_0 u_0 t_0} &\sim 10^{-3}, \quad \frac{u_0 t_0}{\delta} = \epsilon \sim 10^{-1}, \quad \frac{\delta^2}{r_0^2} \sim 10^{-4}, \quad \frac{h^2}{r_0^2} \sim 10^{-2}, \\ \frac{u_0 t_0}{h} &\sim 10^{-2}, \quad \frac{\partial \sigma}{\partial \theta} \frac{\theta_0}{\mu u_0} \frac{l^2}{r_0^2} \sim 10^{-3}, \quad \alpha = \frac{q D h \rho_0}{\delta \lambda \theta_0} \sim 1, \\ \beta \theta_0 &\sim 10^{-3}, \quad \frac{\partial \sigma}{\partial \theta} \sim 10^{-5} \text{ kg/m}^2 \text{ }^0\text{C}, \quad \frac{\rho_0 \beta \theta_0}{c^*} \sim 10^{-2}, \quad \frac{\beta \theta_0 l \rho_0}{t_0 \mu} \sim 10^{-5}. \end{aligned} \quad (5.163)$$

The dimensionless parameters determined in this way in the model (5.145 – 5.155) are not greater in order than unity, which is a necessary condition for the validity of the result from the qualitative analysis.

From (5.163) it is evident that the parameter of the Marangoni effect (5.158) is in order of  $10^{-3}$  and does not influence the velocity, the concentration and temperature field. Similar results have been obtained [54-56] in the analysis of the simultaneous influence of the natural convection and the Marangoni effect in the cases of a fixed thickness of the water column, greater than  $10^{-3}$  m. This result shows that under conditions of an intensive mass transfer the natural convection and the non-linear mass transfer lead to a flow, which characteristic velocity is of two orders greater than the velocity, at which the Marangoni effect may occur.

Another significant result of (5.163) is that  $\beta \theta_0 \ll \frac{c^*}{\rho_0} < 1$ , i.e. the temperature change

does not influence the density  $\rho$  and further will assume  $\beta = 0$ .

The different effects in the complex process take place when their corresponding parameters are  $> 10^{-2}$ , i.e. the problem (5.145 – 5.155) may be expressed in a zero-order approximation regarding the parameters of order lower than  $10^{-2}$  (and smaller). In this way from (5.145 – 5.155) and (5.163) it follows:

$$\frac{\partial^2 V_z}{\partial Z_l^2} + C = 0, \quad \frac{\partial^2 V_r}{\partial Z_l^2} = 0, \quad \frac{\partial^2 V_\phi}{\partial Z_l^2} = 0,$$

$$\begin{aligned}
& (1+\varepsilon C) \left( \frac{\partial V_z}{\partial Z_1} + \frac{V_r}{R} + \frac{\partial V_r}{\partial R} + \frac{1}{R} \frac{\partial V_\varphi}{\partial \Phi} \right) + \varepsilon \left( V_z \frac{\partial C}{\partial Z_1} + V_r \frac{\partial C}{\partial R} + \frac{1}{R} V_\varphi \frac{\partial C}{\partial \Phi} \right) = 0, \\
& \frac{\partial \tilde{C}}{\partial T} + \varepsilon \left( \tilde{V}_z \frac{\partial \tilde{C}}{\partial Z_2} + \tilde{V}_r \frac{\partial \tilde{C}}{\partial R} + \frac{\tilde{V}_\varphi}{R} \frac{\partial \tilde{C}}{\partial \Phi} \right) = \frac{\partial^2 \tilde{C}}{\partial Z_2^2}, \\
& \left( 1 + \varepsilon \tilde{\tilde{C}} \right) \frac{\partial \tilde{\tilde{\Theta}}}{\partial T} = \frac{\partial^2 \tilde{\tilde{\Theta}}}{\partial Z_2^2}; \\
& T = 0, \quad \tilde{C} = 0, \quad \tilde{\tilde{\Theta}} = I; \\
& Z_1 = Z_2 = Z_3 = 0, \quad V_z = -\frac{\partial \tilde{C}}{\partial Z_2}, \quad \frac{\partial V_r}{\partial Z_1} = 0, \quad \frac{\partial V_\varphi}{\partial Z_1} = 0, \\
& \tilde{C} = I, \quad \frac{\partial \tilde{\tilde{\Theta}}}{\partial Z_3} = \varepsilon \alpha_1 (1 + \varepsilon) \frac{\partial \tilde{C}}{\partial Z_2}; \\
& Z_1 = Z_2 = Z_3 \rightarrow \infty, \quad V_z = V_r = V_\varphi = \tilde{C} = 0, \quad \tilde{\tilde{\Theta}} = I; \\
& R = 0, \quad V_r = 0. \tag{5.164}
\end{aligned}$$

The solution of (5.164) depends on two parameters ( $\alpha, \varepsilon$ ), where  $\varepsilon$  is a small parameter and the solutions may be expressed in an expansion of  $\varepsilon$  in the form  $V_r$ :

$$\begin{aligned}
V_z &= V_z^{(0)} + \varepsilon V_z^{(1)} + \dots, \quad V_r = V_r^{(0)} + \varepsilon V_r^{(1)} + \dots, \quad V_\varphi = V_\varphi^{(0)} + \varepsilon V_\varphi^{(1)} + \dots, \\
\tilde{C} &= \tilde{C}^{(0)} + \varepsilon \tilde{C}^{(1)} + \dots, \quad \tilde{\tilde{\Theta}} = \tilde{\tilde{\Theta}}^{(0)} + \varepsilon \tilde{\tilde{\Theta}}^{(1)} + \dots. \tag{5.165}
\end{aligned}$$

The introduction of (5.165) into (5.164) allows to find the zero-order approximations ( $\varepsilon = 0$ ):

$$\begin{aligned}
& \frac{\partial^2 V_z^{(0)}}{\partial Z_1^2} + C^{(0)} = 0; \\
& Z_1 = 0, \quad V_z^{(0)} = -\left( \frac{\partial \tilde{C}^{(0)}}{\partial Z_2} \right)_{Z_2=0}; \quad Z_1 \rightarrow \infty, \quad V_z^{(0)} = 0. \tag{5.166}
\end{aligned}$$

$$\begin{aligned}
& \frac{\partial^2 V_\varphi^{(0)}}{\partial Z_1^2} = 0; \\
& Z_1 = 0, \quad \frac{\partial V_\varphi^{(0)}}{\partial Z_1} = 0; \quad Z_1 \rightarrow \infty, \quad V_\varphi^{(0)} = 0. \tag{5.167}
\end{aligned}$$

$$\frac{\partial V_r^{(0)}}{\partial R} + \frac{V_r^{(0)}}{R} = -\frac{\partial V_z^{(0)}}{\partial Z_1} - \frac{1}{R} \frac{\partial V_\varphi^{(0)}}{\partial \Phi};$$

$$R = 0, \quad V_r^{(0)} = 0 \text{ (finite).} \quad (5.168)$$

$$\frac{\partial \tilde{C}^{(0)}}{\partial T} = \frac{\partial^2 \tilde{C}^{(0)}}{\partial Z_2^2};$$

$$T = 0, \quad \tilde{C}^{(0)} = 0; \quad Z_2 = 0, \quad \tilde{C}^{(0)} = 1; \quad Z_2 \rightarrow \infty, \quad \tilde{C}^{(0)} = 0. \quad (5.169)$$

$$\frac{\partial \tilde{\Theta}^{(0)}}{\partial T} = \frac{\partial^2 \tilde{\Theta}^{(0)}}{\partial Z_3^2};$$

$$T = 0, \quad \tilde{\Theta} = 1; \quad Z_3 = 0, \quad \frac{\partial \tilde{\Theta}^{(0)}}{\partial Z_3} = 0; \quad Z_3 \rightarrow \infty, \quad \tilde{\Theta}^{(0)} = 1. \quad (5.170)$$

The solutions of (5.167), (5.169) and (5.170) are obtained directly.

$$V_\varphi^{(0)} = 0, \quad \tilde{C}^{(0)} = \operatorname{erfc} \frac{Z_2}{2\sqrt{T}}, \quad \tilde{\Theta}^{(0)} = 1. \quad (5.171)$$

From (14) and (50) it is clear that

$$C^{(0)} = \operatorname{erfc} \left( \frac{l}{\delta} \frac{Z_1}{2\sqrt{T}} \right) \approx 1, \quad \alpha_0 = \frac{l}{\delta} \sim 10^{-3}. \quad (5.172)$$

The introduction of (5.172) in (5.166) allows the determination of  $V_z^{(0)}$ , replacing the infinity condition with  $V_z(l) = 0$ :

$$V_z^{(0)} = -\frac{1}{2} Z_1^2 + \left( \frac{1}{2} - \frac{1}{\sqrt{\pi T}} \right) Z_1 + \frac{l}{\sqrt{\pi T}}. \quad (5.173)$$

The substitution (5.171) and (5.173) in (5.168) leads to:

$$V_r^{(0)} = \left[ \frac{1}{2} Z_1 + \frac{l}{2\sqrt{\pi T}} - \frac{1}{4} \right] R. \quad (5.174)$$

The problem for determination of the first approximation of the concentration  $\tilde{C}^{(1)}$  is of the type:

$$\frac{\partial \tilde{C}^{(1)}}{\partial T} = \frac{\partial^2 \tilde{C}^{(1)}}{\partial Z_2^2} - \tilde{V}_z^{(0)} \frac{\partial \tilde{C}^{(0)}}{\partial Z_2};$$

$$T = 0, \quad \tilde{C}^{(1)} = 0; \quad Z_2 = 0, \quad \tilde{C}^{(1)} = 0; \quad Z_2 \rightarrow \infty, \quad \tilde{C}^{(1)} = 0, \quad (5.175)$$

where

$$\tilde{V}_z^{(0)}(Z_2, T) = V_z^{(0)}(Z_1, T), \quad Z_1 = \frac{1}{\alpha_0} Z_2. \quad (5.176)$$

From (5.176) it directly follows that the volume source in (5.175) is:

$$\tilde{V}_z^{(0)} \frac{\partial \tilde{C}^{(0)}}{\partial Z_2} \neq 0 \quad \text{for } 0 \leq Z_2 < \alpha_0 \sim 10^{-3}, \quad (5.177)$$

i.e. its influence on the mass transfer is practically confined to the interface ( $Z_2 = 0$ ) and may be replaced by a surface flow as:

$$S = \int_0^{\alpha_0} \tilde{V}_z^{(0)} \frac{\partial \tilde{C}^{(0)}}{\partial Z_2} dZ_2. \quad (5.178)$$

Thus, the problem (5.175) takes the form:

$$\begin{aligned} \frac{\partial \tilde{C}^{(1)}}{\partial T} &= \frac{\partial^2 \tilde{C}^{(1)}}{\partial Z_2^2}; \\ T = 0, \quad \tilde{C}^{(1)} &= 0; \quad Z_2 = 0, \quad \frac{\partial \tilde{C}^{(1)}}{\partial Z_2} = -S; \quad Z_2 \rightarrow \infty, \quad \tilde{C}^{(1)} = 0; \\ S &= -\sqrt{\frac{T}{\pi}} \frac{\alpha_0 e^{-\frac{\alpha^2}{4T}} - \sqrt{\pi} \operatorname{erf} \frac{\alpha}{2\sqrt{T}}}{\alpha_0^2} - \left( \sqrt{\frac{T}{\pi}} - \frac{2}{\pi} \right) \frac{e^{-\frac{\alpha^2}{4T}} - 1}{\alpha_0} - \frac{1}{\sqrt{\pi T}} \operatorname{erf} \frac{\alpha_0}{2T}. \end{aligned} \quad (5.179)$$

From (5.179) is clear that for small values of  $\alpha_0$  ( $\alpha_0 \sim 10^{-3}$ ),  $S \approx 0$ , therefore

$$\tilde{C}^{(1)} \equiv 0. \quad (5.180)$$

It is not difficult to show that

$$V_z^{(1)} \equiv 0, \quad V_r^{(1)} \equiv 0, \quad V_\phi^{(1)} \equiv 0, \quad \tilde{\theta}^{(1)} \equiv 0. \quad (5.181)$$

The average absorption rate  $J$  (per unit interface) for a time interval  $t_0$  may be expressed by means of the mass transfer coefficient  $k$ . It may be determined from the average mass flux  $I$ :

$$J = kc^* = \frac{1}{\pi r_0^2 t_0} \int_0^{t_0} Idt, \quad I = \pi r_0^2 i, \quad i = -\frac{D\rho^*}{\rho_0} \left( \frac{\partial c}{\partial z} \right)_{z=0}, \quad \rho^* = \rho_0 + c^*, \quad \frac{\rho^*}{\rho_0} = 1 + \varepsilon. \quad (5.182)$$

Thus equation (5.182) may be used to obtain the Sherwood number for a non-stationary diffusion:

$$Sh = \frac{kl}{D} = -(1 + \varepsilon) \sqrt{\frac{\nu}{gt_0}} \sqrt{\frac{1}{Dt_0}} \int_0^{t_0} \left( \frac{\partial \tilde{C}}{\partial Z_2} \right)_{Z_2=0} dT, \quad (5.183)$$

e.g.

$$Sh = 2(1 + \varepsilon) \sqrt{\frac{\nu}{\pi gt_0}} \sqrt{\frac{1}{Dt_0}}. \quad (5.184)$$

The amount of the gas absorbed  $Q$  [kg/m<sup>2</sup>] for the time interval  $t_0$  [sec] is:

$$Q = \frac{1}{\pi r_0^2} \int_0^{t_0} Idt = 2(1 + \varepsilon) c^* \sqrt{\frac{Dt_0}{\pi}}. \quad (5.185)$$

The results reported (5.171, 5.173, 5.174) show that the temperature is of practically constant value and does not influence the fields of velocity and concentration. These results differ from the solution of the Benard problem [32, 52, 53], where  $V_z = V_r = V_\phi = 0$ , because the effect of the non-linear mass transfer does not allow the existence of a mechanical equilibrium, where the liquid may remain stagnant.

The experimental results from the absorption of CO<sub>2</sub> in an immobile layer of water [57] show that the rate of the absorption is significantly greater than the one that can be determined from (5.185). This fact indicates that the non-stationary process that is described by the equations (5.171, 5.173, 5.174) (analogous to the Benard problem) is unstable regarding small periodical disturbances. Their increase may lead to new periodic flows with a constant amplitude, which will evidently change the mechanism and the kinetics of mass and heat transfer.

### 5.5.2. Linear stability analysis

In 5.5.1 it has been shown that in cases of absorption of pure gases in a cylindrical liquid column, a second flow is induced as a result of a natural convection and a non-linear mass transfer. Under these conditions the Marangoni effect is negligible and for the velocity, temperature and concentration the following expressions have been obtained:

$$v_z = \varepsilon \left[ -\frac{g}{2\nu} z^2 + \left( \frac{1}{2} - \sqrt{\frac{t_0}{\pi}} \right) \sqrt{\frac{g}{\nu}} \sqrt{\frac{D}{t_0}} z + \sqrt{\frac{D}{\pi}} \right],$$

$$v_r = \varepsilon \left[ + \frac{g}{2\nu} z - \left( \frac{1}{4} - \frac{1}{2} \sqrt{\frac{t_0}{\pi}} \right) \sqrt{\frac{g}{\nu}} \sqrt{\frac{D}{t_0}} \right] r, \\ v_\varphi \equiv 0, \quad p \equiv 0, \quad c^* = erfc \frac{z}{2\sqrt{Dt}}, \quad \theta \equiv \theta_0, \quad \varepsilon = \frac{c^*}{\rho_0}, \quad \nu = \frac{\mu}{\rho_0}. \quad (5.186)$$

These results differ significantly from the Benard problem [52, 53], where under certain conditions a mechanical equilibrium ( $v_z = v_r = v_\varphi = 0$ ) is possible. The reason for this difference is the non-linear mass transfer, i.e. the big mass flux induces a secondary flow on the phase boundary:

$$z = 0, \quad v_z = \sqrt{\frac{D}{\pi t}} \quad (5.187)$$

and in this way violates the necessary condition for a mechanical equilibrium [8, 32].

The process, described by the expressions (5.186), as may be expected, analogous to the Benard problem, is unstable regarding small disturbances, which makes the usage of the linear analysis [68, 70] possible.

A process, represented as a superposition of the basic process (5.186) and small disturbances in the velocity ( $v_z^{'}, v_r^{'}, v_\varphi^{'}$ ), pressure ( $p^{'}$ ), concentration ( $c^{'}$ ) and temperature ( $\theta^{'}$ ) will be considered:

$$v_z + v_z^{'}, \quad v_r + v_r^{'}, \quad v_\varphi + v_\varphi^{'}, \quad p + p^{'}, \quad c + c^{'}, \quad \theta + \theta^{'}. \quad (5.188)$$

This new process should satisfy (as well as the basic one) the Oberbeck- Boussinesq equations (5.141, 5.142). Introducing (5.186) and (5.188) in the equations (5.141, 5.142) a system of equations concerning  $v_z^{'}, v_r^{'}, v_\varphi^{'}, p^{'}, c^{'}$  and  $\theta^{'}$  is obtained. It will be analysed in a linearised form with regard to these small disturbances:

$$\left( I + \frac{c}{\rho_0} \right) \left( \frac{\partial v_z^{'}}{\partial t} + v_z^{'}, \frac{\partial v_z}{\partial z} + v_z, \frac{\partial v_z^{'}}{\partial z} + v_r^{'}, \frac{\partial v_z^{'}}{\partial r} + v_r, \frac{\partial v_z^{'}}{\partial \varphi} \right) = - \frac{1}{\rho_0} \frac{\partial p^{'}}{\partial z} + \\ + v \left( \frac{\partial^2 v_z^{'}}{\partial z^2} + \frac{1}{r} \frac{\partial v_z^{'}}{\partial r} + \frac{\partial^2 v_z^{'}}{\partial r^2} + \frac{1}{r^2} \frac{\partial^2 v_z^{'}}{\partial \varphi^2} \right) + \frac{g}{\rho_0} c^{'}, \\ \left( I + \frac{c}{\rho_0} \right) \left( \frac{\partial v_r^{'}}{\partial t} + v_z^{'}, \frac{\partial v_r}{\partial z} + v_z, \frac{\partial v_r^{'}}{\partial z} + v_r^{'}, \frac{\partial v_r^{'}}{\partial r} + v_r, \frac{\partial v_r^{'}}{\partial \varphi} \right) = - \frac{1}{\rho_0} \frac{\partial p^{'}}{\partial r} + \\ + v \left( \frac{\partial^2 v_r^{'}}{\partial z^2} + \frac{1}{r} \frac{\partial v_r^{'}}{\partial r} + \frac{\partial^2 v_r^{'}}{\partial r^2} - \frac{v_r^{'}}{r^2} + \frac{1}{r^2} \frac{\partial^2 v_r^{'}}{\partial \varphi^2} - \frac{2}{r^2} \frac{\partial v_\varphi^{'}}{\partial \varphi} \right), \\ \left( I + \frac{c}{\rho_0} \right) \left( \frac{\partial v_\varphi^{'}}{\partial t} + v_z^{'}, \frac{\partial v_\varphi}{\partial z} + v_z, v_r^{'}, \frac{\partial v_\varphi^{'}}{\partial r} + \frac{1}{r} v_r v_\varphi^{'}, \frac{\partial v_\varphi^{'}}{\partial \varphi} \right) = - \frac{1}{\rho_0 r} \frac{\partial p^{'}}{\partial \varphi} +$$

$$+ \nu \left( \frac{\partial^2 v'_\varphi}{\partial z^2} + \frac{1}{r} \frac{\partial v'_\varphi}{\partial r} + \frac{\partial^2 v'_\varphi}{\partial r^2} - \frac{v'_\varphi}{r^2} + \frac{1}{r^2} \frac{\partial^2 v'_\varphi}{\partial \varphi^2} + \frac{2}{r^2} \frac{\partial v'_r}{\partial \varphi} \right); \quad (5.189)$$

$$\begin{aligned} & \frac{\partial c'}{\partial t} + (\rho_0 + c) \left( \frac{\partial v'_z}{\partial z} + \frac{\partial v'_r}{\partial r} + \frac{v'_r}{r} + \frac{1}{r} \frac{\partial v'_\varphi}{\partial \varphi} \right) + \\ & + v'_z \frac{\partial c}{\partial z} + v_z \frac{\partial c'}{\partial z} + v_r \frac{\partial c'}{\partial r} = 0; \end{aligned} \quad (5.190)$$

$$\begin{aligned} & \frac{\partial c'}{\partial t} + v'_z \frac{\partial c}{\partial z} + v_z \frac{\partial c'}{\partial z} + v_r \frac{\partial c'}{\partial r} = D \left( \frac{\partial^2 c'}{\partial z^2} + \frac{1}{r} \frac{\partial c'}{\partial r} + \frac{\partial^2 c'}{\partial r^2} + \frac{1}{r^2} \frac{\partial^2 c'}{\partial \varphi^2} \right), \\ & \left( 1 + \frac{c}{\rho_0} \right) \left( \frac{\partial \theta'}{\partial t} + v'_z \frac{\partial \theta'}{\partial z} + v_r \frac{\partial \theta'}{\partial r} \right) = a \left( \frac{\partial^2 \theta'}{\partial z^2} + \frac{1}{r} \frac{\partial \theta'}{\partial r} + \frac{\partial^2 \theta'}{\partial r^2} + \frac{1}{r^2} \frac{\partial^2 \theta'}{\partial \varphi^2} \right); \end{aligned} \quad (5.191)$$

$$t = 0, \quad v'_z = v'_r = v'_\varphi = c' = \theta' = 0;$$

$$z = 0, \quad v'_z = -\frac{D}{\rho_0} \frac{\partial c'}{\partial z}, \quad \mu \left( \frac{\partial v'_r}{\partial z} + \frac{\partial v'_z}{\partial r} \right) = \frac{\partial \sigma}{\partial \theta} \frac{\partial \theta'}{\partial r},$$

$$\mu \left( \frac{\partial v'_\varphi}{\partial z} + \frac{1}{r} \frac{\partial v'_z}{\partial \varphi} \right) = \frac{1}{r} \frac{\partial \sigma}{\partial \theta} \frac{\partial \theta'}{\partial \varphi},$$

$$c' = 0, \quad \lambda \frac{\partial \theta'}{\partial z} = qD \frac{\partial c'}{\partial z};$$

$$z \rightarrow \infty, \quad v'_z = v'_r = v'_\varphi = c' = \theta' = 0;$$

$$r = 0, \quad v'_z, v'_r, v'_\varphi, c', p', \theta' - \text{finite};$$

$$r = r_0, \quad v'_z = v'_r = v'_\varphi = 0, \quad \frac{\partial c'}{\partial r} = \frac{\partial \theta'}{\partial r} = 0. \quad (5.192)$$

Equations (5.190) are obtained from the equation of continuity using the condition  $\beta < 1$ . Boundary conditions for the pressure are not used, because it will be eliminated in the equations (5.189). Boundary conditions regarding coordinate  $\varphi$  are not included, because disturbances periodical regarding  $\varphi$  will be discussed.

The system of equations (5.189 – 5.192) has partial solutions (“normal” disturbances), which depend exponentially on the time:

$$\begin{aligned} v'_z &= \bar{v}_z(t, z, r, \varphi) \exp(-\omega t), & p' &= \bar{p}(t, z, r, \varphi) \exp(-\omega t), \\ v'_r &= \bar{v}_r(t, z, r, \varphi) \exp(-\omega t), & c' &= \bar{c}(t, z, r, \varphi) \exp(-\omega t), \\ v'_\varphi &= \bar{v}_\varphi(t, z, r, \varphi) \exp(-\omega t), & \theta' &= \bar{\theta}(t, z, r, \varphi) \exp(-\omega t), \end{aligned} \quad (5.193)$$

where the pre-exponential parts depend on the time, because the basic process (5.186) is non-stationary. The presented in this way disturbances decrease or increase with the time, depending on the value of  $\omega$ , and for  $\omega = 0$  the disturbances are “neutral”, i.e. a process which neither slows down nor intensifies with the time. The mathematical description of this process is obtained from (5.189 – 5.192) after introducing (5.193) and  $\omega = 0$ :

$$\begin{aligned} \left(1 + \frac{c}{\rho_0}\right) \left( \frac{\partial \bar{v}_z}{\partial t} + \bar{v}_z \frac{\partial v_z}{\partial z} + v_z \frac{\partial \bar{v}_z}{\partial z} + v_r \frac{\partial \bar{v}_z}{\partial r} \right) &= -\frac{1}{\rho_0} \frac{\partial \bar{p}}{\partial z} + \\ &+ \nu \left( \frac{\partial^2 \bar{v}_z}{\partial z^2} + \frac{1}{r} \frac{\partial \bar{v}_z}{\partial r} + \frac{\partial^2 \bar{v}_z}{\partial r^2} + \frac{1}{r^2} \frac{\partial^2 \bar{v}_z}{\partial \varphi^2} \right) + \frac{g}{\rho_0} \bar{c}, \\ \left(1 + \frac{c}{\rho_0}\right) \left( \frac{\partial \bar{v}_r}{\partial t} + \bar{v}_z \frac{\partial v_r}{\partial z} + v_z \frac{\partial \bar{v}_r}{\partial z} + \bar{v}_r \frac{\partial v_r}{\partial r} + v_r \frac{\partial \bar{v}_r}{\partial r} \right) &= -\frac{1}{\rho_0} \frac{\partial \bar{p}}{\partial r} + \\ &+ \nu \left( \frac{\partial^2 \bar{v}_r}{\partial z^2} + \frac{1}{r} \frac{\partial \bar{v}_r}{\partial r} + \frac{\partial^2 \bar{v}_r}{\partial r^2} - \frac{\bar{v}_r}{r^2} + \frac{1}{r^2} \frac{\partial^2 \bar{v}_r}{\partial \varphi^2} - \frac{2}{r^2} \frac{\partial \bar{v}_\varphi}{\partial \varphi} \right), \\ \left(1 + \frac{c}{\rho_0}\right) \left( \frac{\partial \bar{v}_\varphi}{\partial t} + v_z \frac{\partial \bar{v}_\varphi}{\partial z} + v_r \frac{\partial \bar{v}_\varphi}{\partial r} + \frac{1}{r} v_r \bar{v}_\varphi \right) &= -\frac{1}{\rho_0 r} \frac{\partial \bar{p}}{\partial \varphi} + \\ &+ \nu \left( \frac{\partial^2 \bar{v}_\varphi}{\partial z^2} + \frac{1}{r} \frac{\partial \bar{v}_\varphi}{\partial r} + \frac{\partial^2 \bar{v}_\varphi}{\partial r^2} - \frac{\bar{v}_\varphi}{r^2} + \frac{1}{r^2} \frac{\partial^2 \bar{v}_\varphi}{\partial \varphi^2} + \frac{2}{r^2} \frac{\partial \bar{v}_r}{\partial \varphi} \right); \end{aligned} \quad (5.194)$$

$$\begin{aligned} \frac{\partial \bar{c}}{\partial t} + (\rho_0 + c) \left( \frac{\partial \bar{v}_z}{\partial z} + \frac{\partial \bar{v}_r}{\partial r} + \frac{\bar{v}_r}{r} + \frac{1}{r} \frac{\partial \bar{v}_\varphi}{\partial \varphi} \right) + \\ + \bar{v}_z \frac{\partial c}{\partial z} + v_z \frac{\partial \bar{c}}{\partial z} + v_r \frac{\partial \bar{c}}{\partial r} = 0; \end{aligned} \quad (5.195)$$

$$\begin{aligned} \frac{\partial \bar{c}}{\partial t} + \bar{v}_z \frac{\partial c}{\partial z} + v_z \frac{\partial \bar{c}}{\partial z} + v_r \frac{\partial \bar{c}}{\partial r} = D \left( \frac{\partial^2 \bar{c}}{\partial z^2} + \frac{1}{r} \frac{\partial \bar{c}}{\partial r} + \frac{\partial^2 \bar{c}}{\partial r^2} + \frac{1}{r^2} \frac{\partial^2 \bar{c}}{\partial \varphi^2} \right), \\ \left(1 + \frac{c}{\rho_0}\right) \left( \frac{\partial \bar{\theta}}{\partial t} + v_z \frac{\partial \bar{\theta}}{\partial z} + v_r \frac{\partial \bar{\theta}}{\partial r} \right) = a \left( \frac{\partial^2 \bar{\theta}}{\partial z^2} + \frac{1}{r} \frac{\partial \bar{\theta}}{\partial r} + \frac{\partial^2 \bar{\theta}}{\partial r^2} + \frac{1}{r^2} \frac{\partial^2 \bar{\theta}}{\partial \varphi^2} \right); \end{aligned} \quad (5.196)$$

$$\begin{aligned} z = 0, \quad \bar{v}_z = -\frac{D}{\rho_0} \frac{\partial \bar{c}}{\partial z}, \quad \mu \left( \frac{\partial \bar{v}_r}{\partial z} + \frac{\partial \bar{v}_z}{\partial r} \right) = \frac{\partial \sigma}{\partial \theta} \frac{\partial \bar{\theta}}{\partial r}, \\ \mu \left( \frac{\partial \bar{v}_\varphi}{\partial z} + \frac{1}{r} \frac{\partial \bar{v}_z}{\partial \varphi} \right) = \frac{1}{r} \frac{\partial \sigma}{\partial \theta} \frac{\partial \bar{\theta}}{\partial \varphi}, \quad \bar{c} = 0, \quad \lambda \frac{\partial \bar{\theta}}{\partial z} = qD \frac{\partial \bar{c}}{\partial z}, \\ z \rightarrow \infty, \quad \bar{v}_z = \bar{v}_r = \bar{v}_\varphi = \bar{c} = \bar{\theta} = 0; \end{aligned}$$

$r = 0, \bar{v}_z, \bar{v}_r, \bar{v}_\varphi, \bar{p}, \bar{c}, \bar{\theta}$  – finite;

$$r = r_0, \bar{v}_z = \bar{v}_r = \bar{v}_\varphi = 0, \frac{\partial \bar{c}}{\partial r} = \frac{\partial \bar{\theta}}{\partial r} = 0. \quad (5.197)$$

The problem (5.194 – 5.197) obviously has partial solutions, for which the velocity, the concentration and the temperature depend on  $\varphi$  harmonically, i.e. the following range of neutral disturbances may be introduced in (5.194 – 5.197):

$$\begin{aligned} \bar{v}_z &= \sum_{n=0}^{\infty} v_n(t, z, r) \cos(n\varphi), \quad \bar{v}_r = \bar{v}_\varphi = 0, \quad \bar{p} = \sum_{n=0}^{\infty} p_n(t, z, r) \cos(n\varphi), \\ \bar{c} &= \sum_{n=0}^{\infty} c_n(t, z, r) \cos(n\varphi), \quad \bar{\theta} = \sum_{n=0}^{\infty} \theta_n(t, z, r) \cos(n\varphi). \end{aligned} \quad (5.198)$$

Introducing (5.198) in (5.194 – 5.197) the following eigenvalues problem is obtained:

$$\begin{aligned} (1+\varepsilon) \left( \frac{\partial v_n}{\partial t} + v_n \frac{\partial v_z}{\partial z} + v_z \frac{\partial v_n}{\partial z} + v_r \frac{\partial v_n}{\partial r} \right) &= -\frac{1}{\rho_0} \frac{\partial p_n}{\partial z} + \\ &+ \nu \left( \frac{\partial^2 v_n}{\partial z^2} + \frac{1}{r} \frac{\partial v_n}{\partial r} + \frac{\partial^2 v_n}{\partial r^2} - \frac{n^2}{r^2} v_n \right) + \frac{g}{\rho_0} c_n, \\ (1+\varepsilon) \frac{\partial v_r}{\partial z} v_n &= -\frac{1}{\rho_0} \frac{\partial p_n}{\partial r}, \\ \frac{\partial p_n}{\partial \varphi} &= 0; \end{aligned} \quad (5.199)$$

$$\begin{aligned} \frac{\partial c_n}{\partial t} + \rho_0 (1+\varepsilon) \frac{\partial v_n}{\partial z} + v_n \frac{\partial c}{\partial z} + \\ + v_z \frac{\partial c_n}{\partial z} + v_r \frac{\partial c_n}{\partial r} &= 0; \end{aligned} \quad (5.200)$$

$$\begin{aligned} \frac{\partial c_n}{\partial t} + v_n \frac{\partial c}{\partial z} + v_z \frac{\partial c_n}{\partial z} + v_r \frac{\partial c_n}{\partial r} &= D \left( \frac{\partial^2 c_n}{\partial z^2} + \frac{1}{r} \frac{\partial c_n}{\partial r} + \frac{\partial^2 c_n}{\partial r^2} - \frac{n^2}{r^2} c_n \right), \\ (1+\varepsilon) \left( \frac{\partial \theta_n}{\partial t} + v_z \frac{\partial \theta_n}{\partial z} + v_r \frac{\partial \theta_n}{\partial r} \right) &= a \left( \frac{\partial^2 \theta_n}{\partial z^2} + \frac{1}{r} \frac{\partial \theta_n}{\partial r} + \frac{\partial^2 \theta_n}{\partial r^2} - \frac{n^2}{r^2} \theta_n \right); \end{aligned} \quad (5.201)$$

$$z = 0, \quad v_n = -\frac{D}{\rho_0} \frac{\partial c_n}{\partial z}, \quad c_n = 0, \quad \lambda \frac{\partial \theta_n}{\partial z} = qD \frac{\partial c_n}{\partial z};$$

$$z \rightarrow \infty, \quad v_n = c_n = \theta_n = 0;$$

$$r = 0, \quad v_n, c_n, \theta_n - \text{finite};$$

$$r = r_0, \quad v_n = 0, \quad \frac{\partial c_n}{\partial r} = \frac{\partial \theta_n}{\partial r} = 0; \quad n = 0, 1, 2, \dots, \infty. \quad (5.202)$$

In (5.199 – 5.201)  $c = c^*$ , is accepted because the thickness of the velocity change layer is many times less than the thickness of the concentration change layer.

The pressure in (5.199) may be eliminated, if the second equation is integrated in regard to  $r$  and then differentiated in regard to  $z$ :

$$(I + \varepsilon) \int \frac{\partial v_r}{\partial z} \frac{\partial v_n}{\partial z} dr = - \frac{I}{\rho_0} \frac{\partial p_n}{\partial z}, \quad n = 0, 1, 2, \dots, \infty. \quad (5.203)$$

The introduction of (5.203) and (5.200) into (5.199) and (5.201) leads to the final form of the equations for determination of the “neutral” velocity, concentration and temperature disturbances:

$$\begin{aligned} & (I + \varepsilon) \left( \frac{\partial v_n}{\partial t} + v_n \frac{\partial v_z}{\partial z} + v_z \frac{\partial v_n}{\partial z} + v_r \frac{\partial v_n}{\partial r} \right) = (I + \varepsilon) \int \frac{\partial v_r}{\partial z} \frac{\partial v_n}{\partial z} dr + \\ & + v \left( \frac{\partial^2 v_n}{\partial z^2} + \frac{1}{r} \frac{\partial v_n}{\partial r} + \frac{\partial^2 v_n}{\partial r^2} - \frac{n^2}{r^2} v_n \right) + \frac{g}{\rho_0} c_n, \\ & (I + \varepsilon) \frac{\partial v_n}{\partial z} = \frac{D}{\rho_0} \left( \frac{\partial^2 c_n}{\partial z^2} + \frac{\partial^2 c_n}{\partial r^2} + \frac{1}{r} \frac{\partial c_n}{\partial r} - \frac{n^2}{r^2} c_n \right), \\ & \frac{\partial^2 \theta_n}{\partial z^2} + \frac{\partial^2 \theta_n}{\partial r^2} + \frac{1}{r} \frac{\partial \theta_n}{\partial r} - \frac{n^2}{r^2} \theta_n = 0, \quad n = 0, 1, 2, \dots, \infty \end{aligned} \quad (5.204)$$

with boundary conditions:

$$\begin{aligned} & z = 0, \quad v_n = - \frac{D}{\rho_0} \frac{\partial c_n}{\partial z}, \quad c_n = 0, \quad \frac{\partial \theta_n}{\partial z} = \frac{qD}{\lambda} \frac{\partial c_n}{\partial z}; \\ & z \rightarrow \infty, \quad v_n = c_n = \theta_n = 0; \\ & r = 0, \quad v_n, c_n, \theta_n - \text{finite}; \\ & r = r_0, \quad v_n = 0, \quad \frac{\partial c_n}{\partial r} = \frac{\partial \theta_n}{\partial r} = 0; \quad n = 0, 1, 2, \dots, \infty. \end{aligned} \quad (5.205)$$

The problem (5.204) will be solved through introducing the dimensionless variables (5.144) and a partial separation of the variables:

$$t = t_0 T, \quad z = l Z, \quad r = r_0 R, \quad v_n = u_0 [V_n(Z, T) - B f_n(R)],$$

$$c_n = c^* [C_n(Z, T) + Z f_n(R)], \quad \theta_n = \frac{q D c^*}{\lambda} f_n(R), \quad B = \frac{D \varepsilon}{u_0 l}, \quad n = 0, 1, 2, \dots, \infty, \quad (5.206)$$

where the dependence of the disturbances on the coordinates is supposed to be analogous to the basic process (5.186) for small values of  $z$ .

The introduction of (5.206) in (5.204 – 5.205) leads to:

$$\begin{aligned} & (1 + \varepsilon) \left\{ \frac{u_0}{\alpha_0 g} \frac{\partial V_n}{\partial T} + \frac{u_0^2}{\varepsilon l g} \left[ (V_n - B f_n) \frac{\partial V_z}{\partial Z} + V_z \frac{\partial V_n}{\partial Z} - B V_r f_n' \right] \right\} = \\ & = (1 + \varepsilon) \frac{u_0^2 r_0^2}{\varepsilon l^3 g} \int \frac{\partial V_r}{\partial Z} \frac{\partial V_n}{\partial Z} dR + \frac{\nu u_0}{\varepsilon l^2 g} \frac{\partial^2 V_n}{\partial Z^2} - \frac{\nu u_0}{\varepsilon r_0^2 g} V_n \frac{n^2}{R^2} + C_n + Z f_n, \\ & f_n'' + \frac{l}{R} f_n' - \frac{n^2}{R^2} f_n = 0, \\ & -(1 + \varepsilon) \frac{u_0 l}{\varepsilon D} \frac{\partial V_n}{\partial Z} = \frac{\partial^2 C_n}{\partial Z^2} - \frac{l^2}{r^2} \frac{n^2}{R^2} C_n; \quad n = 0, 1, 2, \dots, \infty; \end{aligned} \quad (5.207)$$

with boundary conditions:

$$\begin{aligned} & Z = 0, \quad V_n = -B \frac{\partial C_n}{\partial Z}, \quad C_n = 0; \\ & R = 0, \quad f_n = \text{finite}; \\ & R = l, \quad f_n' = 0; \quad n = 0, 1, 2, \dots, \infty, \end{aligned} \quad (5.208)$$

where

$$\begin{aligned} & \frac{u_0}{\varepsilon g t_0} \sim 10^{-9}, \quad \frac{u_0^2}{\varepsilon g t_0} \sim 10^{-7}, \quad \frac{u_0^2 r_0^2}{\varepsilon g l^3} \sim 10^3, \\ & \frac{\nu u_0}{\varepsilon g l^2} \sim 1, \quad \frac{\nu u_0}{\varepsilon g r_0^2} \sim 10^{-9}, \quad \frac{u_0 l}{\varepsilon D} \sim 10^{-8}, \quad \varepsilon \sim 10^{-1}, \\ & u_0 = \varepsilon \sqrt{\frac{D}{t_0}} \sim 10^{-7} \text{ m/s}, \quad l = \sqrt{\frac{\nu}{g}} \sqrt{\frac{D}{t_0}} \sim 10^{-7} \text{ m}. \end{aligned} \quad (5.209)$$

The solution of the Euler equation in (5.207) is obtained through Green's functions [5], searching for the eigenvalues and the eigenfunctions for  $n = 0, 1, 2, \dots, \infty$ :

$$f_0 = \text{const};$$

$$f_n = \frac{\xi^n + \xi^{-n}}{2n} R^n, \quad R < \xi;$$

$$\begin{aligned} f_n &= \frac{\xi^n}{2n} (R^n + R^{-n}) \quad R < \xi; \\ f_n &= \frac{\xi^{2n}}{2n} + \frac{1}{2n}, \quad R = \xi, \quad 0 < \xi < 1, \quad n = 1, 2, \dots, \infty, \end{aligned} \quad (5.210)$$

where the eigenvalue  $\xi$  is a parameter that can not be determined in the approximations of the linear stability theory.

Having in mind the order of the dimensionless variables in (5.209), from (5.207) one can directly obtain:

$$\begin{aligned} \frac{\partial^2 C_n}{\partial Z^2} &= 0; \quad Z = 0, \quad C_n = 0; \\ C_n &= \gamma_n Z; \\ \frac{\partial V_n}{\partial Z} &= 0; \quad Z = 0, \quad V_n = -B \frac{\partial C_n}{\partial Z}; \\ V_n &= -B \gamma_n; \quad n = 0, 1, 2, \dots, \infty, \end{aligned} \quad (5.211)$$

where the eigenvalue  $\gamma_n < 0$  can not be determined in the approximations of the linear stability analysis.

The obtained solutions (5.186, 5.210, 5.211) allow to produce the final expressions for the velocity, the concentration and the temperature:

$$\begin{aligned} v_z &= \frac{c^*}{\rho_0} \left\{ -\frac{g}{2\nu} z^2 + \left( \frac{1}{2} - \sqrt{\frac{t_0}{\pi t}} \right) \sqrt{\frac{g}{\nu}} \sqrt{\frac{D}{t_0}} z + \sqrt{\frac{D}{\pi t}} - \right. \\ &\quad \left. - \sqrt{\frac{gD}{\nu}} \sqrt{Dt_0} \left[ \gamma + \sum_{n=1}^{\infty} (\gamma_n + f_n) \cos n\varphi \right] \right\}, \\ c &= c^* \left\{ erfc \frac{z}{2\sqrt{Dt}} + z \sqrt{\frac{g}{\nu}} \sqrt{\frac{t_0}{D}} \left[ \gamma + \sum_{n=1}^{\infty} (\gamma_n + f_n) \cos n\varphi \right] \right\}, \\ \theta &= \theta_0 + \frac{qc^* D}{\lambda} \left[ f_0 + \sum_{n=1}^{\infty} f_n \left( \frac{r}{r_0} \right) \cos n\varphi \right], \quad \gamma = \gamma_0 + f_0. \end{aligned} \quad (5.212)$$

From (5.212) is possible to determine the mass flow at a given moment:

$$\begin{aligned} i &= -\frac{D\rho^*}{\rho_0} \left( \frac{\partial c}{\partial z} \right)_{z=0} = \frac{D\rho^* c^*}{\rho_0} \left\{ \frac{1}{\sqrt{\pi Dt}} - \sqrt{\frac{g}{\nu}} \sqrt{\frac{t_0}{D}} \left[ \gamma + \sum_{n=1}^{\infty} (\gamma_n + f_n) \cos n\varphi \right] \right\}, \\ \rho^* &= \rho_0 + c^*, \quad f_n = f_n \left( \frac{r}{r_0} \right), \quad n = 1, 2, \dots, \infty. \end{aligned} \quad (5.213)$$

The amount of absorbed passed substance through the cross section  $\pi r^2$  is determined directly from (5.213), integrating on  $\varphi$  in the range  $[0, 2\pi]$ , and having in mind that the integrals of the harmonic functions are equal to zero:

$$I = \pi r_o^2 c^* \left( I + \varepsilon \left( \sqrt{\frac{D}{\pi}} - \bar{\gamma} \right) \right), \quad \bar{\gamma} = \gamma D \sqrt{\frac{g}{\nu}} \sqrt{\frac{t_0}{D}}. \quad (5.214)$$

From (5.214) the absorption rate ( $J$ ), the Sherwood number ( $Sh$ ) and the mass of the absorbed substance ( $Q$ ) for a period of time  $t_0$  through a unity surface are directly obtained:

$$J = kc^* = \frac{1}{\pi r_o^2 t_0} \int_0^{t_0} Idt = (I + \varepsilon)c^* \left( 2 \sqrt{\frac{D}{\pi t_0}} - \bar{\gamma} \right), \quad (5.215)$$

$$Sh = \frac{kl}{D} = (I + \varepsilon) \left( 2 \sqrt{\frac{\nu}{\pi g t_0}} \sqrt{\frac{l}{Dt_0}} - \gamma \right), \quad (5.216)$$

$$Q = \frac{1}{\pi r_o^2} \int_0^{t_0} Idt = (I + \varepsilon)c^* \left( 2 \sqrt{\frac{Dt_0}{\pi}} - \bar{\gamma} t_0 \right), \quad \bar{\gamma} = \frac{\gamma D}{l}, \quad (5.217)$$

where  $k$  is the mass transfer coefficient of the non-stationary absorption.

In this way the obtained equations (5.215 – 5.217) allow the determination of the absorption rate with an accuracy defined by the parameter  $\bar{\gamma}$ , which value can not be determined in the approximations of the linear stability analysis. The parameter  $\bar{\gamma}$  may be determined introducing an additional physical condition, or from experimental data.

### 5.5.3. Comparison with experimental data

The study of non-stationary absorption of pure CO<sub>2</sub> in H<sub>2</sub>O [57] provides experimental data for the dependence of  $Q$  on  $\sqrt{t_0}$ . They have been used for the determination of  $\bar{\gamma}$  in (5.217) by means of the least squares method. The value of  $\bar{\gamma}$  was calculated as  $\bar{\gamma} = -1.787 \cdot 10^{-6}$  m/s. On Fig. 5.39 the equation (5.217) is shown for  $\bar{\gamma} = -1.787 \cdot 10^{-6}$  m/s, and the dots are experimental data from [57].

From (5.216) and (5.217) it becomes clear that the increasing of the absorption rate is a result of the loss of stability of the main process (5.186). As a result the small disturbances may increase until reaching a new stable periodic process, i.e. they represent a self-organizing dissipative structure (5.212).

The correctness of the applied linear analysis of the process stability (5.186) may be determined, if a check of the satisfaction of its approximations is carried out. For example, the used of the first equation from (5.189) is legitimate in the cases where:

$$v_z' \frac{\partial v_z'}{\partial z} \ll v_z \frac{\partial v_z}{\partial z}, \quad v_r' \frac{\partial v_z'}{\partial r} \ll v_r \frac{\partial v_z}{\partial r}, \quad v_\varphi' \frac{\partial v_z'}{\partial \varphi} \ll v_\varphi \frac{\partial v_z}{\partial \varphi}. \quad (5.218)$$

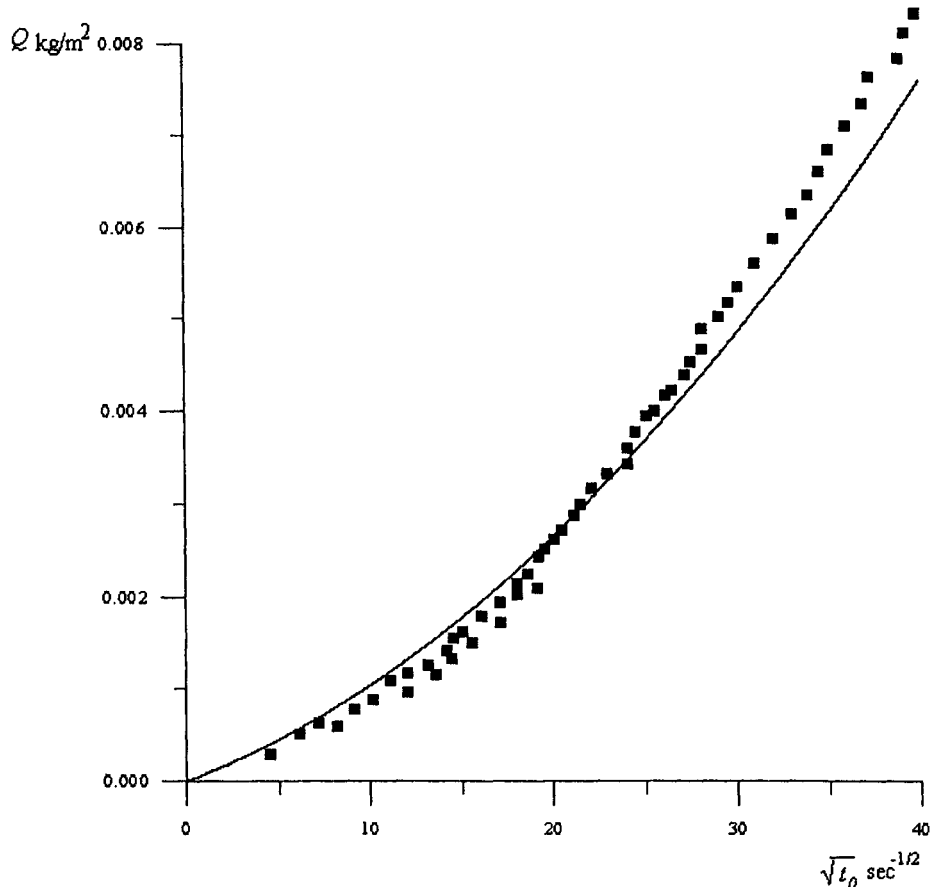


Fig. 5.39. Relation between the amount of the absorbed gas ( $Q \text{ kg/m}^2$ ) and the time ( $\sqrt{t_0} \text{ s}^{-1/2}$ ) ( $D = 1.78 \cdot 10^{-9}$ ,  $c^* = 1.6 \text{ kg/m}^3$ ,  $\bar{\gamma} = -1.787 \cdot 10^{-6} \text{ m/s}$ ,  $\varepsilon = 1.6 \cdot 10^{-3}$ ).

The obtained results for the disturbances (5.206, 5.209 – 5.211) show

$$v_z' \frac{\partial v_z'}{\partial z} = v_r' \frac{\partial v_z'}{\partial r} = v_\varphi' \frac{\partial v_z'}{\partial \varphi} = 0. \quad (5.219)$$

The correctness of the elimination of the rest square terms from the others equations in (5.189–5.191) could be demonstrated in a similar way. Exceptions are the terms:

$$v_z' \frac{\partial c'}{\partial z}, \quad v_z' \frac{\partial \theta'}{\partial z} \quad (5.220)$$

in (5.191) but they will appear also in (5.190) and will be eliminated in the next transformations to obtain (5.204).

The analysis of (5.218 – 5.220) shows that the obtained results (5.212 – 5.217) are correct and are valid not only for very small disturbances, i.e. they satisfy the non-linear form of the system of equations (5.189 – 5.192).

An attempt to explain the discrepancy between the experimental data for a non-stationary absorption of pure CO<sub>2</sub> in H<sub>2</sub>O and the linear theory of mass transfer with the Marangoni effect has been made in [57]. There it has been correctly shown that  $(\theta^* - \theta_0) \approx 0,02^\circ C$  ( $\theta^*$  – temperature of the phase boundary), but the assumption that the fluctuations of  $\theta^*$  as a result of a surface tension gradient are enough to cause the loss of stability are unreasonable. The use of the experimental data for the determination of the characteristic velocity of the flow  $u_0 = 1,12 \cdot 10^{-6} m/s$  shows that obtained velocity is very close to the characteristic one in the cases when it is a result of a non-linear mass transfer :

$$u_0 = \frac{c^*}{\rho_0} \sqrt{\frac{D}{t_0}} = 0,876 \cdot 10^{-6} m/s, \quad t_0 = 10 s.$$

The solution of the Benard problem taking into account the surface tension gradient [8, 64 – 66] shows that the Marangoni effect may occur in layers with thickness not greater than several millimeters. Further it is evident that in the case of a non-stationary absorption at big concentration gradients the occurrence of the Marangoni effect could not be expected.

The interphase mass transfer in a stagnant gas-liquid system has been investigated, as follows: in the case of an irreversible chemical reaction [63]; when an absorbed component is surface active [64]; in the case of stagnant liquid evaporation [65], in the case of presence of waves at the interface [66] etc.

Most of the experimental studies [57,67,68] indicate that under gas absorption the mass transfer rate is significantly greater than the one predicted by the linear theory. On the other hand, under desorption such differences have not been observed. This fact has been explained in different ways [57]. It is possible to demonstrate that the above fact follows directly from the non-linear theory of the mass transfer and the hydrodynamic stability [69].

#### 5.5.4. Comparative analysis of the absorption and desorption rates

Carbon dioxide desorption from a saturated stagnant water solution into a nitrogen gas phase has been investigated experimentally by several research groups [57,67,68]. In this case the CO<sub>2</sub> concentration in the gas phase changes from the equilibrium value at the interface to zero in the bulk of the gas. Thus, it is necessary to use the Oberbeck-Boussinesq (5.141) equations for both phases. As shown in 5.2.1 (see (5.171) and (5.181)) the temperature is practically constant. Thus, (5.141) gives for the gas (1) and the liquid (2) phase, respectively:

$$\begin{aligned} \rho_i \left( \frac{\partial v_z^{(i)}}{\partial t} + v_z^{(i)} \frac{\partial v_z^{(i)}}{\partial z} + v_r^{(i)} \frac{\partial v_z^{(i)}}{\partial r} + \frac{v_\phi^{(i)}}{r} \frac{\partial v_z^{(i)}}{\partial \phi} \right) &= - \frac{\partial p_i}{\partial z} + \\ + \mu_i \left( \frac{\partial^2 v_z^{(i)}}{\partial z^2} + \frac{1}{r} \frac{\partial v_z^{(i)}}{\partial r} + \frac{\partial^2 v_z^{(i)}}{\partial r^2} + \frac{1}{r^2} \frac{\partial^2 v_z^{(i)}}{\partial \phi^2} \right) &+ g(\rho_i - \rho_{0i}), \end{aligned}$$

$$\begin{aligned}
\rho_i \left( \frac{\partial v_r^{(i)}}{\partial t} + v_z^{(i)} \frac{\partial v_r^{(i)}}{\partial z} + v_r \frac{\partial v_r^{(i)}}{\partial r} + \frac{v_\phi}{r} \frac{\partial v_r^{(i)}}{\partial \varphi} - \frac{v_\phi^{(i)2}}{r} \right) &= - \frac{\partial p_i}{\partial r} + \\
+ \mu_i \left( \frac{\partial^2 v_r^{(i)}}{\partial z^2} + \frac{1}{r} \frac{\partial v_r^{(i)}}{\partial r} + \frac{\partial^2 v_r^{(i)}}{\partial r^2} - \frac{v_r^{(i)}}{r^2} + \frac{1}{r^2} \frac{\partial^2 v_r^{(i)}}{\partial \varphi^2} - \frac{2}{r^2} \frac{\partial v_\phi^{(i)}}{\partial \varphi} \right), \\
\rho_i \left( \frac{\partial v_\phi^{(i)}}{\partial t} + v_z^{(i)} \frac{\partial v_\phi^{(i)}}{\partial z} + v_r^{(i)} \frac{\partial v_\phi^{(i)}}{\partial r} + \frac{v_\phi^{(i)}}{r} \frac{\partial v_\phi^{(i)}}{\partial \varphi} + \frac{v_r^{(i)} v_\phi^{(i)}}{r} \right) &= - \frac{1}{r} \frac{\partial p_i}{\partial \varphi} + \\
+ \mu_i \left( \frac{\partial^2 v_\phi^{(i)}}{\partial z^2} + \frac{1}{r} \frac{\partial v_\phi^{(i)}}{\partial r} + \frac{\partial^2 v_\phi^{(i)}}{\partial r^2} - \frac{v_\phi^{(i)}}{r^2} + \frac{1}{r^2} \frac{\partial^2 v_\phi^{(i)}}{\partial \varphi^2} + \frac{2}{r^2} \frac{\partial v_r^{(i)}}{\partial \varphi} \right), \\
\frac{\partial \rho_i}{\partial t} + \frac{\partial (\rho_i v_z^{(i)})}{\partial z} + \frac{\partial (\rho_i v_r^{(i)})}{\partial r} + \frac{\rho_i v_r^{(i)}}{r} + \frac{1}{r} \frac{\partial (\rho_i v_\phi^{(i)})}{\partial \varphi} &= 0, \\
\frac{\partial c_i}{\partial t} + v_z^{(i)} \frac{\partial c_i}{\partial z} + v_r^{(i)} \frac{\partial c_i}{\partial r} + \frac{v_\phi^{(i)}}{r} \frac{\partial c_i}{\partial \varphi} &= D_i \left( \frac{\partial^2 c_i}{\partial z^2} + \frac{1}{r} \frac{\partial c_i}{\partial r} + \frac{\partial^2 c_i}{\partial r^2} + \frac{1}{r^2} \frac{\partial^2 c_i}{\partial \varphi^2} \right), \\
\rho_i = \rho_{0i} \left( 1 + \frac{a^{2-i} c_i}{\rho_{0i}} \right), \quad i = 1, 2, \tag{5.221}
\end{aligned}$$

where  $\rho_{0i}$  is the water density while  $\rho_{02}$  is the density of nitrogen.

Under CO<sub>2</sub> diffusion in N<sub>2</sub> (20° C)  $a$  is determined through the densities of both gases:

$$a = \frac{\rho_{CO_2} - \rho_{N_2}}{\rho_{CO_2}} = 0.367. \tag{5.222}$$

The boundary conditions of (5.221) follow from (5.142) taking into account the interaction between the phases during the desorption process:

$$\begin{aligned}
t = 0, \quad v_z^{(i)} = v_r^{(i)} = v_\phi^{(i)} = c_1 = 0, \quad c_2 = c_{20}; \\
z = 0, \quad v_z^{(i)} = - \frac{D_i}{\rho_{0i}} \frac{\partial c_i}{\partial z}, \quad v_r^{(i)} = v_r^{(2)}, \quad v_\phi^{(i)} = v_\phi^{(2)}, \\
\mu_i \left( \frac{\partial v_r^{(i)}}{\partial z} + \frac{\partial v_z^{(i)}}{\partial \varphi} \right) = \mu_2 \left( \frac{\partial v_r^{(2)}}{\partial z} + \frac{\partial v_z^{(2)}}{\partial \varphi} \right), \\
\mu_i \left( \frac{\partial v_\phi^{(i)}}{\partial z} + \frac{1}{r} \frac{\partial v_z^{(i)}}{\partial \varphi} \right) = \mu_2 \left( \frac{\partial v_\phi^{(2)}}{\partial z} + \frac{1}{r} \frac{\partial v_z^{(2)}}{\partial \varphi} \right), \\
c_1 = \chi c_2, \quad \frac{D_i \rho_i^*}{\rho_{0i}} \frac{\partial c_1}{\partial z} = \frac{D_2 \rho_2^*}{\rho_0^*} \frac{\partial c_2}{\partial z},
\end{aligned}$$

$$\begin{aligned}
z \rightarrow \infty, \quad v_z^{(1)} = v_r^{(1)} = v_\varphi^{(1)} = c_l = 0; \\
z \rightarrow -\infty, \quad v_z^{(2)} = v_r^{(2)} = v_\varphi^{(2)} = c_2 = c_0; \\
r = 0, \quad v_z^{(1)}, v_r^{(1)}, v_\varphi^{(1)}, c_i - \text{finite}; \\
r = r_0, \quad v_z^{(i)} = v_r^{(i)} = v_\varphi^{(i)} = 0, \quad \frac{\partial c_i}{\partial r} = 0; \quad i = 1, 2. \tag{5.223}
\end{aligned}$$

The solution of the problems (5.221) and (5.223) requires dimensionless variables such as (5.144) for both phases:

$$\begin{aligned}
t = t_0 T, \quad z = l_i Z_l^{(i)} = \delta_i Z_2^{(i)}, \quad r = r_0 R, \quad \varphi = 2\pi\Phi, \quad p_i = \rho_{0i} u_{0i}^2 P^{(i)}, \\
v_z^{(i)}(t, z, r, \varphi) = u_{0i} V_z^{(i)}(T, Z_l^{(i)}, R, \Phi) = u_{0i} \tilde{V}_z^{(i)}(T, Z_2^{(i)}, R, \Phi), \\
v_r^{(i)}(t, z, r, \varphi) = \frac{u_{0i} r_0}{l_i} V_r^{(i)}(T, Z_l^{(i)}, R, \Phi) = \frac{u_{0i} r_0}{\delta_i} \tilde{V}_r^{(i)}(T, Z_2^{(i)}, R, \Phi), \\
v_\varphi^{(i)}(t, z, r, \varphi) = 2\pi \frac{u_{0i} r_0}{l_i} V_\varphi^{(i)}(T, Z_l^{(i)}, R, \Phi) = 2\pi \frac{u_{0i} r_0}{\delta_i} \tilde{V}_\varphi^{(i)}(T, Z_2^{(i)}, R, \Phi), \\
c^{(i)}(t, z, r, \varphi) = c_{0i}^* C^{(i)}(T, Z_l^{(i)}, R, \Phi) = c_{0i}^* \tilde{C}^{(i)}(T, Z_2^{(i)}, R, \Phi), \quad i=1, 2, \tag{5.224}
\end{aligned}$$

where the order of the following characteristic scales is known:

$$\begin{aligned}
t_0 \sim 10^2 \text{ s}, \quad r_0 \sim 10^{-2} \text{ m}, \quad \chi = 1.06, \quad c_0 = 1.6 \text{ kg/m}^3, \\
c_{0i}^* = \chi c_0, \quad c_{02}^* = c_0. \tag{5.225}
\end{aligned}$$

The substitution of (5.224) into (5.222) and (5.223) converts the problem in a dimensionless form

$$\begin{aligned}
& \left[ I + \frac{\bar{c}_{0i}^*}{\rho_{0i}} C^{(i)} \right] \left[ \frac{u_{0i} \rho_{0i}}{g t_0 \bar{c}_{0i}^*} \frac{\partial V_z^{(i)}}{\partial T} + \frac{u_{0i}^2 \rho_{0i}}{g l_i \bar{c}_{0i}^*} \left( V_z^{(i)} \frac{\partial V_z^{(i)}}{\partial Z_l^{(i)}} + V_r^{(i)} \frac{\partial V_z^{(i)}}{\partial R} + \frac{V_\varphi^{(i)}}{R} \frac{\partial V_z^{(i)}}{\partial \Phi} \right) \right] = \\
& = - \frac{u_{0i}^2 \rho_{0i}}{g l_i \bar{c}_{0i}^*} \frac{\partial P^{(i)}}{\partial Z_l^{(i)}} + \frac{\mu_i u_{0i}}{g l_i^2 \bar{c}_{0i}^*} \left[ \frac{\partial^2 V_z^{(i)}}{\partial Z_l^{(i)2}} + \frac{l_i^2}{r_0^2} \left( \frac{1}{R} \frac{\partial V_z^{(i)}}{\partial R} + \frac{\partial^2 V_z^{(i)}}{\partial R^2} + \frac{1}{4\pi^2} \frac{1}{R^2} \frac{\partial^2 V_z^{(i)}}{\partial \Phi^2} \right) \right] + C^{(i)}, \\
& \left[ I + \frac{\bar{c}_{0i}^*}{\rho_{0i}} C^{(i)} \right] \left[ \frac{u_{0i} \rho_{0i}}{g t_0 \bar{c}_{0i}^*} \frac{\partial V_r^{(i)}}{\partial T} + \frac{u_{0i}^2 \rho_{0i}}{g l_i \bar{c}_{0i}^*} \left( V_z^{(i)} \frac{\partial V_r^{(i)}}{\partial Z_l^{(i)}} + V_r^{(i)} \frac{\partial V_r^{(i)}}{\partial R} + \frac{V_\varphi^{(i)}}{R} \frac{\partial V_r^{(i)}}{\partial \Phi} - 4\pi^2 \frac{V_\varphi^{(i)2}}{R} \right) \right] = \\
& = - \frac{l_i^2}{r_0^2} \frac{u_{0i}^2 \rho_{0i}}{g l_i \bar{c}_{0i}^*} \frac{\partial P^{(i)}}{\partial R} + \frac{\mu_i u_{0i}}{g l_i^2 \bar{c}_{0i}^*} \left[ \frac{\partial^2 V_r^{(i)}}{\partial Z_l^{(i)2}} +
\right]
\end{aligned}$$

$$\begin{aligned}
& + \frac{l_i^2}{r_0^2} \left( \frac{1}{R} \frac{\partial V_r^{(i)}}{\partial R} + \frac{\partial^2 V_r^{(i)}}{\partial R^2} - \frac{V_r^{(i)}}{R^2} + \frac{1}{4\pi^2} \frac{\partial^2 V_r^{(i)}}{\partial \Phi^2} - \frac{2}{R} \frac{\partial V_\phi^{(i)}}{\partial \Phi} \right) \Bigg], \\
& \left[ 1 + \frac{\bar{c}_{0i}^*}{\rho_{0i}} C^{(i)} \right] \left[ \frac{u_{0i} \rho_{0i}}{gt_0 \bar{c}_{0i}^*} \frac{\partial V_\phi^{(i)}}{\partial T} + \frac{u_{0i}^2 \rho_{0i}}{gl_i \bar{c}_{0i}^*} \left( V_z^{(i)} \frac{\partial V_\phi^{(i)}}{\partial Z_l^{(i)}} + V_r^{(i)} \frac{\partial V_\phi^{(i)}}{\partial R} + \frac{V_\phi^{(i)}}{R} \frac{\partial V_\phi^{(i)}}{\partial \Phi} + \frac{V_r^{(i)} V_\phi^{(i)}}{R} \right) \right] = \\
& = - \frac{l_i^2}{r_0^2} \frac{u_{0i}^2 \rho_{0i}}{gl_i \bar{c}_{0i}^*} \frac{1}{R} \frac{\partial P^{(i)}}{\partial \Phi} + \frac{\mu_i u_{0i}}{gl_i^2 \bar{c}_{0i}^*} \left[ \frac{\partial^2 V_\phi^{(i)}}{\partial Z_l^{(i)2}} + \right. \\
& \left. + \frac{l_i^2}{r_0^2} \left( \frac{1}{R} \frac{\partial V_\phi^{(i)}}{\partial R} + \frac{\partial^2 V_\phi^{(i)}}{\partial R^2} - \frac{V_\phi^{(i)}}{R^2} + \frac{1}{4\pi^2} \frac{1}{R^2} \frac{\partial^2 V_\phi^{(i)}}{\partial \Phi^2} + \frac{1}{2\pi^2} \frac{1}{R^2} \frac{\partial V_r^{(i)}}{\partial \Phi} \right) \right] \\
& \frac{l_i c_{0i}^*}{\rho_{0i} u_{0i} t_0} \frac{\partial C^{(i)}}{\partial T} - \left( \frac{\partial V_z^{(i)}}{\partial Z_l^{(i)}} + \frac{V_r^{(i)}}{R} + \frac{\partial V_r^{(i)}}{\partial R} + \frac{1}{R} \frac{\partial V_\phi^{(i)}}{\partial \Phi} \right) \left[ 1 + \frac{\bar{c}_{0i}^*}{\rho_{0i}} C^{(i)} \right] + \\
& + V_z^{(i)} \frac{\bar{c}_{0i}^*}{\rho_{0i}} \frac{\partial C^{(i)}}{\partial Z_l^{(i)}} + V_r^{(i)} \frac{\bar{c}_{0i}^*}{\rho_{0i}} \frac{\partial C^{(i)}}{\partial R} + \frac{V_\phi^{(i)}}{R} \frac{\bar{c}_{0i}^*}{\rho_{0i}} \frac{\partial C^{(i)}}{\partial \Phi} = 0, \\
& \frac{\partial \tilde{C}^{(i)}}{\partial T} + \frac{u_{0i} t_0}{\delta_i} \left( \tilde{V}_z^{(i)} \frac{\partial \tilde{C}^{(i)}}{\partial Z_2^{(i)}} + \tilde{V}_r^{(i)} \frac{\partial \tilde{C}^{(i)}}{\partial R} + \frac{\tilde{V}_r^{(i)}}{R} \frac{\partial \tilde{C}^{(i)}}{\partial \Phi} \right) = \\
& = \frac{D_i t_0}{\delta_i^2} \left[ \frac{\partial^2 \tilde{C}^{(i)}}{\partial Z_2^{(i)2}} + \frac{\delta_i^2}{r_0^2} \left( \frac{1}{R} \frac{\partial \tilde{C}^{(i)}}{\partial R} + \frac{\partial^2 \tilde{C}^{(i)}}{\partial R^2} + \frac{1}{4\pi^2} \frac{1}{R^2} \frac{\partial^2 \tilde{C}^{(i)}}{\partial \Phi^2} \right) \right];
\end{aligned}$$

$$T = 0, \quad V_z^{(i)} = V_r^{(i)} = V_\phi^{(i)} = \tilde{C}^{(i)} = 0, \quad \tilde{C}^{(2)} = I;$$

$$Z_l^{(i)} = Z_2^{(i)} = 0, \quad V_z^{(i)} = - \frac{D_i c_{0i}^*}{u_{0i} \rho_{0i} \delta_i} \frac{\partial \tilde{C}^{(i)}}{\partial Z_2^{(i)}},$$

$$\frac{\partial V_r^{(i)}}{\partial Z_l^{(i)}} + \frac{l_i^2}{r_0^2} \frac{\partial V_z^{(i)}}{\partial R} = \frac{\mu_2 u_{02} l_i^2}{\mu_i u_{0i} l_2^2} \left( \frac{\partial V_r^{(2)}}{\partial Z_l^{(2)}} + \frac{l_2^2}{r_0^2} \frac{\partial V_z^{(2)}}{\partial R} \right),$$

$$\frac{\partial V_\phi^{(i)}}{\partial Z_l^{(i)}} + \frac{l_i^2}{4\pi^2 r_0^2} \frac{1}{R} \frac{\partial V_z^{(i)}}{\partial \Phi} = \frac{\mu_2 u_{02} l_i^2}{\mu_i u_{0i} l_2^2} \left( \frac{\partial V_\phi^{(2)}}{\partial Z_l^{(2)}} + \frac{l_2^2}{r_0^2 4\pi^2} \frac{\partial V_z^{(2)}}{\partial R} \right),$$

$$C^{(i)} = C^{(2)}, \quad \frac{\partial C^{(i)}}{\partial Z_l^{(i)}} = \frac{D_2 \rho_2 \rho_{0i} \delta_i}{D_1 \rho_1 \rho_{02} \delta_2 \chi} \frac{\partial \tilde{C}^{(2)}}{\partial Z_l^{(2)}},$$

$$Z_l^{(i)} \rightarrow \infty, \quad V_z^{(i)} = V_r^{(i)} = V_\phi^{(i)} = C^{(i)} = 0;$$

$$Z_l^{(2)} \rightarrow -\infty, \quad V_z^{(2)} = V_r^{(2)} = V_\phi^{(2)} = 0, \quad C^{(2)} = I;$$

$R = 0, V_z^{(i)}, V_r^{(i)}, V_\varphi^{(i)}, c^{(i)}$  - finite;

$$R = 1, V_z^{(i)} = V_r^{(i)} = V_\varphi^{(i)} = 0, \frac{\partial C^{(i)}}{\partial R} = 0; i = 1, 2, \quad (5.226)$$

where:

$$\bar{c}_{0i}^* = a^{2-i} c_{0i}^*, \quad i = 1, 2.$$

The qualitative analysis of (5.226) may be performed in a way similar to that employed while considering the absorption (see 5.51). This allows to evaluate the characteristic scales for both phases as:

$$\begin{aligned} \frac{D_i t_0}{\delta_i^2} &= 1, \quad \delta_i = \sqrt{D_i t_0}, \quad \delta_1 \sim 10^{-2} \text{ m}, \quad \delta_2 \sim 10^{-4} \text{ m}, \\ \frac{\mu_i u_{0i}}{g l_i^2 \bar{c}_{0i}^*} &= 1, \quad \frac{D_i \dot{c}_{0i}}{u_{0i} \rho_{0i} \delta_i} = 1, \\ u_{0i} &= \frac{\dot{c}_i}{\rho_{0i}} \sqrt{\frac{D_i}{t_0}}, \quad u_{01} \sim 10^{-4} \text{ m/s}, \quad u_{02} \sim 10^{-8} \text{ m/s}, \\ l_i &= \sqrt{\frac{a^{2-i} \mu_i}{\rho_{0i} g}} \sqrt{\frac{D_i}{t_0}}, \quad l_1 \sim 10^{-5} \text{ m}, \quad l_2 \sim 10^{-7} \text{ m}. \end{aligned} \quad (5.227)$$

The characteristic scales (5.227) permit the evaluation of the parameter orders in (5.226):

$$\begin{aligned} \varepsilon &= \frac{c_i^*}{\rho_{0i}} \sim \bar{\varepsilon}_i = \frac{\bar{c}_i^*}{\rho_{0i}} \sim [l, 10^{-3}], \quad \frac{u_{0i} \rho_{0i}}{g t_0 \bar{c}_i^*} \sim [10^{-7}, 10^{-9}], \\ \frac{u_{0i}^2}{g l_i \bar{\varepsilon}_i} &\sim [10^{-3}, 10^{-7}], \quad \frac{l_i^2}{r_0^2} \sim [10^{-6}, 10^{-10}], \quad \frac{\delta_i^2}{r_0^2} \sim [l, 10^{-4}], \\ \frac{l_i}{t_0 u_{0i} \bar{\varepsilon}_i} &\sim [10^{-3}, 10^{-4}], \quad \frac{u_{0i} t_0}{\delta_i} = \varepsilon_i \sim [l, 10^{-3}], \\ b &= \frac{\mu_2 u_{02} l_1^2}{\mu_1 u_{01} l_2^2} \sim 1, \quad \frac{D_2 \rho_2^* \rho_{01} \delta_1}{D_1 \rho_1^* \rho_{02} \delta_2} \sim 10^{-2}, \end{aligned} \quad (5.228)$$

where the values in the square brackets are for the gas phase (1) and the liquid phase (2) respectively.

The order( $10^{-2}$ ) of the last parameter in (5.228) shows that the mass transfer under desorption of  $\text{CO}_2$  from a saturated water is limited by the mass transfer in the liquid phase. i.e.,  $C^{(i)} \equiv 0$ . Further, only the equations for the liquid phase will be considered. For simplicity the superscript (2) will be omitted. In this way the set (5.226) gives:

$$\begin{aligned}
& \frac{\partial^2 V_z}{\partial Z_1^2} + C = 0, \quad \frac{\partial^2 V_r}{\partial Z_1^2} = 0, \quad \frac{\partial^2 V_\varphi}{\partial Z_1^2} = 0, \\
& \frac{\partial V_z}{\partial Z_1} + \frac{V_r}{R} + \frac{\partial V_r}{\partial R} + \frac{1}{R} \frac{\partial V_\varphi}{\partial \Phi} = 0, \\
& \frac{\partial \tilde{C}}{\partial T} = \frac{\partial^2 \tilde{C}}{\partial Z_2^2}; \\
& T = 0, \quad \tilde{C} = 0; \\
& Z_1 = Z_2 = 0, \quad V_z = -\frac{\partial \tilde{C}}{\partial Z_2}, \quad \frac{\partial V_r}{\partial Z_1} = 0, \quad \frac{\partial V_\varphi}{\partial Z_1} = 0, \quad \tilde{C} = 0; \\
& Z_1 = Z_2 \rightarrow -\infty, \quad V_z = V_r = V_\varphi = 0, \quad \tilde{C} = 1; \\
& R = 0, \quad V_r - \text{finite.}
\end{aligned} \tag{5.229}$$

It follows from (5.229) that the solution for  $\tilde{C}$  is :

$$\tilde{C} = -\operatorname{erf} \frac{Z_2}{2\sqrt{T}} \quad (Z_2 \leq 0), \quad \left\langle \tilde{C} = \operatorname{erfc} \frac{Z_2}{2\sqrt{T}} \quad (Z_2 \geq 0) \right\rangle, \quad Z_2 = \alpha_0 Z_1, \quad \alpha_0 = \frac{l}{\delta} \sim 10^{-3}. \tag{5.230}$$

Here and up to the end of this part of the book, the results concerning absorption will be shown in brackets  $\langle \rangle$ .

The solution (5.230) gives:

$$C = -\operatorname{erf} \left( \alpha_0 \frac{Z_1}{2\sqrt{T}} \right) \approx 0, \quad \left\langle C = \operatorname{erfc} \left( \alpha \frac{Z_1}{2\sqrt{T}} \right) \approx 1 \right\rangle. \tag{5.231}$$

The substitution of (5.231) into (5.229) shows that in the case of desorption of gas from a stagnant liquid there are no conditions allowing a natural convection. Thus, for the flow velocity components (induced by the mass transfer in the liquid phase) are obtained:

$$\begin{aligned}
& \frac{\partial^2 V_z}{\partial Z_1^2} = 0; \quad \left\langle \frac{\partial^2 V_z}{\partial Z_1^2} = 1 \right\rangle; \quad Z_1 = 0, \quad V_z = -\left( \frac{\partial \tilde{C}}{\partial Z_2} \right)_{Z_2=0}; \quad Z_1 = -l, \quad V_z = 0. \\
& \frac{\partial V_r}{\partial R} + \frac{V_r}{R} = -\frac{\partial V_z}{\partial Z_1} - \frac{1}{R} \frac{\partial V_\varphi}{\partial \Phi}; \quad R = 0, \quad V_r^{(0)} - \text{finite.} \\
& \frac{\partial^2 V_\varphi}{\partial Z_1^2} = 0; \quad Z_1 = 0, \quad \frac{\partial V_\varphi}{\partial Z_1} = 0; \quad Z_1 = -l, \quad V_\varphi = 0.
\end{aligned} \tag{5.232}$$

In the above problems the boundary condition at  $(-\infty)$  is substituted by the condition at  $(-l)$ , i.e. at the border of the boundary layer. The solutions are straightforward:

$$\begin{aligned}
 V_z &= \frac{1}{\sqrt{\pi T}} (Z_l + l), \quad (Z_l \leq 0), \quad \left\langle V_z = -\frac{1}{2} Z_l^2 + \left( \frac{1}{2} - \frac{l}{\sqrt{\pi T}} \right) Z_l + \frac{l}{\sqrt{\pi T}} \quad (Z_l \geq 0) \right\rangle, \\
 V_r &= -\frac{l}{2\sqrt{\pi T}} R, \quad \left\langle V_r = \left( \frac{1}{2} Z_l + \frac{l}{2\sqrt{\pi T}} - \frac{l}{4} \right) R \right\rangle, \\
 V_\varphi &\equiv 0. \tag{5.233}
 \end{aligned}$$

The result (5.233) indicates that a larger concentration gradient in the liquid (at the interface) induces the flow in a liquid bulk.

The velocity field (5.233) and the concentration distribution in the liquid (5.230) may be expressed as:

$$\begin{aligned}
 v_z &= \varepsilon_0 \sqrt{\frac{D}{\pi t}} \left( \frac{z}{l} + 1 \right), \quad v_r = -\frac{\varepsilon_0}{2l} \sqrt{\frac{D}{\pi t}} r, \quad \varepsilon_0 = \frac{c_0}{\rho_0}, \\
 v_\varphi &\equiv 0, \quad c = -c_0 \operatorname{erf} \frac{z}{2\sqrt{Dt}}, \quad l = \sqrt{\frac{\mu}{\rho_0 g}} \sqrt{\frac{D}{t_0}}. \tag{5.234}
 \end{aligned}$$

The mass transfer rate may be obtained in the way already employed for (5.182). The relationships for the Sherwood number and the amount of the desorbed substance are similar to those obtained for the absorption process:

$$Sh = \frac{kl}{D} = 2 \sqrt{\frac{\nu}{\pi g t_0}} \sqrt{\frac{l}{Dt_0}}, \quad Q = 2c_0 \sqrt{\frac{Dt_0}{\pi}} \text{ kg/m}^2, \tag{5.235}$$

where in case of desorption  $c' = 0$  and  $\rho' = \rho_0$ .

The stability of the desorption process may be studied by means of small perturbations of the axial velocity, the pressure and the concentration:

$$v_z + v'_z, \quad p + p', \quad c + c', \tag{5.236}$$

in the complete set of equations of Oberbeck-Boussinesq (5.221) and (5.223). The perturbations may be expressed through Fourier series of eigenfunctions, where  $\omega$  and  $n$  are eigenvalues:

$$\begin{aligned}
 v'_z &= \exp(\omega t) \sum_{n=0}^{\infty} v_n(t, z, r) \cos(n\varphi), \\
 p' &= \exp(\omega t) \sum_{n=0}^{\infty} p_n(t, z, r) \cos(n\varphi), \\
 c' &= \exp(\omega t) \sum_{n=0}^{\infty} c_n(t, z, r) \cos(n\varphi). \tag{5.237}
 \end{aligned}$$

There are stable periodic solutions at  $\omega = 0$ . After elimination of the pressure (like in 5.52) the eigenvalue problem takes the form:

$$\begin{aligned}
 & \frac{\partial v_n}{\partial t} + v_n \frac{\partial v_z}{\partial z} + v_z \frac{\partial v_n}{\partial z} + v_r \frac{\partial v_n}{\partial r} = \nu \left( \frac{\partial^2 v_n}{\partial z^2} + \frac{l}{r} \frac{\partial v_n}{\partial r} + \frac{\partial^2 v_n}{\partial r^2} - \frac{n^2}{r^2} v_n \right) + \\
 & + \frac{g}{\rho_0} c \left\langle + \int \frac{\partial v_r}{\partial z} \frac{\partial v_n}{\partial z} dr \right\rangle, \\
 & - \frac{\partial v_n}{\partial z} = \frac{D}{\rho_0} \left( \frac{\partial^2 c_n}{\partial z^2} + \frac{\partial^2 c_n}{\partial r^2} + \frac{l}{r} \frac{\partial c_n}{\partial r} - \frac{n^2}{r^2} c_n \right); \\
 & z = 0, \quad v_n = -\frac{D}{\rho_0} \frac{\partial c_n}{\partial z}, \quad c_n = 0; \\
 & z = -\infty, \quad v_n = -\frac{D}{\rho_0} \frac{\partial c_n}{\partial z}; \\
 & r = 0, \quad v_n, c_n - \text{finite}; \\
 & r = r_0, \quad v_n = 0, \quad \frac{\partial c_n}{\partial r} = 0; \quad n = 0, 1, 2, \dots, \infty. \tag{5.238}
 \end{aligned}$$

The comparison between (5.238) and (5.204) shows that the difference between the absorption and the desorption processes is determined by the velocity distribution in the main flow (under desorption  $\frac{\partial v_r}{\partial z} = 0$ ).

The solution of (5.238) may be presented in the form of (5.206) :

$$\begin{aligned}
 v_n &= u_0 [V_n(Z, T) - Bf_n(R)], \\
 c_n &= c_0 [C_n(Z, T) + Zf_n(R)], \quad n = 0, 1, 2, \dots, \infty, \\
 T &= \frac{t}{t_0}, \quad Z = \frac{z}{l}, \quad R = \frac{r}{r_0}, \quad B = \frac{D\varepsilon_0}{u_0 l}, \quad \varepsilon_0 = \frac{c_0}{\rho_0}.
 \end{aligned}$$

The introduction of new variables into (5.238) leads to:

$$\begin{aligned}
 & \frac{l^2}{\nu t_0} \frac{\partial V_n}{\partial T} + \frac{u_0 l}{\nu} \left[ (V_n - Bf_n) \frac{\partial V_z}{\partial Z} + V_z \frac{\partial V_n}{\partial Z} - BV_r f'_n \right] = \frac{\partial^2 V_n}{\partial Z^2} - \frac{l^2}{r_0^2} \frac{n^2}{R^2} V_n + \\
 & + \frac{\varepsilon_0 l^2 g}{\nu u_0} (C_n + Zf_n) \left\langle + \frac{u_0 l}{\nu} \frac{r_0^2}{l^2} \int \frac{\partial V_r}{\partial Z} \frac{\partial V_n}{\partial Z} dR \right\rangle \\
 & \frac{u_0 l}{\varepsilon_0 D} \frac{\partial V_n}{\partial Z} = \frac{\partial^2 C_n}{\partial Z^2} - \frac{l^2}{r_0^2} \frac{n^2}{R^2} C_n;
 \end{aligned}$$

$$\begin{aligned}
& f_n'' + \frac{1}{R} f_n' - \frac{n^2}{R^2} f_n = 0; \\
& Z = 0, \quad V_n = -B \frac{\partial C_n}{\partial Z}, \quad C_n = 0; \\
& Z \rightarrow -\infty, \quad V_n = -B \frac{\partial C_n}{\partial Z}; \\
& R = 0, \quad f_n \text{ finite;} \\
& R = l, \quad f_n' = 0, \quad n = 0, 1, 2, \dots, \infty,
\end{aligned} \tag{5.239}$$

where (5.210) is the solution for  $f_n$  ( $n = 0, 1, 2, \dots, \infty$ ).

The orders of the dimensionless parameters in (5.239) are as follows :

$$\frac{l^2}{\nu t_0} \sim 10^{-10}, \quad \frac{u_0 l}{\nu} \sim 10^{-9}, \quad \frac{l^2}{r_0} \sim 10^{-10}, \quad \frac{\varepsilon_0 l^2 g}{\nu u_0} \sim 10^{-2}, \quad \frac{u_0 l}{\varepsilon_0 D} \sim 10^{-3}, \left\langle \frac{u_0 l r_0^2}{\nu l^2} \sim 10 \right\rangle. \tag{5.240}$$

The small parameters in (239) may be assumed zero and the resulting set for the determination of  $V_n$  and  $C_n$  ( $n = 0, 1, 2, \dots, \infty$ ) is :

$$\begin{aligned}
& \frac{\partial^2 V_n}{\partial Z^2} = 0 \quad \left\langle \frac{\partial V_n}{\partial Z} = 0 \right\rangle; \quad \frac{\partial^2 C_n}{\partial Z^2} = 0; \\
& Z = 0, \quad V_n = -B \frac{\partial C_n}{\partial Z}, \quad C_n = 0; \\
& Z \rightarrow -\infty, \quad V_n = -B \frac{\partial C_n}{\partial Z}; \quad n = 0, 1, 2, \dots, \infty.
\end{aligned} \tag{5.241}$$

The problem (5.241) has a solution for  $V_n$  ( $n = 0, 1, 2, \dots, \infty$ ) depending linearly on  $Z$ . This leads to a result similar to (5.211):

$$V_n = -B \gamma_n, \quad C_n = \gamma_n Z, \quad \gamma_n \leq 0, \quad Z \leq 0, \quad n = 0, 1, 2, \dots, \infty, \tag{5.242}$$

where the velocity and concentration are determined with an accuracy of an unspecified constant that could not be obtained in the approximation of the linear stability theory.

The result developed shows that under desorption of  $\text{CO}_2$  from a stagnant saturated water the desorption rate may be expressed by a relationship similar to that obtained for the absorption. So, the process rate can be determined from (5.215 - 5.217). This result could be

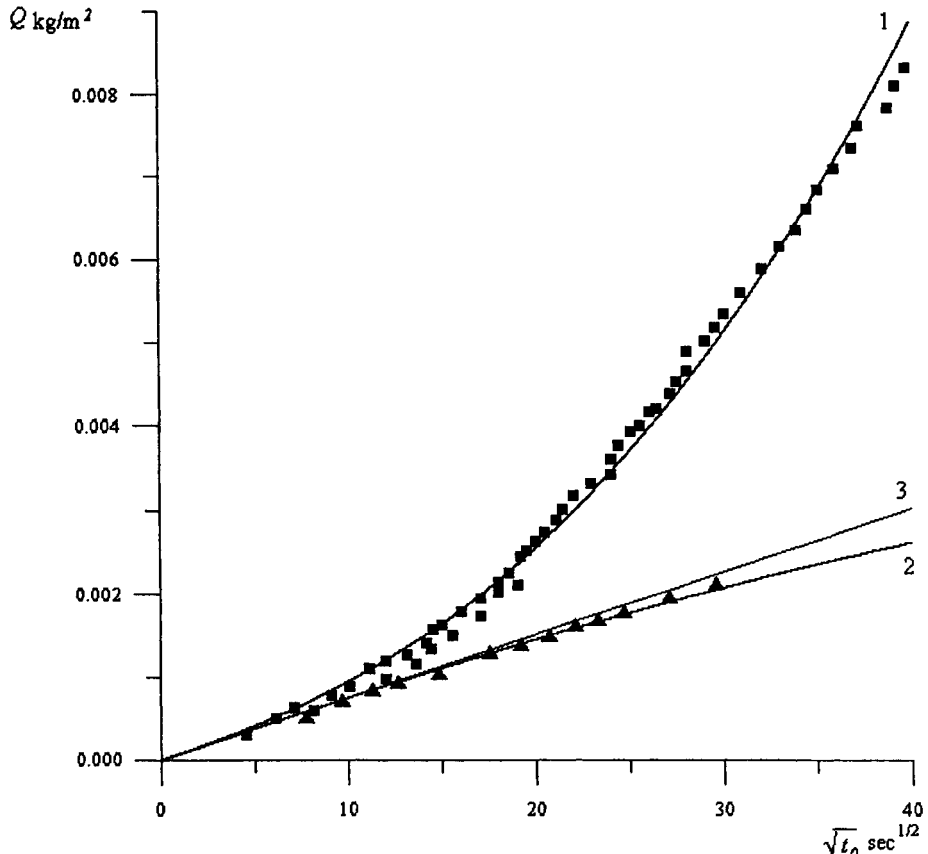


Fig. 5.40. Comparison of the absorption and desorption rates (5.243) of  $\text{CO}_2$  in  $\text{H}_2\text{O}$ :  
 1) absorption ( $\gamma = -4.204 \cdot 10^{-4}$ ); 2) desorption ( $\gamma = 3.029 \cdot 10^{-5}$ ); 3) linear theory ( $\gamma = 0$ );  
 Experimental data: ■ - absorption, ▲ - desorption.

derived more precisely taking into account the weak dependence of  $\bar{\gamma}$  from  $t_0$   $\left(\bar{\gamma} \sim t_0^{\frac{l}{4}}\right)$ .

Thus, from (5.217) and (5.214) it directly follows:

$$Sh = \frac{kl}{D} = 2 \sqrt{\frac{\nu}{\pi g t_0}} \sqrt{\frac{l}{Dt_0}} - \gamma,$$

$$Q = c_0 \left[ 2 \sqrt{\frac{Dt_0}{\pi}} - \gamma \left( \frac{g}{v} \right)^{\frac{1}{2}} D^{\frac{3}{4}} t_0^{\frac{5}{4}} \right]. \quad (5.243)$$

The obtained result (5.243) is valid in case of absorption as well, when  $c_0 = c^*$  ( $\varepsilon \ll 1$ ).

The eigenvalue  $\gamma$  is determined by the least squares method applied to the experimental data obtained in [57, 67, 68]. In case of absorption  $\gamma = -4.204 \cdot 10^{-4}$ , while in case of desorption  $\gamma = 3.032 \cdot 10^{-5}$ . This result indicates that the desorption process is stable in contrast to the absorption. In this case the mass transfer rate may be determined by (5.234). Figure 5.40 presents the relationship  $Q = Q(\sqrt{t_0})$  in (5.243) for absorption (line 1), desorption (line 2) and according to the linear theory of mass transfer, i.e.  $\gamma = 0$  (line 3), compared with the experimental data [57, 67, 68].

The comparative analysis of the both processes shows that under desorption of CO<sub>2</sub> from a stagnant saturated water there are no conditions allowing a natural convection. As a result the axial velocity component depends linearly on the axial co-ordinate (see (5.234)), while the radial component is independent of the same co-ordinate. This result is opposite to that obtained under absorption, where the relationship of the axial co-ordinate is of a power 2. Thus, the axial perturbations of the concentration attenuate and the respective axial perturbations of the velocity attenuate too. The radial perturbations are symmetrical and do not affect the mass transfer rate. The concentration gradient at the interface induces a flow, but its velocity is small and has no effect on the mass transfer rate. This fact together with the absence of a natural convection in desorption make the induced flow stable with respect to the axial perturbations provoked by the perturbations of the concentration.

Due to the stability of the desorption process and the absence of a non-linear mass transfer effect the process rate may be determined by the linear theory of the non-stationary mass transfer (5.235). This result is confirmed by the experimental data [57, 67, 68] shown in Fig. 5.40.



The theoretical analysis of the mechanism and the kinetics of the transport processes in systems with intensive mass transfer shows that in the cases of a gas absorption at great concentration gradients and a chemical reaction in the liquid phase, the mass transfer rate is significantly higher than the one predicted by the linear theory of mass transfer. In the absence of surface active agents and availability of a temperature field, caused by the thermal effect of the chemical reaction, the surface tension gradient is not enough for the occurrence of the Marangoni effect. In the case of a non-stationary absorption of a gas in a stagnant liquid, a flow is induced as a result of a natural convection and a non-linear mass transfer (a density gradient in the volume and a big mass flux through the phase boundary). This problem differs significantly from the Benard problem, as the big concentration gradient at the interphase induces a secondary flow, oriented normally to this surface, and in this way does not allow the existence of a mechanical equilibrium (diffusion in an immobile liquid). In this way the considered basic process (simultaneous momentum, mass and heat transfer) is

unstable regarding disturbances (that may not be small). As a result the process becomes unstable and is transformed into a periodic stable process, i.e. a self-organizing dissipative structure (velocity, concentration and temperature field). The mass transfer rate is significantly greater than that which is predicted by the linear theory. In case of desorption the process is stable and the mass transfer kinetics is determined according the linear theory. These results are confirmed by a large amount of experimental data.

## References

1. V. I. Arnold, *Ordinarily Differential Equations*, Nauka, Moskow, 1984 (in Russian).
2. M. Braun, *Differential Equations and their Applications*, Springer-Verlag, New York, 1978.
3. D. Zwillinger, *Handbook of Differential Equations* (ed. II) Acad. Ress. Inc., Boston, 1957.
4. J. E. Marsden and M. McCracken, *The Hopf Bifurcation and its Application*, Springer-Verlag, New York, 1976.
5. E. Kamke, *Differentialgleichungen*, Leipzig, 1959.
6. D. D. Joseph, *Stability of Fluid Motion*, Springer-Verlag, New York, 1976.
7. H. Shlichting, *Grenzschicht-Theorie*, Verlag G. Broun, Karlsruhe, 1965.
8. G. Z. Gershuni and E. M. Zhuhovitski, *Convective Stability in Compressible Liquids*, Nauka, Moskow, 1972 (in Russian).
9. *Hydrodynamics of Interphase Surfaces*, Notes of mechanics 34, Nauka, Moscow, 1984 (in Russian).
10. R. Betchov and W. O. Criminale, *Stability of Parallel Flows*, Acad. Press, New York, 1967.
11. V. U. Zhigulev and A. M. Tumin, *Arising of Turbulence*, Nauka, Novosibirsk, 1987 (in Russian).
12. L. D. Landau and E. M. Lifshits, *Theoretical Physics*, 4 *Hydrodynamics*, Nauka, Moskow, 1988 (in Russian).
13. Chr. Boyadjiev, *J. Phys. Eng (Russia)*, 60, (1991) 845.
14. M. A. Goldshtik and V. N. Shtern, *Hydrodynamic Stability and Turbulence*, Nauka, Novosibirsk, 1977 (in Russian).
15. A. A. Abramov, *J. Comput. Math. Math-Phys.*, (Russia), 1 (1961) 542.
16. Chr. Boyadjiev, I. Halatchev, B. Tchavdarov, *Int. J. Heat Mass Transfer*, 39 (1996) 2571.
17. K. Bussman, H. Munz, *Absaugung. Jb. dt. Luftfahrtforschung I*, (1942) 36.
18. Chr. Boyadjiev and E. Toshev, *Hung. J. Ind. Chem.*, 18 (1990) 7.
19. Th. L. Van Stijn, *Stability of Almost Parallel Boundary Layer Flows*, Ph. D. Thesis, Royal University of Groningen, 1983.
20. Chr. Boyadjiev and N. Vulchanov, *C. r. Acad. Bulg. Sci.*, 40 (1987) 35.
21. Th. L. Van Stijn and A. I. van de Vooren, *J. Eng. Math. (Netherlands)*, 14 (1980) 25.
22. R. Jordinson, *J. Fluid Mech.*, 43 (1970) 801.
23. Chr. Boyadjiev and V. Beshkov, *Mass Transfer in Liquid Film Flows*, Publ. House Bulg. Acad. Sci., Sofia, 1984, (in Bulgarian).
24. Chr. Boyadjiev and V. Beshkov, *Mass Transfer in Falling Liquid Films*, Mir, Moscow, 1988, (in Russian).

25. W. B. Brown, A stability criterion for three-dimensional laminar boundary layers. -In: *Boundary Layer and Flow Control*. 2. (1961) 913 (London).
26. M. D. Barry and M. A. S. Ross, *J. Fluid Mech.*, 43 (1970) 813.
27. Th. L. Van Stijn and A. I. van de Vooren, *Comput. Fluids* (G.B.), 10 (1983) 223.
28. Chr. Boyadjiev and M. Doichinova, *Hung. J. Ind. Chem.*, 27 (1999) 215.
29. Chr. Boyadjiev and N., Vulchanov *Int. J. Heat Mass Transfer*, 31 (1988) 795.
30. N. Vulchanov and Chr. Boyadjiev, *Int. J. Heat Mass Transfer*, 31 (1988) 801.
31. N. Vulchanov and Chr. Boyadjiev, *Int. J. Heat Mass Transfer*, 33 (1990) 2045.
32. G. A. Ostroumov, *Free Convection under Internal Problem Conditions*, Technika, Moscow, 1952 (in Russian).
33. Chr. Boyadjiev, *Bulg. Chem. Communications*, 26 (1993) 33.
34. Chr. Boyadjiev and I. Halatchev, *Int. J. Heat Mass Transfer*, 39 (1996) 2581.
35. I. Halatchev and Chr. Boyadjiev, *Int. J. Heat Mass Transfer*, 39 (1996) 2587.
36. Ts. Sapundzhiev and Chr. Boyadjiev, *Russian J. Eng. Thermophys* (Russia), 3 (1993) 185.
37. M. Hennenberg, P. M. Bisch, M. Vignes-Adler and A. Sanfeld, *Interfacial instability and longitudinal waves in liquid-liquid systems*. Lecture Notes in Physics, Springer-Verlag, Berlin, No. 105 (1979) 229
38. H. Linde, P. Schwartz and H. Wilke, *Dissipative structures and nonlinear kinetics of the Marangoni-instability*. Lecture Notes in Physics, Springer-Verlag Berlin, No. 105 (1979) 75.
39. H. Savistowski, *Ber. Bunsenges Phys. Chem.*, 85 (1981) 905.
40. Chr. Boyadjiev and I. Halatchev, *Int. J. Heat Mass Transfer*, 39 (1996) 2593.
41. Chr. Boyadjiev, *J. Phys. Eng. (Russia)*, 59 (1990) 92.
42. Chr. Boyadjiev, *J. Phys. Eng. (Russia)*, 59 (1990) 277.
43. M. G. Velarde and J. L. Castillo, *Transport and reactive phenomena leading to interfacial instability. Convective Transport and Instability Phenomena*, edited by Zieper J., Oertel H., Braun Verlag, (1981) 235.
44. Chr. Boyadjiev and I. Halatchev, *Int. J. Heat Mass Transfer*, 41 (1998) 945.
45. Chr. Boyadjiev and I. Halatchev, *Int. J. Heat Mass Transfer*, 41 (1998) 197.
46. J. A. Buevich, *J. Phys. Eng.*, (Russia), 49 (1985) 230.
47. A. Sanfeld, A. Steinchen, M. Hennenberg, P. M. Bisch, D. Van Lamswerde-Galle and W. Dall-Vedove, *Mechanical and Electrical Constraints and Hydrodynamic Interfacial Instability*, Lecture Notes in Physics, Springer-Verlag Berlin, No. 105 (1979) 168
48. L. E. Scriven and C. V. Sterling, *Nature (London)* 127 No. 4733 (1960) 186.
49. T. S. Sorensen and M., Hennenberg, *Instability of a Spherical Drop with Surface Chemical Reaction and Transfer of Surfactants*. Lecture Note in Physics, Springer-Verlag Berlin, No. 105 (1979) 276.
50. Chr. Boyadjiev Proceedings Apollonia'99, 4-th Workshop on "Transport Phenomena in Two-Phase Flow", Sept. 11-16 Sozopol, Bulgaria (1999) 141.
51. Lecture Note in Physics, Springer-Verlag, Berlin, (1979) No. 105.
52. H. Benard, *Revue generale des Sciences, pures et appliquees*, 12 (1900) 1261, 1309.
53. H. Benard, *Ann. Chim. Phys.*, 23, No. 7 (1901) 62.
54. J. K. A. Pearson, *J. Fluid Mech.*, 4 (1958) 489.
55. D. A. Nield, *J. Fluid Mech.*, 19 (1964) 341.
56. D. A. Nield, *ZAMP*, 17 (1996) 226.

57. V. V. Dilman, N. N. Kulov, V.A. Lothov, V.A. Kaminski and V. I. Najdenov, Theoretical Fundaments of Chemical Technology, 32 (1998) 377.
58. .V. S. Krylov, Success. Chem. (Russia), 49, No.11 (1980) 118.
59. C. V. Sternling and L. E. Scriven, AIChEJ, 5 (1959) 514.
60. . Chr. Boyadjiev Proceedings Apollonia'99, 4-th Workshop on "Transport Phenomena in Two-Phase Flow", Sept.11-16 Sozopol, Bulgaria (1999), 141, 155.
61. Chr. Boyadjiev, Int. J. Heat Mass Transfer, (in press).
62. Chr. Boyadjiev, Int. J. Heat Mass Transfer, (in press).
63. K. Warmuzinski and I. Buzec, Chem. Eng.Sci., 45 (1990) 243.
64. P. L. T. Brian and J. R. Ross, AIChEJ, 18 (1972) 582.
65. A. Vidal and A. Acrivos, Eng. Chem. Eng. Fund., 7 (1968) 894.
66. K.Muenz and J. M. Marchello, AIChEJ, 12 (1966) 249.
67. R. E. Plevan and J.A. Quinn, AIChEJ, 12 (1966) 894.
68. V.V. Dilman, V.I. Najdenov and V.V. Olevskii, Chem. Industry (Russia), No.8 (1992) 465.
69. Chr. Boyadjiev, Int. J. Heat Mass Transfer, (in press).

This Page Intentionally Left Blank

## Conclusion

A theoretical analysis of non-linear mass transfer has been developed in the book. The main idea follows from the non-linearity of the convective diffusion equation:

$$\rho(c)W(c)\mathbf{grad}c = \operatorname{div}[\rho(c)D(c)\mathbf{grad}c] + kc^n,$$

The velocity  $W$  is governed by the hydrodynamic equations. However, the principal non-linear phenomenon is due to the concentration effects on the velocity  $W(c)$ , density  $\rho(c)$ , viscosity  $\mu(c)$ , diffusivity  $D(c)$  and on the chemical reaction rate  $kc^n$  (for  $n \neq 0$ ).

It was shown in the Introduction that there are a number of cases with non-linear mass transfer behavior. The well-known linear mass transfer theory could be successfully applied in these cases. However, in case of two-phase interphase mass transfer with a flat interface the above equation permits a non-linear mass transfer model to be derived by means of the boundary layer approximation.

$$\rho_i \left( u_j \frac{\partial u_j}{\partial x} + v_j \frac{\partial u_j}{\partial y} \right) = \mu_j \frac{\partial^2 u_j}{\partial y^2} + A_j, \quad \frac{\partial u_j}{\partial x} + \frac{\partial u_j}{\partial y} = 0,$$

$$u_j \frac{\partial c_j}{\partial x} + v_j \frac{\partial c_j}{\partial y} = D \frac{\partial^2 c_j}{\partial y^2} + B_j, \quad j = 1, 2;$$

$$x = 0, \quad u_j = u_{j0}, \quad c_j = c_{j0};$$

$$y = 0, \quad u_1 = u_2, \quad \mu_1 \frac{\partial u_1}{\partial y} = \mu_2 \frac{\partial u_2}{\partial y}, \quad v_j = 0;$$

$$c_1 = \chi c_2, \quad D_1 \frac{\partial c_1}{\partial y} = D_2 \frac{\partial c_2}{\partial y};$$

$$y = (-I)^{j+1}\infty, \quad u_j = u_{j0}, \quad c_j = c_{j0}; \quad j = 1, 2,$$

where the index 1 is used to denote gas or liquid phase, while the index 2 designates liquid or solid phase. The terms  $A_j$  and  $B_j$  ( $j=1,2$ ) are the contributions of some additional physical effects.

The solution of the above set of equations permits the mass transfer rate to be determined as follows:

$$J = MK_1(c_{10} - \chi c_{20}) = \frac{MD_1}{L} \int_0^L \left( \frac{\partial c_1}{\partial y} \right)_{y=0} dx = MK_2 \left( \frac{c_{10}}{\chi} - c_{20} \right) = \frac{MD_2}{L} \int_0^L \left( \frac{\partial c_2}{\partial y} \right)_{y=0} dx.$$

There are a number of processes where  $u_j$ ,  $v_j$ ,  $\mu_j$ ,  $\rho_j$ ,  $D_j$ ,  $A_j$ , and  $B_j$  are independent of the concentration  $c_j$  ( $j=1,2$ ). These situations are the basis of the linear mass transfer theory.

The mathematical model allows the following principle characteristics of the linear mass transfer to be drawn:

- the mass transfer rate  $J$  does not depend on the mass transfer direction;
- the mass transfer coefficient  $K_j$  does not depend on the concentrations  $c_{j0}$  ( $j=1,2$ ).

The striving to decrease the size of the industrial devices necessitates process intensification. The systems with intensive mass transfer are characterized by a behavior that deviates considerably from the characteristics mentioned above. The main feature is the higher mass transfer rate, which differs significantly from the value predicted by the linear mass transfer theory. The non-linear effects leading to above have been described in the book.

In systems with high concentrations and such exhibiting large concentration gradients the deviations from the linear Fick's diffusion law are significant too. Under such conditions, the higher concentrations could affect both the viscosity and the density of the fluid:

$$D_j = D_j(c_j), \quad \nu_j = \mu_j(c_j), \quad \rho_j = \rho_j(c_j), \quad j = 1,2.$$

The concentration effect introduces a non-linearity in the convective diffusion equation discussed in details in 1.5.1 and 1.5.2.

The other non-linear effect due to the non-uniform concentration distributions

$$A_j = g(\rho_j - \rho_{0j}), \quad \rho_j = \rho_j(c_j)$$

leads to a natural convection commented in 4.5.1.

The next cause that may intensify the mass transfer process is the existence of a chemical reaction with a rate  $B_j$  in the bulk of the phase:

$$B_j = B_j(c_j), \quad j = 1,2.$$

The studies developed in Part 3 and Part 4, show that in the gas-liquid systems with a chemical reaction  $B_1=0$ , while  $B_2=kc^n$ . Moreover, the chemical reaction rate could affect significantly on the mass transfer mechanism between the phases.

The thermal effect of the chemical reactions could lead to the temperature non-uniformity on the phase interface and to consequent surface tension gradients. This calls for new boundary conditions taking into account the equality of the tangential components of the stress tensor on the interface:

$$y = 0, \quad \mu_1 \frac{\partial u_1}{\partial y} = \mu_2 \frac{\partial u_2}{\partial y} - \frac{\partial \sigma}{\partial x}.$$

The investigation of this effect (Marangoni effect) in 1.5.3 and 4.5.1 has shown that it is negligible when there are no surfactants in the system.

One of the most interesting non-linear effects arises from the conditions imposed by the high concentration gradients. The latter induce secondary flows at the phase boundaries

(Part 1). This effect has been discussed in details in the book for a large number of systems taken as examples and it has been termed “non-linear mass transfer effect”.

Under the conditions imposed by high concentration gradients induced secondary flows occur. They provoke convective components of the mass transfer flux additional to the main diffusion flux. In this case the mass transfer rate is:

$$J = \frac{MD\rho^*}{L\rho_0} \int_0^L \left( \frac{\partial c}{\partial y} \right)_{y=0} dx,$$

where the secondary flow affects both the diffusion mass transfer  $D \left( \frac{\partial c}{\partial y} \right)_{y=0}$  and the convective mass transfer  $\frac{M\rho^*}{\rho_0}$ . In gas-liquid and liquid-liquid systems (Chapters 1.3 and

1.4) the non-linearity has been proven to be the effect of the induced secondary flow on the diffusion transfer. In liquid-solid systems the induced flow affects mainly the convective transfer. These effects are clearly demonstrated the electrochemical systems (discussed in Part 2) due to the high molecular mass ( $M$ ) of the metals.

All the non-linear effects influence the velocity fields which leads to changes in the hydrodynamic stability of the system. The loss of stability could cause an increase of the amplitudes of the random disturbances until a new stable state or a stable periodic process is reached. (Part 5). The latter is a self-organizing dissipative structure with a mass transfer rate growing sharply which is not the case in the conventional systems. The problem has been discussed in details in Chapter 5.5 in the case of non-stationary absorption of pure gases in immobile liquid layer with flat interface.

Self-organizing dissipative structures due to the non-linear mass transfer are Schlichting-Tollmien waves in the laminar boundary layer. The study of these waves should be a further development of the theory of both the non-linear mass transfer and the hydrodynamic stability in systems with intensive interphase mass transfer.

This Page Intentionally Left Blank

## INDEX

Abramov method 418.

**absorption**

$\text{Cl}_2$  252.

$\text{CO}_2$  375, 379, 380, 385, 386, 462, 470, 472, 481.

$\text{H}_2\text{S}$  252.

irreversible 195.

mechanism 252.

$\text{NH}_3$  105.

non-stationary 291, 471, 482.

parameters 279, 281, 304, 385.

physical 174, 178, 189, 191, 193, 197, 222, 227, 233, 249, 263, 264, 269, 276, 278, 279, 291, 304, 316, 368.

plane 265, 275, 276, 277, 281, 288, 306, 367, 385.

problem 265, 266, 269, 303, 305.

pure gases 452, 462.

rate 235, 276, 370, 429, 462, 470, 471, 472, 481.

regime 276, 335, 336, 343, 345, 346, 353, 357, 359, 360, 361, 364, 365, 368, 379, 371, 372.

resistance 282.

reversible 187, 189.

$\text{SO}_2$  252.

square 280, 281, 291.

two-phase 252, 261, 263, 264, 265, 271, 291, 304, 305, 306, 307, 353, 367.

**absorption plane quadrants**

first quadrant 288, 307, 328, 330, 332, 334, 335, 336, 337, 340, 343, 344, 345, 349, 350, 353, 357, 362, 364, 365, 373.

second quadrant 234, 288, 350, 357, 358, 361, 362, 363, 364, 365, 367, 371.

third quadrant 288, 309, 310, 315, 318, 323, 326, 328, 336, 340, 343, 344, 350, 352, 353, 354, 357, 358, 362, 365, 367, 371.

forth quadrant 288, 343, 344, 345, 346, 349, 350, 351, 352, 353, 354, 356, 373.

algorithm 91, 93, 94, 97, 98, 103, 262.

**anodic**

concentration 127, 141, 158.

current 118, 125, 133, 141, 142, 148, 156.

current density 120, 125, 127, 128, 135, 143.

dissolution 118, 119, 120, 122, 124, 125, 127, 130, 132, 133, 137, 141, 142, 147, 156, 158.

layer 127.

limiting current 127, 132, 156.

process 156, 164.

**arbitrary**

perturbation 400, 401, 406.

solution 418.

**attractor(s)** 391, 393, 395.

**Benard**

cell convection 407.

problem 462, 463, 472, 482.

**bifurcation**

curve 405.

non-stationary 407.

point 396.

subcritical 396, 405, 406.

supercritical 396, 405, 406.

theory 394, 395, 402.

- Blasius**  
 flow 440.  
 function 6.
- boundary layer**  
 approximation 5, 7, 14, 413, 424, 487.  
 liquid 429.  
 gas 429.  
 diffusion 5, 23, 25, 26, 27, 28, 29, 30, 40, 52, 62, 66, 88, 92, 96, 119, 122, 124, 128, 137, 153, 157, 165, 172, 173, 174, 181, 182, 189, 190, 194, 196, 199, 200, 227, 232, 241, 246, 247, 252, 292, 299, 301, 303, 346, 351, 363, 374.  
 Helmholtz 119.  
 injection 101, 161, 410, 411, 412, 437, 440, 449.  
 laminar 4, 12, 62, 407, 409, 410, 412, 416, 437, 440, 441, 444, 445, 447, 451.  
 Nernst 119.  
 suction 101, 147, 410, 411, 412, 429, 437, 440, 449.  
 temperature 30, 33, 207, 212, 214.  
 theory 4, 10.
- Cauchy**  
 conditions 152.  
 problem 412, 437.
- characteristic scales 92, 453, 454, 457, 458, 474, 476.
- chemical interaction**  
 strong 323, 326, 340, 344, 353, 354, 364, 370, 371, 372.  
 weak 325, 342, 353, 354, 356, 361, 364, 365, 367, 370, 371, 373, 374.
- chemical reaction**  
 effect 272, 277, 278, 281, 367, 452, 482, 488.  
 fast 197, 222, 261, 264, 278, 278, 290, 291, 369.  
 first order 182, 194, 210, 225, 261, 262, 287, 298, 336, 338, 369, 373.  
 homogenous catalytic 194, 198.  
 irreversible 172, 178, 194, 195, 203, 261, 269, 272, 292, 380, 385, 386, 472.  
 kinetics 222, 294.  
 macrokinetics 125, 171, 193, 194, 202.  
 microkinetics 118, 200.  
 pseudofirst order 181, 184, 192, 195, 372.  
 rate 101, 102, 171, 172, 174, 175, 176, 177, 178, 180, 181, 182, 183, 186, 198, 207, 220, 222, 225, 227, 263, 265, 273, 276, 280, 315, 379.  
 reversible 187, 188, 191, 375.  
 second order 291, 294, 336, 369, 372, 375, 385.  
 slow 174, 180, 222, 276, 277, 297, 379, 381.  
 very fast 206, 210, 214, 215, 222, 302.
- chemosorption**  
 $\text{CO}_2$  375.  
 design 265, 277, 290, 307.  
 interval 307, 315, 316, 307, 315, 316, 332, 333, 336, 343, 344, 345, 347, 348, 349, 350, 353, 354, 357, 362, 364, 365, 368, 371, 372, 373, 374.  
 kinetics 197.  
 liquid film 171, 195, 197.  
 parameter 264, 275, 276, 277, 281, 289, 294, 308, 323, 340, 343, 349, 352, 353, 355, 357, 362, 369, 372, 374.  
 plane 306, 307, 328, 336, 357, 369.  
 resistance 279, 315, 318, 319, 332, 369.  
 square 306, 323, 326, 363, 368, 373, 374.  
 two-phase 261, 263, 277, 290, 303, 305, 315, 335, 343, 350, 351, 353, 360, 362, 364, 365, 368, 369, 371, 373.

- constant**
- equilibrium 188, 191, 192, 222, 375, 381.
  - Faraday 118.
  - Henry 7, 55, 173, 176, 191, 193, 202, 222, 250.
  - rate 120, 179, 180, 188, 193, 194, 220, 222, 263, 264, 292, 343, 369, 375, 376, 381, 384.
  - universal gas 118, 254.
- controlling parameters** 275, 318, 328, 337, 343, 344, 345, 354, 351, 352, 357, 358, 361, 362, 364, 369, 370, 373, 385.
- Couett flow** 407, 429, 440.
- current-potential**
- characteristic 130.
  - curve 137.
  - relationship 130.
- cycle**
- limit 394, 395.
  - stable 394, 396.
  - unstable 394.
- Damkohler**
- number 226, 343, 345, 350, 353, 357, 358, 364, 367, 263, 265, 266, 269, 275, 277, 294, 369, 370.
  - number effect 345, 353, 357, 358, 364.
- Danckwerts equation** 264, 275, 276, 279, 292, 298.
- Darcy law** 118.
- Debay-Hukel theory** 137.
- desorption**
- $\text{CO}_2$  472, 476, 480, 482.
  - gas 477.
  - process 473, 478, 482.
  - rate 429, 472, 481.
- dimensionless**
- equation 4, 10, 13, 52, 113, 128, 130, 144, 154, 221, 226, 228, 229, 234, 253, 262, 294, 303, 308, 363, 369, 401, 454, 455, 474.
  - function 173, 288, 362.
  - parameters 148, 174, 212, 229, 249, 264, 290, 305, 310, 343, 350, 369, 455, 458, 480.
  - variables 10, 33, 54, 67, 77, 91, 96, 102, 128, 139, 143, 148, 154, 163, 172, 179, 185, 188, 194, 196, 199, 205, 208, 226, 304, 307, 362, 454, 468, 469, 474.
- dissipate structure** 406, 452, 471.
- distribution**
- concentration 70, 75, 77, 122, 127, 130, 138, 217, 236, 281, 301, 303, 304, 312, 332, 333, 334, 346, 348, 358, 359, 360, 369, 370, 373, 375, 478,
  - density 162.
  - diffusion resistance 175, 176, 177, 182, 190, 193.
  - particle 115.
  - potential 114, 115, 118, 119, 127, 129, 130, 157, 161, 162.
  - spacio-temporal 114.
  - temperature 217.
  - velocity 17, 27, 28, 29, 40, 70, 73, 76, 77, 100, 122, 147, 148, 219, 436, 441, 479.
- disturbance**
- amplitude 415, 442.
  - infinitesimal 416
  - method 34.
  - neutral 465, 466, 467.
  - periodic 413, 414, 441, 442, 446.
  - small 462, 463, 471, 472.
- Dughamel theorem** 149, 150.

**effect**

chemical reaction 272, 277, 278, 281, 367, 452, 482, 488.  
concentration 53, 54, 85, 89, 90, 91, 157, 158, 161, 207, 209, 210, 441, 443, 487, 488.  
convective transport 103, 175, 181, 182, 222.  
Damkohler number 345, 353, 357, 358, 364.  
density 94, 99, 446.  
double electric layer 153.  
hydrodynamic 17, 30, 53, 75, 432.  
gravitational 88.  
Marangoni 1, 14, 59, 75, 77, 100, 101, 105, 106, 107, 108, 407, 429, 435, 440, 449, 450, 451, 452, 457, 458, 462, 472, 482, 488.  
mass transfer 122, 152, 389, 412, 429, 440, 450, 452, 462, 482, 489.  
mechanical impulse 148.  
migration mechanism 156.  
non-linear 1, 14, 15, 22, 23, 26, 33, 40, 43, 46, 47, 59, 60, 64, 73, 75, 76, 77, 82, 206, 207, 225, 389, 424, 429, 430, 431, 432, 440, 450, 452, 462, 488, 489.  
saturation 127, 141.  
slipping 65.  
temperature 161, 207, 210, 211, 212, 218, 219, 220, 222, 249, 252, 255, 449,  
thermal 100, 101, 161, 211, 452, 453, 482, 488.  
thermocapillary 210, 212, 215, 219, 222.  
viscosity 218.

eigenfunction 217, 218, 398, 403, 404, 408, 415, 416, 418, 419, 467, 469, 479, 482.

eigenvalue 218, 398, 403, 415, 469, 478.

**electrochemical**

cell 118, 119, 161.  
dissolution 111, 142, 153, 161.

**gradient 116.**

machining 118, 120, 134, 142.  
potential 117, 120, 123.  
reaction 111, 121, 127, 133, 162.  
recovery 111, 142, 152, 157.  
system 111, 142, 152, 161, 165.

**electroplating 157.****equation**

autonomous 389, 390, 403.  
characteristic 230, 234, 235, 236, 237, 264, 266, 417, 419.  
chemosorption kinetics 197.  
continuity 116, 225, 454, 464.  
convective diffusion 4, 14, 17, 21, 64, 65, 66, 174, 195, 487, 488.  
convective transport 111.  
Danckwerts 264, 275, 276, 279, 292, 298.  
diffusion 296.  
dimensionless 4, 10, 13, 52, 113, 128, 130, 144, 154, 221, 226, 228, 229, 234, 253, 262, 294, 303, 308, 363, 369, 401, 454, 455, 474.  
equilibrium 376.  
evolution 389, 399, 442.  
Gibbs-Duhham 116.  
heat transfer 1, 29, 161.  
hydrodynamic 17, 18, 19, 21, 134, 142, 399, 400, 487.  
hypergeometric 118.  
ionic mass transfer 114, 117, 128, 134.  
kinematics 158.  
kinetic 130, 158, 191, 197.  
Laplace 118.  
Leveque 149.  
local electrical neutrality 114.  
macroscopic balance 64.  
mass balance 229, 294, 304, 307, 308, 310, 313, 314, 316, 320, 338, 346, 348, 359, 368, 369.  
mass convection 121, 134.  
mass transfer 1, 17, 53, 116.  
Maxwell 116.  
momentum 1, 4, 111, 161.

- multicomponent mass transfer 55.
- Navier-Stokes 2, 4, 18, 21, 64, 66, 89, 134, 138, 227, 399, 407, 414, 441.
- Nernst 112.
- Nernst-Einstein 112, 133.
- Nusselt 195.
- Oberbeck-Boussinesq 88, 407, 453, 463, 478.
- Orr-Sommerfeld 407, 408, 409, 415, 416, 427, 432, 437, 442, 443.
- Poisson-Boltzmann 113.
- Prandtl 409.
- quantity of movement 17.
- Sand 158.
- splitting 370.
- transport 135, 136, 145, 153, 154, 235, 236, 238, 273, 278, 295, 303, 304, 317, 338, 351, 352, 363, 364, 368, 369, 376, 379, 380, 381, 384, 385.
- velocity distribution 70.
- equilibrium**
  - chemical 188, 190, 191, 192, 222.
  - equation 376.
  - mechanical 457, 462, 463, 482.
  - physical 191, 222.
  - state 389.
  - thermodynamic 3, 6, 113, 116, 172.
- Euler**
  - equation 469.
  - formula 391.
- extraction 40, 59, 60, 115, 430.
- Faraday constant 118.
- Fick law 488.
- Floke power 404.
- flow
  - almost parallel 407, 408, 409, 412, 417, 427, 442.
  - Blasius 440.
  - connective 20, 54.
  - Couett 407, 429, 440.
  - electrolyte 118, 119, 161, 162, 423.
  - film 15, 65, 171, 195, 198, 436.
  - Hagen-Poiseuille 407.
  - laminar 18, 85, 137, 147, 152, 161, 406, 407.
  - parallel 407, 408, 417,
  - periodic 405, 406, 407, 442, 452, 462.
  - pipe 407,
  - Poiseuille 37, 407.
  - secondary 14, 17, 28, 29, 38, 53, 59, 64, 65, 67, 74, 75, 100, 101, 102, 108, 111, 406, 410, 411, 424, 435, 436, 440, 441, 450, 451, 452, 457, 462, 463, 482, 487, 488, 489.
  - stability 401, 402, 406, 410, 419, 429, 435, 437, 438, 448, 449, 452.
  - stationary 406, 413, 441.
  - Stephan 1, 19.
  - turbulent 152, 406, 423.
- focus**
  - attractor 391.
  - stable 393, 395, 396.
  - unstable 393.
- Fourier**
  - number 174, 226.
  - series 478.
- frequency critical 408, 414.
- Frumkin A.N. 115.
- function**
  - Blasius 6.
  - characteristic 230.
  - composite 315.
  - correlative 114.
  - current 118.
  - dimensionless 173, 288.
  - Green 3, 83, 84, 197, 297, 469.
  - harmonious 470.
  - objective 288, 289, 316, 317, 318, 319, 320, 321, 323, 325, 326, 328,

- 335, 337, 338, 339, 340, 343, 357, 358, 361, 362, 363, 364, 365, 369, 371, 374.
- power 250.
- galvanization 157.
- Gauss successive method 316.
- Gibbs-Dugham equation 116.
- Green function 3, 83, 84, 197, 297, 469.
- Guy length 114, 115.
- Guy-Chapman theory 113, 115.
- heat transfer
  - coefficient 221, 256, 423.
  - convective 29, 161.
  - equation 1, 29, 161.
  - interphase 252, 258, 259, 423.
  - kinetics 29, 452, 462.
  - laminar tube 147.
  - non-linear 21, 29, 32.
  - non-stationary 252, 385.
  - problem 147, 152, 252.
  - rate 32, 33, 102, 221.
  - regime 256, 257, 258, 259, 260, 261.
  - resistance 259.
  - two-phase 253.
- Hagen-Poiseuille flow 407.
- Helmholtz
  - double electric layer 119.
  - plane 130.
- Henry
  - constant 7, 55, 173, 176, 191, 193, 202, 222, 250.
  - law 228, 292.
- increment factor 408, 414.
- instability
  - area 401.
  - hydrodynamic 435
  - solution 390.
  - thermoconnective 407.
- Karman problem 135.
- Kronecker delta 114.
- Landau-Hopf idea 406.
- law
  - Darcy 118.
  - evolution 389.
  - Fick 488.
  - Henry 228, 292.
  - kinetic 171.
  - mass conservation 86, 172, 174.
  - molecular diffusion 304.
  - Ohm 118, 119, 120.
- Laplace
  - equations 118.
  - operator 150.
  - transformation 150, 151.
- Leveque equation 149.
- Lewis number 30.
- liquid film 64, 65, 66, 76, 171, 195, 198, 200, 203, 204, 207, 210, 212, 435, 436.
- mass transfer
  - coefficient 2, 3, 7, 8, 14, 22, 41, 74, 81, 91, 99, 193, 195, 206, 209, 225, 462, 470, 488.
  - convective 5, 17, 52, 134, 153, 164, 489.
  - diffusion 5, 26, 27, 63, 74, 489.
  - effect 122, 152, 389, 412, 429, 440, 450, 452, 462, 482.
  - equation 1, 17, 53, 116.
  - flux 151.
  - intensive 17, 19, 22, 25, 26, 29, 30, 31, 32, 33, 36, 40, 53, 54, 59, 64,

- 66, 75, 76, 84, 85, 111, 135, 137, 138, 147, 165, 204, 205, 389, 409, 412, 416, 419, 423, 424, 429, 430, 432, 435, 436, 440, 441, 451, 452, 457, 482.
- interphase 1, 5, 8, 9, 10, 14, 17, 19, 22, 29, 32, 33, 36, 40, 41, 45, 47, 48, 49, 51, 52, 53, 54, 55, 58, 59, 63, 64, 65, 67, 75, 76, 85, 87, 88, 100, 125, 138, 143, 146, 156, 161, 165, 171, 172, 175, 176, 178, 179, 180, 182, 193, 194, 198, 207, 222, 225, 227, 233, 236, 237, 265, 269, 281, 292, 410, 411, 412, 416, 419, 423, 424, 429, 430, 432, 435, 436, 440, 441, 451, 452, 472.
- ionic 112, 113, 114, 116, 117, 118, 123, 124, 125, 127, 128, 134, 134, 142, 147, 153, 157, 164.
- kinetics 17, 23, 26, 27, 32, 33, 36, 37, 40, 48, 75, 99, 100, 101, 106, 107, 116, 147, 161, 171, 207, 215, 225, 429, 435, 440, 452, 462, 483.
- mechanism 75, 171, 172, 177, 178, 181, 182, 183, 184, 186, 187, 188, 189, 225, 226, 227, 389, 452, 488.
- multicomponent 21, 33, 35, 36, 37, 54, 55, 59, 76, 81.
- non-linear 1, 14, 19, 21, 23, 25, 26, 27, 28, 29, 30, 32, 36, 37, 40, 47, 51, 52, 53, 54, 59, 64, 67, 75, 76, 77, 78, 79, 85, 88, 89, 91, 95, 99, 100, 101, 105, 106, 107, 203, 410, 411, 424, 429, 430, 431, 432, 435, 436, 440, 449, 450, 452, 457, 462, 472, 482.
- non-stationary 225, 226, 227, 228, 482.
- problem 19, 111, 114, 148.
- rate 1, 2, 7, 8, 9, 14, 19, 22, 27, 28, 37, 39, 40, 41, 45, 52, 53, 63, 64, 70, 74, 75, 76, 77, 78, 81, 91, 95, 96, 102, 119, 147, 165, 171, 172, 174, 177, 178, 181, 183, 191, 193, 195, 198, 204, 207, 209, 221, 222, 227, 368, 410, 435, 448, 472, 478, 482, 483, 487, 488, 489.
- resistance 233, 239, 240, 244, 344, 345, 357, 358, 367, 269, 273, 277, 279, 281, 288, 292, 294, 368, 372, 373, 385.
- steady state 225.
- theory 1, 2, 3, 4, 5, 14, 17, 21, 69, 74, 76, 91, 99, 100, 106, 107, 140, 195, 204, 410, 435, 440, 451, 472, 482, 487, 488, 489.
- with chemical reaction 225, 227.
- Marangoni effect 1, 14, 59, 75, 77, 100, 101, 105, 106, 107, 108, 407, 429, 435, 440, 449, 450, 451, 452, 457, 458, 462, 472, 482, 488.
- Maxwell
- equation 116.
  - stress tensor 115.
- method
- Abramov 418.
  - ADI 38.
  - analytical 118.
  - approximation 163.
  - Gauss successive 316.
  - disturbances 34.
  - experimental 137.
  - least square 471, 482.
  - local thermodynamic equilibrium 116.
  - mathematical physics 163.
  - Nernst 118, 128, 134, 156.
  - numerical 25, 31, 38, 74, 118, 124, 156.
  - perturbation 23, 42, 56, 70, 82, 216.
  - potentiometric 132.
  - Runge-Kutta 322, 329.
  - self consistent field 112, 114.
  - variable separation 230, 263.
- natural convection 14, 214, 407, 452, 454, 457, 458, 462, 477, 482.
- Navier-Stokes equation 2, 4, 18, 21, 64, 66, 89, 134, 138, 227, 399, 407, 414, 441.

- Nernst  
 equations 112.  
 layer 119,  
 model 118, 128, 134, 156.
- Nernst-Einstein relationship 112, 134.
- neutral curve 408, 409, 419, 420, 421, 422, 423, 427, 428, 433, 434, 435, 437, 443, 444, 445, 446, 447, 450, 451.
- number  
 critical Reynolds 404, 416, 419, 420, 428, 433, 437, 439, 446, 447, 448, 450.  
 Damkohler 226, 343, 345, 350, 353, 357, 358, 364, 367, 263, 265, 266, 269, 275, 277, 294, 369, 370.  
 Fourier 174, 226.  
 Lewis 30.  
 Nusselt 31, 33, 36, 103, 105, 213, 221, 222.  
 Peclet 147, 148.  
 Prandtl 152.  
 Reynolds 4, 119, 152, 156, 162, 401, 4007, 408, 409, 413, 416, 419, 420, 421, 422, 423, 427, 428, 429, 432, 433, 434, 435, 437, 438, 443, 450.  
 Schmidt 5, 122, 152, 153, 155, 156, 201, 411.  
 Sherwood 2, 6, 8, 9, 10, 13, 24, 35, 38, 41, 45, 54, 57, 59, 60, 61, 63, 67, 69, 70, 74, 77, 80, 84, 103, 105, 194, 195, 196, 200, 202, 203, 213, 220, 222, 462, 470, 478.  
 Struchal 226.  
 wave 408, 414, 419, 420, 421, 427, 428, 433, 434, 437, 438, 442, 443, 446, 447, 450.
- Nusselt  
 equation 195.  
 number 31, 33, 36, 103, 105, 213, 221, 222.
- Oberbeck-Boussinesq equation 88, 407, 453, 463, 478.
- Ohm law 118, 119, 120,
- Orr-Sommerfeld equation 407, 408, 409, 415, 416, 427, 432, 437, 442, 44, 443.
- Peaceman-Rachford scheme 38.
- Peclet number 147, 148.
- perturbation  
 amplitude 400, 404, 405, 408, 409.  
 arbitrary 400, 401.  
 energy 402, 405.  
 evolution 400.  
 method 23, 42, 56, 70, 82, 216.  
 periodic 404.  
 singular 412.  
 small 390, 394, 400, 402, 403, 406, 478.  
 stationary 403.
- point  
 bifurcation 396.  
 saturation 246.  
 singular 390, 391, 393, 396.  
 stable 395, 396.  
 stationary 309, 391, 483.
- Poiseuille  
 flow 37, 407.  
 profile 37, 40, 161.
- Poisson-Boltzmann equation 113.
- Polubarinova-Kotchina P.Ya equation 118.
- Prandtl  
 equation 409.  
 number 152.
- primary amines 262, 292, 380.

**problem**

absorption 265, 266, 269, 303, 305.  
 Benard 462, 463, 472, 482.  
 boundary 12, 23, 24, 56, 68, 93, 96,  
 185, 186, 189, 190, 194, 196, 197,  
 199, 204, 212, 216, 218, 219, 220.  
 Cauchy 412, 437.  
 chemosorption 262, 263, 304, 307,  
 315, 316, 332, 340, 343, 350, 351,  
 360, 369, 375, 384.  
 concentration distribution 217.  
 convective diffusion 19.  
 eigenvalue 398, 403, 408, 416, 418,  
 419, 466, 479.  
 electrochemical machining 118,  
 142.  
 heat transfer 147, 152, 252, 385.  
 hydrodynamic 19, 135, 210, 399,  
 431.  
 Karman 135.  
 mass transfer 2, 19, 111, 114, 148.  
 model 302.  
 spectral 403.  
 stability 399, 400, 401.  
 Stephan 143, 144.  
 temperature distribution 217.  
 transport 307.  
 velocity profile 216.

**profile**

concentration 140, 273, 317.  
 Poiseuille 37, 40, 161.  
 temperature 152.  
 velocity 37, 122, 123, 138, 155,  
 161, 162, 195, 216, 408, 409, 411,  
 412, 415, 424, 426, 430, 431, 432,  
 435, 436, 441.

**rotating disk electrode** 133.**Reynolds**

critical number 404, 416, 419, 420,  
 428, 433, 437, 439, 446, 447, 448,  
 450.  
 number 4, 119, 152, 156, 162, 401,  
 4007, 408, 409, 413, 416, 419, 420,

421, 422, 423, 427, 428, 429, 432,  
 433, 434, 435, 437, 438, 443, 450.

**Runge-Kutta method** 322, 329.**Sand equation** 158.**Schlichting-Tollmien waves** 489.

Schmidt number 5, 122, 152, 153, 155,  
 156, 201, 411.

Sherwood number 2, 6, 8, 9, 10, 13, 24, 35,  
 38, 41, 45, 54, 57, 59, 60, 61, 63, 67, 69,  
 70, 74, 77, 80, 84, 103, 105, 194, 195, 196,  
 200, 202, 203, 213, 220, 222, 462, 470,  
 478.

similarity variables 6, 8, 11, 12, 22, 29, 41,  
 60, 70, 92, 96, 232, 311, 410, 425, 431,  
 436.

**stability**

analysis 399, 407, 413, 436, 441,  
 449, 462, 469, 470, 471.  
 asymptotic 400.  
 flow 401, 402, 406, 410, 419, 429,  
 435, 437, 438, 4448, 449, 452.  
 global 401, 402, 404.  
 hydrodynamic 75, 85, 107, 389,  
 396, 399, 403, 404, 407, 408, 410,  
 412, 416, 423, 429, 430, 432, 435,  
 436, 440, 441, 449, 450, 452, 473,  
 489.  
 linear 410, 441, 447, 449, 462, 469,  
 470, 471.  
 linear theory 402, 403, 412, 469,  
 481.  
 neutral 405, 416, 445, 451.  
 non-linear 400.  
 power (theory) 400, 401, 402.  
 problem 399, 400, 401.  
 theory 389.  
 zone 402.

- Stephan**  
 flow 1, 19.  
 problem 143, 144.
- stress tensor** 65, 73, 114, 115.
- Struchal number** 226.
- sulphuric acid alkylation** 198, 200.
- surface active agent** 106, 482.
- surface tension** 75, 102, 115, 171, 210, 218, 451, 452, 453, 454, 472, 482.
- systems**  
 Cartesian co-ordinate 234, 305.  
 chemical reacting 272.  
 electrical 111.  
 electrochemical 111, 142, 152, 161, 165, 488.  
 gas-liquid 7, 9, 10, 12, 40, 48, 51, 52, 54, 63, 64, 91, 99, 101, 106, 171, 178, 184, 193, 195, 207, 210, 385, 424, 429, 432, 435, 436, 450, 472, 488.  
 gas-solid 5, 21, 48, 91, 410, 423.  
 heterogeneous 116.  
 liquid-liquid 7, 40, 59, 76, 91, 100, 105, 106, 107, 429, 430, 432, 435, 488.  
 liquid-solid 5, 21, 48, 91, 410, 423, 488.  
 multicomponent 33.  
 physical 145.  
 two-phase 17, 19, 64, 106, 225, 227, 241, 343, 353, 364, 370.  
 with intensive mass transfer 17, 85, 88, 99, 147, 389, 410, 435, 440, 441, 451, 452, 482, 488, 489.  
 with semitransparent membranes 147.  
 film flow 435, 436.
- Taylor**  
 expression 298.  
 vortexes 407.
- theory**  
 asymptotic 25, 31, 32, 35, 36, 47, 49, 52, 74, 75, 88.  
 bifurcation 394, 395, 402.  
 boundary layer 4, 10, 21.  
 convective diffusion 125, 158.  
 Debay-Hukel 137.  
 decelerating charge 128.  
 diffusion boundary layer 23, 172.  
 diffusion in multicomponent systems 33.  
 Guy-Chapman 113, 115.  
 kinetics 64, 111.  
 linear mass transfer 1, 3, 4, 5, 14, 17, 21, 26, 28, 32, 33, 53, 63, 69, 74, 76, 99, 487, 488.  
 linear stability 402, 403, 412, 469, 481.  
 mass transfer 17, 21, 69, 74, 76, 91, 99, 100, 106, 107, 140, 195, 204, 410, 435, 440, 451, 472, 482.  
 model 2, 3.  
 multicomponent mass transfer 54.  
 non-linear mass transfer 14, 63, 74, 75, 88, 91, 99, 107, 487, 489.  
 power 400, 401, 402.  
 rotating disk electrode 133.  
 stability 389.
- turbulence** 156, 202, 405, 406, 407, 409, 423, 429.
- wave**  
 length 408, 414.  
 number 408, 414, 419, 420, 421, 427, 428, 433, 434, 437, 438, 442, 443, 446, 447, 450.  
 velocity 419, 420, 422, 423, 428, 433, 437, 443, 446, 447, 450.